Pulp Production and Processing: From Papermaking to High-Tech Products

Editor
Valentin I. Popa

SMITHERS RAPRA

Pulp Production and Processing: From Papermaking to High-Tech Products

Editor

Valentin I. Popa

A Smithers Group Company

Shawbury, Shrewsbury, Shropshire, SY4 4NR, United Kingdom
Telephone: +44 (0)1939 250383 Fax: +44 (0)1939 251118
http://www.polymer-books.com

First Published in 2013 by

Smithers Rapra Technology Ltd

Shawbury, Shrewsbury, Shropshire, SY4 4NR, UK

A catalogue record for this book is available from the British Library.

ISBN: 978-1-84735-633-8 (hardback)
978-1-84735-634-5 (softback)
978-1-84735-637-6 (ebook)

Typeset by Argil Services

Preface

It is known that the pulp and paper industry is based on renewable and recyclable resources. Therefore, this industry can be considered as the only one which corresponds to the criteria of sustainable development. At the same time, the pulp and paper industry can be environmentally friendly if it is developed using a combination of chemical and biotechnological processes; from this point of view a new concept, represented by biorefining, is discussed.

The biorefining concept offers an opportunity to revitalise the pulp and paper industry to produce high-value chemicals and biofuels, develop new technologies and to penetrate new markets. This situation explains the different proposals, at a world level, concerning the implementation of biorefining in the pulp and paper industry, or to create and develop a new technology. The existence of such opportunities is discussed along with the concept of complex biomass processing. Thus, this evaluation could be useful to establish what directions can be identified for practical applications of a biorefinery. The objective of *Future Biorefinery* is to develop new methods, enabling fractionation of wood or annual plants into cellulose, hemicelluloses, lignin and extractives in their native-like form, and to further upgrade these fractions into chemicals and materials.

The conventional procedures to obtain pulp and paper include chemical or mechanical treatments of fibrous raw materials. The resultant pulp yield is a function of the applied technology; the by-products are used to recover chemicals and energy.

Bleaching is the following step connected with pulp manufacturing. This operation is carried out using oxidants as the main reagents to continue the removal of lignin. At present, there is an increasing interest for the bleaching technology to be eco-friendly, which explains why oxygen is utilised on a large scale.

After pulp production, the resultant black liquors contain many valuable products. Among the options concerning the process of biorefining include research presently being carried out involving recovery of the compounds which are formed by the chemical transformation of raw material components during delignification.

The majority of the produced pulp is used for paper manufacture, which is why knowledge of the fibre characteristics and their behaviour during the process of

papermaking represents important aspects. At the same time, we have to take into account the possibilities of developing raw material resources bearing in mind the existing experience of hardwoods; represented by the known species in South America, or new ones proposed to be used in China.

Over recent years, the utilisation of cellulose to synthesise its derivatives has increased. This situation is determined on the one hand by the accessibility of this renewable compound in large quantities, and on the other hand by the possibility of manufacturing high-tech products based on cellulose and its derivatives.

The new solvent (e.g., *N*-methyl-morpholine-*N*-oxide) developed for cellulose, assures the fabrication of cellulosic fibres (lyocell) to substitute cotton fibres in a higher proportion, which explains the increasing dissolving pulp production.

The compatibility of cellulose with the environment and biological systems explains the new utilisation in the high-tech fields as microspheres, nanostructures, optical functional films or antibacterials.

Last but not least, cellulosics as waste materials can be used to produce biofuels; hydrogen being presented as an example.

The initiative to edit this book belongs to Helene Chavaroche who presented me with a challenge. That is why special thanks are extended to Helene and many of her colleagues who were involved in this project, taking the risk to bring out such a book and for ensuring the excellent quality of the publication.

The publishing of this book was accomplished with the contributions of renowned specialists in the pulp, paper and cellulose derivatives production from all over the world. We are very grateful to these scientists for their efforts and dedication to this reference work.

Last but not least, I would like to thank to my wife, Mariana, and my daughters, Liana-Ionela and Ana Maria, for their patience. I sincerely apologise for the many hours I spent in the preparation of this book, which kept me away from them.

This book is a very useful tool for many scientists, students and postgraduates working in the field of pulp, paper and cellulose derivatives, aimed at opening a new era of renewable resources processed by biorefining. It may not only help in research and development, but may also be suitable in the line of teaching.

I hope that you as a reader will enjoy the volume.

Valentin I. Popa

2013

Contributors

Jing Bian

Institute of Biomass Chemistry and Technology, Beijing Forestry University, Beijing 100083, China

Diana Ciolacu

Petru Poni Institute of Macromolecular Chemistry Iasi, 41 A, Grigore Ghica-Voda Alley, 700487 Iasi, Romania

Florin Ciolacu

Gheorghe Asachi Technical University of Iasi, Department of Natural and Synthetic Polymers, Paper Science and Engineering Group, Blvd. Mangeron, No 71, Iasi-700050, Romania

Jorge Luiz Colodette

Pulp and Paper Laboratory, Forestry Engineering Department, Federal University of Viçosa, Viçosa, 36.570-000, Brazil

Monica Ek

Wood Chemistry and Pulp Technology, School of Chemical Science and Engineering, KTH - Royal Institute of Technology, SE-100 44, Stockholm, Sweden

Pedro Fardim

Laboratory of Fibre and Cellulose Technology, Åbo Akademi, FinlandLab. of Fibre and Cellulose Technology, Åbo Akademi University, Porthansgatan 3 FI-20500, Finland

Heinrich Firgo

Lenzing Aktiengesellschaft, 4860 Lenzing, Austria

Dan Gavrilescu

Gheorghe Asachi, Technical University of Iasi, Romania

Martin Gericke

Laboratory of Fibre and Cellulose Technology, Åbo Akademi, FinlandLab. of Fibre and Cellulose Technology, Åbo Akademi University, Porthansgatan 3 FI-20500, Finland

Youssef Habibi

Department of Advanced Materials and Structures, Public Research Centre Henri Tudor, 5 rue Bommel/ZAE Robert Steichen, 4940, Hautcharage, Luxembourg

Josefin Illergård

Wood Chemistry and Pulp Technology, School of Chemical Science and Engineering, KTH - Royal Institute of Technology, SE-100 44, Stockholm, Sweden

Emmanuel G. Koukios

School of Chemical Engineering, National Technical University of Athens, Zografou Campus, GR-15700 Athens, Greece

Mohd Edeerozey Abd Manaf

School of Materials Science, Japan Advanced Institute of Science and Technology, 1-1 Asahidai, Nomi, Ishikawa 923-1292 Japan and Faculty of Manufacturing Engineering, Technical University of Malaysia Malacca, Locked Bag 1752, Durian Tunggal, 76109, Malacca, Malaysia

Daniela Correia Martino

Pulp and Paper Laboratory, Forestry Engineering Department, Federal University of Viçosa, Viçosa, MG Brazil 36.570-000

Miloslav Milichovský

University of Pardubice, Faculty of Chemical Technology, Department of Wood, Pulp and Paper, Studentská 95, CZ 532 10 Pardubice, Czech Republic

Lilana Olaru

Petru Poni Institute of Macromolecular Chemistry Iasi, 41 A, Grigore Ghica-Voda Alley, 700487 Iasi, Romania

Nicolae Olaru

Petru Poni Institute of Macromolecular Chemistry Iasi, 41 A, Grigore Ghica-Voda Alley, 700487 Iasi, Romania

Ioannis A. Panagiotopoulos

Forest Products Biotechnology/Bioenergy Group, Faculty of Forestry, University of British Columbia, 2424 Main Mall, Vancouver BC, V6T 1Z4, Canada

Feng Peng

Institute of Biomass Chemistry and Technology, Beijing Forestry University, Beijing 100083, China and State Key Laboratory of Pulp and Paper Engineering, South China University of Technology, Guangzhou 510640, China

Pai Peng

State Key Laboratory of Pulp and Paper Engineering, South China University of Technology, Guangzhou 510640, China

Valentin I. Popa

Gheorghe Asachi, Technical University of Iasi, Romania

Jun-Li Ren

State Key Laboratory of Pulp and Paper Engineering, South China University of Technology, Guangzhou 510640, China

Dana Suflet

Petru Poni Institute of Macromolecular Chemistry Iasi, 41 A, Grigore Ghica-Voda Alley, 700487 Iasi, Romania

Run-Cang Sun

Institute of Biomass Chemistry and Technology, Beijing Forestry University, Beijing 100083, China and State Key Laboratory of Pulp and Paper Engineering, South China University of Technology, Guangzhou 510640, China

Jani Trygg

Laboratory of Fibre and Cellulose Technology, Åbo Akademi, FinlandLab. of Fibre and Cellulose Technology, Åbo Akademi University, Porthansgatan 3 FI-20500, Finland

Ivo Valchev

Department of Pulp, Paper and Printing Arts, University of Chemical Technology and Metallurgy, 8, Kl. Ohridski Str., 1756 Sofia, Bulgaria

Lars Wågberg

Wood Chemistry and Pulp Technology, School of Chemical Science and Engineering, KTH - Royal Institute of Technology, SE-100 44, Stockholm, Sweden

Patrick A. White

51 Park View, Sharnford, Leicestershire, LE10 3PT, United Kingdom

Feng Xu

Institute of Biomass Chemistry and Technology, Beijing Forestry University, Beijing 100083, China

Masayuki Yamaguchi

School of Materials Science, Japan Advanced Institute of Science and Technology, 1-1 Asahidai, Nomi, Ishikawa 923-1292 Japan

Contents

1 Biorefining and the Pulp and Paper Industry

Valentin I. Popa

1.1 Introduction

Enhanced industrial competition puts pressure on conventional industries, such as the pulp and paper industry. Therefore, the pulp industry must reinforce its competitiveness and produce both products of higher value and large volumes of base chemicals. A pulp mill has excellent prerequisites to be the base for a biomass-based biorefinery due to the large flow of raw materials (wood and annual plants), existing process equipment and good process knowledge. The key strengths of the pulp and paper industry are the wood and biomass sourcing along with the logistic infrastructure, a sustainable existing base of integrated production, and the high efficiency and experience in combined heat and power generation. The industry has unique capabilities in handling very large volumes of biomass, and the synergies in logistics and energy integration are significant. Therefore, biorefining and bioenergy fit well into the integrated business model of forest product companies.

The current chemical pulp process uses approximately 50% of the available organic raw material in the production of paper pulp; the remaining 50% is combusted in the recovery boiler to produce steam. A modern energy-optimised pulp mill has a substantial excess of energy/steam. This excess can be utilised in several different ways:

- The first is to produce electrical power;
- The second is to replace the recovery boiler with a black liquor gasification unit to produce syngas;
- The third is to extract some lignin from the black liquor and sell it as a new product to be used as fuel or raw materials for biobased products; and
- The fourth is to attract other external sources of biomass or wastes and to process them with the aim of obtaining fuels and chemicals [1].

In the pulp mill of tomorrow, the hemicelluloses and extractives, dissolved in process streams, could be extracted and used as chemical raw materials.

According to the American National Renewable Energy Laboratory, a biorefinery is a facility that integrates biomass conversion processes and equipment to produce fuels, power and chemicals from biomass [2]. Biorefining aims for a complete valorisation of the biomass source by performing the overall processes with minimum energy and mass, and to maximise the overall value of the production chain. It consists of an efficient fractionation of biomass into various value-added products and energy, using physical separation processes in combination with biochemical and thermochemical conversion steps. In that sense, the biorefinery concept has similar objectives as today's oil refineries. A plant for the fractionation and refining of biomass, and for the utilisation of its entire components, a 'biorefinery' plant, will have to display a high level of process **integration** and **optimisation** to be competitive in the near future. Forest product companies may increase revenue by producing biofuels and chemicals in addition to wood, pulp and paper products in a so-called Integrated Forest Biorefinery (IFBR). The concept of an IFBR is being advanced by a number of investigators who envision converting cellulose, hemicelluloses and lignin from woody biomass, dedicated annual crops and municipal waste into bioenergy and basic chemicals [3]. As a consequence, the chemical pulp mill could be transformed into an integrated biomass biorefinery producing different chemicals besides traditional pulp and papers [4]. At the same time, the utilisation of biomass as a renewable raw material may have the following advantages:

1. Reduced dependence on imported fossil oil;
2. Reduction in greenhouse gas emissions;
3. Building on the existing innovation base to support new developments;
4. A bioindustry that is globally competitive;
5. The development of processes that use biotechnology to reduce energy consumption and the use of nonrenewable materials;
6. The creation of jobs and wealth;
7. The development of new, renewable materials;
8. New markets for the agriculture and forestry sectors, including access to high-value markets;
9. Underpinning a sustainable rural economy and infrastructure; and
10. Sustainable development along the supply chain from feedstock to products and their end-of-life disposal.

1.2 Biomass for Chemicals and Bioproducts

The term biomass is defined as any organic matter that is available on a renewable basis, including dedicated energy crops and trees, agricultural food and feed crop residues, aquatic plants, wood and wood residues, animal wastes and other materials. The chemical composition of biomass depends strongly on its source. Plant tissue can be divided into various compound classes, including storage materials which are intracellular and structural components that occur in membranes, extracellular or as cell wall constituents.

1.2.1 Intracellular and Storage Materials

1.2.1.1 Proteins

Proteins represent a group of substances in plant cells and consist of polypeptides, which are long chains of various amino acids. Proteins serve a manifold purposes, e.g., as enzymes, transport proteins, regulators, storage substances or as structural proteins. They are usually composed of the 20 most commonly occurring amino acids, which can be subdivided into basic, neutral or acidic amino acids.

1.2.1.2 Starch and Fructans

Starch is an important storage polysaccharide in vascular plants. Starch consists of two different polymers of glucose, amylose and amylopectin, where amylose composes, on average, 25% of the starch.

Fructans are often found as a further storage polysaccharide in grasses. This is a water-soluble polymer of fructose with α-D-glucose as an end group. Besides their storage function, they are essential for osmoregulation and freezing point depression in plant cells. The two most important groups are inulins, composed of β-(2-1)-linked fructose, and levans or phlein, with β-(2-6)-linkage of the fructose units.

1.2.1.3 Chlorophyll and Other Pigments

Chlorophyll consists of four pyrrole rings which, together with a fifth ring, build a porphyrin structure; a long phytol chain is bound to the porphyrin structure. Chlorophyll is present in all photosynthetically active cells. During leaf senescence,

chlorophyll is decomposed, whereas carotenoids (yellow pigments) accumulate and new red anthocyanins are synthesised, giving the autumnal colouration of foliage.

1.2.2 Plant Cell Wall Components

1.2.2.1 Cellulose

Cellulose is the most abundant biopolymer, as it comprises the major structural component of the cell walls, and its quantity is estimated at approximately 2×10^9 tonnes/year [5]. Cellulose is a linear polymer glucan and is composed of glucose units which are linked by β-(1-4)-glycosidic bonds. The regular arrangement of the hydroxyl groups along the cellulose chain leads to the formation of H-bridges and therefore to a fibrillar structure with crystalline properties. Approximately 15% of the cellulose fibrils build a basic structure, which is closely associated with hemicelluloses and in the woody cell wall with lignin [6–8].

1.2.2.2 Noncellulosic Polysaccharides

The noncellulosic polysaccharides are often summarised as hemicelluloses or polyoses. Noncellulosic polysaccharides differ from cellulose in their composition of sugar units (mainly pentoses, hexoses, hexuronic acids and desoxyhexoses), side chain and branching. Hemicelluloses are a group of polysaccharides of different composition, which consist of different cellulose sugar units, bound together by glycosidic linkages, with a variable branching degree and a lower degree of polymerisation than cellulose. The content and composition of hemicelluloses are different in deciduous and coniferous wood and annual plants. Xylans are a widespread hemicellulose group, consisting of (1-4) glycosidic units of β-D-xylose. Additionally, they contain among other sugars, α-L-arabinose and 4-*O*-methyl–D-glucuronic acid, linked in the C2 or C3 position of the xylose. They comprise 5–30% of the polysaccharides in woody tissues. Mannans are composed of chains of (1-4)-glycosidic-linked β-D-mannose, which are partly supplemented with side chains of α-D-galactose (bound by 1,6-glycosidic bonds). Glucomannans, with a glucose-mannose ratio of 1:2, are mainly found in deciduous trees. Coniferous plants possess glucomannans with a galactose side chain. Galactans are water-soluble, highly branched polysaccharides composed of (1-3/6)-glycosidic-bound β-D-galactose. The side chains consist of, among other monosaccharides, L-arabinose and L-rhamnose which are linked *via* (1-6)-glycosidic bonds. Pectins are complex, strongly branched polysaccharides, consisting mainly of galactose, arabinose and hexuronic acids. Pectins form the binding substance between

the cells, especially in herbaceous plants and fruits; additionally, they occur in the primary cell wall. Pectin only composes a small proportion of the plant material in woody tissues and in grasses (approximately 1% in woody material). In contrast to crystalline cellulose, most hemicelluloses are soluble in alkaline solution [9–12].

1.2.2.3 Lignin

Lignin is a high molecular, three-dimensional macromolecule consisting of phenyl propane units. Lignin fills out the cell walls, which consist predominantly of linear polysaccharidic membranes, providing structural rigidity. Lignin is an important element of the cell walls of vascular plants. Along with hemicelluloses, lignin is found in the primary wall, the secondary wall, and in the middle lamella of the voids of the cellulose-microfibrils. After the polysaccharides, lignin is the most abundant biopolymer in nature and a large contributor to the residues of the terrestrial biomass. The primary building units of lignin (monolignols) are the cinnamyl alcohols: coniferyl alcohol, sinapyl alcohol and *p*-coumaryl alcohol. The monomers react through the so-called dehydrogenative polymerisation to a three-dimensional macromolecule, which contains a multitude of C-C and ether-linked compounds. The arylglycerol-β-arylether (β-*O*-4) linkage dominates by far, followed by biphenyl (5-5) and phenylcoumaran (β-5) linkages. Most of the linkages in lignin molecules are not hydrolysable. Lignin in gymnosperms, angiosperms and grasses is classified based on differences in monolignol composition. The lignin of gymnosperms is composed almost exclusively of guiacyl propane monomers, which are derived from coniferyl alcohol. Angiosperm lignin contains approximately equal proportions of guiacyl propane and syringyl propane units derived from sinapyl alcohol. The lignin of grasses is composed of approximately equal proportions of guiacyl propane, syringyl propane and *p*-hydroxyphenyl propane units. Additionally, around 5–10% of *p*-coumaric acid and ferulic acid, which are predominantly esterified to the terminal hydroxyl groups of the propyl side chains, is found in lignin. The proportions of coniferyl, sinapyl and *p*-coumaryl alcohol amount to 94:1:5 in spruce lignin, 56:40:4 in beech lignin and 1:1:1 in grass lignin. Part of the cellulose or hemicelluloses is bound to lignin in the so-called lignocellulose or lignin-polysaccharide-complex. The structure of this complex is far from clear and no detailed structural model can be given. It is supposed to be held together by hydrogen bonds and covalent (ester or ether) linkages [13–15].

1.2.2.4 Tannin and Other Polyphenols

Tannins are defined as polyphenols that occur in higher plants. They precipitate proteins in aqueous solutions and therefore act as tanning substances. Besides tannic substances, plants contain a multitude of other *secondary phenolic substances*. Tannic

substances are distinguished in two groups, the condensed or nonhydrolysable tannin (also termed proanthocyanidine) and the hydrolysable tannins. The condensed tannins are polyphenols from polyhydroxy-flavan-3-ol units, which are linked mostly through C-C bonds between C-4 and C-8, and sporadically between C-4 and C-6 and therefore, not acid or base hydrolysable. Usually, condensed tannins consist of more than one flavan unit and up to 40 monomers have been found. Due to the presence of different functional groups, an immense heterogeneity exists within this compound class. Polymer proanthocyanidines possess two phenolic OH-groups on the B-ring, whereas prodelphinidines possess three OH-groups. The proanthocyanidines are bound to polysaccharides by glycosidic bonds, e.g., on hemicelluloses. Hydrolysable tannins contain units, namely sugar (mostly D-glucose or similar polyoses) and phenolic acids. They yield both units upon acid or alkaline hydrolysis. They are a heterogeneous group of macromolecules, which can be differentiated into gallotannin and ellagitannin. Gallotannin has a central sugar unit, which is esterified with several molecules of gallic acid; whereas, ellagic acid is a basic phenolic unit of ellagitannin. Tannins are quantitatively important components of various plant parts. They occur in various organs of higher plants, especially in dicotyledones. Condensed tannins are found in high concentrations in the bark of trees and also in the shell material of hazelnuts. Tannic substances play an important role as antifeedants, i.e., they are the defence of the plant against chewing phytophagus insects or animals [16].

1.2.2.5 Lipids

Lipids are organic substances that are insoluble in water but extractable with nonpolar solvents, e.g., chloroform, hexane, ether or benzene. Lipids are a heterogeneous group of substances that occur both in plants as well as microorganisms. The surface lipids of plants are comprised of different structural groups. They cover the surface of leaves and needles with a thin layer as a component of the plant cuticle.

1.2.2.6 Cutin and Suberin

Cutin and suberin are polyesters that occur in vascular plants. Cutin composes the macromolecular frame of the plant cuticle in which the low molecular waxes and fats are embedded. The cuticle covers the epidermis and protects the plant surface against desiccation by the atmosphere. In contrast, suberin is a cell wall component of cork cells, which compose the periderm layer of surficial as well as subterranean parts of woody plants. Suberin is also found in bundle sheath cells of grasses. The content of suberin is particularly high in bark and in plant roots. The cutin polymer is composed of di- and trihydroxy and epoxy fatty acids with a C_{16} and C_{18} chain length. In the C_{16} group, dihydroxypalmitic acid dominates, and in the C_{18} group,

oleic acid and hydroxyoleic acid dominate. These are mainly linked by ester bonds and some ether bonds. The individual composition of cutin polymers is dependent on the plant species, stage of development and environmental conditions. Suberin is composed of aliphatic and aromatic components. In contrast to cutin, it contains monomers with a higher chain length of C_{20}-C_{30}, in particular 1-alcanols, fatty acids, ω-hydroxy fatty acids and especially α,ω-dioic acids with a C_{16} or C_{18} chain length. In addition, suberin contains phenolic acids, especially hydroxycinnamic acids [17].

1.2.2.7 Oil Crops

Domesticated oil seed crops are major agricultural commodities used primarily for nutritional applications. Recently, these oils have been used to produce biofuels and chemical feedstocks. The rising cost of petroleum has fuelled concern about the environmental impact of using fossil oil. The reliance on foreign fuels sources has emphasised the need to develop renewable domestic sources of fuel and industrial raw materials. Plant oils are renewable sources of high-value fatty acids for the energy, chemical and health-related industries. The fatty acid composition of plant oil generally defines its value and areas of application. There are several areas where plant oils can have significant impact on the emerging energy, chemical and nutritional demands due to the types of fatty acids required in various applications.

1.2.2.8 Terpenes

Terpenes constitute a large class of some 40,000 structures and form the largest class of all known plant constituents. Their formation is based on the isoprenoid biosynthesis pathway in which higher molecular weight materials are formed from successive incorporation of the fundamental building blocks of isoprene. This five carbon branched molecule leads to the generation of multiples, i.e., monoterpenoids (C_{10}), sesquiterpenoides (C_{15}) and diterpenoids (C_{20}), up to the natural rubber which is a polyterpenoid. *Many industrially relevant chemicals, pharmaceuticals, flavours, fragrances, pesticides and disinfectants, are derived from plant terpenes*. A new awareness of plant terpenoids as valuable resources has developed where the use of these plant chemicals can displace society's reliance on petrochemical resources. Interdisciplinary research ranging from chemistry to biology will be required to harness these plant chemicals as strongly contributing renewable resources. Understanding of biosynthetic pathways and metabolic engineering to improve yields is basic to the endeavours of providing new chemical feedstocks for the production of specialised chemicals and fuels [18].

1.3 Possibilities of Biorefining Implementation into the Pulp Industry

Examples of fractionation technologies are the several biomass pulping processes that are common practice in the pulp and paper industry (e.g., kraft pulping, sulfite pulping, soda pulping, organosolv pulping and so on). Here, the biomass is essentially fractionated into cellulose (for paper) and black liquor, a waste stream that predominantly contains residual carbohydrates and their degradation products (e.g., from the hemicelluloses), partly degraded lignin and inorganics from the pulping process. The main application to date of this black liquor is combustion for heat. In addition, lignin and lignin-containing residues are large side streams from the pulp and paper industry, and from biorefineries that use the carbohydrate fraction of the biomass, e.g., for the production of bioethanol. Globally ~ 50 Mt per year of lignin originates from the pulp and paper industry, predominantly from kraft-, soda- and sulfite-pulping of softwood, hardwood and agricultural residues such as straw, flax and grasses. Only 1 Mt is used for commercial purposes, including lignosulfonates from sulfite pulping, and 0.1 Mt as (chemically modified) kraft lignins from kraft pulping. At present, most of these sulfur-containing lignin streams are combusted to generate power and/or heat, an application with very limited added value. These sizable amounts of lignin are in principle available for valorisation into chemicals and performance products. New developments in soda-pulping technology have resulted in sulfur-free lignins from herbaceous types of biomass such as straw and grass [19, 20]. Furthermore, large amounts of (hydrolytic) lignin will be produced from future bioethanol-based biorefineries by processes such as steam explosion and organosolv pulping. The first process is a thermomechanical treatment that uses sulfuric acid for the hydrolysis and steam explosion for breaking up the fibrous biomass structure. Organosolv pulping of the hardwood, grasses and straw leads to a high-quality lignin that is essentially sulfur-free. Organosolv pulping refers to a thermal and pressurised treatment of the lignocellulosic biomass with water and organic solvents such as ethanol and carboxylic acids. The biomass is fractionated into lignin, cellulose and a hemicellulose-containing side stream. Generally, the hydrolytic lignins are the main fraction in the side stream, which originate from the processing of wood and agricultural residues for transportation fuels and chemical building blocks.

Taking into account the utilisation of different biomass sources as raw materials in a complex integrated pulp mill producing bioproducts and biomaterials, in our opinion we have to consider the following aspects: (1) all kinds of vegetable biomass contain almost the same main compounds; (2) the macromolecular compounds existing in the biomass incorporate biosynthesis energy, and their conversion to useful products seems to be economical; and (3) the complex and total processing technology may be modulated depending on the chemical composition of the biomass sources, as well

as on the utilisation of the obtained chemical compounds [21]. Thus, the specific objectives of this proposal have to be the following:

1. Identification, quantification and characterisation of resources from the chemical composition point of view;
2. Separation and establishment of the optimal conditions for fractionation using an original scheme, which allows isolating chemical compounds as a function of their structure and the raw material accessible to be processed (**Figure 1.1**). Conventional and nonconventional extraction procedures will be used;

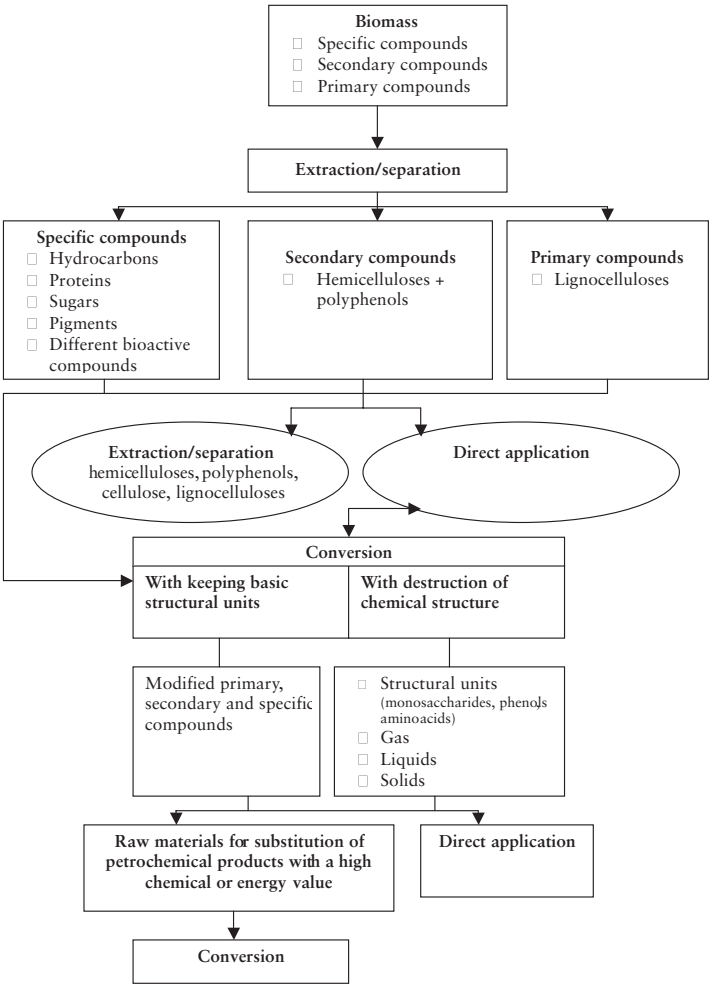

Figure 1.1 Flow sheet of integral and complex processing of phytomass

3. Characterisation of isolated products; comparative studies of extraction methods will be carried out; correlation of the characteristics with the possibility of utilising the obtained products; establishing potential applications;

4. The elaboration of sequential technological procedures to recover separated compounds with the aim of transferring them to the pilot-scale level;

5. Evaluation of the results obtained in technological transfer from the efficiency, economical and social points of view; and

6. Evaluation of the economical feasibility of applications of the proposed technologies; analysis of the cost-benefit ratio.

The world distribution of phytomass evidences huge quantities still unexploited by man (about 89%), together with significant forest, agricultural, industrial and urban wastes.

Wood phytomass is still being incompletely exploited (an important amount is used as fuel (about 50%) for local energy requirements and, only to a certain extent, for chemical ones).

Agricultural phytomass is now being confronted with a new problem: 'limited grounds against an ever increasing number of people', a situation which cannot, by any means, assure new stocks (wastes excepted); consequently, there is no reason to replace valuable food products such as wheat, sugar beet, sugar cane for conversion into liquid fuels (e.g., ethanol). In such circumstances, mention should be made of the efforts to use soil inadequate for agriculture, in order to energetically culture fast-growing plants, species with a high content of biological compounds or hydrocarbons. At the same time, it is known that the processing of agricultural products and plants containing biological compounds, results in a substantial amount of waste This can represent a raw material, allowing the separation and upgrade of different components, with energy and chemical value, using technology proposed by us. Thus, from a pulp mill biorefinery the following products can be obtained besides that of pulp and paper: phenols, adhesives, carbon fibres, activated carbon, binders, barriers, antioxidants, pharmaceuticals, nutraceuticals, cosmetics, surfactants, chelants, solvents, descaling agents, speciality polymers, biofuels (pellets, lignin fuel, methanol, dimethylether, ethanol and so on). New or increased amounts of traditional products can be made from internal/or external biomass (**Figure 1.2**).

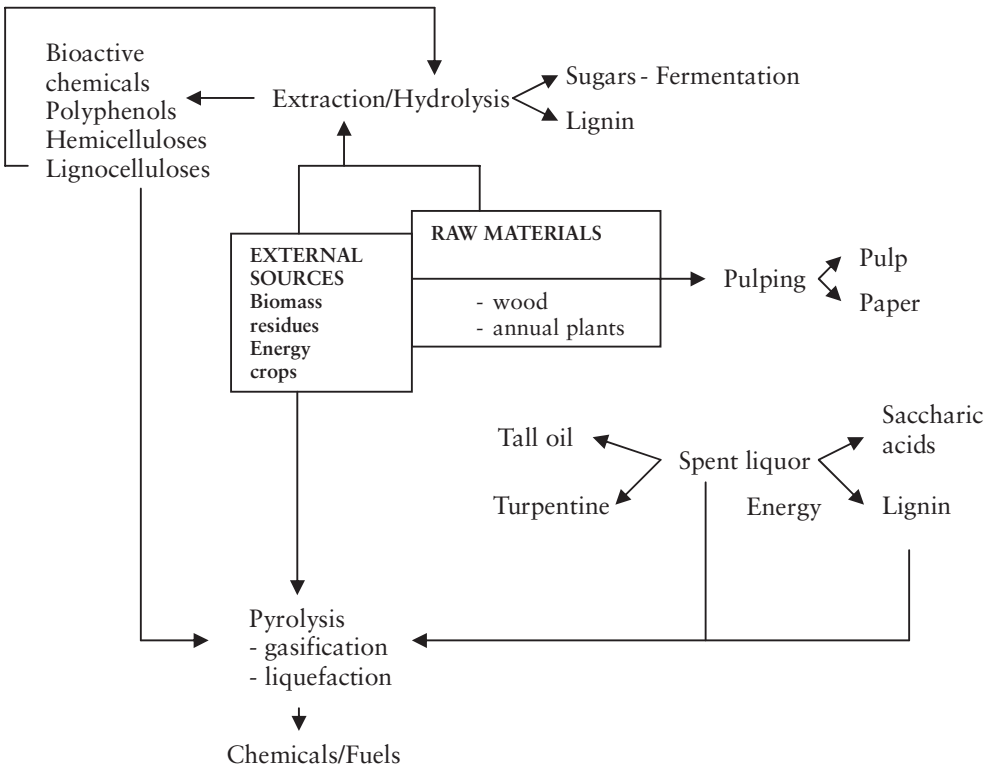

Figure 1.2 Flow sheet for biorefining technology using internal and external biomass sources

Three different levels can be identified:

- A high degree of energy saving in future mills, especially chemical pulp mills, will lead to a large amount of excess internal biomass which can be transformed into the products mentioned above;
- Components in e.g., the black liquor, forest residues and bark can be upgraded to more valuable ones, and the energy balance of the mill can be maintained through fuel import, wholly or partly depending on the level of mill energy efficiency. The imported fuels can be biomass or other types; and
- External (imported) biomass (in some cases together with excess internal biomass) can be upgraded using the synergy effects of docking this upgrading to a pulp mill.

To develop and apply new technology, we took into account the following considerations as a result of our previous research [21–23].

I. *All categories of phytomass contain the same compounds, arbitrarily divided into three large groups*:

- Primary compounds: cellulose and lignin;
- Secondary compounds: hemicelluloses and polyphenols; and
- Specific compounds: pigments, hydrocarbons simple sugars, alkaloids, polyphenols, other bioactive compounds, oils, proteins and so on.

After the selective isolation of the specific and secondary compounds (performed in successive stages), the structural heterogeneity is reduced. Thus, the residual material becomes lignocellulose (cellulose/lignin in variable ratios) characteristic of all higher plants; some examples are presented in **Tables 1.1** and **1.2**.

Consequently, *any category of available vegetable biomass may constitute a source of raw materials in its complex and integral valorification*.

II. *Compounds existing in phytomass store an important amount of energy as a result of their biosynthesis*. Thus, the biosynthesised macromolecular structures in phytomass require an amount of equivalent external energy for their cleavage into energy or chemical compounds (e.g., glucose from cellulose and phenol from lignin). That is why, depending on the available raw materials, investigations have not been restricted exclusively to obtaining ethanol from cellulose *via* 'glucose', or only to phenol separation from lignin, aiming also at the modification of the micro- and macromolecular structures existing in nature, from which valuable products can be obtained. Thus, the main objective is that all specific, secondary and primary constituents isolated from phytomass, modified or not, should functionally substitute the classical chemical products or represent materials with new properties (**Table 1.3**).

III. *The technology of integral and complex valorification which has been proposed is to be performed on several stages and modules, depending on the chemical composition of the available resources and on the corresponding field of application for the obtained products*.

Table 1.1 Specific chemical components from energy cultures							
Species	**Yield t/hectare/ year**	**Primary process**	**Peculiar products**	**% from oven dry (o.d.) material**	**Secondary product of conversion**	**Resultant products yield/hectare/year**	**World stage**
Helianthus tuberosus 1983	40 (5.6 t) hydrolysable sugar	Extraction with hot water	Inulin	12–14	Alcoholic fermentation (invertase)	C_2H_5OH 38% 200–300 waste fodder	The French programme
Asclepiassyriaca (selected from 52 bearing-latex species)	15 (0.690)* Latex 1.770	Extraction with solvents (CH_3OH)	Latex fermentable sugars	4.7	Catalytic cracking alcoholic fermentation	Hydrocarbons 690 Vegetable gasoline 400	California Australia Brazil Japan
*Low-content oil sands – oil = 0.10 kg/kg; bearing- latex plants – latex = 0.047 kg/kg Reproduced with permission from C.I. Simionescu, V. Rusan and V.I. Popa, *Cellulose Chemistry and Technology*, 1987, **21**, 1, 3. ©1987, Romanian Academy Publishing House							

Table 1.2 Secondary and primary chemical components of some raw materials

Chemical components, % o.d. material	Agroenergy culture		Forest and processing waste				Agricultural waste		Industrial waste
	Asclepias sp.	*Helianthus tuberosus*	Spruce bark	Beach bark	Aspen bark	Softwood foliage	Stems of tomato	Stems of potato	*Datura inoxia*
Primary components									
Cellulose	27.45	19.40	25.54	34.67	26.64	19.37	20.0	23.81	31.21
Lignin	15.71	8.8	39.95	33.75	32.11	57.07	12.0	13.92	25.14
Secondary components									
Soluble substances in cold water	-	-	17.93	10.99	19.33	15.40	-	-	-
Soluble substances in hot water	29.94	-	23.98	14.03	23.05	14.69	-	-	12.38
Soluble substances in sodium hydroxide solution, 1%	54.67	-	38.56	31.27	39.29	44.75	-	37.00	41.84
Pentosans	7.69	11.60	11.31	20.75	20.07	4.94	10.30	6.95	16.17
Tannins	-	-	15.26	3.87	6.67	1.00	-	-	-

Reproduced with permission from C.I. Simionescu, V. Rusan and V. I. Popa, *Cellulose Chemistry and Technology*, 1987, **21**, 1, 3. ©1987, Romanian Academy Publishing House

Prior to biomass harvesting, morphological elements destined for different valorification, are isolated. Then, the biomass which has been ground (containing a different content of humidity) is subjected to stepwise processing. The technology we have imagined for the complex and integral processing and valorification implies two distinct stages: *extraction/separation* (*extraction of the specific compounds, extraction of the secondary compounds*) *and conversion* (*with or without maintaining the structural integrity of the initial compounds*) which may be modularly applied, depending both on the species and on the chemical compounds utilised. The raw material may run through certain sequences of this flow sheet (see **Figures 1.1** and 1.2), which may be detached as a single separate technology and

may be applied depending on the available *amount* of phytomass. Some examples are presented in **Figures 1.3**- **1.5**.

Table 1.3 Examples of valorification of some isolated and/or modified components of phytomass

Components	Isolated products	Modified products/modification reaction	Field of valorification
Specific compounds	Photosynthetic pigments	Chlorophyll derivatives Modified carotenes Complex mixtures Vegetable gasoline/cracking Fructose/hydrolysis and inversion.	Medicines, cosmetics, food industry, pharmacy, animal husbandry and so on. Fuel, food industry, alcoholic fermentation.
	Alkaloids		
	Hydrocarbons		
	Inulin		
Secondary compounds	Hemicelluloses	Sugar, hydrolysis, proteins, furfural, hydrolysis, dewatering additives, biological active compounds, antioxidants, adhesives, polyaddition or polycondensation.	Animal husbandry, food industry, chemical industry, papermaking, wood processing, food industry, agriculture, pharmacy, wood industry, electrotechnical industry, metallurgy, textiles, drilling.
	Polyphenols		
Primary compounds	Lignocellulose	Filling active material, compound, mixing, analogue polymer reactions, fertilisers, oxyammonolysis proteinaceous fodder, hydrolysis, proteins.	Building material, agriculture, animal husbandry.
	Cellulose	Derivatives, analogue polymer reactions, filling active material.	Textile, food industry, papermaking, cellulose derivatives.
	Lignin	Fertiliser, oxyammonolysis, additives and adhesives, analogue polymer reactions.	Agriculture, chemical industry, drilling, wood industry.

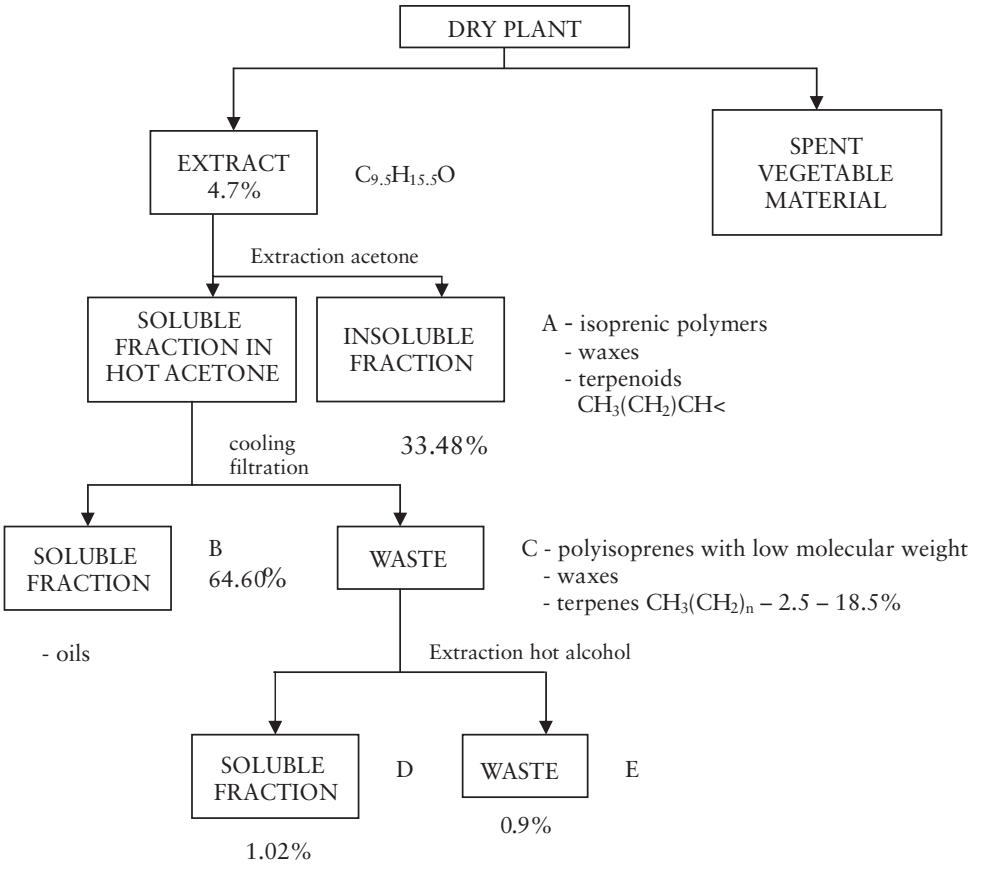

Figure 1.3 Example of the extraction and separation of specific compounds (isolation of hydrocarbons from *Asclepias syriaca*). Reproduced with permission from C.I. Simionescu, V. Rusan and V.I. Popa, *Cellulose Chemistry and Technology*, 1987, **21**, 1, 3. ©1987, Romanian Academy Publishing House [21]

After the separation of the specific compounds from the phytomass, we can apply an alkaline extraction which allows the isolation of a complex consisting of polyphenols and hemicelluloses (**Figure 1.5**). The idea of separating phenolic products from plants, especially from wood bark, is not new; it was proposed many years ago, yet its development has been prevented due to phenol accessibility in petrochemistry. Lately, as a consequence of the newly created economic conditions, the problem of extracting and utilising phenolic compounds has been overcome.

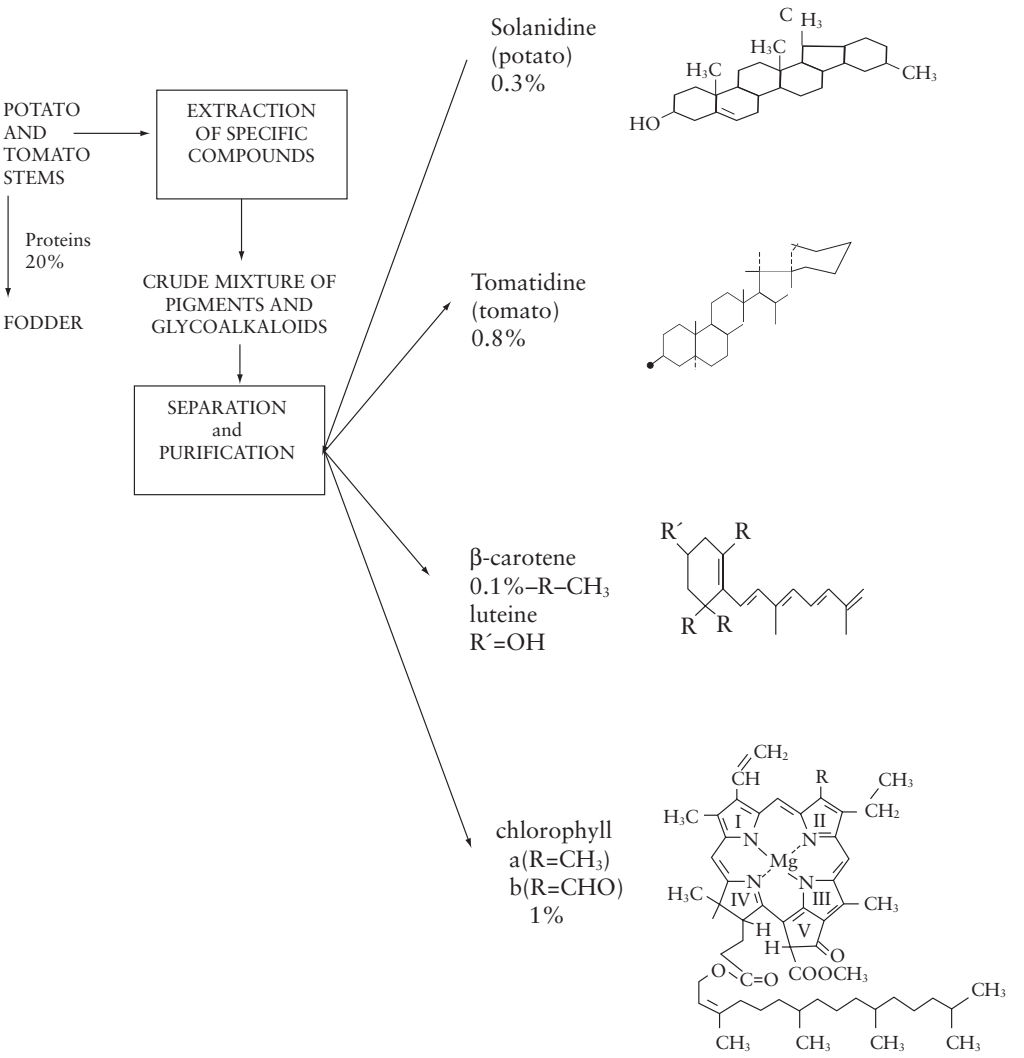

Figure 1.4 Example of the extraction and separation of specific compounds (isolation of pigments and alkaloids from tomato and potato stems). Reproduced with permission from C.I. Simionescu, V. Rusan and V.I. Popa, *Cellulose Chemistry and Technology*, 1987, **21**, 1, 3. ©1987, Romanian Academy Publishing House [21]

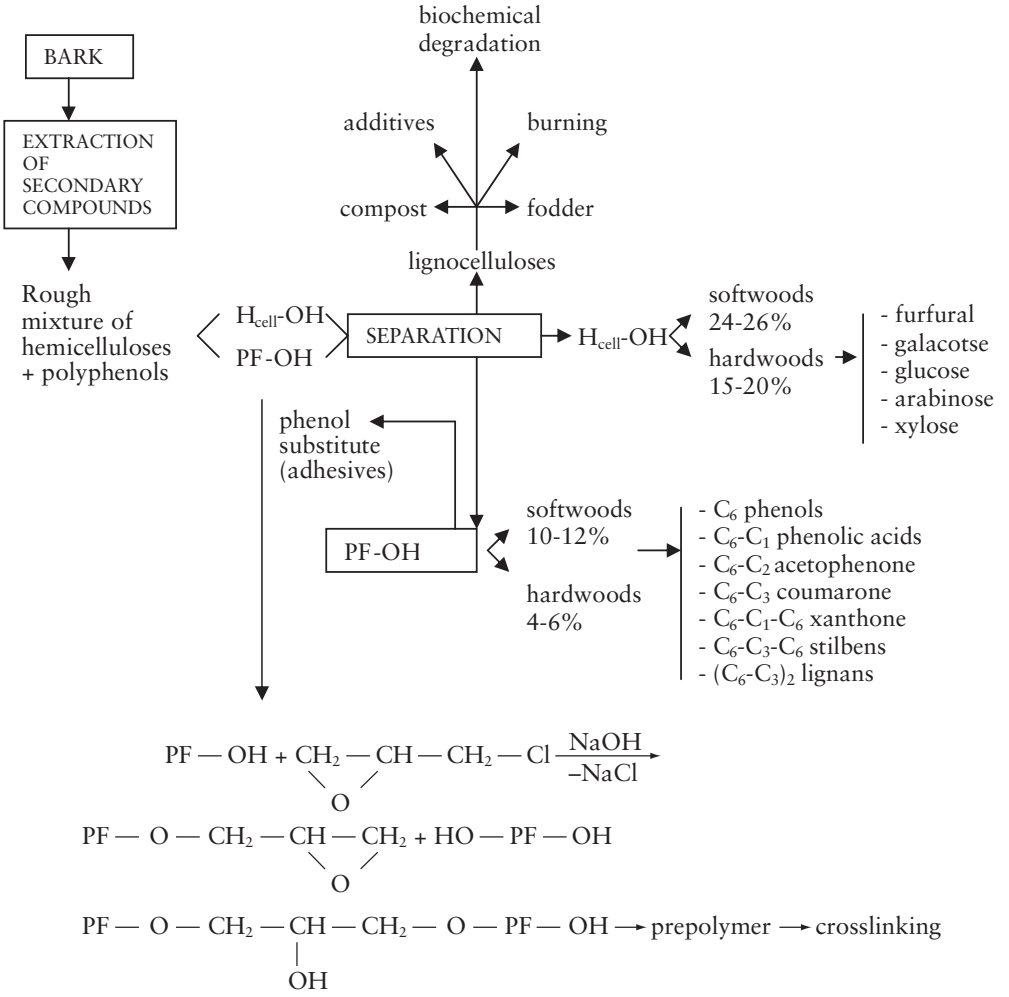

Figure 1.5 Example of the extraction and separation of secondary compounds (isolation of hemicelluloses and polyphenols from wood bark). Reproduced with permission from C.I. Simionescu, V. Rusan and V.I. Popa, *Cellulose Chemistry and Technology*, 1987, **21**, 1, 3. ©1987, Romanian Academy Publishing House [21]

The European pulp mills produce large amounts of bark as by-products, about 5.5 Mt/y. Additional amounts of bark are produced in sawmills. To date, the major use of bark is as a fuel, although alternative use has been sought for a long time. Thus, bark can be used for extraction of useful chemicals and the process can be integrated into the production cycle, allowing them to be implemented industrially (instead

of only being a matter of academic interest) [24]. The alkaline extracts were tested as a phenol substituent in the synthesis of phenolformaldehyde resins, a bisphenol substituent in the synthesis of polyphenol epoxy resins or as a phenolformaldehyde resin substituent [25].

Further conversion could be performed by *synthesis*, using chemical or biochemical procedures which offer the possibilities of transforming the specific, secondary and primary compound whilst maintaining their basic structural units, or processing them by the procedures presented in **Figure 1.6.**

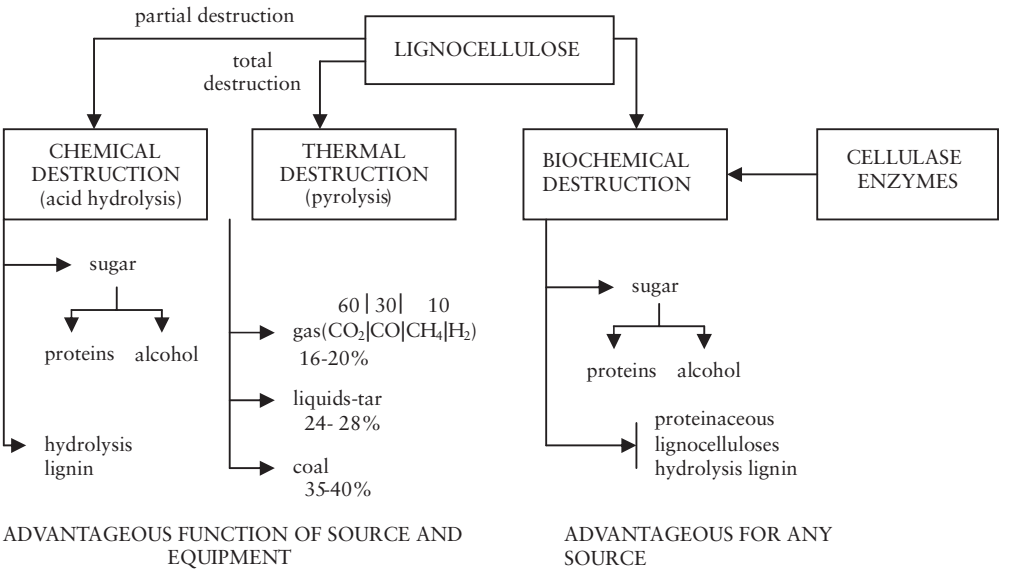

Figure 1.6 Possibilities of lignocellulose complex valorification

During processing, without maintaining the basic structural units, conversion occurs by *degradation,* using chemical, biochemical and thermochemical procedures (**Figure 1.7**) for the destruction of specific (**Figure 1.8** and **1.9**), secondary and primary compounds [21].

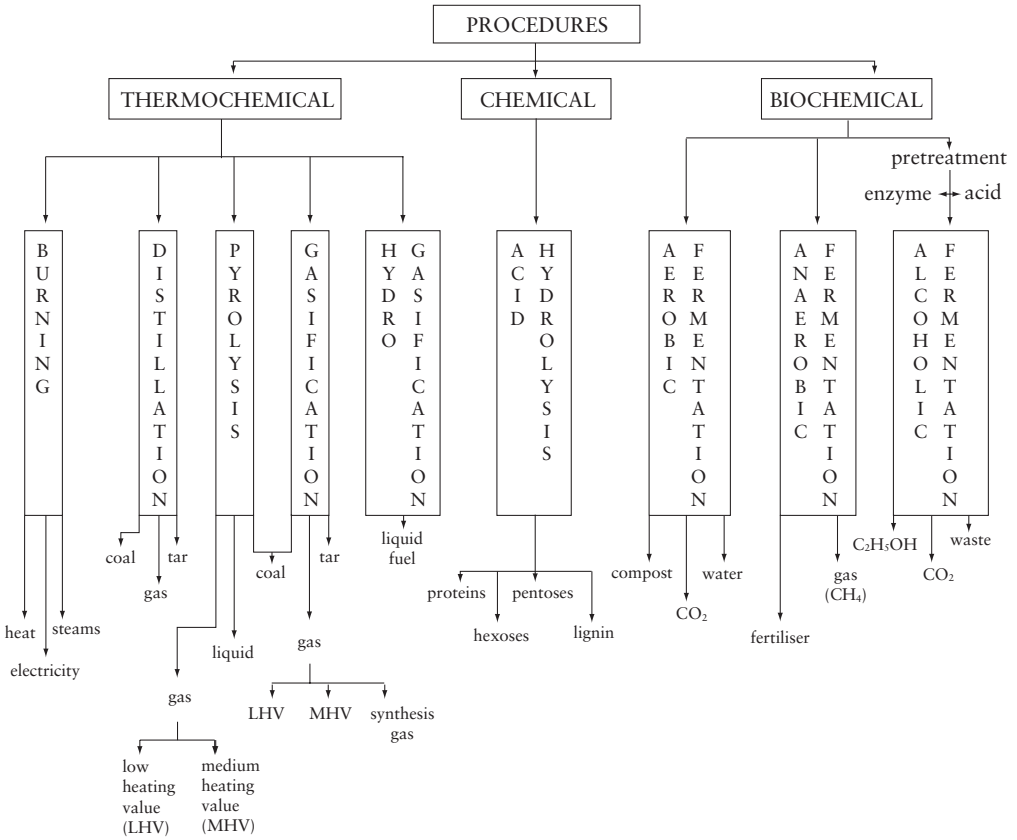

Figure 1.7 Procedures for phytomass conversion

IV. *Products obtained by phytomass chemical processing, using the above mentioned methods may structurally and/or functionally substitute certain raw materials of carbo- and petrochemical origin* (**Table 1.3**).

All these considerations will determine the approach to new directions of research:

- Separation and direct utilisation of the chemical compounds isolated from biosystems;
- Chemical processing of biomass and/or wastes into their components by destruction, thus assuring raw materials for the synthesis of polymers and sources of chemical energy;
- Chemical or biochemical transformation of both components and integral biomass

(functionalisation or functionality) for specific uses;

- Elucidation of structures and functions of natural compounds in biosystems aimed at their utilisation in structures with advanced properties and improving their behaviour against physical, chemical and biological agents; and
- *In vitro* and *in vivo* simulation of the synthesis of natural chemical compounds.

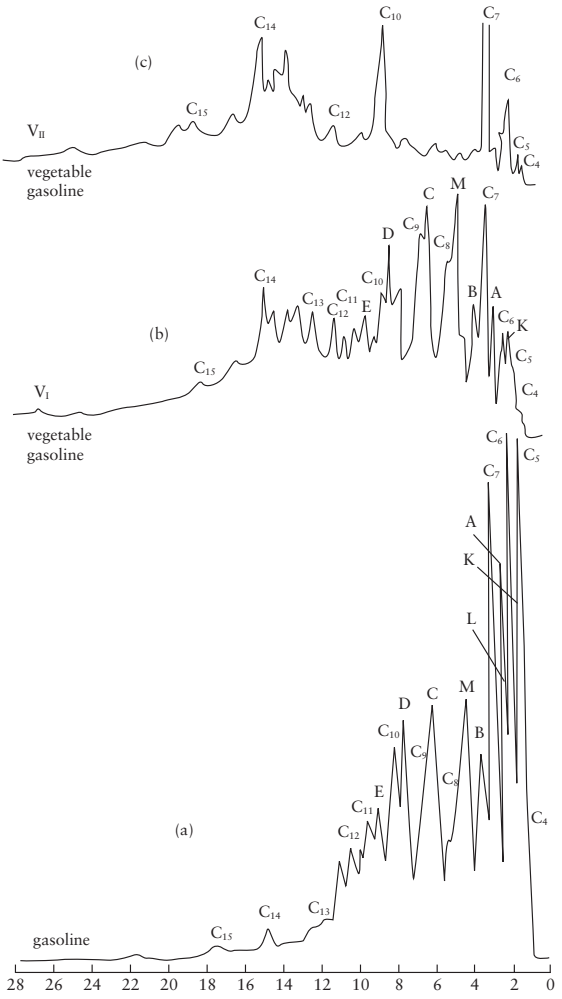

Figure 1.8 Gas chromatogram of gasoline and the cracking products of hydrocarbons obtained from *Asclepias syriaca* stems. Reproduced with permission from C.I. Simionescu, V. Rusan and V.I. Popa, *Cellulose Chemistry and Technology*, 1987, **21**, 1, 3. ©1987, Romanian Academy Publishing House [21]

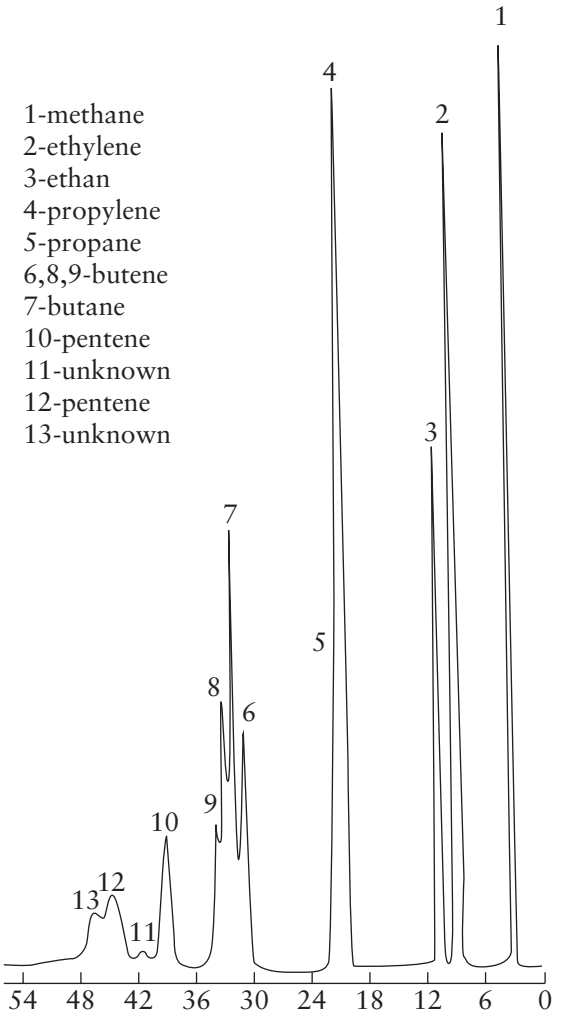

Figure 1.9 Gas chromatogram of gaseous products resulting in pyrolysis of latex from *A. syriaca* stems. Reproduced with permission from C.I. Simionescu, V. Rusan and V.I. Popa, *Cellulose Chemistry and Technology*, 1987, **21**, 1, 3. ©1987, Romanian Academy Publishing House [21]

Using our proposed classification, cellulose and lignin can be considered as primary compounds in the pulp and paper industry. The main utilisation of pulp is to obtain paper and dissolving pulp (for cellulose derivatives, fibres, sponges and films). At the same time, many chemicals can be produced from lignocelluloses, but recently there has been a new preoccupation to find special uses for cellulose. Thus, cellulose micro/

nanofibrils, as a reinforcing material for composites, are becoming more and more attractive to researchers in composite science because of its potential lightweight and high strength [26, 27].

1.3.1 Lignin

Today, wood is converted into pulp, and in chemical pulp mills, steam and electricity are generated in the recovery boiler. In the pulp mill of tomorrow, lignin, hemicelluloses and extractives, dissolved in process streams, will be extracted and used as chemical raw materials.

1.3.1.1 Separation of Lignin

Black liquor from the cooking process in kraft mills contains cooking chemicals and dissolved and degraded wood substances, with about half of the wood organic material dissolved into the black liquor. The liquor is incinerated with the recovery of inorganic cooking chemicals and the production of steam. The modern chemical pulp mill produces an excess of energy in relation to its own needs, but the surplus steam often has no user and is a waste product. The export of biofuels (bark, lignin and so on) from the mill would very often be more efficient than the on-site incineration of all internally generated fuels. The production of kraft black liquor lignin amounts to about 16 Mt/y in Europe [24].

The dissolved organics consist primarily of lignin, hemicelluloses and the degradation products of cellulose and hemicelluloses. Valuable chemical properties and fractions of highly polymeric lignin and hemicellulose compounds are not utilised when the black liquor is simply burnt at the mill site for energy recovery. Many other options exist for energy production, whereas the chemical properties of the renewable lignin and hemicelluloses material are unique. The spectrum of potentially interesting products from hemicelluloses and lignin is wide, ranging from upgraded biofuels to high-value speciality chemicals. Furthermore, withdrawal of lignin and/or hemicelluloses would allow the production capacity of the pulp mill to be profitably increased if the recovery boiler is, as is often the case, the bottleneck of the mill.

One way of utilising the energy surplus in a modern pulp mill is to extract *lignin* from the black liquor. The extraction of lignin is very flexible; lignin is energy rich (26–27 Mj/kg) and can be used as fuel to replace coal or oil in combustion and/or gasification plants; lignin may be also be used as an internal fuel in the pulp mill (e.g., in the lime kiln), or sold either as fuel or raw material to be used for the production of various biobased materials/products (dispersants, various phenols, carbon fibres

and so on). Many of these components have a high market value, implying that lignin demands a high market value. It should also be kept in mind that if lignin is used as a raw material, the end product will have a heat value which, of course, should be utilised after the material has been used. Consequently, the extraction of lignin is not only a very flexible alternative, it is also sustainable especially if the lignin is used as a material before it is used as fuel. Extracting lignin is not, however, a new idea; it was proposed more than 50 years ago and a process for doing so has already been used in a few pulp mills for many years. In this process, the pH of the black liquor is lowered to about 10 and the lignin precipitates. The precipitated lignin is thereafter separated by means of filtration and a simple wash on the filter. Lignin produced using the older process was not very pure; the ash content could vary between 3 and 6% which limited its use. Furthermore, some of the lignin was partly dissolved during the washing stage, which meant the remaining lignin was very difficult to dewater. This dissolution implies that the total yield was reduced. A novel process known as the 'LignoBoost' process was proposed a few years ago and is the result of scientific investigation. This process has now been tested on a pilot as well as demonstration scale and found to work very well; it is possible to produce lignin with a low ash content using the LignoBoost process. Although it lowers the pH of the black liquor to about 10, the separation stage is however, quite different from the old process. The novel process starts with separation without washing. The filter cake from this stage is resuspended in low pH liquor and the lignin is filtered off and washed on a second filter. This particular procedure ensures that no noticeable amount of lignin will be dissolved and reprecipitated during the washing stage; as a result, the filtration resistance will be low throughout the process. The yield loss during washing will also be low. Despite the fact that there are two filters, the total filter area is normally much smaller than that of the older process [28, 29].

Lignin does not possess a true repeating unit which can be selectively produced by degradation of the polymer, either chemically or enzymatically. Therefore, the future use of lignin (except as fuel) will depend on the possibilities of either *degrading* it or as a *multifunctional macromolecule* [30]. Degradation of lignin can be obtained by *pyrolysis* under reductive conditions. Such methods have been tried for the production of phenols or aromatic hydrocarbons respectively. In the latter case, substituted benzene structures can be obtained with properties suitable for *biodiesel ingredients*. Since very harsh conditions are employed in the degradation reaction, the structure of lignin seems to play a minor role, whereas the choice of reaction conditions must be such that tar formation is minimised [31, 32].

1.3.2 Degradation Products of Polysaccharides

Various saccharinic acids and other monocarboxylic acids are formed from

polysaccharides during the alkaline pulping of wood and nonwood raw materials. Their formation depends on the cooking conditions and composition of raw materials, but typically up to 10% of the charged raw materials are converted to these acids. In addition, varying amounts of volatile acids (formic and acetic acids) and different dicarboxylic acids are formed [33]. Although dozens of compounds have been identified so far, usually a few major compounds can be recognised. Among these, the most interesting compounds for the potential applications include: glycolic, lactic, 2-hyroxybutanoic, 2,5-dihydroxypentanoic (3,4-dideoxypentonic), xyloisosaccharinic and glucoisosaccharinic acids. The isolated hydroxyl acids or acid mixtures can find applications in many different fields. The simple hydroxyl acids, glycolic and lactic acids are currently used as industrial chemicals with several applications. The higher homolog, 2-hydroxybutanoic (which is one of the main hydroxyl acids in hardwood black liquors) could find uses in the manufacture of resins and polymers; e.g., after conversion to crotonic or isocrotonic acids. It should also be noted that lactic and 2-hydroxybutanoic acids in the black liquors are of a racemic nature. The studies carried out have demonstrated the strong complexing capabilities of saccharinic acids, especially for many radionuclides and other materials. They have also been used for the preparation of various fine chemicals and as energy sources for aerobic and anaerobic bacteria [34, 35].

1.3.3 Black Liquor as a Feedstock for Synthesis Gas

An opportunity for biobased synthesis gas processes is the integration of biofuel production with pulp and paper manufacture. For many of today's mills, this would enable the high-grade by-product energy of the biofuel plant to be fully exploited in the paper mill. The biofuel plant would also benefit from the existing infrastructure of the paper mill, in particular from that pertaining to feedstock procurement and handling.

Black liquor is a by-product of pulping, which is today used for steam and power production in the pulp mills. Black liquor is a pumpable liquid, which is a significant advantage when the goal is to produce a clean syngas for use in catalytic processing. The challenge with black liquor as a fuel is that it is highly corrosive and that the cooking chemicals in the black liquor must be recovered in a form which is compatible with the pulping process. Black liquor, the spent liquor of kraft mill pulping, is a major potential biofeedstock for synthesis-gas production. However, gasifiers developed for solid biomass cannot be applied, as such, to black liquor. Significant efforts are currently being made to develop the required specialised technology. Synthesis-gas production from black liquor has the potential of being somewhat more economical than synthesis-gas production from solid biomass residues. On the other hand, the latter technology has a greater market potential, possesses a smaller availability

risk for a pulp mill and is technically more certain at the present time [36]. In the gasification process, black liquor is atomised by a gas-assisted nozzle and sprayed into the reactor where it is directly gasified. Gasification of lignin also offers a smart option for the utilisation of other biomass sources, which can be included in the pulp mill allowing a broad range of different feedstocks to be converted into one homogeneous synthesis gas. This product can be used for electricity generation (combined power and heat (CPH) gas engine, gas turbine) as well as for chemical synthesis (production of hydrogen, ammonia, methanol, methane from remethanisation, hydrocarbon formation using Fischer–Tropsch reactions and so on) by conventional technologies.

Wood biomass can also be transformed into a liquid product through pyrolysis. Other products from this process are a solid biomass residue called char and noncondensable gases mainly CO, CO_2 and light hydrocarbons. The liquid product, which is highly oxygenated, can be upgraded by removing oxygen. Application of zeolites during the upgrading removes the oxygen as water at low temperatures, and as CO and CO_2 at higher temperatures, changing the yield of the produced phases. The major products in the resultant biooil, besides water, were 1-hydroxy-2-propanone, 2-methoxy-4-(1-propenyl)-phenol, 2-methoxy-4-methyl-phenol and acetic acid. The phenolic products are formed during the pyrolysis of lignin, while the other two are formed from wood carbohydrates [37].

- Secondary compounds: hemicelluloses and polyphenols.

1.3.4 Separation of Hemicelluloses

The flow of kraft black liquor carbohydrate derived by-products (including degraded sugar acids) amounts to about 12 Mt/y in Europe. In spite of the large amounts available, hemicelluloses have not yet been utilised commercially to any large extent. The main obstacle is the difficulty of extracting them in their native form, since they are intimately associated with cellulose and lignin in the wood structure [38]. During the chemical pulping using the kraft method, most of the hemicelluloses are degraded and dissolved as monomeric and oligomeric sugars or sugar acids in the black liquor. However, xylans – the main constituent of hemicelluloses in e.g., birch and eucalyptus – are preserved in a more native form to a certain extent. When isolated, the hemicelluloses have many potentially valuable properties, such as paper additives, thickeners, food additives, emulsifiers, gelling agents, adhesives and adsorbents. Some hemicelluloses have shown cholesterol-lowering effects and even antitumour effects [12].

The *hemicelluloses* which normally end up in the black liquor of a hardwood kraft mill can be extracted prior to kraft pulping and used for the production of ethanol

and acetic acid. The extracted liquor undergoes evaporation, hydrolysis, separation, fermentation and distillation for the production of acetic acid and ethanol. During the extraction process, the acetyl groups, which are side chains on the xylan hemicelluloses, are cleaved to give dissolved sodium acetate which will be converted to acetic acid in the hydrolysis stage of the plant.

The hardwood biorefining uses green liquor with the addition of antraquinone (AQ) for wood extraction prior to modified kraft cooking to preserve both pulp yield and quality. During extraction, about 10% of the wood goes into solution. The extract contains mostly hemicellulose-derived organic compounds and has a near neutral pH. The extracted chips require 3% lower white liquor (as Na_2O on original oven dry wood) and a lower H factor in the subsequent kraft cook.

Galactoglucomannan (*GGM*) dominates the softwood hemicelluloses. During refining of the mechanical pulp, part of the GGM is dissolved in the process water, which can be recovered from the water by ultrafiltration. The molar mass of GGM depends on the filtration methods, but is typically 20–30 kDa. GGM has been found to stabilise colloidal pitch by forming a hydrophobic layer on the surface of the pitch particles, thus reducing the risk of deposit formation during papermaking. Other possible uses of GGM can also be found, as their sorption property can be utilised together with fillers, cellulosic and mechanical fibres. GGM can be modified by grafting it with other types of functional groups other than hydroxyl groups. It is also an interesting polysaccharide as a food additive, as it may be used as a so-called dietary fibre. GGM has also been studied as a film-forming constituent [38].

- Specific compounds: pigments, hydrocarbons, simple sugars, alkaloids, polyphenols, other bioactive compounds, oils, proteins and so on.

1.3.5 Fine and Speciality Chemicals

Black liquor contains compounds of potential value. Roughly half of the dissolved organic material is lignin and the rest is mainly sugar acids, other organic acids and methanol.

Tall oil and turpentine products from kraft pulping were developed at the beginning of the last century and have been produced ever since. Distillation technology has been improved during the last decades and today, very pure rosin and fatty acid products can be manufactured. Tall oil fatty acids and tall oil rosin have found a wide variety of applications. The fragrance industry largely utilises turpentines, both sulfate turpentines and turpentines distilled from tapped oleoresin. A new use of tall oil fatty acids could be the production of conjugated linoleic acids (CLA). Nordic

tall oil fatty acids are rich in linoleic acid (9,12–18:2), typically containing 40–50% linoleic acid. It is possible to make CLA with the aid of heterogeneous catalysts and in the absence of solvents. Various antioxidant and antitumour properties have been attributed to CLA, and such preparations are marketed as dietary supplements [39].

In addition to naturally occurring constituents, chemical modification of isolated wood compounds provides new options. For example, new physiologically active compounds can be derived from wood using heterogeneous catalysis; *sitostanol* can be produced by catalytic hydrogenation from *sitosterol*, conjugated *linoleic acids* can be synthesised *via* the isomerisation of *linoleic acid*, and other lignans can be obtained from hydroxymataresinol hydrogenolysis [40].

1.3.5.1 Bioactive Compounds

Some ideas concern new high added value applications in the medical field, where these raw materials have not been used before, the driving force being to replace polymers/materials obtained from nonrenewable feedstocks. Xylitol and sitosterol/sitostanol are health-promoting products from wood, both of which have found their own special niche; xylitol promotes mouth hygiene and sitosterol/sitostanol exerts a lowering effect on the cholesterol level of the human coronary flow. However, wood constituents still offer additional new opportunities for health-promoting products, as well as being a raw material of chemicals. For example, knots in spruce, i.e., inner parts of the branches, have been found to contain an extremely high concentration of polyphenols compared to the stem. Generally, these polyphenols are strong antioxidants. The dominating lignan *hydroxymataresinol* (HMR) has been documented to carry favourable properties in the fight against cancer and also coronary heart diseases. The HMR lignan is extracted from spruce knots which are separated from chips of the spruce trees grown in the Northern part of Finland. After purification and formulation of the HMR lignan product, it has been marketed as a health-promoting food supplement since 2006.

Stilbenes are also interesting bioactive constituents in trees; these can be found in the bark of spruce, up to the level of 10%. *Piceatannol*, which is the main spruce bark stilbene, is an efficient antioxidant. The same group of antioxidants is also found in grapes and in red wine [41].

In our studies, different lignins and polyphenols extracted from phytomass sources have been used in model experiments to follow their actions as allelochemicals [42]. Polyphenols extracted from spruce wood bark have been tested as plant growth regulators and the results showed that the isolated compounds exhibited similar effects to the endogenous hormones, cytokinine and auxine [43]. Based on the

obtained results, lignin and polyphenols were used in seed germination, plant tissue culture, plant cultivation, bioremediation or as a substrate for the development of microorganisms [44, 45].

1.4 Conclusions

The plant cell wall biomass is composed of cellulose, hemicelluloses, lignin, protein, lipids and several small molecular weight components with different ratios depending on the raw materials.

The key issue for a successful valorisation of biomass to chemicals is the efficient fractionation into hemicelluloses, cellulose, lignin and the other compounds.

Thus, a plant for the fractionation and refining of biomass, and for the utilisation of all its components, a 'biorefinery' plant, will have to display a high level of process *integration* and *optimisation* to be competitive in the near future. A biorefinery is an installation that can process biomass into multiple products using an array of processing technologies. By integrating *Forest Biorefinery* (*FBR*) activities in an existing plant, pulp and paper mills have the opportunity to generate significant amounts of bioenergy and bioproducts, and to drastically increase their revenues while continuing to produce wood, pulp and paper products. A new generation of technologies based on thermochemical, biochemical and chemical pathways is likely to enable the development FBR. Manufacturing new value added by-products (e.g., fuels, bulk and specialty chemicals, pharmaceuticals and so on) from biomass could represent, for some forestry companies, an unprecedented opportunity for revenue diversification. At the same time, biorefineries in the pulp and paper sector will integrate several biomass raw materials.

In addition to process technology development, product development will be essential for identifying successful new markets for biorefining products and their supply chain management. Therefore, incorporating new products, in addition to the existing pulp and paper product portfolio, is a complex problem and perhaps the key to a company's successful diversification.

Biorefinery technology development will typically be implemented in retrofit and must be accompanied by careful process systems analysis in order to understand the impact on existing processes.

Dedication

This chapter is dedicated to my friend Viorica Rusan. Together we discussed and proposed the complex topic of processing biomass technology.

References

1. H. Theilander in *Proceedings of Nordic Wood Biorefinery Conference*, Stockholm, Sweden, 2008, p.36.

2. National Renewable Energy Laboratory. (NREL is a national laboratory of the US Department of Energy-www.nrel.gov). *http://www.nrel.gov/biomass/biorefinery.html*

3. H. Mao, J.M. Genco, A. van Heiningen and H. Pendse in *Proceedings of Nordic Wood Biorefinery Conference*, Stockholm, Sweden, 2008, p.16.

4. B. Kamm, M. Kamm, P.R. Gruber and S. Kromus in *Biorefineries-Industrial Processes and Products: Status Quo and Future Directions*, Volume 1, Eds., B. Kamm, P.R. Gruber and M. Kamm, Wiley-VCH, Weinheim, Germany, 2006.

5. M. Sasaki, T. Adschiri and K. Arai, *Journal of Agricultural and Food Chemistry*, 2003, **51**, 18, 5376.

6. G. Cazacu and V.I. Popa in *Polysaccharides: Structural Diversity and Functional Versality*, 2nd Edition, Ed., S. Dumitriu, Dekker/CRC Press, New York, NY, USA, 2004.

7. D. Ciolacu and V.I. Popa in *Cellulose: Structure and Properties, Derivatives and Industrial Uses*, Eds., A. Lejeune and T. Deprez, Nova Publishers, New York, NY, USA, 2010.

8. D. Ciolacu and V.I. Popa in *Cellulose Allomorphs: Structure, Accessibility and Reactivity,* Nova Publishers, New York, NY, USA, 2010.

9. V.I. Popa and I. Spiridon in *Polysaccharides: Structural Diversity and Functional Versality*, Ed., S. Dumitriu, Marcel Dekker Inc., New York, NY, USA, 1998.

10. I. Spiridon and V.I. Popa in *Polysaccharides: Structural Diversity and Functional Versality*, 2nd Edition, Ed., S. Dumitriu, Dekker/CRC Press, New York, NY, USA, 2004.

11. I. Spiridon and V.I. Popa in *Monomers, Polymers and Composites from Renewable Resources*, Eds., M. Belgacem and A. Gandini, Elsevier, Oxford, UK, 2008.

12. V.I. Popa in *Polysaccharides in Medicinal and Pharmaceutical Applications*, Ed., V. Popa, Smithers Rapra Technology Ltd, Shrewsbury, UK, 2011.

13. G. Cazacu and V.I. Popa in *Handbook of Polymer Composites*, Volume 4B, Eds., A.K. Kulshreshtha and C. Vasile, Rapra Technology Limited, Shrewsbury, UK, 2003.

14. A. Abäecherli and V.I. Popa, *Environmental Engineering and Management Journal*, 2005, 4, 3, 273.

15. V.I. Popa, A.P. Stingu and I. Volf in *Bioremediation Technology*, 1st Edition, Ed., M.H. Fulekar, Springer, Dordrecht, The Netherlands, 2010.

16. I. Ignat, I. Volf and V.I. Popa, *Food Chemistry*, 2011, **126**, 4 1821.

17. I. Kogel-Knabner, *Soil Biology and Biochemistry*, 2002, **34**, 2, 139.

18. J.A. Glaser, *Clean Technology and Environmental Policy*, 2009, **11**, 4, 371.

19. T. Malutan, R. Nicu and V.I. Popa, *BioResources*, 2008, **3**, 1, 13.

20. T. Malutan, R. Nicu and V.I. Popa, *BioResources*, 2008, **3**, 4, 1371.

21. C.I. Simionescu, V. Rusan and V.I. Popa, *Cellulose Chemistry and Technology*, 1987, **21**, 1, 3.

22. V.I. Popa and I. Volf, *Environmental Engineering and Management Journal*, 2006, 6, 4, 545.

23. V.I. Popa and I. Volf in *Proceedings of Nordic Wood Biorefinery Conference*, Stockholm, Sweden, 2008, p.229.

24. B. Backlund and P. Axegård in *Proceedings of Nordic Wood Biorefinery Conference*, EU Project WACHEUp, Stockholm, Sweden, 2008, p.50.

25. C.I. Simionescu, J. Bulacovschi, V.I. Popa, M. Popa, V. Nuta and V. Rusan, *Holzforschung und Holzverwertung*, 1988, **40**, 6, 136.

26. F.W.C. Herrick, R.L. Hammilton and J.K. Sandberg, *Journal of Applied Polymer Science: Applied Polymer Symposia*, 1983, **37**, 797.

27. T.H. Wegner and P.E. Jones, *Cellulose*, 2006, **13**, 2, 115.

28. F. Ohman, H. Wallmo and H. Theiliander, *Filtration*, 2007, **7**, 4, 309.

29. P. Tomani, P. Axegård, N. Berglin, A. Lovell and D. Nordgren, *Cellulose Chemistry and Technolology*, 2011, **45**, 7–8, 533.

30. V.I. Popa, *Cellulose Chemistry and Technology*, 2007, **41**, 9–10, 591.

31. S.B. Alpert and S.C. Schuman, inventors; no assignee; Canadian Patent 841708, 1970.

32. J.S. Schabtai, W.W. Zimierczak, E. Chornet and D. Johnson, inventors; no assignee; US 0115792 AI, 2003.

33. K. Niemelä and R. Alén in *Analytical Methods in Wood Chemistry, Pulping, and Papermaking*, Eds., S.Sjöström and R. Alén, Springer, Berlin, Germany, 1999.

34. J. Tits, E. Wieland and M.H. Bradbury, *Applied Geochemistry*, 2005, **20**, 11, 2082.

35. S.E. Strand, J. Dykes and V. Chiang, *Applied and Environmental Microbiology*, 1984, **47**, 2, 268.

36. P. McKeough and E. Kurkela in *Proceedings of Nordic Wood Biorefinery Conference*, Stockholm, Sweden, 2008, p.10.

37. A. Aho, K.Eränen, N. Kumar, T. Salmi, M. Hupa, J-P. Mikkola and D.Y. Murzin in *Proceedings of Nordic Wood Biorefinery Conference*, Stockholm, Sweden, 2008, p.184.

38. K. Mikkonen, P. Madhav, P. Yadav, S. Willför, K. Hicks and M. Tenkanen, *BioResources*, 2008, **3**, 1, 178.

39. B. Holbom in *Proceedings of Nordic Wood Biorefinery Conference*, Stockholm, Sweden, 2008, p.105.

40. M. Hupa, M. Auer and B. Holmbom in *Proceedings of Nordic Wood Biorefinery Conference*, Stockholm, Sweden, 2008, p.79.

41. B. Holmbom, S. Willför, J. Hemming, S. Pietarinen, L. Nisula, P. Eklund and R. Sjöholm in *Materials, Chemicals and Energy from Forest Biomass*, Ed., D.S. Argyropoulos, ACS Symposium Series 954, 2007.

42. V.I. Popa, M. Dumitru, I. Volf and N. Anghel, *Industrial Crops and Products*, 2008, **27**, 2, 144.

43. A. Balas and V.I. Popa, *Romanian Biotechnological Letters*, 2007, 12, 3, 3209.

44. A. Stingu, I. Volf, V.I. Popa and I. Gostin, *Industrial Crops and Products*, 2012, 35, 1, 53.

45. A.R. Hainal, A.M. Capraru, I. Volf and V.I. Popa, *Cellulose Chemistry and Technology*, 2012, **46**, 1–2, 87.

2 Pulping Fundamentals and Processing

Dan Gavrilescu

2.1 Introduction to Pulping

Pulping is the process by which plant material (wood, straw, grass and so on) is reduced to a fibrous mass. Pulp refers to a suspension of cellulose fibres in water and represents the raw material for producing paper and boards, and obtaining cellulose derivatives. There are two major pulp grades: paper-grade pulp and dissolving pulp. The properties of paper-grade pulp refer to pulp yield, pulp brightness and strength properties. The properties of dissolving-grade pulp refer to the high cellulose content and to a high reactivity towards derivatising chemicals.

According to the Confederation of European Paper Industries [1], the global production of pulp was 184.8 million tonnes in 2010 and the main pulp producers are North America, Europe and Asia. The pulp and paper capacity survey (2010–2015) of the Food and Agriculture Organization of the United Nations [2], shows that in North America and Europe pulp production in the next few years will remain at a relatively constant level, while pulp production in Latin America will increase due to wood abundance and the low cost of labour. A study of Haley [3] affirms that in 2008, China overtook the US to become the world's largest producer of paper due to the fact that this country has been rapidly expanding its paper-producing capacity. A forecast of domestic paper consumption in China shows that paper demand is projected to grow to 143 million tonnes in 2021 [3].

The aim of all pulping processes is to separate the fibres from the lignocellulosic materials in order to obtain pulp grades that are suitable for papermaking. Cellulosic fibres can be separated from each other by mechanical, chemical or by a combination of both treatments. According to Biermann [4], there are three main categories of pulping processes: mechanical, semichemical and chemical.

Mechanical pulping uses mechanical energy to separate the fibres from the wood matrix. There are several variants of mechanical pulping depending on the process

parameters and equipment. Wood is processed either in the form of logs treated in grinders, or in the form of wood chips that are converted to pulp in a refiner. Lignin or other wood components are not intentionally removed during mechanical pulping. Höglund [5] shows that in order to weaken the strength of the fibre-fibre bonds, steaming or/and a gentle chemical treatment of wood is performed. Classification of mechanical pulping comprises four processes:

- Groundwood pulping includes stone groundwood (SGW) and pressure groundwood methods. Atmospheric grinding and pressure grinding of logs using a pulpstone are the main alternatives of groundwood pulping;
- Refiner mechanical pulping (RMP) consists of the atmospheric refining of wood chips using a dedicated disc refiner;
- Thermomechanical pulping (TMP) consists of refining the steamed chips under pressure and elevated temperature using a disc refiner; and
- Chemithermomechanical pulping (CTMP) involves refining the steamed and chemically pretreated chips, under pressure and elevated temperature, using a disc refiner.

The yield of mechanical pulp grades is high and depends on the process involved, as presented by Sundholm [6]: groundwood pulp and refiner mechanical pulp (96–98%), thermomechanical pulp (94–96%) and chemithermomechanical pulp (90–95%). Besides the high yield, mechanical pulps exhibit a high light-scattering power, a high bulk and a fairly high brightness. These pulps are used in producing papers with good opacity and printability at low basis weight (newsprint and magazine paper). Sundholm [6] also stated that the drawbacks of mechanical pulps refer to their high electrical energy consumption (up to 3.5 MWh/t of pulp) and the fact that high-quality wood is required.

Semichemical pulping is performed in two steps: a mild chemical treatment of wood chips followed by a moderate mechanical refining. A partial removal of both lignin and hemicelluloses takes place, so that the yield of pulp ranges between 60–80%. The chips are chemically treated at an elevated temperature, where around 50% of the initial lignin content of the wood is removed. The softened chips are then processed in a defibrator enabling fibre separation. According to von Koeppen [7], the most frequently employed process is neutral sulfite semichemical (NSSC) pulping, which uses cooking liquor containing Na_2SO_3 and Na_2CO_3. Sodium sulfite is the reagent for lignin sulfonation, while sodium carbonate acts as a liquor pH buffer. A high cooking temperature (160–180 °C) is necessary for both lignin sulfonation and dissolution. Hardwood is usually the best fibre source for NSSC pulp. The high lignin content makes the fibres very stiff, with the NSSC pulp being found to be the best raw material

for a corrugated medium [8]. NSSC pulping generates spent liquor (usually named as red liquor), which contains dissolved lignin and hemicelluloses as well as inorganic substances. Ingruber [9] showed that the red liquor must be processed in order to recover the process chemicals.

Chemical pulping uses chemicals for lignin degradation and dissolving. Due to the fact that lignin is extensively removed, the fibres can be separated with little or no mechanical treatment. The process requires a high temperature and pressure. Pulping chemicals are not selective regarding lignin degradation, as the carbohydrates are also affected during the process. Almost half of the wood material is removed during chemical pulping and the pulp yield ranges from 45 to 55%, depending on the pulping technique. According to Sixta and co-workers [10] it is impossible to remove all lignin in any pulping process hence, the cooking is intentionally stopped at a certain lignin content of the pulp. The residual lignin content represents the most important parameter, which characterises the pulp grade. The properties of chemical pulps must be compared at the same residual lignin content. In a chemical pulp mill, further delignification is achieved by bleaching the pulp. Gullichsen [11] stated that pulping methods are classified according to the composition of cooking liquor and delignification can be performed in an alkaline or acidic domain. Chemical pulping can also be performed in one or two stages.

Kraft pulping strongly dominates the world pulp production due to the following advantages:

- Kraft cooking is able to produce pulp from any kind of raw materials (wood species and nonwood plants);
- Kraft pulp exhibits very good strength properties;
- Cooking chemicals are produced *via* processing of the spent liquor in a recovery plant. Both steam and electrical energy are generated, so that the process is self-sufficient with respect to energy; and
- The large capacity of the kraft pulp mills reduces the specific consumption of materials and energy, and enhances the profitability of pulp making.

Drawbacks of kraft pulping are:

- Pulp yield is lower, compared with other pulping processes; and
- The kraft pulp mill represents a source of polluting materials, which are very different regarding their quantities and characteristics.

2.2 Mechanical Pulping

During mechanical pulping, forces of various magnitude and duration are applied to the wood matrix in order to separate the fibres. Wood is a viscoelastic material, so that its behaviour when mechanical forces are applied is influenced by its moisture, temperature, load intensity and time under load. Water plays a key role in mechanical pulping due to the fact that the softening temperature of the main components of the wood depends on the wood moisture. Salmen and co-workers [12] showed that for water-saturated lignin, the softening takes place at 80–90 °C. Mechanical energy is partially converted into heat as a result of the friction between the wood and pulpstone or refining plates. The fibres are removed from the wood matrix once the lignin from the middle lamella has been heated to the temperature which exceeds its glass transition point. Mechanical pulp is manufactured by mechanical defibration using two procedures: grinding of wood logs using a pulpstone (grinding process) and refining of wood chips in a dedicated disc refiner (refining process). **Figure 2.1** shows the mechanical pulping techniques.

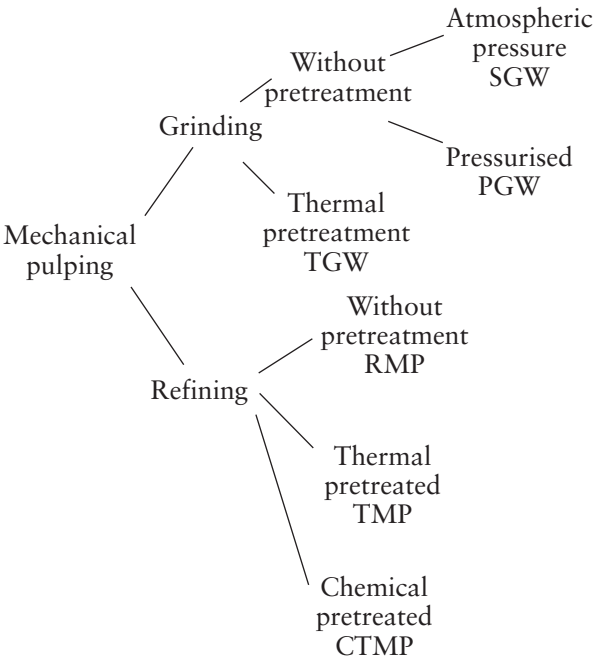

Figure 2.1 Mechanical pulping processes

As shown in **Figure 2.1**, the commercial grinding processes are SGW, pressure groundwood (PGW) and thermogroundwood (TGW). The refiner processes are represented by RMP, TMP and CTMP.

A mechanical pulp mill includes the following stages: log debarking and chipping, grinding of logs or refining of wood chips, and the screening and bleaching of mechanical pulp. The grinding process consists of pressing the wood logs against a rotating pulpstone in the presence of water. According to Karnis [13], the process is divided into two consecutive stages: (I) softening of the wood and breakdown of the wood matrix; and (II) peeling and successive refining of the fibres. The pulpstone contains grits that pass over the wood surface at very high frequencies, yielding a compression/decompression process. The grinding principle is presented in **Figure 2.2**. The wood structure is loosened due to the fatigue work performed by the grits. At the same time, the temperature increases rapidly in the grinding zone causing the lignin to soften. The presence of water reduces the softening temperature of lignin. The high frequency pressure pulsations determine the deformation of the fibres and breakdown of bonds between the fibres. The fibres are peeled from the wood surface and then successively refined in the fibrous layer generated between the wood surface and pulpstone.

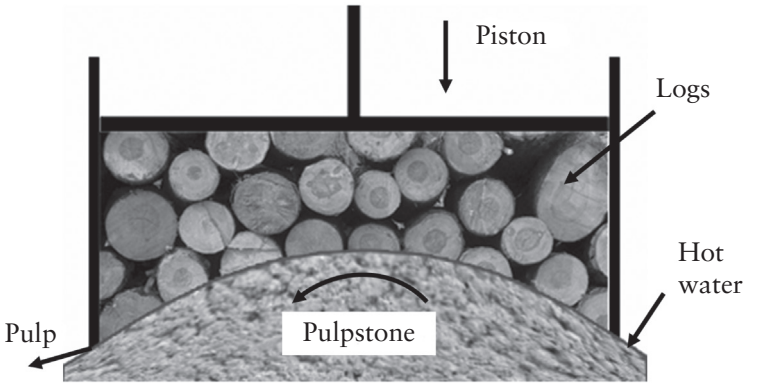

Figure 2.2 Grinding process

There are many parameters influencing the defibration of wood by grinding. Liimatainen and co-workers [14] showed that the most important are: wood moisture, log feeding speed (grinding pressure), pulpstone peripheral speed, water temperature in the grinder pit, surface shape of the pulpstone and specific energy consumption.

The refining process uses wood chips that are fed into a dedicated disc refiner, where these are defibrated by passing through the refining zone. McDonald and co-workers [15] showed that in order to soften the wood matrix before refining, the chips are steamed and/or undergo a mild chemical treatment. A mechanical, thermal or chemical softening of lignin takes place.

The common refining processes are TMP and CTMP. In a TMP process, wood chips are steamed and fed into the refiner, which is pressurised, and the steam pressure corresponds to the temperature of the saturated steam. Berg [16] showed that the friction process between the fibres, and between the fibres and bar edges, causes fibre shortening and fibrillation to take place. The refining process consumes considerable energy that is partially converted into heat which increases the temperature in the refining zone between the plates, as presented by Muhic and co-workers [17]. The additional heating positively influences the chip defibration and fibre fibrillation, and has an important influence on the final pulp quality. According to Miles and Karnis [18], the electrical energy demanded using refining to produce TMP pulp for magazine paper grades is 1,800 to 3,000 kWh/t, newsprint grades demand 1,800 to 2,200 kWh/t and paperboard grades 1,000 to 1,400 kWh/t. TMP is currently the most important mechanical pulping process, and displaced older grinding processes, because similar paper properties could be achieved using a lesser amount of expensive chemical pulp, as shown by Illikainen [19], and Fernando and co-workers [20]. Thermomechanical pulp is mostly used for producing printing papers such as newsprints, and uncoated and coated magazine papers.

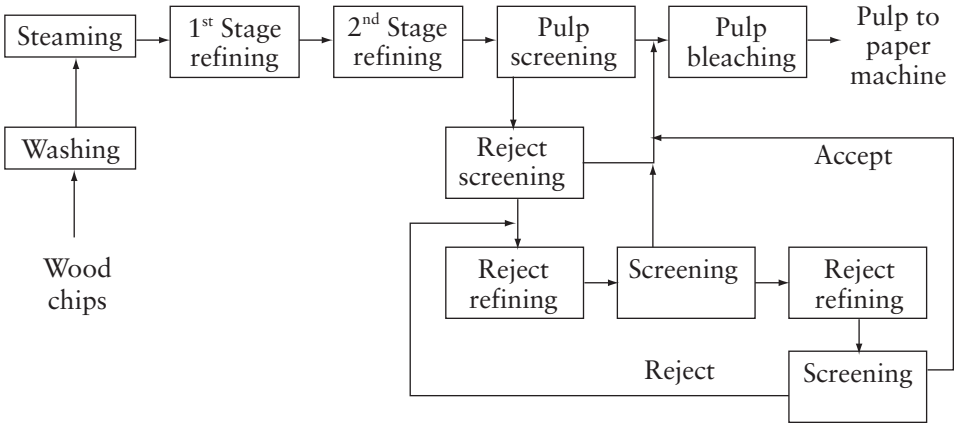

Figure 2.3 Flowsheet of a TMP fibreline

Figure 2.3 presents the flowsheet of a TMP fibreline with a two-stage chip refining. The chips are washed in order to remove sand and are steamed. The steamed chips are fed into the first refining stage, where the wood material is broken into small fragments and shives. After the first refining stage, the semirefined chips feed into the second refiner for fibre separation. After refining, the pulp is screened and enters the bleaching stage. Rejected material is processed in a two-stage refining line and after screening is combined with screened pulp. Bleached TMP pulp is sent to the paper machine.

CTMP uses both steaming and chemical treatment for lignin softening. Chemical softening exhibits a major influence on the properties of fibres liberated from the wood matrix during the refining of chips. When wood chips are impregnated with chemicals, the softening due to the swelling of the reactive middle lamellae and the primary wall regions is predominant, and this is where the defibration fracture zones are located, as stated by Gorski [21]. During CTMP operation, the chemical treatment is carried out by the impregnation of wood chips. Sodium sulfite is the dominating reagent both in hardwood and softwood pulping. Atack and Heitner [22] showed that the softening temperature of lignin depends on the sulfonate content of the wood, which is influenced by the sulfite dose, and the temperature and duration of the chemical treatment of the chips. According to Lindholm and Kurdin [23], during the production of softwood using CTMP, the parameters of the chemical treatment of the chips are: sodium sulfite charge 2–4% on wood; temperature 120–135 °C; retention time 2–15 min. The sulfonate content of the lignin ranges between 0.25–0.75% on pulp. **Figure 2.4** presents a typical flowsheet of a CTMP plant. The major difference between TMP and CTMP processes is the chemical impregnation stage; in this stage, chips are damped and compressed and then are expanded in a sodium sulfite solution. The expansion and condensation effects cause the absorption of the liquid phase into the wood structure.

The chips are refined in two stages and the obtained pulp is screened and bleached. The benefits of CTMP refer to the reduction of specific energy consumption and to an increased level of long fibres in the pulp.

The properties of the mechanical pulp depend on the pulping technique. Blechschmidt and co-workers [24] showed that the strength properties increase in the range SGW, RMP, TMP and CTMP. Regarding the light-scattering coefficient, SGW shows the highest values, followed by RMP, TMP and CTMP. These pulps are the raw material for the production of some of the most significant paper grades. Both softwood and hardwood species are used in mechanical pulping, and **Table 2.1** lists the main end products.

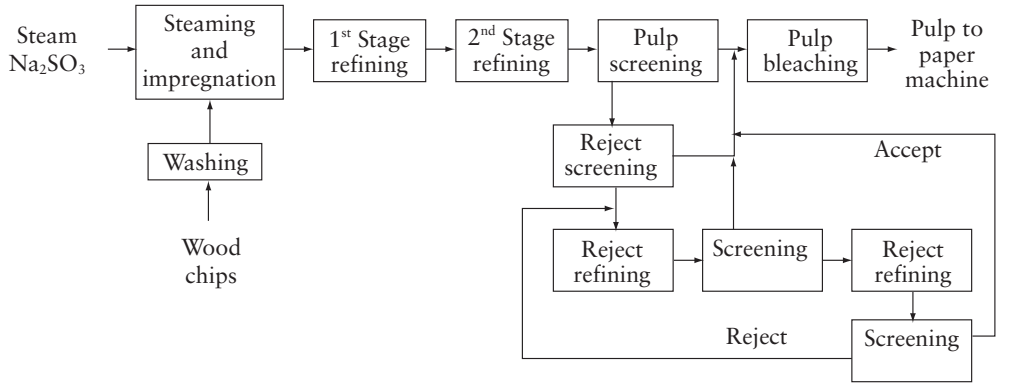

Figure 2.4 Flowsheet of a CTMP fibreline

Table 2.1 Paper grades achieved from the mechanical pulp of softwoods and hardwoods

Wood species	Mechanical process	Paper grade
Softwoods	SGW, TMP	Newsprint, supercalendered (SC), low-weight-coated (LWC)
	CTMP	Tissue, liquid packaging boards
Hardwoods	PGW, CTMP	Tissue, printing
	CTMP	Tissue, fluting

2.3 Semichemical Pulping

The term semichemical pulping suggests that pulp is produced by a chemical treatment of chips followed by a mechanical treatment, and both treatments exhibit a fairly equal contribution to the separation of fibres from the wood matrix. During semichemical pulping, the partial removal of lignin and hemicelluloses takes place, so that the yield of pulp is 60–80%. NSSC is the most important semichemical pulping process. The wood chips undergo partial chemical pulping using sodium sulfite liquor, followed by a treatment in a disc refiner to achieve fibre separation. The sulfonation of the middle lamella lignin causes its partial dissolution so that the fibre-fibre bonds are weakened before the subsequent mechanical treatment. NSSC cooking liquor contains both Na_2SO_3 and Na_2CO_3, as presented by Obrocea and Gavrilescu [25]. Sodium sulfite represents the lignin sulfonation agent, while sodium carbonate acts as a buffer of liquor pH. The Na_2SO_3 consumption ranges between 6–9% on wood, and the ratio

of Na_2SO_3/Na_2CO_3 varies between 3:1–4:1. The liquor pH is 10–11 and cooking time is 0.5–2 h at 160–185 °C.

Hardwoods (beech, poplar, adler) are the best fibre source for NSSC pulp, as found by Nemati and co-workers [26]. Nonwood plant residues (straws especially) are also used, as studied by Ahmadi and co-workers [27], and by Leoponiemi [28]. NSSC pulp is used for the production of papers where stiffness is essential, such as a corrugating medium. These papers show the best value for the flat crush of corrugated medium (Concora flat crush), as found by Gavrilescu and Toth [29].

Norman and Sell [30] studied the spent liquor of NSSC pulping (red liquor) and found that it contains lignosulfonates, hemicelluloses, organic acids and ashes. The concentration of red liquor is quite low (5–8% dry matter) and for this reason its calorific value is small. The NSSC pulping plant is often integrated into a kraft pulp mill to facilitate chemical recovery by a so-called cross-recovery, where the red liquor is processed together with the kraft black liquor.

2.4 Chemical Pulping

On a global scale, pulp is predominantly produced by chemical pulping processes, as presented in **Figure 2.5.** Chemical pulp represents around two-thirds of the total pulp production worldwide.

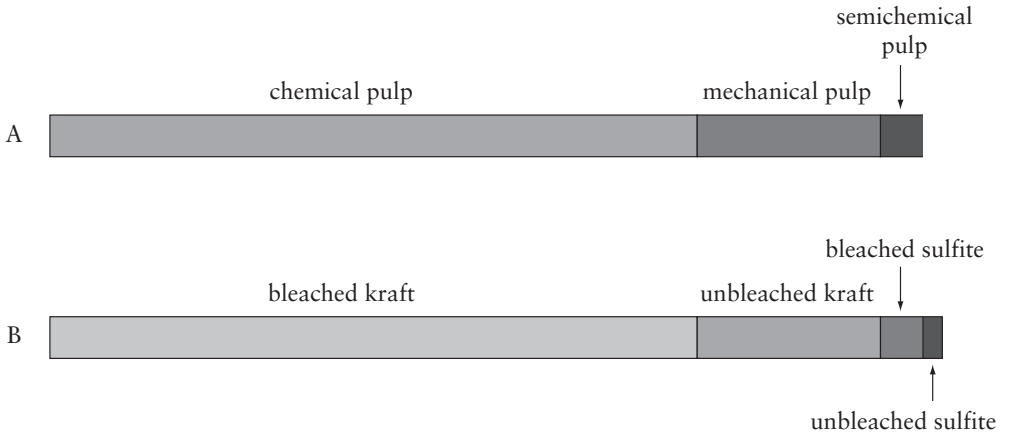

Figure 2.5 Sharing of chemical, semichemical and mechanical pulps (A), and the distribution of chemical pulps (B)

Figure 2.5 also shows that among the chemical pulps, kraft pulp (bleached and unbleached) grades are mostly produced compared with sulfite pulp. During the chemical pulping, reagents are used to split the macromolecule of lignin into fragments that are further dissolved in the cooking liquor. Fibre separation occurs when the lignin from the middle lamella is totally removed and, as a rule, no mechanical action is necessary. Chemical pulping requires a large quantity of reagents and a high temperature and pressure. Besides lignin, polysaccharides are also chemically modified and dissolved, so that the pulp yield ranges between 45–60%. An important volume of spent liquor is generated.

There are two major grades of chemical pulp: papermaking pulp and dissolving pulp. Papermaking pulp includes unbleached and bleached pulp and is characterised by yield, residual lignin content, brightness and strength properties. Dissolving pulp differs substantially from papermaking pulp and it is characterised by high alpha-cellulose content, low noncellulosic carbohydrate content, defined cellulose molar mass and molar mass distribution, low extractives and low ash content, and high reactivity towards derivatising chemicals.

The main stages of a chemical pulping process are: wood preparation, cooking, pulp washing and screening, pulp bleaching and recovery of the cooking chemicals.

2.5 Kraft Pulping Processes

2.5.1 General Description

Kraft (or sulfate) pulping represents the main cooking process, accounting for nearly 90% of the global chemical pulp production as presented by Gavrilescu and Craciun [31]. The term *kraft* refers to the fact that kraft pulp exhibits good strength properties. The cooking liquor (usually called white liquor) contains sodium hydroxide and sodium sulfide as the active alkali, which reacts with lignin and promotes degradation of the lignin polymer into fragments that dissolve in the cooking liquor. **Figure 2.6** shows the flowsheet of kraft pulping. Wood preparation includes log debarking and chipping, and chip screening. Screened chips are temporarily stored in piles and then transported to the digester house.

Cooking is performed in discontinuous or continuous digesters at a high temperature and pressure. After cooking, the pulp is washed and screened, and is finally bleached to obtain the bleached pulp which is used for printable paper grades, while unbleached pulp is used for the production of packaging paper grades. Kraft pulping generates spent liquor (denoted as black liquor) which contains the organic compounds removed

from wood and the inorganic chemicals originating from the white liquor. The black liquor must be processed in order to recover the cooking reagents and to valorise the heat of the organic matter; the alkali recovery process includes black liquor evaporation and burning, causticising of green liquor and lime reburning.

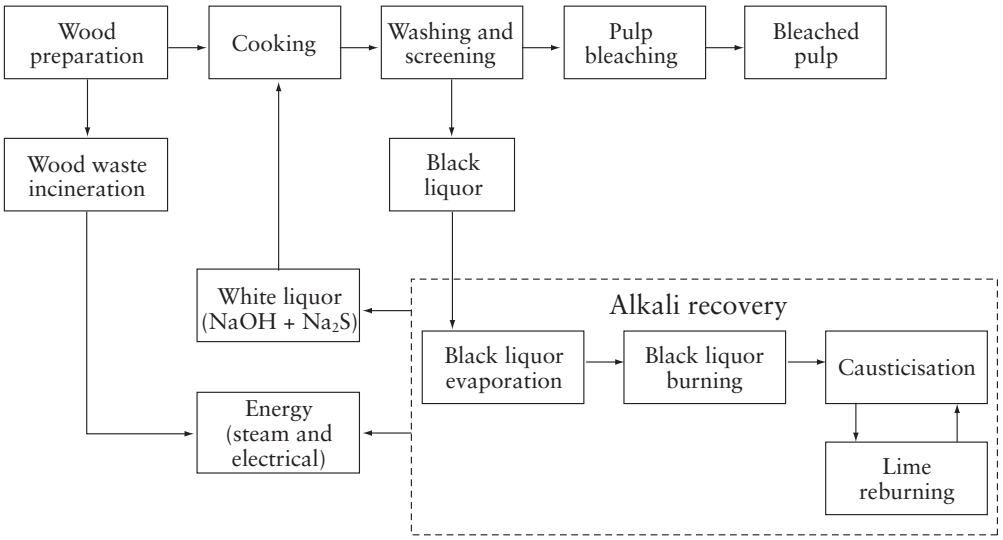

Figure 2.6 Flowsheet of kraft pulping

White liquor is characterised by the quantitative and qualitative parameters presented in **Table 2.2**. The most important are the concentration of active alkali (AA) and sulfidity (S).

Detailed studies were made regarding the composition of kraft cooking liquor. Gullichsen [32] found that in the white liquor, the main ionic species are: Na^+, OH^-, HS^- and CO_3^{2-}. Other ionic species (S^{2-}, HCO_3^-, SO_4^{2-}) are of negligible importance in the electrolyte equilibria of the cooking liquor. Gullichsen also stated that hydroxide ions (OH^-) and hydrogen sulfide ions (HS^-) are the only species that react with lignin during kraft pulping. The typical composition of white liquor is presented in **Table 2.3**. The major components are sodium hydroxide and sodium sulfide, and the minor components are sodium carbonate and sodium sulfate. Under kraft pulping conditions, sodium carbonate and sodium sulfate are not able to react with lignin.

Table 2.2 Parameters of white liquor	
White liquor parameter	**Formula**
Quantitative parameters	
Active alkali (AA)	$NaOH + Na_2S$
Effective alkali (EA)	$NaOH + 0.5\ Na_2S$
Total alkali (TA)	$NaOH + Na_2S + Na_2CO_3 + Na_2SO_4$
Qualitative parameters	
Sulfidity (S)	$S = Na_2S / (NaOH + Na_2S)$
Causticity (C)	$C = NaOH / (NaOH + Na_2CO_3)$
Degree of reduction of sodium sulfate (DR)	$DR = Na_2S / (Na_2S + Na_2SO_4)$

Table 2.3 Typical composition of white liquor (expressed as Na_2O and NaOH)			
Component	**Concentration g/L**	**Concentration (Na_2O), g/L**	**Concentration (NaOH), g/L**
NaOH	100	100(31/40) = 77.5	100
Na_2S	35	35(31/39) = 27.8	35(40/39) = 35.9
Na_2CO_3	20	20(31/53) = 11.7	20(40/53) = 15.1
Na_2SO_4	6	6(31/71) = 2.6	6(40/71) = 3.4
Active alkali concentration	-	105.3	135.9
Total alkali concentration	-	119.6	154.4

Extensive research has been carried out to elucidate the chemistry of kraft cooking. Potthast [33], and Sakakibara and Sano [34] showed that the reactions of lignin during kraft pulping can be divided into two main categories, degradation reactions and condensation reactions, respectively. Degradation reactions split the lignin macromolecule into fragments which are able to dissolve in the cooking liquor. According to Gierer [35, 36] the common degradation reactions occurring during kraft pulping include the cleavage of the α-aryl ether and β-aryl ether bonds of lignin. Condensation reactions are not desirable as they lead to the formation of alkali-stable linkages, thereby increasing the molecular size of lignin fragments, as found by Gellerstedt and Lindfors [37]. These reactions occur if the wood impregnation with white liquor is not finished and/or the cooking temperature is raised too fast. According to the same authors, during a normal kraft cook, no extensive condensation involving the aromatic rings of the lignin takes place [38].

It is known that kraft spent liquor is black in colour and kraft pulp is darker in comparison with pulp obtained by other pulping procedures. Robert and co-workers [39] showed that the reason for this behaviour is the formation of lignin chromophores, such as quinonoide structures and stilbenes. A particular reaction that occurs in kraft pulping studied by Gierer [40], involves the cleavage of methyl aryl ether bonds and the generation of mercaptans, represented by metylmercaptan, dimethylsulfide and dimethyldisulfide. Mercaptans are responsible for the specific smell of the kraft pulp mill.

Sixta [41] studied the pulp yield evolution and the degree of pulp delignification, and found that lignin is eliminated on a large scale during kraft pulping. Besides lignin, nonlignin components, mainly carbohydrates, are removed to some extent and, as a result, the pulp yield decreases.

The reactivity of carbohydrates in kraft pulping depends on their structural features such as morphology, crystallinity and degree of polymerisation. Gentile and co-workers [42] found that hemicelluloses are degraded more than cellulose in alkaline media at a high temperature. Green and co-workers [43] reviewed the alkaline degradation of carbohydrates during kraft cooking and concluded that there are two basic degradation reactions: peeling and alkaline hydrolysis. In the peeling reaction, a step-by-step depolymerisation occurs at the reducing end sites of the carbohydrates. The reaction generates a monosaccharide that finally transforms into an isosaccharinic acid. During the reaction a new reducing end on the remaining carbohydrate is also formed, which can undergo further peeling reactions. The same authors also showed that the carbohydrate material lost in the peeling reaction is converted into various hydroxy acids, which consume active alkali and consequently reduce its concentration in the pulping liquor. Hemicelluloses (glucomannans and xylans) are more engaged in peeling reactions compared with cellulose. About 50–60 monomer units are peeled off from the carbohydrate macromolecule and after that, a stopping reaction occurs. Gustavsson and Al-Dajani [44] showed that the alkaline hydrolysis of cellulose takes place at the end of the cook and determines the degree of cellulose polymerisation reduction. Due to the high temperature and strong alkaline medium, a random cleavage of the cellulose macromolecule occurs. The resulting fragments may dissolve in the cooking liquor or participate in the peeling reactions. The alkaline hydrolysis of cellulose explains the severe loss of pulp yield in the final part of the kraft cook. An important reaction of the carbohydrates in alkaline pulping is the formation of hexenuronic acids, which are formed by the alkaline degradation of 4-*O*-methyl-D-glucuroxylans. It was established that the presence of hexenuronic acids in the kraft pulp, influences the reagent consumption during pulp bleaching and the stability of pulp brightness [45].

Olm and Tistad [46] studied the kinetics of kraft pulping and showed that the

dissolution of lignin and carbohydrates proceeds in three phases denoted as initial, bulk and final delignification. **Table 2.4** shows the characteristics of kraft pulping phases.

Table 2.4 Phases of delignification during kraft pulping

Phases of delignification	Features
Initial	Slow delignification; lignin content is reduced by 15–25% of the initial amount, compared with about 40% of the hemicelluloses (cooking selectivity is low)
Bulk	High delignification rate; about 70% of the lignin is dissolved, compared with 5–7% of the carbohydrates (high selectivity)
Final (residual)	Slow delignification; intensive degradation of carbohydrates. Low selectivity

Initial delignification is a slow phase and only 15–25% of the initial lignin is dissolved. In this stage, around 40% of the hemicelluloses are dissolved so that the cooking selectivity is low. Bulk delignification is the main stage of cooking, with around 70% of the lignin being dissolved. The delignification rate is high, as is the process selectivity. Final delignification begins at a delignification rate of about 90%. To avoid excessive pulp yield loss, the kraft cook is often stopped before the final delignification [47].

Besides the major chemical constituents (cellulose, lignin and hemicelluloses), wood contains a large number of low molecular weight organic compounds, denoted as extractives. The extractives can be separated from wood with hot water or organic solvents. Umezawa [48] found that the extractives are complex mixtures of fats, fatty acids, fatty alcohols, phenols, terpenes, steroids, resin acids, rosin, waxes and other minor organic compounds. During kraft pulping, extractives exhibit a complex behaviour. Some of them are volatile and accumulate in the gaseous phase of the digester; this fraction is recovered from the digester relief condensate and is called sulfate turpentine. Most of the extractives are soluble in the cooking liquor and may react with alkali. Fatty acids and resin acid esters are neutralised and recovered as tall oil soap. Allen [49] found that crude tall oil from pine contains 40–60% resin acids, 40–55% fatty acids and 5–10% neutral constituents. Abietic and dehydroabietic acids cover over 60% of the resin acids, while oleic and linoleic acids predominate in the fatty acid fraction.

2.5.2 Kraft Pulping Parameters

Kraft pulping parameters include those factors influencing the delignification rate, pulping selectivity, pulp properties and specific consumption of raw materials and energy. MacLeod [50] showed that kraft pulping variables can be divided into key factors and minor factors. The key factors exert a significant influence on pulping results and they are: active alkali charge, white liquor sulfidity, cooking temperature and cooking time, wood species and chip quality. The minor factors are: liquor-to-wood ratio, black liquor addition and the presence of sodium carbonate in the white liquor. The active alkali charge represents the ratio between the active alkali quantity (expressed as NaOH or Na_2O) and wood mass. Casey [51] established that the theoretical consumption of active alkali in kraft pulping is 15% NaOH on wood. In order to enhance the delignification rate, the practical active alkali charge is 50–60% higher, so that the cook is performed with an excess of active alkali. At the end of the cook, the concentration of active alkali must be 5–10 g/L NaOH to avoid the reprecipitation of dissolved lignin on the fibres. As the active alkali charge is higher, more lignin dissolves from the wood, so that this parameter determines the degree of pulp delignification. The active alkali charge ranges between 17–19% NaOH for obtaining hard kraft pulps and 20–25% NaOH for bleachable pulp grades. Softwoods require 10–12% more active alkali compared with hardwoods. Casey [51] also showed that the active alkali concentration depends on the active alkali charge and on the liquor-to-wood ratio. The kraft cooking requires at least 25 g/L NaOH active alkali for fibre separation. At higher values, the delignification rate increases at the given temperature. Practically, kraft cooking requires an initial active alkali concentration of 40–60 g/L NaOH.

The sulfidity of white liquor is expressed as the per cent ratio between sodium sulfide and active alkali. According to Kleppe [52], the sulfidity strongly influences the cooking rate and process selectivity. The pulping rate significantly increases if the sulfidity rises up to 16%. The delignification rate continues to increase up to 35–40% sulfidity at a constant active alkali charge. As the sulfidity increases, the cooking selectivity enhances which means that the pulp yield increases at the same pulp lignin content. A high sulfidity is advantageous for other many reasons: it reduces the lime consumption for green liquor causticisation and decreases the fuel consumption of the lime kiln, enhances the sedimentation velocity of the lime particles during white liquor clarification and raises the fluidity of the black liquor. The sulfidity ranges between 25–35% for the cooking of hardwoods and 35–40% for softwoods.

Cooking temperature is the main factor influencing the delignification rate, with the rate approximately doubling for an increase in cooking temperature of 8 °C. Temperature negatively influences the process selectivity, in other words, at the same lignin content, increasing the temperature will decrease the pulp yield. The

cooking temperature depends on the wood species, pulp grade and cooking plant (discontinuous or continuous). The cooking of softwoods uses temperatures of 170–175 °C, while the cooking of hardwoods is performed at 165–170 °C.

The pulping time must be correlated with the cooking temperature in order to obtain pulp with the same properties. The *H*-factor is a kinetics model that combines cooking temperature and time into a unique parameter which measures the degree of cooking. Rantanen [53] found that the degree of delignification can be accurately estimated using the *H*-factor if other pulping parameters, such as active alkali and sulfidity, remain constant. Bleachable kraft pulp grades are obtained for *H*-factor values in the range of 1,000–2,000.

Kraft pulp can be obtained from any kind of raw material, wood species and nonwood plants. Wood species refer to softwoods and hardwoods, while nonwood plants are mainly represented by straw, reed, flax, hemp, kenaf and bamboo [54]. Among wood species, softwoods are preferred by papermakers as softwood pulp has the best strength properties. Hardwoods exhibit higher pulp yield, and assure good optical properties and good printability of paper. Softwoods contain more lignin which is less reactive compared with lignin from hardwoods. For this reason, pulping of softwoods requires stronger conditions (more active alkali addition and higher cooking temperatures). Nonwood plants able to be used in papermaking are very different regarding their morphological structure and chemical composition. According to Sanjoikari-Pakhala [55], nonwood plant fibres can be divided into four categories: grass fibres (cereal straw, reeds, bamboo, sugar cane), bast fibres (flax, hemp, kenaf, ramie), fruit fibres (cotton) and leaf fibres (sisal, abaca). Kraft pulping and other pulping methods (soda, organosolv) are used for the cooking of nonwood plants, as investigated by Leponiemi [56]. Nonwood pulp fibres are used for the production of common paper grades and speciality papers. Panwar and co-workers [57] showed that bast fibres are used for papers when strength, permanence and other special properties are needed; examples include permanent paper, fancy paper, currency and cigarette papers. One of the main problems in the pulping of nonwood plants is their high ash concentration, especially silica. Huang and co-workers [58] established that in alkaline pulping, silica dissolves in the cooking liquor and when the spent liquor is processed, the concentration of silica compounds increase to such an extent that it may form scale deposits.

The bark content in chips is detrimental above a certain level for many reasons: it reduces the pulp yield, increases the energy and chemical consumption and reduces the cleanliness of the pulp; hence, the bark content in chips must be restricted in accordance with the pulp grade. According to Brännvall [59], unbleached kraft pulp can tolerate a certain amount of bark content, but bleachable pulp grades are more restrictive regarding chip bark content.

Chip quality refers to chip dimensions and chip dimensional uniformity, both being of huge importance in all pulping processes. The chip dimensions must be as uniform as possible and the dimension limits of commercial chips are: length 25–40 mm, thickness 3–8 mm and width 15–30 mm. The most important factor among chip dimensions is chip thickness [60, 61]. Gullichsen and co-workers [62] showed that variation of the chip thickness is the main cause of the nonuniformity of the kraft cook. A mixture of thick and thin chips leads to a pulp which contains less delignified fibres and fibres of very low lignin content.

The liquor-to-wood ratio represents the ratio between the volume of liquid phase (sum of the white liquor, black liquor and water from wood moisture) and wood mass in the digester. During kraft cooking, it is necessary to assure the liquor phase is sufficient for the complete impregnation of the chips. The significance of the liquor-to-wood ratio on the reaction kinetics of kraft pulping was recently studied by Gustavsson [63]. It was found that a low liquor-to-wood ratio, at a constant active alkali addition, increases the alkali concentration and raises the rate of the process. At the same time, a low liquor-to-wood ratio reduces the energy consumption for liquor heating and pumping. In the high liquor-to-wood ratio cooks, dissolved wood components could diffuse more easily into the black liquor [63]. The liquor-to-wood ratio also affects the total flow inside the digester and as the liquor-to-wood ratio is increased, the liquor flow through the process is increased. Andersson [64] stated that from a practical point of view, a low liquor-to-wood ratio is preferred and the values range from 2.5–3.5.

White liquor contains variable quantities of sodium carbonate depending on the degree of causticisation. Sodium carbonate is not an effective cooking reactant, being inactive both on lignin and carbohydrates. Carbonate may have a positive effect in the kraft cook due its contribution to the alkalinity of the liquor in the final phase of cooking. However, Lundqvist and co-workers [65] found that under kraft cooking conditions, with a regular addition of white liquor, the contribution of carbonate to the alkalinity is practically zero. Sodium carbonate can precipitate calcium ions from the cooking liquor, yielding calcium carbonate which forms scale deposits on the heating surfaces of the pulp mill [66].

In order to assure a sufficient liquid phase for chip impregnation, a certain volume of black liquor is filled into the digester. The black liquor temperature is high and it contains the excess active alkali charged with white liquor at the begining of the cook. Addition of the black liquor exhibits the following advantages: increases the starting temperature of the cook, reduces the white liquor charge in the digester and increases the dry solid content of the spent liquor.

2.5.3 Kraft Pulping Technology

Kraft cooking is performed in discontinuous (or batch) and continuous processes. Features favouring batch kraft cooking are:

- High availability – one digester down for repair does not stop pulp mill production;
- Good flexibility to switch between softwoods and hardwoods as raw materials for pulping; and
- Easy to add pulp capacity of the fibreline by adding another digester.

Features favouring continuous kraft cooking, compared with batch cooking are:

- Higher capacity of fibrelines has been possible;
- Lower steam and electrical energy consumption;
- Characteristics of the pulp are more uniform;
- Higher black liquor solids and consequent lower evaporation costs in the black liquor recovery cycle; and
- Lower specific investments costs.

A batch kraft cooking cycle consists of the following operations: chip filling, liquor fill, heating and cooking, and pulp discharge. Chip filling must assure as much wood as possible in order to increase the pulp yield per cook. The uniform distribution of chips across the digester is obtained by using steam as a packing medium. The chips are warmed and the air is displaced from inside the chips. The cooking liquor (a mixture of white and black liquors) is charged to the bottom of the digester; once the digester is charged, the heating period starts. The cooking liquor is continuously extracted by the digester strainer and recirculated in a heater. The temperature of the digester content is raised up to the cooking temperature according to the cooking diagram. The digester content is kept at the cooking temperature until the lignin content of the pulp is reached. At the end of the cook, the digester content is transferred into a dedicated pulp tank.

Batch cooking uses a stationary vertical digester with a volume up to 400 m^3. A pulp mill may be equipped with a number of digesters, according to the capacity of the fibreline. An indirect heating system consisting of a liquor heater and a recirculating pump is preferred. **Figure 2.7** shows the conventional batch cooking system.

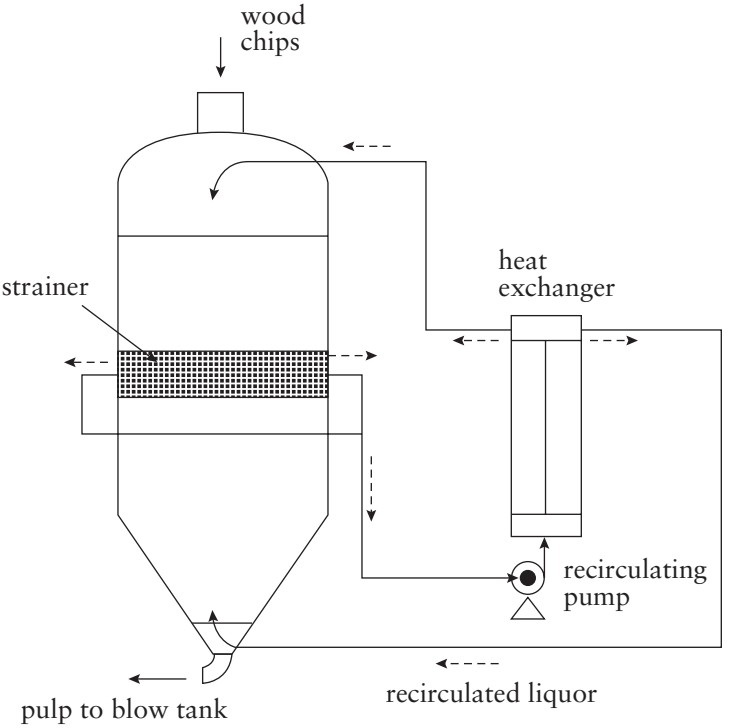

Figure 2.7 Conventional batch cooking

Batch kraft cooking is a high consumer of steam and therefore, effort has been made to reduce the energy consumption. Rapid displacement heating (RDH) is a modification of kraft cooking in a batch digester, which decreases the specific steam consumption. According to Kaiser and Pierre [67], the purpose of the RDH method is to recover the energy of the warm black liquor and to decrease the digester heating time. The RDH process involves impregnation of steam-packed chips with black liquors of increasing temperatures. The final hot black liquor is then displaced with a mixture of hot, white and black liquors at the cooking temperature. Since the liquor is preheated, the heating time is minimal and pulp production is increased [68]. Mathieson and Gustafson [69] found that the key advantage of the RDH process is the decrease in digester steam consumption, with a reduction of 60–80% compared with conventional batch kraft pulping. The energy savings accrue from the shorter steaming time required to reach the white liquor cooking temperature.

Super batch cooking is an improvement of the RDH process, the major difference being that the white liquor is added during the cooking phase. Pursiainen and co-workers

[70] found that the extended cooking of softwoods and hardwoods, to obtain pulps with low lignin content, is completely possible without negative effects on pulp quality.

A recent development of the batch process is continuous batch cooking (CBC), which combines the advantages of batch operation with the continuous preparation of cooking liquors. The impregnation liquor and the cooking liquor are prepared in the tank farm by adjusting their alkali concentration and temperature. During the cook, the liquor continuously circulates between the tanks and digester. Wizani and co-workers [71] showed that the CBC advantages are due to an even alkali profile throughout the cooking stages, a reduced cooking time and an improvement in pulp quality.

Kraft continuous pulping was developed in the 1950s and for decades became the dominant pulping process. The capacity of the pulp mills rapidly increased and now several fibrelines producing 3,000 ton/day of kraft pulp, using a unique digester, are in operation. A unique unit now under construction will produce more than 4,000 ton/day of kraft pulp [72]. During continuous cooking, the chips and chemicals are continuously fed into the top of the digester and pulp is removed from the bottom. The digester is divided to zones, in which cooking phases take place. During conventional continuous cooking, the steamed chips and cooking liquor are fed by a high pressure feeder to the top of the digester. The chips fall into the digester and the transfer circulation liquor returns to the high pressure feeder. The chips gravitationally move down through the following digester zones: impregnation, heating, cooking, hi-heat washing of pulp and pulp discharge. Heat is provided by the indirect heating of cooking liquor extracted through circumferential screens [73]. The resulting black liquor is extracted through screens located about halfway up the digester. **Figure 2.8** shows the principle of conventional continuous cooking.

In order to increase the capacity of the pulp mills and to improve pulp properties, modifications of the conventional kraft continuous cooking have been undertaken. The basic principle is the creation of a countercurrent flow of the pulping chemicals and wood chips. Atalla and co-workers [74] showed that it is feasible to keep the concentration of active alkali lower and more uniform throughout the cooking process, and also to reduce the concentration of dissolved lignin during the cook.

During the modified continuous cooking (MCC) process, white liquor is added at several points, and the cook starts at a lower concentration of active alkali and ends at a higher concentration of active alkali, compared with conventional continuous cooking. In this way, the degradation of carbohydrates is reduced and the delignification is enhanced, as stated by Norden and Teder [75]. Extended modified continuous cooking (EMCC) utilises the washing zone of the digester to further increase delignification. A volume of white liquor is added into the hi-heat washing

circulation and the temperature of the hi-heat washing zone is increased. Isothermal cooking is widely similar to EMCC but uses two sets of wash circulation loops with individual heaters. The delignification is extended by raising the temperature in the washing zone to levels normal for pulp cooking [76].

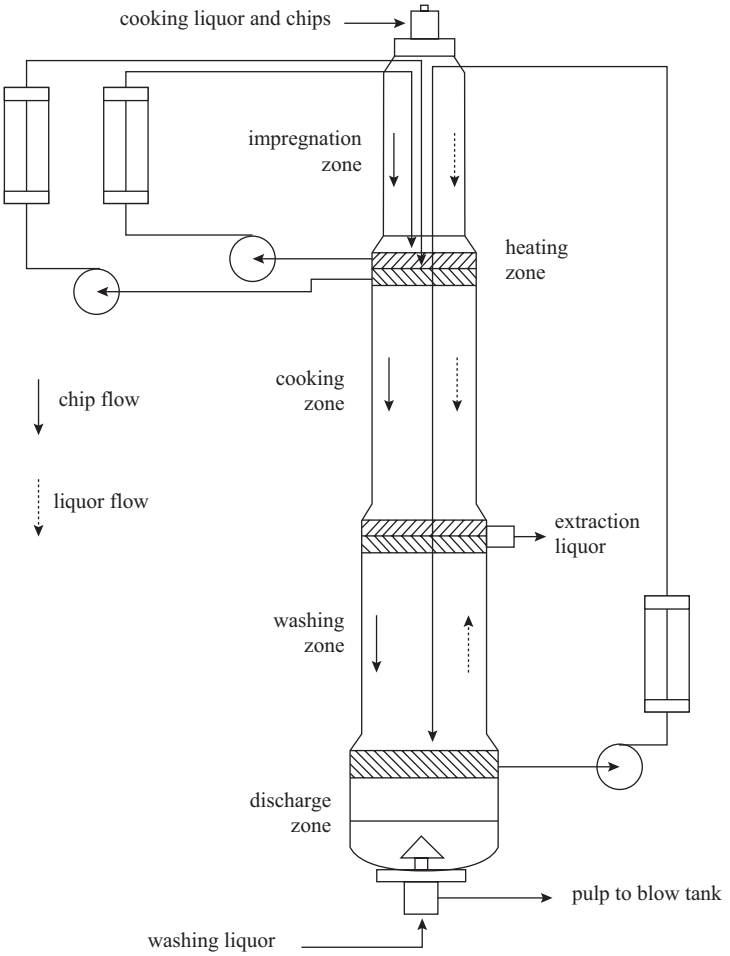

Figure 2.8 Conventional continuous cooking

The latest development of the kraft process is Lo-Solids cooking, which aims to minimise the concentration of dissolved wood solids throughout the cooking stages,

to maintain an even alkali profile and a minimal cooking temperature. Many of these objectives are similar to those of MCC and EMCC processes. According to Marcoccia and co-workers [77], Lo-Solids pulping aims to decrease the concentration of all dissolved wood solids in both the bulk and final stages of cooking, whereas earlier modified continuous cooking methods were mainly designed to decrease the concentration of dissolved lignin in the final stage of cooking. During Lo-Solids pulping, multiple cooking liquor extractions are performed. White liquor and brown stock washer filtrate are added to replace the extracted liquors. An optimum profile of alkali concentration and digester temperature at every cooking stage is maintained; benefits include: improved process selectivity, extended pulp delignification and increased pulp strength, as found by Lindstrom and Lindgren [78].

2.6 Sulfite Pulping

Sulfite pulping includes the following cooking variants: acid sulfite, disulfite, neutral sulfite and alkaline sulfite. The alternatives of sulfite pulping differ by the composition and pH of the cooking liquor, as presented in **Table 2.5**.

Table 2.5 Sulfite pulping alternatives

Sulfite processes	pH of cooking liquor	Active species	Applications
Acid sulfite	1–2	H^+, HSO_3^-	Dissolving pulp, newsprint, tissue
Disulfite	3–5	HSO_3^-	Newsprint, tissue, printing paper
Neutral sulfite	6–9	SO_3^{2-}	Corrugated medium
Alkaline sulfite	10–13	HO^-, SO_3^{2-}	Corrugated medium, package grades

Acid sulfite pulping was the dominant cooking process until the 1940s when it was surpassed by kraft cooking. Acid sulfite pulp is brighter compared with kraft pulp and can be used without bleaching to produce some printing paper grades. Acid sulfite pulp is weaker than kraft pulp and not all species of wood can be cooked easily. In addition, the cooking cycle is long (up to 10–12 hours) and chemical recovery of the cooking chemicals, from sulfite spent liquor, is complicated or impractical. The pollution potential of acid sulfite pulping is much higher than that of kraft, due to the sulfite spent liquor, which is rich in organic dissolved material, and due to a high sulfur dioxide loss in the air.

The cooking liquor is highly acidic and contains a mixture of sulfurous acid and sodium disulfite, the active species being HSO_3^- and H^+. During the cook, the lignin macromolecule is split by hydrolysis and sulfitolysis reactions into smaller fragments which dissolve in the liquid phase. According to Sixta [79], sulfonation is the main reaction of sulfite pulping and renders the lignin sufficiently hydrophilic to dissolve into the cooking liquor. Soluble lignosulfonates are formed in the process. During acid sulfite pulping, lignin condensation reactions may be important if the disulfite ion concentration is low and the cooking liquor acidity is high. Poor chip impregnation will always increase the risk of lignin condensation, which reduces the lignin reactivity and darkness of the pulp and, finally, a so-called 'black cook' can be attained.

Gellerstedt [80] found that the main reaction of carbohydrates during acid sulfite cooking is the acid-catalysed hydrolysis of glycosidic bonds. Hemicelluloses are degraded much more than cellulose, yielding monosaccharides which dissolve into the cooking liquor. At an elevated temperature, monosaccharides are partially dehydrated to furfural and hydroxymethylfurfural.

According to Wolfinger and Sixta [81], the rate of delignification in acid sulfite pulping is highly influenced by temperature and cooking liquor composition. Temperature elevation exerts a complex influence: it increases the pH of the cooking liquor, decreases sulfur dioxide solubility, increases lignin dissolution and carbohydrate decomposition. The delignification rate increases vastly with the increasing concentration of sulfur dioxide in the cooking liquor.

Process variables during acid sulfite pulping are wood species, pH of cooking liquor, and cooking base and temperature. Acid sulfite pulping is sensitive to wood species, due its poor ability to dissolve extractives. Spruce wood is largely used while rich-extractives softwoods (pine wood) cannot be successfully cooked. Before cooking, wood must be stored for a certain period in order to reduce its moisture and extractives content. The most important variable of the sulfite process is the pH of the cooking liquor. Acid sulfite cooking is performed at pH 1–2, the pH at which all bases (calcium, sodium, magnesium and ammonium) are fully soluble. By replacing the insoluble calcium base with a sodium or ammonium base (soluble bases), a better delignification takes place and less scaling problems occur. Young [82] found that soluble bases give pulps with better yield and higher brightness. Cooking temperature determines the reaction rate and process selectivity. Acid sulfite pulping requires a temperature between 130–145 °C. With every increase of 10 °C cooking temperature, the delignification rate doubles, but the cook selectivity is reduced.

Disulfite pulping is carried out at a pH of 3–5 and the disulfite ion is the dominant reagent in the cooking liquor. Disulfite liquor is free from sulfurous acid (H_2SO_3). Under mild acidic conditions, the delignification rate decreases and the acid hydrolysis

of cellulose reduces. In order to compensate for the lower rate of lignin dissolution, disulfite pulping uses higher cooking temperatures (155–170 °C), compared with acid sulfite pulping. The cooking liquor may contain either sodium disulfite or magnesium disulfite, which are fully soluble at the pH of the liquor [83].

The major advantage over acid sulfite pulping is that the strength properties of the disulfite pulp are significantly better than that of the acid sulfite pulp. The advantages over kraft pulping include a considerably higher pulp yield at the same lignin content, higher unbleached pulp brightness and better pulp bleaching capacity. Industrial applications include the Arbisco process, which uses sodium disulfite and Magnefite, which uses magnesium disulfite, as presented by Biermann [84]. Both processes are used to produce pulps for newsprint. The Magnefite process is used at pH 4.5 and a temperature of 160 °C, with $Mg(OH)_2$ as the base. The cooking cycle is 6–8 hours and the pulp yield ranges between 55–65% [84]. Chemical recovery is necessary due to the high cost of the base. Cook [85] showed that Magnefite spent sulfite liquor is concentrated by evaporation and burned in a recovery boiler. The solid phase contains magnesium oxide (MgO) and the flue gases contain SO_2, which is recovered. The MgO is slurried into the water to give a slurry containing $Mg(OH)_2$, which is used to scrub SO_2 from the flue gases.

Alkaline sulfite (AS) pulping uses a cooking liquor containing a mixture of sodium sulfite and sodium hydroxide, with a pH of 10–13. This process was developed during the 1980s as an alternative to kraft pulping, in order to reduce the environmental impact and to maintain pulp strength properties at the level of kraft pulp [86]. If compared with kraft pulping, AS pulping shows a very low rate of delignification and the pulp yield at the same lignin content is lower, as found by Kettunen and co-workers [87]. In addition, the recovery of AS pulping chemicals is more difficult compared with the kraft recovery system. For these reasons, AS pulping wasn't applied on a commercial scale however, interest in AS pulping increased when it was found that the addition of small quantities of antraquinone (AQ) increased the delignification rate [88]. Moreover, if methanol is added, the delignification rate further increases and on this basis, a new pulping method, (alkaline sulfite-antraquinone-methanol – ASAM) was developed [89]. Kordsachia and co-workers [90] found that the presence of methanol in the alkaline sulfite/AQ-system provides pulps with a highly selective delignification, yielding a low lignin content with high viscosity and high strength properties. Despite all of the above mentioned advantages, the ASAM pulping has failed to be applied at the industrial scale for several reasons: the efficiency of the sodium sulfite recovery system is not economically feasible, the presence of methanol needs a dedicated recovery plant, and the concurrent kraft pulping process has been vastly improved over the last few years and has diminished the advantages of the ASAM pulping [91].

2.7 Organosolv Pulping

Kraft pulping is the dominant process used in the production of chemical pulp, due to its advantages related to high pulp strength properties and raw material versatility. However, there are some limitations regarding its environmental impact. The presence of sodium sulfide in the cooking liquor creates the problem of mill odour, originating from the air emission of reduced sulfur compounds (mercaptans and hydrogen sulfide) [92, 93]. In addition, during pulp bleaching, large volumes of wastewaters which contain organic chlorine compounds are generated [94]. During the 1980s and 1990s, the possibilities for substituting the kraft process were widely studied and a number of new pulping processes were developed. The new processes use organic chemicals to dissolve lignin and to separate the fibres from the wood, among their objectives being cited [95]:

- The process should be sulfur free to avoid malodorous gas generation;
- It should be capable of dissolving most of the wood lignin with very little loss of cellulose and hemicelluloses;
- It should not require higher temperatures, pressures or pulping times than used in kraft pulping;
- It should have a simple chemical recovery system;
- The pulp quality should be at least equal to the quality of the kraft pulp; and
- The pulp should be bleached without chlorine chemicals.

The new pulping processes are grouped in the so-called organosolv pulping processes which use different types of organic compounds: alcohols (methanol, ethanol), acids (formic, acetic), phenols (phenol and cresols), esters (ethyl acetate), amines (methylamine, ethylenediamine), ketones (methylethylketone). A classification of the organosolv pulping processes according to the basic mechanism involved in lignin dissolution is given in **Table 2.6.**

Table 2.6 shows that several organosolv pulping methods have been developed, but many of them have not progressed past the laboratory test stages. A limited number of pulping methods, based on organic acids or alcohols, have been tested at pilot level [106, 107]. According to Leponiemi [108], an advantage of organosolv processes is the formation of useful by-products such as furfural, lignin and hemicelluloses.

Most problems of the organosolv processes are related to the pulp quality, which is normally lower than the quality of corresponding kraft pulps, and solvent recovery.

Organic solvents are more expensive than the inorganic reactants used in kraft pulping and for this reason they have to be recovered at high recovery rates.

Table 2.6 Classification of organosolv pulping processes

Pulping method	Main characteristics	References
Autohydrolysis		
Ethanol-water (no catalyst added)	42.5% ethanol, 185 °C; 55% ethanol, 195 °C	[96, 97]
ALCELL	50% ethanol, 195 °C, three displacement stages of pulping	[98, 99]
Acid-catalysed		
Acetosolv	93% acetic acid, 0.5–3.0% hydrochoric acid, 110 °C	[100, 101]
Phenol pulping	Phenols, 100 °C	[102]
Alkaline processes		
Organocell	Methanol, antraquinone, sodium hydroxide	[103]
Ethanol alkali	Etanol, sodium hydroxide	[104, 105]
Oxidative processes		
Milox	80% formic acid, 4% H_2O_2	[106, 107]

Only small organosolv pulp mills are in operation today, mainly producing pulp from wheat straw. A pulping process designed for the manufacture of bleached pulp, lignin and hemicelluloses from cereal straw was developed by Compagnie Industrielle de la Matière Végétale (CIMV process) [109]. According to the CIMV process, wheat straw is treated at atmospheric pressure with a mixture of acetic acid/formic acid/water, 30/55/15 (v/v/v), for a reaction time of 3.5 h at 105 °C. In these conditions, wheat straw lignin dissolves and the hemicelluloses are hydrolysed into oligosaccharides and monosaccharides with a high xylose content. The obtained pulp is screened and bleached. Organic acids are then recycled by concentration of the extraction liquor containing lignin and hemicelluloses. The concentrated extraction liquor is treated with water to precipitate lignin, which is recovered using high pressure filtration. Another organosolv process in operation, which is based on the full utilisation of annually renewable fibres, is the Chempolis process developed at Chempolis Ltd, Oulu, Finland, by Rousu and co-workers [110]. Common nonwood materials, such as wheat and rice straw, bagasse and different reeds and grasses are used in pulp production. Delignification is performed in a single-stage formic acid cooking, which

is carried out at a temperature between 110 and 125 °C, and the cooking time can vary between 20 and 40 min; bleaching of the pulp is performed with hydrogen peroxide in several stages. The chemical recovery comprises the evaporation of spent liquor and distillation of the formic acid. The regenerated acid is circulated back into the cooking stage, while the dissolved solid is dried. Lignin can be further used for processing in the chemical industry or it can be burned in an ordinary power boiler. The ash from the boiler and the nutrients from the pulp bleaching filtrates are returned back to the fields [111].

2.8 Conclusions or Future Trends

Woodpulp will be, for the next decade, the main raw material for producing paper and boards, and to obtain cellulose derivatives. Among pulping processes, kraft pulping will continue to dominate global pulp production.

The large differences in wood and labour costs between world regions determine that new pulp mills will mainly be built in Latin America and Asia. Modernisation of existing mills will dominate in Europe and North America.

Research efforts are still necessary for a better understanding of the mechanisms involved in pulping processes in order to decrease material and energy consumption. Reduction of the environmental impact of pulp manufacture is of huge importance for the competitiveness of pulp mills.

Global challenges such as limited oil supply, increased concern about greenhouse gas emissions and the decreasing competitiveness of traditional pulp and paper producers will boost the need to convert the pulp mills into integrated forest biorefineries which will produce, besides pulp, higher value-added products such as ethanol, polymers, carbon fibres, biodiesel and so on.

References

1. Confederation of European Paper Industries (CEPI) in *Key Statistics 2010, European Pulp and Paper Industry*, Ed., CEPI, Brussels, Belgium, 2012, p.8.

2. Food and Agriculture Organization of the United Nations (FAO), *Pulp and Paper Capacities, Survey 2010–1015*, Ed., FAO, Rome, Italy, 2011, p.1.

3. U.C.V. Haley, Economic Policy Institute (EPI) in *No Paper Tigers, Subsidies to China's Paper Industry From 2002–09*, EPI Briefing Paper 264, Washington, DC, USA, 2010, p.2.

4. C.J. Biermann in *Handbook of Pulping and Papermaking*, 2nd Edition, Academic Press, San Diego, CA, USA, 1996, p.55.

5. H. Höglund in *Pulping Chemistry and Technology*, Volume 2, Eds., M. Ek, G. Gellerstedt and G. Henriksson, Walter de Gruyter, Berlin, Germany, 2009, p.57.

6. J. Sundholm in *Papermaking Science and Technology*, Eds., J. Gullichsen and H. Paulapuro, Fapet Oy, Helsinki, Finland,1999, p.21.

7. A. von Koeppen, *Paper Trade Journal*, 1986, **170**, 11, 49.

8. H.E. Worster in *Pulp and Paper Manufacture*, 3rd Edition, Eds., TAPPI-CPPA, Montreal, Canada, 1985, p.130.

9. O.V. Ingruber in *Pulp and Paper Manufacture*, 3rd Edition, Eds., TAPPI-CPPA, Montreal, Canada, 1985, p.244.

10. H. Sixta, A. Potthast and A.W. Krotschek in *Handbook of Pulp*, Ed., H. Sixta, Wiley-VCH, Weinheim, Germany, 2006, p.109.

11. J. Gullichsen in *Chemical Pulping*: *Papermaking Science and Technology*, Eds., J. Gullichsen and H. Paulapuro, Fapet Oy, Helsinki, Finland, 1999, p.A28.

12. L. Salmen, M. Lucander and E. Harkonen in *Fundamentals of Mechanical Pulping*: *Papermaking Science and Technology*, Eds., J. Gullichsen and H. Paulapuro, Fapet Oy, Helsinki, Finland, 1999, p.41.

13. A. Karnis, *Journal of Pulp and Paper Science*, 1994, **20**, 10, J280.

14. H. Liimatainen, P. Haikkala, M. Lucander, R. Karojarvi and O. Tuovinen in *Mechanical Pulping*: *Papermaking Science and Technology*, Eds., J. Gullichsen and H. Paulapuro, Fapet Oy, Helsinki, Finland, 1999, p.107.

15. D. McDonald, K. Miles and R. Amiri, *Pulp and Paper Canada*, 2004, **105**, 8, 27.

16. J-E. Berg in *Wood and Fibre Mechanics Related to the Thermomechanical Pulping Process*, Mid Sweden University, Sundsvall, Sweden, 2008, p.3. [Doctoral Thesis]

17. D. Muhic, L. Sundström, C. Sandberg, M. Ullmar and P. Engstrand, *Nordic Pulp and Paper Research Journal*, 2010, **25**, 4, 420.

18. K.B. Miles and A. Karnis, *Journal of Pulp and Paper Science*, 1995, **21**, 11, p.J383.

19. M. Illikainen in *Mechanisms of Thermomechanical Pulp Refining*, University of Oulu, Oulu, Finland, 2008, p.15. [Doctoral Thesis]

20. D. Fernando, D. Muhic, P. Engstrand and G. Daniel, *Holzforschung*, 2011, **65**, 6, 777.

21. D. Gorski in *A TMP Process*: *Improved Energy Efficiency in TMP Refining Utilizing Selective Wood Disintegration and Targeted Application of Chemicals*, Mid Sweden University, Sundsvall, Sweden, 2011, p.10. [Doctoral Thesis]

22. D. Atack and C. Heitner in *Proceedings of the International Mechanical Pulping Conference*, Toronto, Canada, 1979, p.1.

23. C-A. Lindholm and J.A. Kurdin in *Chemimechanical Pulping: Papermaking Science and Technology*, Eds., J.Gullichsen and H. Paulapuro, Fapet Oy, Helsinki, Finland, 1999, p.236.

24. J. Blechschmidt, S. Heinemann and H-U. Suss in *Handbook of Pulp*, Ed., H. Sixta, Wiley-VCH, Weinheim, Germany, 2006, p.1069.

25. P. Obrocea and D. Gavrilescu in *Pulping Fundamentals*, Rotaprint Publishers, Iasi, Romania, 1992, p.148. [In Romanian]

26. M. Nemati, A. Samariha and A. Khakifirooz, *American-Eurasian Journal of Agricultural and Environmental Science*, 2011, **11**, 1, 15.

27. M. Ahmadi, A.H. Latibari, M. Faezipour and S. Hedjazi, *Turkish Journal for Agriculture and Forestry*, 2010, **34**, 1, 11.

28. A. Leoponiemi in *Fibres and Energy from Wheat Straw by Simple Practice*, VTT Publications, Espoo, Finland, 2011, p.59. [Doctoral Dissertation]

29. D. Gavrilescu and S. Toth in *Corrugated Board*, T3 Publishers, Sf. Gheorghe, Romania, 2007, p.10. [In Romanian]

30. J.C. Norman and N.J. Sell in *Proceedings of TAPPI Engineering Conference*, Book 1, Nashville, TN, USA, 1991, p.405.

31. D. Gavrilescu and G. Craciun in *Kraft Pulping Processes*, Texte, Dej, Romania, 2012, p.10. [In Romanian]

32. J. Gullichsen in *Fiber Line Operations*, *Papermaking Science and Technology*, Eds., J. Gullichsen and H. Paulapuro, Fapet Oy, Helsinki, Finland, 2000, p.38.

33. A. Potthast in *Handbook of Pulp*, Ed., H. Sixta, Wiley-VCH, Weinheim, Germany, 2006, p.164.

34. A. Sakakibara and Y. Sano in *Wood and Cellulosic Chemistry*, Eds., N-S. David, N-S. Hon and N. Shiraishi, Marcel Dekker, New York, NY, USA, 2001, p.109.

35. J. Gierer, *Wood Science and Technology*, 1980, **14**, 4, 241.

36. J. Gierer, *Wood Science and Technology*, 1985, **19**, 4, 289.

37. G. Gellerstedt and E-L. Lindfors, *Holzforschung*, 1984, **38**, 3,151.

38. G. Gellerstedt and E-L. Lindfors in *Proceedings of the International Pulp Bleaching Conference*, Stockholm, Sweden, 1991, p.73.

39. D. Robert, M. Bardet, G. Gellerstedt and E-L. Lindfors, *Journal of Wood Chemistry and Technology*, 1984, **4**, 3, 239.

40. J. Gierer, *Svensk Paperstidning*, 1970, **73**, 18, 571.

41. H. Sixta in *Kraft Pulping Kinetics*, *Handbook of Pulp*, Ed. H. Sixta, Wiley-VCH, Weinheim, Germany, 2006, p.185.

42. V.M. Gentile, L.R. Schroeder and R.H. Atalla in *The Structure of Cellulose: Characteristics of the Solid State*, Ed., R.H. Atalla, American Chemical Society, ACS Symposium Series, Washington, DC, USA, 1987, p.272.

43. J.W. Green, I.A. Pearl, K.W. Hardacker, B.D. Andrews and F.C. Haigh, *TAPPI*, 1977, **60**, 10, 120.

44. C.A.S. Gustavsson and W.W. Al-Dajani, *Nordic Pulp & Paper Research Journal*, 2000, **15**, 2, 160.

45. J. Buchert, E. Bergnor, G. Lindblad, L. Viikari and M. Ek, *TAPPI*, 1997, **80**, 6, 165.

46. L. Olm and G. Tistad, *Svensk Papperstidning*, 1979, **87**, 5, 458.

47. N. Andersson, D.I. Wilson and U. Germgård, *Nordic Pulp and Paper Research Journal*, 2003, **18**, 2, 200.

48. T. Umezawa in *Chemistry of Extractives*: *Wood and Cellulosic Chemistry*, Eds., N-S. David, N-S. Hon and N. Shiraishi, Marcel Dekker, New York, NY, USA, 2001, p.213.

49. R. Alen in *Basic Chemistry of Wood Delignification*, *Papermaking Science and Technology*, Eds., J. Gullichsen and H. Paulapuro, Fapet Oy, Helsinki, Finland, 2000, p.74.

50. M. MacLeod, *Paperi ja Puu*, 2007, **89**, 4, 1.

51. J.P. Casey in *Pulp and Paper Chemistry and Chemical Technology*, Volume 1, John Wiley and Sons, New York, NY, USA, 1980, p.14.

52. P.J. Kleppe, *TAPPI*, 1970, **53**, 1, 35.

53. R. Rantanen in *Modelling and Control of Cooking Degree in Conventional and Modified Continuous Pulping Processes*, Academic Dissertation, University of Oulu, Oulu, Finland, 2006, p.36.

54. W. Sridach, *Suranaree Journal of Science and Technology*, 2010, **17**, 2, 105.

55. K. Sanjoikari-Pakhala in *Nonwood Plants as Raw Material for Pulp and Paper*, Academic Dissertation, University of Helsinki, Helsinki, Finland, 2001, p.15.

56. A. Leponiemi, *Appita Journal*, 2008, **61**, 3, 234.

57. M.P. Panwar, A.K. Upadhyay, P.N. Sharma and M. Himanshu, *IPPTA: Quarterly Journal of Indian Pulp and Paper Technical*, 2008, **20**, 3, 173.

58. G. Huang, J.X. Shi and T.A.G. Langrish, *Bioresource Technolology*, 2007, **98**, 15, 2829.

59. E. Brännvall in *Wood Handling*, *Pulp and Paper Chemistry and Technology*, Eds., M. Ek, G. Gellerstedt and G. Henriksson, Walter de Gruyter, Berlin, Germany, 2009, p.15.

60. A.F.M. Akhtaruzzaman and N-E. Virkola, *Paperi ja Puu*, 1979, **61**, 9, 578.

61. M. Svedman, P. Tikka and M. Luhtanen, *TAPPI*, 1998, **81**, 7, 157.

62. J. Gullichsen, H. Kolehmainen and H. Sundqvist, *Paperi ja Puu*, 1992, **74**, 6, 486.

63. M. Gustavsson in *The Significance of Liquor-to-wood Ratio on the Reaction Kinetics of Spruce Sulphate Pulping*, Karlstads Universitet, Karlstad, Sweden, 2007, p.17. [Master's Thesis]

64. N. Andersson in *Workshop on Chemical Pulping Processes*, Karlstad University, Karlstad, Sweden, 2006, p.31.

65. F. Lundqvist, L. Olm and D. Tormund, *Nordic Pulp and Paper Research Journal*, 2006, **21**, 3, 290.

66. A. Saltberg, H. Brelid and F. Lundqvist, *Nordic Pulp and Paper Research Journal*, 2009, **24**, 4, 440.

67. M. Kaiser and R. Pierre in *Proceedings of the TAPPI Pulping Conference*, TAPPI Press, Atlanta, GA, USA, 1986, p.627.

68. E.K. Andrews in *Proceedings of the TAPPI Pulping Conference*, TAPPI Press, Atlanta, GA, USA, 1989, p.607.

69. B.A. Mathieson and R.R. Gustafson, *TAPPI*, 1996, **79**, 5, 180.

70. S. Pursiainen, S. Hiljanen, P. Uusitalo, K. Kovasin and M. Saukkonen, *TAPPI*, 1990, **73**, 8, 115.

71. W. Wizani, W.A. Krotscheck, W. Juljanski and R. Bito in *Proceedings of the Pulping Process and Product Quality Conference*, Boston, MA, USA, 2000, p.340.

72. Andritz Group, *PULPAPERnews*. *http://www.pulpapernews.com/2011/01/andritz-supplies-eldorado-pulp-mill*

73. S. Laakso in *Modeling of Chip Bed Packing in a Continuous Kraft Cooking Digester*, Helsinki University of Technology, Espoo, Finland, 2008, p.19. [Doctoral Dissertation]

74. R.H. Atalla, R. Reiner and C.J. Houtman in *New Technology in Pulping and Bleaching*, Elsevier, Madison, WI, USA, 2004, p.918.

75. S. Nordén and A. Teder, *TAPPI*, 1979, **62**, 7, 49.

76. A. Bachlung and J. Svanberg, inventors; Kvaerner Pulping AB, assignee; US 5766413, 1998.

77. B. Marcoccia, R. Laakso and G. McClain, *TAPPI*, 1996, **79**, 6, 179.

78. M. Lindstrom and C. Lindgren, inventors; Kvaerner Pulping AB, assignee; US 5885414, 1999.

79. H. Sixta in *Handbook of Pulp*, Ed., H. Sixta, Wiley-VCH, Weinheim, Germany, 2006, p.392.

80. G. Gellerstedt in *Pulping Chemistry*, *Wood and Cellulosic Chemistry*, Eds., D.N-S. Hon and N. Shiraishi, Marcel Dekker, New York, NY, USA, 2001, p.859.

81. M.G. Wolfinger and H. Sixta, *Lenzinger Berichte*, 2004, **83**, 35. [In German]

82. R.A. Young in *Handbook of Industrial Chemistry and Biotechnology*, Ed., J.A. Kent, Springer, New York, NY, USA, 2007, p.1248.

83. K.N. Lewis in *Summer Sickness of Magnesium Bisulfite Pulp at Fraser Paper's Edmunston Mill*, University of New Brunswick, New Brunswick, Canada, 1994, p.39. [Master's Thesis]

84. C.J. Biermann in *Handbook of Pulping and Papermaking*, Academic Press, San Diego, CA, USA, 1996, p.95.

85. G.G. Cook, *TAPPI*, 1984, **67**, 11, 66.

86. O.V. Ingruber and C.A. Allard, *Pulp and Paper Magazine of Canada*, 1973, **74**, 11, p.T354.

87. J. Kettunen, J.E. Laine, I.Yrjälä and N.E. Virkola, *Paperi ja Puu*, 1982, **64**, 4, 205.

88. J. Kettunen, N.E. Virkola and I. Yrjala, *Paperi ja Puu*, 1979, **61**, 11, 685.

89. K. Fuchs, A. Huber and H-L. Schubert, inventors, Impco-Voest-Alpine Pulping Technologies GmbH, assignee; EP 0777780, 1998.

90. O. Kordsachia, B. Wandinger and R. Patt, *Holz als Roh- und Werkstoff*, 1992, **50**, 3, 85. [In German]

91. R. Patt, H.L. Schubert, O. Kordsachia, E. Oltmann and W. Ridder in *Proceedings of the Sunds Defibrator Symposium*, Pori, Finland, 1990, p.1.

92. J.Y. Hsu, X.S. Chai, X.J. Pan, Q. Luo and J. Li, *Environmental Science and Technology*, 2002, **36**, 10, 2269.

93. C.J.M. Bordado and J.F.P. Gomes, *Journal of Chemical Engineering and Processing*, 2002, **41**, 8, 667.

94. M. Sillanpaa in *Studies on Washing in Kraft Pulp Bleaching*, Academic Dissertation, University of Oulu, Oulu, Finland, 2005, p.20.

95. E. Muurinen in *Organosolv Pulping A Review and Distillation Study Related to Peroxyacid Pulping*, Academic Dissertation, University of Oulu, Oulu, Finland, 2000, p.13.

96. T.N. Kleinert, *TAPPI*, 1974, **57**, 8, 99.

97. H. Sixta and A. Borgards, *Das Papier*, 1999, **53**, 4, 220. [In German]

98. E. Pye and J.H. Lora, *TAPPI*, 1991, **74**, 3, 113.

99. J.H. Lora, *TAPPI*, 1992, **75**, 1,117.

100. H. Nimz, H.A. Berg, C. Granzow, R. Casten and S. Muladi, *Das Papier*, 1989, **43**, 10A, p.V102. [In German]

101. P. Obrocea and D. Gavrilescu, *Celuloza si hartie*, 1988, **37**, 4,157. [In Romanian]

102. A. Vega and M. Bao, *Wood Science and Technology*, 1991, **25**, 6, 459.

103. B. Lonnberg, T. Laxen and R. Sjoholm, *Paperi ja Puu*, 1987, **69**, 9, 758.

104. S. Aziz and K. Sarkanen, *TAPPI*, 1989, **72**, 3, 169.

105. M.A. Gilarrahz, M. Oliet, F. Rodriguez and J. Tijero, *Canadian Journal of Chemical Engineering*, 1998, **76**, 4, 253.

106. J. Sundquist and K. Poppius-Levlin in *Milox Pulping and Bleaching*, *Environmentally Friendly Technologies for the Pulp and Paper Industry*, Eds., R.A. Young and M. Akhtar, John Wiley and Sons, New York, NY, USA, 1998, p.157.

107. P. Obrocea and G. Cimpoesu, *Cellulose Chemistry and Technology*, 1998, **32**, 5–6, 517.

108. A. Leponiemi in *Fibres and Energy from Wheat Straw by Simple Practice*, Aalto University, Espoo, Finland, 2011, p.20. (Doctoral Dissertation)

109. G-H. Delmas, B. Benjelloun-Mlayah, Y. Le Bigot and M. Delmas, *Journal of Applied Polymer Science*, 2011, **121**, 1, 491.

110. P. Rousu, P. Rousu and E. Rousu, inventors; Chempolis Oy, assignee; US 6156156, 2000.

111. P. Rousu, P. Rousu and J. Anttila, *Conservation and Recycling*, 2002, **35**, 1–2, 85.

3 Chemical Pulp Bleaching

Ivo Valchev

3.1 General Aspects

The main objective of bleaching is to remove encrusted substances to obtain a pure white product therefore, the manufacturing process requires further delignification and bleaching of the fibres, as residual lignin is a major contributing factor to colour. Unbleached chemical pulps still contain lignin in an amount of 2–4.5% on oven dry (o.d.) pulp depending on the wood species and process details. The bleaching process can best be regarded as a continued pulping in which a series of alternating oxidation and extraction treatments ultimately lead to an almost lignin-free fibre. During bleaching, the cleanliness of the pulp improves when the fibres of the fibre bundles, or shives, are released as the last of the residual lignin is removed from the pulp and any bark debris dissolves. The chemicals used in bleaching also effectively dissolve extractives contained in the pulp. There is a fundamental difference between bleaching of chemical pulps and mechanical pulps. In the bleaching of chemical pulps lignin is oxidised, decomposed and finally eliminated from the pulp fibres. This results in less chromophores in the pulp. The bleaching process must be carried out as gently as possible, so that the carbohydrate is not attacked. The target brightness cannot be achieved in only one bleaching step without sacrificing pulp strength. Therefore, pulp is bleached in several steps, and the pulp is washed between them. Multistage bleaching gives the best results regarding both quality and economy, and there are alkaline and acidic bleaching stages. With only alkaline or acidic stages, the target brightness would not be attained, so both are always used in bleaching. Using old technology, bleaching was performed with chlorine-containing chemicals: with elemental chlorine (C), hypochlorite (H) or with chlorine dioxide (D). Between stages, the dissolved lignin was extracted with alkali (E). Typical traditional bleaching sequences were CEHDED and CEDED.

During the 1980s and 1990s, environmental concern in the pulp and paper industry increased considerably, and pressure on the industry to become more environmentally friendly came, to an increasing degree, from the final customers. As a result of the

concern regardimg chlorinated organic compounds formed during chlorine bleaching, conventional bleaching concepts were rapidly replaced by the so-called elemental chlorine-free (ECF) bleaching process, and this became the dominant bleaching technology. The complete substitution of chlorine by oxygen and chlorine dioxide is the key step in reducing the levels of organochlorines, measured as adsorbable organic halogens (AOX), in pulp mill effluents. The modern ECF bleaching sequences of today became established with oxygen (O), chlorine dioxide (D) and hydrogen peroxide (P) as the predominant oxidation agents. Some mills have also installed ozone (Z), peracetic acid (T) and xylanase (X) stages. Typically, a bleaching sequences using less than 4 kg chlorine dioxide/o.d. t pulp is referred to as ECF light and that notation is very popular. Pulp can also be totally bleached without chlorine chemicals. This kind of oxygen chemical bleaching is usually known by the abbreviation TCF – totally chlorine free. Bleaching chemicals used during TCF bleaching are oxygen-containing chemicals such as oxygen, peroxides and ozone. Like ECF, TCF never refers to any specific bleaching sequence, but includes Q(PO), (TZQ)(PO) and A(OP)Q(PO), where Q stands for treatment of the pulp with a chelating agent and A with acid. However, very few mills are today producing only TCF bleached kraft pulp. A bleaching stage can be defined as any treatment during the course of the bleaching, which takes place between two subsequent washings. (OO)(DQ)(PO) is thus a 3-stage sequence, where (OO) is the notation of an oxygen delignification process taking place in two subsequent reactors without intermediate washing.

When the bleaching is performed mainly with chlorine-containing chemicals, the active chlorine concept is used to quantify the oxidising power of the different substances. This means that all charges are recalculated as if only chlorine is used, **Table 3.1**. In ECF bleaching sequences, this concept still prevails.

Table 3.1 Active chlorine content and oxidising equivalent (OXE) of bleaching chemicals

Chemical (formula)	Transferred electrons (e^-/mole)	Equivalent weight (g/mole.e^-)	Active chlorine (kg /kg)	Oxidising equivalent (OXE/kg active chlorine)
Chlorine (Cl_2)	2	35.46	1	28.20
Hypochlorite (NaClO)	2	37.22	0.95	26.86
Chlorine dioxide (ClO_2)	5	13.49	2.63	74.12
Oxygen (O_2)	4	8.00	-	125
Ozone (O_3)	6	8.00	-	125
Hydrogen peroxide (H_2O_2)	2	17.01	-	58.29
Peracetic acid (CH_3COOOH)	2	38.00	-	26.32

The oxidising equivalent (OXE) concept suggested by Grundelius [1] is a valuable tool in comparing the efficiencies of all bleaching chemicals, where 1 OXE is equal to that quantity of substance which receives 1 mole of electrons during bleaching (**Table 3.1**). However, in reality this theoretical number should be used with caution as the same bleaching effect cannot always be expected for different chemicals even if the OXE should be the same. The treatment of a pulp with different bleaching chemicals having the same amount of OXE can lead to different brightness values [2].

3.2 Optical Properties of Pulp

The best known and mostly used theory for describing the optical properties of pulp and paper is the Kubelka–Munk theory. This theory was originally developed for paint films and it is the most commonly used and most widely accepted theory for estimating optical constants in pulp and paper [3–7]. The theory is based on the interrelationship between the light-scattering coefficient **s**, light absorption coefficient k and reflectance factor R_∞ – brightness (**Equation 3.1**):

$$R_\infty = 1 + \frac{k}{s} - \sqrt{\frac{k^2}{s^2} + 2.\frac{k}{s}} \tag{3.1}$$

where $100 * R_\infty$ is the brightness, in per cent, measured at 457 nm of an optically thick or opaque sample.

The scattering coefficient **s** depends on the fibre area and the degree of bonding between fibres, and the indices of refraction of the fibres. A sheet of stiff, tube-like fibres scatters light more than slender, collapsed fibres. Both beating the pulp and pressing a paper sheet result in a higher degree of bonding and a denser sheet with less light-scattering interfaces. The ability of a sheet to scatter light is not or slightly affected by the degree of cooking and bleaching of the pulp. The absorption coefficient k is influenced, to some extent, by the degree of bonding between the fibres and the indices of refraction, but to a much greater extent by changes in the cooking process, the degree of bleaching and brightness reversion. The light absorption coefficient is mainly dependent on the chromophoric groups in the pulp. During papermaking operations, it is primarily influenced only by the addition of dyes, clay, dirt and soluble impurities such as iron compounds [8]. It is not or slightly affected by beating or pressing. In the Kubelka–Munk theory, the additivity principle is used to calculate s and k for mixtures (**Equations 3.2** and **3.3**):

$$s = s_1.g_1 + s_2.g_2 + s_3.g_3 + \ldots \tag{3.2}$$

$$k = k_1.g_1 + k_2.g_2 + k_3.g_3 + \ldots \tag{3.3}$$

where g_1, g_2 and g_3 … are the proportions of components 1, 2 and 3.

The additive properties of **k** an **s** can be used for predicting the optical properties for papers with different fibres and fillers. The change in brightness through a bleaching step is not proportional to the reduction in chromophore concentration. The Kubelka–Munk expression (**Equation 3.1**) shows that the reflectance (brightness) is not a linear function of the chromophore concentration. At a high brightness level, the brightness is governed by only a small change in chromophore concentration, while at a low brightness level the same loss in brightness is connected with a significantly higher change in chromophore concentration. In accordance with the Kubelka–Munk theory, the following remission function (**Equation 3.4**) can be used for characterising a colour change in a particular pulp or paper, brought about by an arbitrary treatment that results in a change in the absorption coefficient, but does not affect the scattering coefficient.

$$\frac{k}{s} = \frac{(1 - R_\infty)^2}{2.R_\infty} \tag{3.4}$$

For example, Tongren [9], Giertz [10], Paulsson and co-workers [11], and Li and Ragauskas [12] have used this kind of expression for the study of certain changes in pulps after aging, in the form of the Post Colour number (*Pc*). The *Pc* number is the difference between *k*/*s* values before (*a*) and after (*b*) aging, as shown in **Equation 3.5**. The term Post Colour number is used when the values are determined at a single wavelength (usually = 457 nm):

$$Pc = [(k/s)_a - (k/s)_b].100 \tag{3.5}$$

The decrease in chromophore concentration through bleaching operations can be monitored by the relative change of *k*/*s* values $\alpha_{k/s}$ (**Equation 3.6**):

$$\alpha_{k/s} = \frac{k_a/s - k_b/s}{k_a/s} = \frac{k_a - k_b}{k_a} \tag{3.6}$$

where k_a and k_b are values of the absorption coefficient before (*a*) and after (*b*) bleaching, and **s** is the scattering coefficient, the value of which is assumed to be constant during bleaching. The nondimensional quantity $\alpha_{k/s}$ from **Equation 3.6**, can be used as a kinetic variable for bleaching processes [13–16].

3.3 Residual Lignin and Other Oxidisable Structures

The amount of lignin, the types of oxidisable structures and the metal content of the pulp entering the bleaching stages determine the consumption of bleaching agents. Froass and co-workers [17] showed that the residual lignin, compared with native lignin, is unreactive towards chlorine dioxide due to a low content of aryl ether linkages and prevalence of condensed type structures. Gustavsson [18] reports that the higher the content of β-aryl ether structures in the residual lignin after cooking, the easier it is to bleach in a QPQP sequence. However, it is difficult to establish any clear relationship between the chemical structures of the residual lignin and the bleachability of the pulp [18]. In unbleached kraft pulps, according to Lawoko [19], 85–90% of the residual lignin molecules are somewhere linked to carbohydrates, and mainly to glucomannan and xylan in network structures. The relatively faster delignification of the xylan-rich lignin-carbohydrates complex (LCC) could be explained by the hydrolysis of the predominant β-*O*-4 structures found in the native LCC fraction. Janson and Palenius [20, 21] observed that the lignin redeposited on the fibres at the end of the cook is much darker than the residual lignin left in the pulp. Transition metals can also be attached to lignin and extractives by complex formation. Dyer [22] also showed that pulp washing can have a significant impact on the metal content of the unbleached kraft pulp and that calcium is not likely to be a significant contributor to the chromophoric properties of pulp in this case, since the pulp is completely washed.

The kraft pulp contains not only residual lignin, but also other oxidisable structures. The most important of these are hexenuronic acids which are attached to the xylan, but other nonspecified structures are also present in the unbleached pulp. In both softwood and hardwood, the xylan chain is substituted with 4-*O*-methylglucuronic acid groups located in the C-2 position. Under alkaline conditions, the methoxyl group can be eliminated as methanol resulting in the formation of a hexenuronic acid (HexA) group. Since the HexA group is rather sTable in alkali, the xylan that remains in the pulp after the cook will contain an appreciable amount of such groups. These will influence the pulp properties and contribute to the bleachability of the pulp. The HexA consumes permanganate in the Kappa number analysis of pulps and thereby appears as ‘false lignin’ in the Kappa number measurement. Gellerstedt and Li [23] report that typically 3–6 Kappa number units of an unbleached hardwood pulp and 1–3 Kappa number units of an unbleached softwood pulp are due to HexA.

Vuorinen and co-workers [24], Buchert and co-workers [25], and Bergnor-Gidnert and co-workers [26] report that HexA reacts with several bleaching chemicals, such as ozone, chlorine dioxide or peracids and thus consumes these bleaching chemicals, whereas no significant degradation of HexA has been detected during the oxygen or peroxide stages. If it is present in a fully bleached pulp, HexA has been reported to decrease the brightness stability of the pulp [27–30]. Sevastyanova showed that HexA plays a dominant role in the brightness reversion in bleached kraft pulps [31]. HexA also has a strong affinity for transition metals according to Devenyns and co-workers, and Vuorinen and co-workers [24, 32, 33]. However, according to Laine and Stenius [34], a high surface charge of the pulp, partly provided by the presence of HexA, leads to better paper strength properties. However, Gustavsson [18] could not reveal any clear correlation between the HexA content in the bleached pulps and the yellowing tendency. Moreover, in the case of the D_{HT}(OP)D sequence, Gustavsson determined that a high HexA content, after cooking of the hardwood, has a positive effect in achieving a low bleaching chemical requirement. Furthermore, neither of the strategies to significantly reduce the HexA content in a kraft pulp by altering the cooking conditions is attractive for industrial implementation, since they would result in extensive losses in pulp yield, viscosity and strength [18].

In bleached pulp, resonance-stabilised quinones are the main chromophores surviving bleaching, along with chlorine dioxide and hydrogen peroxide [35–37]. The concentration of chromophores is generally extremely low, mostly in the ppm range, and for fully bleached pulps even lower, but their resonance stabilisation prevents destruction with alkaline peroxide.

Suess and Rosenau demonstrated [36, 38] that chromophores in/on cellulosics can generally be divided into two classes: primary and secondary chromophores. The primary chromophores are formed independently of the respective process chemicals, from monosaccharides, and are thus solely carbohydrate derived. Among the identified primary chromophores, hydroxybenzoquinone, hydroxyacetophenone and naphthoquinone structures are dominant. A second class of chromophores, named secondary chromophores, is formed with the involvement of the process chemicals during bleaching. They are thus process specific, in contrast to the primary chromophores which are based only on the hemicelluloses material.

3.4 Oxygen Delignification

The first commercial installation of an oxygen delignification high consistency (HC) system was started up in a South African mill in 1970 and the first medium consistency (MC) unit has been in operation since 1979. By 2010, the worldwide installed capacity increased dramatically to about 300,000 air dry metric tonnes per

day, representing more of the world's bleachable-grade pulp [39]. At first, the main driving forces for the installation of oxygen delignification in existing mills were environmental regulations and the complete abolition of chlorine during bleaching. The effluent from the oxygen stage could be recirculated as a countercurrent wash liquor, in the washing after the digester, and could be sent to the recovery boiler. The discharge of biochemical oxygen demand (BOD), chemical oxygen demand (COD) and AOX could thus be greatly reduced. The economic advantages of an oxygen delignification stage are the savings in operation costs through the use of lower amounts of other bleaching agents, as oxygen has a lower cost than all other oxidising agents. Oxygen delignification removes about 40–65% of the lignin remaining in the pulp after cooking for softwood and about 35–55% for hardwood. In general, it is difficult to reach a Kappa number below 10 whatever oxygen delignification process is adopted, largely because the Kappa number does not refer only to lignin, but also to structures like HexA which are not reactive towards oxygen. The other advantage of oxygen delignification is that it is more selective in terms of yield and viscosity preservation than low Kappa kraft cooking [40]. However, reductions in pulp viscosity are usually higher compared with chlorine dioxide treatment [41]. Moreover, because high pressures are involved in oxygen delignification, the cost of an oxygen system can require a significant capital investment [39].

3.4.1 Chemistry of Oxygen Delignification

Oxygen is an unusual molecule in that its normal configuration is the triplet state. Oxygen has a strong tendency to oxidise organic substances, under alkaline conditions, simultaneously resulting in its stepwise reduction to water by one electron transfer processes as shown in **Equation 3.7**. Depending upon the pH, this reaction yields different transients, including the superoxide anion radical ($O_2^{\bullet}$), which can combine with a hydrogen ion to form the hydroperoxy radicals ($HO_2^{\bullet}$), hydroperoxide anions (HO_2^-), hydrogen peroxide (H_2O_2) and hydroxyl radicals ($HO^{\bullet}$) [41].

$$O_2 + e^- \rightarrow O_2^{-} + H^+ \rightarrow HO_2^{\cdot} + e^- \rightarrow HO_2^- + H^+ \rightarrow H_2O_2 + e^- \rightarrow HO^{\cdot} + e^- \rightarrow OH^- + e^- \rightarrow OH^- + H^+ \rightarrow H_2O \quad (3.7)$$

Free phenolic hydroxyl groups play a key role during lignin reactions [42]. When ionised by the addition of alkali, they furnish the high electron density that is needed to initiate the reaction with the relatively weakly oxidising molecular oxygen. This, together with the weakly acidic nature of the phenolic hydroxyl groups, explains why strongly alkaline conditions are needed to achieve appreciable delignification rates.

The initial step is the conversion of the ionised phenolic group to a phenoxy radical through the loss of a single electron to a suitable acceptor; this may be molecular oxygen or one of the many other radical species present in the system [43]. Once the radical is produced on the phenolic hydroxyl oxygen, resonance structures may shift the radical to the *ortho* and *para* positions relative to the carbon containing the hydroxyl group. These radicals have now become new sites available for the electrophilic attack of an oxygen molecule, which results in bridging, ring opening and then the formation of carboxylic acids according to the scheme shown in **Figure 3.1**:

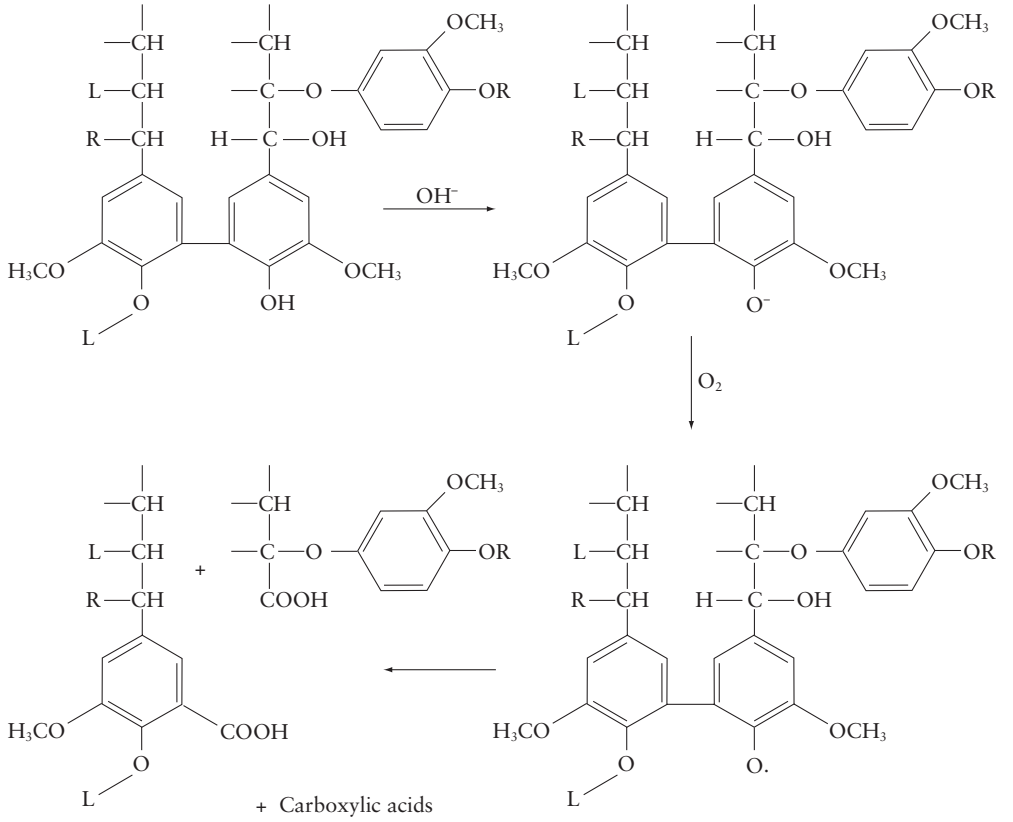

Figure 3.1 Typical reaction of lignin with oxygen in an alkaline media

Eventually, when the lignin undergoes a few of these steps, its aromatic structure breaks down and the number of hydrophilic oxidised groups increases; so the lignin

fragments become water-soluble and can be removed from the pulp. Also, when the initial resonance structure moves to a carbon of an alkene side chain, oxygen will attack the radical, bridge to the adjacent carbon and cleave the carbon-carbon linkage, leaving two carbonyl groups and eliminating part of the side chain [43]. In the oxygen delignification process, carbohydrates are attacked to a greater extent than in the chlorination and alkali extraction processes. Random chain cleavage and endwise secondary peeling reactions are two types of carbohydrate degradation reactions that occur during oxygen delignification. Random chain cleavage can occur at any point along the main chain to lower the degree of polymerisation of cellulose. The viscosity loss is due to an oxidation of one or more of the hydroxyl groups located along the cellulose chain. Thereby, a carbonyl group is created and, due to the alkaline conditions, an elimination reaction occurs resulting in a cleavage of the chain into two shorter units according to the scheme (**Figure 3.2**):

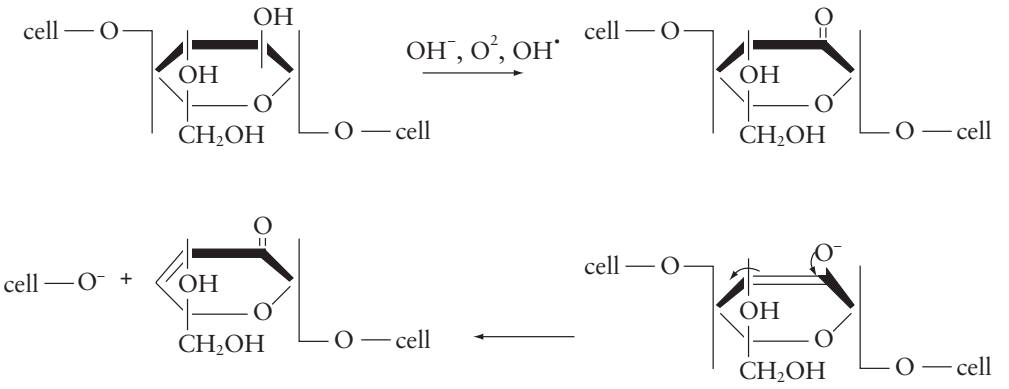

Figure 3.2 Cellulose chain cleavage in the conditions of oxygen delignification

The reaction which causes yield loss in an alkaline media, the peeling reaction, usually has less importance in oxygen delignification than random chain cleavage. This occurs for two reasons. First, pulps (because of their long previous exposure to strongly alkaline conditions in the digester) contain very few end units that have not been converted to the sTable form by stopping reactions. The secondary reason is that oxygen itself converts reducing end groups to the stable oxidised form. However, peeling can become a problem if random chain cleavage is excessive because every chain breakage creates two new chain ends, one of which is a reducing end group. Antonsson and co-workers [44] report that the prehistory of the pulps is a very

important factor in determining the response to oxygen delignification. Sulfite pulps show the greatest yield loss during oxygen delignification, compared with those of kraft and prehydrolysis kraft pulps. It is also shown that the degree of delignification is not due to different amounts of hexenuronic acid. It is likely that lignin-carbohydrate complexes (LCC) play a very important role in limiting the reaction rate of oxygen delignification. LCC is probably native and not formed during cooking [44].

3.4.2 Process Description and Variables

The typical temperature in the technical oxygen delignification process is 90–100 °C, the charge of alkali is 15–25 kg/t o.d. pulp, final pH 10–11, the pressure at the reactor top is 0.4–0.6 MPa, whereas the oxygen charge is in the range of 15–25 kg/t o.d. The process is normally carried out at medium consistency in a single- or two-stage system with a retention time of 40–80 min.

Oxygen delignification is a heterogeneous process involving three phases: solid (fibres), liquid (aqueous alkali solution) and gas (oxygen). As a first step, oxygen dissolves in the aqueous phase and is then transported through the liquid to the pulp fibre interface. The dissolved oxygen subsequently diffuses into the fibre wall and then reacts with the wood components. Agarwal and co-workers [45] determined that the intrafibre mass transfer effect does not influence the delignification rate. Hsu and Hsieh [46] also report that the mass transfer resistance of oxygen in the gas phase is insignificant in comparison with the liquid phase resistance due to the low solubility of oxygen in the liquid phase. Therefore, in order to compensate for the low solubility of oxygen in water, a high oxygen pressure and fluidisation of the pulp suspension are regarded as a prerequisite for oxygen delignification. The effect of pressure on the oxygen delignification of hardwood kraft pulp was studied by Nenkova and co-workers [47]. It has been established that an increase in oxygen pressure from 0.3 to 0.6 MPa leads to a Kappa number reduction of 0.5 units, a viscosity loss of about 30 dm^3/kg, and a brightness increase of nearly 2% without changing the pulp strength (**Table 3.2**). This indicates that the higher oxygen pressure increases the bleaching processes of hardwood pulp only slightly, while the results obtained from Heiningen and Ji [48], for softwood pulp, show a decrease of the Kappa number by more than 2 units without effect on the selectivity. A higher pressure oxygen delignification would certainly be beneficial for the process, but in practice it is not economical due to the higher capital and energy cost.

The results in **Table 3.2,** obtained by varying the sodium hydroxide charge, show that a higher charge leads to more cellulose degradation (a viscosity loss of almost 100 dm^3/kg) as well as to a pulp strength loss, besides a Kappa reduction of 0.7 units [47]. Therefore, a high charge of sodium hydroxide reduces the oxygen delignification

selectivity and leads to a lower pulp strength at the same degree of delignification. These results are consistent with previous reports by Yang and co-workers [49] and that obtained for softwood pulp [48]. In order to increase delignification without dramatically decreasing the selectivity, Heiningen and Ji [48] suggest modification to the oxygen system design so that the alkali concentration and charge should be decoupled, similar to modern cooking systems.

Table 3.2 Effect of oxygen delignification conditions on pulp properties at a temperature of 102 °C and 60 min reaction time

Oxygen delignification conditions			Pulp properties				
NaOH charge %	Pulp consistency, %	Oxygen pressure, MPa	Kappa number	Viscosity, dm^3/kg	Brightness, ISO%	Breaking length, m	Tear index, $mN.m^2/g$
2.5	10	0.3	11.0	816	47.2	8,500	7.50
		0.4	10.9	809	47.6	8,510	7.52
		0.5	10.7	799	48.4	8,520	7.46
		0.6	10.5	787	49.5	8,520	7.45
2.0	10	0.6	10.7	818	48.7	8,700	7.80
2.5			10.5	787	49.5	8,530	7.50
3.0			10.3	755	50.7	8,400	7.70
3.5			10.0	715	52.1	8,340	7.75
2.5	8.0	0.6	10.5	–	49.3	–	–
	10.0		10.5	787	49.5	8,530	7.50
	12.0		10.7	—	48.7	—	—
	14.0		10.7	816	48.7	8,500	7.50

It has been found that the consistency of oxygen delignification has no significant effect on the Kappa number reduction or brightness improvement (**Table 3.2**) [47]. A medium consistency oxygen system operates between 11% and 14% consistency. At a consistency below 10 %, channelling may occur in the reactor, while at about 14%, fluidisation of the pulp slurry becomes difficult.

The carry-over of dissolved solids has little or no impact on the initial rapid phase of oxygen delignification, however, it will increase the overall oxygen and alkali requirements due to their preferred consumption by the dissolved organic and inorganic compounds [50]. In addition, organic unoxidised solids may negatively affect the pulp viscosity. It is theoretically possible to estimate the requirement of

molecular oxygen to be close to 0.3 kg/t per oxygen delignified Kappa number unit of softwood kraft pulp, while mill measurements showed that a consumption of 1 kg O_2/t per oxygen delignified Kappa number unit can be applied, as it includes the molecular oxygen normally required for the oxidation of unoxidised carry-over with the pulp [51].

The effects of oxygen delignification temperature and reaction time on the pulp properties were studied by Nenkova and co-workers [47]. **Figure 3.3** shows that a prolonged treatment and higher temperature leads to a higher lignin removal, as expected. The effect of increasing the temperature from 95 °C to 110 °C is the same as that of doubling the reaction time. When the temperature is increased from 85 °C to 110 °C, the brightness, according to the International Organization for Standardization (ISO), improves by 9% after 60 min. This is expected as a decrease in Kappa number normally leads to an increase in the brightness of the pulp.

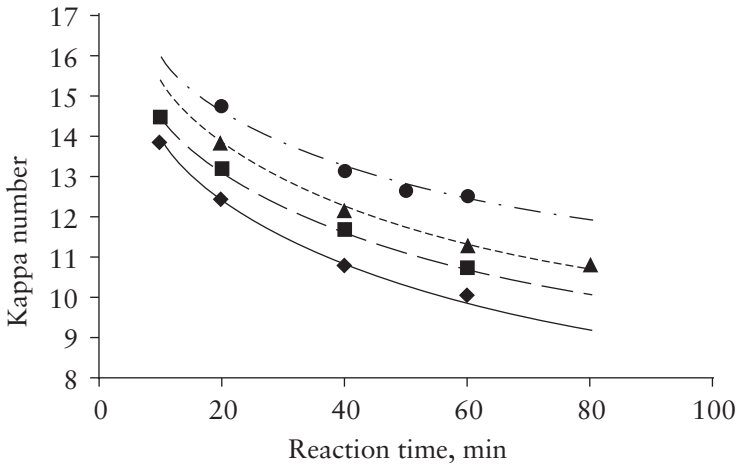

Figure 3.3 Kinetic data of Kappa number (● 85 °C; ▲ 95 °C; ■ 102 °C; and ¨ 110 °C)

The evolution of the pulp viscosity is shown in **Figure 3.4.** It can be seen that increasing the temperature and reaction time leads to an increased viscosity loss of the bleached pulp. The behaviour of the pulp viscosity in **Figure 3.4** is very similar to that of the Kappa number in **Figure 3.3**. The obtained Kappa number – viscosity relationship (**Figure 3.5**) shows that the selectivity (delignification – cellulose degradation) is not

a function of temperature. However, the selectivity decreases upon increasing the alkali charge, as can be seen by the extra viscosity drop at the same Kappa number.

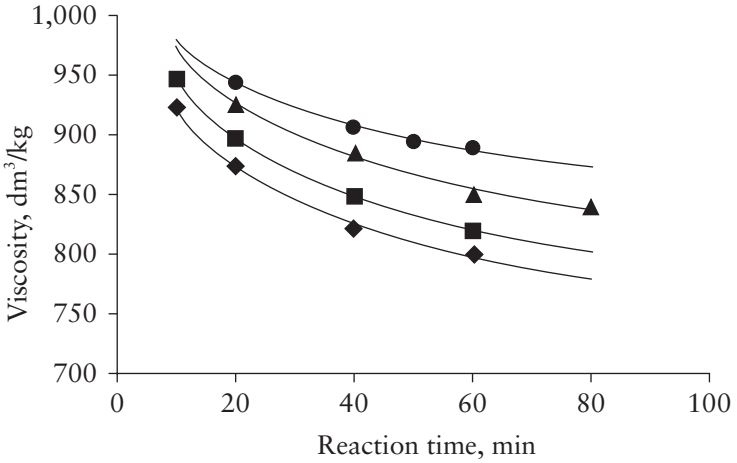

Figure 3.4 Kinetic curves of viscosity (● 85 °C; ▲ 95 °C; ■ 102 °C; and ♦ 110 °C)

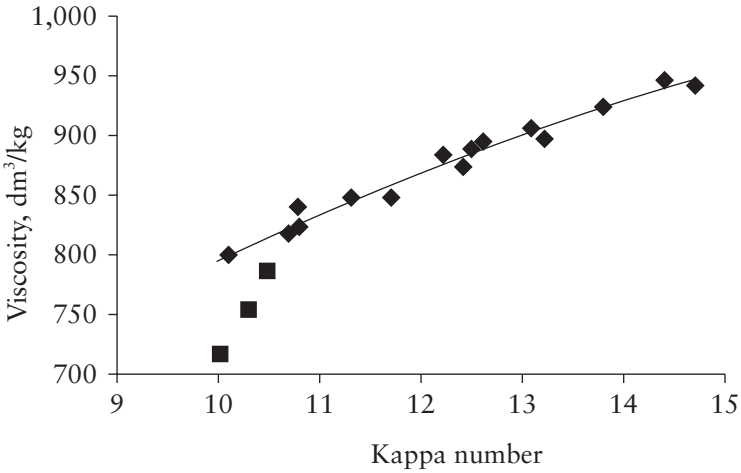

Figure 3.5 Correlation between Kappa number and viscosity (■ 2.5–3.5% NaOH and ♦ 2% NaOH)

The pulp strength properties do not change considerably over the studied temperature – time interval. This result indicates that an increase in temperature can considerably accelerate the bleaching process without affecting the pulp strength properties. Therefore, it is most effective to increase the degree of oxygen delignification by optimisation of the temperature – time profile [47]. Heiningen and Ji [48] report that for softwood oxygen delignification, the selectivity does not change much from 80 °C to 100 °C, while it decreases by 30% to 40% when the temperature is raised to 110–115 °C. The lower selectivity and the higher capital cost (due to higher pressures) of the latter explains why the industry generally does not operate above 100 °C.

3.4.3 Kinetics of Oxygen Delignification

In an effort to optimise the efficiency and selectivity of oxygen delignification, many kinetic studies have been documented. Most kinetic models for oxygen delignification are empirical, in which the rate of delignification is considered to be proportional to the lignin content expressed as the Kappa number (K) and hydroxide ion concentration [OH^-], and oxygen pressure (p_{O2}) expressed in the form of a power law (**Equation 3.8**):

$$-\frac{dk}{dt} = A.e^{-E/RT}.[OH^-]^m.P_{O_2}^n.K^q \tag{3.8}$$

The constants m, n and q are determined empirically from experimental data, while the temperature dependence is given by the Arrhenius equation, where E is the activation energy, A is the preexponential factor, R is the gas constant and T is the absolute temperature. Based on **Equation 3.8,** the rate of oxygen delignification has been described by using one and two region model Equations by Olm and Teder [52], Hsu and Hsieh [53, 54], Iribarne and Schroeder [55], and Agarwal and co-workers [45]. The two different reaction periods, a rapid initial step followed by a long period during which the change in Kappa number is at a very slow rate, are assumed to be related to the various lignin linkages comprising its structure. The most widely accepted kinetic model of the two regions is that of Olm and Teder [52], who assumed pseudo first-order kinetic Equations in terms of the Kappa number. All those studies have an empirical character and that is why they cannot describe the complex heterogeneous oxygen delignification process. Similar empirical power law models have also been proposed for cellulose degradation. The other category of kinetic models is based on the topochemical concept that the delignification rate depends on the number of reactive sites, formed at the beginning of the process, and the growth rate of the transformed lignin from these reactive sites. Valchev and

Christensen [56], and Nguyen and Liang [57] successfully verified the applicability of the topochemical Equation of Avrami–Erofeev in the kinetics of oxygen delignification. The next development of the topochemical delignification model is the applicability of the modified form of the topochemical kinetic Equation of Praut–Tompkins (**Equation 3.9**) [47, 58]. In this kinetic model, the rate of progress of the reaction is determined by the size of the interface between the reacted and unreacted solid. According to this model, the rate of delignification **v** is a function of the amount of oxidised lignin that subsequently becomes soluble, α_k, and of the amount of residual undissolved lignin at any time, $(1 - \alpha_k)$:

$$v = \frac{d\alpha}{dt} = k^1.\chi.\alpha_\kappa^{(\chi-1)/\chi}.(1-\alpha_\kappa)^{(\chi+1)/\chi} \tag{3.9}$$

where the degree of delignification $\alpha_k = (Kappa_{in} - Kappa)/ Kappa_{in}$ and k^1 is the rate constant. The power factors $(\chi - 1)/ \chi$ and $(\chi + 1)/ \chi$ determine the relative contributions by the dissolved and undissolved parts of the lignin, respectively, to the rate of delignification. Based on this topochemical mechanism, the rate of delignification depends on the size and the state of the changing reaction interface. The integrated form of **Equation 3.9** used for the description of the experimental data is:

$$\frac{\alpha_\kappa}{1-\alpha_\kappa} = (k_1.t)^\chi \tag{3.10}$$

where $k_1 = k^1/\chi$ is an apparent rate constant and χ is a power factor.

After rearrangement of **Equation 3.10** and with the inclusion of the Arrhenius temperature dependency of the apparent rate constant, **Equation 3.11** is obtained:

$$Kappa = Kappa_{in}\left[1 - \left[1 + \left(5 \times 10^4.e^{(-5{,}833/T)}.t\right)^{-0.59}\right]^{-1}\right] \tag{3.11}$$

where t is the reaction time in min, and *T* is the temperature in K. The obtained ratio of the activation energy of the process to the universal gas constant, E/R, is 5,833 K. The activation energy E is 48.2 kJ/mol and depends only on the nature of the unbleached pulp. In a mill with relatively constant pulping conditions and wood supply, the

activation energy is practically constant. The same is true for the coefficient χ in the Prout–Tompkins equation, which is 0.59. The preexponential factor, A, includes the effect of all steric factors on the process (charge of reagents, their mixing, the pressure in the system and so on) and was found to be $5.10^4\,min^{-1}$. **Equation 3.11** can be used for process control of the Kappa number. Inclusion of the effect of oxygen pressure and alkali in **Equation 3.11** leads to **Equation 3.12**:

$$Kappa = Kappa_{in}\left[1-\left[1+\left(2.16\times 10^4 . e^{(0.175C+0.8P-5.833/T)} . t\right)^{-0.59}\right]^{-1}\right] \qquad (3.12)$$

where t is the time in min, T is the temperature in K, C is the alkali charge in % and P is the oxygen pressure in MPa.

Equation 3.12 enables one to obtain the Kappa number at any moment during the oxygen delignification as a function of temperature, pressure and alkali charge. This dependence of Kappa number may be used for simulation and control of the oxygen delignification stage.

The variation in pulp viscosity with time at different temperatures has been studied by Valchev and co-workers [58]. The dependence acquires a linear character at the 20^{th} minute from the beginning of oxygen delignification, irrespective of temperature. This shows that the kinetics of viscosity change, which provides information on carbohydrate destruction processes, is described by a zero-order Equation after the first 20 min. The zero order observed shows that the rate of destruction stays unchanged and equals the rate constant. It does not depend on the quantity of carbohydrates undergoing destruction.

3.4.4 Process Technology and Equipment

In a medium consistency one-stage oxygen delignification process, the pulp suspension is pumped to a reactor as presented in **Figure 3.6** [59]. Alkali is added to the pulp suspension prior to the pump. Oxygen and steam are added and thoroughly mixed into the pulp suspension in a mixer positioned immediately after the pump. In the alkaline environment, the oxygen forms a reasonably stable gas dispersion in the pulp. The mixture enters the reactor and passes upwards in a plug flow while the oxygen is consumed in reactions with the lignin in the pulp. The pulp leaves the reactor and enters a blow tank (where off-gases are separated from the pulp suspension), which also serves as a standpipe for a second pump, which pumps the pulp suspension further to washing and bleaching stages.

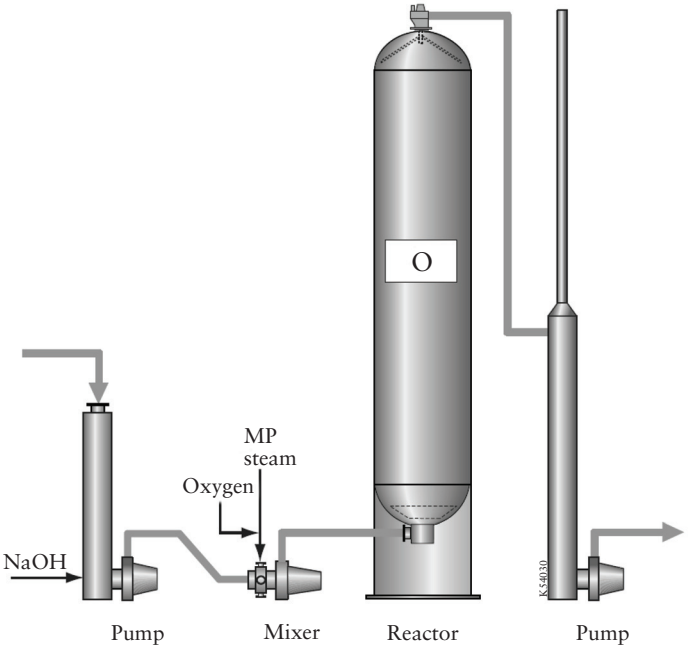

Figure 3.6 One-stage oxygen delignification process

The introduction of two-stage oxygen delignification has further increased the effectiveness of the process (**Figure 3.7**) [59]. Metso introduced the two-stage OxyTrac process [60, 61], with an oxygen pressure and temperature of 0.8–1 MPa and 80–85 °C, respectively, during the first stage of the 20–30 min retention time. During the second stage, the oxygen pressure is 0.3–0.5 MPa, the temperature is 90–100 °C and the reaction time is 60–80 min. According to GLV [59], the optimal conditions for oxygen delignification during the first stage are a lower oxygen pressure, 0.3–0.35 MPa, a temperature of 80–85 °C and a reaction time of only 5 min. The conclusion is based on the kinetics of oxygen delignification reported by Olm and Teder [52]. A high oxygen pressure of 0.6–0.8 MPa and a high temperature of 100 °C or higher during the second stage are recommended. However today, both stages are run at the highest possible pressure to boost Kappa reduction [62]. This system is applied in the industry under the name DUALOX, and its effectiveness is analogous to that of the OxyTrac process (**Figure 3.8**) [59].

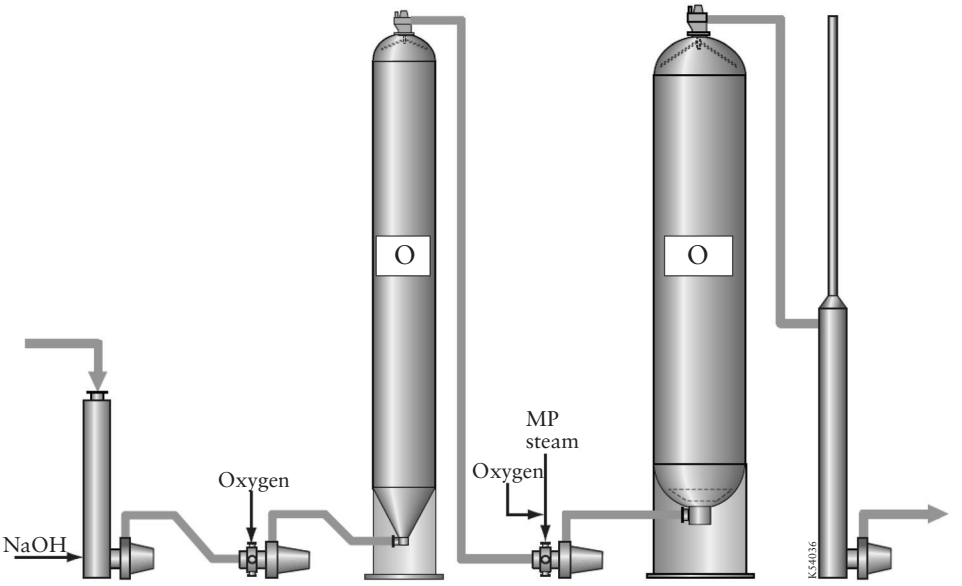

Figure 3.7 Two-stage oxygen delignification process

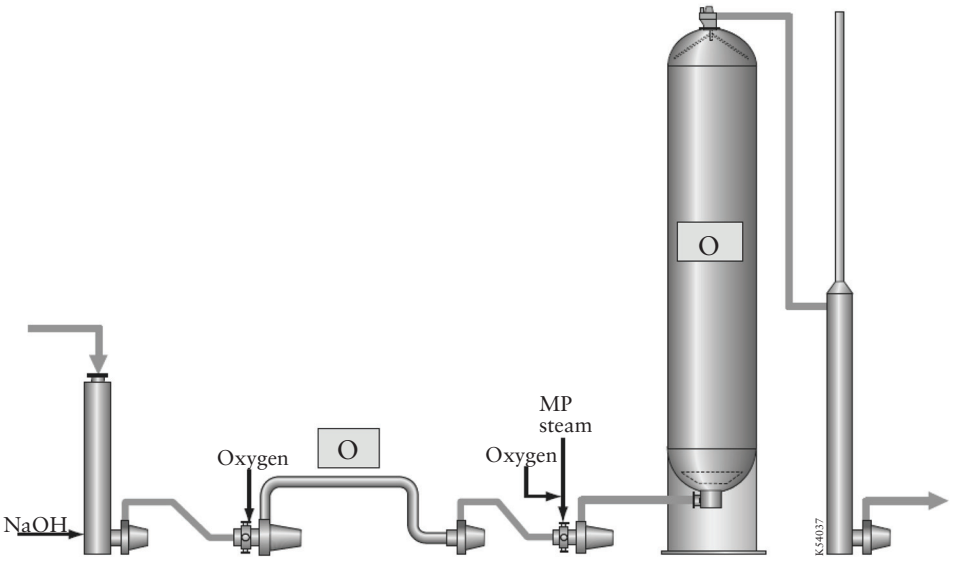

Figure 3.8 DUALOX oxygen delignification process

3.5 Chlorine Dioxide Bleaching

3.5.1 Reactions and Factors in Chlorine Dioxide Bleaching

Since turning from chlorine to ECF bleaching technologies, chlorine dioxide has become the main agent for kraft pulp bleaching. The first chlorine dioxide bleaching stage D_0 and the subsequent extraction, with the addition of oxygen and peroxide, are dominant delignification stages. Chlorine dioxide treatments, to increase the brightness, are also favourable for its stabilisation and are normally final bleaching stages D_1 and D_2. Chlorine dioxide is an efficient delignification agent with high selectivity toward lignin, thus resulting in a high carbohydrate yield in the pulp [63]. Generally, chlorine dioxide reacts with phenolic lignin end groups either by oxidative ring opening, which affords muconic acid structures, or by demethylation, which affords quinone structures [64–65]. The result is a modified lignin with partly oxidised aromatic rings. Subsequently, the modified lignin is solubilised and removed in the extraction stage. The entire oxidising power of chlorine dioxide is utilised in the acid bleach, the reduction proceeding to chlorite ions according to reaction **Equation 3.13**:

$$ClO_2 + 4H^+ + 5e^- \rightarrow Cl^- + 2H_2O \qquad (3.13)$$

There are two different concepts of the performance of the post oxygen D_0 stage. The conventional operating conditions are a temperature of around 60 °C and reaction time of 30–60 minutes, which correspond to the complete consumption of ClO_2 (66, 67). However, the hot chlorine dioxide (D_{HT}) concept involved in the process of bleaching hardwood kraft pulp, supported by Ragnar [66], Lachenal and co-workers [68], is carried out at a temperature of about 90–95 °C and a prolonged reaction time despite the consumption of the ClO_2. Under these conditions, the hexenuronic acids are hydrolysed. The reaction time of chlorine dioxide with pulp lignin is faster than with HexA. Hence, the majority of chlorine dioxide is consumed by the lignin at the beginning of the reaction, while the HexA are eliminated later through pulp acid hydrolysis at a high temperature and long exposure [69]. As a result, bleaching of the pulp is improved, the bleaching agents are saved, and at the same time the heavy metals are removed to a maximum extent without using chelating agents. Although the process may seem like a pure combination of D_0 and A, the results obtained during the D_{HT} stage show many synergies with regards to AOX discharge, chlorine dioxide consumption and yellowing pulp properties. The final pH at the D_0 stage is very important in the bleaching processes during the next stages and for the

final pulp properties. It has been proved by Dahl and co-workers [70], and Valchev and co-workers [71] that the highest intermediate brightness is achieved at pH 4, regardless of the other conditions of the D_0 stage or the type of pulp. However, the highest final brightness is obtained around or below pH 3, which can be explained by the best delignification rate, the better removal of the heavy metals from the pulp and good strength properties of the bleached pulp [70, 71].

The effect of pH on the bleaching efficiency in the final D_1 stage, according to Valchev and co-workers [72], is shown in **Figure 3.9**. The obtained results illustrate that the highest pulp brightness is achieved at a current charge of ClO_2 without preliminary acidifying, i.e., final pH 6.0–7.0, but this required adjusting the final pH for individual samples. However, the higher pH values in the D_1 and D_2 stages cause a loss of pulp viscosity [70, 72]. According to Sevastyanova and co-workers [73], the hypochlorite formation seems to be responsible for the viscosity drop at a higher final pH. At the same time the HexA groups, which are usually degraded during the chlorine dioxide treatment, are present in significantly higher amounts in pulps bleached at higher pH values [73].

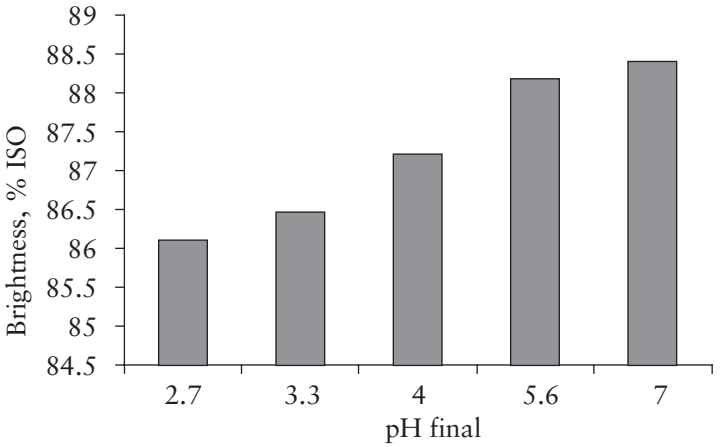

Figure 3.9 Effect of final pH at the D_1 stage on pulp brightness

The real effect of HexA removal can be reported after the D_1 stage, in which ClO_2 reacts very slowly with the residual lignin. The parallel reactions of ClO_2 with the products of HexA hydrolysis impair the bleaching process. Valchev and co-workers [71] presume that the decrease in the chlorine dioxide charge and pH increase

in the D_1 stage, can reduce the negative effects of the HexA content in the pulp. In this way, the competitive harmful reactions are delayed and chlorine dioxide damage decreases. The lower ClO_2 charge in the D_1 stage reduces the efficiency of the D_{HT} stage to only 0.4% ISO brightness (**Figure 3.10**). In the suggested optimum distribution of chlorine dioxide in the hardwood pulp bleaching sequence, the D_0 stage is favourably recommended to be carried out at a lower temperature, for a short time. According to Valchev and co-workers [71] in that case, the positive effect of the D_{HT} stage is negligible, and cannot compensate for the increased power consumption and decrease in the pulp strength properties.

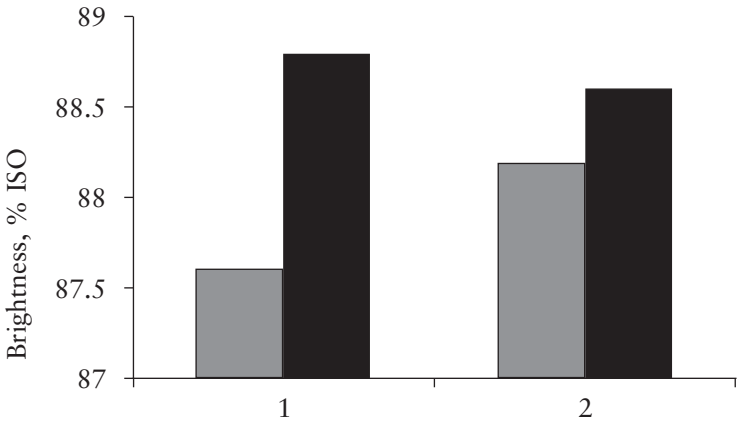

Figure 3.10 The effect of chlorine dioxide distribution on brightness (■–D_0; ■–$D_{HT;}$ (1) = 1.8% D_0+2% D_1 and (2) = 2.5% D_0+0.5% D_1)

3.5.2 Kinetic Dependencies of Chlorine Dioxide Bleaching

The obtained temperature-time dependencies of brightness during the D_0 stage [72] are represented in **Figure 3.11**. The kinetic curves are characterised by a maximum brightness at the shorter reaction times. After the maximum, the brightness decreases and is more obvious at higher temperatures. The observed reduction of brightness can be explained by structural changes and the formation of chromophoric groups in the residual lignin, as this process is better expressed at higher temperatures.

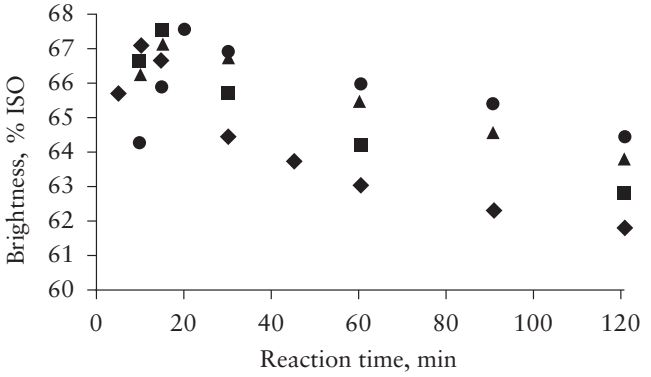

Figure 3.11 Kinetic data of pulp brightness at the D_0 stage (♦ 90 °C; ■ 80 °C; ▲ 70 °C; and ● 60 °C)

It can be seen from **Figure 3.12** that the reaction time necessary for the total consumption of the bleaching agent is identical to the time necessary for achieving the maximal values of brightness. This means that the obtained Kappa number reduction after prolonged bleaching is probably due to the acid hydrolysis of the hexenuronic acids, but not to the lignin extraction [71, 72]. The kinetic curves of the Kappa number are represented in **Figure 3.13**. It can be seen that the delignification is very fast in the first 5 min, when the Kappa number falls under 6.0; after that, the process slows down. At a temperature of 90 °C and for a reaction time of 120 min, the Kappa number is 4. For the same reaction time at 60 °C, the Kappa number stays over 5.

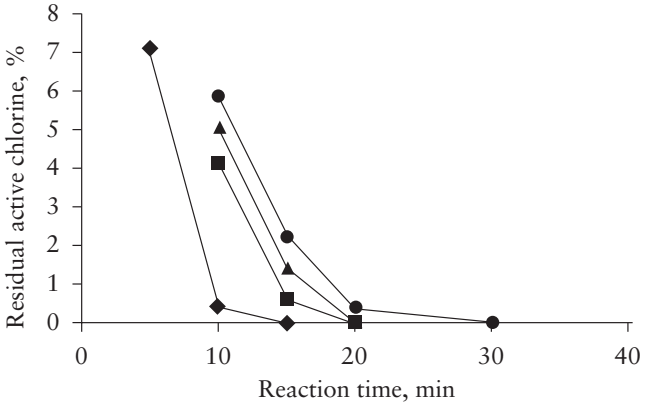

Figure 3.12 Residual active chlorine in the D_0 stage. (♦ 90 °C; ■ 80 °C; ▲ 70 °C; and ● 60 °C)

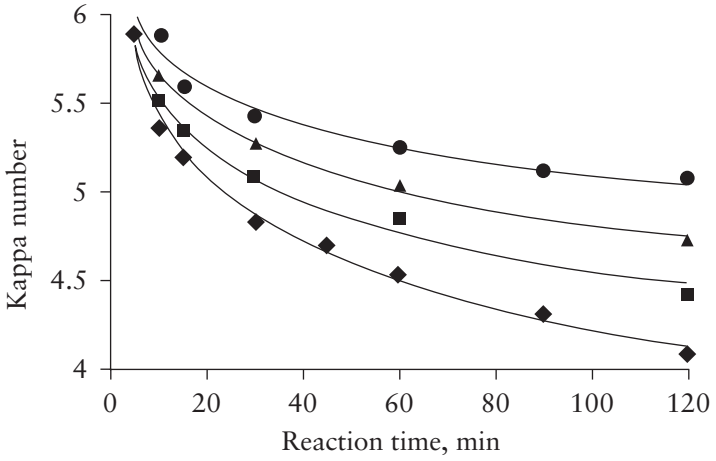

Figure 3.13 Kinetic curves of Kappa in the D_0 stage. (♦ 90 °C; ■ 80 °C; ▲ 70 °C; and ● 60 °C)

The kinetics of HexA hydrolysis was studied by Valchev and Simeonova [15] in order to find the optimal conditions and mechanism of pulp bleaching, with chlorine dioxide, during the first stage – D_0. The relative change of HexA α_H is used as a kinetic variable. Various kinetic Equations have been tested to describe the kinetics of the HexA hydrolysis and the best description has been achieved by the power kinetic equation, which is applied to surface chemical interactions taking place on the exponential uniform surfaces (**Equation 3.14**):

$$v = \frac{d\alpha_H}{dt} = k_1.\alpha_H^{-\frac{1-\chi}{\chi}} \tag{3.14}$$

where k_1 is the apparent rate constant and χ is a coefficient of inhomogeneity.

The process of a HexA hydrolysis, run without changing the activation energy, is shown by obtained kinetic results. The process slowing down is due to decreasing of the preexponential factor, probably because of the exhaustion of reaction groups and difficult accessibility to them. Application of the power kinetic law, at the HexA hydrolysis in pulp bleaching with chlorine dioxide in the D_0 stage, shows that this process is a surface chemical interaction unlike the topochemical processes. One of the reasons can be a low molecular weight of the xylan basic chain and HexA distribution in the side chains. The presented kinetic model, according to Valchev and

Simeonova [15], is common during the whole time interval, including the fast initial phase of the processes. It has been found by Valchev and Simeonova [15] that the Praut–Tompkins topochemical kinetic model (**Equation 3.10**) successfully describes the bleaching process with respect to the light absorption coefficient during the D_1 stage. Application of a modified form of the Praut–Tompkins kinetic equation, on the basis of the kinetic variable $\alpha_{k/s}$ (**Equation 3.6**), can be explained by the distribution and the different accessibility of the chromophore groups during the process. A simplified Equation for the determination of the running absorption coefficient has been achieved, which may be used for control of the bleaching process (**Equation 3.15**):

$$k = k_0\{1 - [1 + [(20 \times 10^6 . e^{-6{,}531/T}).t]^{-0.15}]^{-1}\} \tag{3.15}$$

where k_0 and k are the initial and current absorption coefficient, χ = 0.15, preexponential factor A = 20.10^6 min^{-1} and E/R = 6,531 K.

3.5.3 Technology of Chlorine Dioxide Bleaching

During the D_0 stage, the pulp suspension is pumped to a reactor. Optionally, sulfuric acid is normally added to the pulp suspension prior to the pump. Chlorine dioxide is added and thoroughly mixed into the pulp suspension in a mixer positioned immediately after the pump. The mixture enters the reactor and passes upward in a plug flow, while the chlorine dioxide is consumed in reactions with the lignin in the pulp. Chlorine dioxide bleaching is sometimes carried out in upflow-downflow reactor combinations, where a smaller upflow section is used. This reactor has some operational advantages as it can absorb variations in production rates. The pulp leaves the reactor and enters a second pump, which pumps the pulp suspension further to the washing and bleaching stages. The typical retention time for the D_0 stage is 20–60 min at a temperature of 50–70 °C, while for the D_1 and D_2 stages, the retention time is 1–3 h at a temperature up to 90 °C. The normal retention time for the hot chlorine dioxide process, D_{HT}, is 2 h. The temperature is increased to about 90 °C by the addition of steam in a steam mixer, placed before the chlorine dioxide mixer. The preferred material of construction for the equipment in the chlorine dioxide stage is titanium.

3.5.4 Reactions in the Extraction Stages

The basic idea of the extraction stage E is to extract the oxidised lignin which has been formed in the chlorine dioxide bleaching stage, since the solubility of lignin is low under acidic conditions. The performance of the extraction stage can be somewhat boosted by the addition of a small amount of oxygen – the EO stage, a small amount of hydrogen peroxide – the EP stage or both oxygen and hydrogen peroxide – the EOP stage. The major reactions encountered in an E stage are the neutralisation of carboxyl groups, thereby strongly increasing the water solubility of the oxidised lignin, and the elimination of organically bound chlorine and the formation of a chloride ion. Oxygen and H_2O_2 in the E stages will always either improve the brightnesses of pulp or make it possible to reach the same brightness with less chemicals. Kinetics of the extraction stages, which have been studied by Valchev and Simeonova [15] on the basis of the degree of delignification α_k, are better described by the exponential kinetic Equation (**Equation 3.16**). This Equation is applied to processes which take place on uniformly heterogeneous surfaces:

$$v = \frac{d\alpha_k}{dt} = v_0 . e^{-a.\alpha_k} \tag{3.16}$$

where α_k is the degree of delignification, v_0 is an initial rate and α is a coefficient connected with the inhomogeneity of the surface.

The obtained simplified kinetic expression (**Equation 3.17**) could be used for the fast and precise delignification control:

$$\alpha_k = \frac{1}{a} . \ln(a_k . A_0) + \frac{1}{a} . \left(\ln t - \frac{E_0}{RT} \right) \tag{3.17}$$

The extraction stages are either of the upflow or upflow-downflow type. Typical data for an upflow-downflow (EOP) stage are: temperature 80–90 °C, retention time up to 30 min, pressure 0.3–0.5 Mpa in the top of the upflow tower, and a 60–120 min retention time at atmospheric pressure in the downflow tower, the charge of sodium hydroxide is normally 10–25 kg/ton of pulp.

3.6 Peroxide Bleaching

3.6.1 Chelating Stages

Due to environmental pressure, there is increasing use of hydrogen peroxide as a total or partial substitute for chlorine-based bleaching agents with ECF and TCF sequences. However, to achieve satisfactory brightness all types of transition metal ions have to be removed from the pulp. Transition metals decompose hydrogen peroxide to oxygen and water *via* the intermediate formation of hydroxyl and superoxide radicals. The amount of transition metals in the pulp depends on the wood species and the soil where the wood was grown. Normally, manganese and iron ions dominate, while other metals like copper and cobalt are present only in trace quantities.

Strong acidic stages or treatment with chelants are the standard procedures for successful peroxide bleaching. During standard ECF bleaching, chelants are not required. Transition metals are sufficiently removed by the acidic conditions of the D_0 stage. The pulp cleaning is effective at a final pH <3.0 and the process improves upon an increase in temperature [71]. The highest final brightness can be achieved by the implementation of a preliminary acid treatment of the stage A pulp, with subsequent washing [71]. The strongly acidic conditions during stage A have the disadvantage of removing not only metals like manganese but also magnesium, which provides viscosity protection. Magnesium is therefore normally charged into the pulp to improve pulp quality [74]. During TCF bleaching, the removal of transition metal ions is more important because hydrogen peroxide is applied at much higher charges. The concentration of manganese in the pulp, proceeding into a pressurised PO stage, should not exceed 2 ppm according to Andtbacka [74]. During TCF bleaching, metal removal at the mill scale is typically carried out at the Q stage with chelants at a moderate pH, a temperature between 70 °C and 90 °C and a retention time of about 1 h.

3.6.2 Reactions and Factors in Hydrogen Peroxide Bleaching

Peroxide bleaching is activated with alkali. At higher pH, the equilibrium of **Equation 3.18**, is pushed to right side to the formation of the reactive perhydroxyl anion:

$$H_2O_2 + OH^- \leftrightarrow OOH^- + H_2O \qquad (3.18)$$

The perhydroxyl anion formed according to **Equation 3.18** is primarily responsible for the bleaching effect in pulp and leads to an increase in brightness [75]. Therefore, the bleaching process will certainly be accelerated with higher charges of alkali. On the other hand at higher alkalinity, more peroxide is consumed in side reactions. In addition, high alkali charges have an increasing effect on extraction, and lead to a higher pulp viscosity and simultaneous negative effect on the effluent load and yield. A higher temperature accelerates the bleaching process and the decomposition of hydrogen peroxide into hydroxyl radicals, which in turn leads to the generation of the superoxide anion radicals. The radical species contribute to the oxidation of lignin, but also to a certain extent to the oxidation of the polysaccharides and leads to a drop of the pulp viscosity. Therefore, in ECF bleaching, the mill practice is to keep the temperature level below 90 °C during the peroxide stages. The peroxide bleaching effect most likely occurs by one of two mechanisms: a lignin retaining part, where the perhydroxyl anion reacts with the chromophores resulting in colourless carboxylic acid groups; and a lignin degrading part where radical species, originating from the hydrogen peroxide, oxidise and depolymerise the lignin molecule. Unlike oxygen, hydrogen peroxide in an alkaline medium does not attack phenolic structures. The main reaction pathway of the perhydroxyl anion is nucleophilic addition to enone and other carbonyl structures [76–79]. In this way, the chromophore groups are removed. The two radical species, hydroxyl and superoxide, increase the extent of lignin degradation. The hydroxyl radicals introduce radical sites into the substrate. These substrate radicals may be oxidised, may disproportionate or may combine with superoxide radicals. The superoxide radicals, after coupling with substrate radicals, bring about fission of the C-C bonds and thereby open aromatic rings and cleave ring-conjugated double bonds. In addition, they are intermediates in the formation of hydrogen peroxide and hydroxyl radicals.

3.6.3 Process Variables and Technology of Peroxide Bleaching

In ECF bleaching, hydrogen peroxide is widely used in the EOP extraction stages following chlorine dioxide treatment and is one of the most effective possibilities for the increase of the final pulp brightness [78]. The influence of hydrogen peroxide charge during the EOP stage on the intermediate and final pulp brightness, according toValchev and co-workers [71], is represented in **Figure 3.14**. A significant improvement of the bleaching process selectivity in the EOP stage was obtained by adding up to 0.5% hydrogen peroxide. The higher peroxide charge leads to a relatively lower bleaching effect and can be used to reach a desired brightness, if necessary. In the suggested optimal bleaching conditions, 1 kg peroxide replaces approximately 2.5–3 kg ClO_2 [71].

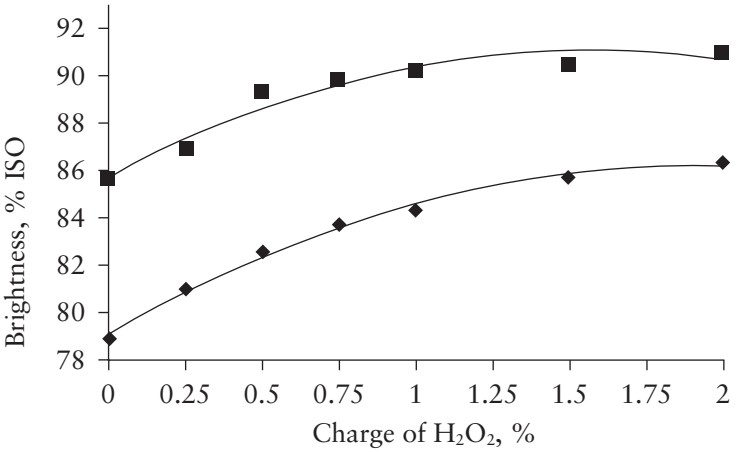

Figure 3.14 Effect of H_2O_2 charge on the pulp brightness (♦ after EOP and ■ after D_1)

The temperature in an EOP stage is between 75 °C and 90 °C and the retention time 60–120 min, while the pH is typically about 11 at the start of treatment and about 10 at the end. A higher pH may result in alkali-induced decomposition of hydrogen peroxide. The charge of sodium hydroxide is normally 10–25 kg per ton of pulp. The equipment used for the EOP extraction stages is very similar to EO extraction equipment. Pressurised hydrogen peroxide bleaching during the PO stage is a very efficient tool for increasing brightness, although the Kappa reduction capability of hydrogen peroxide is decreased, partly because hydrogen peroxide, in contrast to chlorine dioxide and ozone, is not reactive towards HexA. An extensive use of hydrogen peroxide often leads to a somewhat increased yellowing of the fully bleached pulp, especially in the case of hardwood kraft pulp. Extensive use of hydrogen peroxide, as in a PO stage, normally requires a chelating agent treatment (Q) prior to the peroxide stage. Pressurised peroxide bleaching expands the reaction rate by the increase of temperature, peroxide concentration and improving peroxide diffusion [80, 81]. Using the pressure peroxide methods substantially reduces the retention time and increases the brightness ceiling compared with conventional process [81, 82].

Valchev and co-workers investigated the influence of oxygen utilisation during the bleaching processes [13]. It has been established that the initial stage is very important for the bleaching process. The Kappa number of the pulp decreases very quickly in the first 10 min, while in the next stage the delignification is slower. The Kappa number value decreases upon increasing the temperature, but there is not a positive effect on Kappa number reduction at temperatures higher than 100 °C in the presence or

absence of oxygen. This is probably caused by the forced decomposition of peroxide under these conditions.

Oxygen affects the delignification more significantly, especially in the initial stage of the process, but the delignification continues slowly and after full peroxide consumption. Higher brightness (1.5–2%), extended delignification and higher peroxide consumption (5–7%) are reached using pressure peroxide bleaching compared with atmospheric bleaching. Correlations between Kappa number peroxide consumption and brightness show that higher peroxide consumption, in the presence of oxygen, corresponds to an increasing brightness and all experimental data are described with one and the same correlation. However, this increase of peroxide consumption leads to a further extended Kappa number reduction. Consequently, the effect of oxygen during peroxide bleaching is mainly expressed as an improvement of the delignification process [13]. Typical parameter values for a PO stage are normally: temperature of 90–105 °C, retention time of about 2 h, pressure at top 0.3–0.5 MPa and a final pH of 10.0–11.0. The charge of hydrogen peroxide is usually 10–30 kg/ton and depends on the Kappa number of the incoming pulp. The charge of sodium hydroxide is directly proportional to the charge of hydrogen peroxide and is normally 20–30 kg/ton of pulp. The equipment for pressurised peroxide bleaching is very similar to that used in oxygen delignification equipment.

The pulp bleaching history has a great influence on the performance of a final hydrogen peroxide bleaching stage, regarding the bleachability and selectivity parameters, and bleached pulp properties. The final peroxide stage completes bleaching and extracts all remaining potential chromophores. This stage requires temperature and alkalinity to be efficient. The reaction with chromophores or precursors of chromophores is rather fast. A benefit of using peroxide in the final stage of a bleaching sequence is the improved brightness stability. The advantage of the application of hydrogen peroxide can be attributed to the destruction of carbonyl groups and quinoid structures remaining in the pulp after the D stage.

The identified remaining chromophores in fully bleached and aged pulp have a common structural element, hydroxy- and dihydroxyquinones. These compounds are resonance stabilised and have a peculiar reactivity because they can form a dianion under alkaline conditions. They are the main chromophores surviving the ECF bleaching [37, 83]. Traces of quinone compounds are detected in pulp bleached with a final D stage, but no such products were found in pulp bleached with a final peroxide stage [84]. The destruction of quinoid structures is one of the main reactions of alkaline hydrogen peroxide in bleaching processes. For the development of brightness, hydrogen peroxide requires alkaline bleaching conditions. The perhydroxyl anion is a strong nucleophile and cleaves side chains in the residual lignin, thus destructing chromophores. Lignin degradation takes place in addition *via* radicals resulting from

the decomposition of hydrogen peroxide. The disadvantage of these radicals is their unselectivity, the side reactions are cellulose oxidation and the subsequent cleavage of the polymer chains [85].

According to Valchev and co-workers [86], the comparison of the results of pulp post bleaching with xylanase, peracetic acid and hydrogen peroxide shows that the greatest effect on pulp brightness is achieved by the peracetic acid treatment (**Figure 3.15**).

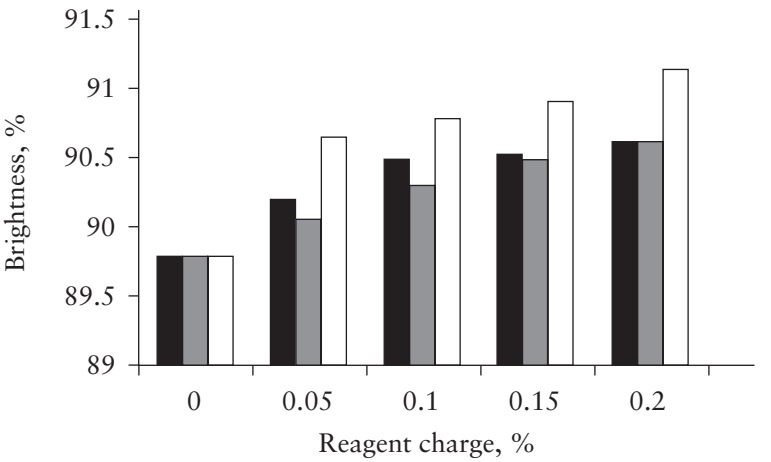

Figure 3.15 Post bleaching effect on the pulp brightness (■–X; ■–P; and □– peracetic acid (Paa))

The peroxide treatment leads to the lowest *Pc* number, but the selectivity of the pulp bleaching with this reagent is also at its lowest (**Figure 3.16**). On the other hand, the decrease in viscosity, observed during peroxide bleaching, does not affect the pulp strength. Typical data for post peroxide bleaching is: temperature about 80 °C, retention time up to 120 min under atmospheric conditions, peroxide charge 1–3 kg/ton of pulp and a final pH of 8.0–10.0. The application of pulp post bleaching does not require additional capital investment, and the effect achieved justifies the expense for bleaching reagents.

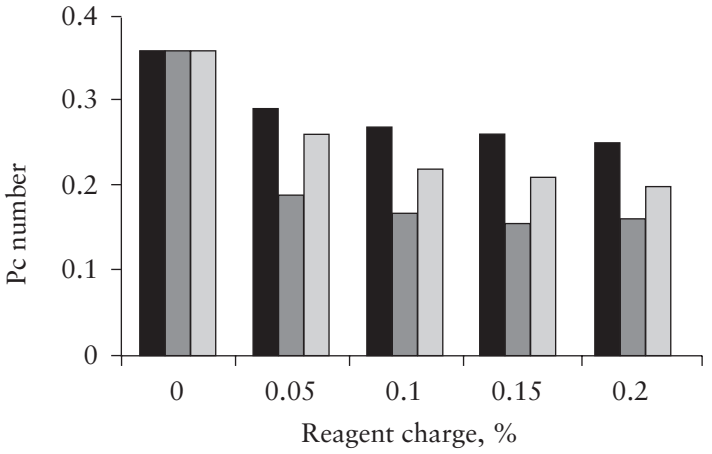

Figure 3.16 Post bleaching effect on the *Pc* number (■–X; ■–P; and □–Paa)

3.6.4 Kinetics of Peroxide Bleaching

The kinetics of the EOP stage, pressure delignification OP and atmospheric peroxide stage P was studied by Valchev and co-workers [13, 15] on the basis of the variation of the Kappa number with reaction time at different temperature values. It has been found that the best description was achieved by the exponential kinetic Equation (**Equation 3.16**), which takes place on uniformly heterogeneous surfaces. The obtained values of activation energy E are independent of the degree of increasing delignification. The preexponential factor A decreases in the process according to the **Equation 3.19**:

$$\ln A = \ln A_0 - a.\alpha \tag{3.19}$$

where a is a coefficient of inhomogeneity of the surface and A_0 is an initial preexponential factor.

Consequently, a higher rate of delignification during pressure peroxide bleaching, compared with atmospheric bleaching, could be due to an increase in the number of interactions between lignin and the reagent species. The pressure peroxide delignification is faster than peroxide bleaching at atmospheric pressure and the effect

of oxygen on the reaction rate corresponds to a nearly 10 °C difference of temperature. The kinetics of peroxide and pressure peroxide bleaching, with respect to absorption coefficients, has also been investigated by Valchev and co-workers [13, 15], and it has been established that the modified Equation of Prout–Tompkins (**Equation 3.10**) gives the best description of the process. The relative change of absorption coefficient $\alpha_{k/s}$ was calculated according to **Equation 3.6**. It is well known that **Equation 3.10** is successfully applied to topochemical reactions of the chain mechanism; a similar Equation can be used in the case of diffusion-controlled heterogeneous processes. Investigation of the processes of peroxide and pressure peroxide bleaching show that the kinetics of delignification is most successfully described by an exponential kinetic Equation (**Equation 3.16**). The activation energy E is independent of the presence of oxygen and does not change during the process. This means that one and the same type of interactions take place. The kinetics of the bleaching process, with respect to the absorption coefficient, is described by the modified topochemical Equation of Prout–Tompkins. The values for activation energy E and preexponential factor A established in this case, confirm the assumption that the effect of oxygen is determined by the value of the preexponential factor and does not depend on the activation energy. The topochemical kinetic mechanism, which describes the change of the absorption coefficient, is determined by the course of two different processes: removal of the lignin from the pulp and transformation of the chromophore groups in the solid phase. These features of pressure peroxide bleaching are confirmed by the obtained correlations. The effect of oxygen action on peroxide bleaching is expressed with some increase in the rate of bleaching processes without changing their kinetic mechanism [13, 15].

3.6.5 Peracetic Acid in Pulp Bleaching

Paa is a highly selective bleaching chemical, the use of which ensures good strength properties of the pulp can be maintained. Today, Paa occupies a niche in TCF bleaching and is also recommended as a final treatment step to boost the brightness of the TCF pulp [87, 88]. Its application is necessary due to the need to modify the residual lignin to allow its destruction during hydrogen peroxide bleaching and to improve the economics of TCF sequences. During pulp bleaching, Paa is consumed by lignin, hexenuronic acids, oxidation reactions and spontaneous decomposition, catalysed by transition metals [89, 90]. In neutral or slightly acid pH, the pulp carbohydrate degradation is mainly dependent on the concentration of peracetic acid [91]. At low pH, acid hydrolysis is probably the main reason for carbohydrate depolymerisation, at neutral pH, decomposition of Paa may produce highly reactive oxygen species, such as hydroxyl radicals, formed by the homolytic cleavage of O-O, which causes the degradation. Peracetic acid is less sensitive to transition metals than hydrogen peroxide. The study of Paa, beyond its use in TCF bleaching, has shown that Paa

removes HexA with an effectiveness equal to chlorine dioxide and ozone [92]. As a final stage, Paa exerts a bleaching effect, but does not necessarily improve the pulp brightness stability. Most likely, the reactions it is involved in, i.e., hydroxylation, as well as oxidation – generates quinones, which cause chromophore formation [83]. Peracetic acid application in the last stage of eucalyptus pulp bleaching caused a slight decrease in pulp viscosity, Kappa number and HexA content, but had no significant effect on pulp reversion [93].

Paa can be used as an equilibrium solution with a mixture of peracetic acid, acetic acid and hydrogen peroxide, or as pure distilled Paa. In order not to waste the hydrogen peroxide content, the equilibrium Paa treatment has to be followed by the peroxide stage without intermediate washing. Following the addition of caustic soda, the unused hydrogen peroxide content in the pulp is reacted in the subsequent P step. This results in an improved delignification and a higher brightness, which is achieved in the following alkaline peroxide stage. Following the investigations of Khristova and co-workers, and Simeonova and co-workers [94, 95], the alkali charge in peracetic acid bleaching has to be selected at an initial pH above 10 in order to finish the process at pH 5.0–6.0. The final pH, around 5, being used for peracetic bleaching is also in accordance with Zawadski's investigations [96]. At that pH, the chromophore groups are easily destroyed and the bleached pulp has a higher brightness. With the increase of pH above 10.8, a sharp decrease of the pulp brightness is observed (**Figure 3.17**) [86], which is due to neutralisation of the Paa. On the other hand, the performance of bleaching in a neutral and low-acid medium does not allow the peroxide to react, which also negatively affects the pulp brightness. The bleaching reagents are entirely consumed in the high-alkali conditions, whereas in an acid medium the peroxide content in the product barely reacts. The comparison of pulp post bleaching with xylanase, peracetic acid and hydrogen peroxide shows that the greatest effect on pulp brightness is achieved by the Paa treatment (**Figure 3.16**). The Paa does not affect cellulose under the applied conditions of the last bleaching stage [86]. An additional advantage of Paa in comparison with other bleaching reagents is its antibacterial action, as well as the reduced consumption of chemicals in the subsequent paper production as a result of the cleaning effect on the pulp fibres.

It has been found by Valchev and co-workers [97], that the modified topochemical Prout–Tompkins Equation most accurately describes the kinetics of the Paa bleaching, with respect to the relative change of the light absorption coefficient. The kinetic investigation shows that the peracetic bleaching, as a final step, is an energetic uniform process. The reaction rate depends on the number of chromophore structures, and the presence of steric and diffusion hindrances which are included in the preexponential factor. For economic reasons, only distilled peracetic acid is of interest, its bleaching effect being equal or slightly better than that for the equilibrium type. Distilled Paa does not need the pH to be changed from the normally slightly

acidic regime to an alkaline one, compared with bleaching using hydrogen peroxide [83]. Tetraacetylethylenediamine (TAED) has also been investigated as a bleaching activator [94]. TAED can react with peroxide over a range of pH conditions; in alkaline conditions, one mole of TAED reacts with two moles of hydrogen peroxide to form two moles of the active bleaching species of the peracetate anion.

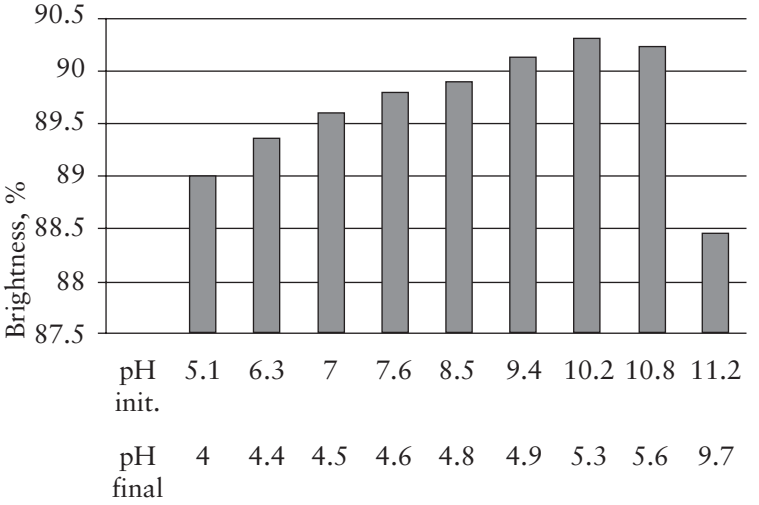

Figure 3.17 Effect of pH on the pulp brightness after the post peracetic acid stage (initial brightness 89.2% ISO, peracetic acid charge 0.15%)

3.7 Ozone Bleaching Chemistry and Technology

Ozone is an extremely powerful oxidant with an oxidation potential of 2.07 V. Ozone has been investigated, on a laboratory scale, for use in the bleaching of chemical pulps for a long time, but for both economic and pulp quality reasons, the first implementation of ozone on an industrial scale wasn't until 1990, when the first installation of an ozone bleaching plant came on stream in Lenzing. Ozone reacts very rapidly with the pulp and the reaction takes place, to a lesser or greater extent, in the mixers. The importance of highly efficient mixing cannot therefore be overestimated. Since ozone decomposes spontaneously into oxygen at high temperatures, ozone stages are run at a low temperature. The stability of ozone in water increases with decreasing pH. This is one of the important reasons why ozone bleaching is performed

under acidic conditions, preferably in the pH range of 2–3. Ozone decomposes *via* the catalytic action of transition metal ions, present in the pulps and bleaching liquors, giving rise to hydroxyl, hydroperoxyl and superoxide anion radical intermediates [98, 99]. The reactions of ozone with lignin involves an initial electrophilic attack by the oxidant, followed by the loss of oxygen, which results in hydroxylation of the aromatic ring. In a subsequent step, ozone reacts with the aromatic ring and finally, this is cleaved [100]. Carbohydrate decomposition during ozone bleaching depends on pH, temperature and the concentration of transition metal ions [101]. The ozone stage leads to the introduction of carbonyl groups and gylcosidic bond cleavage [81]. Thus, alkaline extraction after ozone treatment decreases the molecular weight of the carbohydrates by splitting the alkali-sensitive linkages. As expected, the alkaline treatment of ozone-bleached pulps in general, reduces fibre strength. An advantage of the ozone treatment is that the extractives are removed very efficiently. Another advantage is its ability to efficiently remove HexA in the pulp, which improves the brightness stability of the final bleached pulp and reduces the ClO_2 demand in the bleach plant. Ozone bleaching is normally only used for the bleaching of hardwood kraft pulps and for sulfite pulps. Unfortunately, ozone delignification is accompanied by a concomitant degradation of the polysaccharide fraction. In general, the tearing strength of ozone-bleached softwood kraft pulps is found to be 10–20% lower compared with conventionally bleached pulps of the same provenance [102]. It has been reported that the efficiency of a TCF bleaching sequence is significantly improved when an ozone stage is arranged between two hydrogen peroxide stages [103]. The investigations of Davies and co-workers [83] have shown that the highest brightness and extremely low reversion is obtained after the combination of a small amount of ozone with a subsequent peroxide treatment.

Typical parameter values for the medium consistency ozone Z stage are: a retention time of a few seconds, pH 2–3, temperature about 50 °C, pressure 0.8 MPa and an ozone charge of 3–5 kg/ton. In a medium consistency Z stage, the pulp suspension is pumped into two consecutive mixers. Ozone is added and thoroughly mixed into the pulp suspension in a mixer positioned immediately after the pump (**Figure 3.18**) [59].

Unlike the MC process, high consistency ozone bleaching is carried out under atmospheric conditions, where the pulp meets the gas in a screw reactor. A slightly longer retention time is utilised than in an MC system, but the time is still only about 1 min.

3.8 Xylanases and Laccases in Pulp Bleaching

The use of xylanases for kraft pulp bleaching has been one of the greatest success stories of enzymes in the pulp and paper industry. It is known that a number of

pulp mills continue to use xylanase enzymes to increase the bleaching efficiency. The xylanase treatment of pulp promotes increased efficiency of the subsequent delignification and bleaching processes. Thereby, a 25% saving of bleaching reagents has been achieved, without investment in expensive equipment. The investigations into a pulp enzyme treatment during the bleaching process began in the mid-1990s [104, 106]. The effect of hemicellulases on the pulp brightness is attributed to the removal of xylan from the fibre surface, as well as to the degrading of xylan-lignin complexes in the inner layers of the pulp matrix. The elimination of hemicelluloses makes the pulp fibre structure more accessible to a subsequent bleaching with chemical reagents, such as hydrogen peroxide, chlorine dioxide and ozone, and focuses their action to only the lignin chromophore groups [106, 107]. This improved lignin removal and the removal of the bleach-consuming HexA might explain the mechanism of xylanase prebleaching [108]. The pulp treatment by xylanase also leads to a reduction in the content of heavy metals, such as Cu, Fe and Mn, most likely due to existing bonds between HexA and xylan [109]. According to Valchev and co-workers [14], the xylanase treatment increases the brightness of the peroxide-bleached pulp by about 4% ISO and allows approximately a 1 unit Kappa number decrease upon a 10% lower hydrogen peroxide consumption (**Figure 3.19**). The overall xylanase treatment effect is two times higher than the oxygen effect on the peroxide bleaching.

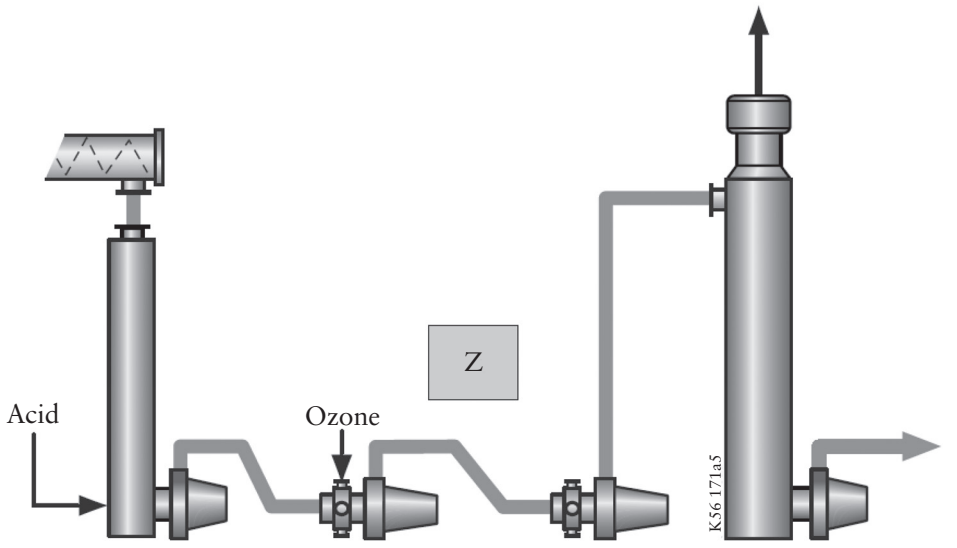

Figure 3.18 Medium consistency ozone process

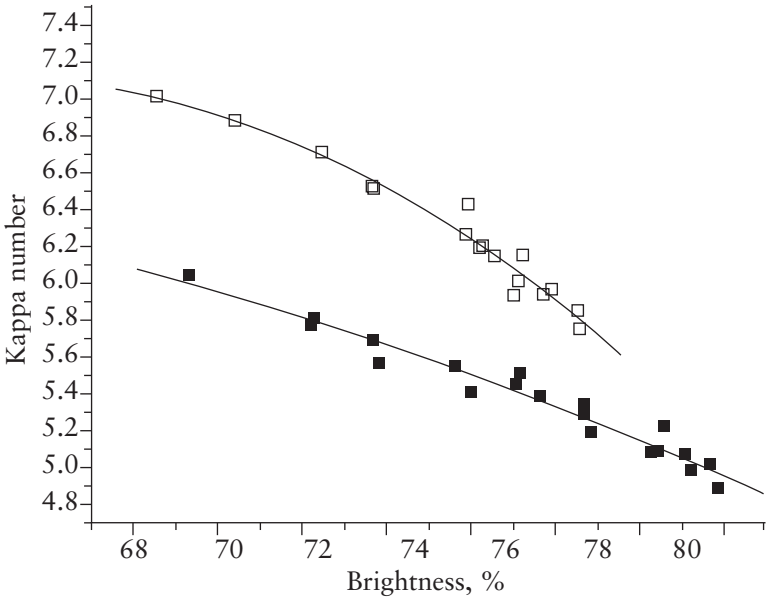

Figure 3.19 Correlation between the Kappa number and brightness. (■–enzyme treated pulp and □–untreated pulp)

There is also variability in the stage of the process where the xylanase treatment is performed. It could be before or after oxygen delignification, or after the bleaching sequence. During ECF bleaching sequences, the best location for the xylanase treatment is in the storage towers of the unbleached pulp. After a continuous xylanase treatment of hardwood pulp under industrial conditions, a 21% reduction of chlorine dioxide is registered [72]. Typical data for a xylanase prebleaching treatment is: temperature about 55–65 °C, retention time up to 120 min, enzyme charge 0.3–1 XU per g of pulp and a pH of 8.0–9.0. Because the kraft process results in pulp which is alkaline and at higher temperatures, enzymes that do not require adjustment of temperature or pH are better suited to the process.

It has been shown that a xylanase post treatment of hardwood kraft pulps, during a final stage, resulted in a significantly reduced yellowing [110]. The enzyme treatment primarily resulted in a degradation of HexA in the pulp, reducing the amount of this structure by up to one-third.

Valchev and Tsekova [111] do not indicate a relation between HexA content and pulp brightness during xylanase post treatment. According to them, the effect on the bleached pulp may be explained by the hydrolysis of the xylan, located on the surface,

and extraction of the stabilised quinone chromophoric structures retained by it. The obtained correlation between the pulp brightness and the enzyme action shows that an optimum bleaching effect is achieved at a low degree of xylan conversion and at a low enzyme charge, which doesn't significantly affect the pulp yield and the strength properties (**Figure 3.20**) [86, 111].

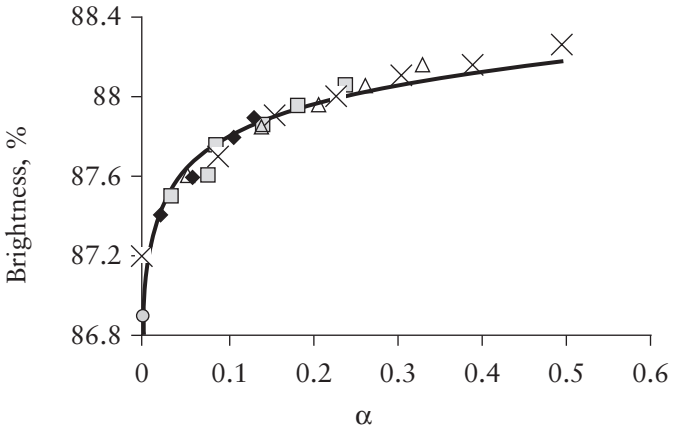

Figure 3.20 Correlation between the brightness and degree of xylan conversion (Pulpzyme HC charge 0.05%)

Kinetic studies of xylan decomposition with different xylanases show quite good results when the modified topochemical Prout–Tompkins **Equation 3.10** is used [112–114]. The nonhomogeneous distribution of xylan, as well as the difference in its structure throughout the pulp matrix, makes the classical Michaelis–Menten rate Equation inadequate to describe the kinetics of enzyme-catalysed decomposition. The application of a modified Prout–Tompkins Equation to the action of xylanase on pulp indicates that the process is connected with a continuous change of reaction area, which is determined by the xylan chain structure and the lignin-carbohydrate bonds. The activation energy does not change during the course of the process, which is an indicator of an interaction with a specific type of xylan. The amount of remaining unreacted xylan in the pulp has a decisive effect on the rate of its removal [111, 115].

While the efforts into the use of xylanase products are directed towards their industrial-scale implementation, the research is aimed at the development of new enzyme technologies with a direct delignification effect.

Laccases (E.C.1.10.3.2.), a group of multicopper oxidases, are the most promising oxidoreductive lignin-degrading enzymes [116]. Laccases oxidise the lignin structure into radicals, which are spontaneously degraded. However, due to the steric hindrances, laccases alone are not very efficient for delignification. Furthermore, their oxidation potential provides the oxidation of lignin's phenolic end groups only. It is recognised that their substrate specificity can be extended to nonphenolic end groups, as well as by adding oxidised low molecular mass compounds (mediators) [117]. 1-hydroxybenzotriazole (HBT) can act as a mediator. Laccase oxidises this mediator, forming an HBT radical during the initial stage of the process [118]. The mediator is small enough to penetrate the lignin network and perform oxidations of the nonphenolic end groups. The application of a laccase-HBT mediator system provides an efficient, selective and completely chlorine-free bleaching stage [119, 120]. It has been discovered that pulp treatment with a laccase-mediator system (LMS) leads to high lignin extraction (40–60%) in the subsequent bleaching stages. In addition, the carbohydrate hydroxyl groups, present in the pulp, remain unchanged and neither a decrease in viscosity nor changes in the content of hexeneuronic acids are observed. Moreover, the enzyme treatment does not directly affect the degree of pulp brightness. Generally, oxygen is required during normal delignification processes. The small size molecules of the oxidised mediator provide a relatively uniform lignin depolymerisation [121]. The investigations of Valcheva and co-workers [122] show the highly selective delignification effect of LMS. A Kappa number decrease of 32% is produced after chlorine dioxide bleaching, while it reaches only 17% after oxygen bleaching. It is evident that the enzyme effect on delignification is more pronounced in the case of chlorine dioxide bleaching [123]. It has been found that the exponential kinetic Equation (**Equation 3.16**), valid for processes taking place on uniformly nonhomogeneous surfaces, provides a good interpretation of the LMS action, when using the kinetic variables of the degree of delignification α_k and the relative change in the light absorption coefficient $\alpha_{k/s}$ [122]. The combination of LMS and ClO_2 leads to the domination of the delignification reaction, while the combination of LMS and O_2 leads to a decrease in the content of chromophoric groups [16]. Some problems related to enzyme stability and the high cost of LMS still exist, but the results obtained provide reasonable optimism for the future application of this type of enzyme system in the pulp bleaching process.

3.9 Conclusions

After the rapid development of pulp bleaching technology in the 1990s, there followed a period in which the individual bleaching processes were mainly optimised, without this being bound to considerable changes in the multistage bleaching sequences. No essential amendments to the environmental legislation are expected in the coming

years, meaning that the main driving force in the development of pulp bleaching technologies will be an economic one.

Since the wood raw material is the main expenditure for a pulp mill, it is more logical to focus on achieving a high pulp yield. An extended and selective oxygen delignification stage would give both a high overall yield and less environmental impact due to the lower requirement for bleaching chemicals. As a result of indepth kinetic studies, the established conditions of the oxygen delignification processes should probably be changed so that in the oxygen system design, the alkali concentration and charge are decoupled, similar to modern cooking systems, to create a more uniform delignification rate throughout the reactor.

Chlorine dioxide will continue to be the main bleaching reagent for kraft pulp bleaching. Through optimisation of the bleaching conditions and temperature-time dependences of the processes in the individual chlorine dioxide bleaching stages, consumption of the bleaching reagent may be considerably reduced and a high final brightness and high carbohydrate yield may be achieved in the pulp.

New efficient catalysts of peroxide bleaching, which will improve the selectivity of the bleaching process, will be sought. The development of production methods for cheap peracetic acid will considerably extend its use in the multistage bleaching sequences.

The development of more selective and efficient enzyme systems, which do not give significant yield losses, might be interesting in pulp treatment in order to break up lignin-carbohydrate complexes.

High final brightness without additional capital investment may be achieved through pulp post bleaching. In the integrated pulp and paper mills, the place of that bleaching will probably be relocated prior to the paper machine.

References

1. R. Grundelius, *TAPPI*, 1993, **76**, 1, 133.

2. M. Ragnar and M. Leite, inventors; Kvaerner Pulping, assignee; WO 2004/079087M, 2004.

3. P. Kubelka and F. Munk, *Zeitschrift für Technische Physik*, 1931, **12**, 593. [In German]

4. F.A. Steele, *Paper Trade Journal*, 1935, **101**, 17, 31.

5. F.A. Steele, *Paper Trade Journal*, 1937, **104**, 8, 157.

6. D.B. Judd, *Paper Trade Journal*, 1938, **106**, 1, 39.

7. J.A. Van den Akker, *TAPPI*, 1949, **32**, 11, 498.

8. H.W. Giertz in *Proceedings of the Transactions of the Symposium on Consolidation of the Paper Web*, Cambridge, UK, 1966, p.928.

9. J.C. Tongren, *Paper Trade Journal*, 1938, **107**, 8, 34.

10. H.W. Giertz, *Finnish Paper Timber Journal*, 1945, **27**, 359.

11. M. Paulsson, L.A. Lucia, A.J. Ragauskas and C. Li, *Journal of Wood Chemistry and Technology*, 2001, **21**, 4, 343.

12. C. Li, D.H. Kim and A.J. Ragauskas, *Journal of Wood Chemistry and Technology*, 2004, **24**, 1, 39.

13. I. Valchev, E. Valcheva and I. Dimitrov, *Cellulose Chemistry and Technology*, 2003, **37**, 1–2, 131.

14. I. Valchev, I. Dimitrov, E. Valcheva and S. Veleva, *Cellulose Chemistry and Technology*, 2004, **38**, 1–2, 67.

15. I. Valchev and G. Simeonova in *Proceedings of the International Pulp Bleaching Conference*, Stockholm, Sweden, 2005, p.272.

16. G. Radeva, I. Valchev and E. Valcheva, *Cellulose Chemistry and Technology*, 2009, **43**, 7–8, 317.

17. P.M. Froass, A.J. Ragauskas, T.J. McDonough and J. Jiang in *Proceedings of the International Pulp Bleaching Conference*, Washington, DC, USA, 1996, **1**, p.163.

18. C. Gustavsson in *Interrelation between Kraft Cooking Conditions and Pulp Composition*: Royal Institute of Technology, Department of Fibre and Polymer Technology, Stockholm, Sweden, 2006. [Doctoral Thesis]

19. 19. M. Lawoko in *Lignin Polysaccharide Networks in Softwood and Chemical Pulps: Characterisation, Structure and Reactivity*, Royal Institute of Technology, Department of Fibre and Polymer Technology, Sweden, 2006. [Doctoral Thesis]

20. J. Janson and I. Palenius, *Paperi ja Puu*, 1972, **54**, 6, 343. [In Finnish]

21. J. Janson, I. Palenius, B. Stenlund and P.E. Sagfors, *Paperi ja Puu*, 1975, **57**, 5, 387. [In Finnish]

22. T. Dyer in *Elucidating the Formation and Chemistry of Chromophores during Kraft Pulping*, Institute of Paper Science and Technology, Atlanta, GA, USA, 2004. (Doctoral Thesis)

23. G. Gellerstedt and J. Li, *Carbohydrate Research*, 1996, **294**, 1, 41.

24. T. Vuorinen, A. Teleman, P. Fagerström J. Buchert and M. Tenkanen in *Proceedings of the International Pulp Bleaching Conference*, Washington, DC, USA, 1996, **1**, p.43.

25. J. Buchert, A. Teleman, V. Harjunpää, L. Viikari and T. Vuorinen, *TAPPI*, 1995, **78**, 11, 125.

26. E. Bergnor-Gidnert, P.E. Tomani and O. Dahlman, *Nordic Pulp and Paper Research Journal*, 1998, **13**, 4, 310.

27. J. Buchert, M. Tenkanen, M. Ek, A. Teleman, L. Viikari and T. Vuorinen in *Proceedings of the International Pulp Bleaching Conference*, Washington, DC, USA, 1996, **1**, p.39.

28. J. Buchert, E. Bergnor, G. Lindblad, L. Viikari and M. Ek, *TAPPI*, 1997, **80**, 6, 165.

29. M. Siltala, K. Winberg, K. Henricson and B. Lonnberg in *Proceedings of the International Pulp Bleaching Conference*, Helsinki, Finland, 1998, **1**, p.279.

30. A. Granström, T. Eriksson, G. Gellerstedt, C. Rööst and P. Larsson, *Nordic Pulp and Paper Research Journal*, 2001, **16**, 1, 18.

31. O. Sevastyanova in *Importance of Oxidizable Structures in Bleached Kraft Pulps*, Royal Institute of Technology, Stockholm, Sweden, 2005. [Doctoral Thesis]

32. J. Devenyns and E. Chauveheid in *Proceedings of the 9th International Symposium on Wood and Pulping Chemistry*, Montreal, Canada, 1997, p.M5-1.

33. J. Devenyns, E. Chauveheid and H. Martens in *Proceedings of the International Pulp Bleaching Conference*, Helsinki, Finland, 1998, **1**, p.151.

34. J. Laine and P. Stenius in *Proceedings of the 8th International Symposium on Wood and Pulping Chemistry*, Helsinki, Finland, 1995, p.589.

35. H. Suess and C. Leporini in *Paper Presented at ABTCP*, Sao Paulo, Brazil, 2007.
http://h2o2.evonik.com/product/h2o2/en/Pages/default.aspx

36. H. Suess, D. Davies and T. Dietz in *Paper Presented at PAPTAC*, Montreal, Canada, 2008.
http://h2o2.evonik.com/product/h2o2/en/Pages/default.aspx

37. T. Rosenau, A. Potthast, P. Kosma H. Suess and N. Nimmerfroh in *Paper Presented at ISWFPC*, Durban, South Africa, 2007.
http://h2o2.evonik.com/product/h2o2/en/Pages/default.aspx

38. T. Rosenau, T. Dietz, A.D. French, U. Henniges and A. Potthast in *Proceedings of the 16th International Symposium on Wood and Pulping Chemistry*, Tianjin, China, **2011**, p.525.

39. J.M. Genco, A. van Heiningen and W. Miller in *The Bleaching of Pulp*, Eds., P. Hart and A. Rudie, TAPPI Press, Atlanta, GA, USA, 2012, p.9.

40. B. Parsad, A. Kirkman, H. Jameel, J. Gratzl and V. Magnotta, *TAPPI*, 1996, **79**, 9, 144.

41. T. J. McDonough in *Pulp Bleaching Principles and Practice*, Eds., C.W. Dence and D.W. Reeve, TAPPI Press, Atlanta, GA, USA, 1996, p.213.

42. S.J. Shin, L.R. Schroeder and Y.Z. Lai, *Journal of Wood Chemistry and Technology*, 2006, **26**, 1, 5.

43. S.M. Violette in *Oxygen Delignification Kinetics and Selectivity Improvement*, University of Maine, ME, USA, 2003. (Doctoral Thesis)

44. S. Antonsson, M.E. Lindstrom and M. Ragnar, *Nordic Pulp and Paper Research Journal*, 2003, **18**, 4, 388.

45. S.B. Agarwal, J.M. Genco, B.J.W. Cole and W. Miller, *Journal of Pulp and Paper Science*, 1999, **25**, 10, 361.

46. C.L. Hsu and J.S. Hsieh, *TAPPI*, 1985, **68**, 11, 126.

47. S. Nenkova, I. Valchev and G. Simeonova, *Journal of Pulp and Paper Science*, 2003, **29**, 10, 324.

48. A. van Heiningen and Y. Ji, *TAPPI*, 2012, **11**, 3, 9.

49. R. Yang, A. Ragauskas and H. Jameel, *Industrial and Engineering Chemistry Research*, 2002, **41**, 24, 5941.

50. J.F. Iijima and H. Taneda, *Journal of Pulp and Paper Science*, 1997, **23**, 12, J561.

51. M. Ragnar and K. Ala-Kaila, *IPW/Papier*, 2004, **8**, T146.

52. L. Olm and A. Teder, *TAPPI*, 1979, **62**, 12, 43.

53. C.L. Hsu and J.S. Hsieh, *TAPPI*, 1987, **70**, 12, 107.

54. C.L. Hsu and J.S. Hsieh, *AIChE Journal*, 1988, **34**, 11, 116.

55. J. Iribarne and L.R. Schroeder, *TAPPI*, 1997, **80**, 10, 241.

56. I. Valchev and P.K. Christensen in *Proceedings of the 7th International Symposium on Wood and Pulping Chemistry*, Beijing, China, **1993**, **1**, p.137.

57. K.L. Nguyen and H. Liang, *Appita Journal*, 2002, **55**, 2, 162.

58. I. Valchev, E. Valcheva and E. Christova, *Cellulose Chemistry and Technology*, 1999, **33**, 3–4, 303.

59. GLV Group, Pulp Techologies. *http://www.glv.com/Pulp_Paper/Pulp_Technologies/Chemical/BusinessCateg.aspx http://www.glv.com*

60. Firmennachrichten-ausland, *Wochenblatt für Papierfabrication*, 1998, **126**, 8, 380. [In German]

61. A. Tuomi, *Balkan Pulp Paper News*, 2000, **1**, 10.

62. M. Ragnar in *Proceedings of the 7th International Conference New Available Technologies*, Stockholm, Sweden, 2002, p.31.

63. M.J.M. Barroca, P.J.T. Marques, I.M. Secom and A.A. Castro, *Industrial & Engineering Chemistry Research*, 2001, **40**, 5680.

64. M.J. Joncort, P. Froment, D. Lachenal and C. Chirat, *TAPPI*, 2000, **83**, 1, 144.

65. B.N. Brogdon and L.A. Lucia, *Journal of Wood Chemistry and Technology*, 2005, **25**, 3, 133.

66. M. Ragnar in *Proceedings of the International Pulp Bleaching Conference*, Portland, ME, USA, 2002, **1**, p.237.

67. T. Dyer and A. Ragauskas, *Pulp and Paper*, 2002, **3**, 49.

68. D. Lachenal, C. Chirat and M.T. Viardin, *TAPPI*, 2000, **83**, 8, 96.

69. K. Eiras and J. Colodette, *Journal of Pulp and Paper Science*, 2003, **29**, 2, 64.

70. O. Dahl, J. Ninimäki, T. Tirri and H. Kuopanportti, *Paperi ja Puu*, 1997, 79, 3, 560. [In Finnish]

71. I. Valchev, G. Simeonova, S. Nenkova and J. Gaidarov, *Cellulose Chemistry and Technology*, 2005, 39, 1–2, 105.

72. I. Valchev, G. Simeonova, S. Nenkova E. Valcheva and J. Gaidarov, *Balkan Pulp and Paper News*, 2004, 5, 12, 25.

73. O. Sevastyanova, A. Forsström, E. Wackerberg and M.E. Lindström, *TAPPI*, 2012, **11**, 3, 43.

74. S. Andtbacka, *Pulp & Paper Canada*, 1998, **99**, 3, 57.

75. D.H. Andrews and R.P. Singh in *The Bleaching of Pulp*, Ed., R.P. Singh, *TAPPI* Press, Atlanta, GA, USA, 1996, p.211.

76. J. Gierer and F. Imsgard, *Svensk Papperstidning*, 1977, **80**, 16, 510.

77. H. Suess, C. Filho and K. Schmidt in *Paper Presented at ABTCP*, Sao Paulo, Brazil, 2000.
http://h2o2.evonik.com/product/h2o2/en/Pages/default.aspx

78. G. Gellerstedt, I. Pettersson and S.E. Sundin in *Proceedings of the International Symposium on Wood and Pulping Chemistry*, *Stockholm, Sweden*, 1981, **1**, p.120.

79. J. Gierer, *Holzforschung*, 1997, **51**, 1, 34.

80. D. Breed, L. Shackford, E. Pereira and J. Colodette in *Proceedings of the TAPPI Pulping Conference*, Chicago, IL, USA, 1995, **2**, p.779.

81. K. Henricson and P. Olavi in *Proceedings of the 9th SPCI New Available Technique Conference*, Stockholm, Sweden, 1996, p.790.

82. K. Peter, K.E. Strom and B.R. Swan in *Proceedings of the 9th SPCI New Available Technique Conference*, Stockholm, Sweden, 1996, p.821.

83. D. Davies, T. Dietz and H.U. Suess, *Pulp and Paper Canada*, 2009, **110**, 8, 25.

84. A.S. Jääskeläinen, A.M. Saariano, P. Matousek, A. Parker, M. Towrie and T. Vuorinen in *Proceedings of the 12th International Symposium on Wood and Pulping Chemistry*, Madison, WI, USA, 2003, **1**, p.139.

85. C.L. Filho and H.U. Suess in *Paper Presented at Iberoamerican Congress on Pulp and Paper Research CIADICYP*, Sao Paulo, Brazil, 2002.

86. P. Tsekova, J. Gaidarov, I. Valchev and V. Blyahovski in *Proceedings of the 16th International Symposium on Wood and Pulping Chemistry*, Tianjin, China, **2011**, p.761.

87. K. Ruohoniemi, J. Heiko, I. Laakso, S. Martikainen, V. Väyrynen and J. Jäkärä in *Proceedings of the International Pulp Bleaching Conference*, Helsinki, Finland, 1998, **1**, p.145.

88. J. Jakara, A. Paren and P. Autio in *Proceedings of the 53rd Appita Annual Conference*, Rotorua, New Zealand, 1999, **2**, p.463.

89. Z. Yuan, Y. Ni and A. van Heiningen, *Canadian Journal of Chemical Engineering*, 1997, **75**, 1, 37.

90. Z. Yuan in *Peracetic Acid Bleaching of Softwood Kraft Pulp*, University of New Brunswick, Canada, 1997. [Doctoral Thesis]

91. A.S. Jääskeläinen and K. Poppius-Levlin in *Proceedings of the International Pulp Bleaching Conference*, Helsinki, Finland, 1998, **2**, p.423.

92. E. Bergnor-Gidnert, P.E. Tomani and O. Dahlman, *Nordic Pulp and Paper Research Journal*, 1998, **13**, 4, 310.

93. D.P. Barros, V.L. Silva, H. Hämäläinen and J.L. Colodette, *BioResources*, 2010, **5**, 2, 881.

94. P. Khristova, J. Tomkinson, I. Valchev and I. Dimitrov, *Bioresource Technology*, 2002, **85**, 1, 79.

95. G. Simeonova, I. Valchev and S. Nenkova, *Journal of the University of Chemical Technology and Metallurgy*, 2003, **38**, 1, 151.

96. M. Zavadzki in *Quantified Determination of Quinone Chromophore during ECF Bleaching of Kraft Pulp*, Institute of Paper Science and Technology, Atlanta, GA, USA, 2004. [Doctoral Thesis]

97. I. Valchev, G. Simeonova and V. Blyahovski in *Proceedings of the 15th International Symposium on Wood and Pulping Chemistry*, Oslo, Norway, **2009**, p.287.

98. G.Y. Pan, C.L. Chen, H.M. Chang and J.S. Gratzl, *Journal of Wood Chemistry and Technology*, 1984, **4**, 3, 367.

99. J. Staehelin and J. Hoigné, *Environmental Science and Technology*, 1985, **19**, 12, 1206.

100. J. Gierer, *Holzforschung*, 1982, **36**, 1, 55.

101. Y. Ni, G.J. Kang and A. van Heiningen, *Journal of Pulp and Paper Science*, 1996, **22**, 2, J53.

102. C.A. Lindholm, *Nordic Pulp and Paper Research Journal*, 1990, **5**, 1, 22.

103. B.V. Lierop, R.M. Berry and B.P. Roy, *Journal of Pulp and Paper Science*, 1997, **23**, 9, 428.

104. L. Viikari, M. Rauna, A. Kantelinen, M. Linko and J. Sundquist in *Proceedings of the 3rd International Conference Biotechnology in the Pulp and Paper Industry*, Stockholm, Sweden, 1986, p.67.

105. L. Viikari, M. Rauna, A. Kantelinen, M. Linko and J. Sundquist in *Proceedings of the 4th International Symposium on Wood and Pulping Chemistry*, Paris, France, 1987, **1**, p.151.

106. L. Viikari, A. Kantelinen, J. Sundquist and M. Linko, *FEMS Microbiology Reviews*, 1994, **13**, 2–3, 335.

107. C. Deneault, C. Leduc and J. L. Valade, *TAPPI*, 1994, **77**, 6, 125.

108. M. Davis, B. Rosin, L.L. Landucci and T.W. Jeffries in *Proceedings of the TAPPI Biological Science Symposium*, San Francisco, CA, USA, 1997, p.435.

109. J. Buchert and L. Viikari, *Paperi Ja Puu – Paper and Timber*, 1995, **77**, 9, 582.

110. G. Simeonova, R. Sjödahl, M. Ragnar, M. Lindström and G. Henriksson, *Nordic Pulp and Paper Research Journal*, 2007, **22**, 2, 172.

111. I. Valchev and P. Tsekova, *Appita Journal*, 2010, **63**, 1, 53.

112. I. Valchev, L. Yotova and E. Valcheva, *Bioresource Technology*, 1998, **65**, 1, 57.

113. E. Valcheva, S. Veleva, I. Valchev and I. Dimitrov, *Reaction Kinetics and Catalysis Letters*, 2000, **71**, 2, 231.

114. E. Valcheva, I. Valchev and L. Yotova, *Biochemical Engineering Journal*, 2001, **7**, 3, 223.

115. I. Dimitrov, I. Valchev and E. Valcheva, *Biocatalysis and Biotransformation*, 2005, **23**, 1, 33.

116. J. Osiadacz, A.J. Al-Adami, D. Bajraszwska, P. Fisher and W. Peczynska-Croch, *Journal of Biotechnology*, 1999, **72**, 1–2, 141.

117. P. Widsten and A. Kandelbauer, *Enzyme and Microbial Technology*, 2008, **42**, 4, 293.

118. A. Potthast, I. Rosenau and K. Fisher, *Holzforschung*, 2000, **55**, 1, 47.

119. C. Crestini and D.S. Argyropoulos, *Journal of Agriculture and Food Chemistry*, 1997, **45**, 4, 1212.

120. K.J. Poppius-Levin, T.L. Tamminen and A. Kalliola in *Proceedings of the 219th ACS National Meeting*, San Francisco, CA, USA, 2000, p.149.

121. S. Camarero, D. Ibarra, A.T. Martinez, J. Romero, A. Gutierrez and J.C. del Rio, *Enzyme and Microbial Technology*, 2007, **40**, 5, 1264.

122. E. Valcheva, S. Veleva, Gr. Radeva and I. Valchev, *Reaction Kinetics and Catalysis Letters*, 2003, **78**, 1, 183.

123. I. Valchev, G. Radeva and E. Valcheva, *Journal of the University of Chemical Technology and Metallurgy*, 2005, **40**, 2, 107.

4 Oxygen Bleaching

Jorge Luiz Colodette and Daniela Correia Martino

4.1 Introduction

Oxygen bleaching, also known as oxygen delignification, is a technology that uses oxygen and alkali under pressure to remove residual lignin from lignocellulosic pulp. The fraction removed from the unbleached pulp corresponds to between 25–65% of the residual lignin. The first industrial installation was launched in South Africa in 1971, based on a successful pilot plant operated in 1968 [1]. The oxygen delignification stage (O-stage) was developed to decrease the environmental impact caused by the effluents from the bleach plant and specifically, regarding the so-called chlorinated organic compounds. This stage is also considered an extension of the pulping process. The oxygen stage has a prebleaching effect, since it promotes both delignification and bleaching. Compared with other oxidising agents used in the bleaching process, oxygen presents low selectivity. Pulps treated with oxygen tend to present low viscosity, but strength is usually not impaired if the stage is run under well-optimised conditions [2]. The oxygen stage allows the pulping process to terminate at a higher Kappa number, thus minimising pulp yield losses, since oxygen delignification is more selective than Kraft cooking at low pulp lignin contents. Furthermore, the oxygen delignification helps to decrease the chemical consumption in subsequent bleaching stages [3]. An advantage of the O-stage is the possibility of reusing its effluent as washing water during brown stock washing. The effluent coming from brown stock washing is sent to the recovery boiler, thus recovering the solids produced in the O-stage. The solid content from O-stage washers is recovered in the brown stock washers (**Figure 4.1**).

For eucalyptus pulps, which usually contain high amounts of hexenuronic acid groups (HexA), the O-stage presents low efficiency, since the oxygen does not react with these groups [4].

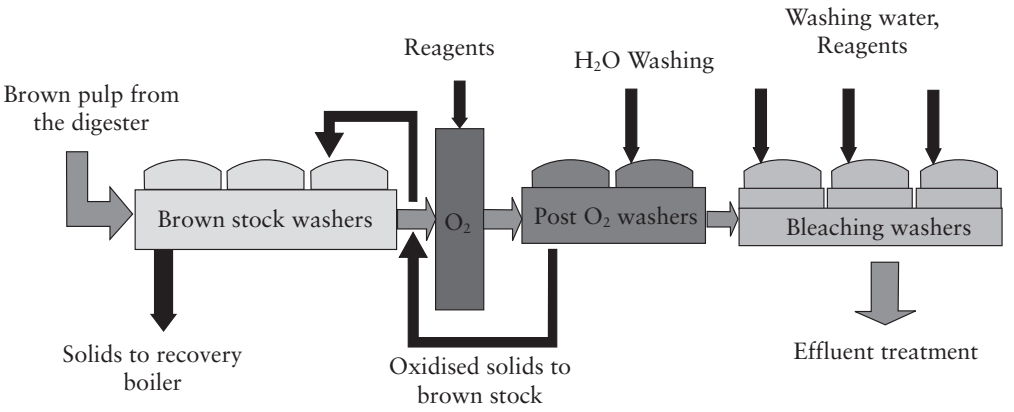

Figure 4.1 Scheme of the brown stock area showing the oxygen delignification stage, with its filtrate being reused for brown stock washing

4.2 Advantages and Disadvantages of Oxygen Delignification

The main advantages of oxygen delignification are improved bleaching effluent quality and decreased bleach chemical costs. The main disadvantages are increased demand for the mill's chemical recovery system, limited selectivity and high capital costs [5, 6]. The implementation of an oxygen delignification stage, ahead of elemental chlorine free (ECF) or standard bleaching processes, reduces the need for chlorine-based oxidants in the bleach plant and, as a consequence, less chlorinated organic compounds are formed. This results in lower quantities of adsorbable organic halides (AOX) in the bleaching effluent and less organic halides in the bleached pulp.

The possibility of recirculating the effluent generated in the oxygen delignification stage to the recovery system has a significant effect on the organic load released in the subsequent bleaching operation. The recovery of such effluent, which otherwise would be released in the bleach plant, reduces the environmental impact related to colour, biological oxygen demand (BOD), chemical oxygen demand (COD) and toxic compounds found in the bleach plant effluents [2]. In addition, the minimisation of the demand for oxidising agents such as chlorine, chlorine dioxide and ozone, allows for a reduction in operational costs. This is due to the fact that the O-stage requires only oxygen and oxidised white liquor to perform the reaction, and these chemicals are of low cost [6].

One disadvantage of oxygen delignification is the potential for overloading the plant chemical recovery system, since the oxidised white liquor, used as the alkali source,

requires additional causticising capacity. Moreover, the solids coming from the O-stage can also bottleneck the evaporation plant and recovery boiler. Another inconvenience of oxygen delignification is its low selectivity towards pulp carbohydrates, in relation to chlorine dioxide delignification, for example. This limits the amount of delignification that can be achieved during such a stage. If delignification is not terminated at the proper Kappa number in the O-stage, severe carbohydrate degradation may occur. The degradation is caused by transient species such as hydroxyl, hydroperoxyl and superoxide anion radicals, which may lead to low viscosity pulps with impaired strength properties [2, 7].

4.3 Oxygen Production

Oxygen is generated through cryogenic and noncryogenic processes. The latter processes include the so-called PSA, VSA and VPSA technologies, where V, P, S and A stand for vacuum, pressure, swing and adsorption, respectively. Cryogenic oxygen is usually produced in large, dedicated plants and is of high purity (>99%), while the noncryogenic oxygen is produced in small, on-site plants and is of low purity (90–95%) [8]. During the cryogenic method, the air is compressed and freed from vapour, dust and carbon dioxide. Subsequently, the air is refrigerated to extremely low temperatures; it is then compressed into a liquid state and fractionated by distillation in which oxygen, nitrogen and other gases are separated. When refrigerated at -183 °C, the oxygen is liquefied and can be stored in stationary tanks. This process, based on distillation, consists of six steps: first, the air passes through a filter for dust removal and is then compressed (18 MPa). Afterwards, the air goes through an oil separator and screen where the water vapour and carbon dioxide are eliminated. In the next step, the purified gas is refrigerated to -30 °C using a heat exchanger. In the distillation column, the gas mixture is comprised mostly of gaseous oxygen and gaseous nitrogen. In the fourth step, the air goes through an expansion machine where it is depressurised from 18 to 0.6 MPa and the temperature is simultaneously reduced to -155 °C, thus becoming liquefied gas. The gas then travels to the distillation column where it is fractionated according to the boiling point of its components and turned into liquid oxygen, liquid argon and liquid nitrogen. The cold gases are heated by a heat exchanger, while the liquid oxygen, liquid argon and liquid nitrogen are fed into different tanks [8].

The most commonly used processes for producing on-site oxygen are the PSA and VSA. The PSA process was developed in the 1950s, but has only been used since the 1970s for commercial production. In this process, the air passes through a molecular sieve of large surface area consisting of small zeolite particles containing large quantities of micropores [8]. Zeolites are aluminium silicate minerals with complex crystal structures made from rings of silicon, aluminium and oxygen ions

interbonded. The chemical composition of the zeolite used for oxygen separation is $Na_{12}[(AlO_2)_{12}((SiO_2)_{12}].27H_2O$. In this form, the mineral is selective towards nitrogen adsorption. The zeolite used in oxygen production has the shape of a cube with holes on each side forming a cage. The sides of the cube forming this structure are made up of SiO_2 and AlO_2. The cations (Na) are exposed through the crystal structures [9, 10].

Adsorption characteristics differ among gases. When nitrogen is close enough to the cations exposed on the zeolite crystal, an induced dipole is formed and the nitrogen is attracted to the zeolite. Nitrogen is more polarisable than oxygen; hence, it is adsorbed by the zeolite while the oxygen passes through it. The internal surface area of the zeolite is high and provides a high degree of adsorption by zeolite volume. In the PSA process, the pressure varies between 0.01 and 0.7 MPa [8–10].

In the VSA process, a vacuum is used for the regeneration of the adsorbent bed and pressure varies between 0.003 and 0.15 MPa. This process can also be referred to as VPSA. In the VPSA system, the absorbents are filled with a bottom layer which removes humidity and carbon dioxide from the injected air, while the upper layer removes nitrogen. Therefore, the oxygen passes through the adsorbent layer along with the argon. The oxygen production is finalised when the upper layers of the absorbents are saturated with nitrogen and the oxygen purity decreases [8]. Each VPSA system has a rotating air blower, a vacuum system (two-bed system), one or two adsorbent vessels, an oxygen tank, two switching valves and a controller. In the one-bed system, the blower draws air, compresses it and sends it to the adsorbent vessel in order to remove the impurities (oxygen purity of 90–94%). The adsorbent is then regenerated and the blower removes the gas by pressure reduction inside the vessel. The residual gas (N_2, H_2O and CO_2) is discharged into the air. Since oxygen is not produced during the regeneration stage, this system includes a low-pressure tank which allows a continuous oxygen supply. In the two-bed system, there is a similar adsorption cycle which is based on the pressure variation of each bed, from adsorption to desorption. Therefore, the beds produce oxygen in one tank, assuring that the product is continuously available at a consistent pressure with high purity [11].

4.4 Delignification Chemistry

4.4.1 Lignin Reactions

The reactions of lignin during pulping and bleaching processes can be divided into two categories, according to the general delignification concept. During pulping, the delignification occurs exclusively *via* nucleophilic reactions, while during the bleaching process, it is initiated primarily by electrophilic reactions which may be followed

by a nucleophilic attack [2, 12, 13]. During oxygen delignification, the molecular oxygen may be converted into a myriad of species that present different reactivities towards the lignin functional groups. The reduction of molecular oxygen advances through four electrons, one by one, or two by two [14]. Some reactions may occur by the species produced during oxygen reduction, with or without the participation of transition metal ions [15].

Hydrogen peroxide is present during oxygen delignification. This means that both hydrogen peroxide and oxygen act cooperatively in the chemistry of delignification. The hydroxyl radicals ($OH^{\bullet}$) and the oxygen biradicals ($^{\bullet}O_2^{\bullet}$) are electrophiles, while the hydroperoxide anions (HOO^{-}) and superoxide radical anions ($^{\bullet}O_2^{-}$) are nucleophiles [15, 16]. Hence, the electrophilic species will react in the centres of the high electron density regions in the lignin and the nucleophiles in the low electron density regions. **Figure 4.2** shows the general reaction of oxygen with a lignin substructure containing a free phenolic hydroxyl group [17]. This reaction leads to ring opening and the formation of dicarboxylic acids, such as muconic acid, with the simultaneous production of hydrogen peroxide and highly reactive free radical transients, such as hydroxyl ($OH^{\bullet}$), superoxide ($^{\bullet}O_2^{-}$) and methanol. The lignin residues containing muconic acid-type groups are much more soluble in alkali than the original unoxidised lignin moiety.

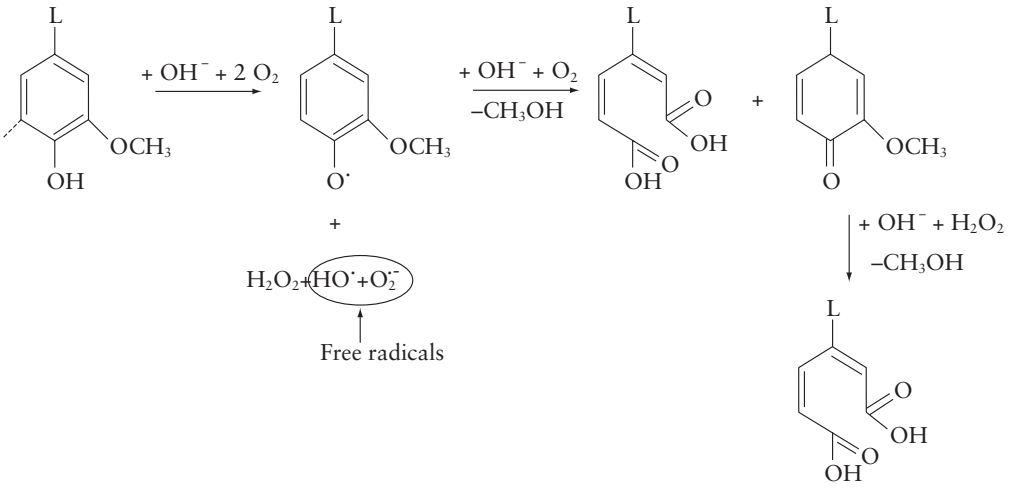

Figure 4.2 Oxidative cleavage of the lignin aromatic ring during oxygen delignification

Under high pressure and alkaline conditions, the lignin phenolic hydroxyl group is deprotonated to produce the phenolate anion, which provides the electron density required to initiate the transference of one electron. The first step in the oxidative degradation of phenolic units is the abstraction, by the biradical oxygen, of one electron from the phenolate anion (high electron density) converting it into a phenoxyl radical and its various mesomeric forms, while the biradical oxygen is converted into superoxide anion radicals ($^{\bullet}O_2^{-}$), which can be protonated giving rise to hydroperoxyl radicals ($HOO^{\bullet}$). The superoxide and hydroperoxyl radicals are strong oxidants and react faster with the lignin units than the molecular oxygen. They attack lignin at the sites of high electron density, producing hydroperoxide cyclohexadienone intermediates. As a side and undesirable reaction, coupling of two phenoxyl radicals at the ring C5 position may occur, thus producing a condensed biphenyl lignin structure, which may be further oxidised to aromatic and aliphatic acids (**Figure 4.3**) [14–16, 18–22]. The hydroperoxide cyclohexadienone radicals may undergo demethoxylation, ring opening and side chain elimination [18].

A study on oxygen delignification kinetics indicated that the reaction between the superoxide anion radical and the phenoxyl radical occurs preferentially at the C3 position of the aromatic ring [24]. These authors have used a model previously proposed [25] to explain the kinetic results (**Figure 4.4**). Other intermediate phenoxyl radicals were proposed in the C1 and Cβ positions of the aromatic ring (**Figure 4.4a**) [6]. These three structures are part of the same resonance structure in which the electron is located in each of the three carbon positions. In **Figure 4.4b**, the reaction leads to both muconic acid and methanol or *ortho* quinone and methanol. Assuming that the hydroperoxide anion is the dominant species at pH > 12–13 (pKa 12–13) and on the basis of the kinetic data, it has been concluded that the carbon at position C3, in the aromatic ring of the lignin, is the most active site for oxygen delignification.

The efficiency of oxygen delignification is affected by the nature of the residual lignin [7]. Among the main lignin chemical characteristics, the most relevant are their content of free phenolic hydroxyl groups and biphenyl substructures, molecular weight and content of lignin-carbohydrate linkages. While a high content of free phenolic hydroxyl groups dramatically favours oxygen delignification efficiency, the presence of biphenyl-type substructures and lignin-carbohydrate complexes slow it down [26]. Lignin fragments of low molecular weight are easier to remove during oxygen delignification [7]. The type of lignin available during oxygen delignification is strongly influenced by pulping conditions and wood raw material.

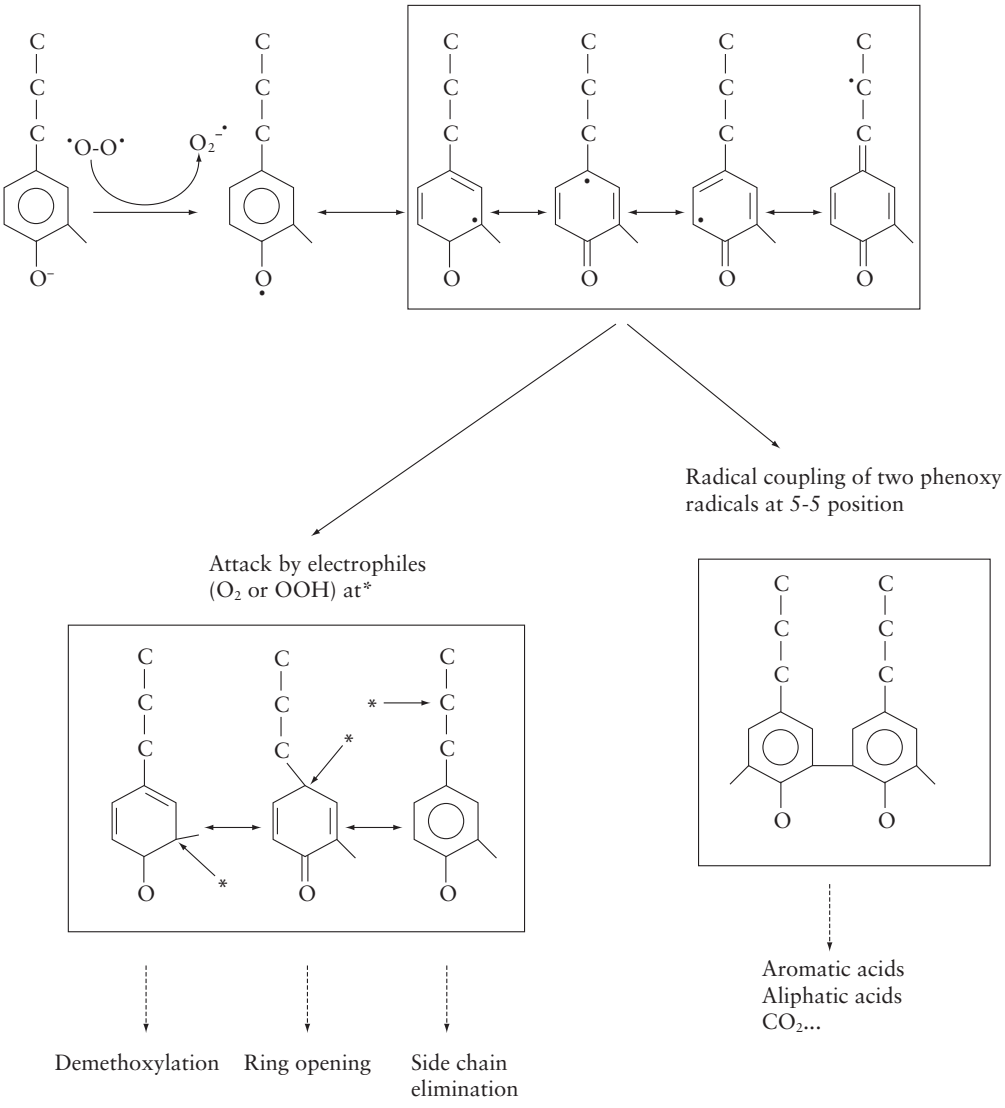

Figure 4.3 Major reactions of free phenolic hydroxyl groups with free radicals during oxygen delignification. Adapted from F. Asgari and D.S. Argyropoulos, *Canadian Journal of Chemistry*, 1998, 76, 1606 [23]

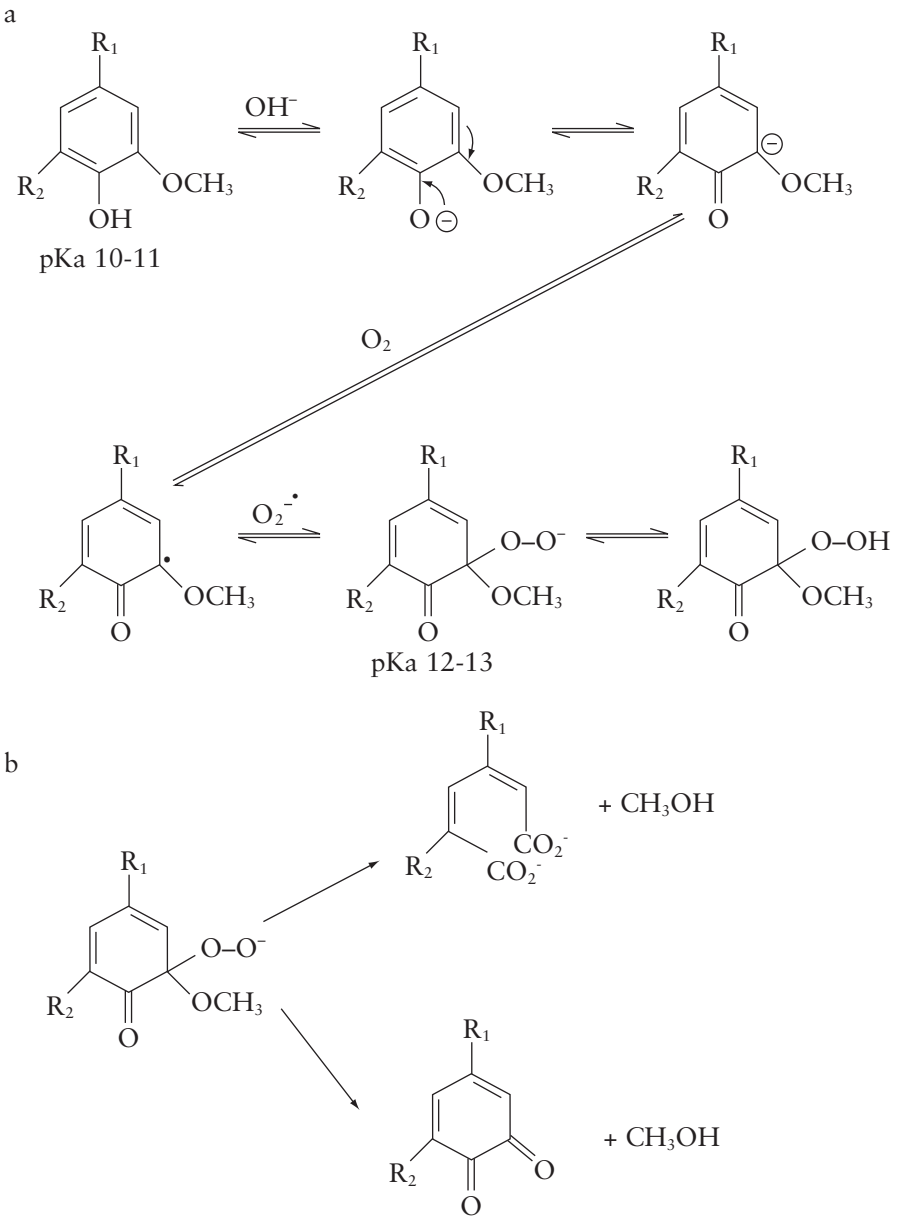

Figure 4.4 Mechanism for the reaction of lignin during oxygen delignification, assuming the C3 of the aromatic ring as the reactive site. Adapted from H. Chang and J.S. Gratzl, *Chemistry of Delignification with Oxygen, Ozone, and Peroxides*,Uni Publishers Co. Ltd, Tokyo, Japan, 1980, p.151 [25]

4.4.2 Carbohydrate Reactions

The attack of carbohydrates during oxygen delignification is more intense compared with that of the chlorine dioxide and alkaline extraction stages, for example. For that reason, the amount of delignification in the O-stage is limited [6]. The reactions of the wood carbohydrates during the alkaline treatment with oxygen can be divided into three categories: i) peeling reactions or endwise depolymerisation, ii) stabilisation of the reducing end groups and iii) cleavage of the polysaccharide chains [27]. Although the peeling reactions are the most important reactions during pulping, they are irrelevant during the oxygen stage. Under oxidative conditions, any reducing end group in the polysaccharide chain will be rapidly oxidised to aldonic acid groups, thus preventing the endwise depolymerisation. Studies have shown that the extension of peeling reactions in the carbohydrates is low in the O-stage [28]. In the presence of oxygen, the peeling reaction rate is higher in xylan than in cellulose and glucomannan, with the opposite occurring in the absence of oxygen [28–30].

Cellulose degradation during oxygen delignification is caused by the attack of free radicals on the sugar units. These radicals are produced by the reaction of oxygen species with the phenolic hydroxyl groups of the lignin [24]. The reduction of the degree of cellulose polymerisation during the oxygen stage is due to the oxidation of one or more hydroxyl groups in the cellulose chain, forming carbonyl groups. Due to alkaline conditions, the elimination reaction occurs *via* oxidative cleavage of the long chains into short chains (**Figure 4.5**). Each one of these new short chains will contain a new reductive end group, but thanks to the oxidative conditions, the terminal depolymerisation reaction will not occur to any great extent because the reducing end groups are stabilised into acid groups.

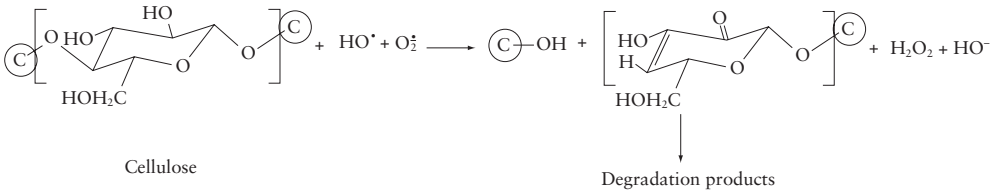

Figure 4.5 Oxidative cleavage of a cellulose chain caused by free radicals

Oxygen attacks cellulose chains both in the crystalline and amorphous regions. A mechanism for crystallinity changes in the cellulose chain during oxygen delignification

has been proposed [31]. The first observation was a rapid initial increase in the crystallinity due to the removal of the amorphous cellulose, which is easily accessible. This depends on the alkalinity of the liquor, but is independent of the gas used (O_2 or N_2) and the type of fibre. The peeling reaction in the amorphous cellulose chain increases the crystallinity/amorphous ratio of the fibres, as the carbohydrate fragments are removed/solubilised [31]. The rapid reduction of crystallinity is a result of direct oxidation caused by oxygen or related radicals. The random cleavage of the glycosidic bonds on the surface of the crystallite, where there are some possible defects in the crystalline structure, allows the penetration of chemical reagents. An attack results in the cellulose chain being gradually 'deglued' from the crystallite. This phenomenon occurs as the intramolecular hydrogen bonding is weakened by the oxygen and the alkali-induced swelling of cellulose [32, 33].

4.4.3 The Role of Hexenuronic Acids in Oxygen Delignification

During alkaline pulping, 4-O-methyl-α-D-glucuronic acid groups react with alkali to form HexA. Thus, hexenuronic acids may be loosely defined as a product of alkaline cooking and its magnitude in the pulp depends upon the amount of 4-O-methyl-α-D-glucuronic acid originally present in the raw material, and the way the alkaline cooking is conducted [34]. HexA contains a double bond which reacts readily with common bleaching chemicals and the $KMnO_4$ used in the Kappa number analysis. Therefore, the Kappa number cannot be used as a true measure of residual lignin in pulps which contain significant amounts of HexA. There are several methods for quantifying pulp HexA and the results are usually expressed in mmoles of HexA per kg of pulp. This unit can be converted into Kappa number by conversion factors that vary in the range of 9.6–11.9 mmoles HexA/ kg pulp per Kappa unit, depending on the method used for HexA quantification [34]. The presence of HexA groups is not of much concern for unbleached pulp grades, but can be significant for bleached pulp grades as they react with electrophilic bleaching chemicals including chlorine, chlorine dioxide and ozone, among others [34]. However, the HexA groups do not react with nucleophilic oxidants which operate under alkaline conditions, such as oxygen and hydrogen peroxide [34]. Currently, the most cost-effective technology to remove HexA is through the so-called hot acid hydrolysis stage [34].

Oxygen delignification has been implemented in a single or double stage. For eucalyptus pulps, which contain significant amounts of HexA, the second stage is rather ineffective. After being treated in the first oxygen stage, the pulp contains very little lignin, with the remaining Kappa number being comprised mostly of HexA, which are unreactive towards oxygen. The second oxygen stage has little impact on Kappa number because the remaining lignin quantity is small and well distributed in the cell wall. However, the second stage improves brightness, which is a useful

asset ahead of the bleaching sequence. The results shown in **Table 4.1** for samples A (high HexA) and B (low HexA), respectively, illustrate the point. Sample B has a low HexA content and benefits from a second oxygen stage, but sample A has a very high HexA content and benefits little from a second stage. The double-stage process is in fact very well suited for softwoods since the Kappa number, after the first oxygen stage, is still quite high and comprised mostly of lignin. For hardwoods, the use of a second oxygen stage is always questionable and depends significantly on the *true* lignin content of the pulp. Since HexA is accounted for in the Kappa number measurement it can be considered as a *false* lignin [35].

Table 4.1 Single (O) *versus* double (O/O) stage oxygen delignification for two well-washed and dichloromethane-extracted eucalyptus Kraft pulp samples containing different amounts of hexenuronic acids

Pulp characteristics before and after oxygen delignification	Sample A			Sample B		
	Brown	O	O/O	Brown	O	O/O
Total Kappa number	17.2	11.7	11.2	17.4	10.8	9.5
Lignin-derived Kappa number	9.9	4.6	4.0	15.1	8.8	7.5
Hexenuronic acid-derived Kappa number	7.3	7.1	7.2	2.3	2.0	2.0
Viscosity, dm^3/kg	1335	1157	1045	1200	1053	988
ISO brightness, %	36.4	51.4	53.4	29.8	48.8	52.5
Kappa reduction in O-stage, %	-	32.0	34.9	-	37.9	45.4
Viscosity reduction in O-stage, dm^3/kg	-	178	290	-	148	347
ISO brightness gain in O-stage, %	-	15.0	17.0	-	19.0	22.7
Yield loss in O-stage, %	-	1.8	2.0	-	2.0	2.2

O: 10% consistency, 100 °C, 45 min, 1.8% O_2, 1.8% NaOH, 0.5 MPa.
O/O: 10% consistency, 100/100 °C, 45/45 min, 1.8/0.9% O_2, 1.8/0% NaOH, 0.5/0.6 MPa.
Adapted from J.L Colodette, C.M Gomes, M.S. Rabelo, K.M.M Eiras, A.F. Gomes and K.D. Oliveira, *TAPPI*, *TJ* Online Exclusive, 2008, p.18A [31]

4.5 Mass Transfer and Reaction Kinetics

The oxygen bleaching rate and its dependence on the process variables, determines equipment size and the choice of optimum process conditions. It is important to

distinguish the physical and chemical phenomena. The physical factors determine the movement of species inside the pulp mass (mass transfer), and the chemical factors regulate the reaction rate between the pulp and the bleaching chemicals once they are in contact with each other (chemical kinetics). It is very important to take into account the mass transfer, since the oxygen bleaching stage is a triphase process. The oxygen needs to cross the gas-liquid interface, diffuse through the liquid film around the fibre, and diffuse into the fibre wall before it reacts with lignin [36]. Diffusion of the oxygen gas through the aqueous film is a determinant for oxygen delignification efficiency, thus making the fluidisation of the cellulose suspension a prerequirement to ensure the good operation of this stage.

The degree of delignification is limited by alkali availability. The removal rate of different lignin types rises with increasing alkali concentration, partial oxygen pressure and temperature. Depending on the conditions and reactor type, the degree of delignification may be determined by the intrinsic chemical reaction rate or by the mass transfer rate of oxygen or alkali to the fibre. If the oxygen and alkali are equally available to all fibres, then the rate of the process is equal to the chemical reaction [37]. While evaluating the effects of oxygen and sodium hydroxide during oxygen delignification, it was found that if only sodium hydroxide or oxygen were used, there was a reduction of three Kappa number units for a given pulp sample. However, a drop of five Kappa units was achieved when both chemical reagents were used together [38]. The lignin degradation proceeds through the phenolate anion, which is produced by the reaction of the hydroxide ion with the lignin phenolic components [39]. Thus, a certain amount of lignin removal by alkali alone should be expected. The reaction of lignin with oxygen requires production of the phenolate anion as a first step and the pKa of lignin phenols (> 10) cannot be met without alkali addition to the pulp.

In order to obtain reasonable delignification rates in the O-stage, a temperature higher than 80 °C is required. Moreover, a lower temperature at the initial phase (5–10 min) favours the selectivity of delignification. If the delignification process occurs in two stages, the temperature should be kept lower in the first stage [1]. At a fixed alkali charge, the Kappa number reduction presents two distinct phases, with the first one being much faster than the second.

In the oxygen stage, both delignification and carbohydrate degradation occurs in two phases: a fast initial phase with high selectivity, followed by a slow and nonselective second phase. This suggests that the selectivity can be optimised by the use of a high alkali charge and oxygen concentration during the initial phase, and by reduction of these two concentrations in the final phase [38]. As shown in **Figure 4.6**, the initial phase of the delignification is more selective when compared with the second phase [40].

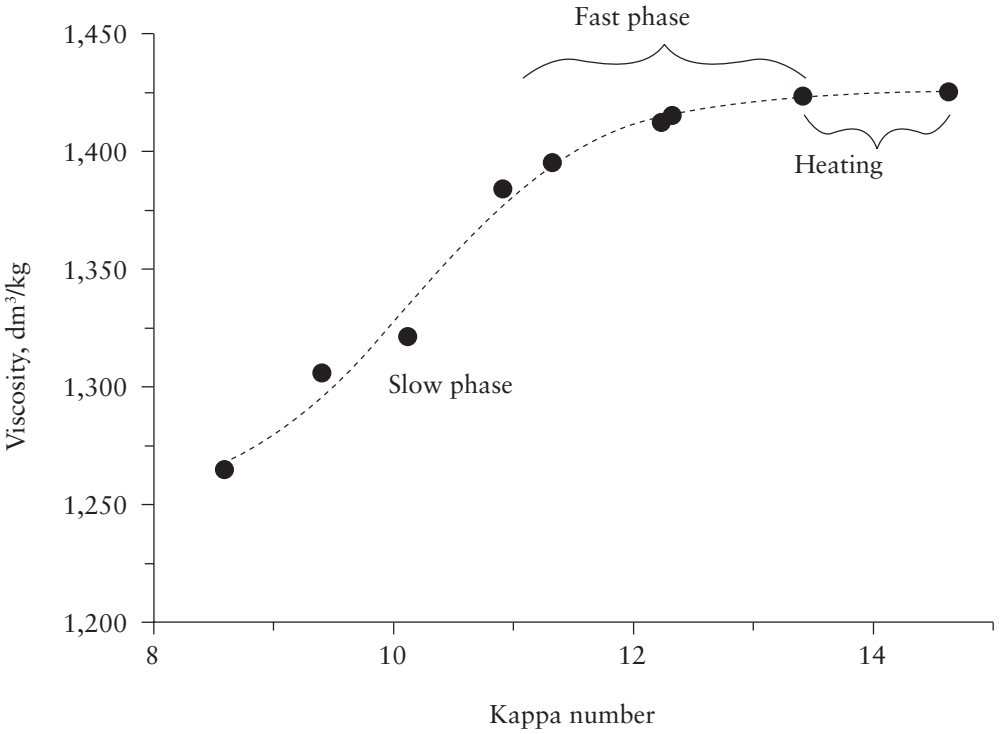

Figure 4.6 Selectivity of the oxygen delignification stage for *Eucalyptus globulus* Kraft pulp. Adapted from M.J.M.C. Barroca, P.J.T.S. Marques, I.M. Seco and J.A.A.M. Castro, *Industrial & Engineering Chemistry Research*, 2001, 40, 24, 5680 [38]

4.6 Oxygen Delignification Technology

Although there are many pulp mills equipped with single-stage oxygen delignification systems of medium or high consistency, the majority of the newer pulp mills operate with double-stage systems of medium consistency [41]. A typical medium-consistency system is shown in **Figure 4.7a**. Pulp discharged from a brown stock washing system (vacuum filter, press, drum displacement washer and so on) is charged with caustic or oxidised white liquor at a 10–14% consistency, preheated in a low-pressure steam mixer, and pumped through one or more medium-consistency gas mixers to an upflow pressurised reactor. Medium-pressure steam and oxygen are added upstream of the medium-consistency mixer or are added directly into it. The reactor bottom may be conical or may have a rotary bottom, and the top is equipped with a discharger.

Medium-consistency reactors operating at atmospheric pressure at the top have been used for delignification of sulfite pulps requiring a relatively small reduction in Kappa number. It has been proposed that atmospheric medium-consistency reactors could also be used with Kraft pulps, particularly hardwood pulps, to obtain a small reduction in lignin content [41].

Figure 4.7b shows a typical high-consistency oxygen delignification system. As the name implies, the pulp is treated at consistencies in excess of 20%, normally in the range of 25% to 28%; a press is used to achieve a consistency of 30%. Fresh caustic or oxidised white liquor is added to the pulp at the discharge of the press. After the press, a thick stock pump transfers the pulp to a fluffer *via* a feed pipe in which a gas-tight plug is formed. The fluffed pulp flows down the pressurised reactor as a loose bed and reacts with oxygen. Steam is injected into the top of the reactor to maintain the temperature. Oxygen gas is added to either the top or bottom of the reactor at a rate required to maintain the oxygen partial pressure. The reacted pulp is diluted with post oxygen filtrate to about 6% consistency and is discharged to a blow tank where small amounts of dissolved gases are released. At the top of the reactor, the pressure is controlled by relieving the gas from the head space. This relief is necessary because inert gases enter the reactor with the pulp, filtrate and oxygen, and because the combustible gases (CO, CH_4, CH_3CH_2OH) which are formed in the reactor must be maintained at safe levels. To reduce oxygen consumption, a portion of the vented gases may be recycled to the reactor *via* a catalyst which converts the combustibles to water and carbon dioxide [41].

Pulp consistency affects the sodium hydroxide concentration and the costs associated with pumping. An increase in pulp consistency results in a reduction in the distance of diffusion and an increase in the alkali concentration, thus increasing the delignification rate. **Table 4.2** presents typical operating data for the high- and medium-consistency oxygen delignification of softwood Kraft pulp. The major differences between the two processes relate to the degree of delignification and steam, alkali, oxygen and power consumption [41]. In spite of its slightly better delignification efficiency, the high-consistency process has become obsolete. No high-consistency systems have been installed worldwide since the early 1990s. The major reasons for the obsolescence have been the high capital cost of installation and the significant maintenance costs. The technology of choice nowadays is the medium-consistency process, particularly in two stages, without interstage washing.

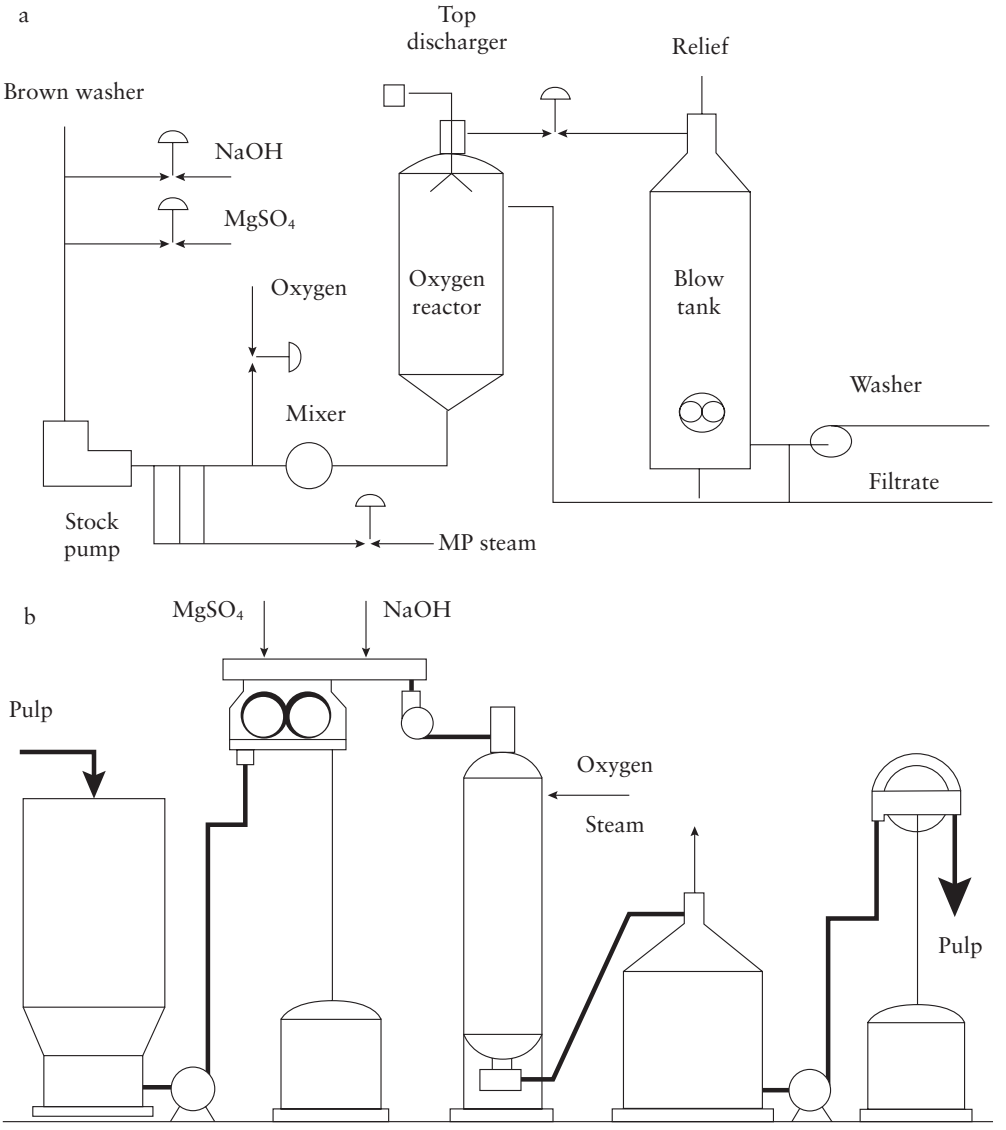

Figure 4.7 Medium- (a) and high- (b) [42] consistency oxygen delignification systems. Adapted from T. McDonough in *TAPPI Bleach Plant*, TAPPI Press, Atlanta, GA, USA, 2012 [42]

Table 4.2 Typical operating data for the oxygen delignification of softwood Kraft pulp at high and medium consistency			
Process parameters	**Unit**	**Consistency, %**	
		High	**Medium**
Pulp consistency	%	25–28	10–12
Kappa reduction across stage	45%	45–50	40-–5
Reaction time	min	30	50–60
Start temperature	°C	100–105	100–105
Pressure IN	MPa	0.5–0.6	0.7–0.8
Pressure OUT	MPa	0.5–0.6	0.45–0.5
Low-pressure steam (0.45 MPa)	kg/o.d.t	-	77.8
Medium-pressure steam (1.14 MPa)	kg/o.d.t	83–111	200–300
Evaporator steam (0.45 MPa)	kg/o.d.t	33–55	90–100
Power consumption	kW.h/o.d.t	44–55	35–45
Alkali consumption	kg/o.d.t	23–26	28–31
Oxygen consumption	kg/o.d.t	22–27	22–27
Magnesium ion	kg/o.d.t	0.55	0.55
Adapted from L. Tench and S. Harper, *TAPPI*, 1987, **70**, 11, *55* [37]			

4.6.1. Double-stage Medium-consistency Oxygen Delignification Systems

Medium-consistency oxygen delignification has been implemented in one or two stages. There are two main types of double-stage oxygen delignification systems, namely: (1) two serial full vertical reactors (OxyTrac™ process) and (2) one pipeline reactor followed by a vertical reactor (DUALOX® Enhanced Process). **Figure 4.8a** shows the OxyTrac™ system, which mirrors the kinetics of oxygen delignification. The basis of the process is that the delignification rate is much higher than the cellulose degradation rate during oxygen delignification. On the other hand, delignification in the initial phase is more dependent on the alkali and oxygen concentration than is the cellulose degradation. The delignification is thus favoured by a high chemical concentration. At the same time, the cellulose degradation is favoured by high alkali concentration at high temperature. The cellulose degradation can be avoided by keeping the temperature at a relatively low level in the first stage. In the second stage, where the final delignification takes place, increased temperature and retention time favours the process selectivity since the alkali concentration is low. In order to maintain adequate

selectivity it is better to extend the time rather than to increase the temperature. There is no improvement of the selectivity by changing the chemical concentrations, but an alkali concentration high enough to avoid significant reprecipitation of lignin is required. The split of oxygen charge between the two stages improves delignification selectivity mainly due to improved mixing. For softwood Kraft pulps, the first reactor operates at temperatures of 80–85 °C, which usually means that the pulp has to be cooled to proceed to the first stage. The total doses of alkali and oxygen are charged to the first reactor, where a pressure of 8–10 bars is maintained at the top of the reactor. With the high pressure, more oxygen is dissolved in the liquor to give a higher concentration of oxygen. At a higher pressure, the gas volume at a given charge of oxygen in a kg/t of pulp is smaller. This facilitates the mixing and decreases the risk of gas channelling in the reactor. The second reactor operates with a longer retention time than the first reactor, since the rate of delignification is slower at the end. To have a reasonable retention time of about an hour, the temperature of the second reactor is usually higher than that of the first reactor. A pressure of about 3 bars is required in the top of the second stage reactor.

Under extended oxygen delignification conditions, where the Kappa number may be reduced by as much as 20 units, both the alkali and the oxygen charges are rather high. This means that efficient mixing before the first stage is very important. The chemical charges are affected by raw material, incoming Kappa number and washing technology preceding the O-stage. For a softwood pulp, a typical value for the alkali charge is about 2–2.5 kg NaOH/Kappa unit removed in the O-stage. The oxygen charge will not exceed 25–30 kg/t pulp, as this is the maximum oxygen charge that can actually be dissolved under normal operating conditions. Magnesium sulfate is usually added in the O-stage with the sole purpose of protecting cellulose degradation and is mostly used for softwood pulps. For hardwood pulps, the NaOH charge factor per Kappa unit removed is usually somewhat higher, 2.4–3.0 kg/t pulp [43, 44]. The degree of delignification achieved using a hardwood pulp is much lower than when using a softwood pulp. The two major factors explaining this fact are the lower out-of-digester Kappa and the high content of HexA in hardwood pulps. In other words, hardwood pulps contain much less *true lignin* than softwoods when they enter the O-stage. The low level of delignification achieved with hardwood pulps minimises the need for using magnesium salts in the O-stage, since cellulose degradation is proportional to the level of delignification in the O-stage.

In the second case, the DUALOX® enhanced oxygen delignification process comprises two reactors with very different reaction conditions regarding retention time, reaction temperature and pressure, thus explaining the word ‘dual’ in the name (**Figure 4.8b**). With this process concept, the main reactor is complemented with a small prereactor, preferably in the form of a thick pipe with a retention time of five minutes. The process design is based on a thorough understanding of the fundamental concepts

of oxygen delignification kinetics [45]; to achieve the maximum delignification rate, the intermediate mixer, as well as the pump, are the key features. This intermediate pump makes the operation at a high pressure in the main reactor feasible, which is an important condition considering the long retention time of this reactor. The benefits of this technology compared with the single-stage process includes: extended oxygen delignification, more selective delignification, simple design and flexibility to choose the pressure and temperature in both reactors. The pulp is fed with a pump. Sodium hydroxide or, more frequently, oxidised white liquor is added to the pulp prior to the pump. A small amount of oxygen is added and thoroughly mixed into the pulp suspension in a mixer positioned after the pump; in the alkaline environment, oxygen forms a stable gas dispersion with the pulp. The mixture enters the prereactor as a plug flow, while the oxygen is continuously consumed in reactions with the lignin in the pulp. After leaving the prereactor, the pulp enters a second pump, where the pressure is increased to a high level. After the pump, the pulp is further treated in a second mixer, where the main portion of oxygen is added, together with medium-pressure steam, to increase the temperature before entering the second larger reactor. The pulp leaves the second reactor and enters a blow tank, which also serves as a stand pipe for a pump. Upon leaving the reactor, the pressure in the pulp flow is released and at the same time the temperature is maximised to the atmospheric boiling point of the suspension. Flash steam and residual gases are vented out. The pulp is fed by a pump to the subsequent washing stage.

In general, double-stage oxygen delignification processes are very appropriate for softwood pulps because the Kappa number after the first oxygen stage is still high and largely comprised of lignin. For hardwood pulps, containing significant amounts of HexA, the second stage is less efficient than in the case of softwoods, and has a low impact on Kappa number as the remaining lignin is very scarce and well distributed in the cell wall. After being treated in the first oxygen stage, the lignin content of the pulp is low and the major part of the Kappa number consists of HexA, which do not react with oxygen [34]. The second oxygen stage improves pulp brightness even in pulps containing large amounts of HexA [48]. It is important to emphasise that even for HexA-rich hardwood pulps, such as those obtained upon Kraft pulping of eucalyptus wood, the development of oxygen delignification technology has centred on the evolution of two-stage systems for increased degrees of delignification. One of the drivers for this is the desire to increase pulp yield, by terminating the Kraft cook at a higher than normal Kappa number, and using the more selective oxygen stage to complete the delignification to Kappa numbers at which other bleaching agents can take over. This is exemplified by work [35] which illustrates the superior selectivity of oxygen delignification relative to that of Kraft pulping. The yield benefit of stopping the cook at Kappa 19 instead of 15.5 and following the delignification with oxygen was 2–2.5%. Furthermore, the study clearly demonstrated that the Kappa number entering the bleach plant is not greatly affected by the out-of-digester Kappa number,

since the oxygen delignification efficiency is much higher for the higher Kappa pulps. Similar trends have been observed by other workers in connection with softwood pulps [43].

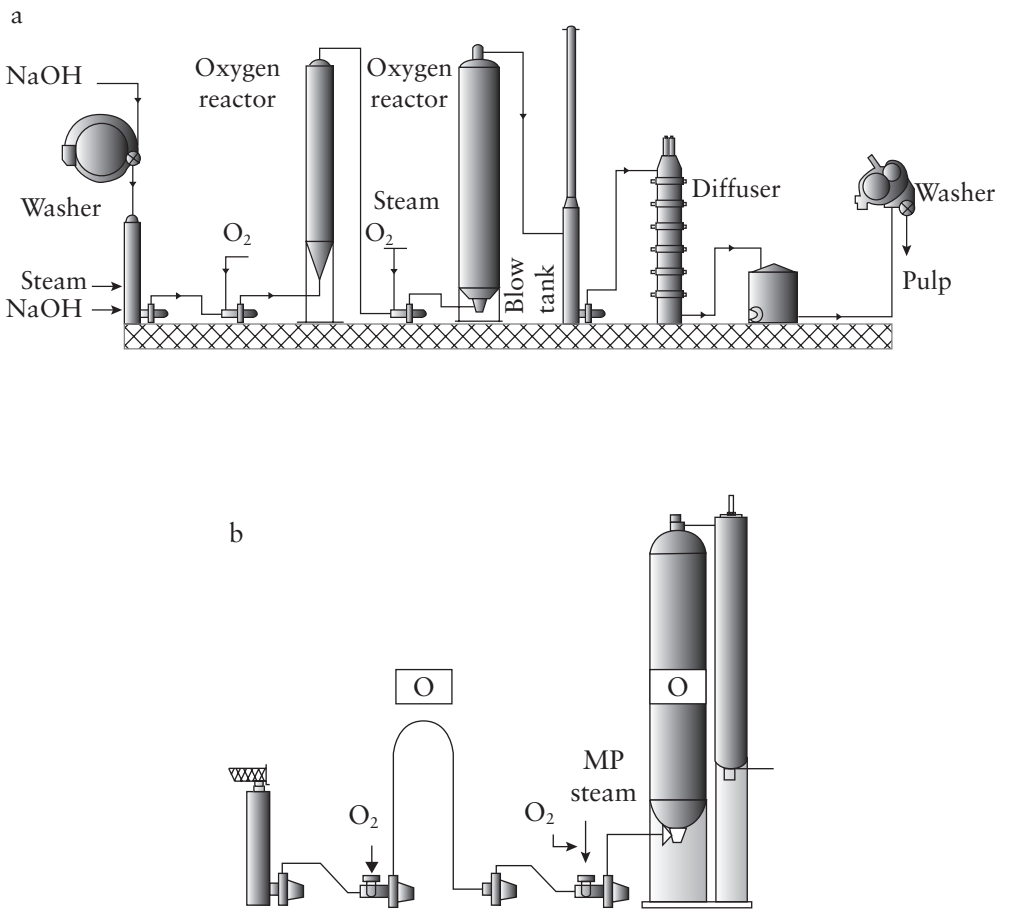

Figure 4.8 Two-stage oxygen delignification systems: a) OxyTrac™ process [46] and b) DUALOX® enhanced oxygen delignification process [47]. Adapted from Ineris, *Techniques to consider in the determination of BAT,* 2012 [46] and Flowtec, *Pulp and Paper Industry/GL&V - Chemical Pulping/Oxygen Delignification*, 2012 [47]

4.7 Process Variables

4.7.1 Pulp Washing

The dissolved solids entering the O-stage derive from two sources: (1) the black liquor carried over from the cooking and (2) the filtrates carried back from the post oxygen delignification washers. Studies have shown that the carry-back from post oxygen washers does not significantly influence the performance of the oxygen delignification. On the other hand, the carry-over from cooking liquor reduces the overall efficiency of the O-stage significantly. As shown in **Figure 4.9**, at a given COD level, the carry-over from cooking is more detrimental to the O-stage delignification efficiency than the carry-back from post oxygen washer filtrates [49].

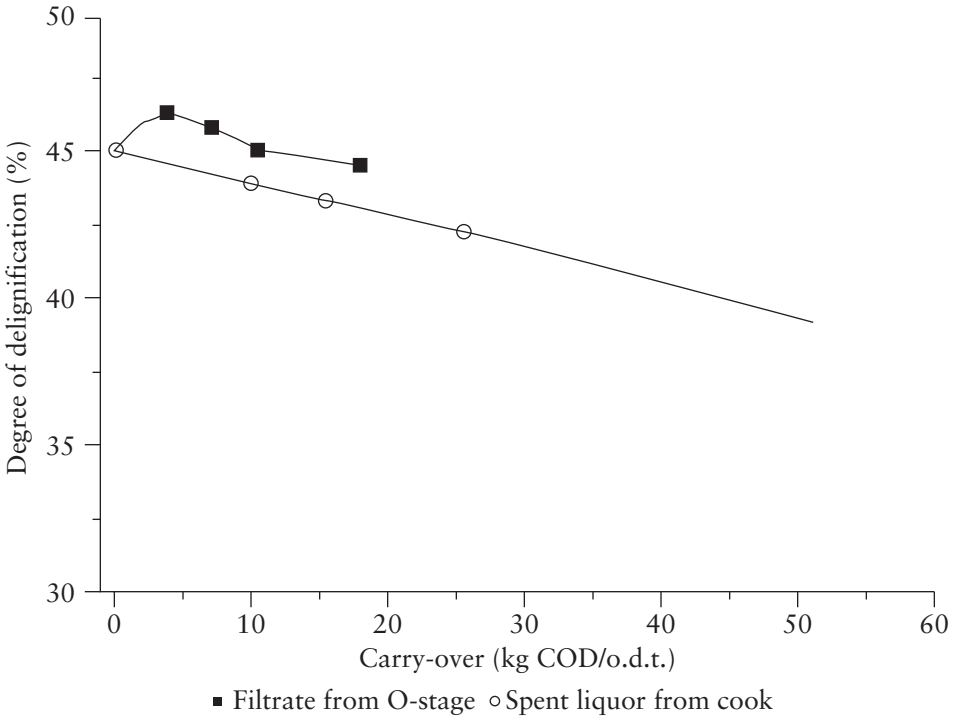

Figure 4.9 The influence of cooking liquor carry-over and post oxygen washer filtrate carry-back on oxygen delignification efficiency. Adapted from J.F. Iijima and H. Taneda, *Journal of Pulp and Paper Science*, 1997, 23, 12, J561 [49]

It has been indicated that there is an increase in active chlorine consumption of 0.085% for each COD unit carried over to the oxygen delignification stage. In other words, efficient washing around the oxygen delignification stage is necessary for cost-efficient bleaching [48].

4.7.2 Incoming Kappa Number

The oxygen delignification performance is significantly affected by the incoming Kappa number from the digester. To a certain limit, pulps of higher Kappa numbers perform better during oxygen delignification. At higher Kappa levels there is more lignin accessible to react with oxygen, which enhances the overall Kappa drop across the stage, particularly considering the mass transfer limitations of the oxygen delignification reaction. On the other hand, pulps of higher Kappa number tend to contain less HexA. These acids negatively affect the overall O-stage efficiency because they do not react with oxygen in spite of accounting for the Kappa number measurement.

It is worth noting that low Kappa Kraft pulps tend to possess residual lignin, rich in free phenolic hydroxyl groups and these groups are the preferred sites for the oxygen reaction with lignin. Hence, the efficiency of the oxygen reaction with lignin should in principle be higher for the low Kappa pulps. However, the effects of HexA plus the better accessibility of lignin in pulps containing larger quantities of this polymer, more than counterbalance the effect of lignin reactivity. The advantage of terminating the cooking at a higher Kappa number and proceeding with the oxygen delignification is illustrated in **Figure 4.10,** where it is observed that oxygen delignification is more yield selective towards residual lignin removal than Kraft pulping itself. In addition, the O-stage delignification performance is substantially higher for pulps cooked to higher Kappa numbers. The solid lines show the efficiency of the O-stage, where more delignification is achieved for the pulp samples with higher incoming Kappa numbers. Furthermore, it is clearly indicated that the overall fibre line yield is much higher when cooking is terminated at a higher Kappa number, with oxygen delignification taking over after that in a more selective way.

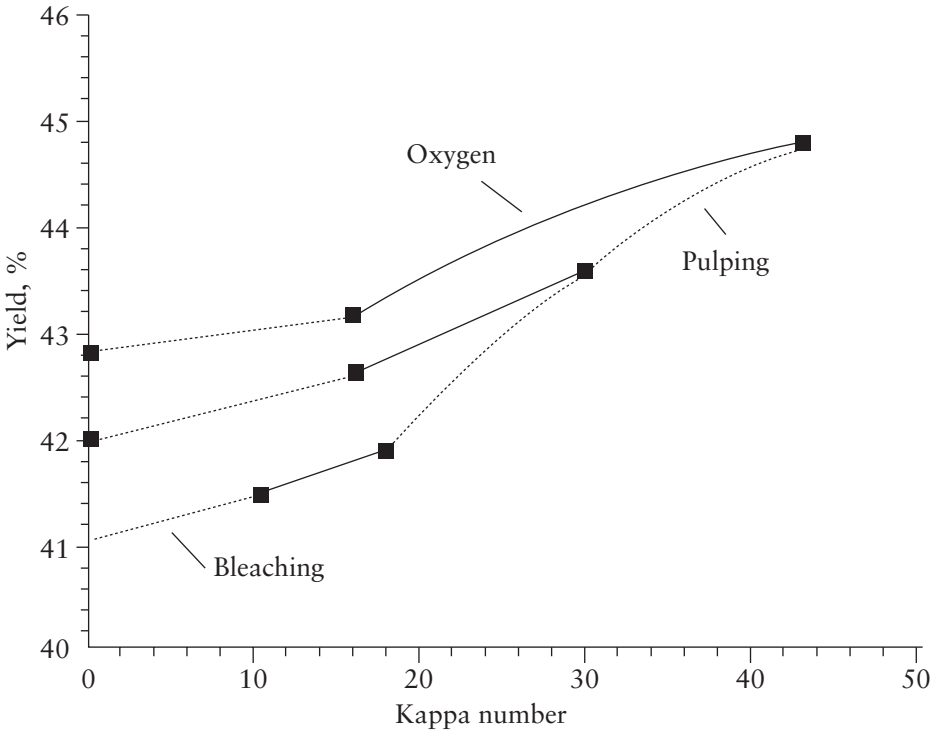

Figure 4.10 Pulp yield after cooking, oxygen delignification and bleaching as a function of the incoming Kappa number. Adapted from P. Axegard and L. Stigsson in *Proceedings of the Breaking the Pulp Yield Barrier Symposium*, Atlanta, Georgia, TAPPI Press, Atlanta, GA, USA, 1998, p.229 [50]

4.7.3 Time and Temperature

At fixed alkali concentration, the decrease of Kappa number with time exhibits two distinct phases, both of which are first-order rate processes. There is an initial and rapid drop followed by a slower one (**Figure 4.6**). This is interpreted as resulting from the presence of two types of lignin which differ in their ease of removal. The two delignification phases are directly paralleled by two corresponding cellulose depolymerisation phases. A consequence of the first-order nature of the delignification process is that given enough alkali, the Kappa number will continue to drop indefinitely [3]. The Kappa number reduction at either the first or second phase is greater at higher temperatures. During the first phase, the delignification rate is fast, but in the second phase, the rate gradually slows down without levelling off [51]. The

temperature obviously enhances overall delignification efficiency but has a negative effect on selectivity. **Figure 4.11** shows the effect of temperature on the oxygen delignification rate for a softwood Kraft pulp. Usually, pulps of higher viscosity, at a given Kappa number, can be obtained by running the process at low temperatures and long retention times [52].

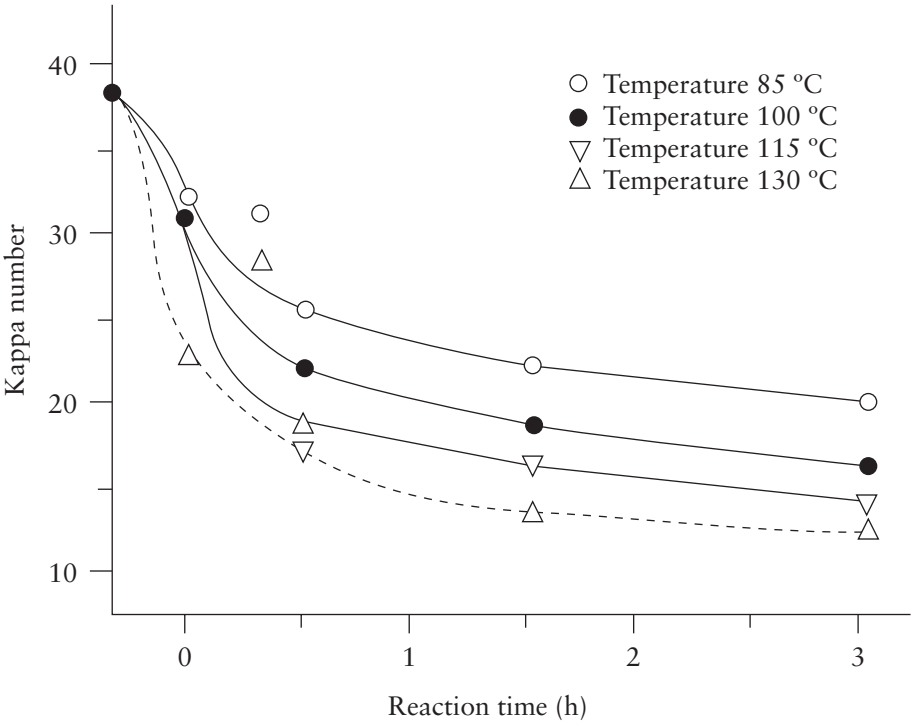

Figure 4.11 The effect of temperature on the delignification rate. Adapted from N. Hartler, H. Norrstrom and S. Rydin, *Svensk Papperstidining*, 1970, **73**, 21, 696 [52]

4.7.4 Reaction Pressure

At high temperatures, oxygen gas solubility in water is very low. Reaction pressure improves the gas solubility in water, thus making more oxygen available for chemical reactions. Therefore, the increase in reaction pressure is expected to influence oxygen

delignification positively. The data in **Figure 4.12** clearly show the improvement of delignification with increasing reaction pressure. The improvement in delignification caused by increasing pressure has no significant impact on selectivity [51]. Overall, increasing pressure is beneficial for oxygen delignification. There is, however, a limit on the maximum pressure that can actually be used on an industrial scale. Since pressure is produced by a pump, the use of high pressures means high energy costs to run the system. In addition, operation at high pressure requires expensive and very robust reactors. Furthermore, operation at pressures which are too high makes consistency control unreliable.

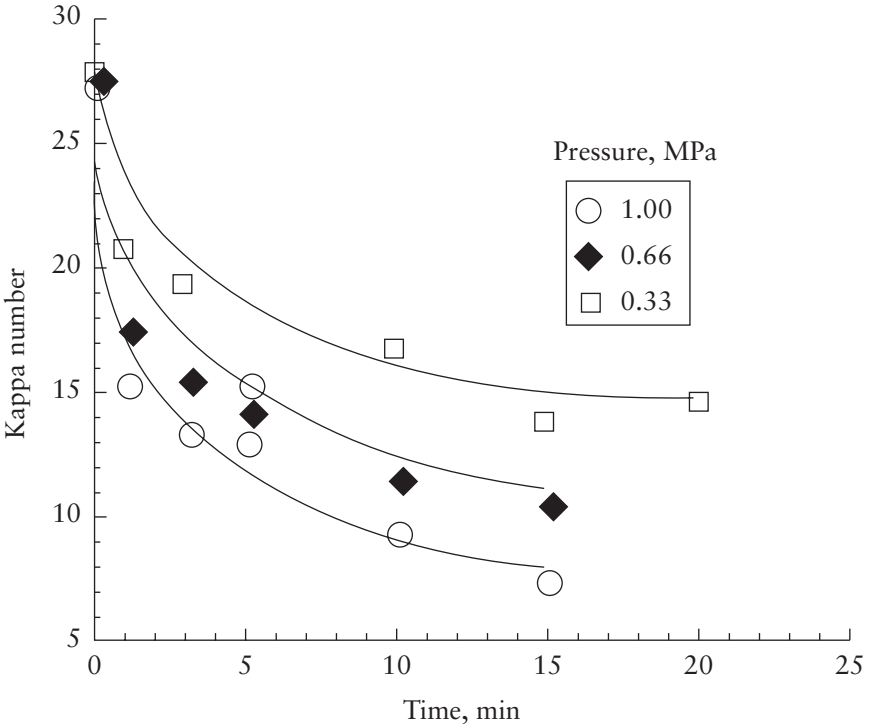

Figure 4.12 Effect of oxygen pressure on the oxygen delignification rate (100 °C, 0.06 mole NaOH/L). Adapted from C.L. Hsu and J.S. Hsieh, *TAPPI*, 1987, p.107 [51]

4.7.5 Oxygen Charge

The oxygen dose is less important than the temperature and alkali charge during oxygen delignification, unless there is an insufficient amount of this oxidant for the reaction to proceed. To avoid oxygen starvation for reactions with lignin, a dose in excess of the required is usually applied (20 and 30 kg/t pulp). By increasing the temperature, the oxygen consumption also increases. However, there is no significant impact on the efficiency of the delignification. Given the limited solubility of O_2 in an alkaline medium, the excess oxygen load remains insoluble in the gas form and thus, occupies a significant fraction of the reactor volume. A reduction in the delignification rate has been observed with increasing oxygen charge, an effect likely caused by a decrease of the retention time in the reactor [53]. This effect is reduced as the oxygen is consumed. Some authors have reported a consumption of O_2 in the range from 1.2 to 1.5 kg/t pulp per Kappa unit removed in the O-stage, if well-washed pulps are used [54, 55]. Thus, a Kappa reduction of 6 units, which is typical for eucalyptus Kraft pulps, for example, would require a maximum of 9.0 kg O_2/t pulp. However, poorly washed pulps containing high COD from cooking will require more oxygen to deal with the COD. For a 50 kg COD/t pulp, which is a typical value for systems with good washing prior to the oxygen delignification stage, a consumption of at least 2 kg O_2/t pulp per Kappa unit has been estimated [54]. In this case, a reduction of 6 Kappa units would require around 12 kg O_2/t pulp. Considering that excess oxygen of about 20% is normally used, a 14 kg O_2/t pulp charge would have to be applied.

4.7.6 Alkali Charge

Oxygen delignification occurs under alkaline conditions [56]. At low alkalinities, lignin starts precipitating over the fibres, thus harming selectivity. In addition, alkali is necessary to abstract the hydrogen from free phenolic hydroxyl groups in the lignin, thus making the reaction of oxygen with lignin possible (**Figure 4.4a**). The pKa of the free phenolic hydroxyl groups in lignin are above 10. Hence, efficient oxygen delignification reactions require a pH at least in this range or higher. In a two-stage oxygen delignification process, the first stage is usually run at a higher pH than the second [57]. Lignin reprecipitation may occur in the O-stage if the pH is not properly controlled. The lignin reprecipitation is primarily influenced by the O-stage final reaction pH; however, it is also influenced by ionic strength, concentration of the dissolved lignin and temperature [58, 59]. Values of 10.5 to 11.0 have been reported for the pKa of industrial Kraft lignins, which allows the assumption that they precipitate at or below these pH values [59]. The final pH of the stage must be higher than 10 to avoid reducing the efficiency and selectivity of the oxygen delignification [1].

The oxygen delignification efficiency increases with increasing alkali charge (**Figure 4.13**) without a major effect on process selectivity [51]. Overall, increasing the alkali charge should be positive for the O-stage. However, there are limitations regarding how much alkali can be added to the system due to complications on the subsequent washing systems and on the recovery of the spent liquor. Excess alkali will hamper subsequent pulp washing and overload the causticising system.

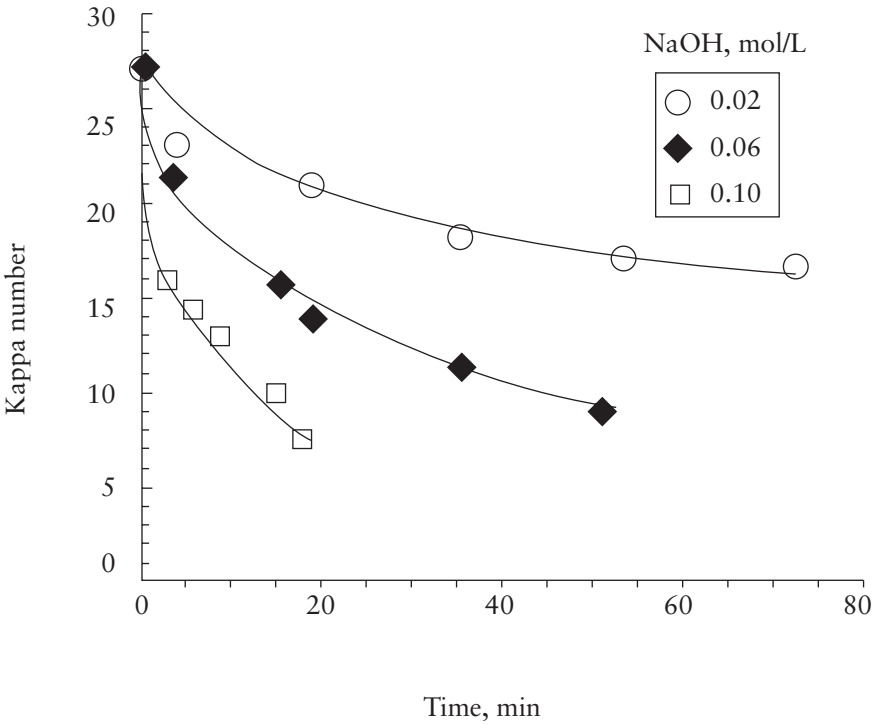

Figure 4.13 Alkali concentration effect on the oxygen delignification rate (100 ºC, 1 MPa). Adapted from C.L. Hsu and J.S. Hsieh, *TAPPI*, 1987, p.107 [51]

Oxygen delignification can be performed with Kraft white liquor, oxidised white liquor or fresh sodium hydroxide as the alkali source. However, fresh sodium hydroxide is relatively expensive and could unbalance the sodium/sulfur ratio in the chemical recovery system. Some studies have indicated no significant change in the delignification rate when oxidised white liquor is used instead of sodium hydroxide in the O-stage [60]. Nonetheless, the unoxidised white liquor reduces the delignification

rate due to the presence of sodium sulfide, which reacts with oxygen. The production of oxidised white liquor is an integral part of any oxygen delignification system, since operation with pure sodium hydroxide is not possible due to the Na/S imbalance. The oxidation of the Na_2S present in the white liquor is carried out at temperatures of 135–170 °C for 30–60 min, and at oxygen pressures corresponding to the temperatures according to **Equation 4.1**. Usually, an excess of oxygen in the order of 50% is applied to guarantee maximum oxidation of the Na_2S into $Na_2S_2O_3$. Full oxidation is usually not possible and a residual Na_2S of 1–2 g/L in the oxidised white liquor is common:

$$2Na_2S + 2O_2 + H_2O \rightarrow Na_2S_2O_3 + 2NaOH \quad (4.1)$$

It has been suggested that the oxidation of Na_2S can be completed all the way to Na_2SO_4. In this case, harsher conditions of temperature and pressure are used, and two reaction vessels may be applied. The reaction mechanism for the oxidation all the way to sulfate is shown in **Equations 4.2–4.5.** The advantage of the oxidised white liquor produced in this manner is that it can be used in the oxygen delignification, as well as in the alkaline extraction stages containing peroxide, which would not be possible if the oxidation was incomplete generating thiosulfate, **Equation 4.1**. The latter reacts with hydrogen peroxide. However, oxidation all the way to sulfate presents the disadvantage of consuming sodium hydroxide as shown in the reaction detailed in **Equation 4.4**:

$$2Na_2S + \frac{1}{2}O_2 + H_2O \rightarrow Na_2S_2 + 2NaOH \quad (4.2)$$

$$Na_2S_2 + \frac{3}{2}O_2 \rightarrow Na_2S_2O_3 \quad (4.3)$$

$$Na_2S_2O_3 + O_2 + 2NaOH \rightarrow 2\,Na_2SO_3 + H_2O \quad (4.4)$$

$$2Na_2SO_3 + O_2 \rightarrow 2Na_2SO_4 \quad (4.5)$$

4.7.7 Magnesium Charge

Selectivity can be defined as the ratio of the attack on lignin to the attack on the carbohydrate. It is affected by the choice of process conditions and by the presence of pulp contaminants. Of the factors governing selectivity in oxygen bleaching, one of the most important is the transition metal content of the pulp, as these metals catalyse the generation of harmful radical species. Most pulps contain appreciable quantities of iron, copper and manganese, all of which have this effect. One approach for dealing with transition metals is to remove them by acid washing or chelation before the oxygen stage; another is to add compounds to the pulp which inhibit carbohydrate degradation. These compounds are called carbohydrate protectors. The protector of greatest commercial importance is the magnesium ion [6].

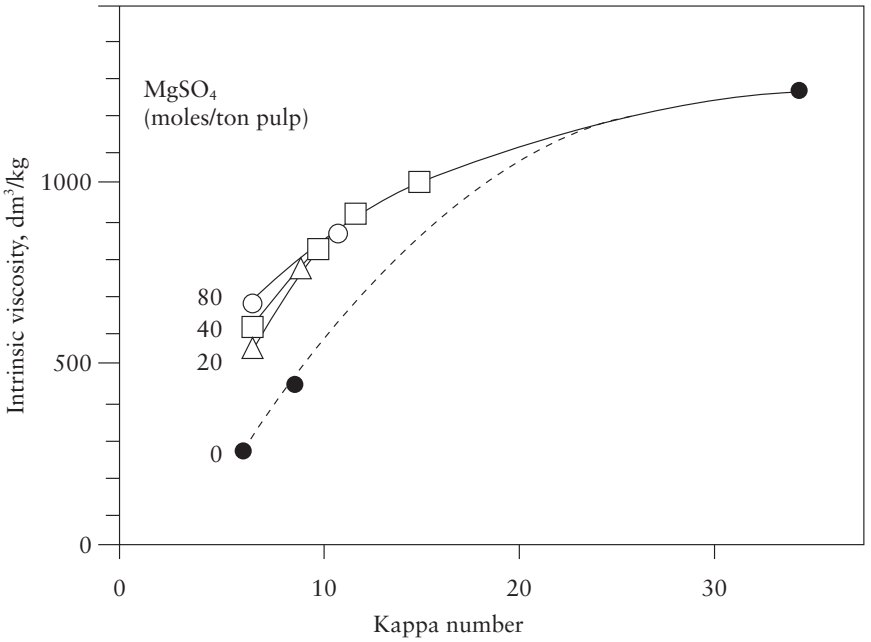

Figure 4.14 Effect of magnesium on oxygen delignification selectivity. Adapted from R.M. Berry in *Proceedings of the 1991 Technical Kraft Pulp Bleaching Course*, Technical Section, CPPA, Montreal, 1991, p.10 [66]

The discovery of its effectiveness in 1963 by Robert and co-workers [61–63] provided a great impetus for the development of oxygen bleaching. Since then, a considerable

number of compounds have been found effective, but none is as economical as magnesium sulfate or its heptahydrate, Epsom salt. It is normally applied at levels as low as 0.05–0.1% Mg^{2+} on oven dried pulp. It is believed to function by precipitating as magnesium hydroxide, which adsorbs the metal ions, making them unavailable for catalysis of peroxide decomposition [64] or by forming complexes with them [65]. Magnesium has also been proposed to function by dismutation of superoxide anion radicals, thus breaking the chain reaction mechanism which increases the concentration of free radicals in the reaction system [48]. **Figure 4.14** show a selectivity plot typical of softwood Kraft pulp oxygen delignification and illustrates the effectiveness of magnesium in preserving pulp viscosity [66].

4.7.8 Consistency

Consistency affects the degree of delignification due to the combination of two factors, the increased concentration of the alkali in the system and increased retention time in the reactor. However, this variable is sometimes disregarded in practice. As it is dependent on the pumping capacity of the system, there is no appreciable cost associated with its optimisation; hence, it is always advisable to operate with the maximum possible consistency, since the higher the consistency, the more efficient the oxygen delignification. In existing oxygen delignification systems, a way to increase consistency is by reducing reactor operating pressure, thus increasing the pumping capacity of the system, but reducing pressure has other negative consequences. Generally, one should operate the system stably at a maximum possible consistency, usually between 11 and 12% consistency [53].

4.8 Impact of Oxygen Delignification on Bleaching Effluent Quality

Oxygen delignification has been one of the most effective technologies developed for decreasing the bleaching effluent load. A significant part of the brown pulp Kappa number is removed during oxygen delignification, along with sizeable amounts of black liquor carry-over from pulping. This material would end up in the bleach plant effluent if not removed during the oxygen delignification stage. Thus, a significant reduction in effluent COD, colour and AOX is observed after the installation of an oxygen delignification stage (**Table 4.3**) [4].

The discharge of bleach plant pollutants and the operating cost of bleaching are reduced by use of an oxygen delignification system. The technology is compatible with new developments aimed at reducing the discharge of bleach plant effluents, such as ozone and peroxide bleaching. Oxygen delignification is expected to play a major role in the industry's efforts to develop an effluent-free bleached pulp mill.

Table 4.3 Bleaching effluent load for the production of a 90% ISO brightness pulp using modified cooking technology to Kappa No. 14-21 and bleaching with the D(PO)DP, A/D(PO)DP and Z/ED(PO) sequences, with and without oxygen delignification

Effluent load parameter	D(PO)DP			A/D(PO)DP			Z/ED(PO)			O/OD(PO)DP			O/OA/D(PO)DP			O/OZ/ED(PO)		
Brown Kappa number	14.1	17.4	20.9	14.1	17.4	20.9	14.1	17.4	20.9	14.1	17.4	20.9	14.1	17.4	20.9	14.1	17.4	20.9
Bleaching filtrate COD, kg O_2/o.d.t	32.5	42.1	51.1	31.5	37.5	40.4	18.9	23.9	29.3	25.7	29.1	30.8	24.5	25.2	26.9	14.2	17.1	20.0
Bleaching filtrate colour, kg Pt/o.d.t	64.0	77.2	85.4	32.3	41.6	50.5	14.1	27.3	41.9	16.6	20.3	25.8	9.1	12.3	14.8	4.9	9.1	13.1
Bleaching filtrate AOX, kg Cl^-/o.d.t	0.45	0.64	0.81	0.47	0.73	1.03	0.17	0.24	0.30	0.16	0.20	0.24	0.19	0.22	0.30	0.09	0.10	0.12

Adapted from J.L. Colodette, J.L. Gomide, D.L. Júnior and C. Pedrazzi, *BioResources*, 2007, **2**, 2, 223 [64]

References

1. H. Sixta, H-U. Süss, A. Potthast, M. Schwanninger and A.W. Krotscheck in *Handbook of Pulp*, Ed., H. Sixta, Wiley-VCH, Verlag GmbH & Co., KGaA, Weinheim, Germany, 2006, **2**, p.609.

2. J. Gierer, *Wood Science and Technology*, 1985, **19**, 4, 289.

3. T.J. McDonough, *TAPPI*, 1986, **69**, 6, 46.

4. J.L. Colodette, J.L. Gomide, D. Longue Júnior and C. Pedrazzi, *Bioresources*, 2007, **2**, 2, 223.

5. J. Gierer, *Wood Science and Technology*, 1980, **14**, 4, 241.

6. T.J. McDonough in *Pulp Bleaching: Principles and Practices*, Eds., C.W. Dence and D.W. Reeve, TAPPI Press, Atlanta, GA, USA, 1996, p.213.

7. S.B. Agarwal, J.M. Genco, B.J.W. Cole and W. Miller, *Journal of Pulp and Paper Science*, 1999, **25**, 10, 361.

8. U. Germgard in *Ljungberg Textbook Pulp and Paper Chemistry and Technology*, Eds., M. Ek, G. Gellerstedt and G. Henriksson, KTH, Stockholm, Sweden, 2006, **2**, p.295.

9. D.M. Ruthven, S. Farooq and K.S. Knaebel in *Pressure Swing Adsorption*, VCH Publishers, New York, NY, USA, 1994.

10. R.Whiting, *Chemistry in New Zealand*, 1991, **55**, 2.

11. Oxygen Producing Vacuum Pressure Swing Adsorption (VPSA) System, Praxair, *http://www.praxair.com/praxair.nsf/7a1106cc7ce1c54e85256a9c005accd7/0a71a43935f77c5285256554007beb79?OpenDocument*

12. J. Gierer, *Svensk Papperstidning*, 1970, **73**, 18, 571.

13. J. Gierer, *Holzforschung*, 1982, **36**, 1, 43.

14. K. Kratzl, J. Gratzl and P. Claus, *Advances in Chemistry Series*, 1966, **59**, 157.

15. J. Gierer in *Proceedings of the International Symposium of Wood and Pulping Chemistry*, Paris, France, 1987, p.279.

16. J. Gierer in *Proceedings of the International Symposium on Wood and Pulping Chemistry Proceeding*, CTAPI, Beijing, China, 1993, p.301.

17. G. Gellerstedt in *Ljungberg Textbook: Pulp and Paper Chemistry and Technology*, Eds., M. Ek, G. Gellerstedt and G. Henriksson, KTH, Stockholm, Sweden, 2006, **2**, p.217.

18. K. Kratzl, P. Claus, W. Lonsky and J. Gratzl, *Journal of Wood Science and Technology*, 1974, **8**, 35.

19. E. Johansson and S. Ljunggren, *Journal of Wood Chemistry and Technology*, 1994, **14**, 4, 507.

20. S. Ljunggren, G. Gellerstedt and M. Petterson in *Proceedings of the 6th International Symposium on Wood and Pulping Chemistry*, 1991, **1**, p.229.

21. G. Gellerstedt, K. Gustafsson and L. Lindfors, *Nordic Pulp and Paper Research Journal*, 1986, **1**, 3, 14.

22. J. Gierer and F. Imsgard, *Svensk Papperstidning*, 1977, **80**, 16, 510.

23. F. Asgari and D.S. Argyropoulos, *Canadian Journal of Chemistry*, 1998, **76**, 1606.

24. Y. Ji, E. Vanska and A. van Heiningen, *Pulp & Paper Canada*, 2009, **110**(**3**), 29.

25. H. Chang and J.S. Gratzl, *Chemistry of delignification with Oxygen, Ozone, and Peroxides*, Eds., J. S. Gratzl, J. Nakanoand and J. P. Singh, Uni Publishers Co. Ltd, Tokyo, Japan, 1980, p.151.

26. L.G. Akin, J.L. Colodette and D.S. Argyropoulos, *Canadian Journal of Chemistry*, 2001, **79**, 201.

27. R. Malinen, *Papper and Timber*, 1975, **4A**, 193.

28. R. Malinen and E. Sjöstrom, *Papper and Timber*, 1973, **55**, 547.

29. H. Kolmodin and O. Samuelson, *Svensk Papperstidining*, 1973, **76**, 2, 71.

30. R. Malinen and E. Sjöstrom, *Papper and Timber*, 1974, **56**, 895.

31. I. J. De Souza, J. Bouchard, M. Méthot, R. Berry and D.S. Argyropoulos, *Journal of Pulp and Paper Science*, 2002, **28**, 5, 167.

32. J.D. Timpa and D.F. Wanjura in *Proceedings of the 10th Cellulose Conference*, New York, NY, USA, 1988, p.1145.

33. E. Sjöstrom in *Wood Chemistry: Fundamentals and Applications*, Academic Press, San Diego, CA, USA, 1993.

34. T. Vuorinen, A. Teleman, P. Fagerstrom, J. Buchert and M. Tenkanen in *Proceedings of the 1996 International Pulp Bleaching Conference*, Washington, USA, 1996, **1**, p.43.

35. J.L. Colodette, C.M Gomes, M.S. Rabelo, K.M.M Eiras, A.F. Gomes and K.D. Oliveira, *TAPPI*, 2008, *TJ* Online Exclusive, p. 18A.

36. C.L. Hsu and J.S. Hsieh, *TAPPI*, 1985, **68**, 6, 92.

37. C.L. Hsu and J.S. Hsieh, *AIChE Journal*, 1988, **34**, 1, 116.

38. M.J.M.C. Barroca, P.J.T.S. Marques, I.M. Seco and J.A.A.M. Castro, *Industrial & Engineering Chemistry Research*, 2001, **40**, 24, 5680.

39. Y-S. Perng and C.W. Oloman, *TAPPI*, 1994, **77**, 7, 115.

40. A.H.D. Vincent, J.F. Mathews and K.L. Nguyen, *Appita Journal*, 1994, **47**, 3, 217.

41. L. Tench and S. Happer, *TAPPI*, 1987, **70**, 11, 55.

42. T. McDonough in *TAPPI Bleach Plant Operations Workshop*, TAPPI Press, Atlanta, GA, USA, 2012.

43. M. Bokström in *Proceedings of the TAPPI Pulping Conference*, TAPPI Press, Atlanta, GA, USA, 1999.

44. J. Iribarne and L.R. Schroeder in *Proceedings of the TAPPI Pulp Conference*, TAPPI Press, Atlanta, GA, USA, 1995, p.125.

45. M. Ragnar in *Proceedings of the 7th International Conference on New Available Technologies*, Stockholm, Sweden, SPCI, Stockholm, Sweden, 2002, p.31.

46. Techniques to consider in the determination of BAT, Ineris. *http://www.ineris.fr/ippc/sites/default/interactive/brefpap/bref_pap/english/bref_gb_kraft_technique.htm*

47. Pulp and Paper Industry/GL&V - Chemical Pulping/Oxygen Delignification, Flowtec.
http://www.flowtec.at/index.php/en/content/view/full/1361

48. J.L. Colodette, C.M. Gomes, M.S. Rabelo, K.M.M. Eiras, A.F. Gomes and K.D. Oliveira, *O Papel*, 2006, **67**, 9, 88.

49. J.F. Iijima and H. Taneda, *Journal of Pulp and Paper Science*, 1997, **23**, 12, J561.

50. P. Axegard and L. Stigsson in *Proceedings of the Breaking the Pulp Yield Barrier Symposium*, Atlanta, Georgia, TAPPI Press, Atlanta, GA, USA, 1998, p.229.

51. C.L. Hsu and J.S. Hsieh, *TAPPI*, 1987, **70**, 12, 107.

52. N. Hartler, H. Norrstrom and S. Rydin, *Svensk Papperstidining*, 1970, **73**, 21, 696.

53. A.Turqueti in *Seminário de Deslignificação com Oxigênio*, ABTCP, Riberão Preto, SP, Brazil, 1995, p.1.

54. J.F. Iijima and H. Taneda in *Proceedings of the International Pulp Bleaching Conference*, Washington, TAPPI Press, Atlanta, GA, USA, 1996, p. 403.

55. S.B. Agarwal, J.M. Genco, B.J.W. Cole and W. Miller in *Proceedings of the Pulping Conference*, San Francisco, CA, TAPPI Press, Atlanta, GA, USA, 1997, p. 963.

56. E. Johansson in *Pulp and Paper Chemistry and Technology*, Royal Institute of Technology, Stockholm, Sweden, 1997. [Doctoral Thesis]

57. A.V. Tran, *Papper and Timber*, 2001, **83**, 5, 405.

58. K. Li and D.W. Reeve in *Proceedings of the International Pulp Bleaching Conference*, Portland, Oregon, TAPPI Press, Atlanta, GA, USA, 2002, p.45.

59. S. Backa and M. Ragnar in *Proceedings of the TAPPI Fall Technical Conference*, Chicago, IL, TAPPI Press, Atlanta, GA, USA, 2003.
http://www.tappi.org/Downloads/unsorted/UNTITLED-fal03143pdf.aspx

60. J.P. Leader, H.H.K. Lim and G.B. Byrom, *Appita Journal*, 1986, **39**, 6, 451.

61. A. Robert, P. Traynard and O. Martin-Borret, no assignee; French Patent 1387853, 1963.

62. A. Robert, P. Rerolle, A. Viallet and O. Martin-Borret, *ATIP Reviews*, 1964, **18**, 4, 151.

63. A. Robert, A. Viallet, P. Rerolle and J-P. Andreolety, *ATIP Reviews*, 1966, **20**, 5, 207.

64. A. Robert and A. Viallet, *ATIP Reviews*, 1971, **25**, 3, 237.

65. A.E. Gilbert, E. Pavlovova and W.H. Rapson, *TAPPI*, 1973, **56**, 6, 95.

66. R.M. Berry in *Proceedings of the 1991 Techical Kraft Pulp Bleaching Course*, Technical Section, CPPA, Montreal, Canada, 1991, p.10.

5 Chemistry and Physics of Cellulose and Cellulosic Substances

Milichovský Miloslav

5.1 Introduction

The unique properties and recent universal focus on natural material resources has put cellulose and cellulose derivatives into the sphere of intensive scientific effort and consequently to the attention of industrial companies. Nature provides wonderful examples of composite structures that involve cellulose. Cellulose is a fibrous, tough, water-insoluble substance, which is found in the protective cell walls of plants, particularly in stalks, stems, trunks and all woody portions of plant tissues. The properties of wood, for instance, result from the unique interplay between nanoscale domains of cellulose, hemicelluloses and lignin [1]. The manner in which such elements are organised into larger structures is critical to the survival of trees and other plants. The hierarchical organisation of wood is based on the natural composite paradigm of providing maximum strength with the minimum amount of material from the most efficient economy of biosynthesis [2]. Even some animal species make use of cellulosic nanostructures, such as some members of the tunicates ('sea squirts') family, the sea alga *Valonia ventricosa* [3], *Chaetomorpha melagonium* [4] and bacterial cellulose, a polysaccharide synthesised in abundance, e.g., by *Acetobacter xylinum* [5]. In all of these organisms, cellulose serves as a 'scaffold' to evolve further mechanical support of highly organised living and growing matter. Knowledge of the supermolecular and hypermolecular structure of cellulose, accompanied by changes during its chemical or mechanical treatment, is important not only for technical or biomedical applications, but predominantly, as a novel approach to better understand and control the aging of cellulose materials, e.g., in paper and paper products and nanocomposites. During the last 150 years of intensive research, an abundance of experimental data and information has been collected concerning the ultrastructure and morphology of cellulose, native cellulosic substances and cellulosic materials. Although the development and utilisation of cellulose have a long history, the understanding of its chemistry and structure is relatively new, and many living polymer scientists have spent their entire working lives developing our present knowledge. Despite the fact that the polymer theory is established and the chemical structure of cellulose is accepted without dispute, the

ultrastructure of cellulose remains controversial on several issues. Despite the degree to which cellulose has been investigated, its structural features have not been identified with absolute clarity and new information is constantly being discovered [6–7]. With regard to the solid state structure of cellulose, progress has been made but a lack of information and theoretical ideas exist involving the behaviour of cellulose in a wet state and water suspensions. Infrared spectroscopy, Raman spectroscopy, single-crystal X-ray studies, high resolution nuclear magnetic resonance (NMR), dark-field electron microscopy and electron diffraction, supported by the recent applications of the solid state, cross polarisation/magic angle spinning (CP/MAS) NMR, ^{13}C-CP/MAS solid state NMR, electron spectroscopy for chemical applications, photoacoustic Fourier transform-infrared spectroscopy (FT-IR), secondary ion mass spectrometry and fast atom bombardment mass spectrometry have added considerable information to our knowledge of the solid state structure of cellulose [8]. However, as we have learned from the past, no single physical method is sufficiently sensitive for all parameters of interest, and no single structural method can give answers to all the questions.

5.2 Basic Chemistry of Cellulose

Materials of a cellulosic nature are typically structured matter exhibiting a characteristic molecular, supermolecular and hypermolecular structure. The supermolecular structure is introduced by molecular chain bundles of cellulose called *elementary fibrils*, connected mutually into *microfibrils*. Elementary fibrils are cemented together by hemicelluloses and lignin. The hypermolecular structures of cellulosic materials are then assembled through microfibrils accumulating into *fibrils*, followed by fibrils forming the fibrous P, S1 and S2 parts of the cellular wall, which display different morphology [1]. The cellulose structure is based on 180 ^{o} turn-screw D-1,4 glucopyranoside units connected with β-glycosidic bonds, which form cellulose polymeric chains, giving rise to amorphous and various crystalline domain formations that are considered allomorphs [9, 10]. It has been shown [11–14] that β-D-glucose exists in a pyranose form and that the latter is in the 4C1 chair conformation, which is the lowest energy structure for β-D-glucopyranose. Degrees of substitution, degree of polymerisation (DP) and distribution of the molecular mass, as well as the distribution of substituents, strongly influence the properties of cellulose and cellulose derivatives, and are also significant factors in their characterisation. According to Schultz and Marx [15, 16], the DP of cellulose depends on the species of wood and other plants, giving a DP of cellulose in the range of 6,200 ± 600 for linters and cotton cellulose, 8,000 for flax fibre, 3,300 for pinewood cellulose and 500–3,000 for dissolving pulp.

Cellulose derivatives are obtained by several functionalisation methods [17]. The acidolysis of carbohydrates is one of the oldest degradation methods for polymeric carbohydrates, but these reactions are very aggressive and lead to a varied

concentration of undesirable degradation products of cellulose oligomers. A milder alternative has been developed using pivalic anhydride/BF_3.Et_2O/CH_2Cl_2 for the degradation of 2,3,6-*tri*-*O*-acetylcellulose (pivaloylysis). Glycosidation reactions allow access to linear products (monodisperse celluloses) as well as to new branched cellulose units [18].

5.3 Supermolecular and Hypermolecular Characteristics of Cellulose and Lignocellulose Materials

Currently, the supermolecular structure of cellulose, in its many forms, remains one of the most studied areas of investigation in polymer science [6]. Cellulose molecules, as a linear macromolecule consisting of anhydroglucose units chain wise interlinked and of coil conformation, are entangled into nanostrands forming so-called *elementary fibrils*. The following arrangement of these fibrillar bundles, called *microfibrils*, is sufficiently regular that cellulose exhibits a crystalline X-ray diffraction pattern. Although the chemical constitution of cellulose has been established, its morphology and crystalline structure continues to be a source of interest and sometimes controversy. Diffraction studies show light and dark areas along a cellulose microfibril, which have been attributed to crystalline and amorphous cellulose, respectively. Another portion of the microfibril consists of less highly ordered cellulose molecules, called the amorphous or paracrystalline region. In general, the 'crystalline' regions alternate with less well-ordered 'amorphous' regions, and there is no connection between the length of the crystalline regions and the molecular chain length. The molecules gradually transition from regions of high-lattice order to regions of low-lattice order. The high strength of the cellulose fibres may be due to the chain ends being held in the lattices by strong hydrogen bonding forces. The simplest conceivable model has 'straight' cellulose chains isotropically distributed in the sample [19]. Cellulose from *Valonia* is a highly crystalline product and consequently it is frequently the object of studies. Verlhac and co-workers [20] suggested that the amorphous material consists mostly of surface chains, which in the large *Valonia* microfibril makes up a low percentage of the total. The surface of crystalline cellulose or indeed areas of 'amorphous' cellulose probably still possess a degree of order. Thus, 'amorphous' cellulose cannot be considered truly amorphous as, by definition, an amorphous material is one which is formless or lacks a definite shape. Evidence has been put forward for the existence of more than one polymorph of cellulose in native samples [7]. Six polymorphs of cellulose (I, II, III_I, III_{II}, IV_I and IV_{II}) were described. Cellulose I, or native cellulose, is the form found in nature, but the crystal structures of native cellulose show structural differences that depend on the source of the cellulose [21]. Simon and co-workers [22] postulated that a form of crystalline cellulose existed near the surface of a crystal, which differed from the structure found at the centre of the crystal. These two crystalline forms were

termed celluloses I_α and I_β [23]. Both allomorphs possess symmetry which is very close to twofold screw symmetry; this leads to the conclusion that the repeating unit along the chain is cellobiose. Celluloses produced by primitive organisms were said to have a dominant I_α component, while those produced by the higher plants have a dominant I_β form. I_α and I_β were found to have the same conformation of the heavy atom skeleton, but differed in their hydrogen bonding patterns. Horii and co-workers [24] suggested that the two ^{13}C-NMR spectra, obtained for polymorphs I_α and I_β, correspond to the resonances for the two-chain and eight-chain unit cell regions of cellulose. The polymorph I_α can be converted to the more stable I_β phase by annealing in various media. Annealing at a temperature of 270 °C converts most of the I_α cellulose to the I_β form. Bacterial cellulose has the highest percentage of I_α polymorph, which is 70%. The existence of I_α and I_β polymorphs in cellulose samples may affect the reactivity of native cellulose, as I_α is metastable and thus more reactive than I_β, according to Yamamoto [25]. The triclinic and the monoclinic structures correspond to I_α and I_β, according to the electron diffraction spectra. The triclinic phase is metastable and annealing it in dilute alkali at 260 °C converts it into the monoclinic form [26, 27]. Essentially, these structures are very similar and interconversion between them is achieved by the slipping of intersheet hydrogen bonds between cellulose sheets, to give a slightly different pattern of cellobiose repeating [26].

In the case of cellulose biosynthesis, the groups or rosettes of particles, or terminal complexes (TC), are seen in the plasma membrane when viewed by freeze fracture techniques [28]. These groups of TC can be seen to be associated with the ends of microfibrils (collections of cellulose chains), and are involved in the elongation of whole cellulose microfibrils. Thus, all the chains in one microfibril would have to be elongated by the complex at the same rate. This requirement means that the complex would need to be comprised of many subunits, each elongating a single chain at a time. Crystalline cellulose I is not the most stable form of cellulose. It is unlikely to be synthesised by the crystallisation of preformed cellulose chains, as such a process carried out *in vitro* gives rise to the thermodynamically more favourable cellulose II. Cellulose II, the second most extensively studied form, may be obtained from cellulose I by either of two processes:

- Regeneration, which is the solubilisation of cellulose I in a solvent followed by reprecipitation upon dilution in water to give cellulose II; or
- Mercerisation, which is the process of swelling native fibres in concentrated sodium hydroxide, to yield cellulose II on removal of the swelling agent. It should be noted that regeneration gives a higher level of conversion of cellulose I to cellulose II [29]. Kuga and co-workers [30] reported a mutant strain of *Acetobacter xylinum* as producing native folded-chain cellulose II. In the mercerisation process (the treatment of cellulose I with alkali, to achieve cellulose II) no solubilisation

occurs, which seems to imply that the fibrous structure of the cellulose would be maintained.

The mechanical properties of natural and regenerated cellulosic fibres have been found to be completely different, with the natural fibres exhibiting near linear behaviour, whereas the regenerated fibres show nonlinear behaviour [8]. Differences in the hydrogen bonding patterns reported for models of cellulose I and II are not solely derived from deviations in hydroxymethyl conformation, but also from the fact that the polarity of the chains are popularly thought to differ; a parallel arrangement [3] is attributed to cellulose I and an antiparallel arrangement is proposed for cellulose II. Celluloses III_I and III_{II} may be obtained reversibly from celluloses I and II, respectively. Celluloses III_I and III_{II}, [31] are formed, in a reversible process, from celluloses I and II, respectively, by treatment with liquid ammonia or some amines, and the subsequent evaporation of excess ammonia [32]. Polymorphs IV_I and IV_{II} [33] may be prepared by heating celluloses III_I and III_{II}, respectively, to 206 °C in glycerol. Cellulose IV is also produced by heating cellulose I or II in glycerol at 280 °C, or by boiling the cellulose-ethylene diamine complex in dimethylformamide. Howsomon and Sisson [34] have suggested that cellulose III and IV can be regarded as disordered forms of celluloses II and I, respectively.

Based on stress-invariance of the cellulose fibre, Eichhorn and co-workers [8] have concluded that the material structure of cellulose can be modelled using a modified series aggregate model structure, composed of parallel orientated and mutual regularly shifting elementary fibrils. In such a structure, the stress is uniform and equal within each element (composed of crystalline and amorphous regions). The surprising result is however, that despite the different crystal structures of natural and regenerated cellulose (cellulose I and II), the rate of shift with respect to stress is equal for each type. Frey-Wysling and Mühlethaler [35–36] indicated that microfibrils are composed of elementary fibrils having an average width of 3.5 nm. The elementary fibrils seem to be crystalline along their entire length. Pozgaj and co-workers [37] described elementary fibrils as having a width in the range of 3.5–10 nm and length of 30–80 nm. Using the ^{13}C-CP/MAS NMR spectroscopy technique, Heux, Dinand and Vignon [38] established that the cellulose extracted from sugar beet pulp exhibited a crystallite size of 4 nm, which was in good agreement with the transmission electron microscopy (TEM) observations. High-resolution solid-state ^{13}C-NMR spectra have been taken using several native cellulosic materials, as well as regenerated low-DP cellulose I, implying that native celluloses exhibit heterogeneous crystalline structures [39]. Therefore, the possibility that native celluloses are biosynthetically tailored composites certainly exists. From an excellent correlation of results obtained separately by the two methods of analysis, it was found highly probable that the chains of *Valonia* cellulose, packed with parallel polarity, maintained a twofold screw axis for the rigid components of the glucose ring, but showed some flexibility of the hydroxymethyl

group rotations. No evidence for crystallite orientation other than parallel to the fibre axis was found [4]. Topographical images of the crystallites (highly crystalline regions of the original cellulose fibre) gained by using atomic force microscopy (AFM) have revealed corrugations across the surface of each crystal, with three spacings relating to: the 0.52 nm glucose interval, the 1.04 nm cellobiose repeat distance and a ~0.6 nm repeat, matching the intermolecular spacing between chains [40]. *A priori* crystal structure prediction of native celluloses, using a chain-pairing molecular model, indicates [41] only a few of all the low-energy three-chain models yield closely packed three-dimensional arrangements. The cellulose chains in the selected models form layers, stabilised by interchain hydrogen bonds. The emergence of several energy minima suggests that parallel chains of cellulose can be paired in a variety of stable orientations. The two best crystal lattice predictions were for a triclinic (P_1) and a monoclinic ($P2_1$) arrangement with the following unit cell dimensions: a = 0.63, b = 0.69, c = 1.036 nm, α = 113.0 °, β = 121.1°, γ = 76.0°, and a = 0.87, b = 0.75, c = 1.036 nm and γ = 94.1 °, respectively. They correspond closely to the respective lattice symmetry and unit-cell dimensions that have been reported for cellulose I_α and I_β allomorphs. At present, the internal structural features of cellulose microcrystals remain undetermined, although some NMR spectroscopic evidence indicates that the inner structure may exhibit [40] a high degree of organisation. Obviously, elementary fibrils, also known as cellulose crystallites, cellulose nanorods, cellulose whiskers and so on, are the smallest elements of all cellulose substances, which are characterised by the highly structured organisation. With respect to the size of C, O and H atoms, length and orientation of the chemical bonds, assuming a 4C1 chair conformation of the anhydroglucopyranose unit it is possible to formulate a model of elementary fibrils. Hydrogen bonding within cellulose chains may determine the 'straightness' of the chain. Interchain hydrogen bonds might introduce order or disorder into the system, depending on its regularity. When considering hydrogen bonding, it is essential to note the conformation of the C(6) hydroxymethyl group [41]. Due to inter- and intramolecular hydrogen bonds among the macromolecular cellulose chains, the nanostrands of elementary fibrils are formed by mutually self-crossing the cellulose macromolecules at an angle of 60° (see **Figure 5.1**) and regularly alternating the entanglement into a half part of opposite cellulose chains, resulting in extraordinary strength of the elementary fibril as similar as a *Czech Easter Monday* whipping tool, the 'pomlazka' (see **Figure 5.2**). The arrangement of both ends of every elementary fibril are a result of the dispersion of cellulose chain lengths, which are more disordered as they are formed after the common connection, resulting in a less compact amorphous part of the cellulosic matter – a microfibril. Evidence exists detailing the varying extent of the compact matter of cellulose and is presented in **Figure 5.3**. Histograms of grey values of pixels measured by Synchrotron X-ray microtomography using a ID19 multipurpose beamline at the European Synchrotron Radiation Facility (ESRF), Grenoble, have revealed the existence of three and two types of matter in papers (bleached linters) with different compactness, which were

prepared from only defibrillated and beaten linter slurry, respectively. In the case of paper made from beaten linters, the disappearance of the high compactness of the third part was most likely due to homogenisation during the beating processing.

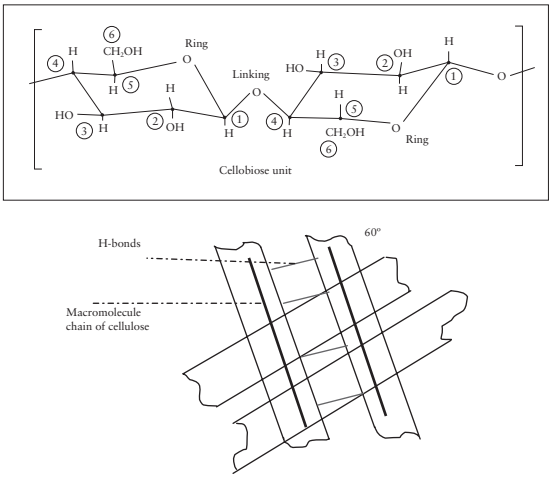

Figure 5.1 Schematic representation of part cellulose chain nanostrands in two planes one located above the other, twisted mutually and forming elementary fibrils

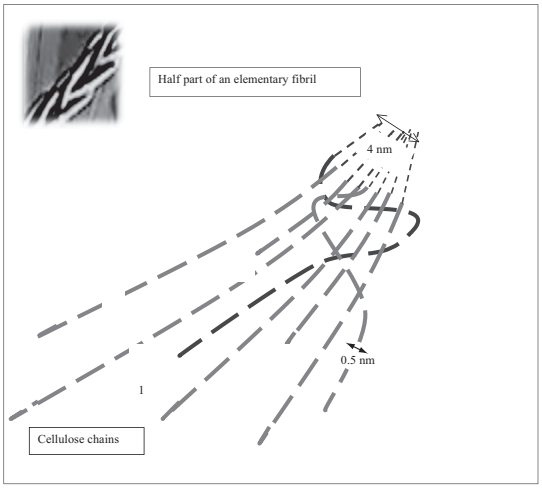

Figure 5.2 Schematic representation of the half part of elementary fibrils formed by ravelling of the individual cellulosic chains into a nanoentanglement

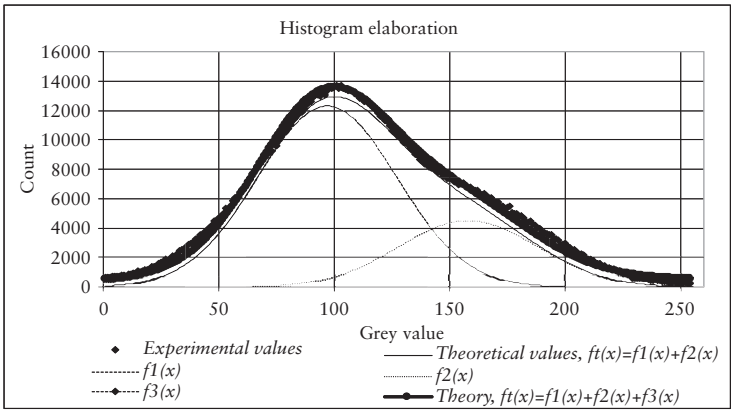

(a)

Figure 5.3 Histogram of grey values verified by use of Gauss probability functions. Bleached linters. Synchrotron X-raymicrotomography using a ID19 multipurpose beamline, ESRF, Grenoble, France. (a) Sample 100628/CZ/Linters/A. Slice 132/256. Std-Dev = 46.29. Results of verification:$f_1(x)$: Mean = 97; Dispersion = 30; $f_2(x)$: Mean = 158; Dispersion = 30; Background $f_3(x)$: Mean = 152; Dispersion = 160. F_1/F_t = 0,655; F_2/F_t = 0,240; F_3/F_t = 0.105 if $\int_1^{255} f_i(x)dx = F_i$ and $\sum F_i = F_t$

The paper was prepared by the dewatering of pulp slurry composed only of *defibrillated linters*.

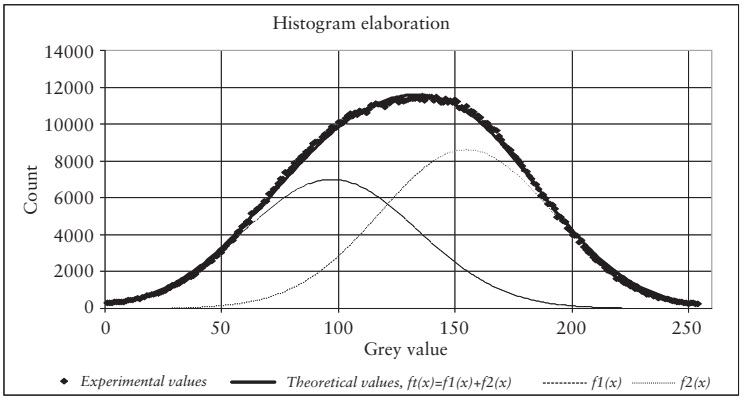

(b)

(b) Sample 100628/CZ/Linters /B. Slice 239/256. Std-Dev = 45.77. Results of verification: $f_1(x)$: Mean = 97; Dispersion = 37; $f_2(x)$:

Mean = 155; Dispersion = 37. F_1/F_t = 0,448;

F_2/F_t = 0.552 if $\int_1^{255} f_i(x)\,dx = F_i$ and $\sum F_i = F_t$

The paper was prepared by dewatering of pulp slurry composed only of *beaten linters*.

Preston [42] proposed a model for the microfibril in which one central crystalline core is embedded in a paracrystalline cortex of molecular chains, which lie parallel along the microfibril length, but otherwise are not stacked in a crystalline array. The dimensions of the crystalline core vary with, but are smaller than, the microfibril width which varies by 30 to 400 nm. Many studies, based on a variety of physical and chemical methods, have indicated that the microfibrils are not completely crystalline, but instead contain two distinctly different regions. The amorphous material in native fibres is composed partly of noncellulosic constituents (e.g., hemicelluloses and lignin). There is also an appreciable amount of cellulose which is in an amorphous state. It is believed that the long cellulose molecules protrude at the surface of the crystallites to give a fringe structure. These protruding chains permit association to take place between the cellulose and noncellulosic constituents of the fibres, thus forming an amorphous mixture of cellulose and noncellulosic substances. Noncellulosic polysaccharides (e.g., hemicelluloses such as xyloglycans, glucomannans and glucuronoxylans) exhibit a strong interaction with the microfibril surface and lead to a further apparent disorder [38]. Owing to intramolecular and intermolecular H-bonds, the cellulose molecules are mutually bound to form the fibre structure of an elementary fibril. The main types of H-bond forming a supermolecular cellulose structure are presented in **Figure 5.4**. Intramolecular H-bonds are formed either between different planes or on the same plane in which separate cellulose chains are found that occupy the most advantageous 4C1 conformation. Two or three types of qualitatively different H-bonds can be distinguished [43, 44], following the scheme presented in **Figure 5.4**:

1. H-bonds of irreversible nature:

- Glycosidic oxygen with hydrogen atoms of several hydroxyl groups C′(6)OH – O(1); and
- Hemiacetal oxygen with hydrogen atoms of several hydroxyl groups [C′(3)OH – O(5), C′(2)OH – O(5), C′(6)OH –O(5)].

2. Reversible H-bonds between amphoteric primary and secondary hydroxyl groups (groups with the ability to form hydrogen bonds with water where both act as the H-donor group and the H-accepting group, depending on the structure and composition of molecules or macromolecules in which they are present):

- [C′(2)OH – C(3)OH, C′(6)OH – C(6)OH].

3. Slightly irreversible type: between primary and secondary hydroxyl groups such as:

- C′(6)OH – C(2)OH.

Intramolecular H bonds
These include:
- C′(2)OH-C(6)OH
- C′(3)OH-O(ring)

Intermolecular H bonds
H-bonds linking up single cellulose chains in the plane located one above the other:
- C′(2)OH-O(ring)
- C′(3)OH-O(ring)
- C′(6)OH-O(ring)
- C′(2)OH-C(3)OH
- C′(6)OH-C(2)OH
- C′(6)OH-C(6)OH
- C′(6)OH-O(linking)

H-bonds linking single cellulose chains located in the same plane:
- C′(6)OH-C(6)OH
- C′(6)OH-C(2)OH
- C′(6)OH-O(ring)

Strength order of particular H bonds
The strength order is:
- Intra C′(6)OH-C′(2)OH >
- Intra C′(3)OH-O(ring) ÷
- Inter C′(6)OH-C(2)OH ÷
- Intra C′(6)OH-C(6)OH ÷
- Intra C′(2)OH-O(ring) ÷
- Intra C′(6)OH-O(linking) >
- Intra C′(6)OH-C(2)OH in the plane >
- Intra C′(3)OH-O(ring) >
- Intra C′(2)OH-C(3)OH

Figure 5.4 The main types of H-bonds possibly participating in the formation of the supermolecular structure of cellulose. Compare with the cellobiose unit in **Figure 5.1**

These qualitatively different H-bonds cause oriented (crystalline), less oriented and nonoriented amorphous zones to occur in cellulose [38]; transitions among these zones are not smooth, but the orientation and degree of coherence differs in various parts of the fibre. Different arrangements can exist even in oriented zones. The destruction of H-bonds with water and water solutions will depend not only on their strength, but also on the nature of the H-bonds. The destruction can be reversible or irreversible. The H-bonds formed by H-amphoteric groups are usually reversible H-bonds, while the groups of only donor or acceptor usually form the irreversible H-bonds [45, 46]. The occurrence of H-amphoteric groups in the system causes a decrease of the crystalline zones. Moreover, cellulose can easily accommodate hydrophobic appending chains to overcome adverse interactions with nonpolar composite matrices [47], and the high melting temperature of cellulose nanocrystals makes it a very attractive feature for designing materials that need to perform at high temperatures.

Intramolecular hydrogen bonds have been found to play an important role in the determination of crystallite modulus and the chain deformation mechanism [48]. The intramolecular hydrogen bonds stiffen the chains along their axis, while the intermolecular hydrogen bonds are responsible for chain packing and aggregation [49]. Recently, increased attention was devoted to nanocellulose, or cellulose nanowhiskers, because of their large modulus of elasticity, strength and large aspect ratio. Cellulose whiskers, made from tunicates, are quasi-perfect crystals with 18 × 9 nm lateral dimensions [17] and an aspect ratio of around 100. They have a tensile modulus (150 GPa) much higher than the usual modulus of polymers (around 3 GPa below the glass transition temperature Tg) and can form hydrogen bonds with their neighbours thanks to the numerous hydroxyl groups on their surface. A crystallite modulus of native cellulose along the chain axis was calculated by Tashiro and Kobayashi [50], based on the X-ray analysed molecular conformation and the force constants used in the vibrational analysis. The calculated values are 172.9 GPa and 70.8 GPa for the cases with and without the intramolecular hydrogen bonds taken into account, respectively. The smallest structural elements of cellulosic fibre, i.e., elementary fibres and microfibres, may still be fused to adjacent structures forming fibrils and fibrillar bundles of thread-like shape, which are then twirled into a hypermolecular structure of varyingly porous walls of fibre with well-defined morphology. These nanosized fibrils stick out of the surface of the cellulose fibre and they are of great importance for their paper-forming ability due to their secure bonding potential [51]. The presence of nanosized fibrils on the surface of intact cellulosic fibres was later demonstrated in a series of scanning electron micrographs published by Alince [52]. These domains possess very high strength, approximately in the order or greater than a comparable steel structure. The density of cellulose crystals, which may be determined by crystallography, is related to the substance structure. The density of crystalline cellulose, as found in a single crystal, is 1.59 g/cm^3, whereas that of pure natural fibre cellulose reaches only 1.55 g/cm^3 [53, 54]. The experimental densities are 1.582 and 1.599 g/cm^3 for the I_α and I_β phases, respectively. The density of the I_α allomorph was very well predicted by Mazeau and Heux [55], using molecular dynamics modelling, and the density of the I_β allomorph is slightly lower than the expected value, by less than 3%. As a general trend for the polymer, the density of the amorphous phase is expected to be 10–20% lower than that of the crystalline phase. The density of the amorphous systems should then be in the range of 1.28 and 1.44 g/cm^3. Generally, in case of a multicomponent material, the overall density is:

$$\rho_s = 1/(\sum X_i/\rho_i), \text{ for } \sum X_i = 1$$

where X_i and ρ_i are the absolute concentration (w/w) and density of the ith component

of the solid part of the material, respectively; as the volume of the multicomponent material V_S is equal to $\Sigma V_i = \Sigma m_i/\rho_i$, all matter m_S equals Σm_i and $\rho_S = m_S/V_S$; $\rho_i = m_i/V_i$; $X_i = m_i/m_S$.

5.4 Water and Cellulose/Cellulosic Substances

Water is the key component controlling the behaviour of all biomaterials, living organisms and so on. We have distinguished that liquid water in porous systems is:

- Self-organised water, i.e., a bulk of water whose behaviour is independent of the character and composition of the porous system; and
- Medium-enforced organised water, i.e., water organised in the porous system, particularly in the microreticular system, which is controlled by the surface molecular properties of the components forming this system. The states of liquid water are dependent on the specific surface area of the pores. The medium-enforced organised water is typical for microporous and nanoporous media, with natural so-called nanostructured polymers being typically hygroscopic.

Undoubtedly, water plays an extraordinary role in the formation, manufacturing, aging and influence of the properties of cellulose and cellulosic materials. The main focus of interest involves cellulose and cellulosic materials in a wet state, predominantly natural or in suspensions, during paper preparation. Formerly, a lot of attention was dedicated to the electrokinetic behaviour of cellulosic fibre slurries during papermaking, i.e., the pulp suspensions [56, 57]. The word 'electrokinetics' implies that an electrical current or potential arises due to the relative movement between two phases, as in the case of anionactive cellulosic fibres or fines suspended in water. Broadly, all prevailing scientific works operate using the concept of Zeta-potential, cationic demand, polyelectrolytes, colloidal stability and so on, because the charged nature of a cellulosic fibre surface is expected to play a major role in such phenomena as fibre dispersion, flocculation, and the adhesion and adsorption of polyelectrolytes [58]. Utilising electrokinetic data, papermakers have used a variety of electrokinetic procedures to control and optimise the levels of additives. Electrokinetic data helped predict the dosages of charged substances needed to achieve different balances of stability *versus* coagulation and flocculation of the suspensions.

5.4.1 Liquid Crystalline Cellulose Suspensions

The era of nanotechnologies and nanomaterials evoked an increased interest of elementary cellulose components with a sophisticated structure, i.e., cellulose

crystallites [40]. The interest was concentrated upon stable colloidal suspensions of cellulose microcrystallites [59] prepared using optimised acid hydrolysis of native cellulose fibres, as above a critical concentration, the suspensions form a chiral nematic ordered phase, or 'colloid crystal' exhibiting chiral nematic (cholesteric) ordering – a liquid crystalline cellulose suspension. Revol and co-workers [60] reported that suspensions of acid-hydrolysed cellulose crystallites can also form an ordered phase displaying chiral nematic orientation. Above critical concentrations, usually greater than ~1.5% (w/w), the suspensions separate into two phases, with the denser lower phase exhibiting birefringence [61] indicative of the chiral nematic phase. The rheology of rigid rod cellulose whisker suspensions has been broadly investigated [61, 62]. Preparation [63] conditions govern the properties of the individual cellulose microcrystallites, and hence the liquid crystalline phase separation of the cellulose suspensions. The typical dimensions of these crystallites are between 10 and 20 nm in diameter for a length of approximately 1 μm [64]. After hydrolysis conditions are optimised, the cellulose colloidal suspensions exhibit nematic liquid crystalline alignment. Nematic ordering is the alignment of fibrils in the same direction along an axis and has long been sought in the fibre industry with the promise of higher tensile strength. Liquid crystalline suspensions of cellulose microfibrils are particularly attractive because of their simplicity, consisting of charged microfibrils that 'self-assemble' into large regions of cholesteric ordering. The microscopic study of algal cellulose [65], using TEM and AFM, supports the presence of such a chiral twist along the microfibrils. Without a magnetic field or a shear field to enhance the liquid crystalline ordering of the cellulose microfibrils, the 2-D small angle neutron spectroscopy (SANS) and X-ray scattering profiles are isotropic 'powder' patterns. Magnetic and shear alignment of the cellulose microfibrils results in anisotropic scattering patterns. The magnetic field induces the orientation of the liquid crystalline phase. In aqueous suspension, these crystals are oriented so that their long axes become perpendicular to the field direction [66]. In addition, the observation that cellulose crystallites align perpendicularly to the direction of a magnetic field is in direct contrast to existing alignment technologies, all of which exhibit positive diamagnetic susceptibility anisotropy and, therefore, align parallel to the field [40]. Observations [65] revealed that the 'fingerprint' patterns, indicative of the chiral nematic phase, are deformed and disappear with increasing shear rate. SANS data obtained from an *in situ* shear cell placed in a neutron beam, provided evidence that as the shear disrupts the chiral nematic phase, microfibrils exhibit nematic ordering with the microfibrils aligned parallel to the flow direction. Additionally, SANS data confirmed that the cholesteric axis of this phase aligns along the magnetic field, with implications that the distance between the microfibrils is shorter along the cholesteric axis than perpendicular to it. This is consistent with the hypothesis that cellulose microfibrils are helically twisted rods. It is hypothesised that the source of the chiral interaction is directly attributable to the packing of screw-like rods. As shown by Orts and co-workers [65], threaded rods can be packed more tightly when their main

axes are offset, such that their 'threads fit within the each other's grooves'. Even a small twist in the cellulose microfibril would be sufficient to induce the observed chiral interaction. A more subtle explanation of this ordering is based on the anionic stabilisation only *via* repulsion forces of the electrical double layers taking place, without any influence of the water molecules. Nevertheless, it was proved that the suspensions of cellulose crystallites were not stable at sufficiently high electrolyte concentrations. Apparently, a decrease in the double layer thickness increases the chiral interactions between the crystallites [67, 68]. The stability of the colloidal suspensions of the rod-like shaped cellulose crystallites with negatively charged sulfate groups, i.e., the isotropic-to-chiral nematic phase equilibrium is sensitive to the nature of the counterions present in the suspension [69]. Although anisotropic phases did form under certain conditions, often either a gel or an isotropic phase was produced. Increasing the total concentration of colloidal suspensions resulted in an increase of the relative proportion of the chiral nematic phase with a higher density. For inorganic counterions, the critical concentration for ordered phase formation increases in the order $H^+ < Na^+ < K^+ < Cs^+$ [69]. Suspensions with H^+ counterions formed an ordered phase at the lowest concentrations of crystallites, i.e., with the highest exclusion tendency. For the inorganic cation series, the hydration number and the hydrated ion size decreased with increasing atomic number in the order $Na^+ > K^+ > Cs^+$. When these hydrated cations bind to the negatively charged particle surface, a hydration force will be generated between the particles. For hydrophilic colloidal suspensions (S), such as cellulose crystallites, the hydration force is repulsive and generally increases with the hydration number of the counterions, so the repulsive hydration force is expected to be in the order S-Na > S-K > S-Cs. Obviously, the relative difference between existing attractive and repulsive forces among rod-like cellulose crystallites in water was disturbed by the presence of additives, and due to this disturbance a new equilibrium is reached, introduced by the formation of the isotropic-to-chiral nematic phase. The phase separation of rod-like polyelectrolytes is among others that are determined by interparticle forces, such as steric repulsion, electrostatic repulsion, and hydration and hydrophobic interactions [67]. The temperature influence connected with the action of the interparticle forces is well known. Dong and Gray [69] observed an anomalous abrupt decrease of the volume fraction of the anisotropic phase at temperatures of 40–50 °C, but only in the H-form of the cellulosic suspension; under the same conditions, the Na-form did not exhibit the same response. The assumed explanation is based on the desulfation reaction of the cellulose crystallites, because for the neutral salt-form suspensions, the desulfation reaction does not occur due to the absence of an acid catalyst; however, in other places of this work it is alleged that at 35 °C for 24 h, the desulfation of the acid form of the suspension is negligible and can be ignored. Unfortunately, a detailed description of the nematic anisotropic denser phase is not reported. Similar liquid crystalline characteristics, which are quite unusual for aqueous suspensions of cellulose microfibrils, have been observed by Dinand and co-workers [70] who noted that the microfibrils of parenchymal cell

cellulose (PCC), prepared from the cell wall of disencrusted sugar beet cell-ghosts, consisted of a loose network of cellulose microfibrils. The PCC suspensions did not flocculate or sediment as long as some hemicelluloses and pectin were maintained at the microfibril surface. However, flocculation occurred if these encrusts were removed by either strong alkali or a trifluoroacetic acid treatment; these observations indicate the formation of a structured microreticular system of cellulosic microfibrils, mutually connected due to the presence of water.

5.4.2 Wet-web Strength and Wet Strength of Cellulosic Materials

The presence of surface functional groups which generate hydrolytically stable covalent bonds in the fibre joint will increase the wet strength. Furthermore, if such bonds can form in the wet end of the paper machine, they will contribute to the wet-web strength. Wet tensile strength is a key functionality for tissue paper, paper towel, paper board for packaging, cellulosic filter sheets and similar paper grades. The chemistry, mechanisms of action and applications of commercial wet strength resins have been extensively studied [71, 72]. Wet strength can be increased by either surface treatment, i.e., the surface modification of fibres, with small molecules, or by surface treatment with macromolecules, called wet strength resins. Conventional wet strength resins contain highly reactive chemical groups, which can crosslink the resin and graft them to the fibre surfaces. Mechanical entanglement, homo-cross and cocrosslinking mechanisms are available [73–79]. By contrast, it is not obvious how polyamines, such as polyvinyl amine, polyethyleneimine and so on, provide wet strength [80]. Laleg and Pikulik [81] working with never-dried webs (wet-web strength) and rewetted sheets (wet strength) made of mechanical pulps, proposed that three possibilities of the fibrous network crosslinking exist: chemical bond by imino-linkage between the carbonyl group and amine group, ionic attraction between the carboxyl and amine groups, and an irreversible H-bond between the -OH group of cellulosic materials and the $-NH_2$ group of the polyamine. It is known that the wet-web strength (initial strength of the paper) or its bond system, respectively, is determined by the mechanical entanglement of fibrous formations and by the mutual physical bonds between them. The extent of the mutual-bonding ability increases with an increase in the degree of beating, but this is detrimental to the mechanical entanglement. If a constant contribution to mechanical entanglement is assured (for instance, by a constant degree of beating) then the changes in the wet-web strength will indicate the changes in the wet state fibre bonds. It was observed [43, 82], that by application of well soluble nonionic urea, which strongly influenced the hydration bond system, i.e., made it weaker, this bond system is negatively influenced. The wet-web strength, measurable under comparable conditions with a relative hydration factor (for further details see **Figure 5.6**), falls with the rise of repulsive hydration forces. DiFlavio and co-workers [83], in their comprehensive laboratory study of the

mechanism of polyvinylamine (PVAm) wet strengthening, have concluded that PVAm should not form many covalent bonds with untreated cellulose. However, PVAm gave low adhesion to untreated cellulose, whereas the 2,2,6,6,-tetramethylpiperidine-1-oxyl radical oxidised cellulose resulting in strong adhesion [84]. This treatment converts the C6 cellulose hydroxyl to carboxyl and aldehyde groups, which will react with the amine groups on PVAm. Amines will couple to aldehydes to form imines but only a few terminal aldehyde groups, which are accessible to PVAm, will react with the amines in PVAm. Therefore, PVAm will not form many covalent bonds with untreated cellulose. They observed [83] that the occurrence of strong adhesion is practically unchanged from pH 3 to 9, which is beyond the range of imine formation. It suggests that physical bonding is also significant. But what bonds occur? DiFlavio and co-workers [83] proposed that PVAm strengthening is due to a combination of covalent bond formation and electrostatic bonding, but they also noted that it is impossible to decouple the effects of electrostatic and covalent bond formation. Or, does another sort of H-bond or physical bond exist?

5.4.3 Interactions in Cellulosic Fibrous Slurries using Enthalpiometric Measurements

Previously, using the microcalorimetric method [85, 86] for the investigation of amine interactions in cellulosic fibrous slurries, it was found that the interactions of nitrogen compounds in water containing aqueous pulp suspensions, exhibit measurable exothermal or endothermal effects. These observations enable us to follow the character of strength of the bonds being formed, as well as the mechanism of their formation. These types of interactions are due to the mechanism of releasing water molecules from active centres on the cellulose substrate and the formation of stronger H-bonds of the 'nitrogen-hydrogen' type with amine groups, instead of the weaker 'oxygen-hydrogen' type with water [86]. It has also been observed [69] that the intermolecular hydrogen bonding, generated from cellulose backbones of the H-form, is much stronger than that of the Na-form.

Two reasons for heat effects exist:

- Formation of strong H-bonds; and
- Formation of strong hydration bonds due to oriented water molecules present at interacting interfaces.

The following conclusions have arisen from the results summarised in **Table 5.1** [85]:

- Measurable heat changes are only exhibited by nitrogen compounds;

- Differential heat and corresponding entropy changes are constant throughout the whole concentrations series of dosed reaction components;
- The interactions lead (except diethylamine (DEtA)) to an increase in the entropy of the system; and
- The ratio between the maximum concentrations of the separate adsorbed reaction components is practically a whole number.

These facts reveal that the mechanism of interactions of monomolecular compounds does not change with their doses. The increase of the system entropy can most likely be accounted for by the increased water mobility and therefore, the state of water molecules being released from the active locations of the cellulose substrate formed by the pulp. The measured heat changes are therefore the result of the released heat coming from the formation of a new, stronger H-bond between the reaction component and the active locations of the cellulose, and the consumed heat during the release of water molecules from these active locations. The level of these resulting heat changes (differential heats, maximum released heat $-\Delta H_{max}$) can therefore be considered to be a relative criterion of the strength of the originating bonds. The results in **Table 5.1** confirm that the strongest bonds are formed by DEtA or secondary amino nitrogen, respectively.

Table 5.1 Sorption data related to the interaction of 1% (w/v) water suspension of unbleached sulfite pulp with 0.5–4% (w/v) water solutions of monomolecular compounds [72]. T = 20 °C

Compound	Max. adsorbed amount, $n_{A\,max}$ (mol/g pulp)	$-\Delta H_{max}$ (J/g pulp)	ΔS (kJ/mol.K)	Differential heat, $d\Delta H_r/dn_A$ (kJ/mol)
Methylethyl-ketone	Nonmeasurable heat			
Ethanol	Nonmeasurable heat			
Acetamide	12.5×10^{-4}	8.4	0.069	- 6.7
Formamide	-	-	-	- 3.3
Urea	24.8×10^{-4}	6.6	0.075	- 2.8
Ammonia	25.5×10^{-4}	15.0	0.094	- 5.9
Ethylamine	13.4×10^{-4}	23.0	0.107	- 15.0
Diethylamine	3.9×10^{-4}	23.0	- 0.034	- 50.0
Triethylamine	13.4×10^{-4}	13.0	0.053	- 12.0
Ethylendiamine	6.7×10^{-4}	20.0	0.013	- 30.8
Diethylentriamine	4.5×10^{-4}	10.0	0.023	- 29.7

Supposing that, during an interaction, one ammonium molecule is substituted by one water molecule, the mechanism and its stoichiometry can be formulated. It follows that the originating H-bonds 'nitrogen-oxygen' are stronger than H-bonds, by which water molecules bond to the cellulose substrate, because the heat of this interaction is exothermal.

5.4.3.1 Interpretation of Enthalpiometric Observations

Heat changes will be greater if bonds other than H-bonds are formed; particularly if they are of different qualities. 'Nitrogen-oxygen' bonds are qualitatively different from the usual 'oxygen-hydration' bonds; H-bonds 'nitrogen-oxygen' can be divided into two groups:

1) The proton-donating group is on the nitrogen compound

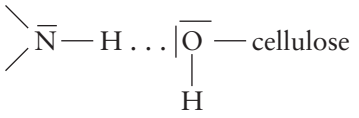

(including ammonium, primary and secondary amino groups)

2) The proton-donating group is on the cellulose or on another compound

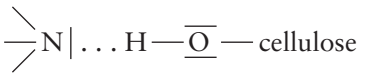

(tertiary amino groups belong there).

These two types of H-bonds enable the formation of a wide spectrum of H-bonds, depending particularly upon their polarity as in the H-bonds 'hydrogen-oxygen'. Continued polarisation of the H-bonds of the 2nd type leads to the formation of highly polarised bonds, which are formed by quaternary amino groups of an ionic type (3rd type). Breaking the hydration layers around the interacting components will occur if the energy level of the originating bonds is the same or greater than the level of bonds within, which are fixed on the interphase of the water molecule or their clusters. The mechanism of this process, in the case of cellulosic material, can be schematically represented in the following way (Cell – representing the cellulosic material, K – the reactive component).

$$\text{Cell-(—H}_2\text{O)}_m + \text{K-(—H}_2\text{O)}_p \rightleftharpoons \text{cell-K-(—H}_2\text{O)}_n + (m–n)\ \text{H}_2\text{O}$$

Due to the interaction of the hydrated molecules of the reactive component K with the surface of the cellulosic material, shifts or the release of water molecules and their clusters, occur from the active locations on the cellulose substrate and within the hydration shell of the reactive component; thus, a more stable bond is formed. The (m - n) value can be positive or negative. The process is naturally accompanied by corresponding energy and entropy changes. The formation of the bond between the cellulosic material and the reactive component K is accompanied by energy release, particularly if a qualitatively different bond is formed, from the original one, with water. The release of water molecules and their clusters or shifts are linked to energy consumption; this is analogous within the ordered state region of separate water molecules and the K component, but in the reverse order. However, it can be assumed that greater entropy changes – increase in entropy – will appear in the water molecules than in the K component molecules – decrease in entropy. As heat effects only occur if energy changes happening within the system are at least on a molecular level (which are linked to the inner energy of the molecules, character and size of the bonds and so on), heat effects will presumably only exhibit interactions leading to changes in hydration layers. This means that the interactions schematically represented above (1) will be accompanied by heat changes of exothermal and endothermal character. If (m - n) = 0 and the energy of the H-bond in the reactive component combined with water is approximately the same as in combination with the cellulose material, then the resulting heat effect will be zero. The amount of exothermal and endothermal heat will depend on the strength of the newly formed bonds and on the relative amount of water molecules, either released or displaced to another energy stage of water molecules and their clusters. The amount of exothermal heat will then relatively indicate the strength of the formed bond. The higher the released heat, the relatively stronger the bond and *vice versa* in the case of the endothermal character of the interaction: the lower the value of the consumed heat, the relatively firmer the bond [85]. The release mechanism of water molecules, as well as hydrogen bond formation, satisfactorily explains the wet-web strength and paper wet-strength when using polyamine substances and other similar processes, such as the heat gelation of proteins and so on.

5.4.4 Existence of Water Inclusions among Cellulosic Chains

Existence of small water inclusions among cellulosic chains of the cellulose membrane with widths about 15 nm, i.e., containing approximately 50 water molecules, was confirmed by the use of wide angle X-ray (WAX) and small angle X-ray (SAX) –

scattering or diffraction methods [49]. The cellulose-water systems were modelled using a water-vapour treated membrane, and soaked in liquid membranes employing light and heavy water. Using these methods, new results were obtained which were coherent for both the applied methods, WAX and SAX. They proved the existence of structural changes in the membrane, on a molecular level, caused by molecular water and that the changes depended on the type of penetrated water. It was also evidence for the existence of oriented water clusters in soaked samples. Simultaneously, the difference at a molecular level between light and D_2O was retained. As a result, water clusters are formed in the soaked samples instead of in the water-vapour-treated samples, where no bulk water exists. Moreover, H_2O vapour modifies the cellulose structure to a greater extent than D_2O. The weaker interaction of D_2O with cellulose corresponds to its lower permeation rate through the cellulose membrane. Inelastic neutron scattering (INS) experiments on various types of cellulose [87] revealed that amorphous cellulose is indeed practically 100% accessible to water, and that a nearly perfect exchange of OH groups into OD groups, after deuteration, is obtained in the accessible (disordered) regions by simple wetting. Hence, swelling and washing of amorphous cellulose in D_2O will lead to a full exchange of OH by OD. This means a 30% exchange of all hydrogen atoms in the cellulose molecule. On removing heavy water by drying the sample, OD groups are preserved as long as the sample is protected against atmospheric humidity or other protonated polar solvents. The explanation is based on additionally perturbing the hydrogen bonds between the cellulose molecules, due to the penetration of water molecules, and increased distance between cellulose molecules because of the swelling. It was also confirmed that all OH groups *inside* the crystalline parts (crystal cores) are unaffected by immersing the sample in D_2O or H_2O, i.e., inaccessible. However, deuteration inside the crystals is possible using a relatively simple hydrothermal treatment technique. Samples were inserted into glass ampoules filled with 0.1 N NaOD/D_2O. The sealed ampoules were kept at 210 °C for 30 min, the morphology of the crystals was shown to be unaffected by this process [87].

5.4.5 Hydrogel Structure of Cellulose

All information and experience have revealed that the smallest cellulosic particles are microcrystallites of rod-like shape (4–10 nm in width; 80–1,000 nm in length), enwrapped with anisotropic hydrogel shells and exhibiting a gradual decrease in viscosity in the direction of bulk to water. These nanosized structured 'submicrohydrogels' of fibrils stick out of the surface of the pulp fibre and have a great importance for their paper-forming ability, due to their secure bonding potential. The results of sorption – desorption hydrocolloid measurements, suggest a permanent evolution of 'submicrohydrogels' from pulps, which are dependent on the type and quality of the pulp (degree of beating), and water composition; these 'submicrohydrogel' substances

predominantly influence the hydration forces. Soluble and colloidal substances, mostly of anionic character (polysaccharides, microcrystallites, monosaccharides, lignosulfonates in the case of sulfite pulp, and other low molecular weight compounds) are bonded by hydration forces to form a vicinal water shell, of quasi-gel structure, with decreasing viscosity around the fibrous surface [88, 89]. These substances are released into the water environment during washing, at a preestablished temperature, in approximately the same amount [90], but depend on the quality and quantity of the acting hydration forces. The increased activity of repulsive hydration forces, i.e., antibonding activity, improved the evolution of colloidal substances into the bulk of the water and *vice versa*. It was found [90] that of the hydrocolloid substances released into the water environment during repeating pulps (bleached sulfite, sulfate and unbleached sulfite pulp, respectively), extraction had a positive influence on the repulsive hydration forces, as a higher amount of substances were released into solution than that corresponding to the predicted value, except in the case of groundwood. More detailed measurements of hydration force activities, by use of the so-called hydration factor, confirmed an increase of the repulsive forces in systems with an increased concentration of released lignocellulosic substances. An increase of the hydration factor, g [43, 82] also indicates a better release of soluble and colloidal substances from the pulp. However, the values for groundwood were in the $g < 1$ range, i.e., in the range of prevailing attractive hydration forces in comparison with distilled water. In this case, the prevailing attractive hydration forces are weakened only upon an increased concentration of the released lignocellulosic substances.

5.5 H-bond Ability and Hydration Bonding/Antibonding Concept

A simple comparison of fibre size (approximate length 2 mm and width 20,000 nm), the length of H-bond (0.27 nm [91]) and water molecule (0.094 nm [92]) signals that it is practically impossible [93, 94] to form a fibrous bonding system of paper without a supporting tool to draw the mutually interacting fibre surfaces near, during the H-bond formation. Without this tool, relatively huge fibres are not able to effectively approach with an accurate orientation of the proton-donor group on one surface and the proton-acceptor group on the other surface. Water molecules allow serviceable tool functioning, which enable the interacting fibres to form an optimal fibre-network structure. The bonding system of paper has been formed due to this unique property of water [5, 93, 94]. Obviously, both the hydration attractive and repulsive forces are responsible for the effective structural fibrous formation, i.e., hydration bonding functions as a predecessor of H-bond formation (see **Figure 5.5**). It is thought that water molecules enable the formation of natural cellulose crystals by favourable alignment of the chains through hydrogen-bonded bridging. This process is connected with the action of attractive hydration forces in the wet state. Part of the cellulose preparation is amorphous between these crystalline sections. The overall structure

is formed of aggregated particles with extensive pores capable of holding relatively large amounts of water by micro- and nanocapillarity. The hydration bonding and antibonding concept (structure change in hydration layers (SCHL) theory) is based on the dipole nature of water molecules and on their two possible orientations in hydration spheres:

- Orientation with the hydrogen atoms of water molecules in the direction of the active surface of the fibre; and
- Orientation with the oxygen atom of water molecules in the direction of the active surface of the fibre.

These two different water molecule orientations are caused by the amphoteric character of water molecules with regard to accepting hydrogen bonds. A water molecule has the ability to join with other molecules or groups with hydrogen bonds, in which it can act as the hydrogen atom donor or acceptor. The intermolecular force field, produced by the formed hydrogen bonds, will then spread by means of the other molecules through the hydration sphere under the influence of this orientation of water molecules, becoming more and more diffuse until it equals a zero value within water. This effect gives rise to forces that cause action between the interacting surfaces – that is, hydration forces [93, 94].

If the water molecule orientation to each of the interacting surfaces is equal, then both surfaces will affect each other with repulsing hydration forces. On the other hand, if the orientation of water molecules is different, the two surfaces will attract. Theoretically, the repulsive forces are effective over a greater distance [46]. This difference appears in the interactions of heterogeneous surfaces, in which repulsive and attractive hydration forces act simultaneously, as a kind of equilibrium is established in which the two surfaces reach a definite optimum distance from each other. During the interaction, a mutual diffusion of hydration spheres takes place, connected with a change of their structure. These structural changes are on the molecular level and should be accompanied by measurable temperature effects [46, 85, 95]. For hydration forces to originate, it is necessary for water molecules to reach a suitable orientation in the hydration spheres. This orientation is determined by H-donor and H-acceptor groups, their amount and by the strength of the hydrogen bond formed with water, or in other words, by the value of the interface tension $\gamma_{1,s}$. All hydrated systems with a high specific surface area behave in this manner; these include various porous systems filled with water and its solutions, gels, quasi-gelantinous systems and so on. According to this theory, the groups forming hydrogen bonds with water can be divided into three types:

- H-donor groups and molecules: such as primary alcoholic OH-groups, secondary amino groups in aliphatic compounds, and partially primary amino groups;

- Amphoteric groups and molecules: such as H_2O, secondary alcoholic OH-groups in polysaccharides, and partially primary amino groups, amide groups and so on; and
- H-acceptor groups: such as hemiacetal oxygen in saccharides, carbonyl groups and tertiary amino groups.

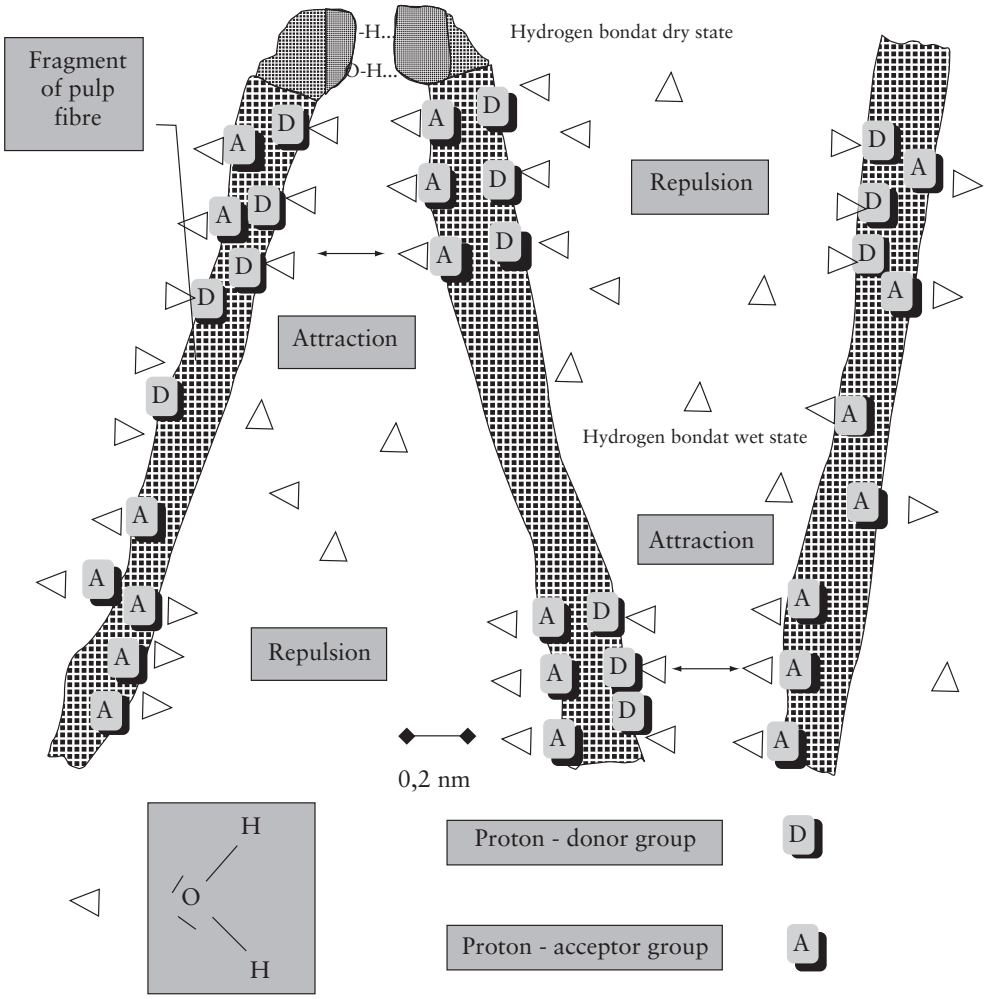

Figure 5.5 Schematic representation of the origin and action of repulsive and attractive hydration forces during the formation of a hydrogen bond system among cellulosic fibre materials in water

The behaviour of these groups depends considerably upon the surrounding groups, which are not necessarily linked to H-bonds. For example, surrounding groups having the -I effect will intensify the donor nature of oxygen in these groups. The mesomeric effect has the opposite influence: the hydroxyl groups will strengthen their acceptor nature and weaken the donor nature [96]. The relationship of this theory to electrokinetic behaviour, following the electrical double layer theory, shows that the adjacent part of the electric double layer, around the hydrated hydrophilic phase interfaces, is formed by hydration layers [46, 96]. The other molecules of ionic and nonionic character are drawn in or expelled by electrostatic, van der Waals or other forces into these layers. However, the thickness of the hydration layers is considerably greater than that of the inner layer, resulting from the classical electrical double layer theory, and due to its diffuse character it is not limited to an exact size; its thickness depends highly on the effect of shear forces, i.e. the velocity gradient. For this reason, the value of the Zeta-potential will be highly influenced by these factors. Under comparable conditions, different Zeta-potential results can be obtained by different experimental methods, which differ both in absolute values and sign.

Coacervation of nanoreticular hydrated systems, composed of hydrophilic anisometric oligomer molecules, during their dilution is a typical phenomenon where the hydration forces play the dominant role. It also seems reasonable to utilise these quasi-hydrogel systems to measure the behaviour of hydration forces using the so-called relative hydration factor [45, 82]. As represented in **Figure 5.6,** under isothermal conditions, the volume of the original hydrated hydrophilic system V_o, e.g., some polyesters or urea-formaldehyde (UF) precondensate, when gradually diluted with water or water solutions respectively, does not undergo any changes until the moment the volume of the diluted sample exceeds the critical value V_k. Consequently, the originally transparent liquid becomes turbid due to precipitated microhydrogel particles; such behaviour is due to the presence of hydrophilic anisometric oligomer molecules. The parts or ends of these molecules influence each other by attractive hydration forces, while other parts of the interacting molecules are influenced by repulsive hydration forces. The effect of the attractive forces among interacting molecules must however, prevail over the repulsive forces. The uniform distribution of the oligomer molecule is thus reached throughout the volume of the water medium. When these systems are diluted, the molecules, their parts and ends are drawn away from each other, and their mutual force of action is thus weakened. After exceeding the critical concentration or critical volume of added diluting water, coacervation takes place, owing to the fluctuation of the affecting mutual forces and kinetic energy of the interacting molecules. In this case, the composition and properties of the separated coacervates correspond to the original concentrated system. The influence of the rate of added substances upon hydration forces can be evaluated by means of the so-called hydration factor $g = CDD/CDD_0$, where CDD and CDD_0 mean the critical degree of dilution in water-solution and distilled water, respectively.

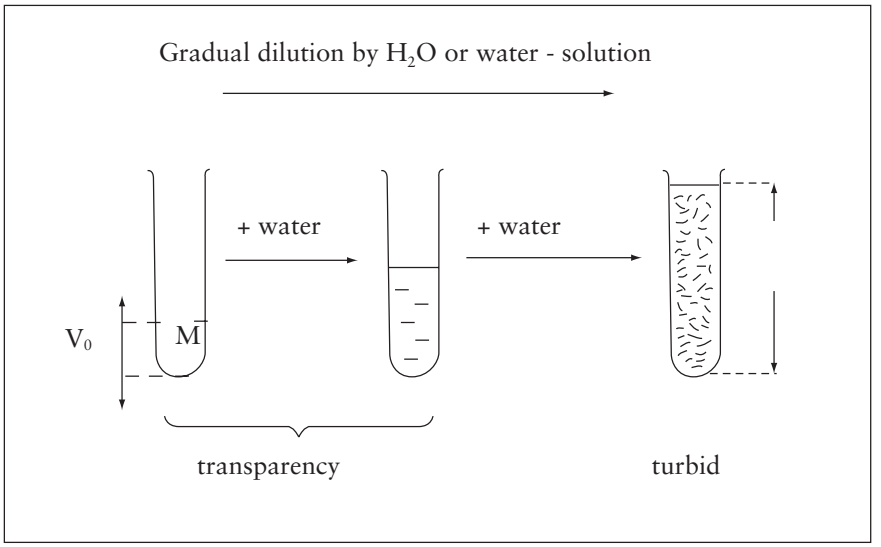

M - Modelling system; CDD = V/V_0; $V = V_0 + V_k$;
$CDD_0 = V_d/V_0$ - Critical degree of dilution i distilled water;
$CDD = V_s/V_d$ - Critical degree of dilution in water-solution;
$g = CDD/CDC_0 = V_s/V_d$ - Relative hydration factor.
If $g < 1$ - increasing of the attractive forces influence in the hydration bonding system; and
If $g > 1$ - increasing of the repulsive forces influence in the hydration bonding system.

Figure 5.6 Evaluation of the effect of hydration forces by means of a hydration hydrophilic modelling system

However, Kim and Yun [97] very interestingly described the discovery of a smart cellulose material that can be used for biomimetic sensor/actuator devices and microelectromechanical systems. This smart cellulose material is termed electroactive paper (EAPap) and it can produce a large bending displacement with low actuation voltage and low power consumption. The authors proposed that electroactive paper is advantageous for many applications, such as microinsect robots, microflying objects, microelectromechanical systems, biosensors and flexible electrical displays. Using this phenomenon it is also possible to explain and simulate muscle movement. EAPap is made from a cellulose film (cellophane) on which gold electrodes are deposited on both sides. An EAPap actuator was supported vertically in a controlled humidity and temperature environment chamber. By excitation of the voltage application to the actuator, a bending deformation is evoked. The authors believe that the actuation is due to a combination of two mechanisms: ion migration (diffusion of sodium ions to the anode?) and dipolar orientation. Again, in spite of the confusing and irrational

explanation of the EAPap movement, the reported results give great inspiration for theoretical potential accompanied by practical challenge. The tip displacement of the EAPap actuator is dependent on the applied electric field, its frequency, EAPap sample thickness and temperature, but predominantly on humidity. The humidity affects the displacement, where a high relative humidity leads to a large displacement; this behaviour can be rationally explained by use of the SCHL theory [98]. The orientation of water molecules in immobilised layers around the cellulose macromolecules, in the layered structure of the EAPap actuator, is determined by the presence of proton-donor groups or proton-acceptor groups at their interacting surfaces. The overall film structure and shape are formed among structural cellulosic units due to hydrogen-bond bridging in the dry state and hydration-bond bridging in the wet state. The extent and intensity of this bonding system is determined by the size, concentration and distribution of nanodomains with either an attractive or repulsive force of action, i.e., among opposite interacting nanosurfaces exhibiting the reverse or identical basic orientation of water molecules, respectively. The basic orientation of a water molecule is determined by the presence of surface proton-donor groups or proton-acceptor groups of cellulose. Whilst hemiacetal and glycosidic oxygen in cellulose are typical proton-acceptor groups, the hydroxyl groups can behave as proton-donor and proton-acceptor groups. Nevertheless, it is supposed that the behaviour of most hydroxyl groups in cellulosic materials have more of a proton-donor character. As a consequence, the domains of prevailing hydration-bond bridging are regularly distributed within the cellulosic material in a flat formation. Any disturbance of this distribution and paper strip curling is evoked because the inner tension equilibrium has been disrupted. Application of an oriented electric field to cellulosic material in a wet state, results in the water molecules in the bonding nanodomains, contained nearest the electrodes, to be reoriented. However, reorientation at the cathode is different to reorientation at the anode – at the anode, reorientation only occurs to the water molecules having been oriented to this pole with hydrogen atoms at the basic original state, and at the cathode it occurs only for those water molecules having been oriented to this pole with oxygen atoms at the basic original state. Moreover, the distribution of attractive forces formed around both the **A** and **D**, and the **D** and **A** nanocentres is not the same – a prevailing **A** - **D** structure orientation in the bonding domains is presumed. In this situation, the application of a DC electric field evokes a weaker bond system in layers near the anode and *vice versa*, a stronger bond system in layers near the cathode. Due to this effect, the paper strip bends towards the anode. Logically, the effect is strongly dependent upon relative humidity, and the reorientation of water molecules is independent of the diffusion process and relatively quick. Obviously a similar effect, but at the microscale, explains the movement of muscles. The main presumption is the nonsymmetrical distribution of attractive forces formed around both the **A** and **D**, and the **D** and **A** nanocentres.

5.5.1 Rheosedimentation

The phenomenon, known as rheosedimentation, is typical of fibrous slurries with papermaking abilities [99, 100]. The macroreticular systems, comprised of a weak bonding system, are represented by papermaking pulp slurries composed of fibres of cellulosic or lignocellulosic character. It is a typical property of components, with marked papermaking properties, that form fibre networks which are only compressed during sedimentation, i.e., this process behaviour is called rheosedimentation [101, 102]. The basic condition of rheosedimentation is an ability of the pulp fibre to form a network displaying special behaviour, i.e., due to a weak bonding system, the fibre network is compressed by gravity [99, 101]. The bonding system of the wet-web state is realised through the so-called Campbell effect followed by the origination of a H-bonding system, but only in water media, i.e., among paper components with so-called hydro-cohesive properties. The ability of these components to form a comprehensive fibre space net in a water medium, i.e., hydrated macroreticular system, has been well documented as typical of this behaviour [98]. It is well known that paper matter exists in three forms:

- The suspension form;
- The wet-web paper form; and
- The dry-web paper form.

Behaviour of the first paper state corresponds to a general formula describing the continuum movement and it is typical for components with marked papermaking properties. Evidence supporting this description is the phenomenon called rheosedimentation as it is observable during sedimentation of diluted fibre slurries. The movement of the fibre space net during rheosedimentation is described by **Equation 5.1**:

$$\frac{t}{(h_0 - h)} = \alpha + \beta \cdot t$$

$\alpha = \frac{1}{v_0}$ for an initial fibre network concentration c_p

$v_s = \frac{1}{\alpha_s}$ standardised rheosedimentation velocity for c_p = 1 kg/m^3

β characterised final concentration of fibre network - c_k as:

$$c_k = h_{00} \cdot x_1 / \left(h_0 - \frac{1}{\beta} \right) \qquad (5.1)$$

which follows from the solution of the General Continuity equation. Symbols h_o and h are the height of the boundary level of a fibre space net in water at time t = 0 and t, respectively. The parameters α and β characterise the velocity of sedimentation at high h_o and a final concentration of the sedimented fibre space net, respectively. It was shown that:

- Rheosedimentation is definative for every fibre component of papermaking ability and it is a useful indicator of this process;
- The sedimentation velocity and final concentration of the sedimented fibre components are dependent on the fibre morphology;
- The final concentration is sensitive to the interbonding ability of the fibre components which create the fibre suspension – it appears that with increasing this ability, the final concentration of the sediment decreases; and
- Both of these parameters, i.e., the sedimentation velocity and final concentration of the sediment are strongly dependent upon the hydration ability of the fibre components – upon increasing this hydration ability, both parameters decrease.

The homogeneous pulp fibre network is formed at a suspension concentration higher than 1 kg/m^3. Dilution of the suspension to a concentration under 1 g/L is accompanied by flocculation and rheosedimentation. However, the rheosedimented fibre network is not in a fully homogeneous state, due to the lack of shear forces (agitation) disturbing the rheosedimenting floccules.

5.5.2 Thermoresponsive Hydrated Macro-, Micro- and Submicroreticular Systems of Cellulose

Hydrated reticular systems, i.e., networks in water environments, characterise all bioentities and the products of their existence. We can identify these structures at the nano- (submicro-), micro- and macroscale as submicro-, micro- and macroreticular hydrated systems, respectively. Supramolecular and hypermolecular structures are typical, e.g., hydrogels based on peptides, and fibre networks based on cellulose; a typical characteristic being the phase transition temperature (lower critical solution temperature (LCST) or upper critical solution temperature (UCST)) of the thermoresponsive hydrated reticular system (TRHRS), exhibiting a unique hydration-dehydration change. As illustrated in **Figure 5.7**, the volume changes are typical in hydrogel TRHR systems. Below the LCST, the uncrosslinked polymer chains are soluble in water, whereas above the LCST the polymer chains form submicro- and microaggregates, which separate from solution. Above the LCST, the polymer starts a complex self-assembling process that leads to an aggregation of polymer chains,

initially forming nano- and microparticles, which segregate from the solution [103]. Below the LCST, the crosslinked hydrogel is swollen and absorbs a significant amount of water, while above the LCST the hydrogel dramatically releases free water and begins to shrink. Thermoresponsive hydrogels composed of crosslinked polymer chains undergo fast [104, 105], reversible structural changes from a swollen to a collapsed state by the expulsion of water. However, other types of thermoresponsive hydrogels exist which are opposite to the LCST hydrogels, i.e., hydrogels with an upper critical solution temperature, UCST. These hydrogels shrink at lower temperatures and swell at higher temperatures.

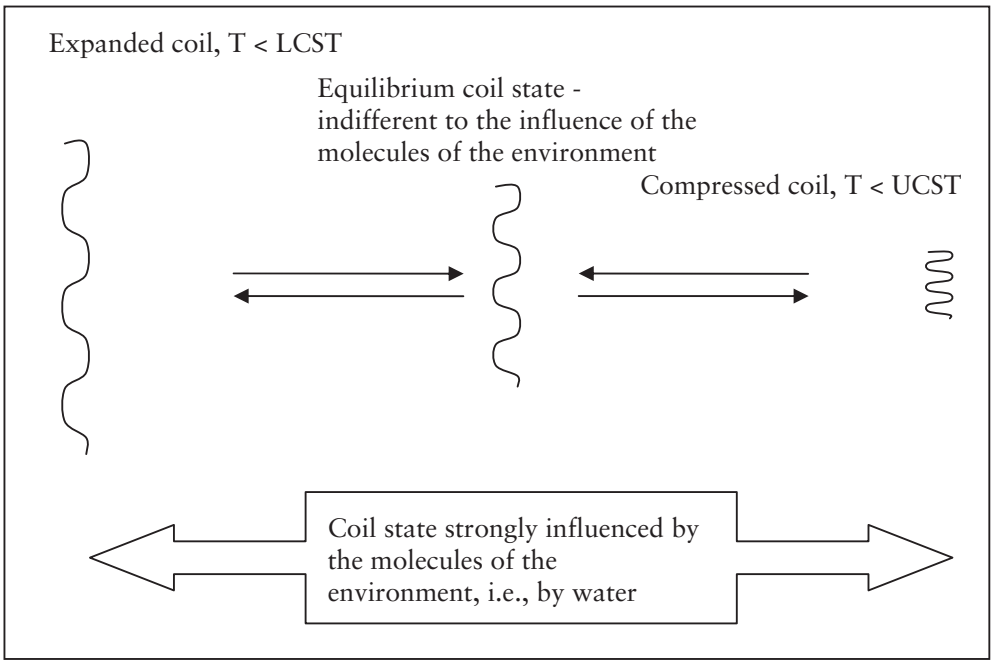

Figure 5.7 Schematic 2-D illustration of linear macromolecule behaviour in hydrated micro- and nanoreticular systems with LCST or UCST, i.e., a lower or upper critical solution temperature, respectively

According to the behaviour of the TRHRS during dilution [98], we can divide the films into water dilutable and nondilutable, crosslinked 3-D networks or crosslinked 2-D networks. Additionally, it is possible to divide the dilutable TRHRS into fully dilutable polymer solutions at T < LCST (or T > UCST), and coacervated

[43, 45, 106] submicro- or microTRHRS, or flocculated macroTRHRS. The dilutable [98] TRHRS coacervate or flocculate in the water environment due to weak bonds among the polymer chains, microparticles, and hydrogel particles or fibres and microfibres, respectively. This is typical for the submicro-, micro- and macronetworks that are disrupted during the dilution process, i.e., the quasi-hydrogels coacervate and the fibre networks flocculate, respectively. As the temperature changes, the transition of the sol-gel reversible hydrogels occurs due to nonchemical crosslinks being formed among the grafted and branched elements of the copolymers.

Poly (*N*-isopropylacrylamide (PNIPAAm), has been the most used polymer in thermoresponsive hydrogels with characteristic LCST. Above the LCST, at around 32 °C in pure water, a reversible structural transition occurs from an expanded coil (soluble chains) to a compact globule (insoluble state) [107–112]. *N*,*N*′-methylenebisacrylamide (MBA) is utilised as a crosslinker [104, 113]. Such a macromolecular design widens the applicability of such systems to a variety of biomedical applications inclusive of the biomineralisation of biodegradable substrates [114]. Such modifications are particularly important to tailor the LCST of PNIPAAm-based systems. Recently, a curiously self-oscillating system of hydrogel particles, rhythmically changing its volume, was described by Yoshida which was based on PNIPAAm, MBA and a covalently immobilised $Ru^{2+/3+}$ redox system utilising the so-called Belousov–Zhabotinsky oscillating reaction [115]. The UCST hydrogels are mainly composed of an interpenetrating polymer network of polyacrylamide and poly(acrylic acid) or poly(acrylamide-*co*-butyl methacrylate) crosslinked with MBA [113]. The formation of helices (double or triple in polysaccharides such as agarose, amylose, cellulose derivatives and carrageenans, or in gelatine, respectively) and the corresponding aggregation upon cooling, form physical junctions which are the basis of hydrogel formation [116]. Dilutable but coacervating quasi-hydrogels with UCST are represented by UF precondensates [43, 45]. We can conclude [98] that under normal conditions, i.e., at room temperature and an inert environment, the PNIPAAm polymer has a preferred thermodynamically advantageous coil conformation because of the hydrophobic interactions among isopropyl pendant groups. However, due to a peculiar water activity, the coil conformation is stretched at temperatures below the LCST, in contradiction with the squeezed original coil conformation above the LCST, as the repulsive domain activity is weakened. The peculiar water activity is accompanied, below the LCST, by the origination of repulsive water action among the polymer chains and its segments, the submicro- and microcolloidal particles and so on, arising from equal water molecule orientation at the interacting interface microdomains due to hetero- followed by homo-H-bonds, i.e., a hydration antibonding system. Obviously, the width of vicinal immobilised water, within the interacting polymer interfaces, decreases with an increase of polymer concentration, because the improving disruptive action of the hydration repulsive forces is dramatically weakened upon an increase in temperature. As a result, the LCST

decreases with increasing polymer concentration [117]. Under normal conditions, i.e., at room temperature and an inert environment, the UCST hydrated crosslinked and uncrosslinked polymers have a preferred thermodynamically advantageous long-chain structure, which is squeezed into a compressed coil conformation in a water environment due to the origination of a weak hydration bonding system. The hydration bonding system [43, 45, 82, 98] among polymer chains, its segments, submicro- and microcolloidal particles and so on, arises from the opposite water molecule orientation at the interacting interface microdomains because of the hetero-H-bonds of the proton-acceptor or proton-donor groups of the polymer chains and homo-H-bonds among water molecules. As the temperature increases, the hydration bonding system is weakened because of the increase in the kinetic energy of the water molecules. Above the UCST, the hydration bonding system is weaker than the inner opposite stress of the compressed polymer chains of the TRHRS and the polymer chains expand. As a result, the crosslinked TRHRS swell and the polymer chains in the noncrosslinked TRHRS are dissolved. Below the UCST, the hydration bonding system is stronger than the inner opposite tension of the compressed flexible polymer chains and the long chains of the polymer compress. The process results in deswelling and coacervating of the crosslinked hydrogel and dissolved polymers, respectively. Obviously, the intrahydration bonds squeeze the long-chain uncrosslinked polymer structure into a compressed coil conformation and the interhydration bonds squeeze the long-chain crosslinked structures to a deswollen form at temperatures below the UCST. However, different characteristic behaviour is observed if a hydrated reticular system is composed of relatively rigid rod-like particles, such as short polymer chains or fibres. The short polymer chains or fibres in hydrated submicro- or macroreticular systems, respectively, are formed through interhydration bonds and the interhydration repulsive domains, i.e., mutually functioning hydration bonding and debonding sites. Typically, due to increased fluctuation of the bonding and debonding activities of the interacting microsites during dilution, the submicroreticular systems coacervate and the macroreticular systems flocculate. The submicro weak bonding of the hydroreticular system, accompanied by coacervation during dilution, is well demonstrated by use of a UF precondensate [43, 45].

We have observed during wet pulp beating that the characteristic decreasing of pulp drainage ability, with increasing input beating energy, is abruptly increased if the temperature of the pulp slurry being beaten is higher than 40 °C. This fact (see **Figure 5.8**) indicates some LCST behaviour of the hydrogels forming the beaten cellulosic fibres. As the temperature is raised above the LCST, the fibre hydrogels deswell, contrary to the swollen state below the LCST, i.e., at temperatures above the LCST of the fibres, the pulp slurry is better drained and *vice versa*. This fact corresponds well with the observation of Dong and Gray [69] of an anomalous abrupt decrease of the volume fraction of the anisotropic phase of colloidal suspensions of cellulose crystallites within the temperature range of 40–50 °C.

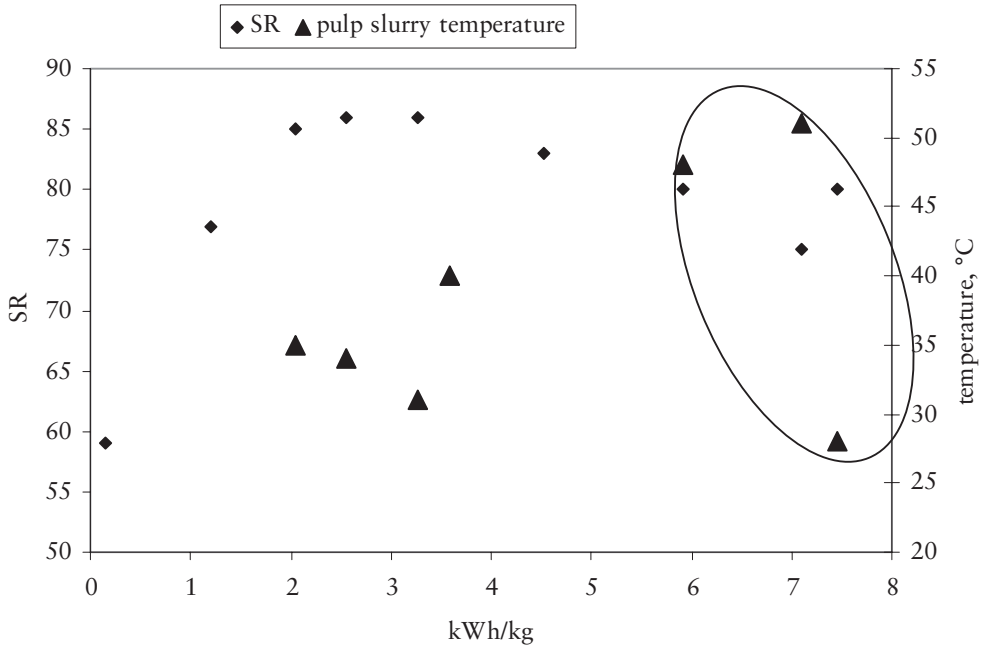

Figure 5.8 Temperature of pulp slurry influence upon drainage ability of beaten hemp pulp

Note:

°SR – degree of pulp beating according to Schopper-Riegler (ČSN EN ISO 5267-1) -

the drainage ability of the pulp slurry decreases with increasing °SR;

Effective beating energy in kWh/kg of oven dried pulp fibre; and

Beating conditions: laboratory toroidal beater; nonbleached hemp pulp prepared by the alkaline cooking method; pulp beaten at 3% consistency for 49 min at an approximately constant operating beater edge load.

It has been concluded that the water inside the pores of the lignocellulosic material is physically created by three sorts of water: the nonmoveable adjacent part of the immobilised water shell with the highest viscosity at a given temperature and flow conditions; transition part of the immobilised water shell flowing with higher viscosity at a given temperature and flow conditions; bulk water in the middle part of the pores flowing with a normal viscosity coefficient at a given temperature.

5.5.3 Swelling

The supermolecular and hypermolecular structure of cellulosic materials is changed upon drying. The pores and lumens collapse and the hydrogel structures are transformed into xerogels. The whole process is well known as the hornification phenomenon. The opposite process – swelling – is not fully reversible and it is characteristic in that water flows into the porous cellulosic matter followed by swelling, i.e., a volume increase of the sample. A few decades ago Dobbins [118] described that pulp swelling is not evoked by the presence of soluble substances, but by water molecules with high polarity. The swelling is often connected with the charging of swollen cellulose predominantly by the dissociation of the carboxylic groups within the cellulose. However, the diminished dissociation of carboxylic groups within the bulk of the cellulose and at its outermost surface was observed. The increased charge density and possibly the ordered water structure are assumed to cause the distinct differences in the behaviour of the carboxylic groups inside the cellulosic layer and at the surface [119].

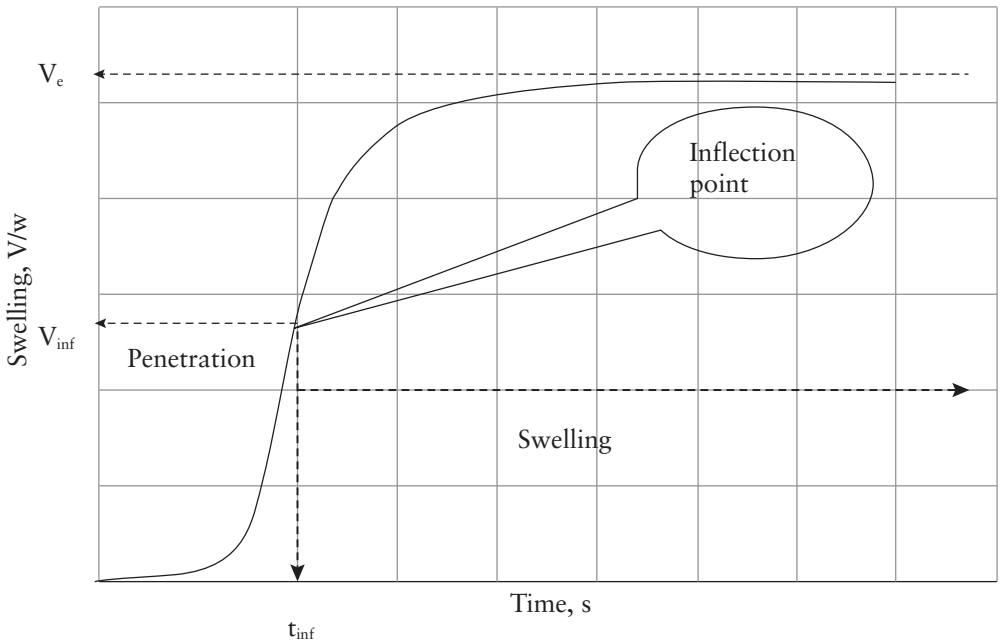

Figure 5.9 Swelling kinetics of cellulosic material; cm^3 of water/g of sample *versus* time

The kinetics of the swelling process is controlled by the water flow into the porous material, Q, which is additively composed of the penetration flow, Q_p and the swelling flow, Q_s. Obviously, water flow in the bulk of the cellulosic porous material is proportional to $(V_e - V)$, **Equation 5.2**:

$$Q = \frac{dV}{dt} = Q_p + Q_s = k(V_e - V) \tag{5.2}$$

where V, cm^3 of water/g of sample is actually the volume of water which had penetrated into the sample during time t; k, kinetic rate of swelling, s^{-1}; V_e, the overall amount of sample water at equilibrium comprises the whole of the penetrated water into the pores, V_{ep} and swollen water V_{es}; $V_e = V_{ep} + V_{es}$. Where V_{es} is given by concentration, c (mol/dm^3) of ionactive and nonionactive hydrophilic soluble and nonsoluble substances, n_e (in mol) embedding of cellulosic interfaces and participation of osmotic pressure, p_{osm} equilibrium with the inner stress of stretched swollen cellulosic matter. Obviously, $p_{osm} \approx c\,RT$, where $c = n_e / V_{es}$;

R – gas constant; T – temperature in K. According to Darcy's equation, the penetration flow, $Q_p = k_p \cdot 1/V$, where:

$k_p \approx \Delta p_c \cdot B \cdot A^2 / \eta$, and B – permeability of porous material with cross-sectional area, A; and

η - viscosity of water; Δp_c – capillary pressure.

By addition, connecting and reassembling of **Equation 5.2**, differential **Equation 5.3** is given in the form:

$$\begin{aligned} &Q_s = \frac{dV}{dt} = k(V_e - V) - \frac{k_p}{V} \\ &\text{or more generally} \\ &Q_s = \frac{dV}{dt} = k(V_e - V)^n - \frac{k_p}{V} \text{ for } n \geq 0 \end{aligned} \tag{5.3}$$

By solution of this equation, the integrating form **Equation 5.4** is given:

$$\begin{aligned} &\frac{V_1^{V_1}(V - V_2)^{V_2}}{(V_1 - V)^{V_1}} = \exp[k(V_1 - V_2)t] \\ &V_{1,2} = \frac{V_e}{2} \pm \frac{1}{2}\sqrt{(V_e^2 - 4(k_p/k))}, i.e., (V_1 - V_2) = \sqrt{(V_e^2 - 4(k_p/k))} \end{aligned} \tag{5.4}$$

The dependence of V *versus* t is depicted in **Figure 5.9**. If $k_p/k << V_e^2/4$ then it follows that $V_1 = V_e$ and $V_2 = 0$. Provided that the start of verification is chosen at the inflection point, i.e., for $t = t_{inf}$, then $V = V_{inf}$, the best verification formula is in the form of **Equation 5.5**.

$$(V - V_{\text{inf}}) = V_e(1 - \exp[-k(t - t_{\text{inf}})]) \tag{5.5}$$

Hornification is known as an irreversible loss of fibre swelling during which most of the macropores and none of the micropores have irreversibly collapsed when the fibres are dried and rewetted [120]. This suggests that hornification is caused by the formation of bonds, stable to water, between adjacent lamellae, i.e., by hydrogen-hydration bonds. When the hornified fibres are refined, the macropores can be almost completely regenerated.

Solár and co-workers [121] have described a simple method for the measurement of the dimensional changes of wood when exposed to an environment composed of water. Geffert and co-workers [122] have studied this process by application of recycled cellulosic fibres. All obtained similar kinetic curves as shown in **Figure 5.9,** except that of recycled pulp fibres. In this case, the kinetic swelling curves display a simple shape without an inflection point, i.e., the swelling process is controlled only by **Equation 5.5**. The majority of the swelling is closely connected with the dissolution of wood cellulose fibres in NaOH-water. The fact that some cellulose chains did not dissolve while others did, although having the same molecular weight, indicates that these chains are less accessible and embedded in cell regions difficult to dissolve. It was shown [123] that the dissolution capacity of cellulose chains is strongly dependent on their localisation within the cell wall structure and the cellulose/hemicelluloses complex. The presence of small amounts of hemicelluloses may prevent or decrease the solubility of cellulose, but it must also be kept in mind that what is called a 'cellulose solution' is not a molecular solution in the thermodynamic sense, and that cellulose aggregates are mainly present [123]. Obviously, hemicelluloses connecting the elementary fibrils in the amorphous part of the microfibrils are the most important.

5.6 Conclusions

Relatively simple macromolecules with a miraculous ability to form an infinite number of supermolecular and hypermolecular structures with fascinating shapes; cellulose represents the most abundant biopolymer of all plants (and also in some

marine animals). Its existence in both an animate and inanimate nature is strongly connected with water. It is formed from water and carbon (carbon dioxide) during photosynthesis at the very beginning of its existence. It dies out during the aging of the lignocellulosic matter of plants *via* degradation and destruction due to the chemical and biochemical influence of the environment; the dehydration process is a typical example. Also typical, is the dehydration process which occurs during the burning of cellulose; its liquefaction to hydrocarbons or condensation reactions occur during the carbonisation of plant matter under appropriate conditions. The cycle of cellulose in nature is so brilliantly closed.

However, water plays the most important role during formation of the hydrogen bonds, i.e., during the formation of supermolecular and hypermolecular cellulosic skeletal structures regardless of whether it is in nature or in industry; the simplest formation of this hypermolecular structure is paper.

References

1. D.N. Hon and N. Schiraischi in *Wood and Cellulosic Chemistry*, 2nd Edition, Marcel Dekker, New York, NY, USA, 2001.

2. T.H. Wegner and P.E. Jones, *Cellulose*, 2006, **13**, 2, 115.

3. K.H. Gardner and J. Blackwell, *Biopolymers*, 1974, **13**, 1975.

4. A. Sarko and R. Muggli, *Macromolecules*, 1974, **7**, 4, 486.

5. W.K. Czaja, D.J. Young, M. Kawecki and R.M. Brown, Jr., *Biomacromolecules*, 2007, **8**, 1, 1.

6. D.N-S. Hon, *Cellulose*, 1994, **1**, 1.

7. A.C. O'Sullivan, *Cellulose*, 1997, **4**, 173.

8. S.J. Eichhorn, C.A. Baillie, N. Zafeiropoulos, L.Y. Mwaikambo, M.P. Ansell, A. Dufresne, K.M. Entwistle, P.J. Herrera-Franco, G.C. Escamilla, L. Groom, M. Hughes, C. Hill, T.G. Rials and P.M. Wild, *Journal of Materials Science*, 2001, **36**, 2107.

9. P. Zugenmaier in *Crystalline Cellulose and Derivatives: Characterization and Structure*, Springer Series in Wood Science, Eds., T.E. Timell and R. Sommer, Springer-Verlag, Berlin, Germany, 2008, p.106.

10. I.M. Saxena, K. Kudlicka, K. Okuda and R.M. Brown, Jr., *Journal of Bacteriology*, 1994, **176**, 18, 5735.

11. A.J. Michell, *Carbohydrate Research*, 1970, **12**, 453.

12. J.T. Ham and D.G. Williams, *Acta Crystallographica*, 1970, **B26**, 1373.

13. H.J. Koch and A.S. Peterlin, *Carbohydrate Research*, 1970, **15**,403.

14. S.O. Rowland and E.J. Roberts, *Journal of Polymer Science, Part A: Polymer Chemistry Edition*, 1972, **10**, 2447.

15. G.V. Schultz and M. Marx, *Makromolekulare Chemie*, 1954, **14**, 52. [In German]

16. G.V. Schultz and M. Marx, *Journal of Polymer Science*, 1958, **30**, 119.

17. Th. Heinze in *Polysaccharide: Structural Diversity and Functional Versatility*, 2nd Edition, Ed., S. Dumitriu, Marcel Dekker, New York, NY, USA and Basel, Hong Kong, China, 2004, p.551.

18. P. Arndt, K. Bockholt, R. Gerdes, S. Huschens, J. Pyplo, H. Redlichl and K. Samm, *Cellulose*, 2003, **10**, 75.

19. H-P. Fink, B. Philipp, D. Paul, R. Serimaa and T. Paakkari, *Polymer*, 1987, **28**, 1265.

20. C. Verlhac, J. Dedier and H. Chanzy, *Journal of Polymer Science, Part A: Polymer Chemistry Edition*, 1990, **28**, 1171.

21. T. Okano and A. Koyanagi, *Biopolymers*, 1986, **25**, 851.

22. I. Simon, H.A. Scheraga and R.T.J. Manley, *Macromolecules*, 1988, **21**, 983.

23. R.H. Atalla and D.L. Vanderhart in *Proceedings of the 10th Cellulose Conference*, Ed., C. Schuerch, John Wiley and Sons, New York, NY, USA, 1989, p.169.

24. F. Horii, A. Hirai and R. Kitamaru, *Macromolecules*, 1987, **20**, 2117.

25. H. Yamamoto and F. Horii, *Cellulose*, 1994, **1**, 57.

26. J. Sugiyama, R. Vuong and H. Hanzy, *Macromolecules*, 1991, **24**, 4168.

27. E.M. Debzi, H. Chanzy, J. Sugiyama, P. Tekely and G. Excoffier, *Macromolecules*, 1991, **24**, 6816.

28. K. Okuda, L. Tsekos and R.M. Brown, Jr., *Protoplasma*, 1994, **180**, 49.

29. F.J. Kolpak and J. Blackwell, *Macromolecules*, 1976, **9**, 273.

30. S. Kuga, S. Takagi and R.M. Brown, Jr, *Polymer*, 1993, **34**, 3293.

31. J. Hayashi, A. Sufoka, J. Ohkita and S. Watanabe, *Journal of Polymer Science: Polymer Letters Edition*, 1975, **13**, 23.

32. A. Sarko in *Wood and Cellulosics: Industrial Utilization, Biotechnology, Structure and Properties*, Ed., J.F. Kennedy, Ellis Horwood, Chichester, UK, 1987, p.55.

33. E.S. Gardiner and A. Sarko, *Canadian Journal of Chemistry*, 1985, **63**, 173.

34. J.A. Howsomon and W.A. Sisson in *Cellulose and Cellulose Derivatives*, 2nd Edition, Interscience, New York, NY, USA, 1954, p.244.

35. A. Frey-Wysling and M. Mühlethaler, *Makromolekulare Chemie*, 1963, **62**, 25. [In German]

36. K. Mühlethaler, *Journal of Polymer Science: Part C*, 1969, **28**, 305.

37. A. Pozgaj, D. Chovanec, St. Kurjatko and M. Babiak in *Struktura a Vlastnosti dreva*, Priroda, Bratislava, Slovakia, 1993, p.57. [In Slovakian]

38. L. Heux, E. Dinand and M.R. Vignon, *Carbohydrate Polymers*, 1999, **40**, 115.

39. D.L. Van der Hart and R.H. Atalla, *Macromolecules*, 1984, **17**, 1465.

40. K. Fleming, D.G. Gray and St. Matthews, *Chemical Europe Journal*, 2001, **7**, 9, 1831.

41. R.J. Viëtor, K. Mazeau, M. Lakin and S. Pérez, *Biopolymers*, 2000, **54**, 342.

42. R.D. Preston in *The Physical Biology of Plant Cell Walls*, Chapman and Hall, London, UK, 1974, p.139.

43. M. Milichovsky, *TAPPI Journal*, 1990, **74**, 10, 221.

44. M. Milichovsky, *Scientific Papers of Faculty of Chemical Technology, Pardubice*, 1994, **57**, 157.

45. M. Milichovsky, *Scientific Papers of Faculty of Chemical Technology, Pardubice*, 1992/93, **56**, 155.

46. M. Milichovsky, *Scientific Papers of Faculty of Chemical Technology, Pardubice*, 1992/93, **56**, 123.

47. M.A. Hubbe, O.J. Rojas, L.A. Lucia and M. Sain, *BioResources*, 2008, **3**, 929.

48. Y. Bréchet, J-Y.Y. Cavaillé, E. Chabert, L. Chazeau, R. Dendievel, L. Flandin and C. Gauthier, *Advanced Engineering Materials*, 2001, **3**, 8, 571.

49. H. Grigoriew and A.G. Chmielewski, *Journal of Membrane Science*, 1998, **142**, 87.

50. K. Tashiro and M. Kobayashi, *Polymer Bulletin*, 1985, **14**, 213.

51. R.D. Neuman, *Nordic Pulp Paper Research Journal*, 1993, **8**, 1, 96.

52. B. Alince, *Nordic Pulp Paper Research Journal*, 2002, **17**, 1, 71.

53. P.H. Hermans in *Physics and Chemistry of Cellulose Fibres*, Elsevier, New York, NY, USA, 1949, p.13.

54. P.H. Hermans and A. Weidinger, *Journal of Polymer Science*, 1949, **4**, 135.

55. K. Mazeau and L. Heux, *Journal of Physical Chemistry*, B2003, **107**, 2394.

56. E. Poppel in *Rheologie und elektrokinetischeVorgänge in der Papiertechnologie*, VEB Fachbuchverlag Leipzig, Germany, 1977, p.294. [In German]

57. M. Milichovsky, *Scientific Papers of Faculty of Chemical Technology, Pardubice*, 1987, **50**, 403. [In Czech]

58. M.A. Hubbe, *BioResources*, 2006, **1**, 1, 116.

59. J-F. Revol, H. Bradford, J. Giasson, R.H. Marchessault and D.G. Gray, *International Journal of Biological Macromolecules*, 1992, **14**, 170.

60. J-F. Revol, L. Godbout, X-M. Dong, D.G. Gray, H. Hanzy and G. Maret, *Liquid Crystals*, 1994, **16**, 1, 127.

61. R.H.Marchessault, F.F. Morehead and M.J. Koch, *Journal of Colloid Science*, 1961, **16**, 327.

62. M. Bercea and P. Navard, *Macromolecules*, 2000, **33**, 6011.

63. X.M. Dong, J-F. Revol and D.G. Gray, *Cellulose*, 1998, **5**, 19.

64. P. Terech, L. Chazeau and J.Y.Cavaille, *Macromolecules*, 1999, **32**, 1872.

65. W.J. Orts, L. Godbout, R.H. Marchessault and J-F. Revol, *Macromolecules*, 1998, **31**, 5717.

66. J. Sugiyama, H. Chanzy and G. Maret, *Macromolecules*, 1992, **25**, 4232.

67. A. Stroobants, H.N.W. Lekkerkerker and Th. Odijk, *Macromolecules*, 1986, **19**, 2232.

68. X.M. Dong, T. Kimura, J-F. Revol and D.G. Gray, *Langmuir*, 1996, **12**, 2076.

69. X.M. Dong and D.G. Gray, *Langmuir*, 1997, **13**, 2404.

70. E. Dinand, H. Chanzy and M.R. Vignon, *Food Hydrocolloids*, 1999, **13**, 275.

71. D. Eklund and T. Lindström in *Paper Chemistry – An Introduction*, DT Paper Science Publications, Grankulla, Finland, 1991, p.89.

72. W.E. Scott in *Principles of Wet End Chemistry*, TAPPI Press, Atlanta, GA, USA, 1996, p.61.

73. L. Westfelt, *Cellulose Chemistry and Technology*, 1979, **13**, 813.

74. B. Fredholm, B. Samuelson, A. Westfelt and L.Westfelt, *Cellulose Chemistry and Technology*, 1981, **15**, 247.

75. B. Haglind, B. Samuelson, A. Westfelt and L.Westfelt, *Cellulose Chemistry and Technology*, 1981, **15**, 263.

76. A. Westfelt and L. Westfelt, *Cellulose Chemistry and Technology*, 1983, **17**, 49.

77. A. Westfelt and L. Westfelt, *Cellulose Chemistry and Technology*, 1983, **17**, 165.

78. B. Samuelson and L. Westfelt, *Cellulose Chemistry and Technology*, 1983, **17**, 179.

79. B. Fredholm, B. Samuelson, A. Westfelt and L. Westfelt, *Cellulose Chemistry and Technology*, 1983, **17**, 279.

80. H.H. Espy, *TAPPI Journal*, 1994, **78**, 4, 90.

81. M. Laleg and I.I. Pikulík, *Nordic PulpPaper Research Journal*, 1991, **6**, 3, 99.

82. M. Milichovsky, *Cellulose Chemistry and Technology*, 1992, **26**, 5, 607.

83. J-L. DiFlavio, R. Bertoia, R. Pelton and R. Pelton in *Proceedings of the 13th Fundamental Research Symposium, Session 7: Chemistry*, Interscience Publisher, Cambridge, UK, September 2005, p.1293.

84. T. Saito and A. Isogai, *TAPPI Journal*, 2005, **89**, 4, 3.

85. M. Milichovsky and Vr. Velich, *Cellulose Chemistry and Technology*, 1989, **23**, 743.

86. N.D. Sanders and A.R. Bashey in *Proceedings of the TAPPI International Paper Physics Conference*, Hawaii, TAPPI Press, Technology Park, Atlanta, GA, USA, September 1991, p.473.

87. M. Müller, Ch. Czihak, H. Schober, Y. Nishiyama and G. Vogl, *Macromolecules*, 2000, **33**, 1834.

88. M. Vodenicarova, M. Milichovsky and Br. Cesek, *Cellulose Chemistry and Technology*, 2001, **35**, 1–2, 59.

89. M. Milichovsky and Br. Cesek, *Adsorption, Science & Technology*, 2002, **20**, 9, 883.

90. Br. Cesek and M. Milichovsky, *Cellulose Chemistry and Technology*, 1996, **30**, 3–4, 297.

91. A.H. Nissan in *Lectures on Fiber Science in Paper*, Ed., W.C. Walker, Joint Textbook from the Committee of Paper Industry, CPPA, Montreal, Canada and TAPPI, Atlanta, GA, USA, 1977.

92. Th. Zeegers-Huyskens and P. Huyskens, *Molecular Interactions*, Volume 2, Ed., H. Ratajczak and W.J. Orville-Thomas, John Wiley & Sons, New York, NY, USA, 1981, p.281.

93. M. Milichovsky, *Scientific Papers of Faculty of Chemical Technology, Pardubice*, 1992/93, **56**, 123.

94. M. Milichovsky, *Scientific Papers of Faculty of Chemical Technology, Pardubice*, 1988, **51**, 71. [In Czech]

95. M. Milichovsky, *Scientific Papers of Faculty of Chemical Technology, Pardubice*, 1988, **51**, 149. [In Czech]

96. M. Milichovsky, *Scientific Papers of Faculty of Chemical Technology, Pardubice*, 1988, **51**, 115. [In Czech]

97. J. Kim and S. Yun, *Macromolecules*, 2006, **39**, 10, 4202.

98. M. Milichovsky, *Journal of Biomaterials and Nanobiotechnology*, 2010, **1**, 17.

99. M. Milichovsky and Br. Cesek, *Cellulose Chemistry and Technology*, 2004, **38**, 5–6, 385.

100. M. Fišerová, J. Gigac and J. Balberčák, *Papír a Celulóza*, 2009, **64**, 11–12, 362.

101. M. Milichovský, *Chemické Listy*, 2000, **94**, 9, 875. (In Czech)

102. M. Milichovský, *Papír a Celulóza*, 1978, **33**, 7–8, V61. (In Czech)

103. P.M. Mendes, *Chemical Society Reviews*, 2008, **37**, 9, 2512.

104. M. Lutecki, B. Strachotova, M. Uchman, J. Brus, J. Plestil, M. Slouf, A. Strachota and L. Matejka, *Polymer Journal*, 2006, **38**, 6, 527.

105. X-Z. Zhang, F-J. Wang and Ch-Ch. Chu, *Journal of Material Science: Materials in Medicine*, 2003, **14**, 3, 451.

106. K. Edelmann in *Lehrbuch der Kolloidchemie*, Band I. VEB, Deutscher Verlag der Wissenschaften, Berlin, Germany 1962, p.147. [In German]

107. J.E. Wong, A.K. Gaharvar, D. Müller-Schulte, D. Bahadur and W. Richtering, *Journal of Colloid and Interface Science*, 2008, **324**, 5, 47.

108. X. Fan, G. Hui, H. Yi, S. Taolei, C. Li, Z. Guangzhao and J. Lei, *Advanced Materials*, 2007, **19**, 8, 2520.

109. F.D. Jochum and P. Theato, *Macromolecules*, 2009, **42**, 7, 5941.

110. X-Z. Zhang, F-J. Wang and Ch-Ch. Chu, *Journal of Material Science: Materials in Medicine*, 2003, **14**, 3, 451.

111. H. Hou, W. Kim, M. Grunlan and A. Han, *Journal of Micromechanical Microengineering*, 2009, **19**, 10, 1.

112. R.M.P. da Silva, J.F. Mano and R.L. Reis, *Trends in Biotechnology*, 2006, **25**, 12, 577.

113. H. Hatakeyma, A. Kichuchi, M. Yamato and T. Okano, *Biomaterials*, 2006, **27**, 9, 5069.

114. X. Xin-Cai, Ch. Liang-Yin, Ch. Sen-Mei and Z. Jia-Hua, *Polymer*, 2005, **46**, 3, 3199.

115. R. Yoshida, *Advanced Materials*, 2010, **20**, 1.

116. J.F. Mano, *Advances in Engineering Materials*, 2008, **10**, 6, 515.

117. S.E. Stabenfeldt, A.J. García and M.C. LaPlaca, *Journal of Biomedical Materials Research Part A*, 2006, **3**, 718.

118. R.J. Dobins, *TAPPI*, 1970, **53**, 12, 2284.

119. U. Freudenberg, R. Zimmermann, K. Schmidt, S.H. Behrens and C. Werner, *Journal of Colloid and Interface Science*, 2007, **309**, 360.

120. T.C. Maloney and H. Paulapuro, *Journal of Pulp and Paper Science*, 1999, **25**, 12, 430.

121. R. Solár, M. Mamoň, St. Kurjatko, R. Lang and Vl. Vacek, *Drvna Industria*, 2006, **57**, 2, 75.

122. A. Geffert, J. Geffertová and Vl. Vacek in *Proceedings of the 8th International Symposium on Selected Processes at the Wood Processing*, Štúrovo, Publishing House of Technical University in Zvolen, Slovakia, 2009, p.45.

123. N. Le Moigne and P. Navard, *Cellulose*, 2010, **17**, 31.

6 Physico-chemical Characterisation of Cellulose from the *Broussonetia papyrifera* Bark and Stem, and *Eucommia ulmoides* Oliver Stem

Feng Peng, Jing Bian, Pai Peng, Xue-Ming Zhang, Feng Xu and Run-Cang Sun

6.1 Introduction

Broussonetia papyrifera (BP), known as paper mulberry, is a dioecious, deciduous and perennial tree or shrub occurring naturally in Asia and Pacific countries such as China, Thailand and USA [1, 2], which is characterised by a higher growth rate and a greater adaptability to adverse environments [3]. It has been cultivated extensively in East, Central and South Asia for papermaking, silk and timber production, and medicinal materials [4, 5]. *Eucommia ulmoides* Oliver, a unique type of plant in China, mainly spreads in the Shanxi, Hunan, Hubei, Sichuan and Yunnan provinces. It has various pharmacological properties including: strengthening tendons and bones, reinforcing muscle, benefiting the liver and kidney, preventing miscarriage, increasing longevity and lowering blood hypertension [6–8]. The leaf and bark of *Eucommia ulmoides* Oliver have been widely used in traditional Chinese medicine for the treatment of hypertension [8, 9], but the remaining stems of *Eucommia ulmoides* Oliver are often burnt as firewood in China. There has been a considerable amount of research based on the traditional medicinal utilisation however, very few investigations report the potential application of the major components of the cell wall.

Cellulose is a linear homopolysaccharide composed of D-glucopyranose units linked together by β-1,4-glycosidic bonds. The β-D-glucopyranose chain units are arranged in a chair conformation, and the secondary OH at the C-2 and C-3, and primary OH at the C-6 position are oriented equatorially. The molecules form microfibrils with partly highly ordered (crystalline) regions and partly less ordered regions (amorphous) by the formation of various strong intermolecular and intramolecular hydrogen bonds [10]. Microfibrils in turn build up into fibrils and finally, into cellulose fibres. The fibrous structure and strong hydrogen bonds give cellulose a high tensile strength and make the fibres insoluble in most solvents [11]. That is, in wood and other higher plants, cellulose is organised mainly into long, thin fibres of the cellulose I allomorph, surrounded by a sheet of hemicelluloses and lignin [12]. Cellulose I consists of two

forms: I_α (triclinic) and I_β (monoclinic). Both are frequently found to coexist in cell wall structures together with amorphous cellulose [13]. There is little consensus regarding the ratio of cellulose I_α to I_β in wood. In general, cellulose I_β is the more abundant form and occurs in an almost pure form in the microfibrils of a wide range of species, from higher plants such as wood, to green algae, to tunicates [14]. In addition, within the fibril, the cellulose chains exist in regions of various degrees of order. Noncrystalline cellulose may be present as distortions in the cellulose lattice and the cellulose chains, located on the fibril surface, are not locked in a three-dimensional structure [15]. It is now well established that when subjected to strong alkali solutions, crystalline native cellulose or cellulose I becomes swollen and upon washing shrinks back to yield a new allomorph, cellulose II [16]. At present, cellulose is the most abundant polymer available worldwide with an estimated annual natural production of 1.5×10^{12} tons and is considered as an almost inexhaustible source of raw materials [17]. As a raw material of an enormously underutilised energy resource for the production of paper, panel products, chemicals and other industrial products, cellulose has received much attention all over the world [18]. Within the lignocellulosic materials, cellulose is embedded in a matrix composed of hemicelluloses, lignin and other components [19]. Due to the recalcitrance of the cell wall, the isolation of highly pure cellulose has been the subject of extensive studies for many years [20]. A combination of chemical and mechanical treatments is necessary for the dissolution of lignin, hemicelluloses and other noncellulosic substances [21]. A protocol based on acidified sodium chlorite is frequently applied to delignify woody materials as an initial step in the isolation of cellulose [22]. Alkali extraction, before or after delignification, is the common method to dissolve hemicelluloses. In this work, α-cellulose was isolated from BP bark and stem, and *Eucommia ulmoides* Oliver stem. The isolated cellulosic preparations were characterised by their yield, content of hemicelluloses, viscosity, molecular weight and thermal stability. In addition, Fourier transform-infrared (FT-IR) and cross polarisation/magic angle spinning (CP/MAS) ^{13}C solid-state nuclear magnetic resonance (^{13}C-NMR) were used to investigate the structural characterisation of cellulosic polymers.

6.2 Experimental

6.2.1 Materials

BP bark and stem (3 and 12 years old) and *Eucommia ulmoides* Oliver stem (3 years old) were obtained from the experimental farm of North-Western University of Agriculture and Forestry, Yangling, China. The air-dried barks and stems of BP and stems of *Eucommia ulmoides* Oliver were cut into small pieces, then ground

and sieved to obtain a 40–60 mesh powder. The powder was dewaxed with toluene-ethanol 2:1 (v/v) in a Soxhlet apparatus for 6 h to remove fats, waxes and oils, and then air dried. All chemicals used in the experiments were of analytical reagent grade and purchased from the Beijing Chemical Reagent Company, China.

6.2.2 Isolation of Cellulose

Figure 6.1 shows the scheme for the isolation of cellulose from the BP bark and stem (3 and 12 years old), and *Eucommia ulmoides* Oliver stem. The dewaxed samples were sequentially subjected to extraction with 70% ethanol for 3 h and water at 80 °C for 3 h in a solid-to-liquor ratio of 1:25 (g/mL), in order to isolate 70% ethanol-soluble materials and water-soluble hemicelluloses, and with acidified water at pH 2.0 (adjusted with HCl) at 80 °C for 3 h to isolate pectin substances. The remaining residues were delignified with 6% sodium chlorite at pH 3.6–3.8 (adjusted with 10% acetic acid) at 75 °C for 2 h [23]. The residue, holocellulose, was subsequently washed with distilled water and ethanol, and dried at 60 °C for 16 h. Then the holocellulose was separately extracted at 25 °C with aqueous potassium hydroxide or sodium hydroxide under different conditions. At the end of the extraction, the insoluble residue (cellulose) was collected by filtration, washed thoroughly with distilled water and 95% ethanol until the filtrate was neutral, and then dried in an oven at 60 °C for 16 h. Note that cellulosic preparations from the BP bark (3 years old) isolated at 25 °C with 10% KOH for 15 h, 8% NaOH for 15 h and 10% KOH for 18 h were labelled as cellulosic preparations C_1, C_2 and C_3, respectively. The cellulosic preparation from the *Eucommia ulmoides* Oliver stem (3 years old) was isolated at 25 °C with 10% KOH for 15 h and labelled as cellulosic preparation C_4. The cellulosic preparations from the BP stem (3 years old) and bark (12 years old) isolated with 10% KOH for 15 h at 25 °C were labelled as cellulosic preparations C_5 and C_6, respectively.

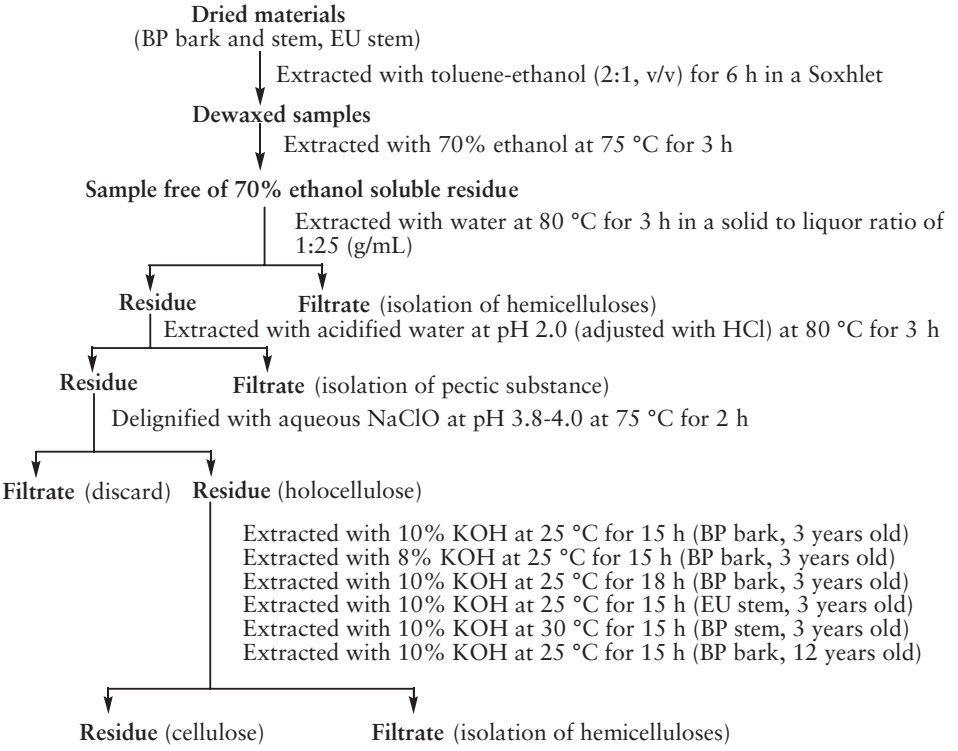

Figure 6.1 Scheme for the isolation of cellulosic preparations from BP bark and stem, and *Eucommia ulmoides* Oliver stem

6.2.3 Structural Characterisation of Cellulose

The average degrees of polymerisation (DP) and molecular weight of the cellulosic preparations were determined using the British Standard Methods for the determination of limiting viscosity number of cellulose in dilute solutions, Part 1: cupriethylenediamine (CED) method (BS 6306: Part 1: 1982). The viscosity-average DP (P) of the samples was calculated by their intrinsic viscosity [η] in a cupriethylenediamine hydroxide (cuene) solution using **Equation 6.1**:

$$P^{0.9}(\text{mL g}^{-1}) = 1.65[\eta] \tag{6.1}$$

where P is an indeterminate average of DP. The molecular weight of the preparations was then calculated from their *P* value using a multiplication factor of 162.

The composition of neutral sugars and uronic acids in the cellulosic fractions was determined by high performance anion exchange chromatography (HPAEC). The neutral sugars and uronic acids in the cellulosic preparations were liberated by hydrolysis with 72% H_2SO_4 for 45 min at 25 °C, followed by a high temperature hydrolysis at 105 °C for 2.5 h after dilution to 1.0 M H_2SO_4. After hydrolysis, the samples were diluted 50-fold, filtered and injected into the HPAEC system (Dionex ISC 3000, USA) with an amperometric detector, AS50 autosampler, a CarbopacTM PA-20 column (4 × 250 mm, Dionex) and a guard PA-20 column (3 × 30 mm, Dionex). Neutral sugars and uronic acids were separated in a 5 mM NaOH isocratic (carbonate free and purged with nitrogen) for 20 min, followed by a 0–75 mM NaAc gradient in 5 mM NaOH for 15 min. Then the columns were washed with 200 mM NaOH for 10 min to remove carbonate, followed by a 5 min elution with 5 mM NaOH to reequilibrate the column before the next injection. The total analysis time was 50 min and the flow rate was 0.4 mL/min. Calibration was performed with standard solutions of L-arabinose, L-rhamnose, D-xylose, D-glucose, D-mannose, D-galactose, glucuronic acid and galacturonic acids.

FT-IR spectra of hemicellulosic samples were obtained on an FT-IR spectrophotometer (Nicolet 510) using a KBr disc containing 1% finely ground samples. Thirty-two scans were taken of each sample recorded from 4,000 to 400 cm^{-1} at a resolution of 2 cm^{-1} using the transmission mode. CP/MAS ^{13}C-NMR spectra were recorded on a Bruker AV-III 400M spectrometer (100 MHz) at 25 °C with a 4 mm MAS probe. About 250 mg of sample was packed into zirconia rotors for MAS. The measurement was performed using a CP pulse program with an acquisition time of 0.034 s, delay time 2 s and with an accumulation of 5,000 scans.

Thermogravimetric analysis (TGA) and derivative thermogravimetry (DTG) were performed on a simultaneous thermal analyser (SDT Q600, TA Instrument, Selb, Germany) under a nitrogen atmosphere. Samples weighing between 8 and 12 mg were heated from room temperature to 600 °C at a rate of 10 °C/min.

6.3 Results and Discussion

6.3.1 Yield of Cellulose

Alkali extraction is the most efficient method for isolating cellulose from delignified materials by releasing large amounts of hemicellulosic polysaccharides into the

alkaline solution [24]. In particular, a delignification step using chlorite prior to isolating cellulose from holocellulose can significantly facilitate the extraction of hemicelluloses, and thus results in high purity residues of the cellulosic polymers. The yield of six cellulosic preparations, obtained using the alkali treatment on the delignified BP bark and stem, and *Eucommia ulmoides* Oliver stem is listed in **Table 6.1**. As can be seen from the table, altering the treatment conditions from 10% KOH to 8% NaOH, resulted in a decrease in the cellulose yield from the delignified BP bark from 50.9% (C_1) to 37.5% (C_2), indicating that the alkali strength played an important role in dissolving the hemicelluloses from the holocellulose of the BP bark, and 8% NaOH was more powerful than 10% KOH for dissolving hemicelluloses. It should be noted that the treatment with 8% NaOH under the given conditions may degrade a small amount of cellulose, giving a lower yield of cellulose. In addition, increasing the treatment time from 15 h to 18 h led to a decrease in cellulose yield from 50.9% (C_1) to 43.9% (C_3), obtained from the delignified BP bark. These results indicate that the relatively higher alkali strength and longer treatment time lead to an increased solubility of the hemicelluloses. The reason for this higher solubility is probably due to the fact that hemicelluloses are mainly present on the outer surface of cellulose, from which they dissolve easily in the alkaline solution. On the other hand, the long cellulose chains are located on the inner parts of the fibres and therefore, are not easily dissolved. Similar results were observed in our previous studies which investigated obtaining cellulose from sugarcane bagasse [25]. Under the same treatment conditions, 10% KOH at 25 °C for 15 h, the yields of cellulose from the delignified BP bark and stem (3 years old), and *Eucommia ulmoides* Oliver stem (3 years old) are 43.9% (C_2) , 42.5% (C_5) and 42.4% (C_4), respectively. In addition, the yield of cellulose obtained from the delignified BP bark (12 years old) is 51.8%, which is higher than the yield (43.9%) of cellulose obtained from the delignified BP bark (3 years old), suggesting that the older BP bark (12 years old) probably had a higher cellulose content or greater number of hydrogen bonds between the hemicelluloses and cellulose than that of the younger BP bark.

6.3.2 Sugar Component Analysis

It is well known that cellulose and hemicelluloses are the major components of the secondary layers of the cell wall in lignocellulosic materials. Hemicelluloses interact with cellulose presumably through hydrogen bonds [26]. The sugar components of the cellulosic preparations are presented in **Table 6.2**. As can be seen, glucose was the predominant sugar component in the six cellulosic preparations, comprising 71.8 to 83.8% of the total sugars, the higher values indicating a higher content of cellulose. While the appearance of a noticeable amount of xylose (5.1–16.9%), and minor amounts of arabinose, rhamnose, galactose and mannose suggest that the cellulosic samples contained noticeable amounts of associated hemicelluloses. The remaining

hemicelluloses, which were inaccessible to the alkali solution, suggest that the hemicelluloses in the cell wall of the BP bark and stem, and *Eucommia ulmoides* Oliver stem are tightly associated with cellulose, probably by hydrogen bonds, coaggregation or chemical linkage [27, 28]. Interestingly, a change in alkali concentration from 10% KOH to 8% NaOH resulted in a distinct enhancement of the glucose content from 71.8 (C_1) to 83.8% (C_2), indicating again that treatment with 8% NaOH was more powerful than with 10% KOH for releasing hemicelluloses from the holocellulose. In addition, a noticeable increase in glucose content from 71.8 (C_1) to 80.1% (C_3), upon increasing the extraction time from 15 h to 18 h during the alkali treatments, corresponded to the higher cellulose content and lower residual hemicelluloses in the cellulosic preparations, which reversed the yield of cellulose. The reason for the increase is obviously due to the significant solubilisation or degradation of the macromolecular hemicellulosic polymers during the alkali treatment. As shown in **Table 6.2**, the cellulosic preparations C_4 and C_5, obtained by extraction with 10% KOH at 25 °C for 15 h from the delignified *Eucommia ulmoides* Oliver and BP stem, contained a relatively high amount of glucose, 73.4 and 77.5%, respectively. In addition, the content of glucose (73.7%) in C_6 obtained from the delignified BP bark (12 years old) was higher than that (71.8%) in C_1 obtained from the delignified BP bark (3 years old). This result showed that the older BP bark (12 years old) probably had a higher content of cellulose, which was in good agreement with the result for cellulose yield.

Table 6.1 Yields and isolating conditions of cellulosic preparations obtained from BP and EU

Fraction No.	Material	Isolating conditions	Yield (% dry matter)
C_1[a]	BP bark, 3 years old	10% KOH, 25 °C,15 h	50.9
C_2[b]	BP bark, 3 years old	8% NaOH, 25 °C, 15 h	37.5
C_3[a]	BP bark, 3 years old	10% KOH, 25 °C, 18 h	43.9
C_4[c]	EU stem, 3 years old	10% KOH, 25 °C, 15 h	42.4
C_5[c]	BP stem, 3 years old	10% KOH, 25 °C, 15 h	42.5
C_6[c]	BP bark, 12 years old	10% KOH, 25 °C, 15 h	51.8

[a]C_1 and C_3 represent the cellulosic preparations obtained by extraction with 10% KOH at 25 °C for 15 h and 18 h from the delignified BP bark (3 years old), respectively.
[b]C_2 represents the cellulosic preparation obtained by extraction with 8% NaOH at 25 °C for 15 h from the delignified BP bark (3 years old).
[c]C_4, C_5 and C_6 represent the cellulosic preparations obtained by extraction with 10% KOH at 25 °C for 15 h from the delignified BP and EU stem (3 years old), and BP bark (12 years old), respectively.

Table 6.2 The content of neutral sugars (relative % cellulosic sample, w/w) in the isolated cellulosic preparations

Sugars (%)	Cellulosic preparation[a]					
	C_1	C_2	C_3	C_4	C_5	C_6
Arabinose	5.5	3.7	4.1	0.4	0.5	5.2
Rhamnose	0.3	0.2	0.5	0.2	0.1	0.4
Galactose	7.4	5.3	6.2	1.1	1.2	7.8
Glucose	71.8	83.8	80.1	73.4	77.5	73.7
Xylose	11.3	5.1	6.7	13.6	16.9	9.3
Mannose	3.7	1.9	2.4	11.3	3.8	2.6

[a]Corresponding to the cellulose preparations in **Table 6.1**.

6.3.3 Intrinsic Viscosity, Viscosity Average Degrees of Polymerisation and Molecular Weight

In general, pulp viscosity is used to estimate cellulose degradation during delignification, although the data obtained using viscosity are relative values. Intrinsic viscosity is a characteristic of macromolecules which is directly related to their ability to disturb flow and indirectly to their size and shape [29]. For molecules that can exist with a variety of molecular weights, the relation between intrinsic viscosity and molecular weight (M_w) is one of the most important properties [30]. The viscosity average DP of a cellulose sample is conveniently estimated from the intrinsic viscosity of its solution in 0.5 M cupriethylenediamine hydroxide by applying the equation $P^{0.9}$ (mL g^{-1}) = 1.65 [η]. The molecular weight of the cellulose was estimated using a multiplication factor of 162, the molar mass of anhydroglucose. **Table 6.3** lists the intrinsic viscosity (η), the viscosity average DP (P) and the M_w of the six cellulosic preparations. Obviously, the intrinsic viscosity, the viscosity average and the molecular weight of the three cellulosic preparations (C_1, C_2 and C_3) obtained from the delignified BP bark (3 years old) followed in this order: C_2 (8% NaOH treatment for 15 h) > C_3 (10% KOH treatment for 18 h) > C_1 (10% KOH treatment for 15 h). The reason for this is presumably due to the removal of some low molecular weight hemicelluloses during the alkaline extraction from the holocellulose, thereby increasing the viscosity and molecular weight of the cellulose. As shown in **Table 6.3**, the C_5 (M_w, 253,560 g/mol) obtained from the delignified BP stem (3 years old) and C_6 (M_w, 273,470 g/mol) obtained from the delignified BP bark (12 years old) had higher molecular weights than that of C_1 (M_w, 232,700 g/mol) obtained from the delignified BP bark (3 years old), under the same extraction conditions. This suggested that the cellulose in the BP stem and older bark had a higher molecular weight than that of cellulose in the younger BP bark (3 years old). In addition, as compared with the molecular weight of

cellulose from the BP stem, the cellulosic preparation C_4 obtained from the *Eucommia ulmoides* Oliver stem had a relatively low molecular weight (244,720 g/mol).

Table 6.3 The intrinsic (η), viscosity average DP (degree of polymerisation) (P) and M_w of the isolated cellulosic preparations

Properties of cellulose	Cellulosic preparation[a]					
	C_1	C_2	C_3	C_4	C_5	C_6
Intrinsic viscosity (η, mL g^{-1})[b]	420.8	615.6	533.5	440.3	454.6	486.6
Viscosity average DP (P)[c]	1,436.4	2,192.1	1,869.8	1,510.6	1,565.2	1,688.1
M_w[d]	232,700	355,120	302,910	244,720	253,560	273,470

[a]Corresponding to the cellulose preparations in **Table 6.1**.
[b]Determined by British Standard Methods for the determination of limiting viscosity number of cellulose in dilute solutions, Part 1. CED method.
[c]Calculated using $P^{0.9} = 1.65[\eta]$.
[d]Calculated using $P \times 162$.

6.3.4 Fourier Transform-infrared Spectra

Fourier Transform-infrared (FT-IR) is the most widely used method to identify chemical constituents and to elucidate their structures. The aim of using FT-IR in this work involved measuring the differences of the structure of the cellulose preparations obtained under various alkaline extraction conditions. **Figure 6.2** illustrates the FT-IR spectra of cellulosic preparations C_1 (spectrum 1), C_2 (spectrum 2) and C_3 (spectrum 3). The absorption at 3,397 cm^{-1} is attributed to O-H stretching, and those of 2,932 and 2,855 cm^{-1} are due to C-H stretching. The absorbed water in the samples gives a signal at 1,628 cm^{-1} [31]. The band at around 1,427 cm^{-1} of all the spectra, indicated that all samples contain a mixture of crystallised cellulose I and amorphous cellulose [32]. The C-H asymmetric deformation oCcurs at 1,380 or 1,372 cm^{-1}. The peak at 1,325 or 1,316 cm^{-1} is assigned to C-C and C-O skeletal vibrations. The absorption bands in the 1,200–1,000 cm^{-1} region are dominated by ring vibration overlapped with stretching of the C-OH side groups. Two peaks at 1,163 and 902 cm^{-1} arise from C-O-C stretching at the β-(1,4)-glycosidic linkages [33]. Two shoulder bands at 1,056 and 1,030 cm^{-1} are indicative of C-O stretching at C-3, C-C and C-O stretching at C-6 [34]. In comparison, the spectral profiles and relative intensities of the signals in spectra 1 and 2 are rather similar, indicating the same structures. On the other hand,

it should be noted that the spectrum of cellulosic sample C_3 (spectrum 3) showed two carboxylic bands at 1,752 cm^{-1} (C=O) and 1,568 cm^{-1} (COO^-). These carboxylic groups are probably due to the oxidation of cellulose and hemicelluloses under the longer treatment time with 10% KOH at 25 °C for 18 h. In addition, all the extraction procedures removed most of the lignin polymers because of the disappearance of the lignin-associated signals at 1,600 and 1,510 cm^{-1}. Similarly, the peaks at: 3,397; 2,919; 2,850; 1,611; 1,423; 1,376; 1,316; 1,167; 1,116; 1,056; 1,026 and 902 cm^{-1} in the spectra of cellulosic samples C_4, C_5, and C_6 (**Figure 6.3**) obtained from the delignified *Eucommia ulmoides* Oliver and BP stem, and BP bark (12 years old), respectively, are associated with the typical value of cellulose. Evidently, the bond intensity of the bands is very similar, indicating similar structures of the cellulosic preparations.

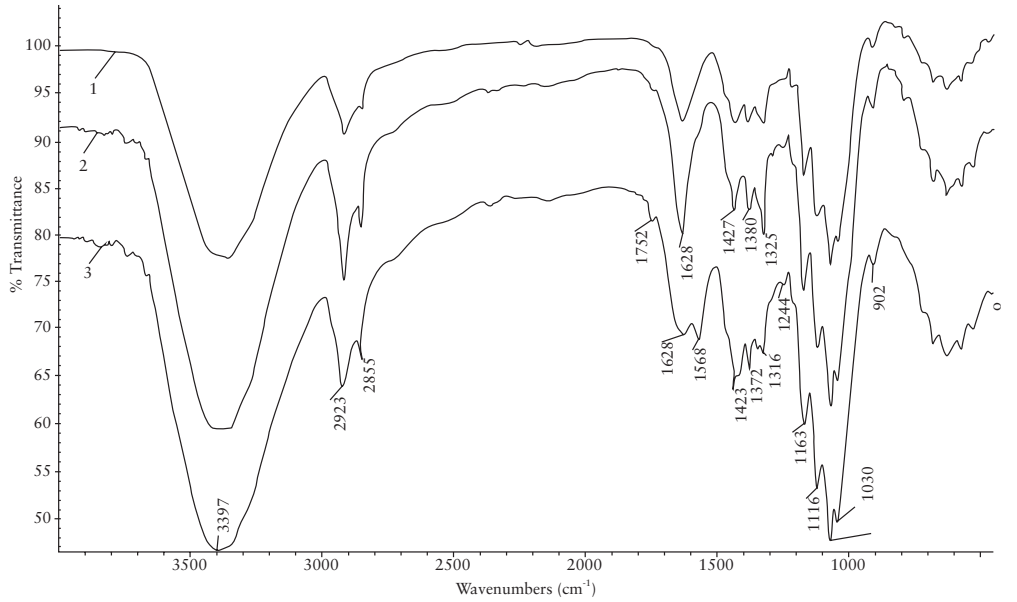

Figure 6.2 FT-IR spectra of cellulosic preparations C_1 (spectrum 1), C_2 (spectrum 2) and C_3 (spectrum 3) isolated from the delignified BP bark (3 years old)

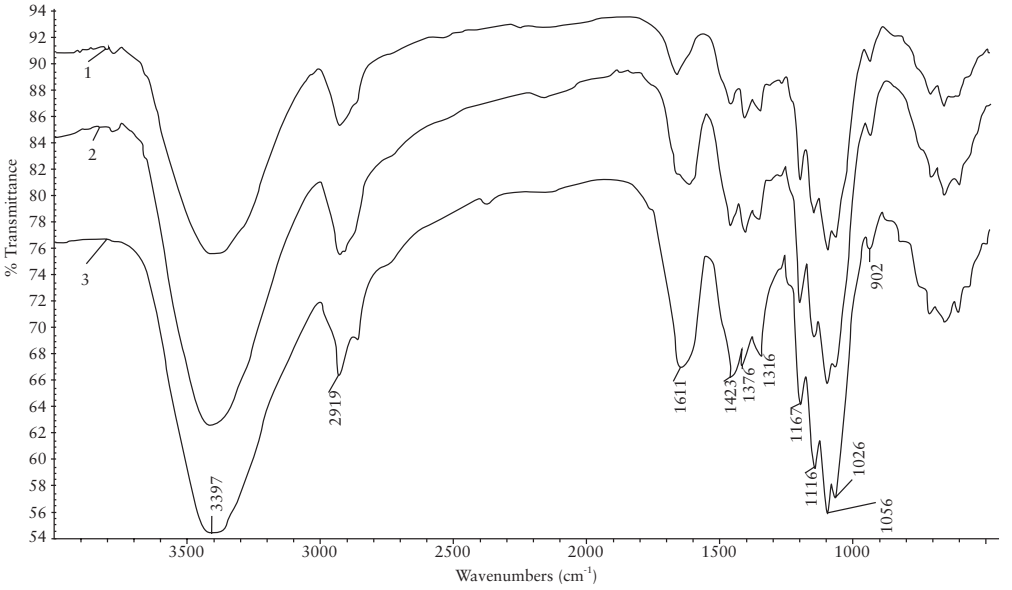

Figure 6.3 FT-IR spectra of cellulosic preparations C_4 (spectrum 1), C_5 (spectrum 2) and C_6 (spectrum 3) from the delignified *Eucommia ulmoides* Oliver stem, BP stem (3 years old) and bark (12 years old)

6.3.5 Cross Polarisation/Magic Angle Spinning ^{13}C Solid-state Nuclear Magnetic Resonance Spectra

Figure 6.4 shows CP/MAS ^{13}C-NMR spectra of cellulosic preparations C_4 (spectrum a), C_5 (spectrum b) and C_6 (spectrum c). The analysis of the three spectra was carried out based on previous literature [35–37]. As can be seen from the spectra, the most intense signals are those from cellulose carbons that appear between 60 and 110 ppm. Starting from the upfield side of the spectra, the region from 60–70 ppm is attributed to C_6, the cluster of resonances from 70–80 ppm is assigned to C_2, C_3 and C_5, the next region from 80–90 ppm is due to C_4 and finally, the region from 100–110 ppm belongs to C_1 [35]. In more detail, the signals at 88.2, 88.4 or 88.5 ppm originate from the C-4 of the highly ordered cellulose of the crystallite interior, whereas the signals at 83.5, 83.2 or 83.7 ppm are attributed to the disordered cellulose. Similarly, the signals at 64.4, 64.6 or 64.7 ppm relate to C-6 in the crystalline cellulose, and at 62.3, 57.8 or 62.4 ppm correspond to crystal surfaces or disordered cellulose. The signals of xylan should be at 103 ppm (C-1), 82 ppm (C-4), 73–79 ppm (C-2, C-3) and 63 ppm (C-5), but the majority of the signals are overlapped by the cellulose

signals [36]. Obviously, in the spectrum of C_6 (spectrum c), the signals at 103.4, 24.5 and 174.9 ppm are attributed to the C-1 of xylose, the carbon of the methyl group and the carbon of the carboxylic group of hemicelluloses, respectively, indicating that the cellulosic preparation C_6 contained a small amount of hemicelluloses. On the other hand, it also suggests that the bonds between hemicelluloses and cellulose in the delignfied BP bark (12 years old) are relatively strong, as during the process of alkaline extraction the side chains of 4-*O*-methyl-glucuronic acid were not completely removed from the backbone of the xylans. In addition, the absence of the signals at 56 and 110–160 ppm, relating to methoxy and aromatic groups of lignin, revealed that the cellulosic preparations were free of the associated lignin, which was consistent with the absence of signal at 1,510 cm^{-1} in the FT-IR spectra.

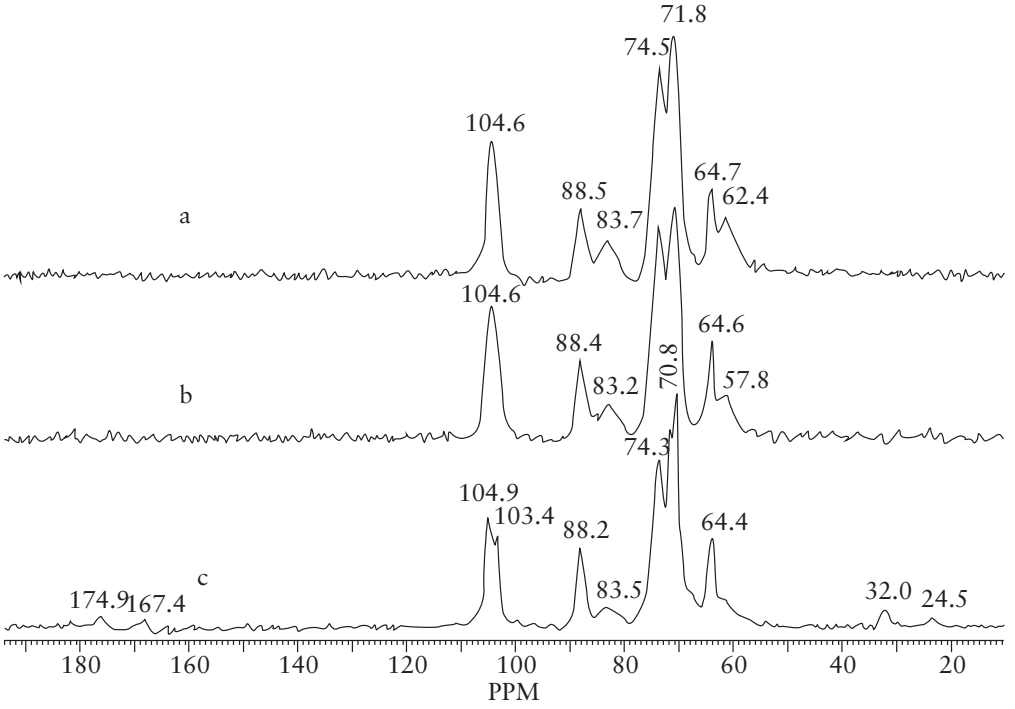

Figure 6.4 CP/MAP ^{13}C-NMR spectra of cellulosic preparations C_4 (spectrum a), C_5 (spectrum b) and C_6 (spectrum c)

6.3.6 Thermal Analysis

Thermal analysis of polymers is an important study covering the field of application and method used for understanding the structure-property relation, and mastering the technology required for the industrial production of different polymeric materials [38]. **Figure 6.5** illustrates TGA and DTG curves of cellulosic preparations C_4 (Curve 1), C_5 (Curve 2) and C_6 (Curve 3). In general, there are three stages of degradation in the TGA curves of the three samples. The initial low temperature mass loss (50–150 °C) corresponds to evaporation of the adsorbed moisture. This loss depends on the initial moisture content of the cellulosic samples. During the second stage, the cellulosic preparations readily start their decomposition, with the severe weight loss mainly oCcuring at 190–380 °C for C_4, 190–360 °C for C_5 and 180–340 °C for C_6, respectively, which was caused by concurrent cellulose degradation processes such as depolymerisation, dehydration and decomposition of glycosyl units followed by the formation of a charred residue. The third stage above 400 °C is due to the oxidation and breakdown of the charred residue into lower molecular weight gaseous products [39–41]. The three cellulosic preparations showed an earlier weight loss at 180 and 190 °C, which was due to the thermal decomposition of unstable hemicelluloses in the cellulosic samples. Hemicelluloses are easily degraded into volatiles at a relatively low temperature because of various saccharides, amorphous structures and branch characteristics [42]. In addition, the maximum weight loss rate reached 2.0 mg/min at 350 °C for C_4, 0.8 mg/min at 320 °C for C_5 and 1.4 mg/min at 350 °C for C_6, which were lower than those reported by Yang and co-workers [42] As can be seen from the TGA curve, when the temperature reached 600 °C, the remaining solid residues are 17% for C_4, 23% for C_5 and 34% for C_6 of the initial weight. The higher amount of the remaining solid residues in C_6, are due to the higher content of ash in the BP bark (12 years old). On the basis of the above results, the thermal stability of cellulosic preparations followed this order: C_4 (*Eucommia ulmoides* Oliver stem) > C_5 (BP stem) > C_6 (BP bark). This indicated that the cellulose obtained from the BP stem had a higher thermal stability than that of the BP bark.

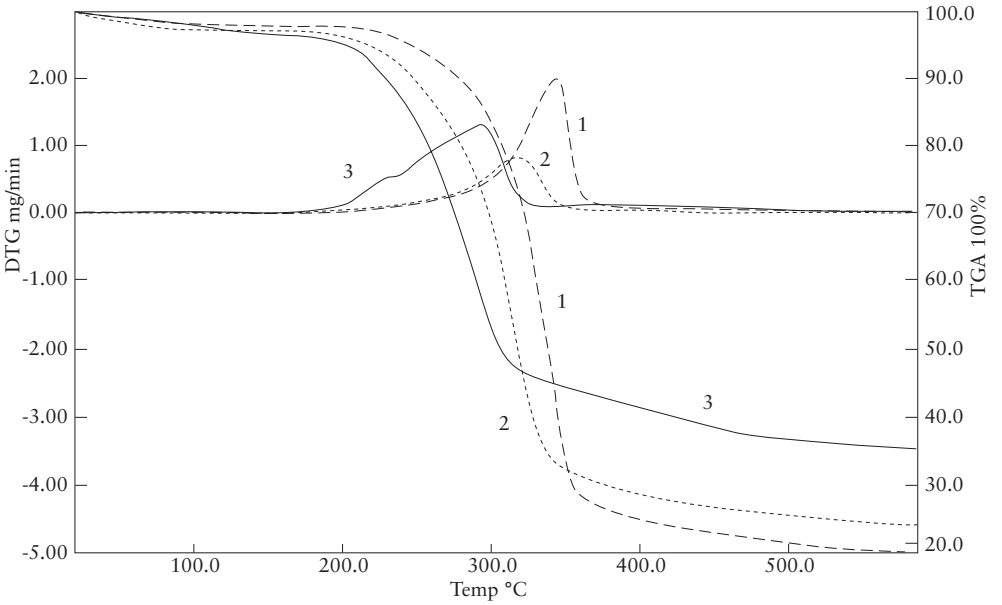

Figure 6.5 TGA/DTG curves of the cellulosic preparations C_4 (curve 1); C_5 (curve 2) and C_6 (curve 3)

6.4 Conclusions

In summary, the BP bark and stem, and *Eucommia ulmoides* Oliver stem were subjected to delignification using chlorite and extraction with alkali, yielding cellulosic fractions of 37.5–51.8%. The results indicated that the relatively higher alkali strength (e.g., 8% NaOH) and longer time of treatment led to an increase of the solubility of the hemicelluloses, and increased the cellulose purity. In addition, the cellulosic polymers in BP stem (3 years old) and older bark (12 years old) had a higher M_w than that of the cellulosic preparation of the BP younger bark (3 years old). The TGA and DTG curves showed three stages of cellulose degradation behaviour. Additionally, the cellulose obtained from the BP stem had a higher thermal stability than that of the BP bark.

Acknowledgements

This work was supported financially from the Major State Basic Research

Projects of China (973-2010CB732203), Ministry of Science and Technology (863-2012AA023204, 10-25 project-2012BAD32B06), National Natural Science Foundation of China (30930073) and Science Foundation for the Excellent Youth Scholars of Ministry of Education of China (20110014120006).

References

1. R.N. Malik and S.Z. Husain, *Pakistan Journal of Botany*, 2007, **39**, 1045.

2. M.A. Huston, *Diversity and Distributions*, 2004, **10**, 167.

3. X.S. Zhang, Z.Y. Wu and Z.Y. Cao in *Flora of China*, Science Press, Beijing, China, 1998, 16, p.23.

4. D. Lee, K.P.L. Bhat, H.H.S. Fong, N.R. Farnsworth, J.M. Pezzuto and A.D. Kinghorn, *Journal of Natural Products*, 2001, **64**, 1286.

5. D. Dutt, A.K. Ray, C.H. Tyagi and V. Kumar, *Journal of Scientific & Industrial Research*, 2005, **64**, 65.

6. K.C. Kin and K.S. Ting, *Acta Physiologica Sinica*, 1956, **20**, 247.

7. T.H. Chien, *Japanese Journal of Pharmacology*, 1957, **6**, 122.

8. T. Deyama, S. Nishibe and Y. Nakazawa, *Acta Physiologica Sinica*, 2001, **22**, 1057.

9. Chinese Pharmacopoeia Commission in *Chinese Pharmacopeia*, Chemical Industry Publishing House, Beijing, China, 2005.

10. J.F. Kadla and R.D. Gilbert, *Cellulose Chemistry and Technology*, 2000, **34**, 197.

11. E. Sjöström in *Wood Chemistry: Fundamentals and Applications*, Elsevier, Academic Press, San Diego, USA, 1993, p.51.

12. G. Daniel in *Wood Deterioration and Preservation: Advances in Our Changing World*, Eds., B. Goodell, D. Nicholas and T. Schultz, American Chemical Society Publishing, Washington, DC, USA, 2003, p.35.

13. T. Imai and J. Sugiyama, *Macromolecules*, 1998, **31**, 6275.

14. A.C. O'Sullivan, *Cellulose*, 1997, **4**, 173.

15. E.L. Hult, T. Iversen and J. Sugiyama, *Cellulose*, 2003, **10**, 103.

16. E. Dinamed, M. Vignon, H. Chanzy and L. Heux, *Cellulose*, 2002, **8**, 7.

17. D. Klemm, B. Heublein, H.P. Fink and A. Bohn, *Angewandte Chemie-International Edition*, 2005, **44**, 3358.

18. C.F. Liu and R.C. Sun in *Cereal Straw as a Resource for Sustainable Biomaterials and Biofuels*, Ed., R.C. Sun, Elsevier, Netherlands Linacre House, The Netherlands, 2010, p.131.

19. S.J. Hanley, J.F. Revol, L. Godbout and D.G. Gray, *Cellulose*, 1997, **4**, 209.

20. O. Brendel, P.P.M. Iannetta and D. Stewart, *Phytochemical Analysis*, 2000, **11**, 7.

21. K. Wang, J.X. Jiang, F. Xu and R.C. Sun, *Polymer Degradation and Stability*, 2009, **94**, 1379.

22. N.J. Loader, I. Robertson, A.C. Barker, V.R. Switsur and J.S. Waterhouse, *Chemical Geology*, 1997, **136**, 313.

23. J. Lundqvist, A. Teleman, L. Junel, G. Zacchi, O. Dahlman, F. Tjerneld and H. Stalbrand, *Carbohyrate Polymers*, 2002, **48**, 29.

24. R.C. Sun, X.F. Sun and J. Tomkinson in *Hemicelluloses: Science and Technology*, Eds., P. Gatenholm and M. Tenhanen, American Chemical Society Publishing, Washington, DC, USA, 2004, p.2.

25. C.F. Liu, J.L. Ren, F. Xu, J.J. Liu, J.X. Sun and R.C. Sun, *Journal of Agricultural and Food Chemistry*, 2006, **54**, 5742.

26. J.P. Vincken, A. Keizer, G. Beldman and A.G.J. Voragen, *Plant Physiology*, 1995, **108**, 1579.

27. J.M. Hackney, R.H. Atala and D.L. Vanderhart, *International Journal of Biology Macromolecule*, 1994, **16**, 215.

28. A. Isogai, A. Ishizu and J. Nakano. *Holzforschung*, 1989, **43**, 333.

29. M. Hirrien, J. Desbriere and M. Rinaudo, *Carbohydrate Polymers*, 1996, **31**, 243.

30. H.K. Johnston and S.J. Sourirajan, *Journal of Applied Polymer Science*, 1973, **17**, 3717.

31. X.F. Xun, R.C. Sun, Y.Q. Su and J.X. Sun, *Journal of Agricultural and Food Chemistry*, 2004, **52**, 839.

32. M.L. Nelson and R.T. O'Connor, *Journal of Applied Polymer Science*, 1964, **3**, 1325.

33. S.Y. Oh, D.I. Yoo, Y. Shin, H.C. Kim, H.Y. Kim, Y.S. Chung, W.H. Park and J.H. Youk, *Carbohydrate Research*, 2005, **340**, 2376.

34. C.Y. Liang and R.H. Marchessault, *Journal of Polymer Science*, 1959, **39**, 269.

35. W.L. Earl and D.L. Vanderhart, *Macromolecules*, 1981, **14**, 570.

36. M.A. Martins, L.A. Forato, L.H.C. Mattoso and L.A. Colnago, *Carbohydrate Polymers*, 2006, **64**, 127.

37. H.R. Tang, Y.L. Wang and P.S. Belton, *Solid State Nuclear Magnetic Resonance*, 2000, **15**, 839.

38. P.V. Joseph, K. Joseph, S. Thomas, C.K.S. Pillai, V.S. Prasad, G. Groeninckx and M. Sarkissova, *Composites Part A: Applied Science and Manufacturing*, 2003, **34**, 253.

39. M. Roman and W.T. Winter, *Biomacromolecules*, 2004, **5**, 1671.

40. A. Demirbas, *Energy Conversion and Management*, 2000, **41**, 633.

41. P. Bjornbom, O. Karlsson, C. Hornell, E. Bjornbom and M. Pirjamali, *International Peat Journal*, 1987, **2**, 137.

42. H.P. Yang, R. Yan, H.P. Chen, D.H. Lee and C.G. Zheng, *Fuel*, 2007, **86**, 1781.

7 Cellulose Fibres in the Papermaking Process

Florin Ciolacu

7.1 Paper and Papermaking Raw Materials

Paper is one of the most valuable inventions of humanity, with significant effects on its evolution and culture. Paper was historically the main communication medium, and for a long time it was the only way to store and transmit information from one generation to another. Over time, there was a broad diversification of paper quality which is used, in addition to writing and printing, as a packaging material and for various technical purposes (filtration of gases and liquids, electrical insulation, building of houses and interior decoration). Some papers, used for packaging or technical goals, require greater thicknesses than those for writing and printing, and are known as paperboard and cardboard. Through its domestic and technical applications, paper also played an important role in increasing the comfort of daily life [1]. Moreover, paper is perceived as an element of art too, not only as a medium for graphics or watercolour masterpieces, but as the result itself in the art of handmade paper manufacturing [2]. Over time, from the famous Tsai Lun to the present day, a variety of fibrous raw materials have been used in paper manufacturing. In fact, identification of new potential raw materials and their processing technology development were the main challenges for papermakers. Until the mid-19th century, rags (based on hemp, linen and cotton) were the only source of raw fibres for papermaking [3]. Along with the development of mechanical and chemical pulping processes, wood became the main raw material for the pulp industry. The use of annual plants is a particularly effective solution for low resource wood regions, for large areas that are not used for agriculture and for large surpluses of agricultural waste products (straw).

Today, paper is made from primary or secondary cellulose fibres, named after the number of manufacturing cycles completed. Primary or virgin fibres are separated from wood or annual plants by various methods – mechanical, chemical or combined – which require weakening or breaking the links which provide structural cohesion. Secondary fibres are produced from recovered paper. In 2011, the world consumption

of pulps was 32.8% for chemical woodpulp, 9.6% for mechanical and semichemical woodpulps, 4.6% for nonwood pulp and 53% for pulp from recovered papers [4].

7.2 Suitability of Cellulose Fibres for Papermaking

During pulping processes, fibres preserve the majority of their original vegetal tissue structure. This is the source of the main explanation of the behaviour of the fibres in the unit operations of papermaking. Obviously the question arises: *what make cellulose fibres suitable for papermaking?* The answer is relatively simple because there are many economical and technical reasons which demonstrate that the cellulose fibres are an ideal raw material for papermaking. The economic arguments are:

- Cellulose fibres are the main constituent of all plants, which are a renewable resource and abundantly available in nature;
- Papermakers are in apparent competition with other users of wood as a raw material, because they mainly use small diameter logs. Wood scrap, sawmill waste, agricultural residue, straw, grasses and/or rags are acceptable sources of virgin fibres;
- Cellulose fibres are reusable/recyclable; and
- Cellulose fibres are biodegradable.

From a technical point of view, cellulose fibres are suitable for papermaking as [5]:

- Lignin, which 'cements' individual fibres in the plant, is physically and chemically weaker than cellulose fibres, making separation of fibres possible by mechanical and/or chemical means;
- Cellulose fibres are made of multilayers of very small thread-like structures called fibrils. These fibrils can be exposed by beating/refining of the fibres and provide a very large area for bonding;
- Cellulose fibres develop physical and chemical bonds with other fibres when changing from wet to dry conditions;
- Cellulose fibres have a high tensile strength, but good flexibility and conformability;
- Cellulose fibres are water-insoluble but are hydrophilic materials at the same time; and
- Cellulose fibres are chemically stable and relatively colourless (white).

Fibres used for papermaking can be classified by their origin as: softwood fibres, hardwood fibres and nonwood fibres. Depending on the original product composition, recycled pulp consists of some or all of the above-mentioned fibre types. Fibre properties affect the formation and consolidation of the paper structure during the papermaking process, and are responsible for the properties of dry paper.

The term 'pulp' is attributed to the fibrous material resulting from complex manufacturing processes involving chemical and/or mechanical treatment of various types of plant material. Pulp is used mainly as the major raw material for paper and board production, where the pulp fibres are mechanically modified to form a paper sheet, but also for chemical conversion to products, such as regenerated fibres and cellulose derivatives. Transformation of fibrous materials into paper as the final product is possible after completion of a technological process flow of varying complexity, depending on the characteristics of paper grade made (**Figure 7.1**).

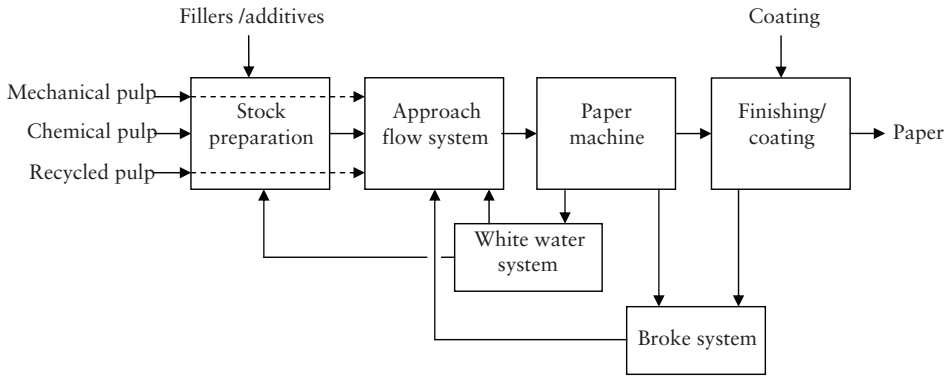

Figure 7.1 Overview of the papermaking process

Paper stock is a complex colloidal system in which the constituent elements (fibres, fine material and fillers) interact with each other. The formation process of paper involves the release of the paper stock on the wire of a paper machine. Water from the paper stock, filtered through the wire, increases in consistency and forms a structure whose strength continuously increases. The strength of this unconsolidated structure is the result of adhesion forces and is not dependent on the fibre strength. During the formation process, paper passes successively through different phases of consolidation during which the moisture and the value of the bonding forces change. By passing the web from the wire section to wet presses and then to the drying stage, the paper

structure gradually moves from a state of coagulation to a network, in which van der Waals forces and weak forces of friction, between the fibre surfaces which are in contact, develop. On drying, paper passes into a consolidated state where the fibres are strongly linked mainly by hydrogen bridges and bonding forces reach the maximum value.

Unlike other engineering materials, paper has the following specific characteristics:

- A heterogeneous composition of structural elements due to the presence of fibres with different lengths and origins, filling and sizing materials;
- Three-dimensional anisotropic distribution of the structural elements due to the different orientation and size of fibres, and auxiliary materials (paper anisotropy is mainly determined by the method and equipment used in manufacturing);
- The porous nature of the structure which controls the paper characteristics such as absorption capacity, permeability to air, hygroscopicity, hygro-expansiveness and the irreversible modification of certain properties during drying;
- Action of bonding forces between the structural elements that determine the mechanical strength of the paper (friction forces, van der Waals forces and hydrogen bonds); and
- The two-sidedness, which is specific to most papers, is determined not only by structural anisotropy, but also by the reality of the manufacturing system (the paper is in contact with the wire on one side and with the press felt on the other).

7.3 Are All Types of Fibres Equally Suitable for Papermaking?

Currently, over 600 grades of paper and paperboard are known and manufactured, and if we take into account the variations on the basis weight, the number exceeds 7,000. For the manufacture of many types of paper and paperboard, only a relatively small number of fibrous raw materials are available, nearly 25 types of sulfite and sulfate pulps, about 10 grades of mechanical pulp, several types of semichemical pulps and a few pulps from rags and recovered paper. Almost all fibrous materials are suitable for the manufacture of most grades of paper if the right technology is applied, but only an optimum composition will allow achieving the desired paper properties at the lowest cost. To determine the optimal composition of pulp it is necessary to know the papermaking properties of the fibrous raw materials.

7.3.1 Papermaking Properties of Cellulose Fibres

No physical or chemical fibre index can solely characterise their papermaking properties, as they depend on a complex number of characteristics reflecting the behaviour of the fibres during refining, the forming and dewatering capacity of the wet paper web, and the effects on the final paper quality. During the refining process, the papermaking capability of the fibres results from their ability to fibrillate, from their shortening and thinning tendency, and from the speed of increasing the beating degree, while key features for paper sheet formation are the pulp drainability and wet strength of the web. Obviously, the papermaking properties of the fibres determine the structural, mechanical, rheological, optical and dielectric characteristics of the paper. The papermaking properties of pulps are extensively described and reviewed in the relevant literature [6–10]. The papermaking properties of the fibres are themselves determined by the chemical composition of the fibres and of course by their morphological characteristics. The properties of fibres in a dry and wet state are also important.

7.3.2 Chemical Composition

The chemical composition of the fibres is important because most of the technical properties of paper are strongly dependent on the chemical components. Of equal importance is the molecular structure and morphology of paper stock components. The chemical composition of cellulosic fibres can be distinguished by major chemical components (more than 1%), minor components (0.1–1%), trace components (0.01–0.1%) and microcomponents (less 0.01%). Of course, the source material and pulping process have a decisive role on the chemical composition of the cellulose fibres. The major components of paper-grade pulps are cellulose, lignin and hemicelluloses. Over time, many studies have tried to demonstrate the influence of the different chemical components of cellulosic fibres on their papermaking properties. Most of them focused on the influence of hemicelluloses and residual lignin content. The content of hemicelluloses in chemical pulps is about half the original quantity existing in wood. Obviously, the chemical composition of the raw materials used to obtain the pulp is variable depending on the wood species and pulping process. Consequently, the content of hemicelluloses will differ. Thus, coniferous wood contains 24–33% lignin, 40–44% cellulose and 25–30% hemicelluloses, to which are added small amounts of resin and extractives substances; hardwood has a lower lignin content (16–24%) and a corresponding higher hemicelluloses content (30–35%) [11]. Due to their high reactivity and distribution in the cell wall structure (in the matrix between the cellulose fibrils in the cell wall, mainly in the outer layers of the fibre [12–14]), hemicelluloses are an important chemical component of paper-grade pulps. They are highly hydrophilic and have a high swelling capacity, promoting fibrillation

and fibre hydration during the refining process. Generally, it was found that sulfite pulps of high hemicelluloses content (about 14%) are easily beaten pulps and form papers with high rigidity, high tensile strength and low greasy permeability. On the other hand, both sulfate and sulfite pulps with only 8% hemicelluloses are beaten easier than those with 12% content. There is an optimum content of hemicelluloses which experience the highest indices of strength. A high content of hemicelluloses is in many cases equivalent to a lower content of alpha-cellulose, a component with long molecular chains which strongly influence fibre strength. The positive effect of the high content of hemicelluloses on the fibre binding capacity is diminished overall by the lower strength of the fibres. In conclusion, it is accepted that pulps have a good beating behaviour and form papers with good resistance, if the alpha-cellulose content does not fall below 94–95% and the pentosans are at least 2.5–3%. It should be noted that not only the quantity, but also the chemical composition and physical state of the hemicelluloses influence the papermaking properties of the chemical pulps. Hexosans, the main component of softwood hemicelluloses have a stronger effect than pentosans, which predominates the hardwood hemicelluloses. In hardwoods, the predominant hemicelluloses are a partially acetylated (4-*O*-methylglucurono) xylan with a small proportion of glucomannan. In softwoods, the major hemicelluloses are partially acetylated galactoglucomannan. A smaller amount of an arabino-(4-*O*-methylglucurono) xylan is also present. This is the main chemical difference between softwoods and hardwoods [15–17]. When comparing two chemical pulps, sulfite and sulfate, from the same wood, with approximately equal yields and close hemicelluloses content, the sulfite chemical pulp is beaten twice as fast, and its strength is between half and three quarters of the strength of the sulfate pulp. This shows that the physical state of hemicelluloses also influence to a great extent, the papermaking properties of the fibres.

Lignin, in the eyes of the papermaker, is an unwanted chemical component of chemical pulps because it prevents fibre softening, limits swelling, reduces the beating rate and the ability of fibres to fibrillate. At high contents of lignin, fibres are rigid, brittle and unable to establish strong links in the paper sheet. Upon wood delignification, the papermaking properties of the chemical pulp continuously improve as the lignin content decreases to a certain value, the phenomenon is then reversed. This is explained by the fact that in the final stages of cooking, a strong degradation of the polysaccharides occurs which has an adverse effect on pulp quality. In terms of mechanical resistance, an optimal content of lignin is about 9% for sulfate pulps, but differs substantially for sulfite pulps depending on the type of strength test used. This makes it difficult to reach a general conclusion in this case. Unbleached sulfite pulps show different properties when compared with sulfate pulps. The residual lignin is sulfonated and therefore rather hydrophilic and is extracted rather easily with effective washing. Because of the acidic pulping conditions, the level of hemicelluloses are very high, therefore the unbleached yield is high. This yield advantage is easily sacrificed

with careless bleaching. Alkaline extraction removes more material from the sulfite pulp in comparison to the sulfate pulp. The resin fraction in unbleached pulp can be quite high, because sulfite pulping does not saponify the resins. In contrast to kraft pulp, the strength of the sulfite fibres depends upon the content of hemicelluloses. Removal of hemicelluloses results in a decrease of pulp strength [18].

The strength of the sulfite pulp is dependent upon the pulping and bleaching conditions. Acidic pulping causes an initial degradation of the fibre structure. This degradation can be severe, despite the relatively high degree of polymerisation of the cellulose chains. Upon beating, the breaking length increases due to the presence of the hemicelluloses which produces good fibre to fibre bonding. In parallel, the tear strength decreases because of the shortening of the fibres. The extraction of the hemicelluloses therefore decreases the strength properties.

7.3.3 Morphological Features of Fibres

Depending on their origin, papermaking fibres differ mainly by morphological characteristics: fibre length, diameter or fibre width, wall thickness, density of the cell wall, and the shape of fibre tips, pits and fenestrations. The morphological properties of the fibres do not essentially change during chemical pulping, but some dimensional changes occur during mechanical pulping.

Fibre properties vary significantly with wood species, growth condition, age, and the pulping and papermaking treatments. Due of the stochastic nature of these variables, the properties of the pulp may have a wide distribution. Each property derives from the contributions of each fibre, and is described by statistical numbers: mean, shape and width of distribution. In order to determine a property of single fibres, many fibres must be measured and the results calculated using a statistical approach.

7.3.3.1 Fibre Length and Fines

There is no doubt that fibre length is one of the most important papermaking characteristics of fibres. A long fibre is able to establish a large number of bonds to other fibres and as such will be anchored more strongly in a fibre network compared with a short fibre; on the other hand, fibres which are too long form papers with a structure of great unevenness (poor formation). The papermaking fibres length is in range 1–6 mm. Hardwood fibres have an average length of around 1 mm whereas the average length of a softwood fibre is 3 mm. Typically, the length of a softwood fibre is 100 times its width, while the width of the open (not collapsed) fibre is approximately ten times the wall thickness. Tensile strength of the wet paper web

increases rapidly with increasing fibre length. The tensile, burst and tear strengths, and elongation at break of the dry paper also improve with increasing fibre length. The influence of the fibre length on the dynamic strength properties, such as tear strength, is much higher than for the equally important interfibre bonds. This is also proved by the well-known relationships established by Clark for the main strength indices [19–24]. So, if the breaking length of the paper is proportional to the square root of the fibre length, the exponent of the fibre length term from the burst index equation increases to 1.0 and to 1.5 for the tear index equation. Fibre length can be assessed either directly or indirectly; the indirect methods split the pulp fibres into different size fractions and give an indication of the fibre length distribution of a pulp and its fines content. This is performed by repeated stepwise screening through screens of decreasing slot size. Fibres are retained predominantly according to their length, but flexibility of the fibres also affects the fractionation result (unsuitable for chemical pulps). Typical screen slots used for mechanical pulp on a Bauer-McNett apparatus are 30, 50, 100 and 200 mesh. The fines content is the material that passes through the screen with the smallest slot (200 mesh). A dynamic drainage jar with a 200-mesh (76 μm diameter holes) wire screen can also be used to measure the fines content [25]. Usually the sample is 500 mL of 0.5% consistency stock.

Determination of the average fibre length can be achieved by different microscopic counting methods [26], image analysis methods [27, 28], or by using various optical devices for measuring dilute fibre suspension movement [29–31]. Counting the fibres and determining their length allows calculation of the arithmetic mean fibre length, but this mean is not always the most useful. For different properties of paper, different averages are more suitable, from the papermaker's point of view. In the case of fibre length, the length-weighted average is the most appropriate. The recent development of optical analysers has made it possible to measure a large amount of fibres in a short time (10,000), including the measurement of fibre morphology parameters such as fibre width, fibre wall thickness and external fibrillation (**Figure 7.2**).

Today, commercial equipment such as the *Kajaani fiber analyser*, *Fiber master* or the *Pulp Expert* provides information regarding the fibre length distribution, average fibre length and the fibre coarseness of a sample. More modern instruments (e.g., *Fiberlab; Metso Automation; Kajaani FS-200*) also provide additional information about fibre width and fibre wall thickness. In addition, shape parameters such as kinks and fibre curl may be quantified by proper image analysis [29–31]. In addition, the fines content can be determined; the measurements were made using two cameras which measure the fibres in a 50μm wide chamber and then deliver the data to the software.

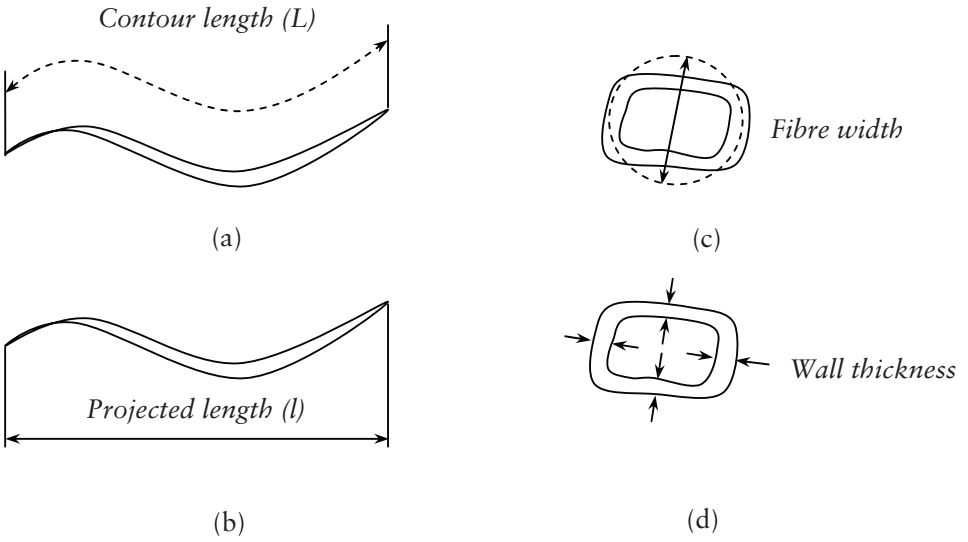

Figure 7.2 Dimensional characteristics of fibres: a) length of strained fibre; b) length of curled fibre; c) dimension of cross section; and d) thickness of fibre wall

The definition of curl index is the result of the difference between the true contour length (L) and the projected length (l) of the fibre divided by the projected length (**Equation 7.1**):

$$Curl\ Index = \frac{L}{l} - 1 \tag{7.1}$$

The curl index is calculated for each individual fibre. A curl index of zero indicates that no curl is present.

The kink is the abrupt change in fibre curvature. The most widely used definition for kink is Kibblewhite's equation. Kibblewhite established that large kinks in fibres had more of an impact on paper properties (i.e., tensile strength, tear and so on) than small kinks. Therefore, his Equation places greater importance on larger angled kinks (**Equation 7.2**):

$$Kink\ Index = \frac{2N_{21-45} + 3N_{46-90} + 4N_{91-180}}{L_{tot}} \quad (7.2)$$

where N is the number of kinks with kink angle values within the three intervals of 21–45, 46–90 and 91–180 degrees respectively, and L_{tot} is the sum of the fibre lengths [32].

The fibre length and coarseness have a large impact on paper properties such as: tensile index [33–35], folding endurance [19], tear index at low-bonding levels [19, 36] and improved formation [37, 38]. On the other hand, fibre curl and kink have been shown to affect the tensile index [39–41], tensile stiffness [42], tear index [39, 40], porosity, bulk, absorbency [41] and burst [42].

7.3.3.2 Cell Wall Thickness and Fibre Coarseness

In geographic areas where the seasons are clearly differentiated, softwood and some hardwood species show seasonal variations in growth and consequently in wood density and fibre size. During the spring season, thin-walled fibres are formed with large lumen called earlywood fibres or springwood. With the change of season, there is a gradual change in fibre size due to the thickening of the walls and decreasing fibre lumen. Thick-walled fibres form sections of latewood or summerwood growth rings (annual). Wood fibre coarseness variations between earlywood and latewood can be larger than those of softwood species [6]. The earlywood fibres collapse more easily, they are more flexible and conform more easily to other fibres.

Fibre coarseness is defined as the weight per fibre length and is normally expressed in units of mg/m or g/m. Coarseness can be calculated from the number of fibres, their average length and the total dry weight of the fibres in a sample. Fibre coarseness can also be obtained by multiplying the cross-sectional area by the density of the fibre cell wall. The fibre coarseness is somewhere around 0.1–0.3 mg/m; the thicker the fibre wall, the higher the coarseness value. Advanced fibre analysers provide direct information on coarseness, the prerequisite being that the total dry weight of the fibres in the sample is known exactly [43]. Fibre length for a given species correlates with their coarseness, as long fibres are appreciated as being coarser than short fibres.

Sometimes, the longest fibres which appear to have the greatest coarseness lead to the strongest papers. In order to more accurately assess the effects of the dimensional characteristics of the fibres, various indices were calculated [44–49] such as (**Equations 7.3–7.8**):

$$Slenderness\ ratio = \frac{L}{D} \tag{7.3}$$

$$Runker\ ratio = \frac{2w}{d} \tag{7.4}$$

$$Flexibility\ ratio = \frac{d}{D} \times 100 \tag{7.5}$$

$$Mühlsteph\ ratio = \frac{D^2 - d^2}{D^2} \times 100 \tag{7.6}$$

$$Rigidity\ coefficient = \frac{w}{D} \times 100 \tag{7.7}$$

$$F\ ratio = \frac{L}{w} \times 100 \tag{7.8}$$

where: w = cell wall thickness; d = diameter of the lumen; D = diameter of the fibre and L = length of the fibre.

The best papermaking pulp fibres are derived from wood species whose fibres do not exceed the Rünkel ratio value of 1 and a value of 80 for the Mühlsteph ratio.

7.3.4 Wet Fibre Properties

The main papermaking characteristics of fibres in the slurry are swelling and specific properties of the swollen fibres: collapsability, flexibility and conformability. These features are defined schematically in **Figure 7.3**.

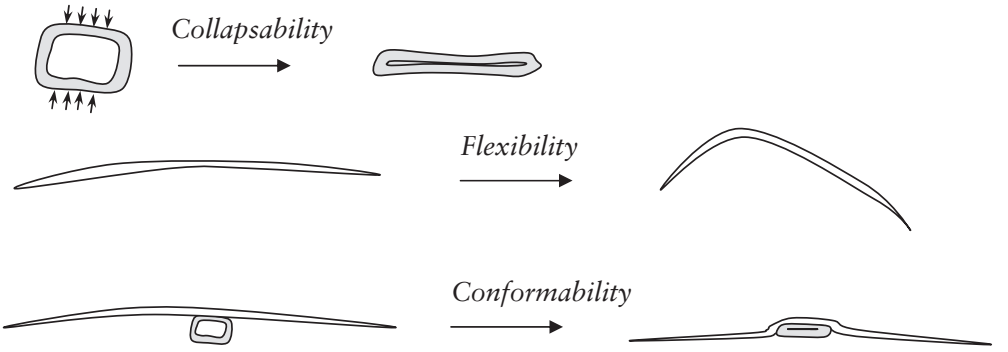

Figure 7.3 Wet fibre properties

Conformability is a combined property which is not directly measurable. Indirect information regarding conformability can be deduced from a combination of swelling (water retention), flexibility and collapsibility measurements. *Conformability* of fibres is a general term that characterises the behaviour of the pulp fibres during the consolidation of the paper structure. Fibres with high conformability bend easily taking the shape of one another and form a dense strongly connected structure. Conformability depends on the cross-sectional dimensions of the fibres, the internal fibrillation, and on the chemical composition and morphology of the cell wall.

Fibres have circular or rectangular sections in wood, but may flatten or collapse during the papermaking process. Under lateral pressure (wet pressing, drying or calendaring), the pulp fibres collapse and change the tube structure into a double-layered strip. When collapsed fibres change, the lumen section alters whereas the value of its perimeter does not. The collapse phenomenon is more specific for chemical pulp fibres rather than those of mechanical pulps. The compression force required to collapse the fibre laterally is in the range of 80–500 Nm^{-1} for a normal pulp and decrease upon increasing the degree of pulping [50]. The main factor of influence on the *collapsability* is the cell wall thickness. Numerous studies have indicated that the springwood fibres are more flexible [51, 52] and collapsible [53–56] than those of summerwood, the latter being stiffer and less collapsible. Furthermore, sulfite fibres collapse more easily than kraft fibres. The noncollapsed lumen of fibres produces an increase in light scattering. Collapsed fibres have a negative effect on the optical properties, but a positive effect on the binding capacity of the fibres and thus on the strength properties of the paper.

The flexibility of wet fibre is a measure of its ability to deform and change shape, to bend or curve, under the action of external forces. Measurement of wet fibre flexibility

is often limited to long fibres. Flexibility or its inverse, called wet fibre stiffness, can be measured by different methods but all are difficult to use and display a rather wide dispersion of results [57, 58]. The wet fibre flexibility decreases rapidly with increasing cell wall thickness, but increases with decreasing pulp yield. Wet stiffness is higher for kraft pulps than for sulfite pulps [59]. Generally, springwood fibres are approximately twice as flexible as summerwood fibres, and the flexibility increases linearly with the degree of beating [60]. Fibres of mechanical pulps have less flexibility than fibres of chemical pulps. The effects of the degree of beating and pulp yield on fibre flexibility are explained by increasing cell wall porosity and wall delaminating. Mohlin and co-workers [61] reported that fully bleached commercial pulps are more deformed than unbleached pulps. Deformation such as kinks, angular folds and twists, which are prone to change the direction of the fibre axis, are found to have a negative effect on the tensile index, compressive strength and so on [62].

7.3.5 Dry Fibre Properties

Despite the difficulties recorded when using measurement techniques, the mechanical properties of single fibres have enjoyed considerable attention [63–68]. By clamping a fibre on a microtensiometer, the tensile strength of single fibres may be measured directly. However, this technique is not easy and may damage the fibre wall such that a predetermined breaking zone is introduced. To determine a significant average value, a large number of fibres must be measured. The large distribution of fibre strength values is a result of the effects of nonuniformity of both the biological raw material and of the pulping processes. Moreover, due to the unfavourable statistics of single fibre measurements, the value of the zero-span strength of paper is commonly accepted as an indirect measure of fibre strength. A sheet is clamped in the tensile apparatus so that the clamps at rest are in contact, and most of the fibres bridging the gap are clamped from both sides. When the clamps separate, these fibres will be under stress. The tensile stress-strain behaviour of various cellulose fibres is similar. Differences are due to the origin and type of fibre, as well as defects relating to the fibre's history, especially pulping and refining. Such weak points may include pores, cracks and dislocations. The elastic modulus of elongation is determined by the initial linear section of the load-elongation curve; beyond the linear section, the fibre offers less resistance towards further stress of elongation. The load-elongation properties of wood fibres are heavily influenced by the wrapping angle of the cellulose fibrils within the secondary S2-layer. For small fibril angles (<10°), the fibres are highly elastic while for high angles, the behaviour is more plastic. Moreover, when the fibrils angle in the S2 layer is small, the load-elongation behaviour of a single fibre is qualitatively similar to that of paper. Bergander [69] demonstrates, by measurements with confocal laser scanning microscopy, that the fibril angle in the springwood varies considerably while in the latewood fibres it is rather constant and smaller.

At the structural level, the tensile behaviour of fibres is more complex. When straining a fibre to a high degree it will tend to twist due to its helical fibrillar structure. This phenomenon cannot happen in paper because of the surrounding network structure. The nonlinearity of the stress-strain dependence of single fibres comes from curling and various defects such as crimps, kinks and microcompressions, which are corrected during fibre elongation. On the other hand, the absence of these defects determines an almost linearly elastic behaviour of the fibres [70, 71].

The cell wall of cellulose fibres can have a large number of dislocations and other unevenness arising from woodchipping, pulping and beating, or other operations from stock preparation (pumping, mixing and cleaning). Also, there may be natural defects such as pits [72]. All these factors reduce the modulus, tensile strength and breaking elongation of the fibre. Only substantial changes in the fibre axis direction (kinks, angular folds, twists) effectively reduce the zero-span strength, the tensile strength and elasticity modulus of paper, as less significant deformations such as fibre curl, just diminish their module and increase the tensile deformation of the fibres [73]. Typical values of the tensile strength of wood fibres are 100–200 mN, springwood fibres require lower values, whereas summerwood fibres require higher values. The breaking force of the summerwood fibre is higher than that required to break springwood fibre because the former have a larger cross-sectional area. The summerwood fibres also have a higher breaking stress (540 MPa compared with only 390 MPa) [6, 74]

Pulping experiments have shown that the gentle removal of lignin during the cooking process does not alter the force required to break the fibres. Pulp may show a comparable fibre strength to wood; this leads to the conclusion that noncellulosic components – lignin and hemicelluloses – do not contribute to the tensile strength of the fibres. The pulping and bleaching reagents can degrade cellulose, reduce the degree of polymerisation, and decrease the stiffness and strength of the fibres. This happens especially when it used in more severe conditions or treatments of extended duration. Kraft pulping provides fibres which are more resistant than sulfite pulping [75, 76].

7.3.5.1 Effects of Drying Stress (Jentzen Effect)

We cannot discuss the properties of dry fibres without mentioning the Jentzen effect. Jentzen [6, 71] showed that drying of never-dried virgin fibres under an axial tension increases the tensile strength and decreases the breaking strain. The opposite occurs when fibres are dried under axial compression. The mechanism of this phenomenon can be explained by the fact that the drying tension reduces fibril angles, aligns molecules parallel to the external load, straightens the fibre, and pulls out dislocations and other defects. A swollen state of the hemicelluloses matrix is necessary for the

structure and molecular rearrangement of fibre to occur, and the high hemicelluloses content is beneficial for the Jentzen effect. But what is more important is that dried and rewetted kraft fibres, which were dried again under load, show no Jentzen effect. This effect demonstrates that drying causes irreversible changes in the fibre wall structure and it also proves the generation of internal stresses during the drying process.

7.4 What happens to Cellulosic Fibres during Papermaking?

The process, in which fibrous cellulosic materials are converted into stock that will later be used on the paper machine, is called stock preparation. The paper stock may be composed of one sort of fibre or a mixture of fibrous raw materials. The nature and extent of the fibrous raw materials used for the paper stock composition depend on the quality characteristics and properties which are required by the final product. Stock preparation consists of several main technological operations: slushing, deflaking and beating or refining by which pulp properties are tailored to fit the final product. The proper choice of technology for stock preparation allows the possibility of manufacturing a wide range of paper grades using a relatively small number of fibrous materials. Balancing the efficiency and reliability of the papermaking process against end-product quality is a crucial factor in stock preparation optimisation.

7.4.1 Cellulose Fibres in the Slushing and Deflaking Processes

Paper mills can be an 'integrated mill' consisting of several pulp and paper manufacturing lines, or a 'nonintegrated mill' with solitary lines of paper or pulp production. Paper mills are integrated with (chemical) pulp mills, mechanical pulp mills and/or deinked pulp mills.

In the cases where a pulp mill is integrated with a paper mill, pulp is pumped through a pipeline from the pulp mill into the paper mill. This eliminates the need for treatment and a pulping system for pulp bales. Moreover, pulp changes due to the drying process known as *hornification* are eliminated. In contrast, dissolved materials coming with the pulp slurry may disturb the wet-end processes of the paper machine [77].

In a nonintegrated paper mill, chemical pulp is supplied in the form of dried pulp sheets or bales, which must be subject to slushing. If necessary, pulp is further disintegrated in a deflaker. The main objective of these operations is to disintegrate cellulose sheets (bale) and turn them into a pumpable fibrous suspension by breaking the bonds created during the pulp dewatering and drying processes. Disintegration of the fibrous suspension ensures there are no visible flakes or bundles of fibres, ensuring a high degree of individualisation of fibrous material which is sent for refining. During

the wet disintegration stage, hydrating and swelling of the fibres also occurs, which improves efficiency and the effects of the subsequent refining operation.

Disintegration of fibrous materials must be performed without shortening the fibres, because their length influences the rate of stock drainage on the machine wire and the mechanical properties of the paper sheet; this condition is thoroughly satisfied by the pulpers. If the paper surface and strength properties are developed during refining, the disintegration and individualisation of the fibres are keys factors for optimal refining. Pulp is always very easy to disintegrate, but some pulps are more difficult to disintegrate into individual fibres than others. The main factors affecting the difficulty of disintegration are: the type of pulp, pulp drying method, and the time and temperature of storage.

Softwood pulps dried in an air flotation dryer or on dryer cylinders are classified as pulps which are easy to disintegrate. On the other hand, the flash dried pulps and in particular, short-fibred nonwood pulps that tend to form clumps (bagasse, reed, straw) are considered difficult to disintegrate [78]. Without any connection to the pulp origin or method of drying, the frozen pulp bales require more intensive use of energy for slushing in comparison to normal pulps. As a general rule, the pulp types that are difficult to slush require deflaking prior to refining. The result of slushing and deflaking, and the degree of defibring are also affected by a wide variety of factors related to stock preparation history, slushing time, and energy and slushing conditions. Undoubtedly, the slushing time and energy have a strong effect on the slushing result. The operating mode of the pulper is also important. The pulpers can operate continuously at low consistency (4–5%) or in a batchwise system at medium or high consistency (6–8% or > 15%). A batch-type pulper yields more homogenous pulp slush than that obtained from a continuously operating pulper since, for instance, variations in the feed flow can be eliminated and all fibres receive the same amount of slushing energy. The specific slushing energy consumption depends on the type of pulp and operating conditions of the pulper; typical values are 10 kWh/t for easily disintegrated pulps and 20 kWh/t for pulps which are difficult to disintegrate. The specific energy consumption is 50% higher in a batchwise operating system. Slushing energy can be described by two parameters, the first is a quantitative one – the amount of energy for slushing and the second is a qualitative one – the intensity of slushing, which is expressed by installed power per cubic metre capacity of the pulper vat (kW/m^3). Increasing the slushing intensity improves the process efficiency, but the specific energy consumption is also raised. A typical value for the intensity of slushing in a medium-consistency pulper is 5–6 kW /m^3. The slushing result is affected by the slushing conditions: water temperature and pH-value as well as consistency. Generally, a higher water temperature results in an acceleration of defibring and reduces the amount of energy needed. For example, an increase in water temperature from 10 to 40 °C reduces the time required for

disintegration and the specific energy consumption by about 50%, while increasing the temperature from 40 to 60 °C has only a minor effect on the slushing rate [79]. The slushing temperature normally depends on the circulation water temperature. Pulp disintegration under alkaline conditions (pH > 7), is easier than under acidic conditions. The penetration of water into the fibres is more difficult when operating at a low water pH stage or if water contains plenty of cations. Sometimes, the water pH-value is raised with sodium hydroxide.

Increasing the slushing consistency will improve the disintegration power up to a certain limit (optimum consistency). The required time for disintegration will also increase with increased consistency. However, at high consistency it can be processed in one batch a larger amount of material and the specific energy consumption is greatly reduced. Increased consistency from 4% to 7–8% reduces the energy consumption by 40–50%, but the use of an appropriate rotor is required. The optimum consistency for pulp slushing depends on the type of pulp as well as the type of pulper. For example, in vertical pulpers running at medium consistency, the optimum slushing consistency for bleached softwood pulp is 6–7%, while for bleached hardwood pulp it is 7–8%. At consistencies of more than 8%, pulp movement starts to slow down markedly, which will reduce the disintegration efficiency. Generally, consistency must be high enough to allow pulp movement and vortex formation. Flotation of pulp sheets or pieces of material on the surface of the slurry indicates a consistency which is too high. For the discharge of a medium consistency pulper, the pulp consistency is reduced to 4–5% by adding dilution water at the bottom of the vat, above the screen plate and in the suction of the discharge pump. Higher consistencies (over 15%) require the use of a specially structured rotor.

In many cases pulp fibres cannot be sufficiently separated from each other by only using the pulper. Completion of the individualisation of the fibres is performed on special equipment, called deflakers. Defibring is more efficient in a deflaker than in a pulper, which saves time and slushing energy. Moreover, deflaking will yield more flexible fibres, which leads to a reduced amount of fibre shortening at the refining stage. On the other hand, due to the break-up of the fibre bundles, pulp cleaning will be easier and the fibre loss is reduced. The operation of the deflaker is based on generating turbulent flows and a pressure pulsation of high frequency by changes in the pulp flow direction using a rotor rotating at a high peripheral velocity (about 40 m/s). Velocity gradients between the liquid layers generate forces that efficiently disintegrate fibre bundles. The energy requirement for deflaking depends on fibre types and their ‘drying history’. A typical energy requirement varies from 20 to 40 kWh/bdmt. An operating consistency for deflaking is from 4 to 5%; a higher consistency value is worth using as it improves the defibring result. Typically, pumps are the factors that set limits for the consistency.

The result of pulp disintegration can be assessed by means of sample sheets by sight, optical methods from sample sheets and stock quality degree (SQD). SQD is a measure of the fibre bundle disintegration efficiency. SQD equals the tensile strength of the laboratory handsheets made from mill stock, expressed as a percentage of the tensile strength of handsheets from the same stock when completely disintegrated in standard laboratory handsheet-making equipment. By 'completely', it is meant that there are no visible fibre bundles and that the tensile strength increases less than 5% during the next 10,000 rotations. Easily disintegrated pulps require an SQD of about 75% after slushing, with the remaining bundle disintegration occurring during refining. Difficult pulps require a higher SQD, which sometimes goes up to 100%, so that they are essentially disintegrated before refining.

Energy savings are possible by optimising the extent of both slushing and refining of the market pulp. Initial trials at mill level found 2 min to be a sufficient time for slushing the softwood pulp. However, for the hardwood pulp, the tensile strength development continued for an optimum slushing time of 10–12 min, reducing its subsequent refining requirement [80]. Tensile index proved a good measure, although other properties may better satisfy the properties sought from the pulp in question. Correct slushing, and in some applications the use of a deflaker, develops the conditions for optimal refining, where the final paper properties such as fibre strength and surface properties of the paper are established. The slushing process in the bale pulping line not only breaks down bales into a pumpable form, but also starts the wetting process required to swell the dried fibres, making them flexible again and releasing the fibre bonds.

7.4.2 Swelling of Fibres

Swelling is a stage of great importance because it greatly influences the intensity of the following process (refining). As a fibre becomes more swollen, the links between the units of the superstructure become weaker, the fibre is more flexible and the shearing processes are lower. Swelling of the fibres favours fibre fibrillation, a transformation that influences decisively the paper strength properties.

The water-fibre interaction absorption refers to the process where water is taken up by the fibres from the external liquid phase. Various mechanisms have been suggested for the absorption process. Three types of water have been defined for water contained inside a fibre: water of constitution, imbibed water (or bonded water) and free water (nonbonded water) [81]:

- *Water of constitution* is that which remains at zero relative vapour pressure. It is water held by fairly strong valence bonds, probably hydrogen bonds. This water forms a monolayer on the cellulose surface;

- *Imbibed water* is all the additional water held by the fibre wall when the relative water vapour is increased from zero to 100%. This water accumulates as further layers on top of the basic monolayer; and
- *Free water* is that held by the fibre, after fibre saturation (at 100% relative water vapour pressure) has occurred. This is held by capillary forces and is not bonded in any way.

Cohesion between the supramolecular structural units of the fibres is ensured by hydrogen bonds established between the hydroxyl groups of the cellulose macromolecular chains. The penetration of water molecules between these units determines their spacing and effective swelling. Fibre swelling under aqueous conditions can be understood in terms of the theories of gel swelling derived by Donnan and Proctor at the beginning of the 20th century. From this starting point, Grignon and Scallan [82] considered that the swelling of the cellulose gel is caused by an osmotic pressure differential, resulting from a difference in concentration of mobile ions between the interior of the gel and the exterior solution. They also showed that a highly charged fibre swells more than a fibre with a lower charge. This was however, later found to be true only for bulk-charged fibres, since Laine and co-workers [83], and Torgnysdotter and Wågberg [84, 85] found that an increase in surface charge of the fibres has no significant influence on the swelling of the fibre wall.

Cellulose fibres are a multiphase body. When immersed in water, the molecules of the water will try to penetrate into the polymer because the osmotic pressure of the water considerably exceeds that of the polymer. The accessibility of the specific domain decreases in the following series: surface of the fibre > surface of the fibrils > open pores and crevices with decreasing size > amorphous domain > crystalline domain. The degree of fibre swelling is determined by the balance between the osmotic pressure and the elastic restraining force of the fibre wall [86, 87]. The partial solubility of hemicelluloses in the cell wall is also an important mechanism of fibre swelling [88].

Many investigations have been focused on studying the swelling properties of the fibre wall, following the introduction of the polyelectrolyte gel concept, as a model for describing the swelling of pulp fibres. Generally, it has been found that the concept works, i.e., the swelling shows changes with pH, fibre charge and salt concentration [89]. The water affinity of the cellulose and fibres depends on the ability of the structural units of glucose to form hydrogen bonds, resulting in the hydrophilicity of these materials. Water can be directly bonded by hydrophilic groups and also indirectly through hydrogen bonds established between water molecules. The degree of fibre swelling is known to be related to the chemical environment and fibre properties [90, 92]. Swelling is influenced primarily by the nature of the fibres, in this case by the content of hemicelluloses and their distribution in the cell wall. Swelling capacity

also depends on the fibre content of the lignin. Pulps with high lignin content swell less because some of the hydroxyl groups of the polysaccharides are engaged in links with the lignin polymer which exhibit high hydrophobicity. Kraft pulps swell more than sulfite pulps and unbleached pulps swell more than the bleached pulps (lower hemicelluloses content).

Simple immersion in water without any mechanical treatment, results in the degree of swelling (% by volume) of 32% for cotton pulp and 30–40% for wood pulps. Depending on the nature of the fibres, the following hierarchy for swelling can be established: cotton linters pulp < bleached sulfite pulp < unbleached sulfite < bleached kraft pulp < unbleached kraft pulp. Swelling depends on drying, pulp consistency, the severity of drying and the fibre hornification. Increasing the degree of hornification results in the swelling occurring to a smaller extent; therefore, papers that are obtained from previously dried celluloses have lower strength properties than those obtained from never-dried pulps. Secondly, the swelling capacity depends not only on the properties of cellulose, but also on the nature of the liquid phase. The swelling of the fibres is strongly influenced by pH [93]; as the pH increases to values above 10, the degree of swelling increases significantly, and a maximum has been recorded between 10.4 and 11.3.

Swelling of the fibres depends on the features of the water or the presence of different cations that favour swelling. The degree of swelling in distilled water is lower than when using industrial process water and the swelling capacity depends on the nature of the cations in the following order: $Al^{3+} < Fe^{3+} < Ca^{2+} < Mg^{2+} < NH^{4+} < Na^{+}$ [82].

The strong connection between swelling and the tensile strength of papers from kraft and sulfite fibres has been shown by Scallan and Grignon [90]. The result of refining is also influenced by fibre swelling as indicated in two recent studies by Hammar and co-workers [94] and Laivins and co-workers [95]. In their studies, the fibre swelling was altered by changing the counter ions, sodium giving a higher swelling than calcium or hydrogen. Both studies reported improved refining efficiency when using sodium.

Well-slushed fibres are flexible, entirely wetted and free of fibre flocs. A uniform and excellent refining result is ensured by these properties [96]. Refining the poorly slushed ‘dry fibres’ will notably increase fibre shortening and impair the bonding ability of the pulp fines.

7.4.3 Cellulose Fibres in the Refining Process

Paper manufacture is based on the ability of fibres to form a network with a desired strength. The strength of the fibre network is first derived from the surface tension

forces and after the solids content has increased (> about 65%), it is derived from interfibre hydrogen bonds. Fibres that have been separated from wood (chemically or mechanically) exhibit poor bond formation ability, since they are stiff and have a smooth surface. In this form, they are unsuitable ingredients for almost any kind of paper-grade production. Papers obtained from unbeaten fibres are characterised by cloudy transparency, high bulk and unsatisfactory strength indices.

During refining, the bonding ability of the cellulose fibres is developed by the mechanical processing (beating) of fibres between the refiner bars. After the collapse of their structure and removal of the poorly soluble lignin-containing primary wall, the cellulosic fibres become more flexible. The breaking of the internal fibre bonds and continued swelling process of the fibres leads to an increase of their fibre-bonding area. Refining is considered one of the most important operations of the papermaking process. During refining, the operator can change the fibre properties and thus, almost all of the properties of the finished paper. The effects of refining on the paper properties are quite different as some of the paper properties are improved (e.g., tensile strength), while others are sacrificed (e.g., opacity) [97, 98]. This is the reason why the refining process is conducted as a compromise between gains and losses, regarding the end product, its conversion and end user needs. The main aspects pursued by refining are closely related to the type of pulp and its role for that paper grade [99]. Thus, the role of the softwood pulp is to improve the strength properties of the paper. The softwood pulp fibres are long, strong and flexible, the ideal properties for reinforcement fibres. The purpose of refining is to improve the reinforcement abilities of softwood pulp without shortening or damaging the fibres to any great extent. In the case of refining softwood pulp, the optimum treatment conditions occur when a specific edge load (SEL) of 2.0 W·s/m is used for an energy level of 80–120 kWh/ton [100]. The main reason for the use of hardwood pulp as a raw material is to improve the paper printability properties. Moreover, short fibres improve the paper formation and optical properties. In this case, the function of refining hardwood fibres is to develop bonding abilities without impairing the optical and printability properties of the fibres. In the case of refining hardwood pulp, the optimum treatment in terms of strength, occurs at a SEL of 0.2 W·s/m over an energy range of 100–150 kWh/ton [100].

Recycled fibre pulp is used to an increasing degree in the papermaking process. The properties of the recycled fibre pulp differ from those of the virgin pulp, due to the irreversible changes that occur during drying and calendaring [101, 102]. The target of refining recycled fibre pulp is to restore the fibre properties, weakened during the recycling and the recycled fibre pulp production process, to a level required by the end product. Generally, recycled fibre pulp is refined with a lower intensity than virgin pulp [103].

7.4.4 Refining Effects on Fibres

The beating or refining process modifies fibre structures in many different ways. For a long time, the effects of refining on fibres were classified into two groups: physical and chemical changes (swelling, removal of the primary wall, hydration, internal fibrillation, external fibrillation) and mechanical changes (shortening and thinning of fibres) [104]. Lately, the literature includes a modern approach to the refining effects on fibres, which are simpler and more scientifically correct. Thus, the basic refining effects on individual fibres can be divided into primary and secondary effects [99]. It should be noted that dividing the refining effects into primary and secondary is based more on conditioning and succession criteria, rather than the importance of the criterion. The primary effects of refining on fibres are as follows: (1) breaking and peeling off of external fibre layers, the creation of fines; (2) external fibrillation; (3) break-up of hydrogen bonds between inner fibre layers, with fibre wall delamination and local collapse; (4) partial dissolution of fibre wall components and the creation of hemicelluloses gel on the fibre surface; and (5) creation of invisible damage and weak points with fibre shortening. As a consequence of the primary effects, the following secondary effects are recorded during refining: (1) water penetration into the fibre wall and fibre swelling by the removal of external plies; (2) creation of new surfaces and fines; (3) elongation and/or compaction of fibres; (4) increase of fibre flexibility; and (5) straightening or curling of fibres (dependent upon if the refining consistency is low or high) [105].

7.4.4.1 Removal of the Primary Fibre Wall

The occurrence of swelling is differentiated across the thickness of the cell wall [106]. The primary cell wall is permeable to water, but swells slightly and acts as a rigid mesh preventing swelling of the secondary wall. The primary wall is more or less resistant to the action of pulping and bleaching reagents, hence paper-grade pulp fibres still contain the primary cell wall. On the other hand, treating the dissolving-grade pulps with alkali generally leads to the loss of the primary cell wall, destroyed by the action of concentrated alkali. The primary cell wall is very sensitive to mechanical action, and under the action of the refiner bars it is immediately removed at the initial refining stage. This creates the possibility of the secondary wall swelling, but it swells in a different manner [107, 108]. The secondary wall, called the S2 layer, swells more than the S1 layer and therefore, due to the swelling pressure which can reach 10^{11} N/m^2, the S1 layer breaks at the weaker areas and allows the S2 layer to swell a greater extent (ballooning effect). As a consequence, the S1 layer detaches.

7.4.4.2 External Fibrillation

After peeling off and delamination of the primary fibre wall and S1 layer, the external surface of the S2 layer is exposed to friction with other fibres, thus resulting in the creation of a fibrillated surface structure. Due to the microfibrillar structure of the S2 layer and the predominant orientation of the microfibrils in the direction of the fibre axis, this leads to strong external fibrillation, which means that a lot of fibrils are partially detached from the fibre surface and results in the build-up of a 'hairy' fibre structure. Upon external fibrillation, the external fibre surface increases significantly and this facilitates interfibre bonding [109, 111].

7.4.4.3 Internal Fibrillation

The action of water is not limited to the fibre surface; it penetrates deep into the amorphous areas of cellulose, acting as a lubricant between the internal fibre layers. It can move under the action of the refiner bars and get into the most convenient position by delamination of the fibre cell wall. Separation of the cell wall structure into fibril layers has the immediate effect of increasing the fibre flexibility and plasticity, and is called internal fibrillation. Due to internal fibrillation, the external fibre area becomes larger and favourable conditions are created for interfibre bonding [112].

7.4.4.4 Fibre Shortening

Under the action of the cutting edges of the refiner bars, fibres are sheared transversally or longitudinally. As a result of the shear action, thinning and shortening of the fibre occurs. The average length of the fibres decreases continuously throughout the refining process. Fibre shortening usually adversely affects the paper characteristics (especially strength properties since the fibre length is an important influential factor), which should be limited by the judicious choice of refining parameters. On the other hand, the shortening of the fibres may also have a positive effect on sheet formation [113]. The shortening of the fibres strongly depends on the refining conditions. In principle, fibre breakage or shortening always occurs when momentary tensile or shear stresses, which develop during refining, exceed the strength of the fibres. As a general rule, a high refining intensity will enhance fibre shortening. There is no weaker or preferential area for fracturing along the fibre length, which means that the shortening of fibres is random and can take place at any point.

7.4.4.5 Creation of New Surfaces and Fines

During refining, new surfaces and fines are created in the pulp suspension due to the peeling off of the outer fibre surfaces, partial delamination of the fibre wall, cutting off of fibre wall parts (lamellar segments and microfibrils) and sections detached during the process of fibre shortening [114]. The creation of fine material does not necessarily exert a negative effect. On the contrary, the creation of fines will improve fibre bonding and paper strength properties. Fine material is composed of particles that have a thickness of 0.1–0.5 μm, a length of several tens of micrometres and can pass through a 200 mesh wire. The fine material generated during refining is called secondary fine material. In addition, two other types of fine material are known: primary and tertiary. Primary fine material is found naturally in the pulp and is represented by parenchyma cells, radial cells and vessel elements. In contrast, tertiary fine material is formed as a result of the action of the pumps and agitator rotor blades of the tanks, and it accumulates into a white water system as a result of 'fractionation' of the paper stock on the machine wire.

7.4.4.6 Partial Dissolution of the Fibre Wall

With the development of refining and exposing the internal structure of the cell wall, new amounts of hemicelluloses and lignin are subjected to the dissolving action of water and refining forces. The amount of dissolution ranges between 0.3 and 1% on weight for paper-grade pulp, but can increase by several points for high-yield pulps. The cyclic action of the compressive forces during refining also contributes to the redistribution of the cell wall components. Since, the hemicelluloses 'migrate' to the fibre surface, and act as a kind of interfibre binder, this type of redistribution has a remarkable effect on the strength of the paper produced from the refined pulp. Numerous studies have demonstrated a strong correlation of the paper strength properties not only with the amount of hemicelluloses present into pulp, but also with its composition [115,116].

7.4.4.7 Increase in Fibre Conformability

Increasing fibre conformability is gained both from the already mentioned refining effects and from the different structural changes and/or damage produced due to mechanical fibre stress.

7.4.4.8 Effects on Pulp Properties

The effects of refining on individual fibres are reflected by changes of the pulp properties and subsequently on the paper properties. The effect of refining on pulp properties is immediately noticed by the papermaker as changes in the drainability and dewatering properties. As refining progresses, the pulp drainability is reduced, which is translated into an increase of the beating degree. A large number of tests are used to control the refining process; some determine the overall transformation of fibres, while others are able to assess the separate effects. The Schöpper-Riegler (°SR) and Canadian Standard Freeness are the main tests which allow the overall assessment of the refining effects based on the dewatering properties of the pulps. Freeness of pulp is the ease with which water drains from the pulp through a wire mesh.

The main influences on pulp freeness are physically, in that the short fibres, vessel elements and fibrils, produced during refining, block drainage more than the long fibres and chemically, in that their affinity for water decreases in the order: hemicelluloses > cellulose >> lignin. Therefore, the unrefined pulps are freer than refined pulps, the long fibre component of a stock is freer than the fine fibres (fines) and the chemical pulps are freer than mechanical pulps. Softwood pulps are freer than hardwood pulps, which in turn are freer than the high hemicelluloses nonwood pulps. Since the freeness measurement is an overall assessment of the effects of refining, it is possible to have two pulps of identical freeness, but with other properties that are very different.

For assessing certain types of fibre transformations, specific tests are used: pulp fractionation to assess mechanical changes, measurement of the external surface area to assess external fibrillation and the water retention value (WRV) as a measure of physical and chemical transformations, and in particular of internal fibrillation. The effect of refining can additionally be detected as a decreasing pulp viscosity value.

During the processes of short circulation (blending, dosage, dilution, cleaning, screening and deaeration), the cellulose fibres do not undergo significant changes. However, the effects of different additives or chemicals on the charging and fibre surface chemistry should not be overlooked. Furthermore, it has been demonstrated that highly charged wet-end additives will continue to contribute to the charge of papermaking fibres, even after they have been recycled [117, 118]. Likewise, the effects of hydrophobic sizing treatments may be passed down to subsequent generations of recycled paper [118].

7.4.5 Cellulose Fibres in the Dewatering and Drying Processes

Papermaking is essentially a dewatering process of a suspension of cellulosic fibres.

During the papermaking process, water is removed by drainage and vacuum in the forming section, by mechanical forces in the press section, and by evaporation and vapour transport in the drying section [119]. Parker [120] believes that paper forming is the result of three basic hydrodynamic processes: drainage, oriented shear and turbulent flow. The main effects of drainage, which can be described as a flow through the wire, are increasing the consistency of the fibrous suspension and felting of the fibres to form a paper web. When the fibres are free to move independently of one another, draining begins with a filtering mechanism and the fibres are deposited on the wire in discrete layers. Filtering is the dominant mechanism of dewatering during paper formation using Fourdrinier-type systems, and the paper web is characterised by a layered structure. When there is no longer the possibility that the fibres can move independently, they flocculate and form coherent networks, and dewatering occurs by thickening, resulting in a cloudy sheet structure. During drainage, fibrous suspensions spontaneously form networks, except when dilution is very high (formation in a laboratory) or when additional mixing energy is provided (which generates turbulence) [121, 122]. Dilution is a great solution for achieving dispersion, but in economic terms cannot be used to control the flocculation into the formation of a paper web on the machine wire. Additional dispersion of the paper stock should be achieved by generating turbulence and/or by initiating oriented shear (shear forces) during drainage. Both shear and turbulence are the result of variations in the flow rate of a fluid. The main difference between these phenomena is that for shear, the velocity vectors are oriented in the same direction, whereas for turbulence they have different directions. Oriented shear can be defined as a flow in layers which has a distinctive profile in the fibrous suspension. This type of flow can occur due to the difference in speed between the wire and the jet, and speed differences between layers of paperstock, determined by contact with a dandy roll or a top wire ('top-former'). Turbulence, defined as an irregular motion, destroys flocks and prevents flocculation, thereby improving formation. Turbulence has selective effects since it only disperses flocks with a fibre length of the same order of magnitude as the scale of the turbulence, while oriented shear affects all flocks. Turbulence can be positive at an early stage of forming (the jet exit from the headbox nozzle), but has an adverse effect on paper formation if it persists in the next stages (forming and dewatering). The hydrodynamic processes of formation, drainage, turbulence and oriented shear occur simultaneously and are not totally independent, being present in both Fourdrinier-forming systems and twin-wire systems.

Although of great importance, the processes of formation and dewatering during the wire section have a negligible effect on the structure and properties of the cellulose fibres. The effects of these processes are confined only to the fibre position within the network under consolidation. The change in the composition of the fibrous suspension, by the lower retention of fines and fillers, can be considered a secondary effect.

Wet pressing is the papermaking operation of expelling water from the paper web by mechanical compression in the nip, formed by two rolls or recently, by a roll and a special part named the 'shoe'. The wet pressing process affects the structure and fibre properties and thus, both the paper properties and papermaking potential of these fibres [123, 124]. In addition to water removal, the fibres are flattened and new bonding conditions develop, which contribute to a permanent densification of the paper sheet. Different studies have demonstrated decreases in the water-holding capacities of fibres which have been pressed under normal or severe conditions [125, 127].

Decreasing the WRV seems to be an effect of the irreversible formation of new semicrystalline regions, as a result of establishing new hydrogen bonds between cellulosic surfaces within parts of the cell wall that come in contact due to the applied force [128]. The use of laser confocal microscopy and swelling measurements led to the conclusion that irreversible hornification (loss of swelling capacity when the fibres are rewetted) began above a solids contents of 30–35% [129].

Drying is the papermaking operation in which the dry content of the paper is brought to an optimum and which largely determines the final characteristics of the paper. In the paper wet web, water is in the form of free water and bound water. Wet pressing removes more than 90% of the free water. The remaining free water and most of the bound water can only be removed by evaporation or by heating. There are three methods normally applied to paper and board drying, which differ in principle from each other by the method of energy supply; contact or cylinder-drying, air-drying and radiation drying. The drying temperature and duration of the process vary widely, depending on the paper basis weight, the speed of the paper machine, and other design and operation parameters. In conventional paper machines, drying takes place under atmospheric pressure. For this reason, the temperature of the paper will tend to remain at the boiling point or lower, as long as the liquid water remains within the pore spaces adjacent to the sheet's surface [130]. When drying freely, the web will shrink. The degree of shrinkage at a paper machine depends, among other things, on the fibre orientation, the length of draws and the tension of the dryer fabric. The shrinking of the paper web during the drying process can result in fibres moving closer to each other and shrinkage of the fibres themselves. Thus, the shrinking process can be divided into interfibre and intrafibre shrinking. The shrinkage of fibre is 1 to 2% in its longitudinal direction and 20 to 30% in its cross-direction. When the dry content is below the saturation point of the fibres, interfibre shrinkage will occur. Neither shrinkage of the fibres nor the formation of interfibre bonds are possible in the presence of free water, whereas the surface tension forces tend to draw each of the fibres closer as well as the fibrils detaching partly or entirely from the fibres.

7.5 Conclusions

Over time, the raw materials used in the papermaking process progressed from simple rags and pasta to bleached chemical pulps, resulting from pulping processes conducted to meet the most stringent quality requirements of the different types of paper and paperboard.

Undoubtedly, cellulose fibres are the most suitable raw material for papermaking. To support this claim, economic and technical arguments were presented in this chapter. It is true that not all pulp grades are equally suitable for making any sort of paper or paperboard hence, a review of papermaking properties was shown to be necessary. Furthermore, proceeding sequentially through the operations of the papermaking process provides an overview, but also a detailed image of the modifications of the cellulose fibres. This review also revealed many phenomena and transformations still not well understood that represent a rich topic of research in the field.

In the near future there are unlikely to be major changes in the raw materials used for papermaking, but use of secondary fibres will further increase achieving a sustainable recycling limit. In addition, new efforts investigating the recovery papermaking potential of secondary fibres will be engaged.

References

1. T-H. Tsien in *Science and Civilization in China*, Volume 5, Ed., J. Needham, University Press, Cambridge, 1985, p.85.

2. M.A. Hubbe and C. Bowden, *BioResources*, 2009, **4**, 4, 1736.

3. T. Barrett in *European Papermaking Techniques 1300–1800*, The University of Iowa, Ames, Iowa, USA, 2012.
http://paper.lib.uiowa.edu/european.php

4. FAO Forestry statistics, Food and Agriculture Organization of the United Nations.
http://faostat.fao.org

5. J. Asunción in *The Complete Book of Papermaking*, Lark Book, New York, NY, USA, 2003, p.104.

6. E. Retulainen, K. Niskanen and N. Nilsen in *Paper Physics: Papermaking Science and Technology*, Eds. J. Gullichsen and H. Paulapuro, Fapet Oy, Helsinki, Finland, 1998, **16**, p.55.

7. E. Hiltunen in *Pulp and Paper Testing: Papermaking Science and Technology*, Eds., J-E. Levlin and L. Söderhjelm, Fapet Oy, Helsinki, Finland, 1999, **17**, p.39.

8. E. Gruber in *Handbook of Pulp*, Ed., H. Sixta, Wiley-VCH, Weinheim, Germany, 2006, p.1211.

9. E. Brännvall and G. Annergren in *Pulping Chemistry and Technology: Pulp and Paper Chemistry and Technology*, Eds., M. Ek, G. Gellerstedt and G. Henriksson, Walter de Gruyter, Berlin, Germany, 2009, **2**, p.429.

10. S.A. Rydholm in *Pulping Processes*, Malabar, Robert E. Krieger Publishing, Florida, FL, USA, 1965, p.1135.

11. D. Klemm, H-P. Schmauder and T. Heinze in *Biopolymers: Biology, Chemistry, Biotechnology, Applications*, Eds., E. Vandamme, S. De Baets and A. Steinbüchel, Wiley-VCH, Weinheim, Germany, 2002, **6**, p.277.

12. A.J. Kerr and D.A.I. Goring, *Cellulose Chemistry and Technology*, 1975, **9**, 6, 563.

13. D. Fengel and G. Wegener in *Wood Chemistry, Ultrastructure, Reactions*, Walter de Gruyter, Berlin, Germany, 1984, p.129.

14. L. Salmén and A-M. Olsson, *Journal of Pulp and Paper Science*, 1998, **24**, 3, 99.

15. A. Teleman in *Wood Chemistry and Wood Biotechnology: Pulp and Paper Chemistry and Technology*, Eds. M. Ek, G. Gellerstedt and G. Henriksson, Walter de Gruyter, Berlin, Germany, 2009, **1**, p.101.

16. H. Meier in *Biosynthesis and Biodegradation of Wood Components*, Ed., T. Higuchi., Academic Press, New York, NY, USA, 1985, p.43.

17. V. I. Popa and I. Spiridon in *Polysaccharides: Structural Diversity and Functional Versality*, Ed., S. Dumitriu, Marcel Dekker Inc., New York, NY, USA, 1998, p.297.

18. H.U. Süss, J.D. Kronis and R. Taylor in *Proceedings of TAPPI Pulping Conference*, Montreal, Canada, 1998, p.851.

19. J. d'A Clark in *Pulp Technology and Treatment for Paper*, 2nd Edition, Miller Freeman, San Francisco, CA, USA, 1985, p.878

20. J. d'A Clark, *TAPPI- Technical Association Papers*, 1943, **26**, 499.

21. J. d'A Clark, *TAPPI*, 1962, **45**, 8, 6.

22. J. d'A Clark, *TAPPI*, 1965, **48**, 3, 180.

23. J. d'A Clark, *Svensk Papperstidning*, 1970, **3**, 15, 54.

24. J. d'A Clark, *TAPPI*, 1973, **56**, 7, 122.

25. *Fines Fraction of Paper Stock by Wet Screening*, TAPPI pm T 261, 1990.

26. *Fiber Length of Pulp by Projection*, TAPPI cm T 232, 1985.

27. *ISO 16065±1: Pulps; Determination of Fibre Length by Automated Optical Analysis. Part 1: Polarized Light Method*, 2001.

28. *Fiber Length of Pulp and Paper by Automated Optical Analyzer using Polarized Light*, TAPPI om T 271, 1998.

29. G. Robertson, J. Olsen, P. Allen, B. Chan and R. Seth, *TAPPI Journal*, 1999, **82**, 10, 93.

30. R.J. Trepanier, *TAPPI*, 1998, **81**, 6, 152.

31. J.A. Olson, A.G. Robertson, T.D. Finnigan and R.R.H. Turner, *Journal of Pulp and Paper Science*, 1995, **21**, 11, J367.

32. P. Sutton, C. Joss and B. Crossely in the *TAPPI 2000 Pulping/Process & Product Quality Conference Proceedings*, TAPPI Press, Boston, MA and Atlanta, GA, USA, 2000, Paper No.133.

33. R.S. Seth, in *Proceedings Materials Research Society Symposium*, San Francisco, CA, USA, 1990, **197**, p.125.

34. E. Retulainen, *Paper and Timber,* 1996, **78**, 4, 187.

35. R.S. Seth, in *Proceedings Materials Research Society Symposium*, San Francisco, CA, USA, 1990, **197**, p.143.

36. R.S. Seth and D.H. Page in *Proceedings of International Paper Physics Conference*, Auberge Mont Gabriel, Mont-Rolland, Quebec, Canada, 1987, p.9.

37. R.J. Kerekes and C.J. Schell, *TAPPI*, 1995, **78**, 2, 133.

38. R.J. Kerekes, R.M. Soszynski and P.A.T. Doo in *Papermaking Raw Materials - Transactions of the 8th Fundamental Research Symposium*, Ed., V. Punton, FRC of Pulp and Paper Fundamental Research Society, London, UK, 1985, p.265.

39. A. Hakanen and N. Hartler, *Paper and Timber*, 1995, **77**, 5, 339.

40. U-B. Mohlin and C. Alfredsson, *Nordic Pulp and Paper Research Journal*, 1990, **5**, 4, 172.

41. D.H. Page, R.S Seth, M. Barbe and B. Jordan in *Papermaking Raw Materials - Transactions of the 8th Fundamental Research Symposium*, Ed., V. Punton, FRC of Pulp and Paper Fundamental Research Society, London, UK, 1985, p.183.

42. U-B. Mohlin and J. Dahlborn, *TAPPI*, 1996, **79**, 6, 105.

43. *ISO 9184-6: Paper, Board and Pulps - Fiber Furnish Analysis. Determination of Fibre Coarseness*, 1990.

44. A. Tutus, N. Comlekcioglu, S. Karaman and M.H. Alma, *International Journal of Agriculture and Biology*, 2010, **12**, 286.

45. A. Tavasoli, M. Dehghani and S. Mahdavi, *World Applied Science Journal*, 2011, **14**, 6, 906.

46. A.A. Watson and H. E. Dadswell, *Appita*, 1961, **14**, 5, 168.

47. H.E. Dadswell and A.J. Watson in *Formation and Structure of Paper - Transactions of the 2nd Fundamental Research Symposium*, Ed., F. Bolam, FRC of Pulp and Paper Fundamental Research Society, London, UK, 1962, p.537.

48. A.A. Watson and H.E. Dadswell, *Appita*, 1964, **17**, 6, 146.

49. D.H. Page, *Journal of Pulp and Paper Science*, 1983, **9**, 1, TR15.

50. N. Hartler and J. Nyrén, *TAPPI*, 1970, **53**, 5, 820.

51. P. Luner in *Proceedings PIRA International Conference 'Advances in Refining Technologies'*, Birmingham, UK, 1986, Paper No.3.

52. T. Hattula, and H. Niemi, *Paperi ja Puu*, 1988, **70**, 4, 356.

53. A. Uhmeier and L. Salmén, *Nordic Pulp and Paper Research Journal*, 1996, **11**, 3, 171.

54. U.B. Mohlin, *Svensk Papperstidning*, 1975, **78**, 11, 412.

55. W.E. Smith and V.L. Byrd, *U.S. Forest Serv*ice, *Research Paper FPL 193*, 1972.

56. F. Huang, R. Lanouette and K-N. Law, *BioResources*, 2012, **7**, 2, 1697.

57. R. Steadman and P. Luner in *Papermaking Raw Materials*, Ed., V. Punton, Mechanical Engineering Publishers Ltd., London, UK, 1985, p.311.

58. P.A. Tam Doo and R.J. Kerekes, *TAPPI*, 1981, **64**, 3, 113.

59. R.J. Kerekes and P.A. Tam Doo, *Journal of Pulp and Paper Science*, 1985, **11**, 2, J60.

60. T. Hattula and H. Niemi, *Paperi ja Puu*, 1988, **70**, 4, 356.

61. U.B. Mohlin, J. Dahlbom and J. Hornatowska, *TAPPI*, 1996, **79**, 6, 105.

62. L. Paavilainen, *Paperi ja Puu*, 1993, **75**, 9, 689.

63. K.W. Hardacker in *The Physics and Chemistry of Wood Pulp Fibres*, TAPPI Special Technical Association Publication No.8, Appleton, WI, USA, 1970, p.201.

64. L. Mott, S.M. Shaler, L.H. Groom and B.H. Liang, *TAPPI*, 1995, **78**, 5, 143.

65. D.H. Page, F. El-Hosseiny and K. Winkler, *Nature*, 1971, **229**, 252.

66. D.H. Page and F. El-Hosseiny, *Journal of Pulp and Paper Science*, 1983, **9**, 1–2, 26.

67. A. Bergander and L. Salmén, *Journal of Materials Science*, 2002, **37**, 1, 151.

68. F. De Magistris and L. Salmén, *Nordic Pulp and Paper Research Journal*, 2008, **23**, 2, 240.

69. A. Bergander and L. Salmén, *Holzforschung*, 2000, **54**, 6, 654.

70. B.A. Jayne, *TAPPI*, 1957, **42**, 6, 461.

71. C.A. Jentzen, *TAPPI*, 1964, **47**, 7, 412.

72. O.L. Forgacs, *TAPPI*, 1961, **44**, 2, 112.

73. U-B. Mohlin and C. Alfredsson, *Nordic Pulp and Paper Research Journal*, 1990, **5**, 4, 172.

74. B. Duncker and L. Nordman, *Paperi ja Puu*, 1965, **47**, 10, 539.

75. B. Leopold, *TAPPI*, 1966, **49**, 7, 315.

76. B. Leopold and J. Thorpe, *TAPPI*, 1968, **51**, 7, 304.

77. L. Sjöström, A. Jacobs, R. Rådeström and M. Nordlund, *Nordic Pulp and Paper Research Journal*, 2006, **21**, 5, 575.

78. J. Lumiainen, *Paper Technology*, 1996, **37**, 6, 22.

79. A. Savolainen, T. Jussila and S. Nikula, *TAPPI*, 1991, **74**, 11, 147.

80. G.H. Nuttall and L. Mott, *Paper Technology*, 1998, **39**, 1, 39.

81. R.W. Hoyland and R. Field, *Paper Technology*, 1976, **17**, 6, 216.

82. J. Grignon and A.M. Scallan, *Journal of Applied Polymer Science*, 1980, **25**, 12, 2829.

83. J. Laine, T. Lindström, C. Bremberg and G. Glad-Nordmark, *Nordic Pulp and Paper Research Journal*, 2003, **18**, 325.

84. A. Torgnysdotter and L. Wågberg, *Nordic Pulp and Paper Research Journal*, 2003, **18**, 455.

85. A. Torgnysdotter and L. Wågberg, *Nordic Pulp and Paper Research Journal*, 2004, **19**, 440.

86. T. Lindström, *Nordic Pulp and Paper Research Journal*, 1992, **7**, 181.

87. L. Wågberg and G. Annergren in *Transactions of the 11th Fundamental Research Symposium* Volume 1, Pira International, Leatherhead, UK, 1997, p.1.

88. K. Luukko and T.C. Maloney, *Cellulose,* 1999, **6**, 123.

89. L. Wågberg in *Pulp and Paper Chemistry and Technology, Paper Chemistry and Technology*, Eds., M. Ek, G. Gellerstedt, G. Henriksson and W. de Gruyter, Berlin, Germany, 2009, **3**, p.39.

90. A.M. Scallan and J. Grignon, *Svensk Papperstidning*, 1979, **82**, 2, 40.

91. T. Lindström and G. Carlsson, *Svensk Papperstidning*, 1982, **85**, R14.

92. A.M. Scallan and A.C. Tigerström, *Journal of Pulp and Paper Science*, 1992, **18**, J188.

93. T. Lindström and M. Kolman, *Svensk Papperstidning*, 1982, **85**, 15, 140.

94. L-Å. Hammar, M. Bäckström and M. Htun, *Nordic Pulp and Paper Research Journal*, 2000, **15**, 3, 189.

95. G. Laivins and T. Scallan, *Journal of Pulp and Paper Science*, 2000, **26**, 6, 228.

96. U-B. Mohlin in *Proceedings of the 2002 TAPPI Technology Summit Conference*, TAPPI, Atlanta, GA, USA, 2002, Paper No. 26.

97. K. Ebeling in *Proceedings of the International Symposium on Fundamental Concepts of Refining*, IPST, Appleton, WI, USA, 1980, p.1.

98. D.H. Page in *Fundamentals of Papermaking - Transactions of 9th Fundamental Research Symposium*, Eds., C.F. Baker and V.W. Punton, FRC of Pulp and Paper Fundamental Research Society, London, UK, 1989, p.31.

99. J. Lumiainen in *Papermaking Part 1: Stock Preparation and Wet End. Papermaking Science and Technology*, Ed., H. Paulapuro, Fapet Oy Publication, Helsinki, Finland, 2000, p.87.

100. C.F. Baker, *TAPPI*, 1994, **78**, 2, 147.

101. R.C. Howard and W.J. Bichard, *Journal of Pulp and Paper Science*, 1992, **18**, 4, J151.

102. N. Gurnagul, S. Ju and D.H. Page, *Journal of Pulp and Paper Science*, 2001, **27**, 3, 88.

103. D. Bergfeld, in *Proceedings of 53rd APPITA International Refining Conference*, APPITA, Rotorua, 1999, **2**, p.787.

104. R.P. Kibblewhite, *TAPPI*, 1977, **60**, 10, 141.

105. R.S. Seth, *Pulp and Paper Canada*, 2006, **107**, 1, 34.

106. K. Olejnik, *Fibres & Textiles in Eastern Europe*, 2012, **20**, 1, 113.

107. T.C. Maloney, H. Paulapuro and P. Stenius, *Nordic Pulp and Paper Research Journal*, 1998, **13**, 1, 31.

108. T.C. Maloney, J.E. Laine and H. Paulapuro, *TAPPI*, 1999, **82**, 9, 125.

109. T. Kang and H. Paulapuro, *Pulp and Paper Canada*, 2006, **107**, 7–8, 51.

110. T. Kang, P. Somboon and H. Paulapuro, *Paperi ja Puu*, 2006, **88**, 7, 409.

111. O. Joutsimo and L. Robertsén, *Paperi ja Puu*, 2004, **86**, 7, 508.

112. O. Joutsimo and L. Robertsén, *Paperi ja Puu*, 2004, **86**, 5, 359.

113. K. Koskenhely, K. Nieminen, E. Hiltunen and H. Paulapuro, *Paperi ja Puu*, 2005, **87**, 7, 458.

114. N.K. Bhardwaj, V.Hoang and K.L. Nguyen, *Bioresource Technology*, 2007, **98**, 1647.

115. T. Lindstrom, *Nordic Pulp and Paper Research Journal*, 1992, **7**, 4, 181.

116. P. Fardim and N. Duran, *Colloids and Surfaces A: Physicochemical and Engineering Aspects*, 2003, **223**, 1, 3, p.263.

117. U. Grau, R. Schuhmacher and S. Kleemann, *Wochenblatt fur Papierfabrikation*, 1996, **124**, 17, 729. [In German]

118. L. Sjostrom and L. Odberg, *Papier*, 1997, **51**, 6A, V69.

119. F.W. Ahrens and H. Xu in *Proceedings of the TAPPI Engineering/Process and Product Quality Conference*, TAPPI Press, Atlanta, GA, USA, 1999, **2**, p.1009.

120. J. Parker and O.M. Hergert, *TAPPI*, 1968, **51**, 10, 425.

121. M.A. Hubbe, *BioResources*, 2007, **2**, 296.

122. A. Celzard, V. Fierro and A. Pizzi, *Cellulose*, 2008, **15**, 803.

123. D.H. Page, *TAPPI*, 1967, **50**, 9, 449.

124. T.C. Maloney, T-Q. Li, U. Weise and H. Paulapuro, *Appita Journal*, 1997, **50**, 4, 301.

125. A.A. Robertson, *Pulp and Paper Magazine of Canada*, 1964, **65**, 3, T161.

126. G. Carlsson and T. Lindstrom, *Svensk Papperstidning,* 1984, **87**, 15, R119.

127. X.L. Luo, J.Y. Zhu, R. Gleisner and H.Y. Zhan, *Cellulose*, 2011, **18**, 1055.

128. A.M. Scallan in *Proceedings of COST Action E1- Improvement of Recyclability and the Recycling Paper Industry of the Future*, Eds., A. Blanco, C. Negro, I. Gaspar, M.C. Monte and J. Tijero, Complutense University of Madrid, La Palmas de Gran Canaria, Spain, 1998, p.312.

129. U. Weise and H. Paulapuro, *Papier*, 1996, **50**, 6, 328. [In German]

130. S.P. Garvin, Jr., and P.F. Pantaleo in *Proceedings of TAPPI Engineering Conference*, Houston, Texas, 1976, TAPPI Press, Atlanta, GA, USA, 1976, p.125.

8 Cellulose Esters - From Traditional Chemistry to Modern Approaches and Applications

Diana Ciolacu, Liliana Olaru, Dana Suflet and Niculae Olaru

8.1 Introduction

Over the years, cellulose, like no other raw or polymeric material has opened a multitude of research topics and interdisciplinary approaches. Its unique structure, of poly(β-1,4-D-anhydroglucopyranose) with three OH groups per anhydroglucose unit, and properties have gathered increasing scientific attention since the second half of the 19th century to the modern age of nanotechnologies. The versatility and wide availability of cellulose could answer various challenges and demands of modern life, and place this natural, biodegradable polymer in a special position amongst other polymers. As a consequence of its high capacity for chemical modification, cellulose can be transformed into a variety of useful products covering a wide range of applications, from traditional plastics and fibres to special devices and innovative products. Maybe the most spectacular feature of modified cellulosics, from the point of view of modern research topics, is their high suitability for nanotechnologies which could significantly broaden, in the coming decades, the applicability of cellulosic polymers for special domains such as top technologies or the biomedical field.

Today, we can consider cellulose chemistry as a distinct discipline in the broad field of polymer science. A cellulose ester, for example, like cellulose acetate, is not a single compound with a unique structure and well-defined properties, as is the case with most of the synthetic polymers. 'Cellulose acetate' (CA) is a generic name covering a multitude of polymers with the same cellulose skeleton and the same functional groups, but various degrees of substitution (DS). Moreover, there are different possible distribution patterns of those groups, both within the glucose unit and along the polymer chain, which generate a wide variety of properties and consequently, applications. This explains the large interest of the scientific world towards cellulose chemistry and the great number of scientific works reported, especially over the last couple of decades. Fundamental aspects and the main topics in cellulose chemistry today refer to structural characterisation and structure-property relationships, new

paths for derivatisation, regioselectivity and products with tailored properties, which have been reviewed in detail in recent years [1–5].

The aim of this contribution is to highlight the present knowledge on some cellulose esters and mixed esters, which are the main points of interest for our research group.

8.2 Cellulose Esters: Heterogeneous or Cvasi-homogeneous Processes

The chemical modification of cellulose, by typical reactions of the hydroxyl groups, can produce esters and ethers with large applications as fibres, films, plastics, coatings and filtration media, as well as additives for food products, cosmetics, pharmaceuticals, the extractive industry and so on [6, 7]. The fibrous nature of cellulose and its strong hydrogen bond network caused serious problems with respect to the reaction conditions and chemical reproducibility. The development of alternative synthesis pathways, including homogeneous derivatisation in novel cellulose solvents, created the possibility to obtain products with tailored structures and properties.

The classical route to obtain organic commercial cellulose esters was, for many years, the esterification of cellulose performed in heterogeneous or cvasi-homogeneous media, using acid chlorides or anhydrides as acylation reagents and a catalyst, usually a strong mineral acid [8, 9]. Other acylation agents could be carboxylic acid or salts of carboxylic acids in media consisting of pyridine/*p*-toluenesulfochloride (TosCl) or *N*,*N*′-dimethylformamide (DMF)/(TosCl) [10, 11].

Inorganic esters of cellulose have also been obtained by classical heterogeneous procedures [12]. Partially substituted cellulose esters, which exhibit specific solubility and certain properties useful for a desired application, could not be synthesised by direct esterification because of the uneven substitution pattern produced under heterogeneous conditions. The most widely used cellulose ester, for example, CA with partial substitution, is produced by the partial hydrolysis of a highly substituted cellulose acetate in aqueous acetic acid media [8, 13–16]. These processes are called ‘cvasi-homogeneous’, because they start in a suspension of cellulose in the reaction medium and end in a solution of the final product.

Several cellulose acetates have been intensively studied for their practical importance. The most attractive are those with DS of 2.50 (acetone-soluble), 1.70 (useful for further derivatisation), as well as water-soluble acetates with partial DS of about 0.5–1.0. The solubility of partially substituted cellulose acetates is known to be one of the most important features governing the properties and applications of these polymers, and has been investigated in relation to different synthesis

methods and the distribution of acetyl groups within the anhydroglucopyranose units (AGU) [17].

The most important drawbacks related to classical procedures are the difficult conditions – such as long reaction times – necessary to obtain a uniform substituent distribution and good solubility in appropriate solvents.

Research efforts have been reported attempting to overcome these disadvantages and make the heterogeneous acylation of cellulose remain attractive from a practical point of view. A process performed at high temperatures, in both the acetylation and hydrolysis steps, leads to acetone-soluble CA with low amounts of gel in solution [18]. For water-soluble cellulose acetates, a solvolysis of CA with a DS of 2.5–3.0 at high temperatures and pressure, using metallic catalysts, has been reported, where the necessary reaction time is considerable shortened [16].

Some of the research was focused on the nature and composition of the hydrolysis medium, and reported that by changing the polarity of this system, the reaction rate could be increased and the necessary amounts of water and catalyst could be decreased [19–21]. These effects were possible by using unconventional hydrolysis systems containing small proportions of a hydrocarbon, such as toluene [19] or benzene [20], which can change the composition of the solvation shell around the CA chains. Thus, products with a DS of 1.70 could be obtained at 60 °C in a reaction system containing 15–34 wt% toluene, in shorter times than in the conventional procedure which was free of toluene [19].

Since the hydrolysis of CA is an equilibrium process and the three hydroxyl groups in AGU present different reactivities, the water concentration in the reaction bath is one of the factors influencing this equilibrium and also the preference of the substituent groups to certain positions in the glucose unit. Consequently, kinetic studies performed in such hydrolysis systems were also able to predict the substituent distribution, performed as a function of the composition of the reaction system [21]. For cellulose acetates with DS higher than 2.00, an increase of the primary hydroxyl content is observed when a system containing 20 wt% toluene is applied.

Contrary to the conventional hydrolysis system, the process performed in hydrocarbon-containing systems follows a pseudofirst-order kinetic law [19, 20], described by a linear relationship of $-\ln (DS/DS_0)$ *versus* time.

The described procedures led to cellulose acetates with a DS of 1.70, useful for further derivatisation, in shorter times than in the absence of the hydrocarbon, and soluble in common solvents such as DMF, acetic acid and dimethylsulfoxide (DMSO). Furthermore, the chain degradation by acetylation could be significantly reduced in

the presence of toluene, due to the lower proportion of acetic acid in the vicinity of the macromolecules [21].

A new, rapid and efficient method recently described in the literature is the heterogeneous acetylation with acetic anhydride in a solvent-free system or in the presence of reduced amounts of solvent and using iodine as a catalyst [22–24].

The solvent-free technique is also reported for CA synthesis in a ball-milling reactor in the presence of a solid superacid SO_4^{2-}/ZrO_2 catalyst [25]. The ball-milling process is aimed to preactivate the cellulose by increasing the surface area and decreasing the crystallinity of the polymer. The DS of the product could reach a value of 1.8.

Attempts were also made to use the solvent-free procedure for modifying celluloses obtained from different natural sources. Sisal cellulose, for example, was successfully acetylated in a heterogeneous medium, using iodine as the catalyst [26].

Heterogeneous acetylation is often cited as an adequate way to reduce the high polarity of cellulose fibres and to increase their hydrophobic character, which can be a valuable feature in order to perform composites with synthetic polymers [27–30].

Thus, the surface properties of fibres from flax have been modified by heterogeneous acetylation with acetic anhydride and sulfuric acid as the catalyst – without changing their morphology – in order to obtain biodegradable fibres for application as polymer composite reinforcements [27]. Cotton cellulose was also acetylated without solvents [28] in order to obtain hydrophobic materials for application in oil spill clean-ups.

Olaru and co-workers [30] studied heterogeneous acetylation without solvents, using acetic anhydride and in the presence of sulfuric acid as a catalyst, which was applied to bleached and unbleached kraft pulps in order to change their polarity and improve their compatibility with synthetic polymers without changing their fibrous structure. Surface acetylation of the fibres to a low extent was able to modify the ratio of the hydrophilic/hydrophobic properties of the cellulose fibres.

Recently, in response to the increasing interest of modern nanotechnologies toward cellulosic polymers, microfibrillated cellulose produced from kraft pulp was heterogeneously acetylated in order to increase the surface hydrophobic properties and to develop films with good barrier properties to water, suitable for packaging applications [31].

The surface modification of cellulose was also performed in the presence of organic solvents [32, 33]. Thus, acetylation to a low extent was achieved in the presence of organic systems containing acetic acid and toluene in order to decrease the hydrophilic character of the fibres [32]. Three cellulosic materials with different crystalline

structures were investigated and it was found that the change in supramolecular structure, and the degree of modification, were both implied in decreasing the hydrophilic properties of the cellulose fibres. At lower DS values, this property is controlled by the crystallinity, while at higher levels of acetylation it is mainly determined by the extent of this transformation. A decrease of crystallinity was observed for all the studied celluloses; however, the crystalline forms of the starting cellulose were maintained. This fact suggests that the acetylation occurs both in the amorphous areas and on the crystalline surfaces of the cellulosic material.

Preparation of CA with certain DS values and the desired properties has been a constant research topic over time. A new approach to predict the solubility of polymers has been very recently been applied to cellulose acetates with various DS values [34].

Cellulose acetate with a DS of about 2.5 has many well-known applications as membranes and fibres. Recently, it was used to produce porous, spherical cellulose particles, called cellulose beads, which are interesting materials as media for separation processes, specific adsorbents and for the controlled delivery of pharmaceutical ingredients [35]. Cellulose beads are regenerated cellulose with the structure of cellulose II.

Ultrathin films of some cellulose esters, e.g., cellulose acetate, cellulose acetate propionate and cellulose acetate butyrate (CAB), have been prepared from their solutions in acetone [36]. The surface properties of these films were changed from hydrophilic to hydrophobic upon annealing in order to use them as a selective support for biomolecules. The protein immobilisation capacity of ultrathin films of CAB and carboxymethylcellulose acetate butyrate obtained by the same procedure was also investigated [37].

The preparation and characterisation of mono- and multilayers of cellulose acetate Langmuir-Blodgett films [38], as well as monomolecular and multimolecular films of cellulose triesters with various chain lengths intended to be well-ordered films, have also recently been reported [39].

The main domains of cellulose ester applications with the greatest research activity over the last decades have recently been reviewed [40] with the focus on their performances in coatings, controlled release, biodegradable plastics, composites and laminates, and separation media.

Apart from their known traditional and modern application areas, partially substituted cellulose acetates are also the necessary intermediates for the synthesis of some mixed derivatives. Mixed esters such as cellulose acetate propionate, butyrate and phthalate are obtained by esterification of CA with anhydrides or acid chlorides in

the presence of acid or basic catalysts [9]. The phthaloylation of CA, for example, can be performed in different media such as acetone, pyridine, dioxin and acetic acid [41–43]. The solubility of cellulose acetate phthalate in mildly alkaline media depends on the substitution degree of the starting CA, as well as on the synthesis conditions. The acetyl and phthaloyl content as well as the distribution of phthaloyl groups are responsible for the solubility behaviour of this derivative. A comparison of different phthaloylation systems in terms of reaction yield and product properties is also provided [42].

The phosphorylation of cellulose could be performed in both, heterogeneous or homogeneous systems. The heterogeneous reactions, which will be discussed in this section, consist of the attachment of the phosphorous groups to the cellulose chain by reactions with the hydroxyl groups from the original polymer, resulting in cellulose esters as monobasic phosphate Cel-O-P(H)(O)(OH), dibasic phosphate Cel-O-P(O)$(OH)_2$ or phosphite Cel-O-P$(OH)_2$. Cellulose ethers with phosphonic acid groups Cel-P(O)$(OH)_2$ could also be synthesised, but this aspect is not the aim of this chapter, which is focused only on the current research of cellulose esters.

The phosphorylation/phosphatation agents such as, phosphoric acid (H_3PO_4), phosphorous acid (H_3PO_3), phosphorous pentoxide (P_2O_5), phosphorous oxychloride ($POCl_3$) and phosphorous trichloride (PCl_3) are the most frequently used for obtaining cellulose phosphates [44]. These phosphorylated agents lead to inorganic cellulose derivatives having a lower reactivity during esterification, but allow obtaining reaction products with far less degradation of the macromolecular chains.

Monobasic cellulose phosphate was obtained by the reaction of cellulose with phosphorous acid in molten urea [45], through a hydrogen bond complex between H_3PO_3, urea and cellulose, according to **Figure 8.1**.

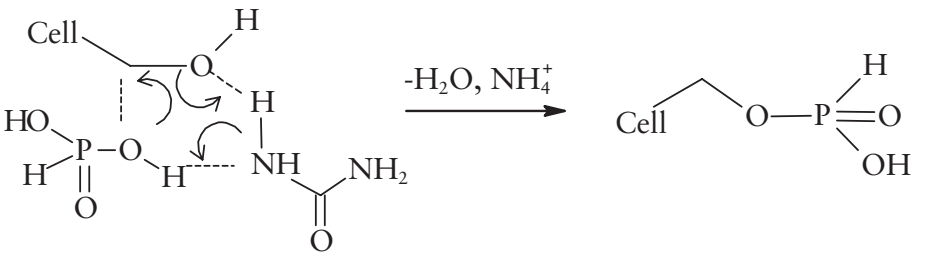

Figure 8.1 The reaction complex in cellulose phosphorylation with H_3PO_3 and urea

The monobasic cellulose phosphate synthesised by this reaction is a white powder, soluble in water with a DS up to 1.5. The intrinsic dissociation constant value, pK_0 was estimated at 2.4, corresponding to the weak acid groups [46]. If the functionalisation leads to polysaccharide derivatives with ionic or ionisable groups they will behave as polyelectrolytes. This derivative could influence the crystallisation/separation of sparingly soluble salts such as calcium carbonate, with an increase of their stability in aqueous dispersions. These monobasic cellulose phosphates could also be used as intermediary products in the synthesis of polyelectrolytes having two different ionisation groups, P–OH and COOH. The reaction is developed in the presence of sodium ethoxide at room temperature by the addition of acrylonitrile to P–H bonds from monobasic cellulose phosphate [47].

The synthesis of dibasic cellulose phosphates was carried out using solutions at a high concentration or water-free orthophosphoric acid as an effective phosphating agent or in different systems (described below), when soluble as well as insoluble derivatives were obtained. *Water-soluble dibasic cellulose phosphate* of a rather high polymerisation degree can be prepared with anhydrous phosphoric acid. The reactivity of the phosphorylation agent can be increased by using a mixture of H_3PO_4 with P_2O_5. In this case, the DS increases with increasing the molar ratio between the phosphorylation agent and the glucosidic unit, and with the reaction time, but these reaction conditions lead to the increase of the degradation of the macromolecular chains. Water-soluble derivatives were also synthesised in ternary systems of H_3PO_4/P_2O_5/DMSO or H_3PO_4/P_2O_5/aliphatic alcohols, when the DS was up to 0.2.

Most synthesis methods of the dibasic cellulose phosphates have led to *water-insoluble* products. The reaction of cellulose with a solution of H_3PO_4/urea or $(NH_4)_2HPO_4$/urea and water at 120 °C leads to derivatives (mono-/diammomium cellulose phosphate salts) with DS values between 0.3 and 0.6, but with a strongly degraded chain [48, 49]. These derivates were used for obtaining matrices or supports for the retention/separation of proteins and enzymes, due to their large hydrophobic area despite their insolubility in common solvents. A high selectivity, over 65.4%, towards protease was reported in the literature [50]. Another application of cellulose phosphates is as ion-exchange materials [51]. The ion-exchange capacity of the cellulose phosphates synthesised by this method, increases with the decrease of hydrated ionic radii, and with the increase in quantity and concentration of metal ions in the following order, for divalent ions: $Ba^{2+} > Sr^{2+} > Ca^{2+} > Mg^{2+}$. Also, these derivatives have shown a high affinity for certain cations, principally Th^{4+}, Ti^{4+}, U^{4+}, Ce^{4+}, Fe^{3+}, ZrO^{2+} and UO_2^{2+} [52]. The same H_3PO_4/urea/water system was used for phosphorylation of cellulose particles. The reaction developed in the presence of a mixture of H_3PO_4 - urea at room temperature and due to the crosslinking reaction, a mixture of insoluble products: noncrosslinked monosubstituted, crosslinked di- or trisubstituted cellulose esters, were formed in the system [53, 54].

These derivatives exhibit interesting properties due to their flame resistance and ion-exchange capacity. They could be potential candidates for the development of anhydrous electrorheological (ER) materials with high performance in dry-base systems [55, 56]. In this respect, phosphate cellulose particles were synthesised from cellulose particles and a H_3PO_4 - urea mixture, and then dispersed in silicone oil to prepare the cellulose-based ER fluid. The results showed not only that the ER properties are enhanced by increasing the particle concentration and electric field strength, but also that cellulose-based ER fluids exhibit viscoelastic behaviour under an applied electric field due to the chain formation induced by the electric polarisation between the particles. The ER properties of the phosphate cellulose/silicone oil suspension were investigated by rheological measurements under both controlled shear rate and shear stress modes. This ER fluid exhibited typical viscoelastic properties under an imposed electric field due to chain formation, and the elasticity increased with the increase in both electric field strength and particle concentration.

The H_3PO_4/urea/DMF system was used for the preparation of cellulose phosphate from various sources such as bacterial cellulose, microcrystalline cellulose, and cotton and cellulose fibres [57–60]. **Figure 8.2** shows the reaction of cellulose with H_3PO_4 in the urea and DMF medium.

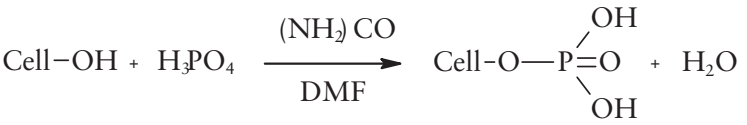

Figure 8.2 The reaction of phosphorylated cellulose with H_3PO_4

Bacterial cellulose phosphate (BCP) was used as an adsorbent material for the retention of metallic ions. The DS of bacterial cellulose is higher than that of plant cellulose under the same conditions. The drying method is also an important factor for this substitution and for maintaining the microfibrous structure. Thus, it was shown that the freeze-drying method is more efficient than the oven drying or alcohol substitution method. This derivative exhibits adsorption behaviour for various transition metal ions and lanthanide ions. The lanthanide ions (La^{3+}, Sm^{3+} and Ho^{3+}) are adsorbed onto BCP under acidic conditions. The pH dependence of adsorption suggests that the mechanism of the process is one of cation exchange. The order of selectivity for studied lanthanide ions was as follows: $Ho^{3+} > Sm^{3+} > La^{3+}$. This selectivity originates from the characteristics of the phosphoric acid groups. Generally, the adsorbents with

phosphoric acid groups exhibit selectivity for heavy rare earth metals in comparison with light rare earth metals. BCP exhibits a high adsorption ability for the 'hard acid' lanthanide ions, on the basis of the high affinity of the 'hard base' phosphoric acid group (the Hard Soft Acid Base principle). Divalent transition metal cations, such as Cu^{2+}, Mn^{2+}, Zn^{2+} and Co^{2+} show similar adsorption behaviour in the presence of BCP; the adsorption percentage increases with the increase of the pH value of the aqueous solution and reaches over 90% at pH values higher than 4.5. The selectivity for adsorbed metals on BCP, at around pH 3, was as follows: $Fe^{3+} > Cu^{2+} > Mn^{2+} > Zn^{2+}$; Co^{2+} [57].

The H_3PO_4/urea/DMF system was also used in order to obtain biomaterials for protein adsorption of cytochrome C [58], bovine serum albumin and lysozyme [59], or for calcium hydroxyapatite growth [60]. The DS was controlled by changing the amount of urea and phosphoric acid in the reaction mixture. All experiments of protein adsorption on various phosphorylated celluloses showed an adsorption *via* electrostatic interaction at a pH lower than their isoelectric points. These cellulosic substrates could be used as implantable biomaterials for faster healing, involving the use of a slow release gel loaded with different active principles, or protein (bone morphogenetic protein) in the vicinity of an implant. The phosphorylated cotton fibres, soaked with a saturated $Ca(OH)_2$ solution at ambient temperature, were used to form thin coatings consisting of deficient calcium apatite by partial hydrolysis of the phosphate groups. The adsorptive properties of the hydroxyapatite from the apatite-cellulose composite may allow drug attachment, which could be useful as a virus filter for medical treatments [60].

The phosphorylation of cellulose was also aimed to improve the strength characteristics of the product and increase its stability in solutions. For this reason, low-substituted cellulose phosphate fibres were obtained by reaction with aqueous solutions of H_3PO_4 - carbamide with concentrations of 0.5–3.33 M and used to study metallic ion retention (Al^{3+} and Cr^{3+}) from their sulfuric acid salt solutions [61].

Another method for the synthesis of cellulose phosphate using the $H_3PO_4/P_2O_5/Et_3PO_4$/hexanol system was reported in the literature for obtaining hydrogels with medical applications [62, 63]. The cellulose powder, after a preliminary drying in vacuum on P_2O_5, and swelling for 24h in hexanol was reacted with a mixture of P_2O_5 in triethyl phosphate and orthophosphoric acid for 72 h at 37 °C [64]. The proposed method proved to be adequate for obtaining products with DS values up to 1.3. The cellulose phosphate was used as an implantable biomaterial able to promote bone regeneration by the formation of calcium phosphates. It was envisaged to take advantage not only of its good matching with the mechanical properties of bone, but also of its hygroexpansivity, therefore allowing a satisfactory fixation to hard tissue [65]. Also, the *in vitro* tests using human bone marrow stromal cells (HBMSC)

were performed on phosphorylated cellulose (cytotoxicity, cell attachment kinetics, proliferation rates and immunohistochemistry) [66]. For this study, the negatively charged cellulose phosphates were neutralised in the form of the calcium salt before contact with the cells. The cytotoxicity tests revealed that all cellulose phosphate derivatives (regardless of DS) were cytocompatible, but due to their negatively charged, highly hydrophilic surfaces they showed poor HBMSC attachment and proliferation, as well as poor alkaline phosphatase-specific activity and expression of osteocalcin and type I collagen. The cellulose from the oil palm biomass was phosphorylated using the $H_3PO_4/P_2O_5/Et_3PO_4$/hexanol system and used as a potential biomaterial. This new type of phosphate cellulose was also found to be noncytotoxic in the culture of human osteoblasts as well as fibroblast cultures, having the ability to induce the formation of an apatite layer under simulated physiological conditions [66].

Phosphorous oxychloride is known as an effective phosphorylation agent for cellulose, from numerous studies, starting from a cellulose suspension in DMF or pyridine. Only partially soluble products are usually obtained by this system, and the reaction is accompanied by an intermediary product of chlorination. The possible reaction of the chlorinated compound formation obtained in the systems containing $POCl_3$ is shown in **Figure 8.3**.

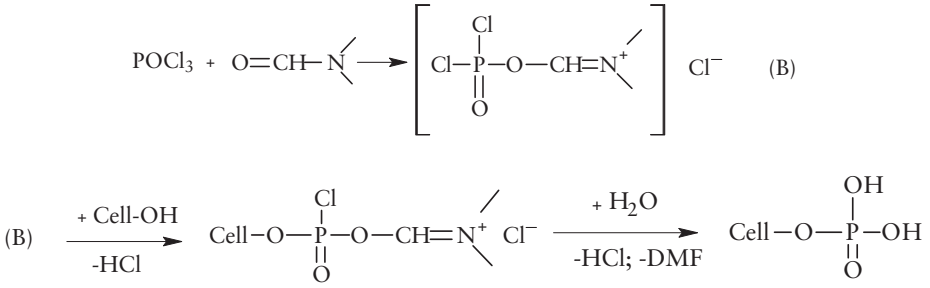

Figure 8.3 Reaction of cellulose with $POCl_3$ in DMF

The phosphorylation reactions with $POCl_3$ in pyridine take place either in the presence or in the absence of a preliminary treatment with sodium hydroxide. After suspending the raw materials in anhydrous pyridine, an amount of phosphorus oxychloride and methylene chloride was added dropwise, and the contents were heated under reflux for 2 h at 115 °C [67–69]. The obtained reaction products are always insoluble in water and they proved to be efficient cation-exchange systems. Other phosphorylated

systems, such as polyol phosphonyl chlorides or phosphochloridates, in the presence of a suitable solvent (DMF) and base (pyridine/NaOH), lead to products with a phosphorus content up to 2.5% (w/w). This is equivalent to phosphorylation yields of up to 22.7%. The phosphorylation efficiency is dependent upon the reaction temperature and the mass ratios between the phosphorylating agent and cellulose. The highest yields occur when reactions are carried out at a mass ratio of 4:1, at 160 °C for 2 h [70].

The phosphorous pentoxide/DMF system was used to introduce the phosphoric groups onto the surface of the cellulose membranes by the reaction between the hydroxyl groups of cellulose and P_2O_5, in order to observe the effect of phosphate groups on cellular behaviour (**Figure 8.4**). These membranes showed a higher adsorption of serum proteins and the growth rate of the Chinese hamster ovary (CHO) cells on the phosphorylated membrane was faster than that on the cellulose membrane. The attachment of CHO cells and their spread was also enhanced by introducing phosphate groups onto the membrane surface [71].

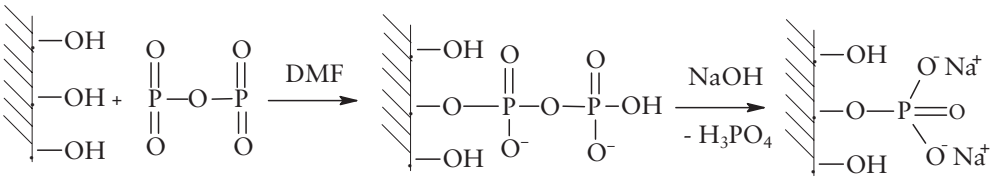

Figure 8.4 The possible mechanism of the phosphorylation of the cellulose membrane

The phosphorylated celluloses were also synthesised using nonconventional methods (called the *green chemistry of polymers*) such as microwave-assisted or enzymatic phosphorylation. The phosphorylation reaction using microwave irradiation was performed at different temperatures with a maximal power output of 12 W. This environmentally friendly process led to monosubstituted phosphorous acid esters of cellulose with various DS of the hydroxyl groups (0.2–2.8), but without a pretreatment stage (swelling in an appropriate solvent) [72]. The enzymatic phosphorylation of cotton cellulose was performed with hexokinase enzymes. These enzymes catalyse the phosphoryl transfer from adenosine-5′-triphosphate to the primary hydroxyl groups of a number of furanose and pyranose compounds [73]. The reaction was carried out at 30 °C for 6 h, with 40 U/mL hexokinase. The ability of the enzyme to initiate

the transfer of phosphate groups suggested the application of this hexokinase to the functional modification of the C6-hydroxyl groups in cellulose. The DS was determined to be about 0.03% of the glucopyranose units (**Figure 8.5**). Phosphorylation occurs on the primary alcohol groups of cellulose, which are most available for the reaction. The secondary 3-OH group forms extra hydrogen bonds with the ring oxygen atom and the chain is additionally coiled protecting the 2-OH groups.

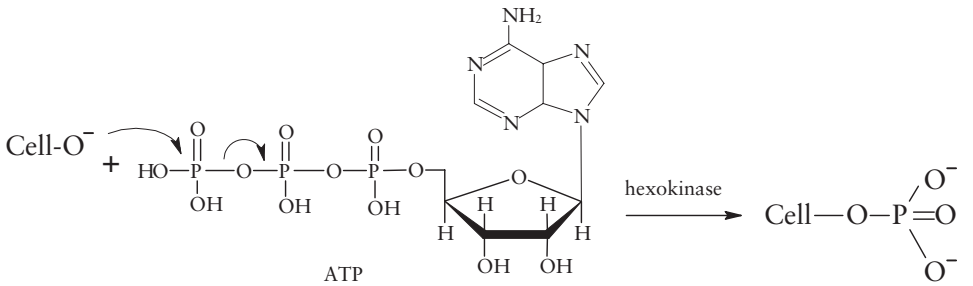

Figure 8.5 Mechanism of hexokinase-catalysed cellulose phosphorylation

This chemical modification of cotton cellulose, by introducing new functional groups (phosphoric groups) could be a way to provide a textile material with improved dye fixation, crease resistance, flame retardance and other properties.

8.3 Cellulose Esters: Homogeneous Processes

8.3.1 Dissolution of Cellulose

One of the most unique and simple structures in the field of polysaccharides, the structure of cellulose, is responsible for the properties of the polymer and has a remarkable and complex influence on the course of its chemical reactions [74].

An important feature of cellulosic materials is their two-phase morphology of crystalline (ordered) and amorphous (disordered) regions, which influence the accessibility and the reactivity of fibres [74]. The presence of these regions is a result of the intramolecular and intermolecular hydrogen-bonding patterns, which are considered the most influential factors related to the conformational and mechanical

properties of cellulose materials. The intramolecular hydrogen bonds are responsible for the shift and rigid nature as well as the 'twofold screw axis' of the cellulose molecule, while the intermolecular hydrogen bonding in cellulose is responsible for the sheet-like nature of native cellulose [75]. A further consequence of hydrogen bonds is the insolubility of cellulose in water, as well as in common organic liquids.

An ideal solvent for cellulose has the following requirements:

- To be safe, inexpensive and easily recycled;
- The dissolution occurs without derivatisation;
- The process takes place without degradation of the cellulosic substrate; and
- The eventual by-products obtained during or after the process are not toxic.

The basic requirement for cellulose dissolution is that the solvent is capable of interacting with the hydroxyl groups of the AGU so as to eliminate, at least partially, the strong intermolecular hydrogen bonding between the polymer chains [76].

In order to systematise cellulose solvents, several proposals have been made, but generally, they are classified into two basic categories (**Figure 8.6**) [76, 77]:

- Nonderivatising solvents – systems dissolving the polymer by intermolecular interactions only; and
- Derivatising solvents – systems where dissolution is achieved *via* a chemical reaction, leading to covalent bond formation, obtaining 'unstable' ether, ester or acetal derivatives.

Both categories of solvents could be divided into aqueous and nonaqueous media.

Before presenting new findings in the field of homogeneous esterification of cellulose, and in particular our results, cellulose solvents will be reviewed pointing out only the more important groups.

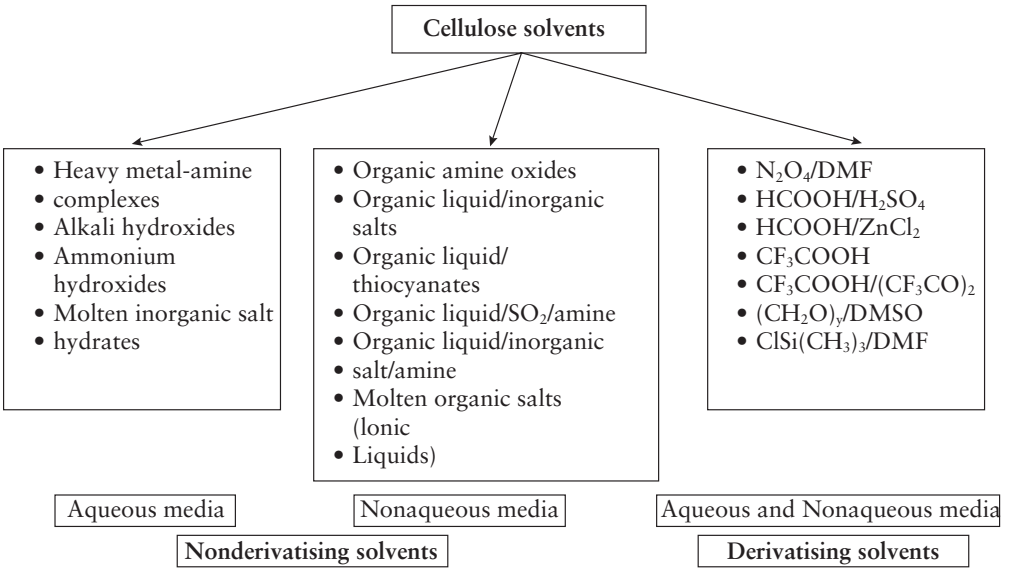

Figure 8.6 Systematisation of the main groups of cellulose solvents

8.3.1.1 Nonderivatising Solvents

8.3.1.1.1 Aqueous Nonderivatising Solvents

Within the group of heavy metal-amine complex solutions there are four important complex systems able to completely dissolve cellulose: the cadmium complex with ethylenediamine, the ferric tartaric acid complex in alkaline aqueous solution, and the most known within cellulose systems, cuprammonium hydroxide (Cuam) and the cupriethylenediamine hydroxide (Cuen). The mechanism of cellulose dissolution consists of the deprotonating and coordinative binding of the hydroxyl groups in the C2 and C3 position of the AGU, displacing either one molecule of diethylendiamine in the Cuen system or two ammonia molecules in the Cuam system [78]. These solvents are utilised for the determination of the molecular mass of cellulose by viscometry. In addition, the Cuam complex had been employed as a medium for the homogeneous derivatisation of cellulose, the further regeneration of cellulose leading to one of the most important commercial products, cuprammonium rayon or to high-quality membranes for haemodialysis [79].

Besides these complex systems there are other alternatives such as the aqueous solutions of the ethylenediamine complex of zinc, cobalt and nickel. It was proved that the efficiency of these solvents was lower than that obtained in the presence of copper and a higher concentration of metal was necessary for a complete dissolution of cellulose [80].

The use of new coordinating solvents appears to be the key to manipulating single strands of underivatised cellulose and could be the tool for the synthesis of supramolecular assemblies with pure cellulose [81]. Some examples in this direction are the (dihydroxo-*tris*(2-aminethyl)amine-nickel(II)-complex) (Nitren) complex which also proved to be an efficient solvent for polysaccharides, like amylose or chitosan, an aqueous solution of the ethylenediamine palladium complex, the zinc/*bis*-(2-aminoethyl)amine complex and the cadmium-*tris*(2-aminoethyl)amine complex (Cdtren). A detailed comparative light-scattering study was published detailing cellulose in Cuoxam, Nitren and Cdtren. All three solvents exhibited good solution properties, but only Cdtren was capable of dissolving even cellulose with the highest degree of polymerisation (DP) namely, cotton linters and bacterial cellulose [82].

In recent years, a new class of aqueous alkali-containing solvents was developed, where the NaOH and NaOH/urea solution system has been found to completely dissolve cellulose of low molecular weight [83, 84]. The dissolution of cellulose in the presence of aqueous NaOH solutions depends on the molecular weight and the degree of crystallinity [85]. Cellulose dissolution in the NaOH/urea solution has the lowest environmental impact, and is faster and has a lower cost than the first method.

More extensive work has been carried out on the LiOH/urea [86, 87] and NaOH/thiourea [88] systems, aiming to regenerate the cellulose by fibre spinning and film casting [81, 89–91]. Jin and co-workers [92] demonstrated that cellulose could be dissolved directly and quickly in a NaOH/urea/thiourea aqueous solvent. This new solvent, with a more powerful ability to dissolve cellulose, could be used to prepare a more stable spinning solution with a higher concentration of cellulose, compared with the NaOH/urea or NaOH/thiourea aqueous solvent systems [93].

Other aqueous nonderivatising solvents are molten inorganic salt hydrates which contain several compounds, such as $LiX{\cdot}nH_2O$ ($X^- = I^-$, NO_3^-, CH_3COO^-, ClO_4^-), $LiSCN{\cdot}2H_2O$, $Ca(SCN)_2{\cdot}3H_2O$ $ZnCl_2{\cdot}4H_2O$, $Zn(NO_3)_2{\cdot}XH_2O$, $FeCl_3{\cdot}6H_2O$, the eutectic mixtures, such as $LiClO_4{\cdot}3H_2O/MgCl_2{\cdot}6H_2O$, $LiClO_4{\cdot}3H_2O/Mg(ClO_4)_2{\cdot}H_2O$ and a mixture between the eutectic melt of NaSCN/KSCN with $LiSCN{\cdot}2H_2O$ [94–96]. These solvents could dissolve celluloses even with a very high DP, although they contain water of hydration and will compete with cellulose for the derivatising agent [76].

8.3.1.1.2 Nonaqueous Nonderivatising Solvents

One of the most important solvents from the group of organic amine oxides is *N*-methylmorpholine-*N*-oxide (NMMO), which is probably the most applied solvent within the industry.

The NMMO system is used for a large number of tailored cellulose modifications leading to highly porous, ultra lightweight materials [96], filled cellulose fibres [98,99], flat cellulose films prepared on precoated substrates [100], cellulose sponge [101] and electrospun cellulose nanofibres [102]. Related to textile fibres, after overcoming problems such as investment costs and recovery of the expensive solvent, the procedure which involves the NMMO solvent is applied on a large scale, under different brand names, such as lyocell (Lenzing), Tencel (Courtaulds), Alceru (TITK Rudolstadt) and Newcell (Akzo Nobel) [81].

Regarding the organic liquid/inorganic salts group, the most versatile and interesting system is *N*,*N*-dimethylacetamide (DMA)/LiCl, an inert and thermally stable solvent system, and an important tool for a homogeneous conversion of cellulose. Advantages claimed for this system in the homogeneous reactions of cellulose are: a full availability of hydroxyl groups, permitting the control of the DS *via* the reagent to AGU molar ratio, a minimal chain degradation at a temperature below 100 °C, a high versatility with regards to the type of reaction intended and a favourable reagent yield due to the rather small consumption by side reactions [103]. Its analytical usefulness (^{13}C-NMR spectroscopy, electrospray mass spectroscopy, size exclusion chromatography and light-scattering techniques) is due to the fact that the solvent is colourless and dissolution succeeds without, or at least with negligible, degradation even in case of high molecular weight polysaccharides, e.g., cotton linters or bacterial cellulose [77].

Due to the incomplete recycling of the expensive DMA/LiCl, this is still not applied on a large scale, but is widely exploited for fundamental research and for the preparation of high value products, representing the most valuable solvent today.

A novel and powerful solvent for cellulose consists of the DMSO/tetrabutylammonium fluoride trihydrate (TBAF) mixture, which can even dissolve cellulose with a DP of 650 within 15 min, without any pretreatment [104]. Cellulose esters of aliphatic, aromatic, bulky and functionalised carboxylic acids are available through the activation of free acids *in situ* with tosyl chloride, *N*,*N*″-carbonyldiimidazole and iminium chloride under homogeneous acylation with DMA/LiCl and DMSO/TBAF [1].

Among the three-component systems of nonaqueous, nonderivatising cellulose solvents, the organic liquid/SO_2/amine combination is one of the most important groups, while the DMSO/SO_2/diethylamine (DEA) mixture is the most versatile

solvent. Isogai and co-workers [105] proved that this solvent is nonderivatising by investigation of the interaction between the cellulose and the solvent system, and arguing that it is a donor-acceptor interaction.

While using the homogeneous preparation of cellulose ethers to synthesis a wide variety of completely functionalised cellulose ethers bearing alkyl- and aryl substituents, the acylation reactions succeed to a limited extent [106, 107]. Also, the regeneration of cellulose from the DMSO/SO_2/DEA system solution is one of the important methods of obtaining amorphous cellulose which is stable even in aqueous media [108–110].

Recently, a new class of solvents was discovered capable of dissolving cellulose over a wide range of DP values, named molten organic salts (ionic liquids (IL)), which contain only ionised species and have a melting point below 100 °C [81, 111, 112]. The IL group are nonaqueous, nonderivatising solvents, as confirmed by ^{13}C-NMR studies demonstrating no covalent bond formation during the dissolution process [113]. The interest of IL as 'green' solvents resides in their attractive properties, such as extremely low vapour pressure, chemical and thermal stability, and nonflammability, which offers advantages such as ease of containment, product recovery and recycling ability [114]. Some of the ionic liquids are liquids even at room temperature (RTIL) and are capable of dissolving numerous polar and nonpolar compounds, offering promise as solvents for the dissolution of carbohydrates [115].

In most cases, ionic liquids are organic salts with one or more cations which are typically ammonium, imidazolium or pyridinium ions [78]. Among the RTIL, 1-*N*-butyl-3-methylimidazolium chloride (BMIMCl) exhibited the best dissolving capability, while 1-*N*-allyl-3-methylimidazolium chloride (AMIMCl) was also found to be a powerful solvent for cellulose [116]. Among BMIMCl, 3-methyl-*N*-butylpyridinium chloride and benzyldimethyl (tetradecyl) ammonium chloride, BMIMCl was demonstrated to be the most appropriate cellulose solvent, because of its strong ability to dissolve cellulose with a DP from 290–1,200 up to very high, and also its capability to barely degrade cellulose after dissolution [117]. Cellulose is also soluble in 1-*N*-butyl-3-methylimidazolium bromide and 1-*N*-butyl-3-methylimidazolium sulfocyanate, but with less than half the solubility of BMIMCl. Regarding AMIMCl, a solution containing up to 14.5 wt% cellulose with a DP of 650 was prepared in only 30 min at 80 °C [118]. Moreover, a series of 1,3-dialkylimidazolium formate compounds, demonstrating superior solubility values, has been found and among these, 1-allyl-3-methylimidazolium formate dissolved cellulose at lower temperatures and reached larger concentrations in comparison with AMIMCl [119]. In the last few years, more cellulose-dissolving IL have been reported based on dialkylimidazolium cations, pyridinium- and quaternary ammonium salts, while the most frequently reported anions are chloride and acetate, but also carboxylates, alkyl phosphate and alkyl phosphonates [120].

IL have been exploited for shaping cellulose into fibres, films, sponges, beads and other cellulosic objects [121–123]. In addition, they are intensively studied for 'biorefinery applications', which include fractionation of lignocellulosic biomass, IL-pretreatment of cellulose for improving enzymatic hydrolysis with the conversion of cellulose dissolved in IL into mono/disaccharides, platform chemicals and biofuels [124–126]. One of the most promising applications of cellulose dissolving IL is their use as a reaction media for the homogeneous preparation of highly engineered polysaccharide derivatives [120]. Moreover, IL might overcome the limitation of other cellulose solvents, used so far for homogeneous derivatisation, regarding recyclability and cost efficiency. They are also intensively studied for the production of commercial bulk derivatives, such as cellulose esters, e.g., acetates, propionates, butyrates and mixed esters [120, 127–129]. At the same time, the RTIL solvents offer a unique opportunity to study the structure and properties of carbohydrates, using a variety of modern spectroscopic and analytical methods. These are solvents in which carbohydrates can be chemically and enzymatically converted into useful new chemicals and materials with many potential applications including textiles, building materials and paper [115].

8.3.1.2 Derivatising Solvents

Derivatising solvent systems involve solvents which react with cellulose leading to a disruption of the hydrogen bonding, by a combination of steric interactions, and a decrease in the number of available hydroxyl groups [76]. The covalent bond formed should be easily cleavable by hydrolysis or a change of pH. The major disadvantage of the dissolution with derivatising solvents is the lack of reproducibility due to the side reactions and formation of undefined structures [130].

Even so, few of these solvents work very efficiently. For example, cellulose has been dissolved in DMSO/paraformaldehyde and esterified by acetic, butyric and phthalic anhydride, as well as by unsaturated methacrylic and maleic anhydride, in the presence of pyridine, or an acetate catalyst [76]. DS values from 0.2 to 2.0 were obtained, being higher for cellulose acetate at 2.5. Other representative examples of derivatising solvents are N_2O_4/DMF, $HCOOH/H_2SO_4$, F_3CCOOH and $Cl_2CHCOOH$, $ClSi(CH_3)_3$; a comprehensive description is discussed elsewhere [76, 77].

Of importance is the fact that the obtained intermediaries during the dissolution of cellulose could be isolated prior to the conversion into final derivatives. On the one hand, there is an increasing reproducibility due to the fact that structural analysis of the intermediates is possible. On the other, these intermediates can be dissolved in a wide variety of common organic solvents, which drastically decreases the tendency

towards side reactions (especially degradation). Therefore, reactive intermediates can be the starting material for a variety of highly engineered derivatives [77].

8.3.2 Homogeneous Esterification of Cellulose

The regioselective introduction of two or three different substituents, as well as the search for new protecting or activating substituents, are topics considered to be at the centre of interest in the near future [131]. A controlled functionalisation of different positions within the AGU can be performed by the homogeneous esterification of cellulose, which is still one of the most versatile reactions in order to obtain new functional polymers. During the derivatisation process under homogeneous conditions, the DS can be controlled by adjusting the molar ratio of the derivatising agent to cellulose and the substituent groups can be introduced regularly, along the natural polymer backbone. The physico-chemical properties of these products are much better controlled than those prepared under heterogeneous conditions.

Besides aqueous, nonderivatising solvents, a relatively new group was used for the *acetylation of cellulose*, the molten inorganic salt hydrates. Several molten systems have been applied as media for the acetylation of cellulose however, only the melt in which the acetylation was successful, the eutectic mixture of NaSCN and KSCN with the addition of 10% $LiSCN{\cdot}2H_2O$, was mentioned [96]. The most important condition in order to perform the reaction is the minimisation of the water content from the melt. The acetylation was carried out at a temperature of 130 °C, using different acetylation reagents such as, acetic anhydride, vinyl acetate, ethylene glycol diacetate and vinyl laurate [132]. Acetylation of cellulose with a high excess of acetic anhydride leads to a DS in the range of 1 and 2.5, which depends on the molar ratio between the AGU and acetic anhydride, as well as the reaction time. Acetylation experiments involving the mixture of $NaSCN/KSCN/LiSCN{\cdot}2H_2O$ with vinyl acetate, ethylene glycol diacetate and vinyl laurate did not yield cellulose esters during a reaction time of 10 h [132].

The solvent $DMSO/TBAF{\cdot}3H_2O$ is highly efficient as a reaction medium for the homogeneous esterification of polysaccharides by transesterification or by the *in situ* activation of complex carboxylic acids [81]. Transesterification with vinyl acetate is more effective than acetylation with acetic anhydride, which is due to the formation of acetaldehyde during this conversion, shifting the equilibrium towards the product side. On the other hand, the lower DS in the case of the application of acetic anhydride is caused by the comparatively fast hydrolysis of the reagent due to the water content of the DMSO/TBAF solvent. Experiments investigating the dewatering of the solvent were also carried out [77, 133, 134]. The conversion of cellulose in DMSO/TBAF with more complex carboxylic acids (e.g., furoyl carboxylic acid) *via in situ* activation with

N,*N*-carbonyldiimidazole was demonstrated [135]. It was also successfully applied as a reaction medium for the synthesis of allyl cellulose by conversion of the polymer with allyl chloride in the presence of solid NaOH [136]. In addition, the solvent is a useful medium for the esterification of crude lignocellulosic materials, for example, Sisal cellulose which contains about 14% hemicelluloses [81, 133].

The binary system DMA/LiCl has proven to be the most suitable nonaqueous, nonderivatising solvent for the preparation of a wide variety of cellulose derivatives and has been extensively studied over the last decades [137]. Moreover, acylation in the homogeneous phase has the advantage of excellent control of the DS and a uniform distribution of the functional groups along the polymer chain [138].

The first experiments regarding the homogeneous esterification of cellulose in DMA/LiCl were carried out using carboxylic acid anhydrides and chlorides [139, 140]. Regarding the utilisation of acid anhydrides as esterification agents, an order of reactivity of acetyl anhydride > phthalic anhydride > maleic anhydride > succinic anhydride was observed [141]. The preparation of acetates, propionates, butyrates and mixed acetates/propionates with a stoichiometric control of the acetyl content can be obtained by reacting with acid anhydride. The negligible effect on the DP and the stoichiometric conversion make this synthesis path a very reliable and reproducible process [138, 142].

A broad variety of halogenated, alicyclic, aromatic and unsaturated esters can be synthesised *via* the reaction with acyl chlorides in a homogeneous phase including adamantoyl- [143], 2-furoyl- [144] and 4-phenyl-benzoyl cellulose [81, 145].

The *esterification of cellulose with bulky ester moieties*, as adamantoyl functions, has received considerable attention due to its tailored properties. The unusual structure of adamantane leads to many chemical and physical properties, such as high thermal and oxidative stability, extreme lipophilicity, low surface energy, high density and hydrophobicity [146]. Furthermore, various adamantane derivatives posses antimicrobial, antibacterial and antiviral activity, and are utilised to combat neurological disorders, e.g., Parkinson's and Alzheimer's diseases, cancer therapy and as antiHIV inhibitors [131].

The synthesis of adamantoyl cellulose proceeded by reacting cellulose with adamantoyl chloride, adamantane carboxylic acid with TosCl, 1,1′-carbonyldiimidazole activation in DMA/LiCl solution [143] or by the reaction of adamantane carboxylic acid in the presence of carbonyldiimidazole in DMSO/TBAF [147]. Cellulose derivatives were obtained with a DS up to 2.1, depending on the reaction stoichiometry and conditions.

Ciolacu and co-workers [131] have synthesised adamantoyl cellulose esters using a two-step process. First, trimethylsilylcellulose (TMSC) was synthesised by a homogeneous reaction of cellulose with chlorotrimethylsilane and hexamethyldisilazane, in the presence of DMA/LiCl (**Figure 8.7a**), and then the adamantoyl esters of cellulose were obtained by reacting the TMSC with adamantoyl chloride (AdCl) (**Figure 8.7b**).

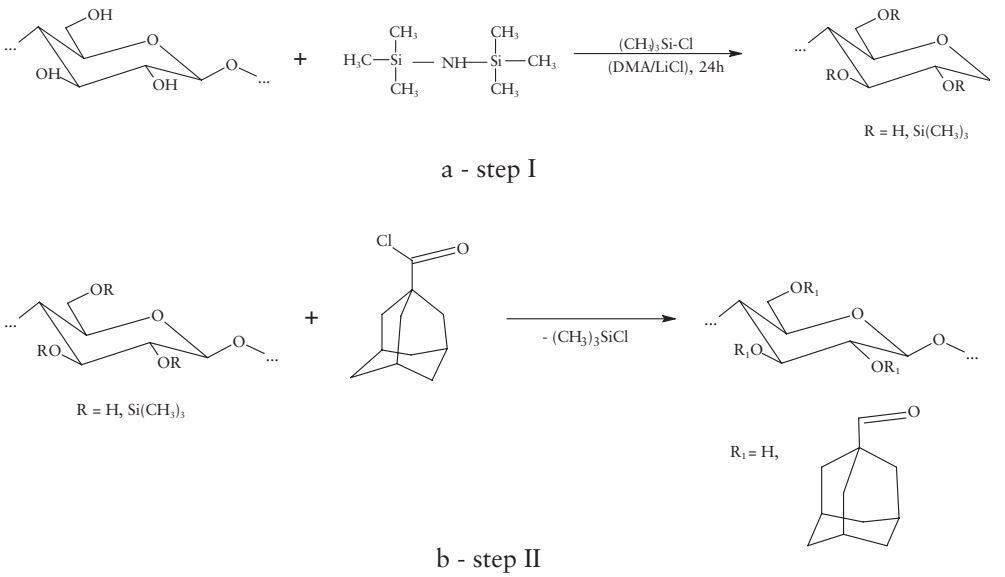

Figure 8.7 Synthesis of (a) trimethylsilylcellulose and (b) adamantoyl cellulose esters. Reproduced with permission from D. Ciolacu, V.I. Popa and H. Ritter, *Journal of Applied Polymer Science*, 2006, **100**, 105. ©2006 Wiley Periodicals, Inc. [131]

The intermediary step was chosen because of its well-known regio- and stereoselective character, and the simple removal of the silicon-containing structural units from the original organic compounds. Consequently, the distribution of the functional groups may be controlled by the previous distribution of the trimethylsilyl ether groups. This fact led to a higher DS of the cellulose ester obtained through the two-step procedure than that obtained by the methods mentioned in the literature [143, 148]. Thus, at a TMSC/AdCl molar ratio of 1:4 and a reaction temperature of 130 °C, a sample with a DS of 2.41 was obtained.

Moreover, the cellulose esters containing bulky acyl groups including pivalate, adamantate and 2,4,6-trimethylbenzoate were investigated in order to compare the effects on the DS and selectivity of these reagents, and were used in three different cellulose solvent systems, such as DMA/LiCl, DMSO/TBAF and the ionic liquid, AMIMCl [148]. It is worth mentioning that the obtained cellulose adamantoyl esters in AMIMCl exhibited a relatively low DS value of 0.89.

Very recently, it has been demonstrated that RTIL can be an efficient media for cellulose acetylation [116, 149, 150]. Some ionic liquids such as AMIMCl and BMIMCl can be used as solvents for acetylation. When using AMIMCl, for example, cellulose acetates with DS values between 0.4–3.0 and good solubilities in some organic solvents have been obtained in one step, in mild conditions and without any catalyst [149]. The same acetylation system could provide an acetone-soluble CA with predominant substitution of the acetyl groups at the C6 position within AGU [150].

Surprisingly, pure CA samples have been reported to be obtained by the homogeneous conversion of cellulose in 1-ethyl-3-methylimidazolium acetate with 2-furoyl chloride, *p*-toluenesulfonyl chloride and triphenylmethyl chloride [151]. The DS values of CA were in the range of 0.55 to 1.86.

Based on the homogeneous acetylation of cellulose using IL, a 'one-pot' process for the production of CA fibres, with controlled DS values and properties, has been investigated [152]. In this process, after the acetylation of cellulose dissolved in BMIMCl, a direct shaping of the obtained CA into fibres was performed. The results are discussed in terms of rheological behaviour of the polymer solutions, which are dependent on the molar ratios of acetic anhydride to AGU.

The regioselectivity of acetylation processes performed in ionic liquids has been demonstrated. The distribution of acetyl groups within the AGU is dependent on the reaction medium and the conditions employed. Thus, differences in solubility may occur for CA with the same DS value, obtained in different ionic liquids, as a consequence of different distributions of substituent groups [116].

Regarding the *homogeneous phosphorylation of cellulose,* one of the most well-known agents is $POCl_3$. In this particular case, cellulose is dissolved in the N_2O_4/DMF system [153]; the reaction leads to products with a DS up to about 1, but only the derivatives with a DS between 0.3–0.6 were found to be soluble in water.

Furthermore, trivalent phosphorus can be introduced into the cellulose chain by reaction with PCl_3 or by transesterification with dimethylphosphite [154]. In the first step, the reaction leads to an intermediate compound and then cellulose phosphite is formed in the systems presented in **Figure 8.8**.

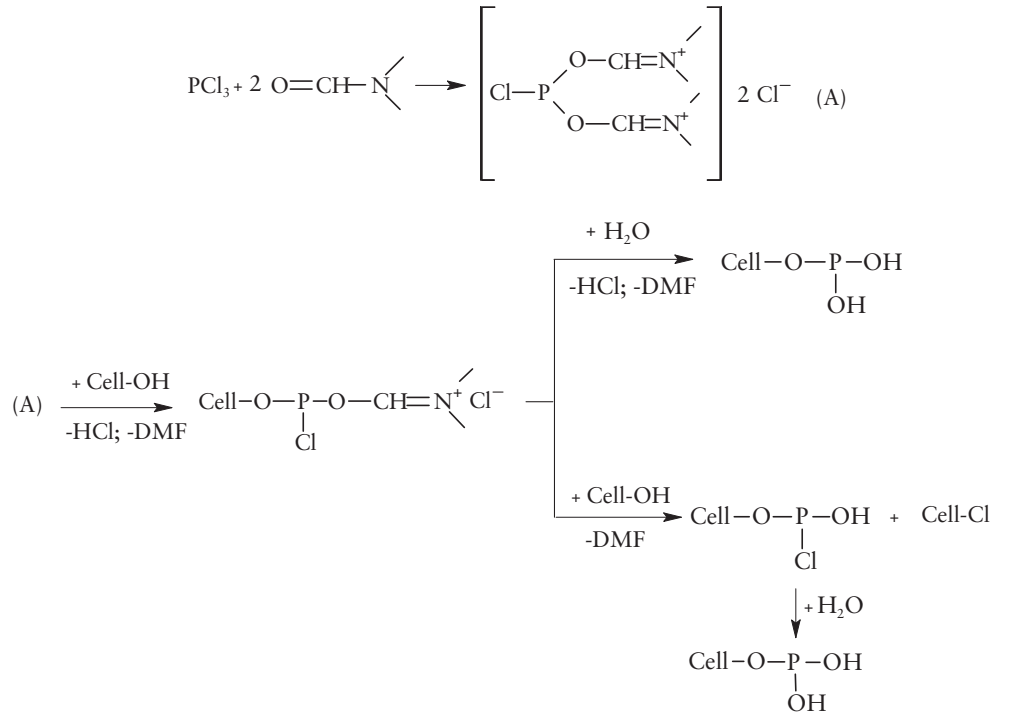

Figure 8.8 Reaction of cellulose with PCl_3 in DMF

The synthesis of cellulose phosphites has also been reported by employing mixed anhydrides of hydrophosphorus and acetic acid.

Other cellulose derivatives with phosphorus groups were obtained by phosphorylation reactions of partially substituted cellulose derivatives such as carboxyalkyl cellulose, acetate, nitrate and so on. Stable ether groups like the carboxymethyl and the acetyl group of cellulose acetates act as efficient protecting groups in the nonaqueous systems involved, and only free hydroxyl groups are converted to phosphate groups. Carboxymethylcellulose (CMC) with a DS of 0.8 was converted to a derivative with a DS in phosphorous of 0.3 using the H_3PO_4/urea system, with the phosphate groups again preferentially located at C6 [155]. CMC containing one phosphate group for each disaccharide unit (CMCP) was also prepared using a 1% solution of CMC in alkaline conditions (pH 12, 2M NaOH) and trisodium trimetaphosphate as the phosphating agent, in amounts sufficient to activate two hydroxyl groups per disaccharide unit, in order to functionalise titanium oxide (TiO_2) surfaces to increase the osseointegration of the host bone tissue. The reaction mixture was stirred for 2 h, the solution was then dialysed against water for 48 h and lyophilised. The TiO_2

surface discs were ultrasonicated in order to remove macroscopic contamination, dipped into a H_2SO_4/H_2O_2 mixture and then rinsed with plenty of double-distilled water. The discs were finally dried and immediately dipped into a CMCP-5 mM sodium salt aqueous solution. The surfaces were maintained for 48 h at room temperature to allow the polymer to bind to the surface, rinsed with double-distilled water and then dried with a filtered nitrogen flow. The functionalised surfaces were completely covered by a homogeneous layer of CMCP, which is bound to the titanium oxide through the phosphate groups of the polymer. The coating was demonstrated to be stable under physiological conditions at least for 7 days. Thanks to the presence of the phosphate groups, which induce osseointegration, the modified TiO_2 surfaces are able to induce bone cell growth and metabolic activity [156]. The carboxyethylcellulose was also phosphorylated and a considerable higher DS in phosphorous of 0.6 was obtained with the H_3PO_4/urea system.

The phosphate groups were also introduced in the form of alkyl-spacers form to obtain a suitable solubility necessary for coating surfaces. Therefore, the hydroxypropyl cellulose was phosphorylated to introduce new functional groups which could increase the adhesion promotion on metallic substrates. The reaction was carried out using the H_3PO_4/DMF/ triethylamine system. The hydroxypropyl cellulose was dissolved overnight in DMF, triethylamine and a solution of poly(phosphoric acid) in DMF were then added. The reaction mixture was heated slowly to 120 °C for 6 h. The phosphorylated hydroxypropyl celluloses were used for the deposition of ultrathin layers on metal surfaces like aluminium, titanium or steel for adhesion promotion and corrosion inhibition [157] with application in the medical field. The authors demonstrated by atomic force microscopy (AFM) obtaining more homogeneous surfaces when the titanium and titanium alloy $TiAl_6V_4$ surfaces were covered with the derivatives containing phosphate groups compared with other cellulose derivatives [158, 159].

The synthesis of soluble cellulose acetate phosphates by the reaction of CA after dissolution in acetone with $POCl_3$ in the presence of an aliphatic amine has been reported in the literature [160]. Polytetraphosphoric acid in combination with tri-n-butylamine in DMF was used for esterification of free hydroxyl groups of cellulose acetate with low DS. Unstable primary substituents (ether or ester groups) can act as the leaving group in a subsequent phosphorylation with P_2O_5 or $POCl_3$ in the absence of an amine, as shown by our results in the cellulose nitrate system or in the case of TMSC. Trimethylsilyl cellulose with a DS of 1.5, with the silyl groups predominantly in the C6 position, could be reacted with an excess of phosphating agent in DMF/ triethylamine to give an insoluble cellulose phosphate with a DS in phosphorous of 0.3–0.6 [160]. The TMS-celluloses were used as intermediary products to obtain cellulose phosphates with a DS in phosphorous of up to 0.7 and a preferential C2/ C3 substitution, using $POCl_3$ or $PO(OH)Cl_2$ in DMF. After desilylation, an optimum

solubility of the alkali cellulose phosphates was obtained at DS values of about 0.5. The cellulose trinitrite solution in DMF, prepared by dissolving the cellulose in N_2O_4/DMF under strictly anhydrous conditions, was susceptible to phosphorylation by P_2O_5 or $POCl_3$, with a selective substitution at the C6 position only in the presence of excess tertiary amine [161].

8.4 Cellulose Esters in Nanotechnology

Cellulose derivatives, mainly cellulose esters, have considerably broadened their fields of applications in the past decades due to the development of nanotechnologies. By means of these techniques, new advanced materials and composites based on cellulosic polymers could be produced for a multitude of domains. Cellulose esters obtained as powders and fibres, with dimensions in the submicrometre range, have high specific surface areas and interesting properties that make them suitable for a wide range of advanced applications in filtration, catalysis, sensors, biomedicine, protective clothing, affinity membranes, hygienic purposes and so on.

The most intensively studied cellulose derivatives from this point of view are esters like cellulose acetate [162–167] and ethers like ethylcellulose [168–170], carboxymethylcellulose, hydroxypropylmethylcellulose and methylcellulose [171]; while few studies have been reported so far on some mixed esters such as cellulose acetate phthalate [172] and cellulose acetate-butyrate [173].

The most versatile way to produce nanostructured cellulose derivatives is electrospinning or electrospraying of their solutions in adequate solvents. The electrospinning process, theory and experimental conditions, as well as properties and applications of nanostructured materials have been largely reviewed in the last decade [174, 175]. In principle, the process consists of spinning a polymer solution with certain characteristics in a high voltage field. The electrostatic force produced on the surface of the liquid allows the formation of a stable jet flowing to the opposite electrode. The solvent evaporates and the polymer is deposited on a collector plate as a nonwoven fibre mat. The solution properties (viscosity, conductivity, surface tension) and the process conditions are known to influence the characteristics of the obtained nanostructures.

In the case of cellulose polymers, many investigations are focused on the influence of the polymer concentration and solvent system on the morphology and dimensions of nanofibres or nanopowders. Electrospinning of cellulose and its derivatives was recently reviewed [176]; particular attention is given to CA, which has been electrospun under various conditions.

Cellulose acetate uniform nanofibre mats are usually produced at polymer concentrations of about 15–20 wt%, while at concentrations lower than 10 wt% only beaded nanofibres or beads could be obtained, dependent also on the solvent employed. As cellulose derivatives are soluble in different organic solvents depending on their molecular characteristics, reports on the importance of the solvent nature or composition of multicomponent solvent systems are also available [177]. Some solvents like acetone, chloroform, DMF, dichloromethane (DCM), methanol, formic acid and pyridine have been investigated as single-solvent systems for CA, but although they formed clear solutions at a polymer concentration of 5% (w/v), only small beads could be obtained by electrospinning [177]. Acetone, when used as a solvent for the electrospinning of CA at a polymer concentration of 8%, produced small nanofibres with beads, but the poor electrospinnability of the system is also reported [178].

When small amounts of a cosolvent were used along with acetone, the spinnability was considerably improved and smooth nanofibres with diameters in the range 100–1,000 nm could be produced. Thus, a mixed solvent of acetone/water with 10–15 wt% water content provided ultrafine CA fibres of 460 nm under alkaline pH conditions [166]. Other binary mixtures successfully used as solvents for electrospinning of CA were acetone/DMA [162, 163, 177], chloroform/methanol, DCM/methanol [177] and DMA/acetic acid [162]. The 2:1 mixture of acetone/DMA is considered the most versatile for the continuous electrospinning of 12.5–20% CA solutions into fibrous membranes [162], but 1:1 and 3:1 ratios of these two solvents are also cited as producing smooth filaments [177]. CA solutions in a 4:1 mixture of DCM/methanol could be electrospun into smooth filaments at even smaller polymer concentrations (8–12% w/v), but the average fibre diameter was slightly higher compared with acetone/DMA systems [177].

The ternary solvent system 3:1:1 acetone/DMF/trifluoroethyleneare has also been reported for obtaining electrospun fibres in the submicrometer range, which were suitable as affinity membranes [167].

The effect of the processing parameters on the structure and morphology of CA fibre mats has been explored in order to find optimal conditions for a certain purpose [179, 180]. In addition, properties of CA solutions in various solvent systems (shear viscosity, surface tension and conductivity) have been investigated, and the influence of polymer concentration and solvent ratios on the resulting fibre diameters is presented by Tungprapa and co-workers [177].

Recently, preparation of CA nanofibrous membranes by electrospinning with a single solvent has been reported [181, 182], as well as their potential as an affinity membrane. DCM, formic acid, acetic acid and trifluoroacetic acid (TFA) were investigated as

single solvents, and it was shown that using TFA as solvent resulted in continuous and smooth CA nanofibres with a fibre diameter of 100–300 nm [181]. Membranes exhibited high porosity and high water permeability, and could be efficient for the separation of particles.

It is also shown that the water retention capacity of the electrospun porous membranes is many times higher than that of common fabrics, which makes these structures representative of a new class of absorbent materials [162].

Beside the suitability of CA nanofibrous mats as separation and affinity membranes, they are also under investigation as materials for biomedical applications. One of the useful directions in this field is the development of carriers for the delivery of drugs based on electrospun CA nanofibres. Thus, vitamin-loaded electrospun cellulose acetate nanofibre mats are reported for the release of vitamins A and E [183], gallic acid-loaded cellulose acetate fibres were prepared for use in topical delivery systems due to the biological activities of gallic acid [184], silymarin-loaded CA fibres gained attention because of the hepatoprotective properties of silymarin [185], and ester prodrug-loaded CA nanofibre mats have been studied as a transdermal drug delivery system [186]. Also, ultrafine cellulose acetate fibre mats were loaded with curcumin, well known for its antitumour, antioxidant and antiinflammatory properties [187]. The release characteristics of some model drugs from drug-loaded electrospun cellulose acetate fibre mats have also been studied and are reported to be better than those from the corresponding as-cast films [188].

The applicability of cellulose polymers to the biomedical field is a common feature due to their nontoxicity and biocompatibility, which allowed the development of various materials particularly useful for medical purposes. This is also the case for a mixed ester of cellulose, cellulose acetate phthalate, which has been recognised for several decades as a pharmaceutical excipient used for the enteric coating of tablets and capsules. Recent literature revealed a new and interesting potential of cellulose acetate phthalate for this domain, since it has been proved that this polymer exhibits antimicrobial and antiviral properties when used as a micronised powder [189–195]. As an alternative way to improve these properties, the possibility of obtaining micro- or nanostructures of cellulose acetate phthalate with high specific surface areas *via* the electrospinning procedure has been recently investigated [172]. Several solvent systems, such as a 2-methoxyethanol, acetone-water mixture 85/15 (v/v) and a 2-methoxyethanol-acetone-water mixture 50/42.5/7.5 (v/v/v), were applied for this purpose and it has been shown that by variation of the solvent system and the polymer concentration, powders and fibres of cellulose acetate phthalate, with sizes in the submicrometer range and different morphologies, can be easily obtained using a simple electrospinning laboratory set-up.

The morphologies of the obtained nanostructures of cellulose acetate phthalate depending on the conditions applied are presented in **Figure 8.9**.

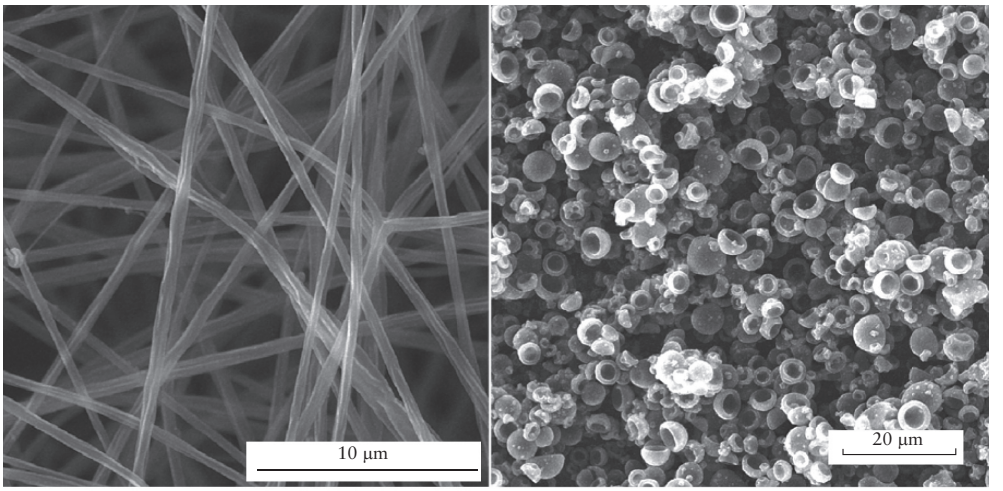

Figure 8.9 Scanning electron microscopy micrographs of (a) cellulose acetate phthalate nanofibres obtained from acetone-water 85/15 (v/v) at a 12.5% (w/v) polymer concentration and of (b) cellulose acetate phthalate micro-/nanoparticles obtained from 2-methoxyethanol solution at a 12.5% (w/v) polymer concentration. Reproduced with permission from N. Olaru and L. Olaru, *Industrial and Engineering Chemistry Research*, 2010, **49**, 1953. ©2010 American Chemical Society [172]

A possible mechanism for the formation of void hemispheres is also suggested. The potential use of electrospun cellulose acetate phthalate fibres for preventing HIV transmission has been very recently discussed [196].

Information on electrospinning of CAB in mixtures of acetic acid and acetone has also recently been made available [173], and the effects of the polymer concentration and processing parameters on CAB electrospinnability are discussed. Furthermore, CAB nanofibres were very recently prepared by a needleless electrospinning technique using a disc as a spinneret, compared with the conventional needle process, and the resulting electrospun fibres were characterised for their morphology, crystallinity and fibre diameter distribution [197]. The matrix obtained by the needleless

electrospinning method exhibits a three-dimensional tissue scaffold feature and enhanced cellular growth performances, which recommends this material for tissue engineering applications.

Cellulose polymers are also intensively studied for their potential use in numerous composite materials designed for various applications.

In the recently developed field of nanocomposites, metal nanoparticles (Ag, Au, Rh, Ru, Pd, Fe, Cu) embedded in solid, polymeric matrices have gained special attention as a result of their antimicrobial properties [198–201]. Cellulose derivatives and particularly cellulose esters exhibit physical and chemical properties that make them suitable for such an approach. Furthermore, their biocompatibility and biodegradability constitute important advantages for many purposes.

Numerous applications within biomedical fields are reported for such composites, including wound dressings, tissue scaffolds, protective clothing, hygienic purposes, environmental protection and so on. Other domains include top technologies, chemistry, electronic devices, catalysis, separation processes, biotechnology, analytical methods and so on.

Cellulose acetate is one of the most studied cellulosic polymers from this point of view [38–41]. Composites of CA with nanoparticles of silver, iron and copper have recently been realised as films and fibres [198, 202, 203]. In principle, a solution of CA containing metal ions is used to obtain films or fibres, which are subsequently subjected to thermal treatment or UV irradiation to produce metal nanoparticles of about 20–200 nm and narrow distribution. The particle size can be controlled by the metal concentration and/or by reaction conditions.

Cellulose acetate nanofibres obtained by electrospinning and containing silver nanoparticles are new products with remarkable properties and very promising applications. Literature reports the preparation of these composites from solutions of CA in adequate solvents with small amounts of $AgNO_3$ [204]. Silver nanoparticles are produced by photoreduction of the obtained nanofibres. Transmission electron microscopy (TEM) images of a typical CA nanofibre showing silver nanoparticles are presented in **Figure 8.10**.

It is assumed that the polymer structure can influence the physical and chemical properties of the composite, and that the silver nanoparticles are stabilised by electrostatic interaction with oxygen atoms of the carbonyl groups of CA. The same procedure was applied to embed Fe [199] or Cu [198] nanoparticles into matrices of CA, using $FeCl_3 \cdot 6H_2O$, γ-Fe_2O_3, $Fe(CO)_5$, $Fe_3(CO)_{12}$ and $CuCl_2$, $Cu(OAc)_2$, respectively, as metal salts, and tetrahydrofuran or 2-methoxyethanol as cosolvents.

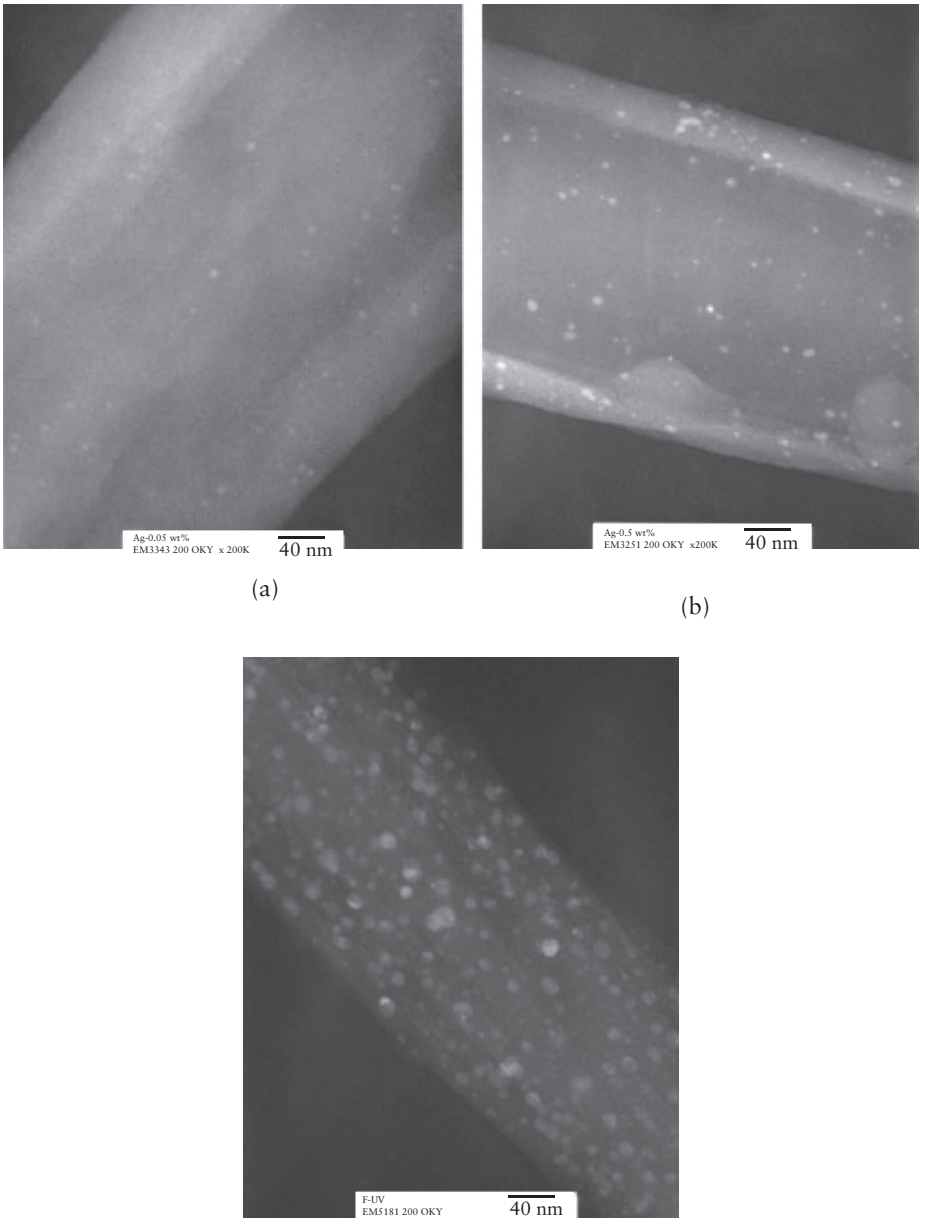

Figure 8.10 TEM images of ultrafine CA fibres electrospun from 10 wt% CA solutions with (a) 0.05 wt% $AgNO_3$, (b) 0.5 wt% $AgNO_3$, (c) 0.5 wt% $AgNO_3$ and subsequently UV irradiated for 3 h. Reproduced with permission from W.K. Son, J.H. Youk, T.S. Lee and W.H. Park, *Macromolecular Rapid Communications*, 2004, **25**, 1632. ©2004 Wiley-VCH Verlag GmbH & Co. KGaA, Weinheim [204]

The polymer and metal concentration, and the processing parameters such as the voltage potential, the distance between the spinneret and the collector plate, and the flow rate of the solution are the main factors which influence the morphology of such composites.

In other methods, water-soluble silver nanoparticles are dispersed in a solution of CA in acetone and acetic acid, and the solution is then electrospun to obtain CA ultrafine fibres containing dispersed silver nanoparticles [205]. A similar method is used to prepare CA ultrafine fibres containing quasi-spherical gold nanoparticles, which are prepared during the first step by trisodium citrate reduction of $HAuCl_4$, then added to the CA solution in acetone and dimethylformamide, and subsequently electrospun into nanofibres [206]. Nanocomposite fibres of CA containing metal (CdTe) quantum dots have also recently been prepared by electrospinning [207]. These types of composites are cited as having many novel and interesting applications in medical and engineering fields.

In other work, CA hollow fibres containing silver and exhibiting antimicrobial activity are produced by a dry spinning procedure with the aim of obtaining membranes for water treatment [208].

8.5 Conclusions

The reevaluation of natural resources became one of the main topics in modern science and technology in the context of the necessity to develop new, environmentally friendly products and processes. Over several decades of interdisciplinary research, cellulose emerged as the most attractive and renewable material, and opened many areas of practical applicability due to its spectacular properties. Thus, the high versatility, hydrophilicity, stereoregularity, biodegradability and nontoxicity of this polymer, as well as its large potential to be transformed into materials with various and useful properties by chemical modification, constitute very promising features from the point of view of the new trends, remarkable today in the field of cellulose chemistry.

Cellulose esters have been known and investigated for a long time as suitable materials for various applications, including fibres, plastics, films, coatings, separation media and so on. Apart from these traditional areas, in the past few years new directions and possibilities for the design of advanced materials based on this natural polymer have been prospected.

Most cellulose esters are still produced for industrial purposes by heterogeneous processes using acid chlorides or anhydrides as acylation reagents in the presence of a catalyst. Partially substituted cellulose acetates of practical importance are traditionally

obtained in two steps consisting of the complete acetylation of cellulose, followed by the partial hydrolysis of the highly substituted product in acetic acid media. Attempts to overcome the difficult reaction conditions related to these processes were reported, one of them being the shortening of the reaction time by using a hydrocarbon in the hydrolysis medium. New and efficient methods for the heterogeneous acetylation of various celluloses imply the use solvent-free systems and/or new catalyst systems, such as iodine. The heterogeneous acetylation of cellulose is also cited as a suitable way to modify the surface properties of cellulose fibres – such as hydrophilicity – in order to use them in composites with synthetic polymers.

The new solvents for cellulose, discovered in the past decades, allowed the development of more diverse synthesis pathways for various derivative types. Homogeneous processes enable the selective functionalisation of cellulose, which generates new derivatives with a controlled chemical and supramolecular structure, and with new and special properties making them suitable for high-value applications in technological, fine chemical or medical fields. In this respect, studies on structure-property relationships are developed as an important tool to evaluate the potential of various homogeneous derivatisation systems.

Cellulose functionalisation in solution can be generally assessed by procedures involving dissolution with nonderivatising or with derivatising solvents. Derivatisation in solvent systems such as DMA/LiCl, DMSO/TBAF, DMSO/paraformaldehyde, ionic liquids or molten inorganic salt hydrates, leads to esters with various DS values and substitution patterns, and with defined solubility. It is recognised that homogeneous modification is the most suitable method of producing cellulose derivatives with tailored properties, which is one of the future trends in cellulose chemistry.

In this context, cellulose esters, and particularly cellulose acetates, are placed among the most promising polymers for the future development of novel materials with superior and attractive properties for top technologies, biomedicine, health care and environmental protection.

Furthermore, new advanced materials and composites could be produced for a multitude of domains by processing cellulose polymers at the nanoscale level. Cellulose esters obtained as fibres and powders with dimensions in the submicrometer range have high specific surface areas and interesting properties which make them suitable for a wide range of advanced applications in filtration, catalysis, sensors, biomedicine, protective clothing, affinity membranes, hygienic purposes and so on. Recent reports reveal the high potential of hybrid materials containing silver or other metal/metal oxide nanoparticles embedded in the solid matrices of cellulose derivatives, especially for biomedical applications such as wound dressings or tissue engineering scaffolds.

Based on numerous research efforts emphasised in recent literature, it may be assumed that important future trends in cellulose esters chemistry will be closely related to the development of modern top nanotechnologies.

References

1. D. Klemm, B. Heublein, H.P. Fink and A. Bohn, *Angewandte Chemie International Edition*, 2005, **44**, 3358.

2. T. Heinze, *Macromolecular Symposia*, 2009, **280**, 1, 15.

3. T. Heinze, T.F. Liebert, K.S. Pfeiffer and M.A. Hussain, *Cellulose*, 2003, **10**, 3, 283.

4. D. Klemm, B. Philipp, T. Heinze, U. Heinze and W. Wagenknecht in *Comprehensive Cellulose Chemistry*: *Fundamentals and Analytical Methods*, Wiley-VCH Verlag GmbH, Weinheim, Germany, 1998, **1**, p.145.

5. T. Heinze and T. Liebert, *Macromolecular Symposia*, 2004, **208**, 167.

6. H. Thielking and M. Schmidt in *Cellulose Ethers: Ullmann's Encyclopedia of Industrial Chemistry*, Wiley-VCH Verlag GmbH & Co. KGaA, Weinheim, Germany, 2006.

7. K. Balser, L. Hoppe, T. Eicher, M. Wandel, H.J. Astheimer, H. Steinmeier and J.M. Allen in *Cellulose Esters: Ullmann's Encyclopedia of Industrial Chemistry*, Wiley-VCH Verlag GmbH & Co. KGaA, Weinheim, Germany, 2004.

8. L.J. Tanghe, L.B. Genung and J.W. Mench in *Methods in Carbohydrate Chemistry*, Ed., R.L. Whistler, Academic Press, New York, NY, USA, 1963, **3**, p.198.

9. A. Ishizu in *Wood and Cellulosic Chemistry*, Eds., D.N.S. Hon and N. Shiraishi, Marcel Dekker Inc., New York, NY, USA, 1992, **16**, p.757.

10. Y. Shimizu and J. Hayashi, *Cellulose Chemistry and Technology*, 1989, **23**, 661.

11. Y. Shimizu, A. Nakayama and J. Hayashi, *Cellulose Chemistry and Technology*, 1991, **25**, 275.

12. G.N. Bruxelles and V.R. Grassie in *Encyclopedia of Polymer Science and Technology*, Eds., H.F. Mark, N.G. Gaylord and N.M. Bikalesds, John Wiley & Sons, Inc., New York, NY, USA, 1965, **3**, p.307.

13. R.T. Bogan, C.M. Kuo and R.J. Brewer in *Kirk-Othmer Encyclopedia of Chemical Technology*, 3rd Edition, Ed., J.I. Kroschwitz, John Wiley & Sons, Inc., New York, NY, USA, 1979, **5**, p.118.

14. C.J. Malm, L.J. Tanghe and B.C. Laird, *Journal of American Chemical Society*, 1950, **72**, 2674.

15. C.J. Malm, K.T. Barkey, M. Salo and D.C. May, *Journal of Industrial and Engineering Chemistry*, 1957, **49**, 79.

16. C.M. Buchanan, K.J. Edgar and A.K. Wilson, *Macromolecules*, 1991, **24**, 3060.

17. K. Kamide, K. Okajima, K. Kowsaka and T. Matsui, *Polymer Journal*, 1987, **19**, 1405.

18. K. Ueda and S. Saka in *Cellulose and Wood: Chemistry and Technology*, Ed., C. Schuerch, John Wiley & Sons, Inc., New York, NY, USA, 1988, p.309.

19. N. Olaru, L. Olaru, A. Andriescu and N. Tudorachi, *Angewandte Makromolekulare Chemie*, 1996, **241**, 67.

20. N. Olaru and L. Olaru, *Journal of Applied Polymer Science*, 2004, **94**, 1965.

21. N. Olaru, A. Andriescu and L. Olaru, *European Polymer Journal*, 2001, **37**, 865.

22. A. Biswas, R.L. Shogren and J.L. Willet, *Biomacromolecules*, 2005, **6**, 1843.

23. A. Biswas, G.S. Selling, M. Appell, K.K. Woods, J.L. Willett and C.M. Buchanan, *Carbohydrate Polymers*, 2007, **68**, 555.

24. A. Biswas, G.S. Selling, R.L. Shogren, J.L. Willett and H.N. Cheng, *Chemistry Today*, 2009, **27**, 33.

25. L. Yan, W. Li, Z. Qi and S. Liu, *Journal of Polymer Research*, 2006, **13**, 375.

26. M.P. de Paula, T.M. Lacerda and E. Frollini, *eXPRESS Polymer Letters*, 2008, **2**, 423.

27. G. Frisoni, M. Baiardo, M. Scandola, D. Lednicka, M.C. Cnockaert, J. Mergaert and J. Swings, *Biomacromolecules*, 2001, **2**, 476.

28. M.O. Adebajo and R.L. Frost, *Spectrochimica Acta, Part A: Molecular and Biomolecular Spectroscopy*, 2004, **60**, 10, 2315.

29. M.O. Adebajo and R.L. Frost, *Spectrochimica Acta, Part A: Molecular and Biomolecular Spectroscopy*, 2004, **60**, 1–2, 449.

30. N. Olaru, L. Olaru, C. Vasile and P. Ander, *Polimery*, 2011, **56**, 11–12, 834.

31. G. Rodionova, M. Lenes, O. Eriksen and O. Gregersen, *Cellulose*, 2011, **18**, 127.

32. N. Olaru, D. Ciolacu, D. Tampu and L. Olaru, *Journal of Optoelectronic and Advanced Materials,* 2007, **9**, 12, 3917.

33. J. Geurden, *Pure and Applied Chemistry*, 1967, **14**, 3, 507.

34. A. Elidrissi, S. El barkany, H. Amhamdi, A. Maaroufi and B. Hammouti, *Journal of Materials and Environmental Science*, 2012, **3**, 2, 270.

35. S. Fischer, K. Thümmler, B. Volkert, K. Hettrich, I. Schmidt and K. Fischer, *Macromolecular Symposia*, 2008, **262**, 891.

36. P.M. Kosaka, Y. Kawano, M.C. Salvadori and D.F.S. Petri, *Cellulose*, 2005, **12**, 4, 351.

37. J. Amim Junior, D.F.S. Petri, F.C.B. Maia and P.B. Miranda, *Quimica Nova*, 2010, **33**, 2064.

38. M. Cohen-Atiya, P. Vadgama and D. Mandler, *Soft Matter*, 2007, **3**, 8, 1053.

39. T. Kawaguchi, H. Nakahara and K. Fukuda, *Thin Solid Films*, 1985, **133**, 29.

40. K.J. Edgar, C.M. Buchanan, J.S. Debenham, P.A. Rundquist, B.D. Seiler, M.C. Shelton and D. Tindall, *Progress in Polymer Science*, 2001, **26**, 1605.

41. C.J. Malm, J.W. Mench, B. Fulkerson and G.D. Hiatt, *Journal of Industrial and Engineering Chemistry*, 1957, **49**, 84.

42. W. Wagenknecht, D. Paul, B. Philipp and T. Ludwig, *Acta Polymerica*, 1987, **38**, 10, 551.

43. N. Olaru and L. Olaru, *Iranian Polymer Journal*, 2005, **14**, 12, 1058.

44. D. Klemm, B. Philipp, T. Heinze, U. Heinze and W. Wagenknecht in *Comprehensive Cellulose Chemistry*: *Fundamentals and Analytical Methods*, Wiley-VCH Verlag GmbH, Weinheim, Germany, 1998, **2**, p.133.

45. D.M. Suflet, G.C. Chitanu and V.I. Popa, *Reactive and Functional Polymers*, 2006, **66**, 11, 1240.

46. D.M. Suflet, A. Nicolescu, I. Popescu and G.C. Chitanu, *Carbohydrate Polymers*, 2011, **84**, 3, 1176.

47. N. Inagaki, S. Nakamura, H. Asai and K. Katsuura, *Journal of Applied Polymer Science*, 1976, **20**, 2829.

48. A.C. Nuessle, F.M. Ford, W.P. Hall and A.L. Lippert, *Textile Research Journal*, 1956, **26**, 32.

49. J.D. Reid and L.W. Mazzeno, Jr., *Industrial and Engineering Chemistry*, 1949, **41**, 12, 2828.

50. R.K. Sharma, J. Singh and G.S. Chauhan, *BioResurses*, 2010, **5**, 4, 2547.

51. N.A. Sharma, P.N. Singh and M.G. Shet, *Research Journal of Chemistry and Environment*, 2002, **6**, 1, 47.

52. A.J. Head, N.F. Kember, R.P. Miller and R.A. Wells, *Journal of the Chemical Society*, 1958, **10-12**, 3418.

53. D.P. Park, J.Y. Hwang, H.J. Choi, C.A. Kim and M.S. Jhon, *Materials Research Innovations*, 2003, **7**, 3, 161.

54. G. Ahn, U.S. Choi and O.K. Kwon, *Polymer International*, 2000, **49**, 6, 567.

55. S.G. Kim, H.J. Choi and M.S. Jhon, *Macromolecular Chemistry and Physics*, 2001, **202**, 4, 521.

56. S.G. Kim, J.W. Kim, W.H. Jang, H.J. Choi and M.S. Jhon, *Polymer*, 2001, **42**, 11, 5005.

57. T. Oshima, K. Kondo, K. Ohto, K. Inoue and Y. Baba, *Reactive and Functional Polymers*, 2008, **68**, 376.

58. M.R. Mucalo, K. Kato and Y. Yokogawa, *Colloids and Surfaces B: Biointerfaces*, 2009, **71**, 1, 52.

59. T. Oshima, S. Taguchi, K. Ohe and Y. Baba, *Carbohydrate Polymers*, 2011, **83**, 2, 953.

60. Y. Yokagawa, M.R. Mucalo, M. Toriyama, T. Suzuki, Y. Kawamoto, F. Nagata, K. Nishizawa and T. Kameyama, *Reports of the National Industrial Research Institute of Nagoya*, 1996, **45**, 8, 449.

61. N.K. Yurkshtovich, T.L. Yurkshtovich, F.N. Kaputskii, N.V. Golub and R.I. Kosterova, *Russian Journal of Applied Chemistry*, 2009, **82**, 6, 963.

62. P.L. Granja, B. de Jeso, R. Bareille, F. Rouais, C. Baquey and M.A. Barbosa, *Reactive and Functional Polymers*, 2006, **66**, 728.

63. W.D. Wan Rosli, H.M.K. Mohamad and S. Azman, *BioResources*, 2011, **6**, 2, 1719.

64. P.L. Granja, L. Pouysegu, M. Petraud, B. De Jeso, C. Baquey and M.A. Barbosa, *Journal of Applied Polymer Science*, 2001, **82**, 13, 3341.

65. P.L. Granja, L. Pouysegu, D. Deffieux, G. Daude, B. De Jeso, C. Labrugere, C. Baquey and M.A. Barbosa, *Journal of Applied Polymer Science*, 2001, **82**, 3354.

66. P.L. Granja, B. De Jeso, R. Bareille, F. Rouais, C. Baquey and M.A. Barbosa, *Reactive and Functional Polymers*, 2006, **66**, 728.

67. S.H. Zeronian, S. Adams, K. Alger and A.E. Lipska, *Journal of Applied Polymer Science*, 1980, **25**, 519.

68. A.M.A. Nada, M.A. Eid, R.M. El Bahnasawy and M.N. Khalifa, *Journal of Applied Polymer Science*, 2002, **85**, 4, 792.

69. A.M.A. Nada, M.A. Eid, A.I. Sabry and M.N. Khalifa, *Journal of Applied Polymer Science*, 2003, **90**, 97.

70. A.R. Horrocks and S. Zhang, *Polymer*, 2001, **42**, 8025.

71. S.S. Kim, W.Y. Jeong, B.C. Shin, S.Y. Oh, H.W. Kim and J.M. Rhee, *Journal of Biomedical Materials Research*, 1998, **40**, 3, 401.

72. N. Gospodinova, A. Grelard, M. Jeanin, G.C. Chitanu, A. Carpov, V. Thiery and T. Besson, *Green Chemistry*, 2002, **4**, 220.

73. T. Tzanov, M. Stamenova and A. Cavaco-Paulo, *Macromolecular Rapid Communication*, 2002, **23**, 962.

74. D. Ciolacu and V.I. Popa in *Cellulose Allomorphs: Structure, Accessibility and Reactivity*, Nova Science Publishers, Inc., New York, NY, USA, 2010.

75. D. Ciolacu and V.I. Popa in *Cellulose: Structure and Property, Derivatives and Industrial Uses*, Eds., A. Lejeune and T. Deprez, Nova Science Publishers, Inc., New York, NY, USA, 2010, p.1.

76. O.A. El Seoud and T. Heinze, *Advances in Polymer Science*, 2005, **186**, 103.

77. T. Heinze and A. Koschella, *Polímeros: Ciência e Tecnologia*, 2005, **15**, 2, 84.

78. J-L. Wertz, O. Bédué and J.P. Mercier in *Cellulose Science and Technology*, EPFL Press, Laussane, Switzerland, 2010, p.147.

79. N.J. Ofsthun, S. Karoor and M. Suzuki in *Advanced Membrane Technology and Applications*, Eds., N.N Li, A.G. Fane, W.S.W. Ho and T. Matsuura, John Wiley & Son, Inc., Hoboken, NJ, USA, 2008, p.19.

80. D. Klemm, B. Philipp, T. Heinze, U. Heinze and W. Wagenknecht in *Comprehensive Cellulose Chemistry: Fundamentals and Analytical Methods*, Wiley-VCH, Weinheim, Germany, 1998, **2**, p.73.

81. T. Liebert in *Cellulose Solvents: For Analysis, Shaping and Chemical Modification*, Eds., T.F. Liebert, T.J. Heinze and K.J. Edgar, ACS Symposium Series 1033, American Chemical Society, Washington, DC, USA, 2010, p.3.

82. K. Saalwäechter, W. Burchard, P. Klűfers, G. Kettenbach, P. Mayer, D. Klemm and S. Dugarmaa, *Macromolecules*, 2000, **33**, 11, 4094.

83. A. Isogai and R.H. Atalla, *Cellulose*, 1998, **5**, 309.

84. J. Zhou and L. Zhang, *Polymer Journal*, 2000, **32**, 10, 866.

85. D. Ciolacu and V.I. Popa, *Cellulose Chemistry and Technology*, 2005, **39**, 3–4, 179.

86. S.L. Liu and L.N. Zhang, *Cellulose*, 2009, **16**, 189.

87. J. Cai, L. Zhang, C. Chang, G. Cheng, X. Chen and B. Chu, *ChemPhysChem*, 2007, **8**, 1572.

88. D. Ruan, A. Lue and L. Zhang, *Polymer*, 2008, **49**, 1027.

89. J. Cai, L. Zhang, J. Zhou, H. Qi, H. Chen, T. Kondo, X. Chen and B. Chu, *Advanced Materials*, 2007, **19**, 821.

90. J. Cai, L. Zhang and L. Wang, *Cellulose*, 2007, **14**, 205.

91. Y. Mao, J. Zhou, J. Cai and L. Zhang, *Journal of Membrane Science*, 2006, **279**, 246.

92. H.J. Jin, C.X. Zha and L.X. Gu, *Carbohydrate Research*, 2007, **342**, 851.

93. S. Zhang, F.X. Li, J.Y. Yu and G. Li-Xia, *Cellulose Chemistry and Technology*, 2009, **43**, 7–8, 241.

94. S. Fischer, H. Leipner, E. Brendler, W. Voigt and K. Fischer in *Polysaccharide Applications, Cosmetics and Pharmaceuticals*, Eds., M.A. El-Nokaly and H.A. Soini, ACS Symposium Series 737, Washington, DC, USA, 2000, p.143.

95. H. Leipner, S. Fischer, E. Brendler and W. Voigt, *Macromolecular Chemistry and Physics*, 2000, **201**, 2041.

96. S. Fischer, H. Leipner, K. Thuemmler, E. Brendler and J. Peters, *Cellulose*, 2003, **10**, 227.

97. F. Liebner, A. Potthast, T. Rosenau, E. Haimer and M. Wendland, *Holzforschung*, 2008, **62**, 129.

98. S. Zikeli, *Chemical Fibers International*, 2001, **51**, 272.

99. A. Nechwatal, C. Michels, B. Kosan and M. Nicolai, *Cellulose*, 2004, **11**, 265.

100. C.W. Kim, D.S. Kim, S.Y. Kang, M. Marquez and Y.L. Joo, *Polymer*, 2006, **47**, 5097.

101. D. Ciolacu and V.I. Popa in *Proceedings of 10th Meeting of Pulp and Paper Industry of the Balkan (Southeast European) Countries*, Agia Triada, Thessaloniki, Greece, 2003. p.2.

102. S. Yokota, T. Kitaoka and H. Wariishi, *Applied Surface Science*, 2007, **253**, 4208.

103. D. Klemm, B. Philipp, T. Heinze, U. Heinze and W. Wagenknecht in *Comprehensive Cellulose Chemistry*: *Fundamentals and Analytical Methods*, Wiley-VCH Verlag GmbH, Weinheim, Germany, 1998, **1**, p.155.

104. T. Heinze and T. Liebert, *Progress in Polymer Science*, 2001, **26**, 1689.

105. A. Isogai, A. Ishizu and J. Nakano, *Journal of Applied Polymer Science*, 1987, **33**, 1283.

106. A. Isogai, A. Ishizu and J. Nakano, *Journal of Applied Polymer Science*, 1984, **29**, 2097.

107. A. Isogai, A. Ishizu and J. Nakano, *Journal of Applied Polymer Science*, 1986, **31**, 341.

108. A. Isogai and R.H. Atalla, *Journal of Polymer Science, Part A: Polymer Chemistry Edition*, 1991, **29**, 1, 113.

109. A. Isogai in *Cellulose Polymers, Blends and Composites*, Ed., R.D. Gilbert, Hanser Publishers, New York, NY, USA, 1994, p.1.

110. D. Ciolacu, F. Ciolacu and V.I. Popa, *Cellulose Chemistry and Technology*, 2011, **45**, 1–2, 13.

111. R.P. Swatloski, S.K. Spear, J.D. Holbrey and R.D. Rogers, *Journal of the American Chemical Society*, 2002, **124**, 4974.

112. M.E. Gibril, *International Journal of Engineering Science and Technology*, 2012, **4**, 7, 3556.

113. R.C. Remsing, R.P. Swatloski, R.D. Rogers and G. Moyna, *Chemical Communications*, 2006, **12**, 1271.

114. Z. Zhao and Y. Dai in *Green Solvents II: Properties and Applications of Ionic Liquids*, Eds., A. Mohammad and Dr. Inamuddin, Springer, Dordrecht, The Netherlands, 2012, p.33.

115. S. Murugesana and R.J. Linhardt, *Current Organic Synthesis*, 2005, **2**, 4, 437.

116. Y. Cao, J. Wu, J. Zhang, H. Li, Y. Zhang and J. He, *Chemical Engineering Journal*, 2009, **147**, 13.

117. T. Heinze, K. Schwikal and S. Barthel, *Macromolecular Bioscience*, 2005, **5**, 520.

118. H. Zhang, J. Wu, J. Zhang and J.S. He, *Macromolecules*, 2005, **38**, 8272.

119. Y. Fukaya, A. Sugimoto and H. Ohno, *Biomacromolecules*, 2006, **7**, 3295.

120. M. Gericke, P. Fardim and T. Heinze, *Molecules*, 2012, **17**, 7458.

121. B. Kosan, C. Michels and F. Meister, *Cellulose*, 2008, **15**, 59.

122. F. Wendler, B. Kosan, M. Krieg and F. Meister, *Macromolecular Symposia*, 2009, **280**, 112.

123. Y. Cao, H. Li, Y. Zhang, J. Zhang and J. He, *Journal of Applied Polymer Science*, 2010, **116**, 547.

124. A. Stark, *Energy & Environmental Science*, 2011, **4**, 19.

125. M. Mora-Pale, L. Meli, T.V. Doherty, R.J. Linhardt and J.S. Dordick, *Biotechnology and Bioengineering*, 2011, **108**, 1229.

126. N. Sun, H. Rodriguez, M. Rahman and R.D. Rogers, *Chemical Communications*, 2011, **47**, 1405.

127. K. Massonne, V. Stegmann, G. D'Andola, W. Mormann, M. Wezstein and W. Leng, inventors; BASF AG, assignee; WO 2008/000666A1, 2008.

128. C.M. Buchanan, N.L. Buchanan, M.E. Donelson, M.G. Gorbunova, T. Kuo and B. Wang, inventors; Eastman Chemical Company, assignee; WO 2010/019245 A1, 2010.

129. R.T. Hembre, N.L. Buchanan, C.M. Buchanan, J.L. Lambert, M.E. Donelson, M.G. Gorbunova, T. Kuo and B. Wang, inventors; Eastman Chemical Company, assignee; WO 2010/019244A1, 2010.

130. T. Heinze and K. Petzold in *Monomers, Polymers and Composites from Renewable Resources*, Eds., M.N. Belgacem and A. Gandini, Elsevier, Oxford, UK, 2008, p.343.

131. D. Ciolacu, V.I. Popa and H. Ritter, *Journal of Applied Polymer Science*, 2006, **100**, 105.

132. K. Thümmler, S. Fischer, J. Peters, T. Liebert and T. Heinze, *Cellulose*, 2010, **17**, 161.

133. G.T. Ciacco, T. Liebert, E. Frollini and T. Heinze, *Cellulose*, 2003, **10**, 125.

134. B.A.P. Ass, E. Frollini and T. Heinze, *Macromolecular Bioscience*, 2004, **4**, 1008.

135. M.A. Hussain, T. Liebert and T. Heinze, *Macromolecular Rapid Communications*, 2004, **25**, 916.

136. T. Heinze, T. Lincke, D. Fenn and A. Koschella, *Polymer Bulletin*, 2008, **61**, 1.

137. T.R. Dawsey in *Cellulosic Polymers, Blends and Composites*, Eds., R.D. Gilbert, Hanser/Gardner Publications, Cincinnati, OH, USA, 1994, p.157.

138. T. Heinze in *Polysaccharides: Structural Diversity and Functional Versatility*, Ed., S. Dumitriu, Marcel Dekker, New York, NY, USA, 2004, p.551.

139. C.L. McCormick and T.R. Dawsey, *Macromolecules*, 1990, **23**, 3606.

140. C.L. McCormick and T.S. Chen in *Macromolecular Solutions - Solvent-property Relationships in Polymers*, Eds., R.B. Symor and G.A. Stahl, Pergamon Press, New York, NY, USA, 1982, p.101.

141. M. Diamantoglou and H. Kuhne, *Das Papier*, 1988, **42**, 690. [In German]

142. A.M. Regiani, E. Frollini, G.A. Marson, G.M. Arantes and O.A. El Seoud, *Journal of Polymer Science, Part A: Polymer Chemistry Edition*, 1999, **37**, 1357.

143. D. Graebner, T. Liebert and T. Heinze, *Cellulose*, 2002, **9**, 193.

144. D.N. Hon and H.J. Yan, *Journal of Applied Polymer Science*, 2001, **81**, 2649.

145. M. Terbojevich, A. Cosani, B. Focher, G. Gastaldi, W. Wu, E. Marsano and G. Conio, *Cellulose*, 1999, **6**, 71.

146. A. Matsumoto, S. Tanaka and T. Otsu, *Macromolecules*, 1991, **24**, 4017.

147. M.A. Hussain, T. Liebert and T. Heinze, *Macromolecular Rapid Communications*, 2004, **25**, 9, 916.

148. D. Xu, B. Li, C. Tate and K.J. Edgar, *Cellulose*, 2011, **18**, 405.

149. Y. Cao, J. Zhang, J. He, H. Li and Y. Zhang, *Chinese Journal of Chemical Engineering*, 2010, **18**, 515.

150. Y. Cao, J. Wu, T. Meng, J. Zhang, J. He, H. Li and Y. Zhang, *Carbohydrate Polymers*, 2007, **69**, 665.

151. S. Kohler, T. Liebert, M. Schobitz, J. Schaller, F. Meister, W. Gunther and T. Heinze, *Macromolecular Rapid Communication*, 2007, **28**, 2311.

152. B. Kosan, S. Dorn, F. Meister and T. Heinze, *Macromolecular Materials and Engineering*, 2010, **295**, 676.

153. W. Wagenknecht, I. Nehls, B. Philipp, M. Schnabelrauch, D. Klemm and M. Hartmann, *Acta Polymerica*, 1991, **42**, 11, 554.

154. W. Wagenknecht, B. Philipp and H. Schleicher, *Acta Polymerica*, 1979, **30**, 108

155. I. Nehls and F. Loth, *Acta Polymerica*, 1991, **42**, 5, 233.

156. D. Pasqui, A. Rossi, F. Di Cintio and R. Barbucci, *Biomacromolecules*, 2007, **8**, 3965.

157. T. Kowalik, H.J. Adler, A. Plagge and M. Stratmann, *Macromolecular Chemistry and Physics*, 2000, **201**, 2064.

158. A. Plagge, H.J. Adler, M. Rohwerder and M. Stratmann, *Thin Solid Films*, 2008, **516**, 2130.

159. E. Jaehne, T. Kowalik, H.J.P. Adler, A. Plagge and M. Stratmann, *Macromolecular Symposia*, 2002, **177**, 97.

160. D. Klemm, Z. Heinze, B. Philipp and W. Wagenknecht, *Acta Polymerica*, 1997, **48**, 277.

161. W. Wagenknecht, B. Philipp, I. Nehls, H. Schnabelrauch, D. Klemm and M. Hartmann, *Acta Polymerica*, 1991, **42**, 213.

162. H. Liu and Y.L. Hsieh, *Journal of Polymer Science, Part B: Polymer Physics Edition*, 2002, **40**, 2119.

163. H. Liu and C. Tang, *Polymer Journal*, 2007, **39**, 65.

164. D. Han and P.I. Gouma, *Nanomedicine: Nanotechnology, Biology and Medicine*, 2006, **2**, 37.

165. L. Chen, L. Bromberg, T.A. Hatton and G.C. Rutledge, *Polymer*, 2008, **49**, 1266.

166. W.K. Son, J.H. Youk, T.S. Lee and W.H. Park, *Journal of Polymer Science, Part B: Polymer Physics Edition*, 2004, **42**, 5.

167. M. Zuwei, M. Kotaki and S. Ramakrishna, *Journal of Membrane Science*, 2005, **265**, 115.

168. X. Wu, L. Wang, H. Yu and Y. Huang, *Journal of Applied Polymer Science*, 2005, **97**, 1292.

169. J.Y. Park, S.W. Han and I.H. Lee, *Journal of Industrial and Engineering Chemistry*, 2007, **13**, 1002.

170. J.P. Jeun, Y.M. Lim, J.H. Choi, H.S. La, P.H. Kang and Y.C. Nho, *Solid State Phenomena*, 2007, **119**, 255.

171. A. Frenot, M.W. Henriksson and M.P. Walkenstrom, *Journal of Applied Polymer Science*, 2007, **103**, 1473.

172. N. Olaru and L. Olaru, *Industrial and Engineering Chemistry Research*, 2010, **49**, 1953.

173. X. Zhu, J. Pang, Z. Zhou and X. Shi, *Synthetic Fiber in China*, 2006, **11,** 15.

174. S. Thandavamoorthy, G.S. Bhat, R.W. Tock, S. Parameswaran and S.S. Ramkumar, *Journal of Applied Polymer Science*, 2005, **96**, 557.

175. A. Greiner and J.H. Wendorff, *Angewandte Chemie International Edition*, 2007, **46**, 5670.

176. M.W. Frey, *Polymer Reviews*, 2008, **48**, 378.

177. S. Tungprapa, T. Puangparn, M. Weerasombut, I. Jangchud, P. Fakum, S. Semongkhol, C. Meechaisue and P. Supaphol, *Cellulose*, 2007, **14**, 563.

178. R. Jaeger, M.M. Bergshoef, C. Martin, I. Batlle, H. Schoenherr and G.J. Vancso, *Macromolecular Symposia*, 1998, **127**, 141.

179. H. Wang, X. Qin and J. Cao, *Advanced Materials Research*, 2011, **175-176**, 242.

180. S. Plianwong, K. Su-utha, P. Opanasopit, T. Ngawhirunpat and T. Rojanarata, *Advanced Materials Research*, 2012, **506**, 242.

181. W. Zhou, J. He, S. Cui and W. Gao, *The Open Materials Science Journal*, 2011, **5**, 51.

182. W. Zhou, J. He, S. Cui and W. Gao, *Advanced Materials Research*, 2011, **148-149**, 1408.

183. P. Taepaiboon, U. Rungsardthong and P. Supaphol, *European Journal of Pharmaceutics and Biopharmaceutics*, 2007, **67**, 387.

184. T. Phachamud and M. Phiriyawirut, *Research Journal of Pharmaceutical, Biological and Chemical Sciences*, **2**, 85.

185. M. Phiriyawirut and T. Phachamud, *Research Journal of Pharmaceutical, Biological and Chemical Sciences*, 2012, **3**, 432.

186. X.M. Wu, C.J. Branford-White, L.M. Zhu, N.P. Chatterton and D.G. Yu, *Journal of Materials Science: Materials in Medicine*, 2010, **21**, 2403.

187. O. Suwantong, P. Opanasopit, U. Ruktanonchai and P. Supaphol, *Polymer*, 2007, **48**, 7546.

188. S. Tungprapa, I. Jangchud and P. Supaphol, *Polymer*, 2007, **48**, 5030.

189. T. Gyotoku, L. Aurelian and A.R. Neurath, *Antiviral Chemistry & Chemotherapy*, 1999, **10**, 327.

190. A.R. Neurath, N. Strick, Y.Y. Li and A.K. Debnath, *BMC Infectious Diseases*, 2001, **1**, 17.

191. R. Duncan, *Nature Reviews Drug Discovery*, 2003, **2**, 347.

192. A.R. Neurath, N. Strick and Y.Y. Li, *BMC Infectious Diseases*, 2003, **3**, 27.

193. A.R. Neurath, N. Strick, S. Jiang, Y.Y. Li and A.K. Debnath, *BMC Infectious Diseases,* 2002, **2**, 6.

194. K.H. Manson, M.S. Wyand, C. Miller and A.R. Neurath, *Antimicrobial Agents and Chemotherapy,* 2000, **44**, 3199.

195. A.R. Neurath, N. Strick and Y.Y. Li, *BMC Infectious Diseases*, 2002, **2**, 27.

196. C. Huang, S.J. Soenen, E. Van Gulck, G. Vanham, J. Rejman, S. Van Calenbergh, C. Vervaet, T. Coenye, H. Verstraelen, M. Temmerman, J. Demeester and S.C. De Smedt, *Biomaterials*, 2012, **33**, 962.

197. C. Huang, H. Niu, C. Wu, Q. Ke, X. Mo and T. Lin, *Journal of Biomedical Materials Research Part A*, 2013, **101A**, 115.

198. I.W. Shim, W.T. Noh, J. Kwon, J.Y. Cho, K.S. Kim and D.H. Kang, *Bulletin of Korean Chemistry Society*, 2002, **23**, 563.

199. I.W. Shim, S. Choi, W.T. Noh, J. Kwon, Y. J. Cho, D.Y. Chae and K.S. Kim, *Bulletin of Korean Chemistry Society*, 2001, **22**, 772.

200. I.W. Shim, J.Y. Kim, D.Y. Kim and S. Choi, *Reactive & Functional Polymers*, 2000, **43**, 71.

201. I.W. Shim, D.Y. Kim, S. Choi, K.H. Kong and J.I. Choe, *Reactive & Functional Polymers*, 2000, **43**, 287.

202. J.W. Kwon, S.H. Yoon, S.S. Lee, K.W. Seo and I.W. Shim, *Bulletin of Korean Chemistry Society*, 2005, **26**, 837.

203. Z. Zhang, L. Zhang, S. Wang, W. Chen and Y. Lei, *Polymer*, 2001, **42**, 8315.

204. W.K. Son, J.H. Youk, T.S. Lee and W.H. Park, *Macromolecular Rapid Communications*, 2004, **25**, 1632.

205. D. Zhao, Q. Feng, L. Lv and J. Li, *Advanced Materials Research*, 2011, **337**, 116.

206. D. Zhao, L. Sun, L. Lv and J. Li, *Advanced Materials Research*, 2012, **391-392**, 400.

207. D. Zhao, L. Sun, M. Wang and J. Li, *Applied Mechanics and Materials*, 2012, **174-177**, 140.

208. W.L. Chou, D.G. Yu and M.C. Yang, *Polymers for Advanced Technologies*, 2005, **16**, 600.

9 Lyocell Processes and Products

Patrick A. White and Heinrich Firgo

9.1 Overview

Lyocell is the generic name of a generation of cellulosic fibres made by a direct dissolution process. It is commercially available under the trade name of TENCEL® and is supplied by the Austrian company, Lenzing AG, which has manufacturing plants in Austria, the UK and the USA. Small-scale pilot lines have more recently been started by other companies in India, South Korea and China. This chapter will describe the processes operated by Lenzing – which are based on the research carried out separately by Courtaulds and Lenzing. The two businesses merged in 2004 when Lenzing took ownership.

The contents, data and illustrations shown in this chapter have been supplied by Lenzing AG and are published with their permission.

9.1.1 Reasons for a New Cellulose Fibre

The development of TENCEL® was initiated in the 1970s with the objective of making a cellulosic fibre which gave an improved cost/performance profile compared with the established viscose rayon fibres. Other driving forces were the increased demand for industrial processes to become safer to operate and more environmentally responsible. It was understood that the development costs would be high and spread over a long timescale, but it was expected that a fibre based on cellulose, a major renewable resource, would have a long-term advantage over synthetic fibres based on oil, which was expected to increase in cost.

It was also correctly anticipated that the demand for cellulose fibres would continue to grow rapidly because of the comfort characteristics that it bestows on apparel due to its moisture absorption. The worldwide consumption of fibres has increased significantly both because of the population growth and also because of increased

prosperity – textile products are one of the first consumables that people buy when they obtain a higher disposable income. Cotton is the dominant cellulose fibre, but we expect the output growth of this fibre will not be able to meet demand due to the constraints of available agricultural land and the high level of chemicals required to achieve good yields. Hence, we expect a cellulose gap to develop that a new fibre could ideally meet.

Furthermore, the need for biodegradable nonwoven products is growing significantly and man-made cellulose fibres are the ideal feedstock for this market. This market has been extended to include pulp-based products that use cellulosic fibres as reinforcement.

9.1.2 Lyocell / TENCEL® Outline Profile

The forms and applications of TENCEL® were evaluated in the early 1980s. The first samples that were made for commercial evaluation were produced in 1984 by Courtaulds in the UK. They were supplied as staple (cut) fibres for textile, nonwoven and paper applications. All of these end uses have subsequently become commercially successful.

AKZO also developed a continuous filament version called Newcell and evaluated it for textile and industrial applications, but did not subsequently commercialise them.

TENCEL® is a 100% cellulosic fibre made from purified wood pulp produced from sustainably managed forests. The wood pulp is directly dissolved in hot hydrated *N*-methylmorpholine-*N*-oxide (NMMO) and the solution is then spun into fibres. The solvent is removed as the fibres pass through a washing process and the manufacturing process is designed to recover > 99% of the solvent. The NMMO solvent is nontoxic and the effluent produced is nonhazardous.

It is the direct dissolution of cellulose in an organic solvent without the formation of an intermediate compound, which differentiates this new generation of cellulosic fibre from other cellulosic fibres such as viscose. This led to the new generic name ‘lyocell’ being accepted for labelling purposes.

TENCEL®/lyocell has all the benefits of being a cellulosic fibre – particularly of being water absorbent and biodegradable. For textile applications it is therefore comfortable to wear either on its own or in a blend with a wide range of fibres. The water absorbency also makes it ideal for many nonwoven and paper applications, and its ease of biodegradation enhances its attraction in these markets.

The high strength of the fibres in both dry and wet conditions allows the handling of the fabrics to be significantly optimised by the use of enzymes or a wide variety of finishing techniques. This strength also allows the production of finer yarns and lighter fabrics. The physical characteristics of TENCEL® also result in its excellent blending characteristics with fibres such as linen, cashmere, silk and wool.

The highly orientated structure of the fibres results in a fibril structure – this also occurs with cotton, cupro and polynosic fibres but to a lesser degree. Fibrillation becomes apparent when the fibre is abraded in the wet state and surface fibrils (small fibre-like structures) peel away from the main body of the fibre but remain attached. The fibrillation behaviour of the fibres can be positively exploited by using a variety of different mechanical, chemical and enzyme treatments to produce an attractive range of fabric aesthetics. However, inadequate control of fibrillation in textile dyeing/finishing processes can lead to poor fabric appearance and this was a constraint on initial exploitation of the fibre. For nonwoven and paper applications, the fibrillation characteristic is mainly an advantage. The control of the fibre's fibrillation behaviour is a major area of continuing research.

In this chapter we will describe the manufacturing processes and explain some of the key technological features of the process that must be fully developed to allow commercial-scale factories to be successfully built and safely operated. We will also describe the key properties of the fibre and the technologies that had to be developed to commercially manufacture attractive end products.

9.2 TENCEL® Development Timescale

The development of the process and product can be traced over very many years, and involved four major international companies and a series of key milestones.

The first patent on the use of amine oxides to dissolve cellulose was issued in 1939 and this was further refined in 1968 by D.L. Johnson of Eastman Kodak, who identified that cyclic amine oxides had the best dissolution power. American Enka/AKZO, from 1969 to 1979, patented routes of producing fibres using NMMO but had problems scaling-up the process. AKZO decided to exit the staple fibre business for strategic reasons and subsequently licenced their patents to Courtaulds and Lenzing.

In 1979, Courtaulds in the UK started research using different technology and in 1988 started up a semicommercial plant in the UK (150 t/yr). The first full-scale commercial factory was commissioned in Mobile, USA in 1992 (**Figure 9.1**) and rapidly expanded to 41 kt/yr in 1996. Courtaulds also opened a factory of 37 kt/yr in the UK in 1998.

At the same time, Lenzing of Austria developed its own technology for the process which led to a pilot line in 1990 and then a full-scale production factory of 40 kt/yr in 1997 at Heiligenkreuz, Austria.

The key factor in this rapid expansion was the commercial success in Japan, where TENCEL® Kai achieved very attractive and unique textile products that commanded an excellent price premium. However, the combined annual capacity of these three factories in 1998 exceeded market demand and so remained at this level for several years, as the technologies to use the fibres were fully developed and the best market opportunities were identified. They have subsequently been uprated to a total capacity of 150 kt/yr (2013) and Lenzing has now started to build a further factory with a capacity of 67 kt/yr.

Figure 9.1 The first commercial TENCEL® factory in Mobile

During the 1990s there was a patent battle between the two rivals which resulted in both companies issuing very many patents. Eventually, an accommodation was reached that allowed both to continue and finally, in 2004, Lenzing purchased the TENCEL® business. The combined patent portfolio is very comprehensive and has acted as a significant deterrent to new entrants.

9.3 Process Description

The process depends on the dissolving power and chemical stability of NMMO.

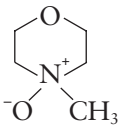

This chemical is soluble in water and its dissolving power for cellulose is maximised when the water content is around 10%. When the water content is increased to around 20% it can cause cellulose to swell and if is reduced much below 10%, the melting point increases significantly and the cellulose solutions become difficult to process and chemically unstable at the higher temperatures.

The outlines of the processes developed by both Lenzing and Courtaulds are the same, but there are significant differences in the manner in which they are applied. Essentially, the wood pulp is mixed with the NMMO solvent, processed to achieve dissolution and then extruded through small holes to generate fibres. These are washed in water then dried, **Figure 9.2**.

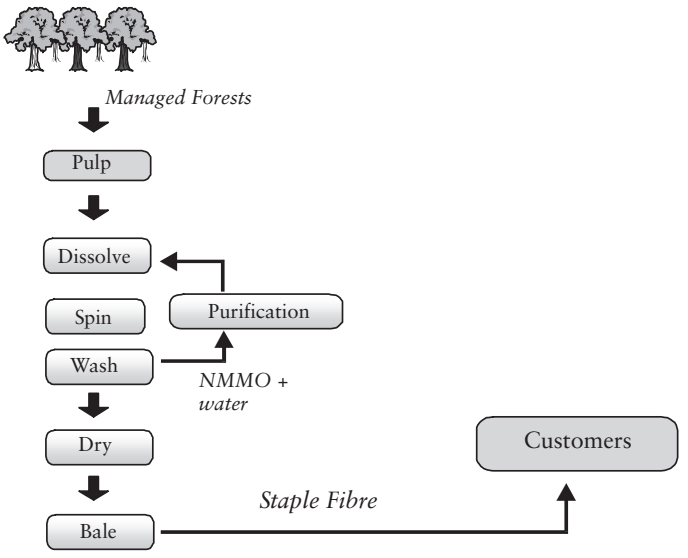

Figure 9.2 TENCEL® – production route

To achieve effective dissolution, the pulp is firstly wetted out with dilute aqueous NMMO to fully penetrate the pulp fibres. The excess water is then removed by heat and vacuum to give a homogenous solution with a minimum of undissolved pulp particles and air bubbles. The high viscosity of the solution leads to higher operating temperatures and pressures than in the viscose process. Cellulose fibres are formed by extruding the solution into an air gap, coagulating and washing in water, and then drying. The NMMO is recovered and recycled after the dilute aqueous solution has been purified and concentrated.

9.3.1 Pulp and Premix

Good quality dissolving pulp is used to facilitate both the consistent operation of the manufacturing plant and the production of optimum properties of the TENCEL® fibre. Typically, the degree of polymerisation (DP) of the pulp is in the range of 400 to 1,000 units and the TENCEL® made by Lenzing fibres have a DP > 600.

The pulp is firstly fed into a shredder, which cuts it into small pieces, and these are then accurately metered into a plough-shear mixer together with a 76–80% NMMO solution in water. A degradation inhibitor (usually propyl gallate) is also added at this stage. The mixture is processed at 70 to 90 °C in the mixer where a number of high speed refiners break the pulp down and aid solvent wetting. The resultant mix consists of swollen pulp fibres and has the consistency of dough. It is then metered to the dissolution stage of the process.

9.3.2 Dissolution Stage

In this stage of the process, the premix is heated and agitated under vacuum to remove sufficient water to obtain the cellulose solution. The solutions are viscous, amber coloured, sticky to the touch and contain 10 to 18% cellulose.

At Lenzing, this process is carried out in a wiped thin film evaporator called a Filmtruder, **Figure 9.3**. This consists of a vertical cylindrical vessel with heated jackets around the outside and a rotating shaft down the centre. Blades attached to the shaft smear the material around the inner surface to accelerate the evaporation process and to transport the solution down the vessel. The configuration of these blades is designed to maximise the output of the unit. The process is carried out under vacuum to reduce the temperature of the solution (to approximately 90 to 120 °C) to avoid chemical degradation of the solution.

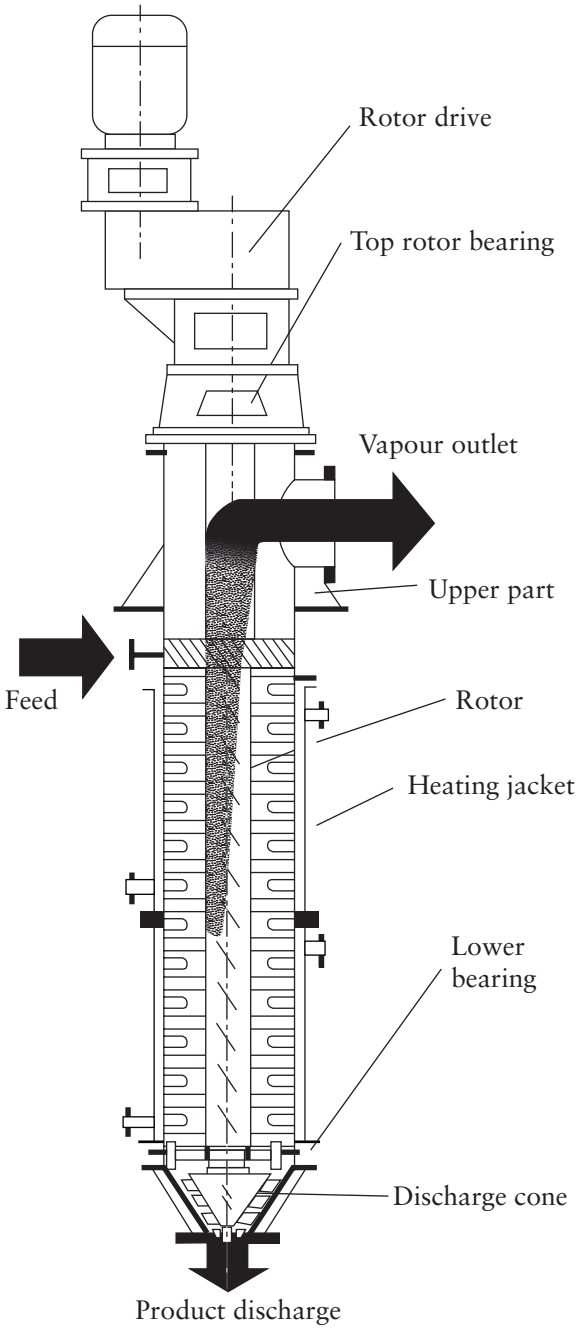

Figure 9.3 Buss Filmtruder

A horizontal mixer with surface wiping can also be used for this process. Courtaulds successfully carried out its early developments using a single shaft kneader reactor supplied by LIST AG, but when it came to quickly scaling-up the process it was found that the Filmtruder configuration was more capital efficient. Furthermore, there were safety concerns about the kneader reactor because significant quantities of the partly dissolved material were held up in the vessel. This material had a high viscosity and could be rapidly heated, by the mechanical action of the mixing rotors, if there was any disturbance of the process flow rate. Conversely, it was difficult to cool this material because of the relatively low heat transfer area. Thus, we felt that internal temperature control was more difficult and the operation needed to be carried out at lower overall temperatures – which further reduced its capital efficiency. As will be explained later, overheating of the material in the reactor could result in a violent decomposition, so a practical method of venting the large quantity of decomposition gases would add significant complexity and cost.

We should add that these considerations were made about 20 years ago, so they may well have been addressed by the latest LIST machines.

9.3.3 Solution Transport

The solution leaving the Filmtruder is transported to the spinning machine *via* a cooler, a buffer tank and the main filters using a series of specialised pumps. Pressures of up to 180 bar are required, so the steel piping system must be made to the highest standards. It is also necessary to include bursting discs at strategic points along the transport system because of the risk that an exothermic runaway reaction can occur due to the chemical degradation of the solution. This reaction can generate volatile compounds which cause a rapid increase in process pressure and must be relieved safely to avoid serious damage to the equipment and the operating staff. This aspect is described in more detail in **Section 9.6.1.**

9.3.4 Filtration

In common with all fibre processes, it is essential to remove particulate impurities from the solution before spinning. In this process, most of these come from the wood pulp and consist of undissolved fibres and inorganic compounds such as sand and ash.

In the TENCEL® process there are two stages of filtration, a) large centrally located units and b) single filter elements on each spinning position. The filters themselves are sintered stainless steel candles and because of their high cost they must be reused after they become blocked with impurities. In the Courtaulds process, they are washed by

an off line process using NMMO followed by ultrasonic washing. Lenzing developed a novel design for their first stage filters where the dirty filters are 'back flushed' with fresh solution which is then discarded from the filter units – see Lenzing patent EP 0915729 [1].

9.3.5 Spinning

A commercial spinning unit consists of many tens of spinning jets arranged in rows, **Figure 9.4**. The fibre threads (tows) are collected together as they pass down the machine and are then passed through to the washing machine.

The cellulose solution is split into substreams and supplied to each jet using a metering pump from which it is spun through an air gap into a spin bath containing a dilute NMMO solution. The jets each have many of thousands of tiny holes through which the solution is extruded and just below each jet face is a small air gap above the surface of the spin bath. Across the air gap, a forced air flow is supplied to stabilise the spinning. The fibres that are then formed are pulled down through the spin bath where the cellulose is regenerated in the dilute solvent. The fibres are usually stretched, in the air gap, by the pull of traction units.

The arrangements of the spinning cells that were developed by Courtaulds consisted of rectangular jets feeding into spinning baths in which the fibres are discharged through the bottom of the bath. The resulting fibres have a circular cross section. Lenzing uses doughnut-shaped jets and feeds the fibres underneath a guide within the bath, so that they can be removed from the surface of the bath (dip spinning). The passage of the fibres under the guide whilst they are still being formed gives them a slightly deformed, less regular cross section

The technology of air gap spinning was the most critical factor in being able to scale-up the process and is described in more detail later.

9.3.6 Fibre Washing

The fibres are next washed in water until all of the NMMO is removed.

In the Courtaulds process, the fibre is washed as a continuous tow (**Figure 9.4**) through a series of wash troughs, which consist of a shallow bath containing a number of wedges that deflect the tow band to improve washing efficiency. The aqueous solution moves countercurrent to the fibre and is fed into the spin bath system. The fresh water feed rate is adjusted to achieve the required concentration of the spin bath.

(a)

(b)

Figure 9.4 Stages of the TENCEL® process. (a) Spin machine and (b) fibre band before washing

In the Lenzing process, the fibres are first cut to their required length (usually 38 mm) and then sluiced onto a moving porous bed which transports the bed of fibre down the washing machine. Squeeze rollers are used along the line to improve its efficiency and the same countercurrent wash flow is used to build-up the NMMO concentration for feeding into the spin bath.

9.3.7 Fibre Treatments

After the fibre has been washed to remove all of the NMMO it can be treated in a number of ways depending on the market requirements:

- Chemical treatments can be applied to control fibrillation – these are described in detail later;
- The fibre could be bleached if required; and
- Soft finish and antistatic agents are applied to make processing easier.

9.3.8 Fibre Drying

In both the Lenzing and Courtaulds processes, the fibre is dried using conventional fibre drum dryers. The fibre is transported through the drier on the outside of the drums and is held in place by the passage of the hot air from the outside to the inside of the drums.

Steps must be taken to ensure that the fibres do not become stuck together in clumps during drying and that they leave the drier in a suitable condition for further processing. Thus in the tow process, the tow must be overfed into the drier to allow a waviness to form and during the staple process, the fibres must be opened before the drier, using pin openers. The choice of fibre finish is obviously very important.

9.3.9 Crimping, Cutting and Baling

In the Courtaulds process, the dry fibre is crimped using stuffer box technology in which steam is injected into the stuffer box to plasticise the fibres. This proved to be technically demanding as the fibres need to be uniformly distributed and of equal tension. Fibre damage can also occur if any wet patches form on the fibre in the stuffer box. Adequate crimp has to be imparted onto the fibres otherwise the fibre has insufficient cohesion to allow high-speed carding.

The crimped tow band is fed directly into a radial blade cutter and then airveyed to the automatic baling presses. The bales of staple fibre are then dispatched to the customers. This process yields fibres that are very open so that the individual fibres can be readily separated out in the next stages of processing. The form of the fibre mass is similar to that of the polyester staple.

The process used by Lenzing to cut the fibres after spinning is essentially the same as that used in the viscose process and in the TENCEL® process it results in the fibres having improved properties as described in Lenzing patent EP 0823945 (US 5863478) [2]. This washing process also generates crimp in the fibres as they are crushed together by the mangle rollers. This has proved very effective in giving the fibres a good processing performance in customers' mills and is described in Patent US 6117378 [3]. The wet bed of fibres must be passed through pin openers to prevent the fibres sticking together in clumps during the drying stage. After drying, the fibres are opened and then airveyed to the automatic baling presses. The form of the fibre mass is very similar to that of viscose fibres and distinctly different to those made via the crimping route.

9.3.10 Solvent Recovery

Diluted NMMO solvent from the spinning machine, from spillages and from waste recovery must all be collected to ensure that the expensive solvent is not lost – over 99% of the solvent used is recycled and recovered by the process. The entire spinning and washing area has to be contained so that spillages can be retained and then recovered. All the waste cellulose solution must be shredded and washed so that all the NMMO can be recycled.

The recovered NMMO will retain a range of carbohydrates and other soluble products from the original wood pulp, plus those generated by the chemical degradation that occurs during the dissolution and spinning stages. The NMMO oxidises cellulose during the process, which will reduce the DP of the cellulose and form coloured compounds that will discolour the fibres unless they are removed. Carboxylic acids are also generated that would reduce the pH of the solution and destabilise it if they were not removed. The NMMO degrades to *N*-methylmorpholine plus a wide range of other amines – it can react with itself or with the carbohydrates in the solution. These reactions are catalysed by transition metals such as copper and iron, so it is therefore essential that the levels of metal ions be maintained at very low levels. Propyl gallate is usually added to the solvent to stabilise the system during normal processing. It appears to act as both an antioxidant and a chelating agent, and is effective at both stabilising the pulp DP and reducing solvent decomposition.

Solvent recovery consists of filtration and ionic purification of the dilute solvent and then evaporation of the excess water to increase the concentration to that required in premixing. Typically, the dilute solution will be in the range of 20 to 35% NMMO and the concentrated solution is in the range of 60 to 80%.

The purification process consists of both cation and anion ion-exchange beds. These remove various transition metal ions that would destabilise the solution and other metal ions that could build-up to generate insoluble salts. They also remove the carboxylic acid and coloured contaminants that would otherwise discolour and destabilise the solvent.

The NMMO is concentrated in a multiple effect falling thin film evaporator that is steam heated. This stage of the process also removes the volatile impurities, such as amines, that had built-up earlier in the process. The water that is removed is reused in the process.

9.3.11 Fibre Properties

The cellulose fibres produced by this route differ very significantly from those made by the traditional viscose route in that they are stronger, particularly in the wet state, see **Figure 9.5,** and have a greater stiffness (see **Table 9.2** in **Section 9.8.4.1**). This means that they give excellent yarn strengths, and can yield very good wash stability and durability in textile products. The wet strength is particularly valuable in nonwoven and paper products when combined with the excellent water absorption.

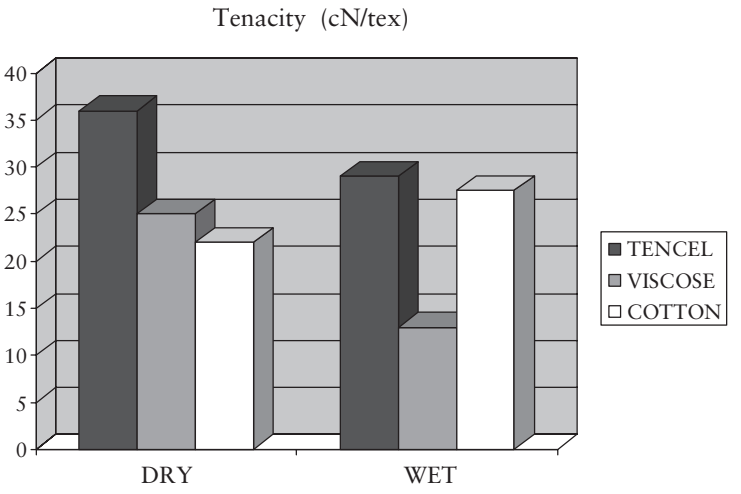

Figure 9.5 Fibre properties

The fibres are more highly orientated and crystalline than viscose, and this leads to the fibrillation tendency that will be discussed below.

9.3.12 Environmental Factors

As the reader will readily appreciate from the above, the TENCEL® process is environmentally very attractive for future investments. The solvent has a very low toxicity and the solvent recovery rates are extremely high. Almost all of the wood pulp is converted into the finished fibre. Most of the water used is also recycled and the low level of effluent is readily purified by conventional techniques. We have emphasised that there are safety considerations that must be designed into the factory, but also

that there are highly effective design features to safeguard the safety of all concerned and that these have been proven in practice.

The TENCEL® fibre itself is readily biodegradable and is made from wood pulp that is itself a renewable resource. The forests that are the ultimate beginning of the supply chain are all managed to ensure sustainability and high environmental standards.

Comprehensive studies of the LIFE CYCLE impacts of cellulose and synthetic fibres were published by Shen and Patel in 2010 [4]. These clearly showed the overall benefits of the TENCEL® process in all environmental aspects. The viscose processes operated by Lenzing in Austria, also scored highly because of the efficient process integration of their factory. Cotton scored relatively poorly because of high ecotoxicity impacts, eutrophication, water use, land use, and relatively low land use efficiencies.

9.4 Key Technological Factors

As indicated earlier, there are fundamental difficulties in the technology for manufacturing TENCEL® fibres that must be understood and overcome before a commercially viable factory can be operated efficiently and safely. For the core process these are the *air gap spinning* of the fibres and *the safe control* of the *chemical reactions* that occur during the process.

Another key feature is the quality, specification and price of the *wood pulp* that can be used in the process, since it differs in a number of significant ways to that supplied by the industry at the time TENCEL® was being developed.

The other fundamental challenge is the control and *manipulation* of the tendency of the fibres to *fibrillate* during wet processing.

9.5 Air Gap Spinning

Spinning the fibres into an air gap before they are coagulated is fundamental to the lyocell process and product: stretching of the filaments after extrusion is necessary to reduce their diameter to a commercially acceptable level. This is because relatively large spinneret hole diameters (> 70 micron) are required to accommodate the high viscosity and viscoelastic characteristics of the cellulose solution. Stretching also orientates the molecules in the fibre so that the fibre has the sufficient strength and extensibility necessary for commercial uses in the textile and nonwovens industries [5].

Attempts to extrude the solution directly into an aqueous coagulant are difficult (because of the 80 °C melting temperature of the solution) and invariably produce fibres that are weak and brittle. This is because the coagulation of the fibres is so rapid that they cannot be sufficiently stretched once immersed in the coagulation solution.

Stretching of the extruded filaments in the air gap is fundamentally difficult when the process is scaled up to a commercial level: significant development work was required by both research teams before practically viable processes could be achieved. These are described in the key patents taken out by these companies and in the following sections we will explain the basic principles that underlie the processes.

In order to achieve the necessary fibre strength, the solution is stretched at a so-called 'draw ratio' of 4 to 10 (**Table 9.1** [5]). This means that the extruded filaments are accelerated up to a speed 10 times the speed at which they leave the spinneret.

The *viscosity of the cellulose solution reduces very significantly when it is drawn* at its extrusion temperature (this effect is called 'elongation viscosity thinning') [6, 7]. This means it is prone to unstable drawing or rupture if high rates of draw are attempted at the extrusion temperature. *In order to render the filaments stable against this stretching they must be cooled down.* This is because the cooler the solution is, the higher is its viscosity. Higher viscosity means more stability during stretching.

On a laboratory scale, if only one filament or a small number of well-spaced filaments are spun into air that is at a lower temperature (ambient temperature), the filaments will cool down on their own by way of two mechanisms [8]:

- They lose heat by radiation; and
- Water is evaporated from the filament surface (the extruded solution contains water) so the latent heat of evaporation further cools the filament.

This 'natural' cooling makes spinning possible because it causes a very significant increase in viscosity.

In order to produce commercial quantities of staple fibre at an economically viable rate, it is necessary to extrude a large number (> 20,000) of closely packed filaments per spinneret. Typically, the speed at which such large bundles of fibres can be spun is limited to 20–100 m/min because of the fluid drag on the fibres, caused by their passage through the aqueous coagulation bath. At higher speeds this drag becomes excessive, and limits both the overall productivity and the fibre quality.

The high number and area density of spun filaments mean that the temperatures of the filaments, in the central regions of the array in the air gap, are close to the temperature

of the extruded solution because the air is stagnant between the filaments and heat loss by radiation is severely hampered.

Furthermore, the water evaporated from the filaments cannot be transported away from the dense filament array. Thus, high air gap humidity builds up in these central regions of the array. This means that further evaporation of water from the filaments is also limited.

Thus, both 'natural' cooling effects as discussed above are severely impaired – in fact, the filaments in the centre of the array will not cool down at all. This means that the necessary reduction in viscosity cannot be achieved and the filaments are prone to unstable drawing or rupture upon stretching.

To achieve stable drawing of the filaments in the air gap, when there is a dense array of fibres, it is therefore necessary to force air across the air gap to cool the fibres and to thereby increase their viscosity.

Effect of the transfer of the filaments into the precipitation bath: there is also another fundamental reason why forced air flow is required – to overcome the disruptive forces imposed on the filaments by the liquid in the precipitation bath. The downward movement of the filament into the aqueous bath generates a flow of the bath liquor in the direction of the fibre movement, i.e., the fibre drags the liquor down with it. This is not a difficulty when spinning a single filament, but even if there are only a small number of filaments that are closely spaced they can easily form a vortex (whirlpool) which will twist the filaments together and cause them to stick to each other.

The basic laws of physics dictate that the way to overcome this problem is to increase the stiffness of the filaments so that they are not easily deflected. In practice, we find that hot filaments of the solution have such a low stiffness that they easily stick together – unless they are physically well separated (say 10 mm). However, if they are cooled in the air gap they become much stiffer and can be spun in much closer proximity (less than 1 mm).

In order to have a commercially viable factory, it is essential that a very large number of the filaments are spun in close proximity (about 1 mm – see last section). This amplifies the technical problem in the precipitation bath since the movement of so many fibres downward from the bath surface acts as a very powerful pump, so that high flows of liquor must flow across the bath surface to replace the liquor removed, as shown in **Figure 9.6.**

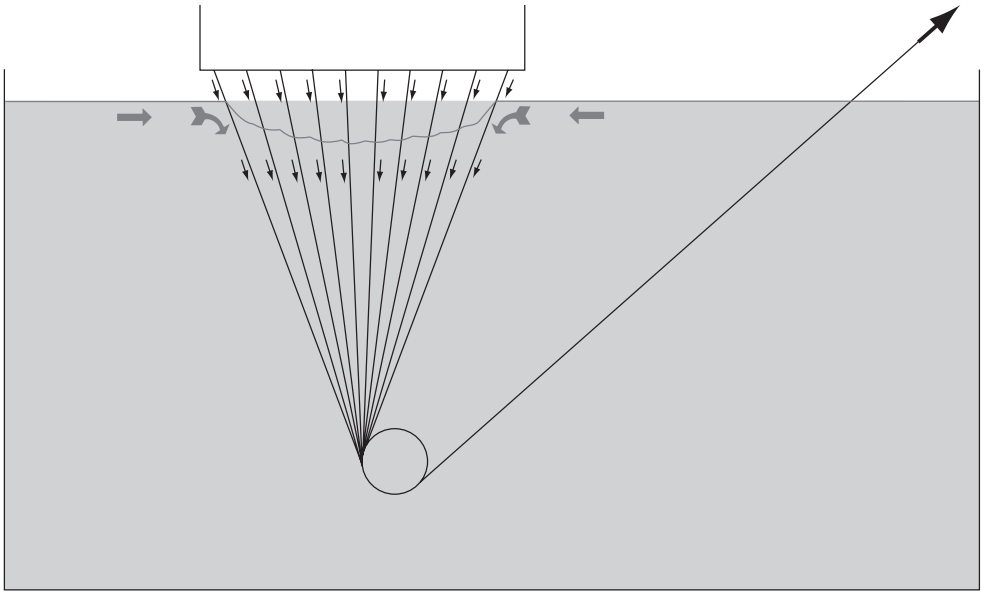

Figure 9.6 Liquor flows in a spinning bath

If the filaments have a low rigidity this liquor flow becomes very turbulent causing the filaments to swing so that they will very rapidly stick together. Filaments being stuck or fused are of no commercial use.

Thus, it is essential that the filaments are given sufficient stiffness in the air gap to resist the strong forces caused by the liquor flows in the precipitation bath.

Practical solutions in the air gap: the only practical solution to the basic physical problem of achieving stable spinning at a high output rate is to cool the filaments by forcing air across the air gap. This forced air will cool the filaments by removing both the heat flux from the filament flow and the water vapour that is emitted. The filaments can then be drawn in a more stable manner and become much more rigid so that they do not touch. In practice, it is also found that the turbulence in the coagulation bath is very significantly damped down when the filaments are stabilised in this manner.

A wide variety of practical options were tried in the early stages of the process development – low spin temperatures (80 °C to 100 °C), extrusion hole sizes of 70 microns to 300 microns, filament velocities of 10 to 300 m/min, air gap distances of 5 mm to 300 mm and spinneret hole spacing of 5 mm to 0.5 mm. In all cases, it was

found to be essential to establish air gap cooling in order to achieve an output rate that would allow us to construct an economically viable production plant.

This is fundamental because in all cases, where a high output of fibres was achieved, there was a high heat and water vapour flux from the filaments in the air gap, and a large pumping action by the filaments in the precipitation bath. Unless this heat and moisture are removed by the forced flow of air, the spinning is very unstable.

Configurations of spinning jets: forced cooling of the filaments in the air gap also dictates that the flow of air over the filaments is as uniform as is practical. Thus, if some of the fibres are cooled more rapidly than the others their draw profile in the air gap is different and this can lead to their premature breakage. When this occurs, globules of undrawn solution build-up on the jet face and cause the neighbouring filaments to break as well. The resultant undrawn mass of solution eventually drops into the spinning bath, gets taken up within the moving bundle of fibres and finds its way into the final bale of fibre. It then causes defects in the customer's process and they rightfully complain!!! This undrawn mass of fibres is called 'trash' and stringent technological methods are used in all the Lenzing factories to prevent it occurring.

The most important method of avoiding trash is the optimum design of the spinning jet and the air feed to ensure uniform cooling of the filaments. The technology used by Courtaulds was based on the use of rectangular jets together with a uniform air feed, in combination with an extraction system that helped to maintain the flow of air close to the jet face. Lenzing developed a configuration based on a ring of filaments in which the air is fed into the centre of the centre of the ring by means of a shaped nozzle.

Practical solutions in the precipitation bath: as already mentioned above, TENCEL® fibres are formed by precipitation and washing of the extruded solution in an aqueous solution. For practical purposes, the solution filaments are drawn downwards into the coagulation bath where cellulose is very rapidly precipitated and the fibre strength increases rapidly.

Lenzing and Courtaulds developed different configurations for coagulating the fibres and then removing them from the spinning bath. The Lenzing process is the dip spinning configuration, where the tow bundle passes under a guide and is then removed from the surface of the bath. In the Courtaulds process, the tow bundle passes downwards and is removed through the base of the bath. In both processes, configurations of the fibre bundle are condensed rapidly as it moves from the bath surface to either the bath exit hole or the guide bar within the bath. This generates a very significant flow of spin of the bath fluid as explained earlier and the net result is to generate very significant circulation flows within the bath. These must be controlled

by bath unit design otherwise erratic turbulent flows will disrupt the spinning process. Ultimately, these flows will act as a significant factor in determining the maximum productivity that can be achieved by each spinning unit.

When the fibres are removed from the coagulation bath they also carry-over significant volumes of liquor that is thus lost from the bath. This liquor must therefore be replaced in such a way as to maintain the optimum air gap distance. If this distance is increased (which is the result if liquor in the bath is constantly carried over by the filaments, i.e., the liquor level gets lower and lower), the spinning stability deteriorates and the incidence of breaks and stuck filaments increases. This is because as the filaments in the air gap become longer they become much more easily displaced by the air flow and the coagulation bath turbulence. On the other hand, if the distance is reduced below the optimum, the spinneret surface can become contaminated by coagulation liquor (e.g., from splashes) which will cause a breakdown in the spinning process.

The coagulation liquor also picks up the NMMO solvent from the filaments. Therefore, the concentration of the NMMO in the bath needs to be maintained at a suitable level by adding more dilute liquor. If the concentration becomes too high, the fibres in the coagulation bath become weaker and more easily damaged by rubbing on the guides and other surfaces that they pass over. In an extreme case the fibres can be so weak that they break when they rub over the guide surfaces.

Thus, it is necessary to take measures to keep both the level of the liquor in the coagulation bath and the concentration of the NMMO constant.

Patent status: as will be obvious from the above description, the development of a commercially viable process for air gap spinning of lyocell fibres was very technologically challenging and so it will be of no surprise that many of the features, particularly the use of a cooling cross draught, were the subject of patents owned by Lenzing which are still in force [9–12].

9.6 Safe Control of Reactions between Cellulose and *N*-methylmorpholine-*N*-oxide

Good control of the chemical reactions that occur during the lyocell process is essential for both safety and economic reasons.

9.6.1 Chemical Reactions occurring in the Process

NMMO is an oxidising agent and can react with itself at elevated temperatures –

particularly if it contains trace metal catalysts. The reaction is exothermic and the formed by-products (e.g., morpholine and *N*-methylmorpholine) are volatile and flammable. Thus, there is a serious risk of fires or explosions if these by-products are not correctly vented.

Cellulose and NMMO also react together at normal operating temperatures – the NMMO oxidises both cellulose and itself. The dissolution of cellulose in NMMO occurs at an elevated temperature and the resulting solution must be maintained at > 80 °C to avoid solidification or getting too viscous to be pumped. At temperatures above 120 °C, the reaction becomes rapid. Copper, iron and other metal ions in the solution will catalyse this reaction very significantly, therefore reducing the temperatures at which severe dope degradation and exothermic runaway reactions will occur [13].

Degradation of cellulose in the solution reduces its molecular weight and generates a wide variety of highly coloured impurities and carboxylic acids. If these are not removed they will reduce the pH value of the solvent and this will *further* destabilise the system – as well as discolour the fibres produced by the process. It is therefore essential to follow the maintaining of the solution pH as described in Lenzing patent EP 0695324 (US 5628941) [14].

Degradation of the NMMO component in the solution generates a range of amines and eventually the degraded product becomes solid as the dissolving power of the solvent is lost. Generally, this is seen as a dark brown or black solid or powder.

As stated earlier, it is essential to incorporate chemical stabilisers into the cellulose solution otherwise the cellulose degradation and solvent discolouration become excessive, even during the short processing times experienced during normal operation. Clearly, any process interruption can cause even worse problems and result in a very inconsistent product.

The reaction that occurs generates heat (it is exothermic) [13]. If the reaction gets out of control in a well-vented vessel it will generate a large volume of dark smoke that contains flammable chemicals with a relatively low flashpoint – thus a serious fire can occur. If the reaction occurs in a sealed unit then there will be a very rapid increase in both temperature and pressure, since the reaction products are volatile. The pressure generated can burst high-pressure pipes and other process units such as pump seals. The force generated can be explosive, since once rupture occurs there is a serious risk of conflagration.

The risks of an exothermic rupture occurring are made worse by the fact that the thermal conductivity of the cellulose solution is very low, so that removal of the

reaction heat is difficult. In the case of a commercial-scale plant, there is a need to transport literally tonnes of spinning solution per hour from the dope production unit(s) to the spinning machine(s). Therefore, in such a large-scale commercial plant relatively large diameter pipes are required and this makes handling the solution difficult. Furthermore, the filtration units and dope buffer tanks have large diameters.

The plant must be designed such that if there is a process interruption and the residence time of the solution in the process equipment is extended from minutes to hours, the process plant must remain stable and safe. There is a very real risk that if a large mass of solution is left stationary, hot regions in that mass can become thermally unstable and eventually exotherm.

There is also a serious risk in a commercial plant that the solution may become overheated in the dissolution unit. These units use high-powered rotating mixing rotors which can impart a very significant degree of heating energy into the solution. Under steady operating conditions this is not a problem, but interruptions can and do occur and these can result in rapid increases in solution temperature. This was one of the reasons why Lenzing preferred to use the Filmtruder – as discussed earlier.

The most serious risk can occur if metal salts from, e.g., iron or copper get into the NMMO system. This can occur from a variety of accidental causes (e.g., small pieces of copper wiring dropping into the system from electrical repairs), from corrosion of process equipment or from a build-up in level as the solvent is repeatedly recycled.

Usually, the first sign of an uncontrolled exotherm occurring is a rapid rise in process pressure. At this point it is too late to initiate emergency cooling. It is thus essential that any lyocell plant has a pressure relief system that will protect the integrity of the process plant and the operating staff, as well as safely venting the by-product vapours.

The problems described above can all be controlled by suitable process designs and control of operating conditions as described below. It must be emphasised that *all* of the above factors must be adequately controlled in a full-scale process plant if it is to be operated safely and economically.

9.6.2 Practical Solutions for Control of the Cellulose Reaction with N-methylmorpholine-N-oxide

9.6.2.1 Cellulose Solution Temperature Control

As explained earlier, a commercial-scale lyocell plant uses large diameter (50 to

300 mm) high-pressure jacketed pipes to transport the solution from the cellulose dissolution unit to the filtration and spinning equipment. The use of large diameter equipment poses the problem of controlling the stability of the solution as explained earlier. The problem is exacerbated by the fact that the solution will solidify if the cooling jacket temperature is below around 80 °C, so the cooling gradient is only low.

The solution to this problem is to work within carefully defined temperature ranges in the pipes – these are described in Lenzing patents. Patent EP 0668941 B2 [15], defines a temperature range at which a solution to be transported through a pipe in the lyocell plant is to be controlled. One claim refers to the temperature in the centre of the pipe, whereas the second refers to the temperature at the interior wall of the pipe. More precisely, these claims define maximum temperatures that should not be exceeded. This maximum temperature is defined by way of an empiric formula that is based on the diameter of the pipe as the variable parameter.

As an example, if one employs a pipe with a diameter of 250 mm, the temperature in the centre of the pipe must be controlled to be equal or less than about 125 °C and the temperature at the interior wall of the pipe must be controlled to be equal or less than about 111 °C.

By controlling the temperature of the solution to remain in the range as defined in the patent, not only can the transport of the solution during continuous production be conducted safely, but also in case of process intermissions (such as for plant maintenance) it is possible to safely keep the high amounts of solution within the pipes for a longer time.

Experiences with production plants show that the penalty for not controlling the temperature of the transported solution, according to the defined thresholds, will sooner or later lead to exothermic reactions, with the risk of explosions and danger for the health of the people working there. This means that whilst an exothermic reaction will not necessarily occur within only minutes, hours or may also be some days of operating at temperatures higher than defined, it will occur eventually. In no commercial production plant, can one afford an inherent risk of explosions.

It is therefore essential to take measures to control the temperature of the solution as it passes through the transport system.

9.6.2.2 Pressure Relief to Accommodate an Exothermic Reaction

Extensive experience in operating commercial-scale plants has taught us that there is a very significant risk of serious exothermic events occurring. The causes of these

events were only determined by thorough research into the individual designs of the operating plants and cannot be divulged here. It has been concluded that in practice it is not possible to ensure that runaway reactions will never occur.

Thus, the plant must incorporate a pressure release system that will allow the degraded materials to be discharged safely. This pressure release system comprises a disc which is connected to the transport pipe and which is displaceable under the action of (increased) pressure caused by the runaway reaction. These 'bursting discs' will rupture once the pressure reaches a certain limit, allowing the pipe to be vented and to release the pressure.

Since the cellulose solution has a very high viscosity, the design of the plant has to incorporate the complex physical details of how the gaseous degradation product can be vented to the nearest pressure release point, through significant lengths of the solution, as well as how the large volumes of solution and gas can be safely discharged.

There are further serious design challenges to achieving this because the discs must remain clear of degraded and/or solidified material during normal process operation. If there is an unheated, dead area in front of the disc, the polymer solution will cool below its melting point and solidify. If there is a 'dead' area that is heated, the solution will decompose to the solid residue described earlier, which will block off the disc such that it will not perform its function in case of a runaway reaction.

Thus, other Lenzing patents EP 0662204 (US 5337776) and EP 0789822 (US 5890504) [16, 17] show that the disc must be arranged such as to be continually washed by the flow of the solution to prevent the build-up of solidified degraded solution. According to these patents at least part of a disc used in an overpressure relief device is flushed by the solution passing through the pipeline.

Thus, it is not only absolutely essential to have a pressure relief system in a lyocell plant, but it is also important to employ a design that ensures the bursting disc is flushed by the solution passing through the pipeline.

9.6.2.3 Operation of Pumps used to Transport the Cellulose Solution

The cellulose solution must be pumped through the transfer pipes and filters, as well as through the metering pumps that supply the spinning jets. These pumps are invariably designed using the solution itself as a lubricant for the moving components. However, there is a major problem in this respect with the solution because it degrades to a dark powder when subjected to excessive or prolonged heating. This can result in the pumps seizing up and overheating. To remedy this problem it is necessary to design

the pumps such that there is a free flow of the solution through the pump bearings and this is described more fully in Lenzing patent EP 0781356 (US 5795488) [18].

9.7 Wood Pulp Requirements

The NMMO solvent is capable of dissolving a very wide range of wood pulps, so in theory there should be fewer constraints on the choice of pulp than for the viscose process. In particular, NMMO can dissolve all the main cellulose components plus other organic compounds such as lignins and resins. However, it will not dissolve inorganic impurities, and the process economics and product quality requirements inevitably need to be considered, reducing the number of commercial options.

The specification of the wood used for the TENCEL® process was derived over many years by a process of iteration with the pulp suppliers. When the TENCEL® developments were in their infancy at the pilot scale there was insufficient demand on the suppliers to justify the large investments required to make a special variant. This changed once TENCEL® manufacturing plants became established, but the evolution is still proceeding.

The essential requirements for the pulp were a relatively low degree of polymerisation (DP) – around 600 units, a 'suitable' DP distribution and a high purity – all at a very minimum of cost. The low DP requirement was primarily driven by the capital and operating cost targets for the TENCEL® process. This is because there are practical limits to the viscosity of the solution that can be processed. If a typical viscose pulp (over 1,000 DP units) is used then the cellulose content of the solution has to be lower to compensate. (It should be noted that in the viscose process there is a very significant degradation of the pulp DP during the dissolution and spinning process, whereas this does not occur in the TENCEL® process.) When a lower pulp DP is used, the cellulose content of the solution can be increased, leading to a very significant increase in the capacity of the solution-making equipment and a reduction in the solvent recovery costs. The fibre properties are not significantly affected by this move to a lower DP.

Both Courtaulds and Lenzing therefore started their commercial developments using the limited numbers of low DP prehydrolysed kraft (PHK) pulps that were available at the time. The hardwood pulps proved easier to process and dissolve at the time and were therefore used initially. The option of using irradiated pulp was also investigated, but would have involved a significant capital investment and the trial lots used in the evaluation gave a poorer performance.

The rheological characteristics of the cellulose solution are also significantly affected by the DP distribution of the pulps. A higher DP component tends to increase the elongational viscosity of the solution, which can aid the stability of the spinning in the air gap – i.e., the drawn filaments have greater rigidity and stability. Thus, the first pulps used by Courtaulds were a mixture of low and high viscosity PHK pulps. It was found that optimisation of these pulp formulations was most easily and accurately performed by measurements of spinning stability rather than measurements of DP distribution. These factors are fully described and covered by Lenzing patents EP 0918894 (US 6241927) and US 6093355 [19, 20].

The range of pulps that can be used commercially has increased significantly in the last 15 years because of close collaboration with various pulp suppliers who could see the potential of the TENCEL® process. Thus, the sulfite and kraft processes, in combination with both hardwood and softwood species, have been successfully developed to produce pulps with lower DP that have performed well in both processing performance and fibre properties.

The process is tolerant to the level of hemicelluloses in the pulp in that most are retained within the resultant fibre and not lost into the solvent system. However, in certain circumstances there can be some loss in fibre properties and an increase in fibre discolouration. A high copper number' of the pulp can also be associated with poorer fibre whiteness.

Inorganic impurities proved to be a significant problem with some pulps. The cellulose solution filtration system uses relatively low capacity sintered metallic gauzes, which can rapidly become blinded if the impurity level is too high. Obviously, the particle size distribution can have a significant impact so it's not just the ppm levels that must be considered. Silica is a particular problem but fortunately, the level can be controlled during the pulping process by using centricleaners.

Metallic impurities must also be avoided as they can destabilise the NMMO – pieces of rust dropping from a drier was one example that caused problems at one stage.

The process stability during the manufacture of TENCEL® is an issue that needs to be addressed within the pulp quality specification. The rheology of the cellulose solution is significantly affected by the cellulose content, average DP and DP distribution, so these parameters need to be maintained at a steady level both in the very short term and over a period of days. This can be achieved by suitable pulp-blending regimes in the TENCEL® factory, but good testing and supply coordination with the pulp supplier is essential to minimise disruption.

9.8 Control and Manipulation of Fibrillation

9.8.1 Background

There are two main applications and market routes for TENCEL® fibres – textiles and nonwovens. The early stages of market evaluation quickly established that the textile market commanded higher prices for a new fibre with the properties of TENCEL®. However, textile applications all involved converting the fibres into coloured fabrics and there were some challenges in using some of the processes in common use in dye houses. These technical issues were mainly due the tendency of the fibres to fibrillate (or split) when subjected to wet abrasion. We will now elaborate on the nature of this effect and the many avenues that were developed to successfully exploit it.

The early commercial success of TENCEL® in Japan was due to the development of fabrics that exploited the unique characteristic of fibrillation – the so-called peach skin touch. A low and uniform level of fibrillation on the surface of the fabrics gave them a very attractive handle and soft touch, and led to a very rapid growth in the market for soft denim jeans. This approach was then rapidly broadened into a wider range of fabrics in Japan and a very lucrative business was created. This business model was then reproduced worldwide and launched TENCEL® into the success that it now is.

The tendency of the fibre to fibrillate reflects its highly orientated and crystalline structure. It is this same structure that gives the fibre its high strength in both dry and wet conditions, and which is the basis of many of its key market attributes. Hence, exploiting its novel performance characteristics has been the basis of many technical and commercial developments.

It must also be emphasised that fibrillation does not pose technical problems for nonwoven markets and can be a benefit for certain applications, such as papers. Thus, a very successful business in nonwovens products has been developed in parallel with the textile one.

9.8.2 What is Fibrillation?

Fibrillation is the longitudinal splitting of a single fibre filament into microfibres as shown in **Figure 9.7** and occurs as a result of wet abrasion, i.e., when the fibres are rubbed against another surface. The fibrils themselves are so fine that they become virtually transparent, but they can give a frosty appearance to a finished fabric.

Figure 9.7 TENCEL® fibrillation

In cases of extreme fibrillation, the loose fibres on the surface of the fabric fibrillate and tangle together to form very light coloured pills **Figures 9.8** and **9.9**. The appearance of the fabric becomes totally unacceptable. Another issue is that the fabrics sometimes crease during the dyeing process and the edges of the creases can abrade more harshly than the surrounding fabric, so that the finished fabric has permanent crease markings.

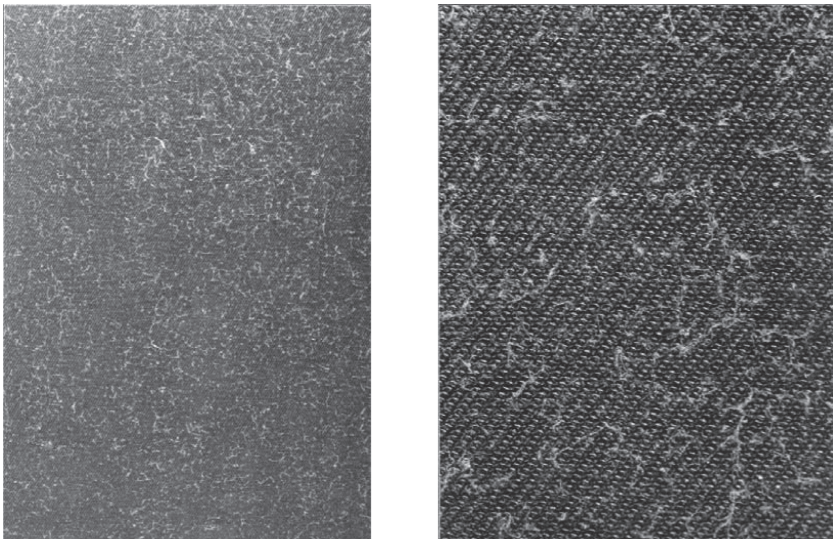

(a) (b)

Figure 9.8 Surface of a fibrillated fabric

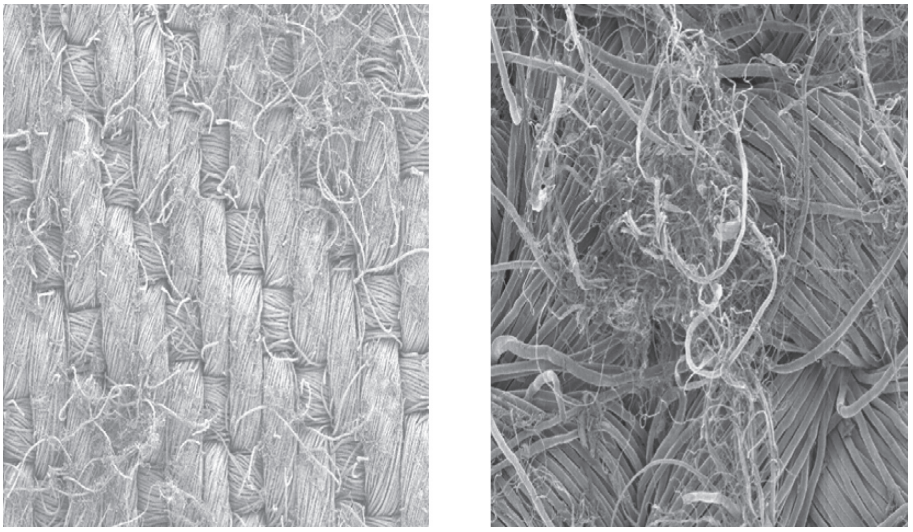

(a) (b)

Figure 9.9 Micrographs of a fabric surface

Any process that abrades the fibre in a wet condition will generate some fibrillation. Processing of the fabric in rope dyeing equipment (jets, winches), where the fabric rubs against itself and the metal, can lead to fibrillation.

9.8.3 Approaches to Manipulation of Fibrillation

Three approaches have been taken to manipulate fibrillation for textile applications as outlined below. Within each approach there are a wide variety of differing technologies and these will be described in turn.

The fibre-manufacturing process can be modified to produce fibres with a much reduced tendency to fibrillate. The superficially simple approach of modifying the spinning process has proved to be extremely difficult to achieve in practice, and small-scale development has so far only generated fibres with an uneconomic balance of performance and cost. The most successful results have come from chemically treating the fibres and this has led to two commercial products – TENCEL® A100 and TENCEL® LF. These will be described below.

The approach taken commercially during the early years of development was to exploit the characteristic of fibrillation to make aesthetically attractive fabrics that have a unique and useful balance of properties. The thrust of this approach was to broaden the range of equipment and techniques that can be used to produce these fabrics. In doing this, the other main driver has also been met – to drive down the costs of producing these attractive fabrics.

It is also possible to suppress or prevent fibrillation during the dyeing and finishing process, and these measures are very widely available to the industry. The challenge here has been to commercialise the inherent strength of the fabrics in order to sell the fibre into more technically demanding applications, such as sheeting and work wear. This approach has longer lead and development times, along with lower price points, but it has also been successful now that the fibre has been available for many years.

9.8.4 Fibre Modification

It was known from the earliest stages of development that the application of 'easy-care' resins to TENCEL® would stop fibrillation. These resins are in common use for cotton and viscose fabrics since they impart both wash stability and crease resistance that are essential in today's market. They act by forming chemical crosslinks to the fibre and are the basis of the third fabric treatment approach described above.

Unfortunately, the easy-care resins used as fabric treatment cannot simply be used as a fibre treatment. Early experiments quickly established that TENCEL® fibres which were treated in such a manner were both brittle and could not be dyed – two lethal disadvantages. The search therefore started for chemicals that could crosslink the fibres without these defects and which could be economically applied during the manufacturing process.

There is a wide variety of potential crosslinking chemicals so it is necessary to reduce the number of options by including key screening factors such as ease of on-line application, additive safety, resultant fibre properties, resistance to the chemical treatments used in dyeing/finishing and total process cost.

Many reactive dyestuffs have two or more reactive groups and these are effective at stopping fibrillation, so the principle of using colourless dyes was patented; this led to the development of the sodium salt of dichlorotriazine (NDT) as an effective treatment of the fibre (see **Section 9.4.2**). There are, of course, many other derivatives of the dichlorotriazine ring and these are fully described in the Lenzing patents US 6241933 and US 6033443 [21, 22]. A development from this is to have two reactive triazine rings linked together as described in Lenzing patent US 6203746 [23].

Two chemicals have so far been successfully used and these make the TENCEL® A100 and TENCEL® LF products described next.

9.8.4.1 TENCEL® A100

This was the first commercial nonfibrillating TENCEL® fibre and was launched in 1998, based in the newly commissioned factory in Grimsby, UK. The manufacturing process was developed as an extra process step during the tow-based washing/drying process and the fibre production lines were able to make both standard and A100 fibres – an essential feature whilst the new fibre was being launched into the market.

The process for manufacturing TENCEL® A100 is in essence a relatively simple procedure, involving the application of trisacryloylhexahydrotriazine (TAHT) to the TENCEL® tow as a crosslinking agent. You can see from the formula in **Figure 9.10** that this chemical has three reactive sites to link the cellulose chains together.

The use of this chemical to treat TENCEL® is described in Lenzing patents US 5882356 and US 5779737 [24, 25].

In more detail, the process starts with washed TENCEL® tow (in the never-dried state), then the crosslinking agent (TAHT) is applied, followed by an alkali and it is

then cured by heating in steam. The treated fibre is washed to remove the unreacted chemicals, and then finished, dried and the tow is crimped as per the standard fibre (**Figure 9.11**).

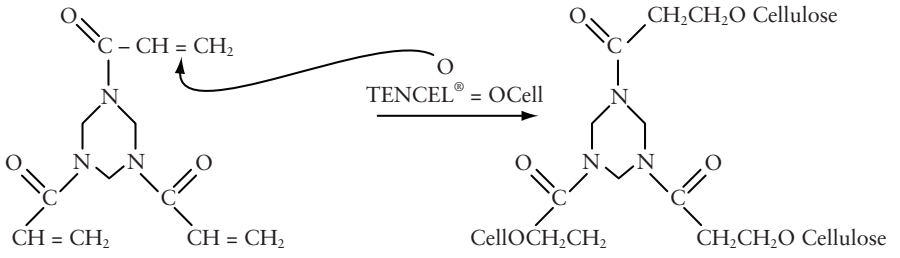

Figure 9.10 Reaction of TAHT with cellulose

TAHT is supplied as a fine powder which is difficult to meter into the process accurately and caused some problems with dust respiration in the workplace. This was overcome by developing a stable suspension – described in Lenzing patent US 6110978 [26].

The important aspects of this process are that the presentation of the fibre as a uniform band enables the chemicals to be applied uniformly, but achieving an adequate curing time is more difficult. The technical challenge was that the curing time in the manufacturing process took several minutes, so a cost-effective method needed to be developed to accumulate the fibre for that length of time. The crosslinking occurs when the fibres are still in a highly swollen state, so that the resultant fibre structure is readily accessible to dyestuff molecules.

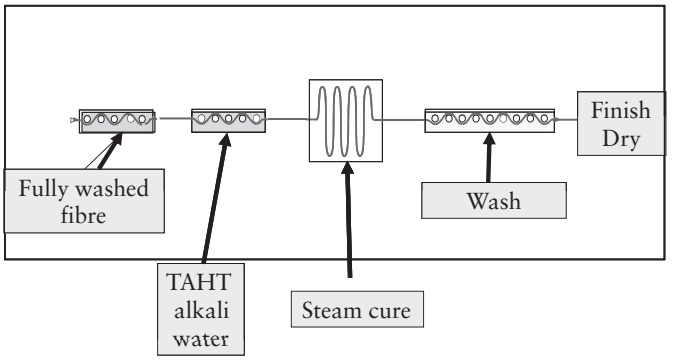

Figure 9.11 TENCEL® A100 - a low fibrillation fibre

Table 9.1 Fibre structure		
Properties	**TENCEL® A100**	**TENCEL®**
Crystallinity (nuclear magnetic resonance)	45	45
Water porosity (g/g)	0.8	0.65
Swelling % on wetting	40–45	30–35
Fibre diameter (μm)	12	11
Dyeability (Q competitive)	120	100

The crystalline structure has remained the same, but there has been a change in both the fibre diameter and the pore width as would be expected from this type of crosslinking process. This leads into the increase in water imbibition and swelling that is observed. Most importantly, the dye affinity of the fibre is significantly higher than that of standard fibre.

Table 9.2 below demonstrates the wet and dry tenacity characteristics of TENCEL® in comparison with other cellulosic fibres. In common with other man-made cellulosic fibres, the tenacity falls when the fibre is wet, but only by 10–15%, compared with a drop of 40–50% in conventional viscose and TENCEL® has a significantly higher dry starting point.

Table 9.2 TENCEL® A100 physical properties					
Properties	**Units**	**A100**	**TENCEL®**	**Cotton**	**Modal**
Dry tenacity	cN/tex	36	36	20–40	35
Wet tenacity	cN/tex	25	29	25–50	20
Dry extension	%	10	11	6.0–9.0	13
Wet extension	%	10	15	-	15
BISFA modulus	cN/tex/5%	10	10	-	6

The A100 is slightly weaker than standard TENCEL®, being about 10% lower in both tenacity and modulus, but still has a very good balance of properties compared with cotton and modal viscose.

A100 can be processed to finished fabrics in the same manner as other cellulose fibres, and can be blended with a wide range of other fibres to broaden its appeal

and performance profile. Of particular note, the excellent dye affinity allows fabrics to be made with deep and vivid colours [27]. Most importantly the fabrics also show excellent appearance retention during use and after repeated washing – significantly better than cotton fabrics. The fabrics are soft and warm to the touch, and retain the good comfort characteristics of cellulose fibres due to their moisture absorbency.

Good market acceptability has led to a doubling of the A100 capacity at Grimsby by the conversion of the second production line to its manufacture.

9.8.4.2 TENCEL® LF

This fibre was developed by Lenzing using a different crosslinking chemical – NDT – see **Figure 9.12**. This is a simple derivative of a class of triazine reactive dyes that are widely used commercially. It has two functional groups to crosslink with the cellulose so a more complete reaction is necessary to give fibrillation protection. However, the chemical is easier to manufacture and has a lower material cost than the one used for A100.

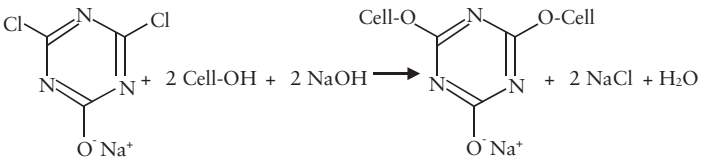

Figure 9.12 Crosslinking of cellulose with NDT

As with the A100 manufacturing route, the NDT can be applied to the TENCEL® fibre whilst it is in the never-dried state and can be included as an optional modification to the wash line. The fibre is processed in a wash bed which means that care must be taken to ensure uniform application of the NDT and alkali. The fibre can then be washed, finished and dried as normal.

The physical properties (**Table 9.3**) are very similar to those of A100 and the fibre can be successfully processed through a wide variety of dyeing and finishing process routes [28]. It does not have the enhanced dye uptake of the A100. The stability and appearance of the LF fabrics during extended wearing and washing use have proved to be very good.

Table 9.3 TENCEL® Comparative properties					
Properties	**Units**	**A100**	**LF**	**TENCEL®**	**Modal**
Dry tenacity	cN/tex	36	34	36	35
Wet tenacity	cN/tex	25	28	29	20
Dry extension	%	10	10	11	13
Wet Extension	%	10	12	15	15
BISFA modulus	cN/tex/5%	10	10	10	6

The A100 and LF fibres tend to compliment each other in that the LF has excellent resistance to alkaline treatments, whereas the A100 has particularly good acid resistance. These factors can be important for certain dyeing processes used when the fibres are blended with other fibres. Thus, the LF gives a good performance with cotton blend fabrics where highly alkaline conditions are often used to give enhanced dyeing of the cotton. The A100 has proved an excellent companion to the synthetic fibres and wool where highly acidic conditions can be used for certain dyeing routes.

The largest markets for the A100 and LF fibres are in jersey and other knits where their softness, warm handle and excellent appearance retention give them a premium market position.

9.9 Dyeing and Finishing Technology – Manipulation of Fibrillation

Many important commercial applications for TENCEL® utilise the fibrillation property to generate fabrics that have a balance of appearance, handle, comfort and performance which cannot be easily achieved by other fibres. The principle by which this is achieved is to generate a fibrillated fabric surface and then remove the surface fibres and fibrils, so that the pilled and frosted appearance is no longer present. The fabric is then like a very fine suede. The processing must be achieved at an economical cost and without generating crease marks that would render the fabrics second quality.

9.9.1 Using Fibrillation to give Peach Touch Fabrics

The characteristic handle of the successful TENCEL® fabrics developed in Japan came from the presence of many fine microfibrils on the surface of the fabric which gave the so-called ‘peach skin’ aesthetic. Much of the early development of the dyeing/finishing technology was aimed at economically achieving this touch without suffering the loss of fabric appearance caused by uncontrolled fibrillation.

When the fabric is first processed in the wet state, the loose fibres that are on the fabric surface fibrillate and form pills. The reflection of the light on the fibrils makes these fibrillated fibres and pills very light coloured and visible, as shown earlier. This fibrillation can be removed by a combination of enzymes (or other chemicals) and surface abrasion so that a fabric with a clean surface can be produced. If this fabric is then further abraded in the wet state, short fine fibrils are formed on the apex of the yarns in the fabric. This type of fibrillation is only visible as a slight frost on the fabric surface and is aesthetically attractive. The short fibrillation also gives the fabric its characteristic 'peach skin' touch. This handle can be modified to the required aesthetic by the use of a variety of softeners, e.g., silicones. Particular attractive finished fabrics are achieved by using a tumbling process to generate bulk and softness in the fabric.

9.9.2 Processing Routes to Making 'Peach Touch' Fabrics

It is important that the fabric produced to give a 'peach touch' has a good performance after laundering – particularly appearance retention and dimensional stability.

The yarn and fabric constructions should be sufficiently tight so that loose fibres do not easily form in use as these can fibrillate and pill. This is difficult to achieve in knitted fabrics so most of the commercial applications are with woven products.

Pretreatment of the fabric in caustic soda is effective in improving both fabric performance and aesthetic. In caustic soda, TENCEL® increases very significantly in its diameter, but very little in length and this will cause the fabric to shrink and its thickness to increase. Upon washing, the fibres become set into this new configuration with significantly improved bulk and flexibility. The stiffness of the fabric when wet is significantly reduced so that it becomes less prone to crease damage marks during the dyeing processing. The caustic treatment also gives more rapid fibrillation removal in processing, and an improved performance and appearance retention in domestic use.

When the fabric is subjected to abrasion during preparation and dyeing, the surface fibres receive the majority of the abrasive action and thus, suffer the greatest degree of fibrillation. The fibrils formed are relatively long and are able to become entangled leading to an extremely matted appearance. It is important that the fabric is processed until the surface fibres are fibrillated to their maximum extent otherwise there will be an unstable surface appearance in the finished fabric.

Cellulase enzymes are used to clean the fibrillated hairs from the surface of the fabric. There is some loss in weight and the surface fibres are weakened, but the latter reduces the tendency of these fibres to cause pills – they simple wash off the fabric surface.

The final peach finish to the fabric is developed by further abrasion of the fabric surface after the surface cleaning has been completed. In the absence of surface hairs, fibrillation is confined to the yarn cross-over points, and the high points of the fabric construction and the position of these fibrils means that they are physically unable to entangle so pilling does not occur **Figure 9.13**.

The absence of surface hairs also causes the fabrics to have a cooler touch.

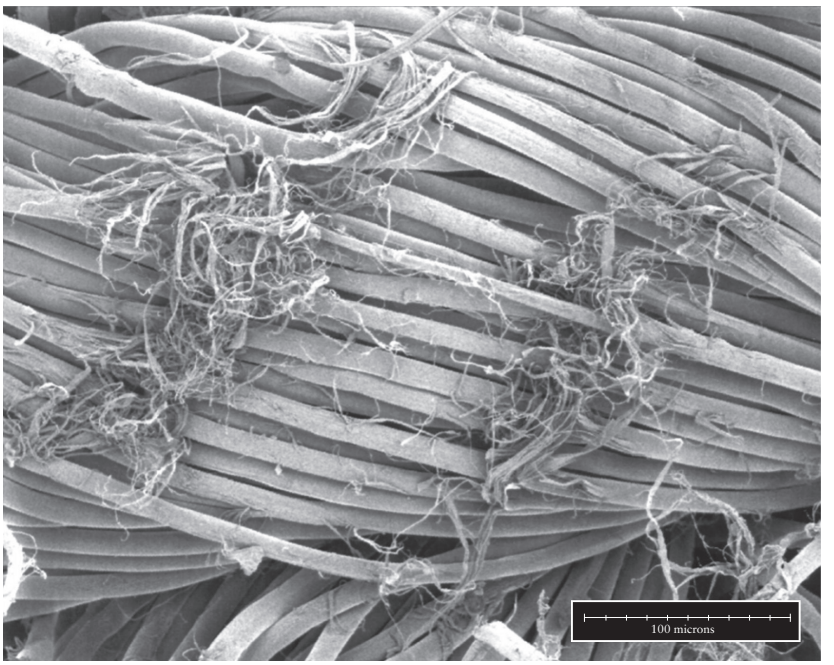

Figure 9.13 Fibrillation on peach skin fabric

This so-called secondary fibrillation can be produced by either a simple washing treatment or during jet dyeing the fabric.

9.9.3 Machinery Selection and Process Methodology

The choice of processing route and the type of equipment used have been important to the commercialisation of TENCEL®. These two factors are very interrelated and this has given a great source of variety to the market.

TENCEL® fibre has unusual swelling characteristics: on immersion in water the high degree of swelling causes a pronounced increase in fabric stiffness, which makes the fabric vulnerable to creasing in rope processes. The apex of the crease is susceptible to fibrillation during the mechanical agitation that occurs during most wet processing and this fibrillation can show up as white lines on the fabric after it is dried. Since this is unacceptable, it can be appreciated that careful machine selection is important. Treatment of the fabric in caustic soda can be very effective in reducing the tendency of the fabric to crease damage, as explained in the last section.

Peach skin processes rely on surface abrasion and the machinery must be capable of giving evenly distributed abrasion to the fabric surface. Machines which have a gentle action require more severe chemical and temperature conditions to achieve the desired result compared with machines which are more aggressive.

9.9.3.1 Garment Processing

(As the title implies, this route involves dyeing/washing or treating the fabrics once they have been made into a garment. They often exhibit abraded or puckered seams.)

Garment processing gives an ideal combination of the physical conditions for processing TENCEL® in that the abrasive action is quite severe, but it is uniform so that white line damage can be readily avoided. Most of the early commercial fabrics were processed by this route. In particular, the processing of indigo denim was an established industry for tumbling and enzyme treating cellulosic garments. This was then extended to whole garment dyeing in these machines [29].

Most machine types designed for garment washing have been found to be suitable and the processing routes described in **Section 9.9.2** work very well with these.

9.9.3.2 Piece Dyeing

(The fabrics are dyed and finished in their full width so that the seams of garments made from piece-dyed fabrics are clean and uniform.)

The early success of apparel made by the garment route generated a demand for fabrics to be made by the piece route. This is because the abrasion on the garment seams, inherent in that route (with all fibre types), makes these products more suitable for casual wear.

The first ‘large-scale’ piece fabrics were developed in Japan using Nidom machines,

which were basically large-scale barrel machines that had a very similar mechanical action to the garment machines. They were commercially very successful in the early days of TENCEL® when the products commanded a very high price in the Japanese market. However, the machines have a low productivity and high labour costs which has restricted the extent of their adoption.

The most common type of machines for dyeing apparel fabrics are jet machines as they generate bulk and softness in the fabric, and can be used for the relatively short production runs demanded by a fashion-conscious market. Unfortunately, many of the machines in use in the early 1990s caused creasing damage to TENCEL® fabrics. Rope processing machines must be capable of frequent reorientation of the fabric otherwise fibrillation will not be uniform across the surface of the fabric, and white lines and marks will become apparent. The most successful jet machines for processing woven TENCEL® fabrics in this way proved to be air jets and they are now used extensively in the industry [30].

Wet tumbling machines need to be utilised for the fibrillation and enzyme processes. In order to achieve the best aesthetics, secondary fibrillation should be enhanced by a final tumbling process. This can be carried out dry or with water present – tumbling under wet conditions gives additional bulk to the fabric.

Progressive technical developments have significantly reduced processing costs and improved fabric performance and aesthetics so that good market acceptability has been achieved in peach skin fabrics made by both garment and piece-dyed routes.

9.10 Dyeing/Finishing Routes that Avoid Fibrillation

Easy-care resins are frequently used after dyeing fabrics containing cellulosic fibres to improve wash stability and crease recovery. These resins crosslink the cellulose fibres and when they are used with TENCEL® they effectively prevent fibrillation.

The resination process is particularly suited to woven fabrics which have been prepared and dyed open width, and so are free of fibrillation. The type of resin and other additives can have a significant influence on the final aesthetic of TENCEL® fabrics, but as the amount of finish required to give resistance to fibrillation and easy-care performance is lower than for cotton, the natural softness of TENCEL® can be retained [31].

TENCEL® woven fabrics produced by this route have clean bright colouration, a full, soft aesthetic and an excellent performance in use. They have proved very comfortable to wear, are durable, retain their ‘as new’ aesthetic and are now widely

used in both apparel and sheets. In blend with polyester they are proving to be excellent for applications such as work wear.

Jersey knitted fabrics can also be made by the same routes as above to give stable, resin-finished fabrics.

An additional option has been developed for jersey based on using air jets for dyeing the fabric. The dyeing stage develops fibrillation across the fabric surface so it is then resin treated and dried in an air tumbler. The fibrillated surface is cleaned by this process as the fibrils have been significantly embrittled by the resin and fall off during the tumbling action. This route is called Mechanical Polishing and gives fabrics with an attractive, clean surface finish that have good washing performance [32].

9.11 TENCEL® Conversion to Yarns and Fabrics

TENCEL® is stronger than all of the other staple fibre cellulosics and has a higher strength than cotton both wet and dry. The dry strength is comparable to typical polyester fibre. These properties allow customers wide scope for making strong yarns in a blend with virtually all the other commercially available staple fibres. The most common form of TENCEL® is as 1.3 dtex fibres cut to 38 mm since this fits well into the major cotton-spinning market sector. This fibre is converted into a spun yarn using machinery developed for handling cotton fibres. TENCEL® also runs very well on more recently developed airjet spinning machines. Courser and longer fibres are also made – often for blending with wool for processing *via* the woollen spinning sector.

Conversion of the yarns into woven and knitted fabrics is achieved using all the conventional routes employed by the industry – their high strength ensures that good efficiencies are achieved.

9.12 TENCEL® in Nonwovens

TENCEL® offers significant advantages in nonwoven fabrics due to its high dry strength, exceptional wet strength, water absorption, biodegradability and potential for fibrillation.

A nonwoven is a ‘textile structure made directly from fibre rather than yarn’. The fabric is usually made by producing a ‘web’ of fibres, which is then strengthened by ‘bonding’ using various techniques such as resin binders and hydroentanglement. The latter is now very important commercially and is achieved by entangling the fibres using very fine jets of high-pressure (up to 200 bar) water. The fabrics made by

hydroentanglement, as in **Figure 9.14,** are much softer and exhibit better drape than those made by using binders. TENCEL® has proved ideal for this process.

A major application for nonwoven fabrics is in 'wipes'. The combination of properties of TENCEL® that make it ideal for wipe applications are the high wet strength, high wet cohesion, water absorption and good processing performance. Fabrics made from viscose fibres become significantly weaker when wet, as shown in **Figure 9.15**. The hydroentanglement of cotton is difficult because of the impurities in the fibre, such as seed and very short fibre. Environmental considerations are also important so the fact that TENCEL® is readily biodegradable gives it a big advantage over synthetic fibres such as polypropylene.

There is a wide range of wipe types, manufacturing technologies and target markets – from everyday domestic kitchen wipes to highly specialised industrial wipes. TENCEL® is an ideal fibre for a large number of these and has found success where the application is technically demanding. Wet wipes are proving to be a rapidly growing market where the attributes of TENCEL® are particularly useful.

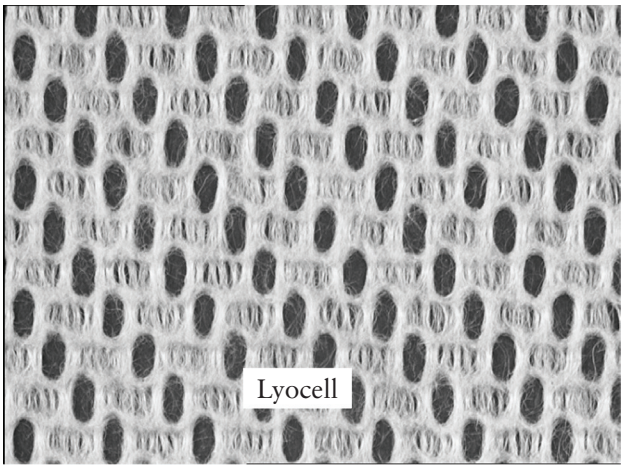

Figure 9.14 TENCEL® hydroentangled fabric

9.13 TENCEL® in Papers

TENCEL® can be used to make high-performance products *via* the processes

commonly used in the pulp and paper industries. The ability of TENCEL® to fibrillate means that it can be processed and made into a paper, like wood pulp, and it can be used either alone or in combination with other pulps to give a wide range of products with novel or enhanced performance. The TENCEL® used is supplied as a 'short cut' fibre of around 5 mm length – most readily made from the continuous fibres obtained by the tow processing route.

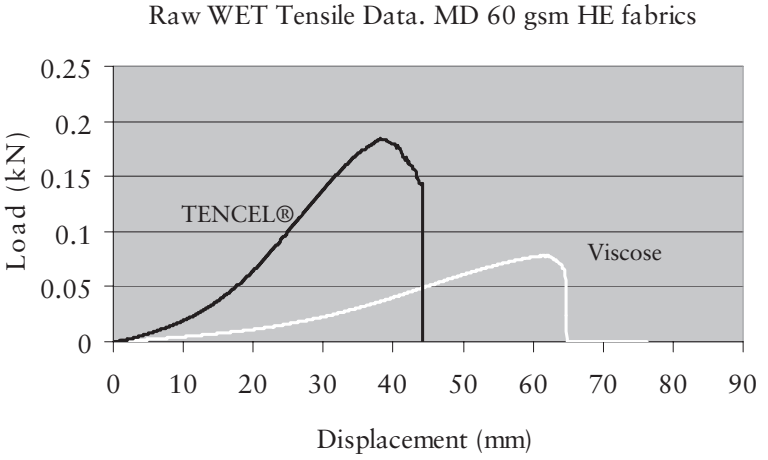

Figure 9.15 Fibre comparison after hydroentanglement (HE)

The key process routes for making paper-type products are:

- Beating and/or refining – a dilute suspension of short fibre is mechanically treated to fibrillate it, either by passing it between a plate and a large grooved roller (beating) or pumping it through a pair of rotating grooved discs (refining). The forces exerted on the fibres cause the fibre to fibrillate and can also cut the fibre; and
- Sheet forming – the refined stock is pumped to the paper machine where it is deposited onto a porous metal belt or 'wire'. The water is sucked through the belt, leaving the fibre on top as a paper sheet. The paper is then passed through a series of drying cylinders and presses before being wound on a roll.

TENCEL® can be processed into a strong paper – usually in a blend with other pulp fibres to upgrade the strength and other properties of the paper. These depend

upon the level of TENCEL® inclusion and the amount of fibrillation generated. In general, TENCEL®-based papers are strong, with good opacity and low air resistance due to the circular nature of the fibres and fibrils. The end uses include a range of filtration applications, electrical separator papers and carbonised products for thermal insulation.

TENCEL® is also used as a very effective reinforcement for pulp which is processed by air laying. These products are proving very successful as wet wipes for toilet tissue.

9.14 Conclusions

The fundamental reasons for the development of lyocell fibres are being vindicated. There is an increased demand for cellulose fibres as the world population and its wealth increases, and customers demand both comfort and performance in textile products. The pressures for sustainable sources of raw materials, safety in factory operation, environmental responsibility and biodegradability are increasing all the time. The process for making lyocell and the resultant products all successfully meet these requirements.

The scale-up of the manufacturing process was technically challenging in many key aspects and this has led to many patents being granted worldwide. As a result there is only one major commercial supplier at this time – Lenzing AG. The fibres produced are widely known under the TENCEL® brand name.

The high wet strength, water absorption and biodegradability of the fibres make them ideal for a very wide range of nonwoven and paper-based applications – particularly industrial and domestic wipes.

The fibres can fibrillate when subject to wet abrasion and manipulation of this characteristic has been a key factor in the development of the fibre for textile applications. Early commercial success was achieved using fibrillation to generate very attractive 'peach skin' touch fabrics, but expansion of the overall market was limited by the speed with which customers obtained suitable dyeing and finishing equipment, and learned the necessary techniques. Successful techniques are now in widespread use to make a wide range of very attractive textile products.

TENCEL® A100 and TENCEL® LF products have also been developed that have good resistance to fibrillation, and these have proved very successful in jersey textile products.

References

1. W. Kalt, F. Schwenninger, M. Longin, R. Stude and J. Kreyenborg, inventors; Lenzing AG, assignee; EP 0915729, 1999.

2. H. Ruf and C. Schrempf, inventors; Lenzing AG, assignee; EP 0823945 and US 5863478, 1999.

3. M. Eibl and D. Eichinger, inventors; Lenzing AG, assignee; PL0219 US 6117378, 2000.

4. L. Shen and M.K. Patel, *Lenzinger Berichte*, 2010, **88**, 1.

5. S.A. Mortimer and A.A. Peguy, *Cellulose Chemistry and Technology*, 1996, **30**, 1, 117.

6. R. Liu, H. Shao and X. Hu, *Macromolecular Materials Engineering*, 2001, **286**, 3, 179.

7. Z. Lewandowski, *Journal of Applied Polymer Science*, 2001, **79**, 1860.

8. V. Simon, *International Journal of Heat Mass Transfer*, 1994, **37**, 7, 1133.

9. P. White, M. Hayhurst, A. Owens, I. Roughsedge, R. Davies, A. Sellars, J. McDonald, M. Quigley, R. Draper and R. Payne, inventors; Lenzing AG, assignee; US 5951932A1, 1999.

10. S. Zikeli, E. Rauch, H. Koberger, F. Ecker, H. Ruf, R. Jurkovic and F. Schwenniger, inventors; Lenzing AG, assignee; EP 0584318 and US 5589125, 1996.

11. P. White, M. Hayhurst, A. Owens, A. Sellars, I. Roughsedge, R. Davies, J. McDonald, M. Quigley, R. Draper and R. Payne, inventors; Lenzing AG, assignee; US 5939000, 1999.

12. S. Zikeli and F. Eker, inventors; Lenzing AG, assignee; EP 1463851 and US 7364681, 2008.

13. F.A. Buijtenhuis, *Das Papier*, 1986, **40**, 12, 615. [In German]

14. W. Kalt, H. Firgo, J. Manner, E. Mulleder, B. Mangen, A. Nigsch, F. Schwenniger and C. Schrempf, inventors; Lenzing AG, assignee; EP 0695324 and US 5628941, 1997.

15. A. Wykes and M. Quigley, inventors; Lenzing AG, assignee; US 5354371, 1994.

16. M. Perry and A. Wykes, inventors; Lenzing AG, assignee; EP 0662204 and US 5337776, 1994.

17. S, Zikeli, K. Weidinger, F. Ecker and M. Longin, inventors; Lenzing AG, assignee; EP 0789822 and US 5890504, 1999.

18. W. Kalt, J. Manner, H. Firgo and F. Schwenniger, inventors; Lenzing AG, assignee; EP 0781356 and US 5795488, 1998.

19. E. Mulleder, C. Schrempf, H. Ruf and W. Feilmar, inventors; Lenzing AG, assignee; EP 0918894 and US 6241927, 2001.

20. J. Newbury and T. Dovey, inventors; Lenzing AG, assignee; US 6093355, 2000.

21. B. Koll, P. Bartsch and E. Mulleder, inventors; Lenzing AG, assignee; US 6241933, 2001.

22. P. Aeschlimann, inventor; Lenzing AG, assignee; US 6033443, 2000.

23. P. Aeschlimann and B. Muller, inventors; Lenzing AG, assignee; US 6203746, 2001.

24. C. Potter, inventor; Lenzing AG, assignee; US 5882356, 1999.

25. C. Potter and P. Dobson, inventors; Lenzing AG, assignee; US 5779737, 1998.

26. I. Graveson, K. Phillip, G.R. Ross and D.S. Towlson, inventors; Lenzing AG, assignee; US 6110978, 2000.

27. Lenzing Fibres, *Processing Guidelines – Processing of Jersey Knit Fabrics in TENCEL® A100*, Technical Marketing Department, A4860, Lenzing, Austria, 2012.

28. Lenzing Fibres, *Processing Guidelines – Processing of Jersey Knit Fabrics in TENCEL® LF*, Technical Marketing Department, A4860, Lenzing, Austria, 2012.

29. Lenzing Fibres, *Processing Guidelines – Garment Processing TENCEL®,* Technical Marketing Department, A4860, Lenzing, Austria, 2012.

30. Lenzing Fibres, *Processing Guidelines – Piece Finishing of 'Peachskin' TENCEL® Standard Woven Fabric*, Technical Marketing Department, A4860, Lenzing, Austria, 2012.

31. Lenzing Fibres, *Processing Guidelines – General Process Route – Continuous Finishing of TENCEL® Standard Woven Fabric*, Technical Marketing Department, A4860, Lenzing, Austria, 2012.

32. Lenzing Fibres, *Processing Guidelines – General Process Routes – Clean Finishing of TENCEL® Standard Jersey*, Technical Marketing Department, A4860, Lenzing, Austria, 2012.

10 Functional Cellulose Microspheres

Jani Trygg, Martin Gericke and Pedro Fardim

10.1 Introduction

Cellulose is a polysaccharide of remarkable interest for researchers and engineers due to its well-known chemical and mechanical properties, abundance, biocompatibility and sustainable applications in material science and technology. A multitude of chemical modification routes are well known and cellulose derivatives with different active sites, ionic charges and hydrophilic character can be prepared [1]. Cellulose microspheres (**Figure 10.1**) are one of the novel products with great potential in market applications. In order to introduce the reader to this field, it is important to define the terminology involved. *Cellulose microspheres* are spherical particles with cellulose as the main component and a diameter above 10 μm. They can be prepared *via* the regeneration or coagulation of cellulose solutions. Thus, similarly shaped cellulose particles, when prepared from dispersions or physically shaped to be spherical, are excluded from this definition. Additionally, composite materials with polymers other than cellulose having a higher than 50% content are not discussed in this chapter.

Functional cellulose microspheres are chemically or physically modified with or without other components, such as other polymers or particles, which give specific attributes to the microsphere. The mechanical stability and matrix has to be mainly cellulose based, other components merely giving the new desired attributes to the sphere. In the case of physical modification, only cellulose is used but the desired properties are gained using physical methods. Functional cellulose spheres can be prepared and functionalised in various ways. Depending on the desired properties, the choice of the preparation method is essential. Starting with the solvent, there are many known solvents for cellulose, some of them derivatising and some direct, causing cellulose to regenerate or coagulate from the solution. In this chapter, a brief review of conventional solvents is given, but the main focus will be on green and direct solvents, and pretreatment methods. In addition, an overview of different shaping techniques will be given.

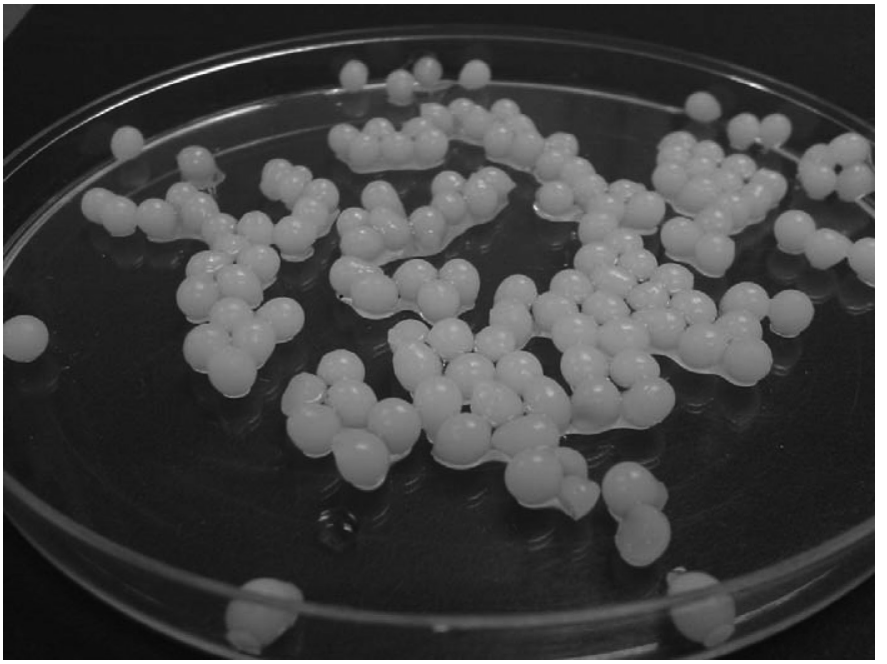

Figure 10.1 Cellulose microspheres prepared by the dropping method. Average diameter is approximately 3 mm

10.2 Challenges in the Dissolution of Cellulose

Cellulose is known to be insoluble in water and most common organic solvents. This is commonly agreed to be due to a strong inter- and intramolecular hydrogen bonding network [1]. To make cellulose soluble, these interactions have to be disrupted and the resulting solution stabilised. Solvents can be divided into two main categories; derivatising and nonderivatising (direct solvents). Nonderivatising solvents disrupt and prevent the hydrogen bonding network from forming, whereas derivatising solvents modify the hydroxyl groups so that the hydrogen bonding network cannot form. Dissolution in conventional solvents usually involves several steps, including cellulose activation, formation of intermediates, processing and shaping, and finally, regeneration. Their by-products are often toxic or their reuse is difficult and the whole process is energy demanding. However, novel solvents are environmentally friendly and recyclable, but are usually too viscous even with low amounts of cellulose, or they are weak solvents requiring intensive pretreatments and activation before being able to penetrate the fibre structure and dissolve cellulose fibrils.

10.2.1 Conventional Solvents

A viscose solution is the most common process which uses a derivatising solvent [2]. After alkalisation, cellulose is treated with CS_2 which reacts with the hydroxyl groups of cellulose forming cellulose xanthate, which is soluble in sodium hydroxide. Xanthate is not isolated from the reaction mixture, but it is directly processed. After shaping the solution into spherical droplets, cellulose is regenerated in acid with the release of toxic CS_2.

Another well-known derivative is cellulose acetate. Esterification of cellulose with acetic acid anhydride or chloride forms a cellulose derivative, which is soluble in nonpolar solvents [1]. Regeneration is achieved by forming the sphere-shaped droplets in water and evaporating the volatile solvents; after shaping, the acetyl group can be cleaved by the saponification reaction, yielding cellulose spheres.

Some of the nonderivatising conventional solvents have been known for decades [3]. They are often heavy metal hydroxides and salts, which form complexes with the hydroxyl groups of cellulose and their ligands. Environmental restrictions strongly limit the use of these chemicals on an industrial scale, but their use is common, e.g., among standards. Cupriethylenediamine is used to measure the limiting viscosity number of pulp (standard ISO 5351). Since these solvents cannot be utilised in novel applications, cellulose spheres are not prepared from heavy metal hydroxides and salts.

N,*N*-dimethylacetamide (DMA)-containing lithium chloride (LiCl) is used for cellulose dissolution and modification [4]. After dissolution, a homogeneous modification can be utilised, yielding a higher degree of substitution than *via* heterogeneous modification. DMA/LiCl is capable of dissolving high amounts of cellulose however, its recyclability is challenging, it is expensive and the viscosity is very high even at low amounts of cellulose [5, 6].

N-methylmorpholine *N*-oxide monohydrate (NMMO) is nowadays the most common nonderivatising solvent [7]. Commercial products from NMMO-cellulose solutions are known as lyocell fibres. However, the solution is rather sensitive to moisture and temperature; cellulose dissolves when the dispersion is heated above 85 °C and crystallites appear again at around 20–40 °C [9]. In particular, the presence of additives causes the solution to become thermally unstable [10]. On the other hand, these sensitivities allow precipitation and coagulation in water or by cooling the solution.

10.2.2 Green Cellulose Solvents

Green cellulose solvents are defined by their properties which are superior to

conventional solvents mainly in three areas; environmental, health and safety (EHS) [11]. Together these properties should indicate better biocompatibility and decreased environmental impact. These are often water-based solvents, but since many of the ionic liquids (IL) also fulfil these EHS requirements, they are also considered as green solvents for cellulose. Ionic liquids are molten organic salts, which have melting points below 100 °C. They are capable of dissolving cellulose concentrations even as high as 25% [12]. Imidazolium-based IL are probably the most studied compounds and cellulose spheres have also been made from IL-cellulose solutions [13]. However, high viscosity and challenging processing are limiting factors for large-scale production. In addition, an efficient and cheap recycling plan has to be implemented in order to make the process profitable [14].

Water-based solvents have gained more attention among researchers recently [15, 16]. Aqueous NaOH solutions, with or without additives, like urea [16], thiourea [15] or zinc oxide [17], are relatively weak cellulose solvents compared with conventional solvents and IL. However, they are capable of dissolving cellulose with a lower degree of polymerisation. As a benefit, they are widely used, readily available, environmentally friendly and fulfil EHS requirements. Also, the residues are water-soluble so product purification is easy. Dissolution in a water-based solvent usually occurs at low temperatures [18]. It is shown that cellulose dissolves when the metal hydroxide (usually sodium) destroys the inter- and intrahydrogen bonds between the cellulose molecules; urea and zinc hydroxide prevent the reassociation of the molecules by occupying the hydrogen bonding sites and hence stabilise the solution, and prolong the gelation and aggregation time [17, 18].

Since NaOH-water cannot dissolve cellulose with a high degree of polymerisation [20], additives are needed [15, 16, 17]. But even with additives, such as urea, some areas of the cellulosic fibres are more resistant to dissolution [21]. Weak solvents cannot easily dissolve the outer layer of the cellulosic fibre (primary cell wall) and this causes ballooning. If the solvent system is too weak, undissolved fragments are left behind after dissolution or dissolution is completely restricted.

10.2.3 Pretreatments of Cellulose Fibres

Pretreatments can be categorised roughly into three different classes; physical, chemical and biological. Generally, it can be said that all pretreatments are intended to break the original structure or composition of the biomass. The accessibility of chemicals to the fibre wall layers plays an important role in dissolving the cellulose and it can be enhanced by utilising these different pretreatment methods [22].

In physical methods, thermal or mechanical energy is used to open the fibre structure. Reduction of the cellulose crystallinity and an increase of accessible surface area can also take place, e.g., in ball milling [23]; on the downside, it is very energy demanding [24].

Physico-chemical methods are more cost effective. Steam explosion and hot water treatments degrade hemicelluloses and disrupt or modify lignin chemical structures [25, 26], but they can also produce compounds that inhibit biological methods of biomass conversion [27]. An ammonia fibre explosion (AFEX) and a CO_2 explosion do not produce inhibitory compounds and they increase the surface area of the biomass material, but AFEX is not effective against lignin and CO_2 is not effective against lignin or hemicelluloses [24]. However, these are often used as a first pretreatment method, followed by more specific steps of chemical or biological methods [28], such as enzyme treatments.

Biological (enzymatic) methods are usually specific to certain components and the presence of other than targeted component hinders the efficiency of the enzyme [29]. Depending on the targeted biomolecule, different microorganisms can also be utilised, e.g., fungi [24]. Hydrolysis rates are relatively low, so enhancement is needed from other methods. Chemical methods, on the other hand, are not completely specific, but can favour certain active sites in their reactions [30] and reaction rates are high. A common factor for biological and chemical treatments, from the dissolution point of view, is that they tend to degrade the cellulose chains to a suitable length so that dissolution would be possible.

Chemical treatments such as organosolv, alkaline hydrolysis, dilute acid treatment and ozonolysis are aimed at degrading or disrupting the structure of lignin and hemicelluloses [22, 24]. Organosolv residues in pulp might inhibit enzymatic processes, so the removal of the solvent is necessary and hence the method is quite expensive. In ozonolysis, a large amount of ozone is needed and the cost benefit balances are not very attractive. Alkaline and dilute acid hydrolysis exposes cellulose for further hydrolysis by removing the lignin and hemicelluloses. However, they require a long treatment time and elevated temperatures.

Acid hydrolysis is the most common method of the chemical treatments. As mentioned, it can be performed even with low concentrations of acid if the appropriate temperature and pressure are applied [24, 31]. Nevertheless, most of the research regarding hydrolysis is performed for biofuel conversion purposes; the effect of acid hydrolysis in an ethanol environment, at relatively low temperatures, on cellulose solubility has also been studied [32].

10.3 Preparation of the Microspheres using a Green Solvent Sodium hydroxide-urea-water system

Cellulose exhibiting a low degree of polymerisation can be dissolved in 8–9% sodium hydroxide at lowered temperatures [20]. However, the solution is not complete as it is unstable and the cellulose molecules are aggregated [33]. Additives, such as urea [16], zinc oxide [21] and thiourea [15] enhance the solubility [17]. These additives act as aggregation inhibitors by blocking the reformation of broken hydrogen bonds. At the same time they delay gelation, which would normally occur rapidly when the temperature is elevated [34]. Dissolution is commonly carried out at temperatures between -12 and -5 °C for NaOH-water and NaOH-urea-water systems, but temperatures between -7 and 5 °C can also be used for the NaOH-urea-water system [19]. When coagulating cellulose from the solution, the solvent conditions should be altered to allow recombination of the cellulose chains through the formation of new intermolecular hydrogen bonds. The most common way to achieve this is to neutralise the dissolving component, sodium hydroxide, by adding acid [35]. Instead of neutralising, concentrations of NaOH can be diluted by coagulating cellulose in water or saline water [34, 36]. The concentration gradient between the sodium hydroxide (and urea) and water causes diffusion, hence diluting the solvent and coagulating the cellulose. Cellulose is also soluble in this solvent system only when using lower temperatures; at higher temperatures it first gelates and eventually coagulates [37, 38].

10.3.1 Techniques for the Preparation of Microspheres

Several techniques can be used to gain the spherical shape after dissolving the pulp in NaOH-urea-water. Roughly, these techniques can be divided into two categories; dropping and dispersion techniques. In the *dispersion technique* (**Figure 10.2a**), the cellulose solution is mixed with an immiscible liquid, such as oil [35]. The control of the oil-solution ratio and mixing speed leads to different spheres that are coagulated by adding acid into the mixture. The particle diameter can vary from micrometres to millimetres. The dispersion technique produces smaller cellulose particles compared with dropping techniques. This procedure can be carried out at relatively large scales, even with basic laboratory equipment, unlike the dropping techniques. Different commercial cellulose spheres prepared by dispersion techniques are available on the market [39, 40].

Dropping techniques are based on droplet formation by cutting the viscous cellulose solution into droplets using gravity, pressure and possibly mechanical appurtenance (**Figure 10.2B–E**). On a laboratory scale, the easiest approach is to use a simple dropping technique, where the solution is extruded through a needle by gravity or by applied pressure. A droplet forms on the top of the needle and when the weight

increases over the critical level, the droplet detaches. If the coagulation medium is too close, the droplet can retain its tear shape. On the other hand, if the coagulation medium is placed at longer distances, impact with the surface will flatten the sphere and lenses are obtained [36]. Spheres of different sizes, with a wet diameter of approximately 0.5 to 3 mm, can be prepared by varying the viscosity (cellulose concentration) and needle size. Several needles can be used simultaneously. Even though the technique is very easy and the parameters are easy to control, it has several limitations. Since the droplet size is practically constant, if the cellulose concentration is too low, the droplets cannot form solid spheres in the coagulation medium due to a lack of building material in the constant droplet volume. On the contrary, if the viscosity is too high, the droplet does not break loose from the needle as the cellulose solution can bear its weight, resulting in a continuous stream of cellulose solution [34].

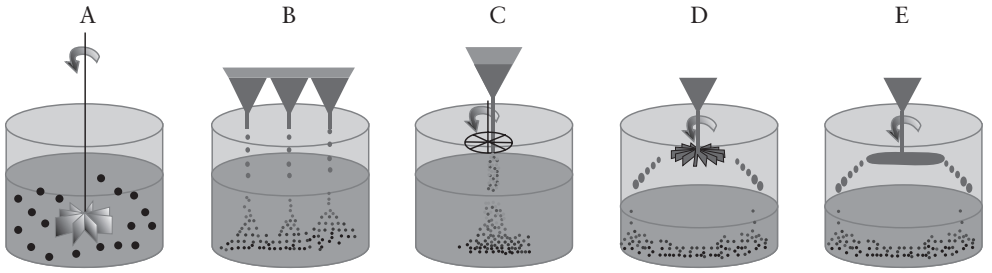

Figure 10.2 Preparation of cellulose spheres by the dispersion technique (A); simple dropping (B); jet-cutting (C); spinning drop atomiser (D) and spinning disc (E). Adapted from M. Gericke, J. Trygg, and P. Fardim, *Chemical reviews*, 2012 [41]

During the jet-cutting technique, a stream of cellulose solution is cut with a rotating knife apparatus [42]. Since the droplet formation is performed by mechanical force, it is possible to carry out the cutting in the coagulation medium. Strong deformations and deviations from the spherical shape can be expected if this method is used. Uniform spherical particles in larger fabrication batches can be obtained by using atomisers [43, 44]. Spinning drop atomisers use a set of nozzles of various diameters and lengths to produce droplets. The solution is pushed through the nozzles by centrifugal force. During spinning disc atomisation, the same forces are used to force the droplet to break-off from the film onto the disc. The size of the cellulose spheres can be controlled when varying the speed of the viscous stream and rotating apparatus, as well as the geometry of the different atomisers. The minimum size can be estimated

to be somewhere around 50 μm, but the upper limit is probably the same as found at the laboratory scale when using the relevant needles.

10.3.2 Tailoring of Cellulose Microspheres using Physico-chemical Design

As pointed out earlier, the choice of the droplet formation technique to a large extent defines the physical dimensions of the cellulose sphere. Cellulose concentration, coagulation media, temperature and concentration of the coagulation media, and additives are other variables that can be utilised when targeting functional spheres towards certain applications. Cellulose can be coagulated by neutralising the alkaline conditions with acid or by diluting with water, hence making conditions unsuitable for dissolving cellulose [19, 34]. It is reasonable to presume that elevated temperature or higher acid concentration would yield more rapid coagulation and give different properties than slower coagulation. It has been reported that slow coagulation gives cellulose chains time to 'pack' more densely [37]. The physical dimensions of the spheres increase slightly with increasing coagulation kinetics. It has been suggested that the physical dimensions are defined by the fast skin formation during the first contact between the cellulose solution droplet and the antisolvent [34]. However, if the coagulation is slow, cellulose chains packing under the skin layer may 'pull down' the exterior skin layer.

Preparation of spheres with smaller physical dimensions, using a constant amount of cellulose, leads to materials of lower porosity and higher density [37]. However, the surface area increases when coagulation is slower [34]. This is also due to the packing of the cellulose molecules; when cellulose coagulates slowly, it fills up the voids and forms a greater amount of smaller pores, while simultaneously maximising the surface area. Fast coagulation favours the formation of larger pores and voids, densely packed cellulose and lower surface area.

Since the physical dimensions are rather constant, the addition of cellulose into the solution increases the density of the material. It also lowers the porosity [34] and decreases the average pore diameter [37]. The effect on the surface area is contradictory; cellulose dissolved in sodium hydroxide, gelated and coagulated in water, yields a lower surface area of materials than when the cellulose concentration is higher [37], whereas cellulose dissolved in calcium thiocyanate, gelated and coagulated in methanol [45] and cellulose in 7% NaOH-12% urea-water coagulated in 2 M nitric acid [34], both yielded a higher surface area when the cellulose concentration was increased. However, the mentioned procedures are not comparable with each other due to the different solvents and coagulation media employed; in addition, the direct relation between processing and the diverse surface areas obtained is not straightforward. Moreover, pore size distribution can be tailored by altering the coagulation conditions.

Macropores can be favoured over smaller pore types when the acid concentration is increased [34, 37]. Faster coagulation forms larger cavities, whereas slower coagulation kinetics allows cellulose to arrange itself in the form of small meso- and micropores, simultaneously increasing the surface area. Pore size distribution tuning can be helpful when targeting certain applications, e.g., size exclusion chromatography. Maximising the surface area by allowing the self-assembling cellulose chains to create a network with voids is again useful when benefiting from the electrostatic forces of the anionic cellulose surface to bind other molecules, e.g., drugs or dyes. It has also been suggested that the addition of surfactants in the cellulose solution would increase porosity and vary the pore size distribution [37].

10.4 Applications of Cellulose Microspheres

Besides the physico-chemical modification during coagulation, cellulose spheres can be chemically modified before or after coagulation. Reactions before coagulation are preferably homogeneous, yielding higher reaction rates, but also heterogeneous reactions are used mainly due to their simplicity. Blending other polymers into the structure of the cellulose microsphere is easy to perform as long as both polymers are soluble in a common solvent. However, in the case of blends it is advisable to ensure that the cellulose matrix and functional polymer are evenly distributed, in addition to being bound to each other physically or chemically. If distribution is not even, structural integrity and mechanical stability can be diminished and the spheres would be unstable. Also, during coagulation, the desired functional groups might prefer certain locations, e.g., surfaces of the sphere or on the contrary, the interior parts away from the coagulation medium.

10.4.1 Chromatography

Cellulose microspheres are suitable for several chromatographic column types due to their size and shape. They have excellent flow properties and they are relatively strong and easy to pack [46]. As a stationary phase in columns, the modified cellulose surface can act *via* different types of interactions with target molecules.

During affinity chromatography, targeted molecules are delayed in the eluent flow or even completely bonded by adsorption onto cellulose microspheres. In the case of binding, target molecules can later be released by changing the pH, salt concentration or the other counterpart of the target molecules (see **Figure 10.3**). 'Dye-ligand chromatography' is a specific application of affinity chromatography. Many textile dyes have specific binding sites for several proteins and they can be used for purification [47]. Whereas unmodified cellulose is able to bind only nonspecifically

via its hydroxyl groups, cellulose can be modified to contain dye-ligands as active binding sites [48, 49].

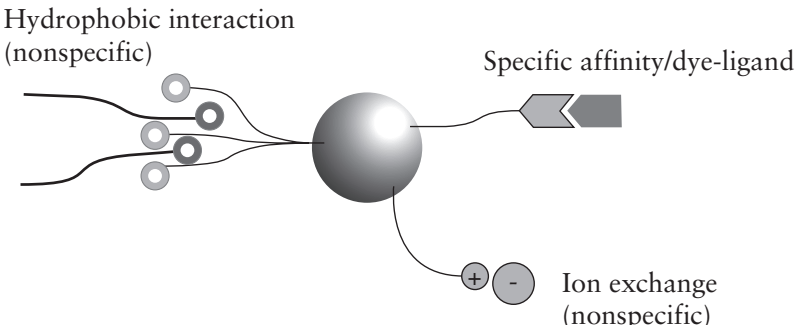

Figure 10.3 Chromatographic separation by different functional groups attached on cellulose microspheres. Adapted from M. Gericke, J. Trygg, and P. Fardim, *Chemical reviews*, 2012 [41]

Hydrophobic interaction chromatography is based on selectivity towards hydrophobic regions, e.g., in protein molecules [50]. Cellulose spheres can be derivatised to contain alkyl or aryl moieties [51], which would interact with the hydrophobic regions of the proteins. Compared with affinity chromatography, removal of the adsorbed protein is easier since the adhesion strongly depends on the salt concentration; the adsorption rate is high when the salt concentration is also high and removal of the protein can be made simply by decreasing the salt concentration rather than introducing the counterion parts, as in dye-ligand chromatography.

Cellulose spheres can be modified to work as ion-exchangers. By adding functional groups, e.g., carboxylates, it is possible to bind metal cations such as copper, silver and lead from water [52]. Cellulose blended together with chitosan has been reported to have a high affinity towards cadmium and copper [8]. Multivalent cations are strongly bound to these functional groups and hence these templates can be utilised as columns for wastewater treatment.

10.4.2 Protein Immobilisation

The immobilisation of proteins or enzymes has limited operational parameters

and optimising the performance of proteins requires additional tools besides the common variables, such as the concentration and temperature of the reaction medium. Immobilisation of enzymes has proven to be an adequate way to enhance the performance of the enzymes [53]. Generally, there are three categories of immobilisation: binding to a support (carrier), entrapment and crosslinking. Cellulose is an ideal material for all these categories and furthermore it is biocompatible, sustainable and easy to modify. Microspheres, on the other hand, provide good flow properties, high surface area and adjustable porosity, and protection from physical exposure. Proteins are usually immobilised onto the cellulose surface *via* their amino groups [54]. Also, functional cellulose microspheres with oxiranes and isocyanate groups may bind proteins *via* their hydroxyl or thiol groups. High selectivity towards the target molecules, i.e., enzymes and proteins, can be achieved by using covalently attached antibodies on cellulose spheres [55, 56]. Besides purifying and adsorbing the proteins, cellulose-enzyme microspheres can be used in sensor applications. Usually, this means that the enzymatic conversion of the analytes yields some measurable properties, such as an amperometric response. It is even possible to simultaneously measure several components, such as glucose, ethanol and lactate [57].

10.4.3 Drug Loading and Release

Cellulose microspheres, dissolved in a water-based solvent, provide a biocompatible material with nontoxic by-products during the production process and are hence a good alternative to microspheres prepared from other materials e.g., viscose. Compared with traditional granulate materials currently used in tableting, microspheres have at least a tenfold higher surface area [34, 58]. Together with high porosity, it is possible to load a high concentration of drugs into the microspheres. The uniform structure enables an even distribution of the drugs and it plays an important factor in the release profiles [59]. The above-mentioned parameters can be adjusted in the preparation of the microspheres. With post processing, i.e., adding fillers, film formers and solubilisers, it is possible to further adjust the release of the drug [60]. Functional microspheres, e.g., additional anionic groups can be utilised to improve the release of poorly water-soluble drugs [61].

10.5 Conclusions

Conventional preparation routes of modifying cellulose have disadvantages due to their troublesome precursors and by-products. New developments in the area of cellulose dissolution allow the construction of the whole process chain, from dissolving pulp to novel cellulose products, by using environmentally friendly methods. While

the research into ionic liquids as a novel alternative solvent for cellulose continues, water-based solvents offer a direct and green alternative to conventional solvents.

Cellulose microspheres provide biocompatiblity and are a highly versatile template which is easy to functionalise for several applications. The flow properties of the microspheres enable their use as a chromatographic material, and their large surface area and high porosity as drug or enzyme carriers. These properties are fairly easy to modify even during the coagulation stage. Using chemical modification, new functions can be added to the microspheres. It is also possible to blend cellulose with another polysaccharide to obtain some of the desired properties. However, basic and innovative research is needed in order to fully understand the potential of these materials. The feasibility of process upscaling and product functionalisation is expected to lead to the emergence of new studies on hybrid materials.

References

1. D. Klemm, B. Philipp, T. Heinze, U. Heinze and W. Wagenknecht in *Comprehensive Cellulose Chemistry 2: Functionalization of Cellulose*, Wiley-VCH, Weinhein, Germany, 1998.

2. D. Klemm, B. Heublein, H-P. Fink and A. Bohn, *Angewandte Chemie*, International Edition, 2005, **44**, 22, 3358.

3. H. Fink, H. Ebeling and W. Vorwerg, *Chemie Ingenieur Technik*, 2009, **81**, 11, 1757. [In German]

4. L. Tim in *Cellulose Solvents: Remarkable History, Bright Future*, American Chemical Society, Washington, DC, USA, 2010, p.29.

5. C.L. McCormick, P. A. Callais and B.H. Hutchinson, *Macromolecules*, 1985, **18**, 2394.

6. J.A. Kaster, W. de Oliveira, W.G. Glasser and W.H. Velander, *Journal of Chromatography A*, 1993, **648**, 1, 79.

7. H-P. Fink, P. Weigel, H. Purz and J. Ganster, *Progress in Polymer Science*, 2001, **26**, 9, 1473.

8. Y-K. Twu, H-I. Huang, S-Y. Chang and S-L. Wang, *Carbohydrate Polymers*, 2003, **54**, 4, 425.

9. O. Biganska, P. Navard and O. Bédué, *Polymer*, 2002, **43**, 23, 6139.

10. A. Konkin, F. Wendler, F. Meister, H-K. Roth, A. Aganov and O. Ambacher, *Spectrochimica Acta Part A*, 2008, **69**, 3, 1053.

11. C. Capello, U. Fischer and K. Hungerbuhler, *Green Chemistry*, 2007, **9**, 9, 927.

12. R.P. Swatloski, S.K. Spear, J.D. Holbrey and R.D. Roger, *Journal of American Chemical Society*, 2002, **124**, 4974.

13. K-F. Du, M. Yan, Q-Y. Wang and H. Song, *Journal of Chromatography A*, 2010, **1217**, 8, 1298.

14. M. Gericke, P. Fardim and T. Heinze, *Molecules*, 2012, **17**, 6, 7458.

15. H. Jin, C. Zha and L. Gu, *Carbohydrate Research*, 2007, **342**, 6, 851.

16. J. Cai and L. Zhang, *Macromolecular Bioscience*, 2005, **5**, 6, 539.

17. W. Liu, T. Budtova and P. Navard, *Cellulose*, 2011, **18**, 911.

18. H. Qi, C. Chang and L. Zhang, *Cellulose*, 2008, **15**, 779.

19. H. Qi, Q. Yang, L. Zhang, T. Liebert and T. Heinze, *Cellulose*, 2011, **18**, 237.

20. A. Isogai and R. Atalla, *Cellulose*, 1998, **5**, 4, 309.

21. C. Cuissinat and P. Navard, *Macromolecular Symposia*, 2006, **244**, 1, 19.

22. N. Mosier, C. Wyman, B. Dale, R. Elander, Y. Lee, M. Holtzapple and M. Ladisch, *Bioresource Technology*, 2005, **96**, 6, 673 .

23. T. Tassinari, C. Macy, L. Spano and D.D.Y. Ryu, *Biotechnology and Bioengineering*, 1980, **22**, 8, 1689.

24. P. Kumar, D.M. Barrett, M.J. Delwiche and P. Stroeve, *Industrial & Engineering Chemistry Research*, 2009, **48**, 8, 3713.

25. J.D. McMillan in *Pretreatment of Lignocellulosic Biomass*, American Chemical Society, Washington, DC, USA, 1994, p.292.

26. J. Weil, A. Sarikaya, S-L. Rau, J. Goetz, C. Ladisch, M. Brewer, R. Hendrickson and M. Ladisch, *Applied Biochemistry and Biotechnology*, 1997, **68**, 21.

27. E. Palmqvist and B. Hahn-Hägerdal, *Bioresource Technology*, 2000, **74**, 1, 25.

28. B. Yang and C.E. Wyman, *Biotechnology and Bioengineering*, 2006, **94**, 4, 611.

29. J. Schilling, J. Tewalt and S. Duncan, *Applied Microbiology and Biotechnology*, 2009, **84**, 465.

30. J. Quesada, M. Rubio and D. Gomez, *Journal of Wood Chemistry and Technology*, 1999, **19**, 1–2, 115.

31. A.M. Adel, Z.H.A. El-Wahab, A.A. Ibrahim and M.T. Al-Shemy, *Bioresource Technology*, 2010, **101**, 12, 4446.

32. J. Trygg and P. Fardim, *Cellulose*, 2011, **18**, 987.

33. C. Roy, T. Budtova and P. Navard, *Biomacromolecules*, 2003, **4**, 2, 259.

34. J. Trygg, P. Fardim, M. Gericke, E. Mäkilä and J. Salonen, *Carbohydrate Polymers*, 2012.
http://dx.doi.org/10.1016/j.carbpol.2012.03.085

35. X. Luo and L. Zhang, *Journal of Chromatography A*, 2010, **1217**, 38, 5922.

36. R. Sescousse, R. Gavillon and T. Budtova, *Journal of Materials Science*, 2011, **46**, 759.

37. R. Gavillon and T. Budtova, *Biomacromolecules*, 2008, **9**, 1, 269.

38. R. Sescousse and T. Budtova, *Cellulose*, 2009, **16**, 417.

39. JNC Corporation.
http://www.jnc-corp.co.jp/fine/en/cellufine/index.html

40. Iontosorb.
http://www.iontosorb.cz

41. M. Gericke, J. Trygg, and P. Fardim, *Chemical Reviews*, 2012. [In press]

42. M. Pinnow, H-P. Fink, C. Fanter and J. Kunze, *Macromolecular Symposia*, 2008, **262**, 1, 129.

43. P. Rosenberg, I. Suominen, M. Rom, J. Janicki and P. Fardim, *Cellulose Chemistry and Technology*, 2007, **41**, 243.

44. Y. Senuma and J.G. Hilborn, *Polymer Engineering & Science*, 2002, **42**, 5, 969.

45. H. Jin, Y. Nishiyama, M. Wada and S. Kuga, *Colloids and Surfaces A: Physicochemical and Engineering Aspects*, 2004, **240**, 1–3, 63.

46. W.D. Oliveira and W.G. Glasser, *Journal of Applied Polymer Science*, 1996, **60**, 1, 63.

47. A. Denizli and E. Piskin, *Journal of Biochemical and Biophysical Methods*, 2001, **49**, 1–3, 391.

48. D. Mislovicová, P. Gemeiner and A. Breier, *Enzyme and Microbial Technology*, 1988, **10**, 9, 568.

49. R.E.F. Boto, P. Almeida and J.A. Queiroz, *Biomedical Chromatography*, 2008, **22**, 3, 278.

50. J. Queiroz, C. Tomaz and J. Cabral, *Journal of Biotechnology*, 2001, **87**, 2, 143.

51. W-D. Schwidop, P. Klossek, R. Müller and R. Claus, *Journal of Chromatography A*, 1990, **520**, 325.

52. M. Hirota, N. Tamura, T. Saito and A. Isogai, *Cellulose*, 2009, **16**, 841.

53. R. Sheldon, *Advanced Synthesis & Catalysis*, 2007, **349**, 8–9, 1289.

54. H-F. Boeden, K. Pommerening, M. Becker, C. Rupprich, M. Holtzhauer, F. Loth, R. Müller and D. Bertram, *Journal of Chromatography A*, 1991, **552**, 389.

55. V. Weber, I. Linsberger, M. Ettenauer, F. Loth, M. Höyhtyä and D. Falkenhagen, *Biomacromolecules*, 2005, **6**, 4, 1864.

56. P. Gemeiner and A. Breier, *Biotechnology and Bioengineering*, 1982, **24**, 11, 2573.

57. K. Matsumoto, H. Matsubara, M. Hamada, H. Ukeda and Y. Osajima, *Journal of Biotechnology*, 1990, **14**, 1, 115.

58. M. Balaxi, I. Nikolakakis and S. Malamataris, *Journal of Pharmaceutical Sciences*, 2010, **99**, 4, 2104.

59. A. Gómez-Carracedo, C. Souto, R. Martínez-Pacheco, A. Concheiro and J.L. Gómez-Amoza, *European Journal of Pharmaceutics and Biopharmaceutics*, 2008, **69**, 2, 675.

60. B. Wolf, *International Journal of Pharmaceutics*, 1997, **156**, 1, 97.

61. B. Volkert, B. Wolf, S. Fischer, N. Li and C. Lou, *Macromolecular Symposia*, 2009, **280**, 1, 130.

11 Processing Cellulose Fibres to the Micron and Nanoscale

Youssef Habibi

11.1 Introduction

Cellulose is the most abundant organic raw material produced in the biosphere with an annual production estimated to be over 7,500 tonnes. Currently, due to its renewability and biodegradability, this fascinating and almost inexhaustible sustainable biopolymer still attracts a lot of interest for the production of biofuels, numerous products and chemicals. In addition, recent applications in the field of materials science have appeared, arising from the low density and the excellent thermal and mechanical properties of cellulose, particularly in the production of composites. Nowadays, further attractive chemical and physical attributes of cellulose are being 'rediscovered' through the singular emergence of micro/nanosized cellulosic substrates known as micro/nanocelluloses, as attested by the abundant reviews published in the last couple of years [1–12]. Indeed, cellulose fibres can be processed through mechanical shearing or chemical treatments, or a combination of these to yield elongated (micro) nanofibrillar defect-free, rod-like micro/nanoparticles respectively. Due to their low cost, availability, renewability, lightweight, nanoscale dimension and unique morphology, these micro/nanosized cellulosic substrates are receiving a great deal of attention as precursors to design biomaterials for advanced applications. Intermediate products, with an average size in the micron scale, are also obtained and present a considerable interest for many applications ranging from food to composite materials.

In conjuncture with the growing interest in developing sustainable economies through the substitution of fossil carbon by renewable resources, interest in micro- and nanocellulose products does not seem to wane and they will continue to attract considerable attention within the materials community as fillers or building blocks for new materials. The large number of papers and patents dealing with micro- and nanocellulose substrates, estimated to be in the hundreds over the last ten years, attest to this huge interest from industry, academia and government laboratories. Additionally, a few industrial ventures for the production of nanocellulose were

initiated in 2012 [13]. But in spite of this huge interest, there is still a considerable discrepancy in terminology and definition of these products dictated by the large variability of starting raw materials and processing methodologies. TAPPI is attempting to regularise this situation through the establishment of Standard Terms and Their Definition for Cellulose Nanomaterial, which are not yet available.

Although huge interest is being sparked, there are still some major drawbacks to processing and using cellulose as a building block at the nanoscale. Therefore, the objective of this chapter is to collate key advances achieved in the processing of cellulose fibres at the micro- and nanoscale, with an emphasis on their distinctive morphologies and characteristics, and to end with a few examples of their potential applications.

11.2 Ultrastructure and Morphology of Cellulose Fibres

Discovered and isolated by Anselme Payen in 1838 [14], cellulose is considered the most important structural element in plants and serves to maintain the cell structure. Cellulose is also important to other living species such as bacteria, fungi, algae, amoebas and even animals. It is a ubiquitous structural polymer that confers its mechanical properties to higher plant cells.

Regardless of its origin, cellulose is a high molecular weight homopolysaccharide composed of β-1,4-anhydro-D-glucopyranose units (**Figure 11.1**). These units do not lie exactly in the plane with the structure, rather they assume a chair conformation with successive glucose residues rotated though an angle of 180 ° about the molecular axis and hydroxyl groups in an equatorial position. This repeated segment is frequently taken to be the cellobiose dimer [5]. The degree of polymerisation (DP) of the cellulose chains varies depending on its origin, and it's estimated that approximately 10,000 glucopyranose units are present in wood cellulose and 15,000 in native cotton cellulose [15]. One of the most specific characteristics of cellulose is that each of its monomers bears three hydroxyl groups. The ability of these hydroxyl groups to form hydrogen bonds plays a major role in the formation of the fibrillar and semicrystalline packing, which governs the important physical properties of these highly cohesive materials.

In plant cell walls, the exquisite architectural arrangement of cellulose microfibrils results from the combined action of biopolymerisation spinning and crystallisation. All these events are orchestrated by specific enzymatic terminal complexes (TC), which adopt a rosette configuration behaving as precise biological spinnerets that are credited with synthesising up to 36 glucan chains simultaneously and in close proximity to each other. The architectural precision of the complex itself is the template for the growing glucan chains to cocrystallise into microfibrils, which adopt a linear and

rigid conformation *in lieu* of an amorphous array of β-glucans. On the one hand, the polymer chains are assembled through van der Waals forces and both intra- and intermolecular hydrogen bonds, in a hierarchical order, to form elementary nanofibrils, which have a cross dimensional thickness of 2–5 nm that in turn aggregates laterally into larger macrofibres [16, 17].

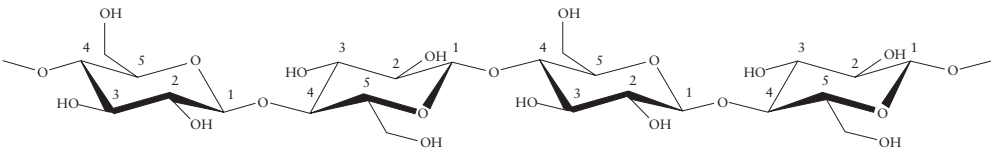

Figure 11.1 Chemical structure of cellulose

On the other hand, if the TC are not perturbed, they can generate an interminable number of microfibrils with a limited number of defects or amorphous regions [18, 19]. These regions are distributed on segments of the elementary fibril, which are distorted by the internal strain in the fibre to undergo tilt and twist [20].

11.3 Processing of Micro- and Nanocelluloses

According to their morphology, cellulose fibres can be dissociated transversely at the amorphous regions present along their axis to yield defect-free, rod-like nanoparticles, referred to hereafter as cellulose nanocrystals (CNC), or laterally to yield bundles of their elementary protofibrils known as nanofibrillated cellulose (NFC). Intermediate processing conditions yield intermediate products with sizes in the micron range.

11.3.1 Processing of Microcrystalline Cellulose

Known since the 1800s as hydrocellulose [21–23], its production was optimised by Battista [24–26]; microcrystalline cellulose (MCC) results from the hydrochloric acid-assisted degradation of cellulose fibres derived from high-purity wood pulps, followed by sonication treatment. The relatively low acid concentration (2.5 N HCl) and the short treatment time (15 min) allow only partial degradation of the amorphous zones of the cellulosic fibres, leading to particles with an average size ranging between 50 and 350 μm. Stable, chemically inactive and physiologically inert

with attractive binding properties, MCC offers significant attributes for multiple uses in the pharmaceutical industry as a tablet binder, in food applications as a texturising agent and fat replacer, and also, as an additive in paper and composite applications. MCC has been commercialised for more than 50 years and approved for use in food products by main regulatory organisations, such as the FDA (USA) and European Commission, and also in drugs by the World Health Organization.

11.3.2 Processing of Cellulose Nanocrystals

Simultaneously to the development and commercialisation of MCC by Battista during the 1950s, Rånby was the first to report that colloidal suspensions of cellulose could be obtained by the controlled sulfuric acid-catalysed degradation of cellulose fibres [27, 28]. Transmission electron microscopy (TEM) images of dried suspensions revealed for the first time the presence of aggregates of needle-shaped particles, while further analyses of these rods with electron diffraction demonstrated that they had the same crystalline structure as the original fibres [29, 30].

The extraction or isolation of crystalline cellulosic regions, in the form of rod-like nanocrystals, is a simple process based on acid hydrolysis which cleaves the cellulose fibres transversely. Lignocellulosic fibres are first subjected to purification and bleaching processes and, after the removal of noncellulosic constituents such as lignin and hemicelluloses, the bleached material is submitted to a hydrolysis treatment with acid under controlled conditions. The amorphous regions of cellulose act as structural defects and are responsible for the transverse cleavage of the cellulose fibres into short nanocrystals during acid hydrolysis. This transformation consists of the disruption of the amorphous regions surrounding the microfibrils, as well as those embedded between them, while leaving the crystalline segments intact; this is ascribed to the faster hydrolysis kinetics of amorphous domains compared with crystalline ones. The hydronium ions penetrate the cellulosic material in the amorphous domains, promoting the hydrolytic cleavage of the glycosidic bonds and releasing individual crystallites. The resulting suspension is subsequently diluted with water and washed by successive centrifugations. Dialysis against distilled water is then performed to remove the free acid in the dispersion. Disintegration of the aggregates and complete dispersion of the whiskers is obtained by a sonication step. These suspensions are generally more diluted because of the formation of a gel of low nanoparticle content. The exact determination of the whisker content can be performed by gravimetric methods before and after drying aliquots of the suspension. The dispersions are stored in the refrigerator after filtration to remove residual aggregates. This general procedure has to be adapted depending on the nature of the substrate.

The actual occurrence of the acid cleavage event is attributed to differences in the kinetics of hydrolysis between the amorphous and crystalline domains. In general, acid hydrolysis of native cellulose induces a rapid decrease in its DP to the so-called level-off DP (LODP). The DP subsequently decreases much more slowly, even during prolonged hydrolysis times [31–36]. The LODP is thought to correlate with crystal sizes along the longitudinal direction of the cellulose chains, present in the original cellulose, before the acid hydrolysis. This hypothesis was based on the reasonable assumption that disordered or *para*-crystalline domains are regularly distributed along the microfibres and therefore they are more susceptible to acid attack (in contrast to crystalline regions that have higher resistance). Also, homogeneous crystallites were supposed to be generated after acid hydrolysis. These assumptions were actually confirmed by X-ray crystal diffraction [37], electron microscopy with iodine staining [37], small-angle X-ray diffraction [33] and neutron diffraction analyses [38]. It was shown that the LODP values obtained by the acid hydrolysis of cellulose correlated well with the periodic crystal sizes along the cellulose chains. The value of LODP has been shown to depend on the cellulose origin, with typical values of 250 being recorded for hydrolysed cotton [39], 300 for ramie fibres, [38] 140–200 for bleached wood pulp [31] and up to 6,000 for the highly crystalline *Valonia* cellulose [40]. However, a wide distribution of the DP is typically observed for different cellulose sources, even at the LODP. Such a disparity in the quoted distributions has stimulated vigorous discussion up to the present day. In fact, the acid hydrolysis of bacterial cellulose, tunicate, *Valonia* or cotton, results in a higher polydispersity in the molecular weight, without any evidence of the LODP, probably because these cellulosic materials have no regular distribution of the less organised domains.

Typical procedures currently employed for the production of CNC consist of subjecting pure cellulosic material to strong acid hydrolysis under strictly controlled conditions of temperature, agitation and time. The nature of the acid and the acid-to-pulp ratio are also important parameters that affect the preparation of CNC. Specific hydrolysis and separation protocols have been developed that depend on the origin of the cellulosic fibres. Most common sources include among others, cellulose fibres from cotton [41, 42], ramie [43–45], hemp [46], flax [47, 48] sisal [49, 50], wheat straw [51], palm [52], bleached softwood [53] and hardwood [54] pulps, cotton linters pulp [55, 56], microcrystalline cellulose [57–60], sugar beet pulp [61], bacterial cellulose [62–64] and tunicates (a type of marine organism) [65–67].

Sulfuric and hydrochloric acids have been extensively used for CNC preparation, but phosphoric [68–71] and hydrobromic [72, 73] acids have also been reported for such purposes.

Dong and co-workers [41] were among the first researchers to study the effect of hydrolysis conditions on the properties of the resulting cellulose nanocrystals. They

proved that a longer hydrolysis time led to shorter monocrystals and to an increase in surface charge. The acid concentration was also found to affect the morphology of the whiskers prepared from sugar beet pulp as reported by Azizi Samir and co-workers [61]. Beck-Candanedo and co-workers [54] reported the properties of cellulose nanocrystals obtained by hydrolysis of softwood and hardwood pulp, and investigated the influence of the hydrolysis time and acid-to-pulp ratio. It was found that the reaction time is one of the most important parameters to consider in the acid hydrolysis of wood pulp. Moreover, it was observed that too long a reaction time will completely digest the cellulose to yield its component sugar molecules. On the contrary, a lower reaction time will only yield large undispersable fibres and aggregates. It was reported that an increase in the hydrolysis time of pea hull fibres resulted in a decrease of both the length and diameter of the nanocrystals, while their aspect ratio first increases and then decreases [74]. The effect of the reaction conditions on the cellulose nanocrystal surface charge and sulfur content was not significant, and it was assumed to be controlled by factors other than hydrolysis conditions. However, the chiral nematic pitch decreases when increasing the cellulose concentration and decreasing the length of the nanocrystals. An attempt to find optimised conditions to prepare cellulose nanocrystals from MCC derived from Norway spruce (*Picea abies*) was also reported [57].

It was also shown that the hydrolysis of amorphous cellulosic chains can be performed simultaneously with the esterification of accessible hydroxyl groups to produce surface functionalised whiskers in a single step [75]. The reaction was carried out in an acid mixture composed of hydrochloric and an organic acid (acetic or butyric). The resulting nanocrystals are of similar dimensions compared with those obtained by hydrochloric acid hydrolysis alone. Narrower diameter polydispersity indices indicate that the surface groups aid in the individualisation of the nanowhiskers. The resulting surface-modified cellulose whiskers are dispersible in ethyl acetate and toluene, indicating increased hydrophobicity and presumably higher compatibility with hydrophobic polymers.

Cellulose nanoparticles are obtained as aqueous suspensions; the stability depends on the dimensions of the dispersed species, size polydispersity and surface charge. The use of sulfuric acid to prepare CNC leads to a more stable aqueous suspension than that prepared using hydrochloric acid [76]. It was shown that the H_2SO_4-prepared nanoparticles present a negatively charged surface, while the HCl-prepared nanoparticles are not charged. During acid hydrolysis utilising sulfuric acid, acidic sulfate ester groups are formed on the nanoparticle surface. This creates electric double layer repulsion between the nanoparticles in the suspension, which plays an important role in their interaction with the polymer matrix and each other. The density of charges on the cellulose nanocrystal surface depends on the hydrolysis conditions and can be determined by elementary analysis or conductometric titration to precisely

determine the sulfur content. The sulfate group content increases upon increasing acid concentration, acid-to-fibre ratio or hydrolysis time. Based on the density and size of the cellulose whiskers, Araki and co-workers [76, 77] estimated for a nanocrystal with dimensions of $7 \times 7 \times 115$ nm^3, that the charge density is 0.155 e.nm^{-2}, where e is the elementary charge. With the following conditions: cellulose concentration of 10 wt% in 60% sulfuric acid at 46 °C for 75 min, the charge coverage was estimated at 0.2 negative ester groups per nm [78]. Other typical values of the sulfur content of cellulose whiskers prepared by sulfuric acid hydrolysis were reported [79, 80]. It was shown that even at low levels, the sulfate groups caused a significant decrease in degradation temperature and increase in char fraction, confirming that the sulfate groups act as flame retardants [81].

If the CNC are prepared using hydrochloric acid hydrolysis, the resulting dispersability is limited and their aqueous suspensions tend to flocculate. Habibi and co-workers [82] performed 2,2,6,6-tetramethylpiperidine-1-oxyl (TEMPO)-mediated oxidation of CNC, obtained *via* the HCl hydrolysis of cellulose nanoparticles from tunicin, to introduce negative charges on their surface. They showed that after hydrolysis and TEMPO-mediated oxidation, the nanoparticles kept their initial morphological integrity and native crystallinity, but at their surface, the hydroxymethyl groups were selectively converted to carboxylic groups, thus imparting a negative surface charge to the whiskers. When dispersed in water these oxidised cellulose nanocrystals did not flocculate, and their suspensions appeared birefringent.

11.3.3 Processing of Micro/Nanofibrillated Cellulose

The process for isolating (micro) nanofibrillated cellulose (MFC)/NFC consists of the disintegration of cellulose fibres along their long axis. They include simple mechanical methods sometimes in combination with enzymatic or chemical pretreatments. Three main technologies exist, e.g., the Manton Gaulin homogeniser, microfluidiser and microgrinder, are commonly used for mechanical treatment.

MFC were first developed in 1983 by Turbak and co-workers [83] using, as starting materials, purified cellulose fibres from wood pulp after high-pressure mechanical homogenisation *via* the Manton Gaulin homogeniser. Pulp fibres are defibrillated under the combined action of rapid pressure drops and high shear, provoking impact forces against a valve and an impact ring. The pressure drop is typically 8,000 psi (55 MPa) in Manton Gaulin 15MR homogenisers and the fibres are cycled through the homogeniser approximately 10–20 times. Cellulosic fibres disintegrate into their substructural fibrils and microfibrils with lengths in the micron scale and widths ranging from 10 to a few hundred nanometres, depending on the nature of the plant cell walls. The resulting aqueous suspensions exhibit gel-like characteristics in water

with pseudoplastic and thixotropic properties even at low solid content.

A few years later, microfluidisation, which is most commonly utilised in the cosmetic and pharmaceutical industries, was introduced to produce MFC/NFC. Materials are defibrillated during processing using a large pressure drop in an interaction chamber, which exposes the fibres to shear forces and impact against the channel walls and colliding streams. The interaction chamber can be designed with different geometries to produce different sized materials and plugging, often encountered with homogenisers, can be resolved using reverse flow through the chamber. The microfluidiser operates at a constant shear rate compared with the homogeniser, which operates at a constant processing volume.

Another method, called microgrinding, is based on ultrafine friction grinding technology during which cellulose fibres are forced through a gap between a rotary and stator discs [84]; these discs have patented bursts and grooves which make contact with the fibres causing them to disintegrate into the substructural components. Contact with the hard surfaces and repeated cyclic stresses result in defibrillation of the fibres. Typically, the material used for the discs is silicon carbide with a grit class of 46. The discs can be produced using different grit classes and different groove configurations to alter flow patterns during processing.

Other methods were also developed, but they are still at a very early stage and far from being amenable to scale up:

- High-speed blender: successfully used to produce NFC with a uniform diameter of 15–20 nm from never-dried pulp. The treatment consisted of blending pulp slurries with a concentration of 0.7 wt% at 37,000 rpm for 30 min. Upon observing the nanofibrillation process, it was clear that the straw-like pulp was fibrillated in a very characteristic way, by forming many balloon-like structures. As the balloons extended to the edges, the fibrils were rapidly individualised. However, the pulp fragments with ripped cell walls were split into finer fragments and gradually disintegrated into nanofibres. This method showed the same degree of fibrillation with less damage to the NFC compared with treatment in a grinder [85].
- Cryocrushing was also tested to facilitate disintegration of the cellulose fibres into MFC, but this method is rarely utilised. Cryocrushing consists of freezing the water in the wood pulp, using liquid nitrogen, and a mortar and pestle are used to produce a high impact force to liberate the fibrils from the cell wall [86].
- High-intensity ultrasonication during which cellulose fibres are subjected to very strong oscillating mechanical power, resulting in the separation of cellulose fibrils by the action of the hydrodynamic forces of the ultrasound [87–92].

11.3.4 Pretreatments

The major obstacle for industrial production has been related to the very high energy consumption involved in processing pure cellulosic fibres. Homogenisation, using a Manton Gaulin-type homogeniser, is estimated to consume approximately 4,000 kJ of energy per kilogram of NFC [93]; in comparison, microfluidisation consumes approximately 200, 390 and 630 kJ/kg at processing pressures of 10, 20 and 30 kpsi, respectively, whereas microgrinding is estimated to consume approximately 620 kJ/kg of MFC/NFC. Another issue associated with these processing methods is that the wood fibres tend to tangle during processing, causing equipment clogging. Pretreatments are required for these methods to decrease the initial fibre length and to reduce energy consumption. Alkaline steam explosion was combined with high-pressure homogenisation in order to facilitate the individualisation of the fibres [94]. Spence and co-workers used a Valley Better refiner to reduce the fibre length and soften the fibres prior to mechanical individualisation [95, 96]. Chemical and/or enzymatic pretreatments were introduced in order to facilitate the fibrillation and mechanical shearing. NFC was produced *via* an environmentally friendly method by combining enzymatic hydrolysis, using endoglucanases or cellulase from *Aspergillus* species, and the mechanical shearing of wood pulp [97–100]. Treatment of natural fibres with a genetically modified fungus, isolated from an Elm tree infected with Dutch elm disease, was used as the enzyme source for the fibre treatment. This pretreatment has been found to substantially alleviate the high energy requirement associated with the isolation of cellulose nanofibres *via* high shear refining and subsequent cryocrushing [101]. The enzyme-assisted pretreatment of waste cotton cellulose fibres, to produce nanofibrils, was optimised using an experimental design methodology, i.e., a Box-Behnken design [102]. According to the fitted model, the optimal conditions, i.e., hydrolysis time, substrate concentration and enzyme loading were suggested as 175 h, 5 g/L and 2.3%, respectively.

A cost-effective chemical pretreatment was also attempted, prior to mechanical shearing, by oxidising the cellulose fibres using TEMPO-mediated oxidation, creating carboxyl groups on the fibre and microfibril surfaces [103–105]. The TEMPO-oxidised cellulose fibres can be converted, utilising mechanical shearing, to transparent and highly viscous dispersions in water, consisting of highly crystalline individual nanofibres [106–108]. At a pH of 10, optimal conditions were reached, giving cellulose nanofibres of 3–4 nm in width and a few microns in length. Other TEMPO analogues were also tested and the results showed that 4-acetamide-TEMPO and 4-methoxy-TEMPO were more efficient in the oxidation of wood cellulose, and were comparable to TEMPO. On the contrary, the use of 4-hydroxy-TEMPO and 4-oxo-TEMPO resulted in the lowest efficiency in oxidation, and consequently in yields of NFC [109]. Carboxymethylation was also successfully used to chemically pretreat cellulose fibres, before mechanical processing, in order to generate NFC

[110–113]. Sequential regioselective periodate-chlorite oxidation was employed as an efficient pretreatment to enhance the nanofibrillation of hardwood cellulose pulp through homogenisation. With this method, only one to four passes were required to achieve NFC with a diameter of around 25 nm [114]. The processing of cellulosic materials, extracted from primary cells such as parenchyma cells from sugar beet pulps [115, 116] or cactus cladodes [117] and fruits [118], were shown to be easier to mechanically process without any enzymatic or chemical pretreatment.

11.4 Morphological Properties of Nanocelluloses

The origin of the cellulose fibres, mainly the nature of the plant cell wall, e.g., primary or secondary, determines the morphology of the generated NFC. They are elongated nanoparticles with widths ranging from 3 to 20 nm and lengths of a few microns. NFC from primary cell walls, such as sugar beet pulps or *Opuntia ficus indica*, are generally thinner and longer, and much easier to produce compared with those extracted from secondary walls, such as wood. **Figure 11.2** shows an example of MFC/NFC extracted from primary or secondary cell walls.

CNC can be prepared from any botanical source containing cellulose. In the literature, different cellulosic sources have been used as shown in **Figure 11.3**. Regardless of the source, cellulose nanocrystals occur as elongated nanoparticles. The persistence of the spot diffractogram when the electron probe is scanned along the rod, during transmission electron microscopy observation, is evidence of the monocrystalline nature of the cellulosic fragment [120]; therefore, each fragment can be considered as a cellulosic crystal with no apparent defect. Their dimensions depend on several factors, including the source of the cellulose, the exact hydrolysis conditions and ionic strength.

The typical geometrical characteristics for nanocrystals derived from different species and reported in the literature are presented in **Table 11.1**. Although, if often composed of a few laterally bound elementary crystallites that are not separated by the conventional acid hydrolysis and sonication process [124], the length and width of the hydrolysed cellulose nanocrystals is generally in the range of a few hundred nanometres to a few nanometres, respectively. It was observed that the length polydispersity has a constant value, whereas the diameter polydispersity depends on the acid used during the isolation [125]. A smaller diameter polydispersity was obtained when using sulfuric acid instead of hydrochloric acid, because of the electrostatic charges resulting from the introduction of the sulfate ester groups when using the former.

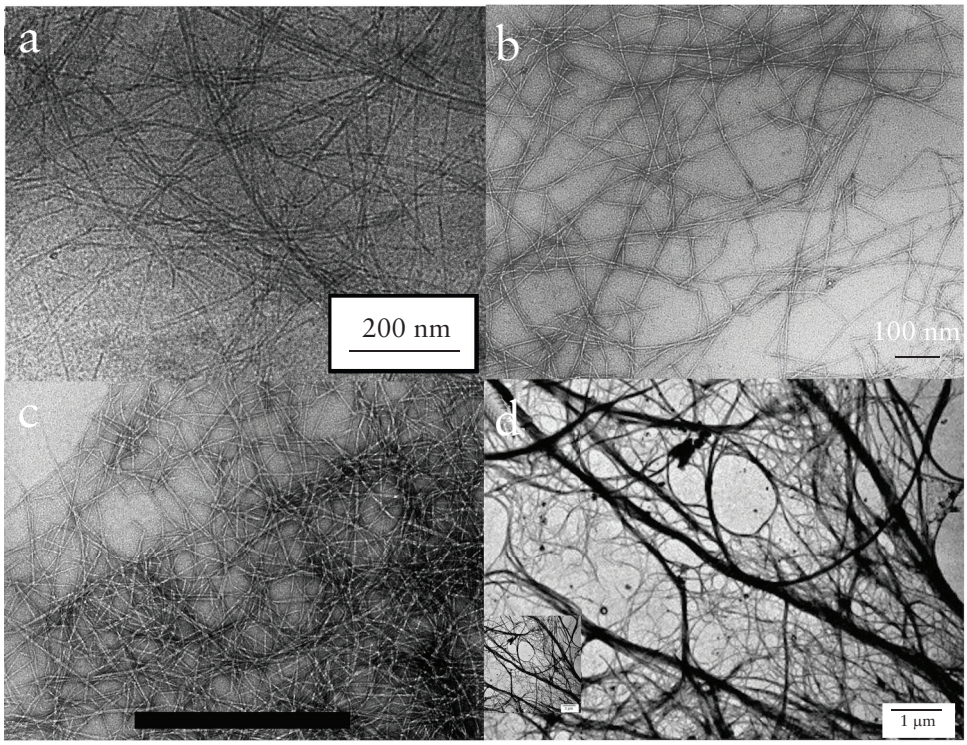

Figure 11.2 Transmission electron micrographs from a dilute suspension of NFC obtained from wood fibres by mechanical processing combined with (a) enzymatic pretreatment. Reproduced with permission from M. Pääkk, M. Ankerfors, H. Kosonen, A. Nykänen, S. Ahola, M. Österberg, J. Ruokolainen, J. Laine, P.T. Larsson, O. Ikkala and T. Lindström, *Biomacromolecules*, 2007, **8**, 6, 1934. ©2007, American Chemical Society [99]; (b) TEMPO-mediated oxidation. Reproduced with permission from T. Saito, S. Kimura, Y. Nishiyama and A. Isogai, *Biomacromolecules*, 2007, **8**, 8, 2485. ©2007, American Chemical Society [107]; (c) carboxylmethylation pretreatment. Reproduced with permission from L. Wågberg, G. Decher, M. Norgren, T. Lindström, M. Ankerfors and K. Axnäs, *Langmuir*, 2008, **24**, 3, 784. ©2008, American Chemical Society [111]; and (d) extracted from *Opuntia ficus-indica*. Reproduced with permission from M.E. Malainine, M. Mahrouz and A. Dufresne, *Composites Science and Technology*, 25, **65**, 10, 1520. ©2005, Elsevier [119]

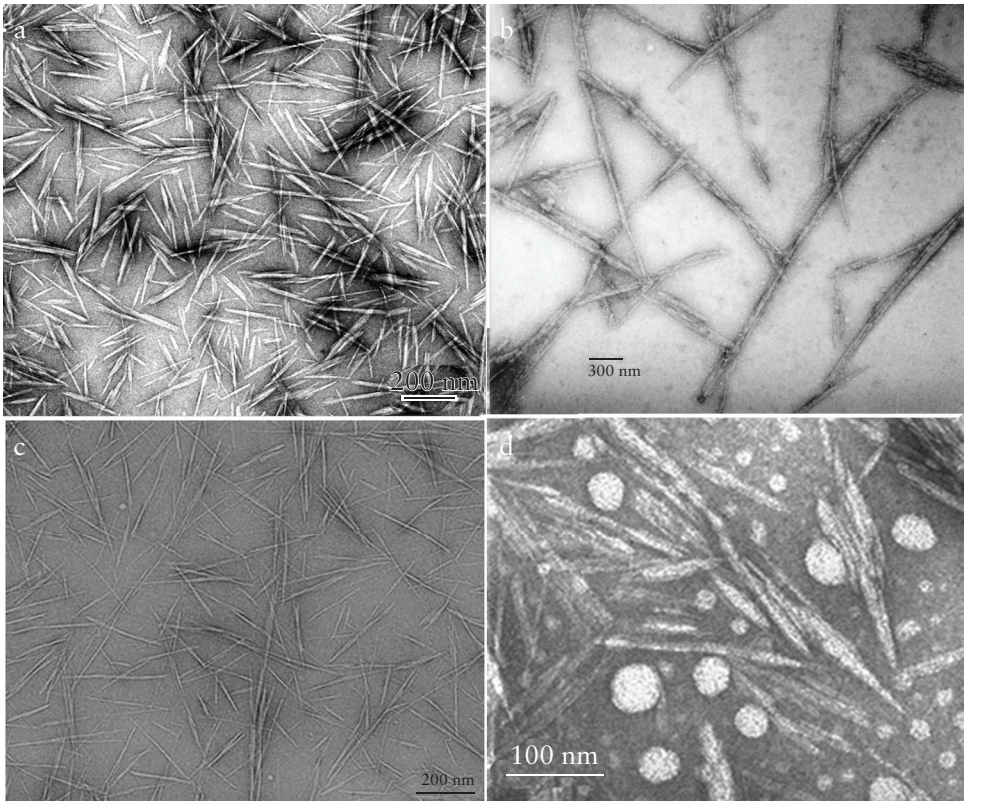

Figure 11.3 Transmission electron micrographs of a dilute suspension of cellulose nanocrystals from: (a) ramie [121]; (b) bacterial. Reproduced with permission from M. Grunert and W.T. Winter, *Journal of Polymers and the Environment*, 2002, **10**, 1–2, 27. ©2002, Science and Business Media [122]; (c) sisal. Reproduced with permission from N.L. Garcia de Rodriguez, W. Thielemans and A. Dufresne, *Cellulose*, 2006, **13**, 3, 261. ©2006, Springer Science and Business Media [49] and (d) microcrystalline cellulose. Reproduced with permission from I. Kvien, B.S. Tanem and K. Oksman, *Biomacromolecules*, 2005, **6**, 6, 3160. ©2005, American Chemical Society [123]

An important parameter for CNC is the aspect ratio, defined as the ratio of the length to the width (**Table 11.1**), which determines the anisotropic phase formation and reinforcing properties. The average length ranges between 1 μm for nanocrystals prepared from tunicate, for instance, to around 200 nm for cotton. The cellulose extracted from tunicate, a sea animal, is referred to as tunicin. The diameter ranges between 15 nm for tunicin and 4–5 nm for sisal or wood. The high value reported for

cotton seed linter corresponds to aggregates. The aspect ratio varies between 10 for cotton and 67 for tunicin. Relatively large and highly regular tunicin whiskers are ideal for modelling rheological and reinforcement behaviours, and were extensively used in the literature. The shape and dimensions of CNC can be assessed from microscopic observations or scattering techniques. The cross sections of microfibrils, observed by TEM, are square whereas their atomic force microscopy (AFM) topography shows a rounded profile due to convolution with the shape of the AFM tip [126]. AFM images of the surface of highly crystalline cellulose microfibrils showed periodicities along the microfibril axis of 1.07 and 0.53 nm, which were assumed to correspond to the fibre and glucose unit repeat distances, respectively. Scattering techniques include small-angle light [127] and neutron [128] scattering.

Table 11.1 Geometrical characteristics of cellulose nanocrystals from various sources: length (L) and cross section (D)

Source	L (nm)	D (nm)	References
Alfa	200	10	[129]
Algal *(Valonia)*	> 1,000	10–20	[126, 130]
Bacterial	100 to several 1,000	5–10 × 30–50	[81, 122, 131]
Cladophora	-	20 × 20	[132]
Cotton	100–300	5–10	[41, 42, 133–135]
Cotton seed linters	170–490	40–60	[136]
Flax	100–500	10–30	[48]
Hemp	Several 1,000	30–100	[137]
Luffa cylindrica	242	5.2	[138]
MCC	150–300	3–7	[123]
Ramie	200–300	10–15	[121, 139]
Sisal	100–500	3–5	[49]
Sugar beet pulp	210	5	[61]
Tunicin	100 to several 1,000	10–20	[120]
Wheat straw	150–300	5	[140]
Wood	100–300	3–5	[54, 76, 77, 134]

11.5 Industrial Production of Micro- and Nanocelluloses

MCC has been commercially available for decades from different producers and at various grades, which differ greatly in purity and particle size. However, industrial

production of other micro/nanocellulose products is still in its early development stage. Different industrial ventures are implemented:

Producers of CNC: CelluForce (Canada), which is a joint venture between FPInnovations and Domtar, claims a production capacity of 1 ton/day of CNC. Producers of MFC/NFC: Innventia (Sweden), with a production capacity of 100 kg/day; Daicel (Japan); Rettenmaier & Sohne Inc. (Germany); Borregaard Biorefinery (Norway) and Stora Enso (Finland), for which production capacities are unknown.

11.6 Examples of Nanocellulose-based Materials

11.6.1 Foams and Aerogels

Aerogels are materials that have been known since the 1930s when silica aerogels became well-established first generation aeromaterials. In general, they are highly porous, extremely lightweight materials having only 1–15% of solid material, a very high specific surface area of up to 1,600 $m^2 g^{-1}$, extremely low thermal conductivity, and good strength and dimensional stability. Aerogels are composed of materials with diameters of a few nanometres, which can be linked to each other to form stable three-dimensional networks. Aerogels have received extensive attention as storage media for gases, catalysts, insulation or as sorbents, mainly because of their high porosity, and the accessible and connected open pore system. Cellulosic aerogels are particularly exemplary aerogels that, in addition to the above-noted benefits, also display the additional advantages of being a renewable, biodegradable, sustainable and eco-friendly biomaterial. Nanocellulose-based foams are currently being studied mainly for packaging applications to replace petroleum-based polymeric foams. Nanocelluloses, especially NFC, alone or incorporated into composite formulations, can be used to prepare foams/aerogels. As thin as the cells in starch foam, NFC has demonstrated the ability to enhance the mechanical performance of starch-based foams prepared with successive freeze-drying techniques [141]. By controlling the density and interaction of the nanofibril obtained by varying the concentration of the nanocellulose in aqueous suspensions before freeze-drying, Sehaqui and co-workers [142] prepared tough foams with tuned porosity. Similarly, Aulin and co-workers [143] prepared structured porous aerogels from nanocellulose by freeze-drying. The resulting aerogels were further chemically modified with fluorinated silane to uniformly coat them and thus tune their wetting properties towards nonpolar liquids and oils. The authors demonstrated that it is possible to switch the wettability behaviour of the aerogels between super-wetting and super-repellent using different aerogel textures.

Recently, cellulose nanocrystal-based aerogels have been prepared through the self-assembly of CNC in a benign manner [144]. Preparation of these aerogels only requires sonication in water to form a hydrogel, solvent exchange with ethanol, followed by supercritical carbon dioxide drying, which results in a very limited shrinkage of the hydrogel. These aerogels display very low densities down to 78 mg/cm^3 with high specific surface areas of up to 605 m^2/g.

11.6.2 Films and Nanopapers

The incorporation of a limited amount of TEMPO-mediated oxidised NFC has been shown to improve to some extent, the wet strength of paper made with cellulose fibres [145–147]. Yet the first films, with a high content of nanocelluloses were prepared by Nagaito and co-workers by impregnating dried sheets made out of bacterial cellulose nanofibres [148] or wood-sourced NFC [149] with phenolic resins. The resulting films displayed a dense paper-like organisation with nanoorder-scale-interconnected network structures. They were porous and exhibited outstanding mechanical properties, but were brittle; similarly, nanocellulose-based films impregnated with melamine formaldehyde resins displayed comparable properties [150]. Full nanocellulose-based paper sheets have been prepared by drying suspensions of NFC in various media other than water. These suspensions were obtained by exchanging water with organic solvents such as methanol, ethanol and acetone. The resulting porous films obtained from carboxymethylated NCF show remarkably high toughness in relation to their large strain-to-failure, which is as high as 10%. Other studies have shown that NFC-based films were found to meet the requirements for packaging applications because at a 35 g/m^2 basis of weight, NFC-based films were found to have the requisite mechanical properties: tensile index of 146 Nm/g, elongation of 8.6%, an elastic modulus of 17.5 GPa and low oxygen transmission rates of 17 mL/m^2 day, which were comparable to synthetic packaging derived from oriented polyester ethylene vinyl alcohol [151]. These properties were further enhanced when these films were produced from NFCs containing residual lignin [95].

11.6.3 Polymeric Nanocomposites

Nanocelluloses have attracted a great deal of interest in the nanocomposites field since the first publication relating to the use of CNC as reinforcing fillers in poly-(styrene-*co*-butyl acrylate) (poly(S-*co*-BuA))-based nanocomposites by Favier and co-workers [152, 153]. They demonstrated a spectacular improvement in the storage modulus, as measured by dynamic mechanical analysis, above the glass-rubber transition temperature range, even at low CNC loading. The use of nanocelluloses, especially CNC, as fillers in polymeric nanocomposite materials is among the most studied

fields in biomaterials science. For more detailed information, the cited reviews are recommended [3, 154, 155].

The nanoscale dimensions, low density and extremely attractive mechanical properties of CNC make them ideal candidates to improve the mechanical properties of polymeric materials. They comprise a generic class of biomaterials that display mechanical strength that is approximately in the order of the binding forces of the adjacent atoms. The tensile strength properties of CNC are far in excess of current high-volume content reinforcement materials and allow access to among the highest attainable composite strengths. In fact, the axial Young's modulus of a CNC is theoretically stronger than stainless steel and similar to that of Kevlar. For CNC, the theoretical value of Young's modulus for the native cellulose perfect crystal has been estimated to be 167.5 GPa [156]. Recently, Raman spectroscopy was applied to measure the elastic modulus of native cellulose crystals from tunicate and cotton to yield values of 143 GPa [157] and 105 GPa [158], respectively. In fact, this technique was also recently applied by Hsieh and co-workers to determine the Young's modulus of a single filament of bacterial cellulose (BC). Their measurements provided a value of 114 GPa, which is not as high as values obtained by Šturcova and co-workers (although the authors offer reasoning based on crystallinity and structural differences), but nevertheless represents a great advancement in our ability to probe the overall physical properties of these unique nanocelluloses [159].

Due to their hydrophilic nature, nanocelluloses have been easily incorporated into waterborne systems containing hydrophilic or hydro-dispersible and latex-based polymer matrices. These composite systems are usually processed by casting-evaporation techniques, but alternative processing methods such as freeze-drying combined with hot-pressing or extrusion/hot pressing have also been reported. Fibre spinning and electrospinning are techniques that are now seeing many more applications.

Examples of polymer-based latex include, but are not limited to: poly-(styrene-*co*-butyl acrylate) (poly(S-*co*-BuA)) [152], poly(hydroxyoctanoate) [160, 161], poly(vinyl acetate) [49, 162], poly(ethylene-vinyl acetate) (PVA) [163], poly(vinyl chloride) [164–167], waterborne epoxy [168], natural rubber [169–171] and poly(styrene-*co*-hexyl-acrylate) [129]. Several hydrosoluble or hydro-dipersible polymers are reported where CNC were incorporated, such as poly(oxyethylene) [172–175], carboxymethylcellulose [176], poly(vinyl alcohol) [177–180] waterborne polyurethane [181], hydroxypropyl cellulose [179, 180], starch [46, 47, 182–186], soy protein [187], chitosan [188] or regenerated cellulose [189].

However, the main challenge of incorporating nanocellulose particles into the most common nonpolar polymeric matrices is interfacial compatibility issues, which

control the homogenous dispersibility within the matrix. It has been demonstrated that tunicin CNC could be dispersed in dimethylformamide without additives or surface modifications [190]. The clear message from this result is the possibility of using hydrophobic polymers as a matrix in addition to permitting additional chemical modifications of CNC, especially those incompatible in water. Different strategies such as surfactant surface coating, covalent or noncovalent chemical modifications (acetylation, esterification, silylation, polymer grafting and so on) have been pursued to improve the dispersibility/compatibility of nanocelluloses within nonpolar media. Following these strategies, nanocelluloses have been incorporated into a wide range of nonpolymer matrices, including thermoplastics, thermosets and urethanes. Examples of such polymers include: acrylic-based resins [191–193], siloxanes [194] polysulfonates [195], poly(caprolactone) [43, 121, 196], cellulose acetate butyrate [62, 197], polyethylene [198], polypropylene [199], polyurethane [200], poly(lactic acid) [201–207] and poly(hydroxybutyrates) [208].

11.7 Conclusions and Future

Micro/nanocelluloses are currently the subject of extensive worldwide research and development efforts to establish sustainable production technologies, and also the pursuit of novel applications in a diverse range of fields, which can be ascribed to their inherently attractive chemical and physical attributes. They can be obtained from a wide number of cellulosic sources which ultimately provide products that display various aspect ratios (length/width). They also constitute a very good platform for chemical functionalisation with a wide range of functional chemical moieties, therefore extending their application window. Although the field is still in its early stage, the knowledge accumulated and the continuous identification of end-use applications are going to further streamline development because the accrued benefits are extremely high. The reduction of production costs is the strongest driver to the growth of this area, although there are still significant scientific and technological challenges to address including uniformity of manufacture, and chemical compatibilisation for composite applications.

References

1. H.P.S. Abdul Khalil, A.H. Bhat and A.F. Ireana Yusra, *Carbohydrate Polymers*, 2012, **87**, 2, 963.

2. S.J. Eichhorn, *Soft Matter*, 2011, **7**, 2, 303.

3. Y. Habibi, L.A. Lucia and O.J. Rojas, *Chemical Reviews*, 2010, **110**, 6, 3479.

4. W. Hamad, *The Canadian Journal of Chemical Engineering*, 2006, **84**, 5, 513.

5. D. Klemm, B. Heublein, H-P. Fink and A. Bohn, *Angewandte Chemie International Edition*, 2005, **44**, 22, 3358.

6. D. Klemm, F. Kramer, S. Moritz, T. Lindström, M. Ankerfors, D. Gray and A. Dorris, *Angewandte Chemie-International Edition*, 2011, **50**, 24, 5438.

7. D. Klemm, D. Schumann, F. Kramer, N. Hessler, M. Hornung, H-P. Schmauder and S. Marsch, *Advances in Polymer Science*, 2006, **205**, 49.

8. D. Klemm, D. Schumann, F. Kramer, N. Heßler, D. Koth and B. Sultanova, *Macromolecular Symposia*, 2009, **280**, 1, 60.

9. N. Lavoine, I. Desloges, A. Dufresne and J. Bras, *Carbohydrate Polymers*, 2012, **90**, 2, 735.

10. R.J. Moon, A. Martini, J. Nairn, J. Simonsen and J. Youngblood, *Chemical Society Reviews*, 2011, **40**, 7, 3941.

11. K. Spence, Y. Habibi, and A. Dufresne in *Cellulose Fibers: Bio- and Nano-Polymer Composites*, Eds., S. Kalia, B.S. Kaith and I. Kaur, Springer, Berlin, Germany, 2011, p.179.

12. S. Eichhorn, A. Dufresne, M. Aranguren, N. Marcovich, J. Capadona, S. Rowan, C. Weder, W. Thielemans, M. Roman, S. Renneckar, W. Gindl, S. Veigel, J. Keckes, H. Yano, K. Abe, M. Nogi, A. Nakagaito, A. Mangalam, J. Simonsen, A. Benight, A. Bismarck, L. Berglund and T. Peijs, *Journal of Materials Science*, 2010, **45**, 1, 1.

13. Anon, *Nanocellulose: A Technology and Market Study*, Future Markets Inc., 2012.

14. A. Payen, *Comptes Rendus Hebdomadaires des Seances de l Academie des Sciences*, 1838, **7**, 1052.

15. E. Sjöström in *Wood Chemistry: Fundamentals and Applications*, Academic Press, New York, NY, USA, 1981.

16. A.D. French, N.R. Bertoniere, R.M. Brown, H. Chanzy, D. Gray, K. Hattori and W. Glasser in *Kirk-Othmer Encyclopedia of Chemical Technology*, 5th Edition, Ed., A. Seidel, John Wiley & Sons, Inc., Hoboken, NJ, USA, 2004, p.360.

17. L. Donaldson, *Wood Science and Technology*, 2007, **41**, 5, 443.

18. R.M. Brown, *Journal of Macromolecular Science, Part A*, 1996, **33**, 10, 1345.

19. R.M. Brown, *Journal of Polymer Science, Part A: Polymer Chemistry Edition*, 2004, **42**, 3, 487.

20. S.P. Rowland and E.J. Roberts, *Journal of Polymer Science, Part A: Polymer Chemistry Edition*, 1972, **10**, 8, 2447.

21. R. Nickerson, *Industrial & Engineering Chemistry Analytical Edition*, 1941, **13**, 6, 423.

22. R.F. Nickerson, *Industrial & Engineering Chemistry*, 1941, **33**, 8, 1022.

23. R.F. Nickerson and J.A. Habrle, *Industrial & Engineering Chemistry*, 1946, **38**, 3, 299.

24. O.A. Battista and S. Coppick, *Textile Research Journal*, 1947, **17**, 8, 419.

25. O.A. Battista, S. Coppick, J.A. Howsmon, F.F. Morehead and W.A. Sisson, *Industrial & Engineering Chemistry*, 1956, **48**, 2, 333.

26. O.A. Battista in *Cellulose Technology Research*, American Chemical Society, Washington, DC, USA, 1975, p.1.

27. B.G. Rånby, *Discussions of the Faraday Society*, 1951, **11**, 158.

28. B.G. Rånby, *Acta Chemica Scandinavica*, 1949, **3**, 5, 649.

29. S.M. Mukherjee, J. Sikorski and H.J. Woods, *Journal of the Textile Institute Transactions*, 1952, **43**, 4, T196.

30. S.M. Mukherjee and H.J. Woods, *Biochimica et Biophysica Acta*, 1953, **10**, 0, 499.

31. O.A. Battista, S. Coppick, J.A. Howsmon, F.F. Morehead and W.A. Sisson, *Industrial and Engineering Chemistry*, 1956, **48**, 333.

32. A. Sharples, *Transactions of the Faraday Society*, 1958, **54**, 913.

33. T. Yachi, J. Hayashi, M. Takai and Y. Shimizu, *Journal of Applied Polymer Science: Applied Polymer Symposium*, 1983, **37**, 325.

34. H. Håkansson and P. Ahlgren, *Cellulose*, 2005, **12**, 177.

35. C. Martin, *Journal of Polymer Science, Part C: Polymer Symposia*, 1971, **36**, 1, 343.

36. M.Y.C Martin, *Journal of Polymer Science, Part A: Polymer Chemistry Edition*, 1974, **12**, 7, 1349.

37. J. Schurz and K. John, *Cellulose Chemistry and Technology*, 1975, **9**, 493.

38. Y. Nishiyama, U.J. Kim, D.Y. Kim, K.S. Katsumata, R.P. May and P. Langan, *Biomacromolecules*, 2003, **4**, 4, 1013.

39. O.A. Battista, *Industrial & Engineering Chemistry Research*, 1950, **42**, 502.

40. A. Kai, *Sen-i Gakkaishi*, 1976, **32**, T326. [In Japanese]

41. X.M. Dong, J-F. Revol and D.G. Gray, *Cellulose*, 1998, **5**, 1, 19.

42. J. Araki, M. Wada, S. Kuga and T. Okano, *Langmuir*, 2000, **16**, 6, 2413.

43. Y. Habibi and A. Dufresne, *Biomacromolecules*, 2008, **9**, 7, 1974.

44. Y. Habibi, L. Foulon, V. Aguié-Béghin, M. Molinari and R. Douillard, *Journal of Colloid and Interface Science*, 2007, **316**, 388.

45. Y. Habibi, A-L. Goffin, N. Schiltz, E. Duquesne, P. Dubois and A. Dufresne, *Journal of Materials Chemistry*, 2008, **18**, 41, 5002.

46. X. Cao, Y. Chen, P.R. Chang, M. Stumborg and M.A. Huneault, *Journal of Applied Polymer Science*, 2008, **109**, 6, 3804.

47. X. Cao, Y. Chen, P.R. Chang, A.D. Muir and G. Falk, *Express Polymer Letters*, 2008, **2**, 7, 502.

48. X. Cao, H. Dong and C.M. Li, *Biomacromolecules*, 2007, **8**, 3, 899.

49. N.L. Garcia de Rodriguez, W. Thielemans and A. Dufresne, *Cellulose*, 2006, **13**, 3, 261.

50. G. Siqueira, J. Bras and A. Dufresne, *Biomacromolecules*, 2009, **10**, 2, 425.

51. W. Helbert, J.Y. Cavaillé and A. Dufresne, *Polymer Composites*, 1996, **17**, 4, 604.

52. A. Bendahou, Y. Habibi, H. Kaddami and A. Dufresne, *Journal of Biobased Materials and Bioenergy*, 2009, **3**, 1, 81.

53. J. Araki, M. Wada, S. Kuga and T. Okano, *Journal of Wood Science*, 1999, **45**, 3, 258.

54. S. Beck-Candanedo, M. Roman and D.G. Gray, *Biomacromolecules*, 2005, **6**, 2, 1048.

55. M. Roohani, Y. Habibi, N.M. Belgacem, G. Ebrahim, A.N. Karimi and A. Dufresne, *European Polymer Journal*, 2008, **44**, 8, 2489.

56. X. Cao, Y. Habibi and L.A. Lucia, *Journal of Materials Chemistry*, 2009, **19**, 38, 7137.

57. D. Bondeson, A. Mathew and K. Oksman, *Cellulose*, 2006, **13**, 2, 171.

58. L. Pranger and R. Tannenbaum, *Macromolecules*, 2008, **41**, 22, 8682.

59. J.R. Capadona, K. Shanmuganathan, S. Trittschuh, S. Seidel, S.J. Rowan and C. Weder, *Biomacromolecules*, 2009, **10**, 4, 712.

60. D. Bondeson, I. Kvien and K. Oksman in *ACS Symposium Series*, Eds., K. Oksman and M. Sain, American Chemical Society, Washington, DC, USA, 2006, p.10.

61. M.A.S. Azizi Samir, F. Alloin, M. Paillet and A. Dufresne, *Macromolecules*, 2004, **37**, 11, 4313.

62. M. Grunnert and W.T. Winter, *Journal of Polymers and the Environment*, 2002, **10**, 1/2, 27.

63. J. Araki and S. Kuga, *Langmuir*, 2001, **17**, 4493.

64. A. Hirai, O. Inui, F. Horii and M. Tsuji, *Langmuir*, 2009, **25**, 1, 497.

65. M.N. Anglès and A. Dufresne, *Macromolecules*, 2000, **33**, 22, 8344.

66. M.N. Anglès and A. Dufresne, *Macromolecules*, 2001, **34**, 2921.

67. M.M. de Souza Lima and R. Borsali, *Langmuir*, 2002, **18**, 992.

68. T. Koshizawa, *Kami Pa Gikyoshi*, 1960, **14**, 455. [In Japanese]

69. T. Okano, S. Kuga, M. Wada, J. Araki and J. Ikuina in *Cellulose Particles Hydrolyzed in Aqueous Solutions Containing Inorganic Acids and Showing Good Dispersibility in Water and Thickening, Emulsification and Hydrophilization Properties and their Manufacture*, Nisshin Oil Mills Ltd., Japan, 1999, p.6.

70. H. Ono, T. Matsui and I. Miyamato in *Stable Cellulose Dispersion and its Uses*, Asahi Kasei Kogyo Kabushiki Kaisha, Japan, 1999, p.77.

71. M. Usuda, O. Suzuki, J. Nakano and N. Migita, *Kogyo Kagaku Zasshi*, 1967, **70**, 3, 349.

72. I. Filpponen in *Department of Forest Biomaterials*, North Carolina State University, Raleigh, NC, USA, 2009, p.202.

73. H. Sadeghifar, I. Filpponen, S. Clarke, D. Brougham and D. Argyropoulos, *Journal of Materials Science*, 2011, **46**, 22, 7344.

74. G. Chen, A. Dufresne, J. Huang and P.R. Chang, *Macromolecular Materials and Engineering*, 2009, **294**, 1, 59.

75. B. Braun and J.R. Dorgan, *Biomacromolecules*, 2009, **10**, 2, 334.

76. J. Araki, M. Wada, S. Kuga and T. Okano, *Colloids and Surfaces A*, 1998, **142**, 1, 75.

77. J. Araki, M. Wada, S. Kuga and T. Okano, *Journal of Wood Science*, 1999, **45**, 3, 258.

78. J.F. Revol, H. Bradford, J. Giasson, R.H. Marchessault and D.G. Gray, *International Journal of Biological Macromolecules*, 1992, **14**, 170.

79. R.H. Marchessault, F.F. Morehead and M.J. Koch, *Journal of Colloid Science*, 1961, **16**, 327.

80. J.F. Revol, L. Godbout, X.M. Dong, D.G. Gray, H. Chanzy and G. Maret, *Liquid Crystals*, 1994, **16**, 1, 127.

81. M. Roman and W.T. Winter, *Biomacromolecules*, 2004, **5**, 5, 1671.

82. Y. Habibi, H. Chanzy and M.R. Vignon, *Cellulose*, 2006, **13**, 679.

83. A. Turbak, F. Snyder and K. Sandberg, *Journal of Applied Polymer Science: Applied Polymer Symposium*, 1983, **37**, 815.

84. A.N. Nakagaito and H. Yano, *Applied Physics A: Materials Science & Processing*, 2004, **78**, 4, 547.

85. K. Uetani and H. Yano, *Biomacromolecules*, 2010, **12**, 2, 348.

86. A. Chakraborty, M. Sain and M. Kortschot, *Holzforschung*, 2005, **59**, 1, 102.

87. S. Wang and Q. Cheng, *Journal of Applied Polymer Science*, 2009, **113**, 2, 1270.

88. S. Kalidhasan, A. Santhana KrishnaKumar, V. Rajesh and N. Rajesh, *Journal of Colloid and Interface Science*, 2012, **367**, 1, 398.

89. W. Chen, H. Yu and Y. Liu, *Carbohydrate Polymers*, 2011, **86**, 2, 453.

90. W. Chen, H. Yu, Y. Liu, P. Chen, M. Zhang and Y. Hai, *Carbohydrate Polymers*, 2011, **83**, 4, 1804.

91. Q. Cheng, S. Wang and Q. Han, *Journal of Applied Polymer Science*, 2010, **115**, 5, 2756.

92. S.P. Mishra, A.S. Manent, B. Chabot and C. Daneault, *Bioresources*, 2012, **7**, 1, 422.

93. K. Spence, R. Venditti, O. Rojas, Y. Habibi and J. Pawlak, *Cellulose*, 2011, **18**, 4, 1097.

94. A. Kaushik and M. Singh, *Carbohydrate Research*, 2011, **346**, 1, 76.

95. K. Spence, R. Venditti, O. Rojas, Y. Habibi and J. Pawlak, *Cellulose*, 2010, **17**, 4, 835.

96. K.L. Spence, R.A. Venditti, Y. Habibi, O.J. Rojas and J.J. Pawlak, *Bioresource Technology*, 2010, **101**, 15, 5961.

97. M. Henriksson, G. Henriksson, L.A. Berglund and T. Lindström, *European Polymer Journal*, 2007, **43**, 8, 3434.

98. T. Lindström, M. Ankerfors and G. Henriksson, inventors; STFI-Packforsk AB, assignee; WO 2007/091942 A1, 2007.

99. M. Pääkkö, M. Ankerfors, H. Kosonen, A. Nykänen, S. Ahola, M. Österberg, J. Ruokolainen, J. Laine, P.T. Larsson, O. Ikkala and T. Lindström, *Biomacromolecules*, 2007, **8**, 6, 1934.

100. S. Yoo and J.S. Hsieh, *Industrial & Engineering Chemistry Research*, 2010, **49**, 5, 2161.

101. S. Janardhnan and M. Sain, *Journal of Polymers and the Environment*, 2011, **19**, 3, 615.

102. T. Meyabadi and F. Dadashian, *Fibers and Polymers*, 2012, **13**, 3, 313.

103. A. Isogai, T. Saito and H. Fukuzumi, *Nanoscale*, 2011, **3**, 1, 71.

104. T. Isogai, T. Saito and A. Isogai, *Cellulose*, 2011, **18**, 2, 421.

105. R. Qian, A. Tang and G. Chen, *Journal of Biobased Materials and Bioenergy*, 2011, **5**, 2, 253.

106. T. Saito, Y. Nishiyama, J. Putaux, M.R. Vignon and A. Isogai, *Biomacromolecules*, 2006, **7**, 6, 1687.

107. T. Saito, S. Kimura, Y. Nishiyama and A. Isogai, *Biomacromolecules*, 2007, **8**, 8, 2485.

108. H. Fukuzumi, T. Saito, T. Iwata, Y. Kumamoto and A. Isogai, *Biomacromolecules*, 2008, **10**, 1, 162.

109. S. Iwamoto, W. Kai, T. Isogai, T. Saito, A. Isogai and T. Iwata, *Polymer Degradation and Stability*, 2010, **95**, 8, 1394.

110. C. Aulin, I. Varga, P.M. Claesson, L. Wågberg and T. Lindström, *Langmuir*, 2008, **24**, 6, 2509.

111. Wågberg, G. Decher, M. Norgren, T. Lindström, M. Ankerfors and K. Axnas, *Langmuir*, 2008, **24**, 3, 784.

112. C. Eyholzer, N. Bordeanu, F. Lopez-Suevos, D. Rentsch, T. Zimmermann and K. Oksman, *Cellulose*, 2010, **17**, 1, 19.

113. C. Eyholzer, A. Borges de Couraça, F. Duc, P.E. Bourban, P. Tingaut, T. Zimmermann, J.A.E. Månson and K. Oksman, *Biomacromolecules*, 2011, **12**, 5, 1419.

114. H. Liimatainen, M. Visanko, J.A. Sirviö, O.E.O. Hormi and J. Niinimaki, *Biomacromolecules*, 2012, **13**, 5, 1592.

115. E. Dinand, H. Chanzy and M.R. Vignon, *Cellulose*, 1996, **3**, 1, 183.

116. E. Dinand, H. Chanzy and R. Vignon, *Food Hydrocolloids*, 1999, **13**, 3, 275.

117. M.E. Malainine, M. Mahrouz and A. Dufresne, *Compososites Science and Technology*, 2005, **65**, 10, 1520.

118. Y. Habibi, M. Mahrouz and M. Vignon, *Food Chemistry*, 2009, **115**, 2, 423.

119. M.E. Malainine, M. Mahrouz and A. Dufresne, *Composites Science and Technology*, 2005, **65**, 10, 1520.

120. V. Favier, G.R. Canova, J.Y. Cavaillé, H. Chanzy, A. Dufreshne and C. Gauthier, *Polymers for Advanced Technologies*, 1995, **6**, 5, 351.

121. Y. Habibi, A-L. Goffin, N. Schiltz, E. Duquesne, P. Dubois and A. Dufresne, *Journal of Materials Chemistry*, 2008, **18**, 41, 5002.

122. M. Grunnert and W.T. Winter, *Journal of Polymers and the Environment*, 2002, **10**, 1/2, 27.

123. I. Kvien, B.S. Tanem and K. Oksman, *Biomacromolecules*, 2005, **6**, 6, 3160.

124. S. Elazzouzi-Hafraoui, Y. Nishiyama, J-L. Putaux, L. Heux, F. Dubreuil and C. Rochas, *Biomacromolecules*, 2008, **9**, 1, 57.

125. B. Braun, J.R. Dorgan and J.P. Chandler, *Biomacromolecules*, 2008, **9**, 4, 1255.

126. S.J. Hanley, J. Giasson, J.F. Revol and D.G. Gray, *Polymer*, 1992, **33**, 21, 4639.

127. M.M. de Souza Lima, J.T. Wong, M. Paillet, R. Borsali and R. Pecora, *Langmuir*, 2003, **19**, 1, 24.

128. W.J. Orts, L. Godbout, R.H. Marchessault and J.F. Revol, *Macromolecules*, 1998, **31**, 17, 5717.

129. A. Ben Elmabrouk, T. Wim, A. Dufresne and S. Boufi, *Journal of Applied Polymer Science*, 2009, **114**, 5, 2946.

130. J.F. Revol, *Carbohydrate Polymers*, 1982, **2**, 2, 123.

131. C. Tokoh, K. Takabe, M. Fujita and H. Saiki, *Cellulose*, 1998, **5**, 4, 249.

132. U.J. Kim, S. Kuga, M. Wada, T. Okano and T. Kondo, *Biomacromolecules*, 2000, **1**, 3, 488.

133. T. Ebeling, M. Paillet, R. Borsali, O. Diat, A. Dufresne, J.Y. Cavaillé and H. Chanzy, *Langmuir*, 1999, **15**, 19, 6123.

134. D. Fengel and G. Wegener in *Wood, Chemistry, Ultrastucture, Reactions*, Walter de Gruyter, New York, NY, USA, 1983.

135. P. Podsiadlo, S-Y. Choi, B. Shim, J. Lee, M. Cuddihy and N.A. Kotov, *Biomacromolecules*, 2005, **6**, 6, 2914.

136. Y. Lu, L. Weng, and X. Cao, *Macromolecular Bioscience*, 2005, **5**, 11, 1101.

137. B. Wang, M. Sain and K. Oksman, *Applied Composite Materials*, 2007, **14**, 2, 89.

138. G. Siqueira, J. Bras and A. Dufresne, *BioResources*, 2010, **5**, 2, 0727.

139. Y. Habibi, L. Foulon, V. Aguié-Béghin, M. Molinari and R. Douillard, *Journal of Colloid and Interface Science*, 2007, **316**, 388.

140. W. Helbert, J.Y. Cavaillé and A. Dufresne, *Polymer Composites*, 1996, **17**, 4, 604.

141. A.J. Vagan, M.A.S.A. Samir and L.A. Berglund, *Advanced Materials*, 2008, **20**, 7, 1263.

142. H. Sehaqui, M. Salajkova, Q. Zhou and L.A. Berglund, *Soft Matter*, 2010, **6**, 8, 1824.

143. C. Aulin, J. Netrval, L. Wågberg and T. Lindström, *Soft Matter*, 2010, **6**, 14, 3298.

144. L. Heath and W. Thielemans, *Green Chemistry*, 2010, **12**, 8, 1448.

145. T. Saito and A. Isogai, *Industrial & Engineering Chemistry Research*, 2007, **46**, 3, 773.

146. T. Saito and A. Isogai, *TAPPI*, 2005, **4**, 3, 3.

147. T. Saito and A. Isogai, *Industrial & Engineering Chemistry Research*, 2006, **46**, 3, 773.

148. A.N. Nakagaito, S. Iwamoto and H. Yano, *Applied Physics A: Materials Science & Processing*, 2005, **80**, 1, 93.

149. A.N. Nakagaito and H. Yano, *Applied Physics A: Materials Science & Processing*, 2005, **80**, 1, 155.

150. M. Henriksson and L.A. Berglund, *Journal of Applied Polymer Science*, 2007, **106**, 4, 2817.

151. K. Syverud and P. Stenius, *Cellulose*, 2009, **16**, 1, 75.

152. V. Favier, G.R. Canova, J.Y. Cavaille, H. Chanzy, A. Dufreshne and C. Gauthier, *Polymers for Advanced Technologies*, 1995, **6**, 5, 351.

153. V. Favier, H. Chanzy and J.Y. Cavaille, *Macromolecules*, 1995, **28**, 18, 6365.

154. I. Siró and D. Plackett, *Cellulose*, 2010, **17**, 3, 459.

155. M.A.S. Azizi Samir, F. Alloin and A. Dufresne, *Biomacromolecules*, 2005, **6**, 2, 612.

156. K. Tashiro and M. Kobayashi, *Polymer*, 1991, **32**, 8, 1516.

157. A. Šturcova, G.R. Davies and S.J. Eichhorn, *Biomacromolecules*, 2005, **6**, 1055.

158. R. Rusli and S.J. Eichhorn, *Applied Physics Letters*, 2008, **93**, 3, 033111.

159. Y.C. Hsieh, H. Yano, M. Nogi and S. Eichhorn, *Cellulose*, 2008, **15**, 4, 507.

160. D. Dubief, E. Samain and A. Dufresne, *Macromolecules*, 1999, **32**, 18, 5765.

161. A. Dufresne, *Composite Interfaces*, 2000, **7**, 1, 53.

162. M. Roohani, Y. Habibi, N.M. Belgacem, G. Ebrahim, A.N. Karimi and A. Dufresne, *European Polymer Journal*, 2008, **44**, 8, 2489.

163. G. Chauve, L. Heux, R. Arouini and K. Mazeau, *Biomacromolecules*, 2005, **6**, 4, 2025.

164. L. Chazeau, J.Y. Cavaillé, G. Canova, R. Dendievel and B. Boutherin, *Journal of Applied Polymer Science*, 1999, **71**, 11, 1797.

165. L. Chazeau, J.Y. Cavaillé and P. Terech, *Polymer*, 1999, **40**, 5333.

166. L. Chazeau, J.Y. Cavaillé and J. Perez, *Journal of Polymer Science, Part B: Polymer Physics Edition*, 2000, **38**, 383.

167. L. Chazeau, M. Paillet and J.Y. Cavaillé, *Journal of Polymer Science, Part B: Polymer Physics Edition*, 1999, **37**, 16, 2151.

168. M. Matos Ruiz, J.Y. Cavaillé, A. Dufresne, C. Graillat and J-F. Gerard, *Macromolecular Symposia*, 2001, **169**, 211.

169. A. Bendahou, Y. Habibi, H. Kaddami and A. Dufresne, *Journal of Biobased Materials and Bioenergy*, 2009, **3**, 1, 81.

170. A. Bendahou, H. Kaddami and A. Dufresne, *European Polymer Journal*, 2010, **46**, 4, 609.

171. G. Siqueira, H. Abdillahi, J. Bras and A. Dufresne, *Cellulose*, 2010, **17**, 2, 289.

172. M.A.S. Azizi Samir, F. Alloin, J-Y. Sanchez and A. Dufresne, *Polymer*, 2004, **45**, 12, 4149.

173. M.A.S. Azizi Samir, L. Chazeau, F. Alloin, J.Y. Cavaillé, A. Dufresne and J-Y. Sanchez, *Electrochimica Acta*, 2005, **50**, 19, 3897.

174. M.A.S. Azizi Samir, A.M. Mateos, F. Alloin, J-Y. Sanchez and A. Dufresne, *Electrochimica Acta*, 2004, **49**, 26, 4667.

175. M.A.S. Azizi Samir, F. Alloin, J-Y. Sanchez and A. Dufresne, *Polimeros: Ciencia e Tecnologia*, 2005, **15**, 2, 109.

176. Y. Choi and J. Simonsen, *Journal of Nanoscience and Nanotechnology*, 2006, **6**, 3, 633.

177. J. Lu, T. Wang and L.T. Drzal, *Composites Part A*, 2008, **39A**, 5, 738.

178. S.A. Paralikar, J. Simonsen and J. Lombardi, *Journal of Membrane Science*, 2008, **320**, 1–2, 248.

179. T. Zimmerman, E. Poehler and T. Geiger, *Advanced Engineering Materials*, 2004, **6**, 9, 754.

180. T. Zimmermann, E. Pöhler, and P. Schwaller, *Advanced Engineering Materials*, 2005, **7**, 12, 1156.

181. X. Cao, Y. Habibi and L.A. Lucia, *Journal of Materials Chemistry*, 2009, **19**, 38, 7137.

182. M.N. Anglès and A. Dufresne, *Macromolecules*, 2001, **34**, 2921.

183. W.J. Orts, S.H. Imam, J. Shey, G.M. Glenn, M.K. Inglesby, M.E. Guttman and A. Nguyen, *Annual Technical Conference – Society of Plastics Engineers*, 2004, **62**, 2, 2427.

184. I. Kvien, J. Sugiyama, M. Votrubec and K. Oksman, *Journal of Materials Science*, 2007, **42**, 19, 8163.

185. Y. Lu, L. Weng and X. Cao, *Macromolecular Bioscience*, 2005, **5**, 11, 1101.

186. Y. Lu, L. Weng and X. Cao, *Carbohydrate Polymers*, 2006, **63**, 2, 198.

187. Y. Wang, X. Cao and L. Zhang, *Macromolecular Bioscience*, 2006, **6**, 7, 524.

188. Q. Li, J. Zhou and L. Zhang, *Journal of Polymer Science, Part B: Polymer Physics Edition*, 2009, **47**, 11, 1069.

189. Q. Li and S. Renneckar, *Cellulose*, 2009, **16**, 6, 1025.

190. M.A.S. Azizi Samir, F. Alloin, J-Y. Sanchez, N. El Kissi and A. Dufresne, *Macromolecules*, 2004, **37**, 4, 1386.

191. S. Ifuku, M. Nogi, K. Abe, K. Handa, F. Nakatsubo and H. Yano, *Biomacromolecules*, 2007, **8**, 6, 1973.

192. M. Nogi, K. Abe, K. Handa, F. Nakatsubo, S. Ifuku and H. Yano, *Applied Physics Letters*, 2006, **89**, 23, 233123/1.

193. F. Khelifa, Y. Habibi, F. Benard and P. Dubois, *Journal of Materials Chemistry*, 2012, **22**, 38, 20520.

194. M. Grunnert and W.T. Winter, *Polymeric Materials Science and Engineering*, 2000, **82**, 232.

195. S. Noorani, J. Simonsen and S. Atre in *ACS Symposium Series: Cellulose Nanocomposites: Processing, Characterization and Properties*, Eds., K. Oksman and M. Sain, American Chemical Society, Washington, DC, USA, 2006, p.209.

196. A.L. Goffin, J.M. Raquez, E. Duquesne, G. Siqueira, Y. Habibi, A. Dufresne and P. Dubois, *Polymer*, 2011, **52**, 7, 1532.

197. L. Petersson, A.P. Mathew and K. Oksman, *Journal of Applied Polymer Science*, 2009, **112**, 4, 2001.

198. A. J. de Menezes, G. Siqueira, A.A.S. Curvelo and A. Dufresne, *Polymer*, 2009, **50**, 19, 4552.

199. C. Bonini in *Mise en Évidence du Rôle des Interactions Fibre/fFbre et Fibre/ Matrice Dans des Nanocomposites à Renfort Cellulosique et Matrice Apolaire (Atactique et Isotactique)*, Joseph Fourier University, Grenoble, France, 2000. [In French]

200. N.E. Marcovich, M.L. Auad, N.E. Bellesi, S.R. Nutt and M.I. Aranguren, *Journal of Materials Research*, 2006, **21**, 4, 870.

201. D. Bondeson and K. Oksman, *Composite Interfaces*, 2007, **14**, 7–9, 617.

202. D. Bondeson and K. Oksman, *Composites, Part A: Applied Science and Manufacturing*, 2007, **38A**, 12, 2486.

203. K. Oksman, A.P. Mathew, D. Bondeson and I. Kvien, *Composites Science and Technology*, 2006, **66**, 15, 2776.

204. L. Petersson, I. Kvien and K. Oksman, *Composites Science and Technology*, 2007, **67**, 11–12, 2535.

205. A.L. Goffin, Y. Habibi, J-M. Raquez and P. Dubois, *ACS Applied Materials & Interfaces*, 2012, **4**, 7, 3364.

206. A.L. Goffin, J-M. Raquez, E. Duquesne, G. Siqueira, Y. Habibi, A. Dufresne and P. Dubois, *Biomacromolecules*, 2011, **12**, 7, 2456.

207. J-M. Raquez, Y. Murena, A.L. Goffin, Y. Habibi, B. Ruelle, F. DeBuyl and P. Dubois, *Composites Science and Technology*, 2012, **72**, 5, 544.

208. L. Jiang, E. Morelius, J. Zhang, M. Wolcott and J. Holbery, *Journal of Composite Materials*, 2008, **42**, 24, 2629.

12 Optical Properties of Cellulose Esters and Applications to Optical Functional Films

Masayuki Yamaguchi and Mohd Edeerozey Abd Manaf

12.1 Optical Properties of Polymeric Materials

The refractive index is one of the most important optical properties for transparent materials, which is defined as the ratio of the optical velocity in vacuum to that in a medium. Therefore, the value is always larger than 1 and decides the refractive angle as expressed by the well-known Snell's law. Materials with a high refractive index are preferably employed as lenses, whereas clothes made of fibres with a low refractive index provide a 'deep' colour, due to the low level of reflection. Since cellulose esters have a relatively low refractive index, which is similar to that observed in silk, some of them are employed for specific clothes that require a 'deep' black effect.

Cellulose esters are also employed for optical displays such as a liquid crystal display. In this application, various types of polymer films are required to construct a display, such as antiglare film, retardation film, protective film, brightness enhancement film and diffusion film. In particular, polarisation is an extremely important property for retardation and protective films.

This property is expressed by birefringence Δn. In the case of oriented polymer films, the birefringence can be controlled by varying the stretching ratio. Consequently, it is always used for a retardation film that gives a specific retardation ($\Gamma = d\,\Delta n$; d is the film thickness). Another important optical film used in displays is the protective film, which is used to protect a polariser from moisture. Therefore, it has to be free from birefringence so that the polarised light will not be disturbed.

In the case of retardation films used in a colour display, retardation not only at a specific wavelength, but also in the broad range of visible light has to be controlled. For example, the absolute value of birefringence must show an increase with increasing the wavelength for wavelength phase difference plates, such as a quarter-wave plate and a half-wave plate. This property is known as 'extraordinary wavelength dispersion' of birefringence. These days, a multiband quarter-wave plate, one of the retardation

films that gives a retardation of a quarter of a wavelength, is required because it is used for advanced display devices, i.e., as glasses for a 3D-display and antifilms for an electroluminescent display. Conventional polymers however, show ordinary dispersion, in which the orientation birefringence increases with the wavelength. This behaviour can be expressed by the following equation which was proposed based on the Sellmeier relation, **Equation 12.1**:

$$n(\lambda)^2 = 1 + \sum_i \frac{A_i}{\lambda^2 - B_i} \tag{12.1}$$

where λ and $n(\lambda)$ are the wavelength of light and the average refractive index, respectively. A and B are the Sellmeier coefficients.

Based on the Kuhn and Grün model proposed for the stress-optical behaviour of crosslinked rubbers, the orientation birefringence $\Delta n(\lambda)$ of an oriented polymer is expressed as follows [1–6]:

$$\Delta n(\lambda) = \frac{2\pi}{9} \frac{(n(\lambda)^2 + 2)^2}{n(\lambda)} N \, \Delta\alpha(\lambda) \left(\frac{3\langle \cos^2\theta \rangle - 1}{2} \right) \tag{12.2}$$

where N, $\Delta\alpha(\lambda)$ and θ are the number of chains in a unit volume, the polarisability anisotropy and the angle that a segment makes with the stretch axis, respectively. The last bracketed term $(3\langle\cos^2\theta\rangle\text{-}1)/2$ is identically equal to the Hermans orientation function [3, 7], whereas the other part in the right hand side of the term is called intrinsic birefringence, which is independent of the molecular weight and determined by the chemical structure of the monomer unit. Consequently, **Equation 12.2** can be written as:

$$\Delta n(\lambda) = \Delta n^0(\lambda) F \tag{12.3}$$

where $\Delta n^0(\lambda)$ is the intrinsic birefringence and F is the Hermans orientation function.

Considering that stress in the rubbery state is originated from the entropy loss by chain orientation, the following stress-optical rule is derived:

$$\Delta n(\lambda) = C\sigma \tag{12.4}$$

$$C = \frac{2\pi}{45k_BT}\frac{(n(\lambda)^2 + 2)^2}{n(\lambda)}\Delta\alpha(\lambda) \tag{12.5}$$

where σ is the stress, C is the stress-optical coefficient and k_B is the Boltzmann constant.

Regarding the wavelength dispersion, the following simple relation is derived:

$$\frac{\Delta n(\lambda)}{\Delta n(\lambda_0)} = \frac{\Delta n^0(\lambda)}{\Delta n^0(\lambda_0)} = const. \tag{12.6}$$

where λ_0 is the arbitrary standard wavelength.

According to **Equation 12.6**, the wavelength dispersion of birefringence, i.e., normalised birefringence $\Delta n(\lambda)/\Delta n(\lambda_0)$, is a constant and determined by the chemical structure.

Both **Equation 12.1** and **Equation 12.6** demonstrate that it is extremely difficult to obtain a polymeric film exhibiting extraordinary wavelength dispersion of the orientation birefringence. For example, the orientation birefringence of stretched films of polycarbonate (PC) is shown in **Figure 12.1**. As seen in the figure, the absolute values of the birefringence decrease with the wavelength. The wavelength dispersion of the birefringence is therefore, contrary to that of an ideal wavelength phase different plate. Furthermore, the wavelength dispersion of birefringence is also independent of the draw ratio as demonstrated in **Figure 12.1**, in which both curves of the normalised orientation birefringence fall on one line.

However, some stretched films of cellulose esters are known to show extraordinary wavelength dispersion. In this chapter, the wavelength dispersion of orientation birefringence for cellulose esters is discussed in detail, after a brief introduction on the concept of controlling the optical anisotropy. Finally, an advanced method to obtain the extraordinary dispersion of the orientation birefringence is proposed.

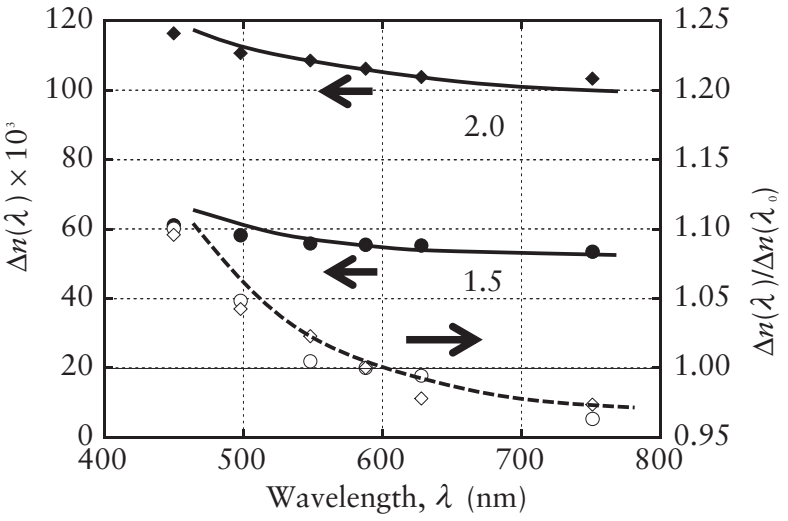

Figure 12.1 Wavelength dependence of (closed symbols) orientation birefringence and (open symbols) normalised orientation birefringence for stretched PC films at draw ratios of (circles) 1.5 and (diamonds) 2.0

12.2 Wavelength Dispersion of Orientation Birefringence

An ideal wavelength phase difference plate shows a consistent retardation value, e.g., quarter wavelength ($\lambda/4$), over a wide range of visible light. As retardation is given by the product of birefringence and thickness, a retardation film must show an increase in birefringence with increasing wavelength. Industrially, the so-called extraordinary dispersion of the orientation birefringence is achieved by piling together two or more polymer films of different wavelength dispersion, with their fast axes set to be perpendicular to each other, as illustrated in **Figure 12.2**. By rotating one of the films at 90°, its fast direction is converted into the slow one ($B_{\parallel} \rightarrow B_{\perp}$) and the combination of the birefringence from these films yields extraordinary wavelength dispersion of orientation birefringence. However, as two or more films are stuck together to produce the required retardation, the adhesion process requires intense care regarding the direction of the optical axes and is rather costly. Thus, having a single material that shows extraordinary dispersion of orientation birefringence is desired as the cost production and thickness can be reduced.

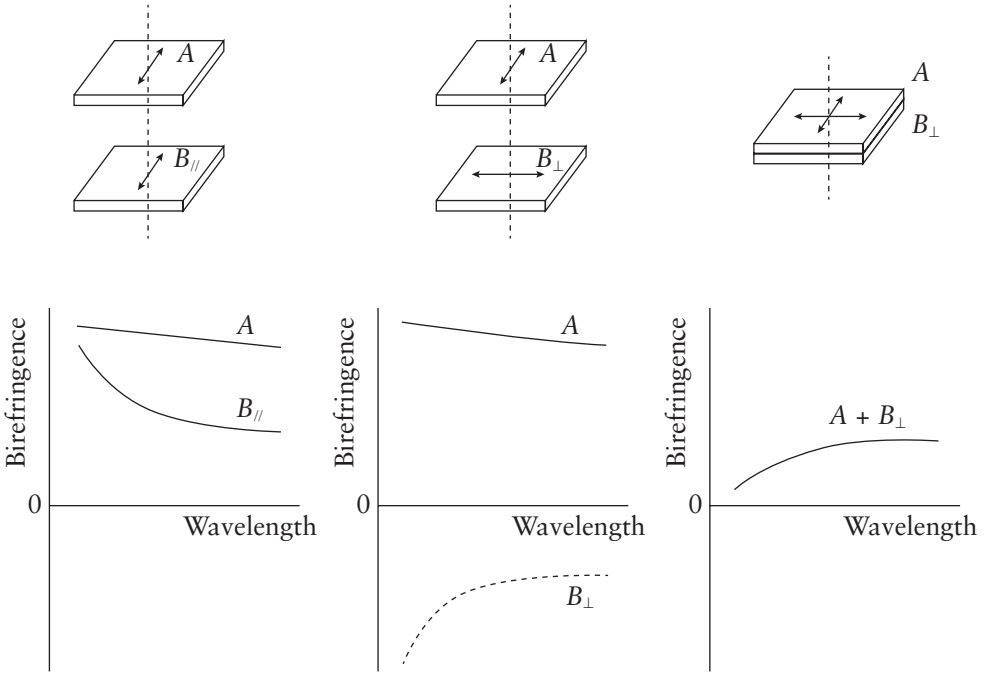

Figure 12.2 Combination of two films having different wavelength dispersion to produce an extraordinary wavelength dispersion of orientation birefringence

The polymer blend method has been employed as a means of controlling birefringence in polymers. Uchiyama and Yatabe [8, 9] have successfully produced polymer films with extraordinary wavelength dispersion of orientation birefringence by using a miscible blend of poly(2,6-dimethyl-1,4-phenylene oxide) (PPO) and atactic polystyrene (PS). In the blend system, PS shows negative birefringence with strong wavelength dependence, whereas PPO exhibits a positive birefringence with weak wavelength dependence. Although both polymers show ordinary wavelength dispersion, blends of certain composition exhibit extraordinary wavelength dispersion due to the summation of the contributions from both polymers as follows:

$$\Delta n = \Delta n_F + \sum_i \phi_i \Delta n_i \tag{12.7}$$

where i refers to the i-th component, ϕ_i is the volume fraction and Δn_F is the birefringence arising from structural or deformation effects.

Additional research carried out in Japan, conducted by Professor Ougizawa and co-workers [10], obtained a transparent polymer film with extraordinary wavelength dispersion from a miscible blend comprising of polynorbornene (NB) and poly(styrene-*co*-maleic anhydride) (SMA) at appropriate blend ratios. As predicted from the chemical structure, NB has a positive birefringence with weak wavelength dispersion, while SMA has a negative birefringence with strong wavelength dispersion.

A specific copolymer also shows extraordinary wavelength dispersion, which was first demonstrated by Uchiyama and Yatabe [11], when employing two monomers such as 2,2-*bis*(4-hydroxyphenyl)propane (BPA) and 9,9-*bis*(4-hydroxy-3-methylphenyl) fluorine (BMPF). Similar to the blend method, one monomer (BPA) has a positive birefringence with weak wavelength dispersion, while the other (BMPF) has a negative birefringence with a strong dispersion for the copolymer.

In principle, the extraordinary wavelength dispersion of birefringence produced by the blend and copolymerisation techniques is achieved by using a similar concept to that of the piling method (**Figure 12.2**) as illustrated in **Figure 12.3** below.

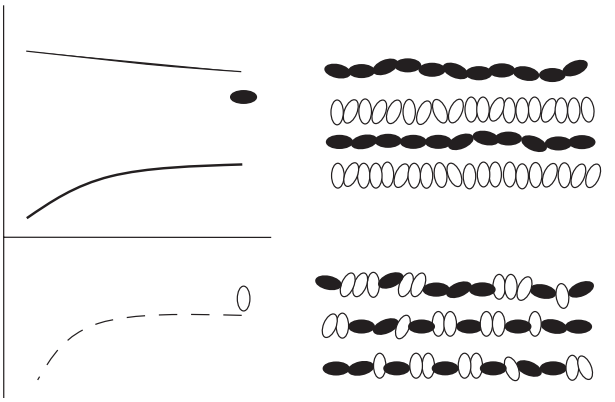

Figure 12.3 Illustration of the miscible blend and random copolymerisation methods to produce extraordinary wavelength dispersion of orientation birefringence. Reproduced with permission from M. Yamaguchi, M.E.A. Manaf, K. Songsurang and S. Nobukawa, *Cellulose*, 2012, **19**, 3, 601. ©2012, Springer [12]

Addition of needle-shaped solid particles demonstrating strong optical anisotropy also modifies the orientation birefringence and its wavelength dispersion, as reported by Koike and co-workers [13].

12.3 Orientation Birefringence of Cellulose Esters

Interestingly, some cellulose esters have been known to show extraordinary wavelength dispersion of orientation birefringence. The wavelength dispersions of orientation birefringence for various types of films of cellulose esters stretched at a draw ratio of 2.0 are shown in **Figure 12.4** [14]. The numerals in the cellulose acetate butyrate (CAB) samples represent the weight fraction (wt%) of the butyryl group. All samples were uniaxially stretched at a temperature where the storage modulus at 10 Hz was 10 MPa, in order to provide the same stress level for all samples having different glass transition temperatures. Except for cellulose triacetate (CTA), all CAB, cellulose acetate propionate (CAP) and cellulose diacetate (CDA) samples employed in this experiment exhibited a positive birefringence with extraordinary wavelength dispersion. Among them, CDA showed the largest value of orientation birefringence indicating the significant contribution of the hydroxyl group to positive birefringence. CTA shows negative birefringence with ordinary dispersion, in agreement with the result by El-Diasty and co-workers [15]. The result demonstrates that the acetyl group provides negative birefringence.

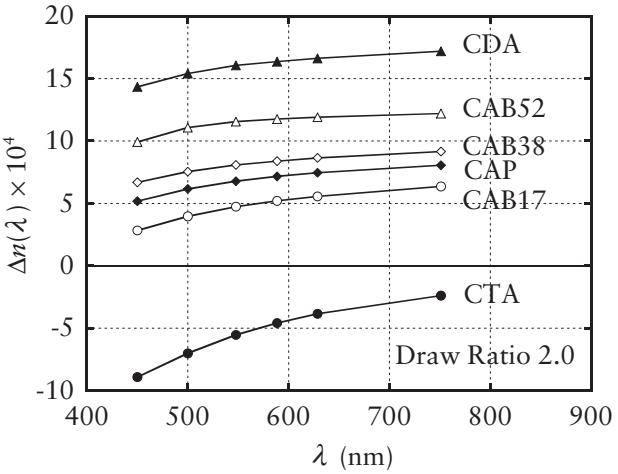

Figure 12.4 Wavelength dependence of orientation birefringence for stretched films of various cellulose esters. The numerals in the CAB label represent the weight concentration of the butyryl group. The degree of substitution of the propionyl group in CAP is 2.58, and those of the butyryl group are 0.73, 1.74 and 2.64 for CAB17, CAB38 and CAB52, respectively. Reproduced with permission from M. Yamaguchi, K. Okada, M.E.A. Manaf, Y. Shiroyama, T. Iwasaki and K. Okamoto, *Macromolecules*, 2009, **42**, 22, 9034. ©2009, ACS Publications [14]

The contribution of the hydroxyl and acetyl groups in CDA were calculated from the experimental results of CTA and CDA using the same relation as **Equation 12.6**, assuming: (i) orientation relaxation is ignored; (ii) contribution of the main chains is ignored; (iii) contribution of the crystalline part of CTA is ignored; and (iv) both hydroxyl and acetyl groups have the same orientation function in CTA and CDA at a constant draw ratio. As seen in **Figure 12.5**, the considerable contribution of the hydroxyl group is confirmed, although the molar content in CDA is lower than that of the acetyl group.

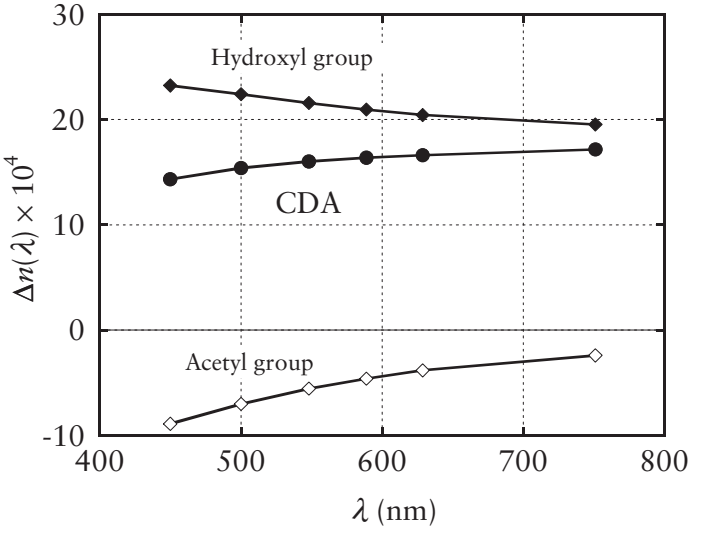

Figure 12.5 Contribution of (closed diamonds) hydroxyl and (open diamonds) acetyl groups to the orientation birefringence of (closed circles) CDA at a draw ratio of 2.0. The birefringence values of both groups are derived from the experimental results of CTA and CDA. Reproduced with permission from M. Yamaguchi, K. Okada, M.E.A. Manaf, Y. Shiroyama, T. Iwasaki and K. Okamoto, *Macromolecules*, 2009, **42**, 22, 9034. ©2009, ACS Publications [14]

Furthermore, it was found that the positive birefringence increases upon increasing the butyryl content, as evidenced in **Figure 12.6** (plotted against the degree of substitution of butyryl or propionyl, S_b) [16]. The figure indicates that CAB with an S_b of 0.35 of the butyryl group content shows no birefringence. Moreover, the figure shows that the butyryl group has a stronger impact on the birefringence than the

propionyl group, since the data of CAP is displaced downward from the solid line. As mentioned in **Figure 12.5** however, the hydroxyl group significantly affects the orientation birefringence. Therefore, the concentration of the hydroxyl group should always be considered in addition to the butyryl or propionyl content.

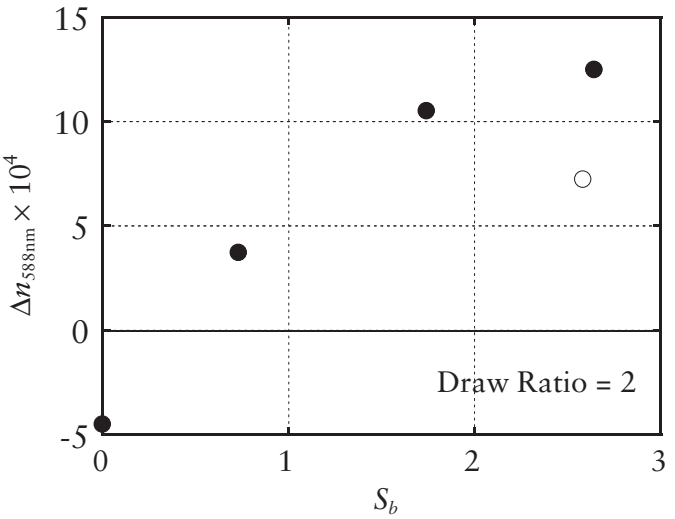

Figure 12.6 Orientation birefringence at a draw ratio of 2 plotted against the degree of substitution of the butyryl group, S_b, for CAB (closed symbols). The open symbol denotes the data for CAP plotted against the degree of substitution of the propionyl group. Reproduced with permission from M. Yamaguchi, M.E.A. Manaf, K. Songsurang and S. Nobukawa, *Cellulose*, 2012, **19**, 3, 601. ©2012, Springer [12]

The effect of the species of ester groups on the wavelength dispersion is evaluated from the normalised orientation birefringence as shown in **Figure 12.7**. Data for CAB38, which is located between those for CAB17 and CAB52, is omitted in the figure for a better view of the results. It is obvious that the acetyl group shows the strongest wavelength dependence. As shown in the figure, the slope of the normalised orientation birefringence of CAP is larger than that of CAB52, although both contain a similar level of the degree of substitution of ester groups. This suggests that the propionyl group provides a stronger wavelength dependence of the birefringence than the butyryl group. Furthermore, the wavelength dependence of the normalised

orientation function becomes weaker as the butyryl content is increased. This is reasonable due to the weak wavelength dependence of the butyryl group.

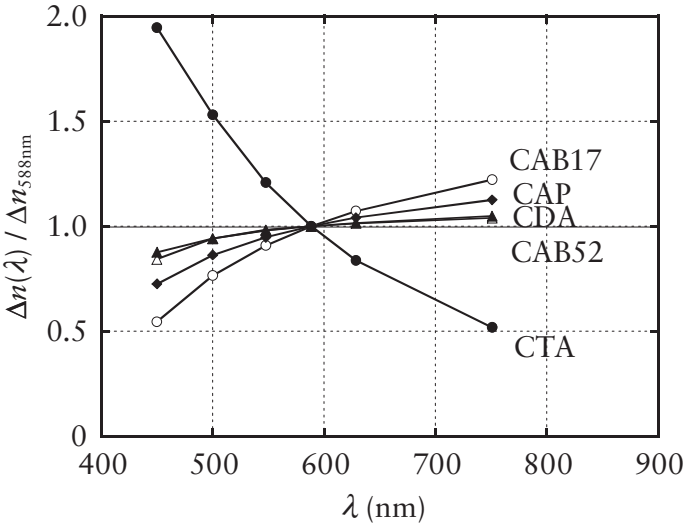

Figure 12.7 Wavelength dependence of orientation birefringence for stretched films of various cellulose esters. The numerals in the CAB label represent the weight concentration of the butyryl group. The degree of substitution of the propionyl group in CAP is 2.58, and those of the butyryl group are 0.73 and 2.64 for CAB17 and CAB52, respectively. Reproduced with permission from M. Yamaguchi, K. Okada, M.E.A. Manaf, Y. Shiroyama, T. Iwasaki and K. Okamoto, *Macromolecules*, 2009, **42**, 22, 9034. ©2009, ACS Publications [14]

Regarding the wavelength dependence of the ester groups, the following relation is expected:

$$-\frac{d(\Delta n(\lambda))}{d\lambda}\bigg|_{\text{Acetyl}} > \frac{d(\Delta n(\lambda))}{d\lambda}\bigg|_{\text{Propionyl}} > \frac{d(\Delta n(\lambda))}{d\lambda}\bigg|_{\text{Butyryl}} \tag{12.8}$$

The orientation function F of the pyranose ring in the CAP film was evaluated by the infrared dichroic ratio D ($= A_{//}/A_{\perp}$) of the absorption band at 880 cm^{-1}, whose electric

vector is perpendicular to the main chain. It was found not to be proportional to -(D-1)/(D+2), as seen in **Figure 12.8** [14]. As (D-1)/(D+2) is proportional to the Hermans orientation function, the result suggests that the stress-optical rule is not applicable to CAP. In other words, the orientation birefringence of CAP is determined not by the orientation of the main chains, but rather by the species and the concentration of the hydroxyl and ester groups. Consequently, the orientation birefringence of CAP is mainly determined by the following relation:

$$\Delta n(\lambda) = \Delta n_A^0(\lambda) F_A + \Delta n_P^0(\lambda) F_P + \Delta n_{OH}^0(\lambda) F_{OH} \tag{12.9}$$

where $\Delta n_A^0(\lambda)$, $\Delta n_P^0(\lambda)$ and $\Delta n_{OH}^0(\lambda)$ are the intrinsic birefringences, and F_A, F_P and F_{OH} are the orientation functions of the acetyl, propionyl and hydroxyl groups, respectively. The contribution of the hydroxyl group is of course neglected, when esterification is completed for all hydroxyl groups in the initial cellulose.

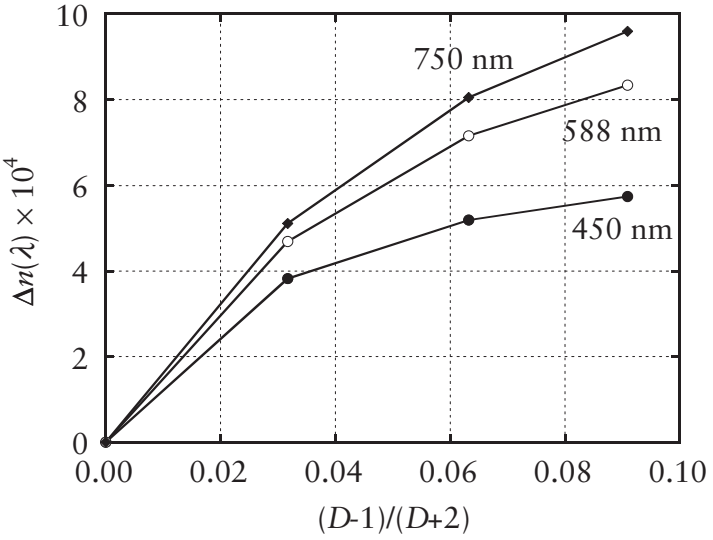

Figure 12.8 Relation between (D-1)/(D+2) and orientation birefringence at various wavelengths. Reproduced with permission from M. Yamaguchi, K. Okada, M.E.A. Manaf, Y. Shiroyama, T. Iwasaki and K. Okamoto, *Macromolecules*, 2009, **42**, 22, 9034. ©2009, ACS Publications [14]

As mentioned previously, the fact that CTA shows negative orientation birefringence with ordinary dispersion suggests that the acetyl group provides negative orientation birefringence. On the contrary, the propionyl and butyryl groups, as well as the hydroxyl group, provide positive birefringence with weak wavelength dispersion. Therefore, it can be concluded that the extraordinary wavelength dispersion, as observed in some cellulose esters, is attributed to the combination of negative and positive birefringences having different wavelength dependence. Furthermore, it is indicated that the flexible and bulky methylene parts of the ester groups with longer alkyl chains, such as propionyl and butyryl, lead to the parallel orientation of the polarisability anisotropy along the flow direction, whereas those of the acetyl group orient perpendicular to the flow direction.

The formation of the extraordinary wavelength dispersion of orientation birefringence in cellulose esters such as CAP is illustrated in **Figure 12.9** [14]. In the figure, the polarisability anisotropy of the ester groups, i.e., acetyl and propionyl are represented by ellipsoids. As depicted in the figure, the addition of both components, denoted by a bold line, gives the extraordinary dispersion with a positive orientation birefringence, when the wavelength dependence of the propionyl group is weaker than that of the acetyl group. This is similar to the formation of the extraordinary wavelength dispersion of birefringence as observed in the miscible blend as well as random copolymerisation methods. In the case of CDA, the dark circles represent the hydroxyl groups.

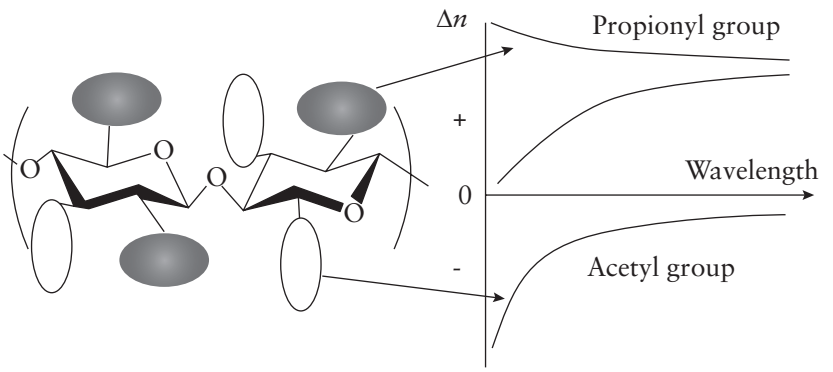

Figure 12.9 Illustration of CAP molecules and the contribution of each ester group to the orientation birefringence. Reproduced with permission from M. Yamaguchi, K. Okada, M.E.A. Manaf, Y. Shiroyama, T. Iwasaki and K. Okamoto, *Macromolecules*, 2009, **42**, 22, 9034. ©2009, ACS Publications [14]

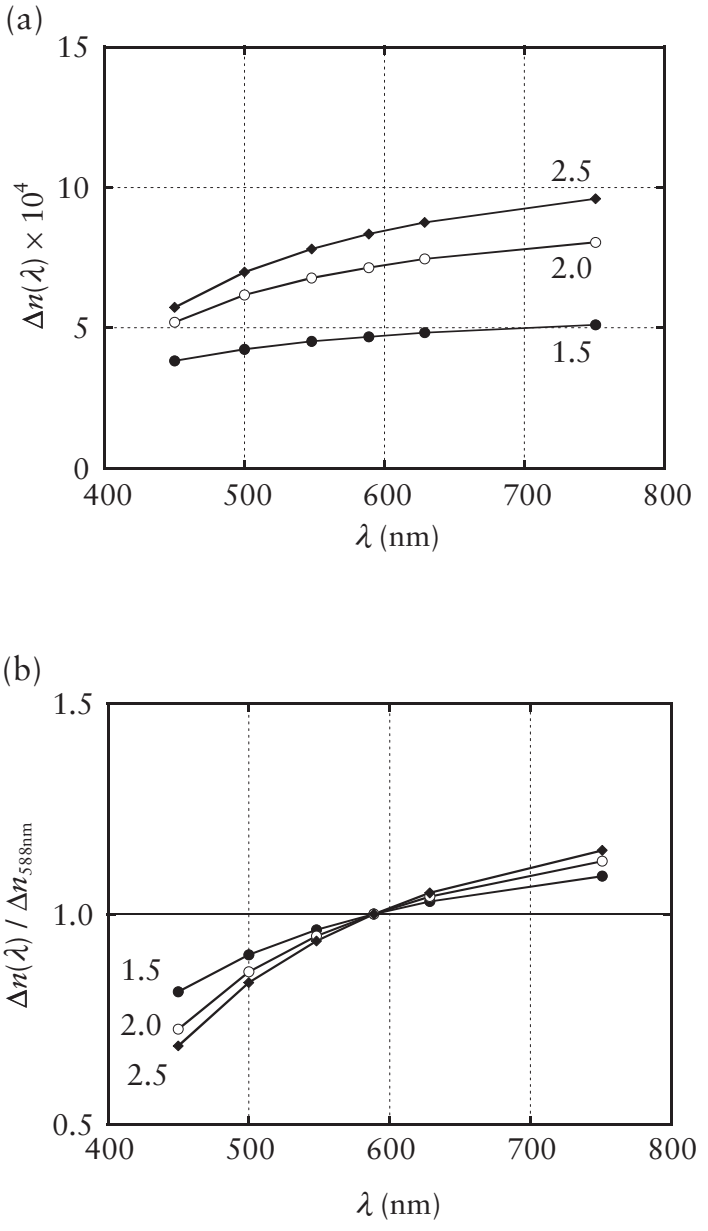

Figure 12.10 Wavelength dependence of (a) orientation birefringence and (b) normalised orientation birefringence of stretched CAP at various draw ratios: (closed circles) 1.5, (open circles) 2.0 and (closed diamonds) 2.5. Reproduced with permission from M. Yamaguchi, K. Okada, M.E.A. Manaf, Y. Shiroyama, T. Iwasaki and K. Okamoto, *Macromolecules*, 2009, **42**, 22, 9034. ©2009, ACS Publications [14]

The wavelength dispersion of the orientation birefringence in cellulose esters is also dependent upon the draw ratio as shown in **Figure 12.10** [14]. It is obvious that the extraordinary dispersion becomes pronounced upon increasing the draw ratio, which is not observed in a conventional polymer as discussed earlier (**Figure 12.1**). Considering that the acetyl group shows a strong wavelength dispersion, the result indicates that the contribution of the acetyl group, i.e., $F_A/(F_A+F_P)$, increases with the draw ratio. From an industrial point of view, the phenomenon indicates that the wavelength dispersion can be controlled by stretching conditions such as the degree of stretching (draw ratio), stretching temperature and stretching speed, which is extremely important information for the actual application.

12.4 Advanced Methods to Control Orientation Anisotropy

It has been revealed that the orientation birefringence of a polymer film is modified by the addition of a low-mass compound exhibiting strong optical anisotropy. Upon stretching, low-mass compounds, which are dissolved in a polymer matrix, are forced to orient in the same direction as the polymer chains by intermolecular orientation correlation called 'nematic interaction' [17, 18]. This intermolecular interaction was originally used to explain the orientation relaxation of a short chain in a polymer melt with a broad molecular weight distribution. It has since been clarified that the nematic interaction is expected to occur in a polymer blend system as long as the system is miscible. Quantitative studies on the nematic interaction in miscible polymer blends have been carried out by Urakawa and co-workers [19–22] based on the orientation coupling theory [23]. This technique uses miscible blends which can be employed to modify the wavelength dispersion of orientation birefringence. Yamaguchi and co-workers studied the effect of a small addition of poly(lactic acid) (PLA) on the orientation birefringence of CAP. They found that PLA is miscible with CAP on a molecular scale when the amount of PLA is less than 3 wt% [24]. Moreover, the orientation birefringence of CAP is greatly enhanced even upon a small addition of PLA as shown in **Figure 12.11**. Considering that the relaxation times are 0.045 s for PLA and approximately 1,000 s for CAP at the stretching temperature, the high level of orientation of PLA chains without relaxation is attained by the cooperative alignment (nematic interaction) with CAP chains. The study indicates that a retardation film having a high level of birefringence, leading to a thin film, can be designed by polymer blends composed of only biomass-based materials. Furthermore, the blends with more than 3 wt% of PLA exhibit large haze values, indicating the existence of phase-separated morphology, as previously reported by Tatsushima and co-workers [25]. As a result, the blends lose transparency and show a similar level of orientation birefringence to the blend with 1 wt% of PLA. This is reasonable because PLA chains in the dispersed phase have no nematic interaction

with CAP chains, thus the orientation will relax immediately when compared with CAP, as illustrated in **Figure 12.12**. As demonstrated for this method, attention has to be focused on the miscibility. Yamaguchi and Masuzawa found that CAP is miscible with poly(vinyl acetate) (PVAc) which has a negative orientation birefringence [26]. Although they only showed that the birefringence at a specific wavelength decreases with the PVAc content, the wavelength dispersion must be modified. They also revealed that poly(epichlorohydrin), having a negative birefringence, is miscible with CAP [27]

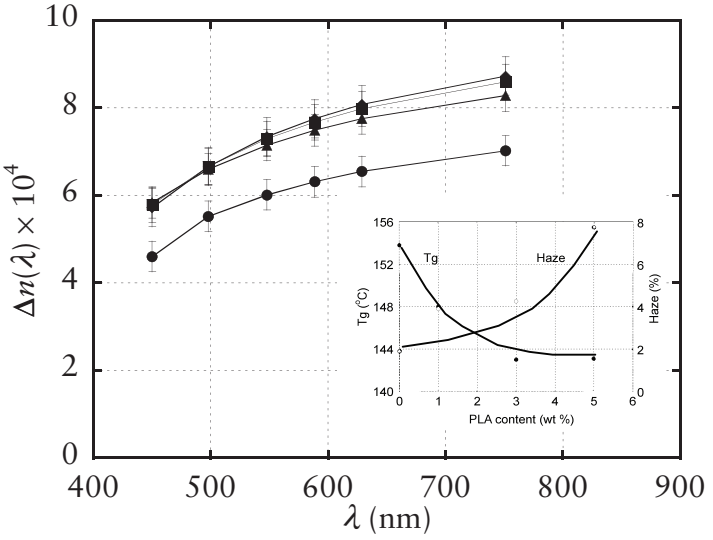

Figure 12.11 Wavelength dependence of orientation birefringence for CAP and CAP/PLA blends stretched at a draw ratio of 2.0: (circles) PLA, (diamonds) 1 wt% of PLA, (triangles) 3 wt% of PLA and (squares) 5 wt% of PLA. The relation between PLA content with regard to the Tg and haze value of the blend are shown in the subfigure. Reproduced with permission from M. Yamaguchi, S. Lee, M.E.A. Manaf, M. Tsuji and T. Yokohara, *European Polymers Journal*, 2010, **46**, 12, 2269. ©2010, Elsevier [24]

Besides polymeric materials, plasticisers such as diethyl phthalate (DEP) and tricresyl phosphate (TCP) are effective in modifying the orientation birefringence of cellulose esters [28–30]. This phenomenon is also attributed to nematic interaction. The degree of modification depends on the intrinsic birefringence of the plasticiser, as well as the nematic interaction coefficient between the plasticiser and the host polymer. Such a

phenomenon is also observed in a solution-cast film [29]. Moreover, some low-mass compounds contribute negative orientation birefringence, when the optical slow axis is perpendicular to the long axis of the low-mass compound [30]. Using a low-mass compound such as a plasticiser is of great benefit, because there are numerous miscible systems due to the large mixing entropy. Because both TCP and DEP contribute to positive orientation birefringence, their incorporation into CTA, which has a negative birefringence with ordinary dispersion, results in the blends having extraordinary wavelength dispersion. **Figure 12.13** shows the orientation birefringence of pure CTA and CTA with 5 and 10 wt% of TCP. CTA with 10 wt% of TCP shows extraordinary wavelength dispersion, in which the orientation birefringence shows almost an ideal dispersion (indicated by the straight dotted line) as required for a multiband quarter-wave plate [31]. Since the molecular shape of TCP is disc-like, more effective rod-shaped low-mass compounds with strong optical anisotropy will be found in the near future. Preliminary experimental results have been reported by our research group [32].

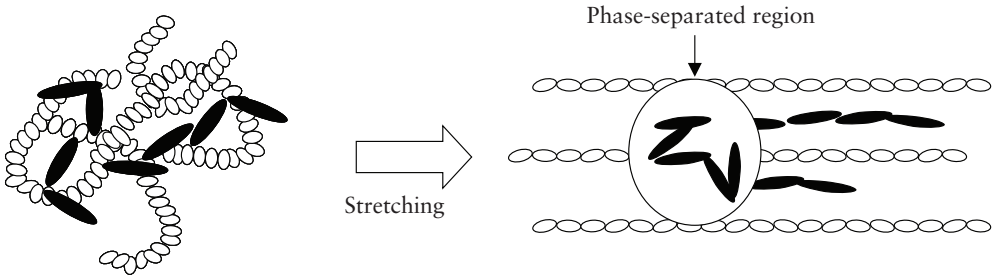

Figure 12.12 Phenomenon of the relaxation of PLA in the phase-separated region for the CAP/PLA blends with above 3 wt% of PLA, illustrated using polarisability anisotropy of (open ellipsoids) CAP and (closed ellipsoids) PLA

Although the orientation of the main chain does not directly affect the orientation birefringence of cellulose esters, it has an impact on the orientation of the ester groups as well as the hydroxyl group. Furthermore, the orientation of the main chain strongly affects the nematic interaction with low-mass compounds. Therefore, the main chain orientation, which is proportional to the stress, should be considered even for cellulose esters. For a better understanding, the effect of stress relaxation on the orientation birefringence was studied by holding the stretched sample in a hot chamber at various residence times [31]. We found that the orientation birefringence decreases monotonically with increasing holding time after stretching. Furthermore, there is

no further decrease in the orientation birefringence above a 30 min holding time. The results suggest that the TCP molecules relax the orientation when left at a high temperature without being quenched. In order to further confirm the contribution of TCP, the stretched sample of the CTA/TCP (95/5) blend was immersed in methanol for 24 h to remove TCP, and the orientation birefringence was measured. There was no considerable change in the dimension of the sample after 24 h of immersion, suggesting there is almost no alteration in the degree of stretching upon immersion in methanol. Furthermore, it was confirmed by IR spectral analysis that TCP was completely removed. Orientation birefringence of the CTA/TCP (95/5) before and after the methanol immersion is shown in **Figure 12.14** [31]. After the immersion, the orientation birefringence of the CTA/TCP blend decreases and approaches that of pure CTA. Therefore, the removal of TCP is reflected in the change of the orientation birefringence from positive to negative values. This result suggests that the positive birefringence in the CTA/TCP blend is strongly attributed to the orientation of TCP.

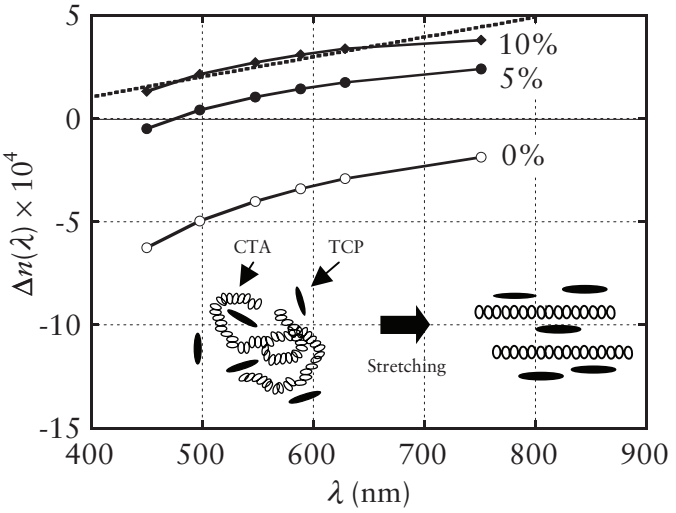

Figure 12.13 Wavelength dependence of orientation birefringence for (open circles) CTA, (closed circles) CTA/TCP (95/5) and (closed diamonds) CTA/TCP (90/10), stretched at a draw ratio of 1.5. In the figure, the straight dotted line represents the ideal wavelength dispersion for a multiband quarter-wave plate with a thickness of 400 μm. The polarisability ellipsoids of the CTA/TCP blends are shown below the curves. Reproduced with permission from M.E.A. Manaf, M. Tsuji, Y. Shiroyama and M. Yamaguchi, *Macromolecules*, 2011, **44**, 10, 3942. ©2011, ACS Publications [29]

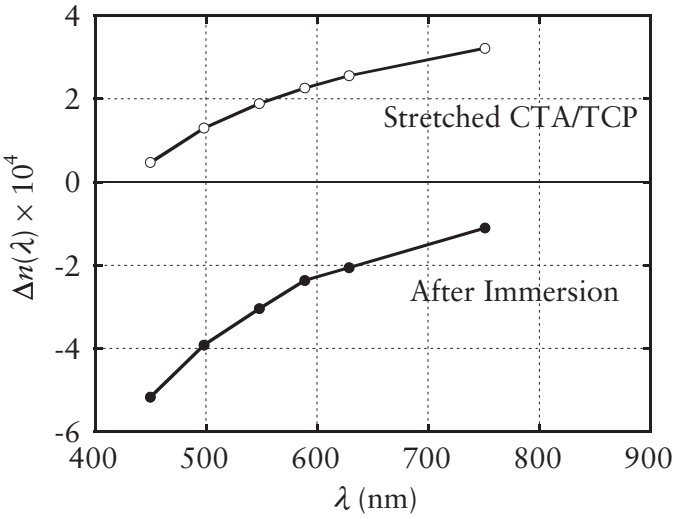

Figure 12.14 Wavelength dependence of orientation birefringence for CTA/TCP (95/5) (open circles) prior to immersion and (closed circles) after the extraction of TCP. Reproduced with permission from M.E.A. Manaf, M. Tsuji, Y. Shiroyama and M. Yamaguchi, *Macromolecules*, 2011, **44**, 10, 3942. ©2011, ACS Publications [29]

12.5 Conclusions

Cellulose esters, which have been used as photographic film and polariser protective film due to their high transparency and excellent heat resistance, have a huge potential as a high-performance optical film. Some cellulose esters such as CAP and CAB show extraordinary dispersion of orientation birefringence, i.e., the magnitude of birefringence increases with the wavelength, a property essential for retardation films such as quarter-wave plate. Although this property can be provided by various techniques – through the piling of two films, blending of two polymers of opposite birefringence or by random copolymerisation, these techniques involve an adhesion or combination of two different types of polymers. In the case of cellulose esters, the orientation birefringence is mainly determined by the type and amount of substitution groups, so it is possible to tailor the retardation/birefringence by manipulating the degree of substitution of the ester groups with intense focus on the hydroxyl group. We found that certain ester groups such as propionyl and butyryl as well as the hydroxyl group contribute to positive birefringence, while the acetyl group contributes to negative birefringence. Furthermore, addition of a suitable plasticiser is also effective

in modifying the orientation birefringence of cellulose esters, provided the blend is miscible.

Acknowledgements

The authors would like to express their gratitude to Taihei Chemicals Limited for their valuable advice and the kind supply of samples employed in this study. Furthermore, the authors gratefully acknowledge financial support from the Japan Science and Technology Agency (Regional Research and Development Resources Utilization Program). One of the authors, Mohd Edeerozey Abd Manaf, would like to extend his gratitude to Universiti Teknikal Malaysia Melaka and the Ministry of Higher Education of Malaysia for funding his studies.

The authors would also like to express his gratitude to Mr Kenji Masuzawa, Mr Takuya Iwasaki, Ms Kyoko Okada, Mr Yasuhiko Shiroyama, Ms So Young Lee and Ms Manami Tsuji for their effort in accomplishing this work.

References

1. W. Kuhn and F. Grün, *Kolloid-Z*, 1942, **101**, 3, 248.

2. L.R.G. Treloar in *The Physics of Rubber Elasticity*, Clarendon Press, Oxford, UK, 1958.

3. B.E. Read in *Structure and Properties of Oriented Polymers*, Applied Science Publishers, London, UK, 1975.

4. F.A. Jenkins and H.E. White in *Fundamental of Optics*, McGraw-Hill, New York, NY, USA, 1981.

5. G.F. Harding in *Optical Properties of Polymers*, Applied and Science, London, UK, 1986.

6. J.E. Marks and B. Erman in *Rubberlike Elasticity: A Molecular Primer*, Wiley, New York, NY, USA, 1988.

7. P.H. Hermans and P. Platzek, *Kolloid-Z*, 1939, **88**, 1, 68.

8. A. Uchiyama and T. Yatabe, *Japanese Journal of Applied Physics*, 2003, **42**, 6, 3503.

9. A. Uchiyama and T. Yatabe, *Japanese Journal of Applied Physics*, 2003, **42**, 11, 5665.

10. K. Kuboyama, T. Kuroda and T. Ougizawa, *Macromolecular Symposia*, 2007, **249–250**, 1, 641.

11. A. Uchiyama and T. Yatabe, *Japanese Journal of Applied Physics*, 2003, **42**, 11, 6941.

12. M. Yamaguchi, M.E.A. Manaf, K. Songsurang and S. Nobukawa, *Cellulose*, 2012, **19**, 3, 601.

13. Y. Koike, K. Yamazaki, H. Ohkita and A. Tagaya, *Macromolecular Symposium*, 2006, **235**, 1, 64.

14. M. Yamaguchi, K. Okada, M.E.A. Manaf, Y. Shiroyama, T. Iwasaki and K. Okamoto, *Macromolecules*, 2009, **42**, 22, 9034.

15. F. El-Diasty, M.A. Soliman, A.F.T. Elgendy and A. Ashour, *Journal of Optics A: Pure and Applied Optics*, 2007, **9**, 3, 247.

16. M. Yamaguchi in *Cellulose: Structure and Properties, Derivatives and Industrial Uses*. Nova Science Publishers, New York, NY, USA, 2010.

17. W.W. Merrill, M. Tirrell, J.F. Tassin and L. Monnerie, *Macromolecules*, 1989, **22**, 2, 896.

18. M. Doi and H. Watanabe, *Macromolecules*, 1991, **24**, 3, 740.

19. O. Urakawa, E. Ohta, H. Hori and K. Adachi, *Journal of Polymer Science, Part B: Polymer Physics Edition*, 2006, **44**, 6, 967.

20. O. Urakawa, S. Nobukawa, T. Shikata and T. Inoue, *Nihon Reoroji Gakkaishi*, 2010, **38**, 1, 41.

21. S. Nobukawa, O. Urakawa, T. Shikata and T. Inoue, *Macromolecules*, 2010, **43**, 14, 6099.

22. S. Nobukawa, O. Urakawa, T. Shikata and T. Inoue, *Macromolecules*, 2011, **44**, 20, 8324.

23. J.A. Zawada, G.G. Fuller, R.H. Colby, L.J. Fetters and J. Roovers, *Macromolecules*, 1994, **27**, 23, 6861.

24. M. Yamaguchi, S. Lee, M.E.A. Manaf, M. Tsuji and T. Yokohara, *European Polymers Journal*, 2010, **46**, 12, 2269.

25. T. Tatsushima, N. Ogata, K. Nakane and T. Ogihara, *Journal of Applied Polymer Science*, 2005, **96**, 2, 400.

26. M. Yamaguchi and K. Masuzawa, *European Polymer Journal*, 2007, **43**, 8, 3277.

27. M. Yamaguchi and K. Masuzawa, *Cellulose*, 2008, **15**, 1, 17.

28. M. Yamaguchi, T. Iwasaki, K. Okada and K. Okamoto, *Acta Materialia,* 2009, **57**, 3, 823.

29. K. Songsurang, A.M. Mohd Edeerozey, A. Miyagawa, P. Phulkerd, S. Nobukawa and M. Yamaguchi, *Cellulose*, 2013, **20**, 1, 83.

30. M.E.A. Manaf, A. Miyagawa, Y. Aoki, S. Nobukawa and M. Yamaguchi, *Optical Materials*, 2013, **35**, 7, 1443.

31. M.E.A. Manaf, M. Tsuji, Y. Shiroyama and M. Yamaguchi, *Macromolecules*, 2011, **44**, 10, 3942.

32. H. Hayashi, S. Nobukawa and M. Yamaguchi in *Proceedings of the 8th International Symposium on Advanced Materials in Asia Pacific*, Busan, Korea, November 2011.

13 Antibacterial Fibres

Josefin Illergård, Lars Wågberg and Monica Ek

13.1 A Brief Introduction

Not long ago, it was common for people to die from bacterial infections. Around the period of World War II, natural as well as the synthetic antibiotics were discovered, which revolutionised health care and life in general. Since then, antibiotic-resistant bacteria have emerged, which is most probably linked to the daily misuse of antibacterial substances. Today, we are yet again facing a situation where a bacterial infection is incurable; in Europe, about 25,000 people die every year as a result of antibiotic-resistant bacteria [1].

As a necessary measure, new antibacterial methods are developed in which antibacterial materials are suggested as a means to prevent the spread of disease-causing microorganisms. Cellulose fibres are an interesting material alternative, as they are a renewable, carbon dioxide-neutral material and have a widespread field of applications.

Besides the desired disease-preventing properties, an antibacterial cellulosic material can also meet the high hygienic standards of today. Antibacterial hygiene products, such as incontinence pads, can decrease the malodour caused by microbial growth and thus have an increased value for the consumer. Using an antibacterial cloth to wipe the benches in your kitchen may prevent the bacterial contamination of food. A prolonged shelf life of food may be possible by using antibacterial packaging and can, in turn, have environmental benefits by leading to less food waste.

13.2 Bacteria and Antibacterial Substances

Bacteria are the smallest known organisms, with a typical cell size of one or a few micrometres. They are generally divided into two groups, Gram-positive and Gram-negative based on the differences in the cell wall and membrane; together

commonly called the bacterial cell envelope (**Figure 13.1**). In the Gram-positives, the cross-linked peptidoglycan cell wall is thick and protects a phospholipid bilayer cell membrane. Common genera in this group are the *Bacillus* species and bacteria belonging to *Staphylococcus*, to which the infamous antibiotic-resistant methicillin resistant *Staphylococcus aureus* (MRSA) belongs. The Gram-negative bacteria instead have an outer membrane and a thin cell wall to protect the inner cell membrane. In addition to peptidoglycan and phospholipids, the quite complex cell envelope consists of several other macromolecular compounds, such as proteins and polysaccharides. The ubiquitous *Escherichia coli* belong to this group. Both Gram-positive and Gram-negative bacteria, named after a staining method, have a negative charge at physiological pH as a consequence of mainly phosphate and carboxyl groups on the cell envelope.

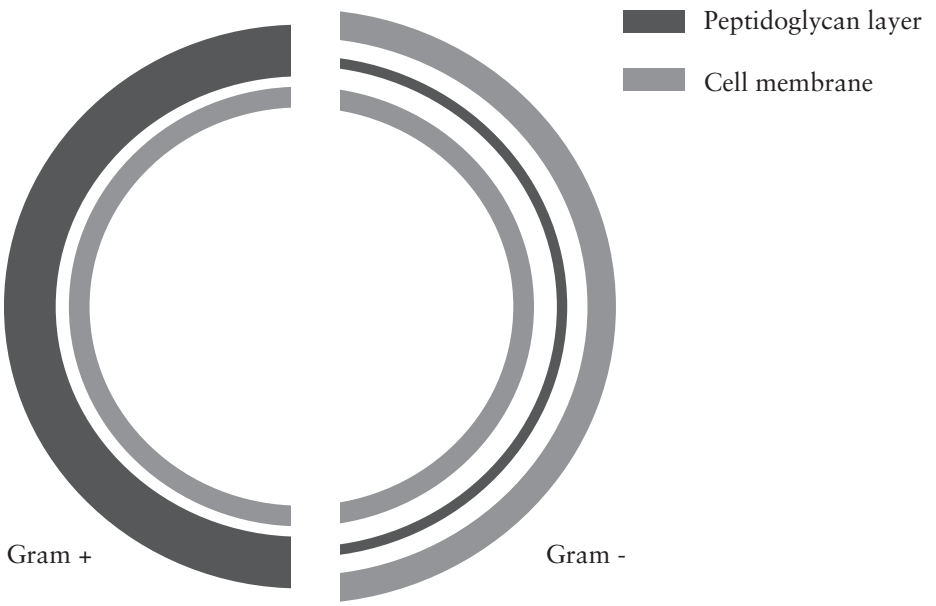

Figure 13.1 Schematic illustration of the differences in the cell envelope of the two main bacterial groups; the Gram-positive and the Gram-negative bacteria

Bacteria belong to the prokaryotes, literally meaning 'before nucleus', as they lack a cell nucleus and organelles. Instead they have deoxyribonucleic acid (DNA) and all vital functions occur freely in the inner of the cell, the cytosol. In this aspect they are

relatively simple compared with the eukaryotic cell, such as our own, and in fact carry only 10% to 40% of the number of genes, depending on the bacterial strain, that a human cell contains. What is interesting though is that despite, or maybe thanks to, bacteria having all the functions contained to one cell they have a remarkable ability to adapt. This has made them evolutionary successful and on Earth today, hardly any natural spot is free from bacteria. Bacteria flourish even in hostile environments, such as underwater black smokers. Bacteria play an important role in the ecosystem where they, e.g., degrade materials and form nutrients in the nitrogen cycle. Bacteria also live in symbiosis with higher organisms; a classical example is bacteria which are active in the digestion of food in both humans and animals, the importance of which is highlighted when we travel and encounter foreign microbial flora. However, a fraction of bacterial species are pathogenic and cause diseases such as pneumonia and tuberculosis, to mention two of the most serious examples; bacteria can also cause less serious infections such as skin infections. As one of the traits of bacteria is fast growth *via* cell division, with generation times as low as 20 min, the disease can spread rapidly. In addition to causing diseases, bacteria also cause other problems such as degradation of, e.g., food and construction materials. Bacterial growth is also associated with unwanted effects such as bad smell and discolouration. Various means have therefore been invented to prevent and treat bacterial growth, both for medical use, where we have antibiotics such as penicillin, and for industrial and household use, e.g., triclosan. These substances work either on the structures inside the bacteria, such as intracellular enzymes and DNA, or on the outside of the cell, i.e., on the cell envelope. Moreover, the mechanism of an antibacterial substance can be classified as being specific by affecting a sole target, such as an enzyme in a metabolic pathway, or general by affecting multiple targets or a broad group of targets, e.g., alcohols that work on the cell envelope. An antibacterial substance can be group specific with regards to the targeted organisms. A good example is penicillin which affects the build-up of peptidoglycan in Gram-positive bacteria, whereas Gram-negative are more resistant, as they only rely on a thin peptidoglycan layer. Bacteria can have different defence mechanisms against antibacterial substances, e.g., by altering the targeting compound or by affecting transportation channels. It is these defence mechanisms that we normally call antibiotic resistance, when the substance in question is an antibiotic compound. Bacteria can also be resistant to other antibacterial agents, such as silver. Antibiotic resistance is now spreading fast, which is thought to be an effect of the misuse of antibiotics in both medical and industrial applications.

So what makes an antibiotic different from other antibacterial agents? There is no clear dividing line, other than that antibiotics are usually small molecules which can be medically used for ingestion, while the term antibacterial includes other substances as well as the antibiotics and has a larger molecular weight spread. It should be noted that 'classical' antibiotics can be used for technical applications, e.g., for disinfecting surfaces. Antibiotics are also often focused on an intracellular bacterial target, which

makes them efficient in small concentrations, but also makes it easier for bacterial adaptation. The group of antimicrobials is more diverse in this aspect as well, as the target spectrum is wider.

13.3 Cellulose as an Antibacterial Material

Both in the literature and in commercial products a number of different materials have been rendered antibacterial, including glass, plastics and cellulose-based material. Cellulose is of special interest for new antibacterial products, notably as it is biorenewable. Moreover, fibres from lignocellulose are used in a vast span of products, stretching from personal hygiene products to packaging materials, as the fibres are relatively inexpensive and easy to modify to obtain new and enhanced properties.

Today, commercially available antibacterial products exist, which are based on cellulosic fibres, with some examples listed in **Table 13.1**. Most examples of antibacterial cellulose are found within the textile industry, which has a long history of making antibacterial fabrics in order to reduce odour. Many of the techniques which are used to confer antibacterial properties onto textile fibres can be applied to other cellulosic fibres, as well and textiles, and have thus been a source of inspiration for the development of antibacterial wood-based materials and consequent testing methods. Wood-based textile fibres also exist which are claimed to impart antibacterial properties, such as bamboo and certain rayon fibres. This antibacterial property is most likely a consequence of the good moisture transport properties of the material, which make the fabric dry quickly. As bacterial growth requires a moist environment to grow well, a 'false', or preventive, antibacterial effect will be obtained. For example, in the case of sports clothes this effect might be sufficient to decrease bacterial growth and can thus be a sustainable alternative.

Table 13.1 Antibacterial cellulose-based products

Product	Antibacterial agent
Wet wipes	Benzalkonium chloride, alcohols, triclosan
Wallpaper	Silver
Sponges	Triclosan
Band aids	Silver compounds
Office paper	Silver compounds, TiO_2
Hand towels	*Unspecified*

Prevention of disease is a strong motivation for the research of new antibacterial modifications. Practically however, the development also has other driving forces. An antibacterial product is usually designed with one or several objectives in mind:

- Protect the product itself;
- Protect another product in, e.g., packaging materials;
- Protect the user; and
- Avoid unpleasant effects, e.g., smell.

The first, protection of the product itself, is valid when it comes to long-term use products, such as wood in the construction or filter membranes, the function of which might be seriously damaged by microbial attack. When it comes to lignocellulosic products, most articles are used over a relatively short period, and often as single-use products. However, certain products would benefit from an increased resistance towards microbial growth; by preventing microbial growth in overseas shipping, where the increased humidity often causes microbial growth on the cardboard, better protection of the containing product, as well as a better work environment, can be achieved. Another example is papers used in archives, which are attacked by bacteria and mould if stored under inappropriate conditions.

More important are the aspects of protecting products and users. Cardboard and paper are commonly used as packaging materials, not least as an environmentally friendly alternative to fossil-based plastics. Paper-based packaging exists, which claims to increase the shelf life of the contained products due to antibacterial properties. Functioning as an absolute barrier may be beneficial in, e.g., the food industry and pharmaceutical packaging, although certain care and consideration must be taken if the antibacterial agent migrates from the packaging into the product. An antibacterial product can also function to protect the user by preventing disease-causing bacteria from spreading by, e.g., using antibacterial cleaning wipes. This objective is becoming increasingly important in health-care environments, where antibiotic-resistant bacteria are spreading from patient to patient.

The last objective is to reduce the inconvenient side effects associated with bacterial growth. A typical example is to reduce the smell caused by bacterial growth, a smell that humans for evolutionary reasons find repelling. This effect can be sought in hygienic products and clothes.

The use of antibacterial products is, however, not without problems and is constantly subjected to intense debate. The marketing of such products relies on the fear of bacteria, but the products may not even have a detectable effect outside the laboratory. There is also the suspicion that homes which are too clean, with regards to both

microorganisms and dust, are negative for the development of the immune system in children and thus lead to allergies. Depending on the type of antibacterial modification there can be adverse effects on nature, by contamination with toxic substances as many antibacterial materials leach out toxic substances.

13.4 Classification of Antibacterial Materials

The term 'antibacterial materials' describes a group of modified materials with the ability to reduce bacteria by 99.9% or more in laboratory tests; the term is usually considered to be a synonym for killing bacteria, though it should be noted that according to the definition, the material can be bacteriostatic, i.e., bacterial growth-inhibiting properties, as well. An antibacterial material can work *via* different antibacterial mechanisms. Generally, the working mechanisms of the antibacterial material fall under one of two categories; leaching or contact-active.

Leaching materials are sometimes referred to as *controlled release materials* and are, as the name suggests, continuously releasing antibacterial substances into the surroundings (**Figure 13.2**). These materials are the most efficient when it comes to affecting bacterial viability and also extend away from the surface. However, leaching materials have the largest environmental impact, as the released substances are often harmful. There is also an obvious risk of material depletion during the lifespan of the product. In the case of cellulose-based products, the majority of the products are intended for short-term usage.

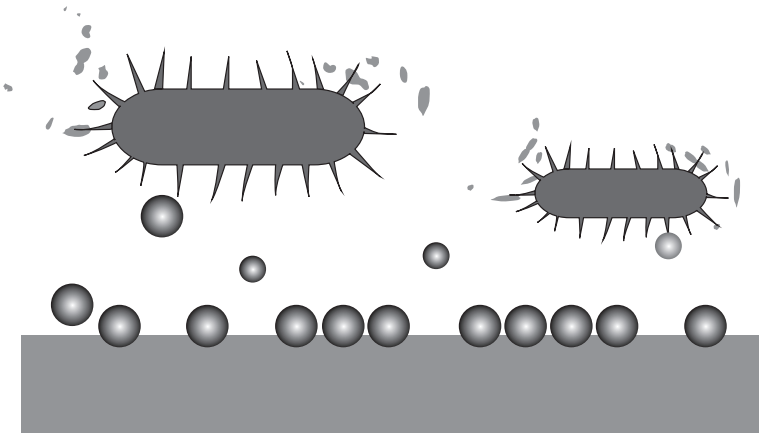

Figure 13.2 A leaching material continuously releasing antibacterial agents

The *contact-active materials* have the antibacterial substance irreversibly attached to the material surface and the bacteria needs to come into direct contact to be affected (Figure 13.**3**). No substance is released or leached into nature and these materials are therefore also referred to as *nonleaching*. The contact-active antibacterial materials are a safer and more environmentally friendly antibacterial alternative than conventional leaching materials. Their effect is on the outer cell envelope, which is thought to be difficult for the bacteria to adapt to, in other words to become resistant against. The antibacterial efficiency of the material is linked to the available surface area and this will be the capacity limiting factor.

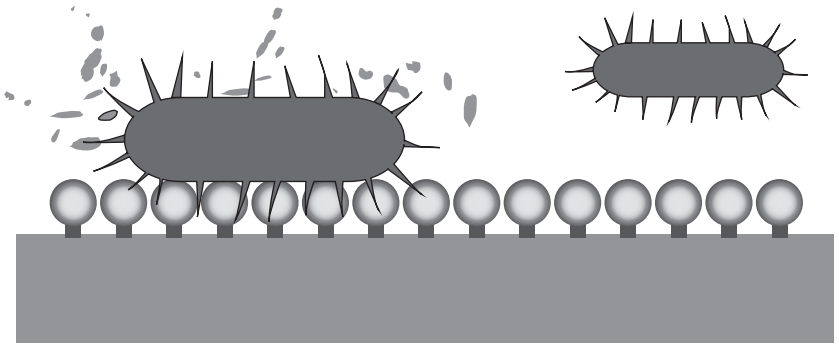

Figure 13.3 A contact-active antibacterial material has the antibacterial agent immobilised on the material surface and does not release harmful compounds

Photocatalytic materials are a special type of nonleaching material, which generate free radicals upon exposure to light. These surfaces are obviously only suited for uses where there is light available, for instance, wallpaper.

Antifouling materials are another type of material often mentioned in this context, but are not truly antibacterial (**Figure 13.4**). These materials repel bacteria, usually by being either superhydrophobic or superhydrophilic, and thus locally prevent bacterial growth. The antifouling materials are more a way of protecting a material which would otherwise be subjected to heavy microbial growth, a so-called biofilm, e.g., ship hulls or in water-treatment plants. There are also examples of commercially available band-aids working *via* this mechanism. This review will, however, focus on materials capable of reducing bacterial numbers according to the definition of antibacterial materials.

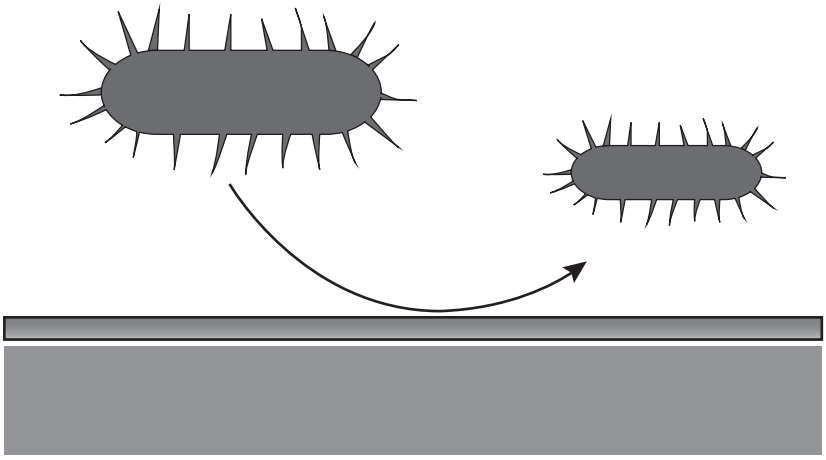

Figure 13.4 An antifouling surface repels bacteria and thereby hinders colonisation

So how do you make antibacterial cellulose? Again, this is strongly dependent on the type of surface. The following section will therefore be divided into two parts: leaching materials and contact-active fibre materials.

13.5 Fabrication of Leaching Materials

In general, the use of leaching antibacterial materials has a long history, dating back to ancient Greece where they used silver for preservation, as silver surfaces continuously leach out silver ions [2]. Numerous examples of leaching materials then followed, including plastics, textiles and wood-based products. The simplest form of creating a leaching cellulosic fibre-based product is to impregnate the ready-made product with an antibacterial agent, which will then leach out during use. This approach is simple, but the effect will only last for the first few washes, as nothing binds the antibacterial substance to the material. Common antibacterial substances used in this manner are silver and triclosan, but wet wipes can also contain benzalkonium chloride as well as alcoholic solutions. The use of these compounds is questionable, both from environmental and toxicological perspectives, especially in products intended for household use. Furthermore, evidence shows that the impregnating process should be avoided, due to the high amounts released during use. For silver and triclosan, an increasingly intense debate is taking place. Below is a description of these two substances.

13.5.1 Silver

While the worldwide use of silver initially decreased as a consequence of the introduction of digital photography, the amount of silver being used has yet again started to increase due to the increasing amount of silver-based antibacterial products. This is naturally not without consequences, especially since silver is long-lived and has adverse effects on fish and crustaceans in concentrations down to 1 µg/L. Its antibacterial properties may disturb natural biological processes and local ecosystems, where bacteria play a vital part. The same adverse effects can also occur in man-made biological processes, such as in sewage plants and constructed wetlands. A second alarming consequence is the possible negative effect on health. There are suspicions that silver can induce resistance in bacteria, not only towards silver but also to antibiotics. The sublethal exposure of silver can make bacteria adapt their efflux system to simply pump out the toxic compound (see **Figure 13.5** for a schematic view of the process); the efflux system is also commonly active in antibiotic resistance. Bacterial species, where silver resistance has been found, includes *Staphylococcus, Pseudomonas* and *Enterobacter*, all species frequently associated with multidrug resistance. The direct exposure of silver can also have an effect on human health. Extreme amounts may cause argyria, an irreversible skin condition where the skin displays a blue-greyish tone. The amount of silver needed to exhibit this symptom is presumably higher than the level the user of the silver-impregnated product is exposed to, but may be a hazard during the manufacturing process.

Recently, more focus has been placed on silver nanoparticles, which are engineered clusters of metallic silver atoms, Ag_0. These nano-sized (5–50 nm) particles have enhanced activities due to the large ratio of surface-to-bulk; however, society is seemingly unprepared to handle nanoparticles. For instance, the water-treatment plants are not designed to remove nanoparticles. More importantly, the question of toxicity of the nanoparticles, as the small-sized particles easily penetrate into cells, has not been fully evaluated. On the contrary, some studies suggest that the particles are toxic [3]. The public debate is unfortunately often driven by tabloids and seldom objective.

13.5.2 Triclosan

Triclosan is a chlorinated aromatic antibacterial compound (**Figure 13.6**) which has been found in consumer products such as toothpaste since the 1960s. Despite its widespread use, the benefits of triclosan addition to products are questionable, since there is a lack of evidence for many products, e.g., triclosan-containing soaps. The usage of triclosan is also thought to add to the development of antibiotic-resistant bacteria. This mainly goes back to triclosan targeting an intracellular enzyme, similar

to many antibiotics and silver, but also to the chemical stability of triclosan. The chemical is highly resistant to changes in pH and this stability is reflected in the triclosan concentrations found in our environment and in our bodies. A survey of the effluent water in coastal cities in Sweden in 2009 showed that the triclosan content exceeded the European Union directive (2008/105/EG) by up to 23,000% [4]. The compound bioaccumulates and has been found in human breast milk, thus exposing infants to the substance [5]. Although triclosan is not known to be hazardous to humans, the exposed environmental concentrations are high enough to affect bacteria and select the triclosan-resistant cells. Despite being stable in water, triclosan can be photolytically degraded, and broken down in the presence of ozone and chlorine, to products with enhanced toxicity. These products are not however, as long-lived as triclosan; contradictorily, triclosan can be degraded by certain bacteria.

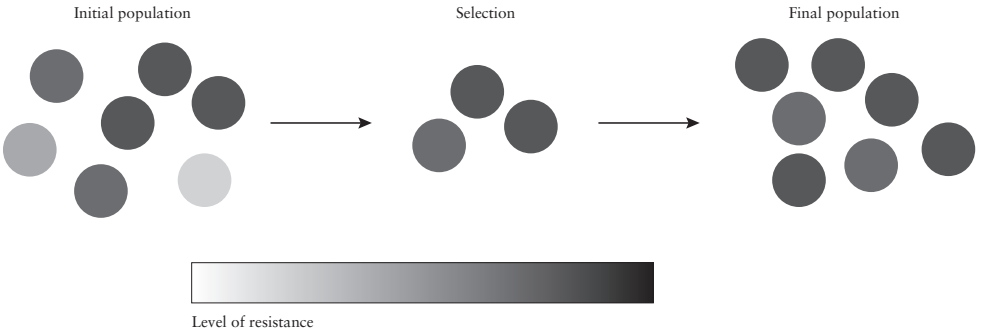

Figure 13.5 How resistant bacteria is selected in sublethal concentrations

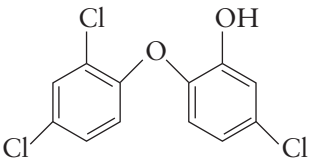

Figure 13.6 Chemical structure of triclosan

13.5.3 Controlled Release of Antibacterial Substances

To reduce the amount of toxic compound used both in the manufacturing and in the final product, a further development of leaching materials, by incorporation of antibacterial substances in the material itself or by partly binding leaching substances to the surface of the material, has been developed. As a result, a slower release sometimes referred to as controlled release can be achieved. The slower release leads to the possibility of a longer lifespan of the product, although the antibacterial substance will be depleted after a period of use. An established method to trap silver nanoparticles on the surface of cellulosic fibres is by reducing $AgNO_3$ with $NaBH_4$. Dankovich and Grey used this approach on absorbent blotting paper from bleached softwood kraft pulp with the aim of obtaining antibacterial filter material [6]. The filter showed good antibacterial properties while the silver effluents were below the World Health Organization limit for drinking water, 0.1 ppm; not only paper has been modified using this method. For medical reasons, antibacterial bacterial cellulose is of interest; this cellulose is very pure and shows good biocompatibility. *In situ* reduction of silver nitrate onto bacterial cellulose has been performed by several researchers (e.g., [7–9]). Pinto and co-workers obtained good antibacterial properties of silver nanoparticles on both chlorine free (ECF) bleached eucalyptus kraft pulp and bacterial cellulose [8]. In the same study, the efficiency of the direct application of the nanoparticles was compared with post-deposition in a layer-by-layer assembly (LbL) with poly(diallyldimethylammonium chloride) and poly(sodium 4-styrenesulfonate) on the pulp fibres. It was found that the LbL required a higher amount of silver to obtain the same action as the directly deposited particles, which was probably due to a slower leaching. No studies on the durability of the materials were performed, but clearly the method of deposition has an impact on the release, where a slower release is expected to prolong the active lifespan of the product.

Silver nanoparticles can also be applied onto fibres by first grafting polymers onto the fibre surface, and then trapping and reducing the silver found on the polymers. Tankhiwale and Bajpai [10] grafted acrylamide, using ceric ammonium nitrate initiated graft copolymerisation, onto cellulose-based filter paper, followed by the entrapment of silver nanoparticles. The method does not involve organic solvents or harsh conditions, such as high temperatures, and was therefore suggested to be suitable for the manufacture of antibacterial food-packaging material, although the silver leaches and might potentially migrate into the food. A similar approach by first grafting and then trapping silver was made by Tang and co-workers [11] *via* surface-initiated atom transfer radical polymerisation (ATRP), grafting poly(*tert*-butyl acrylate) brushes onto filter paper. The brushes were then transferred into poly(acrylic acid) in the presence of trifluoroacetic acid, a chelating agent for silver ions. The Ag^+ was reduced *in situ* to obtain silver nanoparticles. Other metallic nanoparticles can also be used to impart antibacterial properties onto cellulosic fibres. Copper nanoparticles on regenerated

cellulose films were shown to have activity against both *Staphylococcus aureus* and *Escherichia coli* [12].

There have also been initiatives for the controlled release of triclosan from cellulosic fibres. Within the Canadian bioactive paper network (SENTINEL), Qian and co-workers adsorbed triclosan-cationic β-cyclodextrin complexes onto sulfite pulp. The use of the complexes increased the water solubility of the triclosan. The same procedure also worked on the preservative butylparaben, a common antibacterial preservative.

13.5.4 Leaching Natural Compounds

The debate of the negative effects of antibacterial substances is focused around silver and triclosan, though it should be noted that other antibacterial agents also have negative impacts. Butylparaben, mentioned in the example above, is believed to affect the endocrine system in humans and animals, owing to the structural similarities of the compound to the hormone estrogen [13]. Benzalkonium chloride, a common name for mixtures of alkylbenzyldimethylammonium chlorides with varying alkyl chain lengths and commercially used in wet wipes, is highly toxic to water-living organisms, and cause allergic and toxicological reactions in humans as well. There is thus a need for new, innovative antibacterial substances. For paper-based materials intended for food packaging, it is especially important to have nontoxic, environmentally friendly antibacterial compounds; hence, the search in both plants and animals, for natural compounds with antibacterial properties. Several herbs contain antibacterial essential oils, and filter paper impregnated with essential oils from sage and oregano has been shown to have an antibacterial effect [14], while at the same time being edible.

In the light of increasing antibiotic resistance, antimicrobial peptides have gained considerable attention. These short sequences of peptides are found among all life forms and generally have a broad antibiotic spectrum, which is effective on several bacterial species. Antimicrobial peptides commonly target the components of the cell membrane and though there are cases of bacterial resistance, these cases are still scarce. In the food industry, the antibacterial peptide nisin has been used since the 1960s and is also used to produce antibacterial packaging material. Nisin is produced by the bacterium *Lactococcus lactis* and is used to inhibit the growth of the virulent food pathogens *Listeria* and to some part *Clostridium*, although *Clostridium* outbreaks are seemingly rare nowadays. These species are capable of growing in the absence of oxygen, which means that they can survive vacuum packaging of, e.g., charcuterie products. Cellulose casings, e.g., intended for the coating of sausages, have mostly been used to produce antibacterial packaging material [15, 16], but bacterial cellulose has also been used [17]; in addition, the antibacterial peptide pediocin has been used.

However, the use of nisin in cellulosic products appears to be limited to the food industry. A drawback of the use of peptides is that they can be sensitive to pH and heat, which puts constraints on their applications. However, considerable research is focused on discovering and engineering stable antimicrobial peptides.

Another biocompatible component with antibacterial properties that has been getting a lot of attention is the polysaccharide chitosan, which is obtained by the deacetylation of chitin, the structural component of the crustacean exoskeleton. The polysaccharide can then be quarternised into trimethylchitosan, which exhibits an increased antibacterial effect and better water solubility [18]. Though being intensely studied within other areas, such as textiles, the use of chitosan to confer antibacterial properties to lignocellulosic fibres is rather unexplored. However, Bordenave and co-workers obtained antibacterial effects with chitosan-palmitic acid emulsions or with a blend of chitosan and O,O′-dipalmitoylchitosan, on two different papers as well as increased hydrophobicity and wet strength [19]. A coating based on chitosan in lactic acid has been found to exhibit activity against *Bacillus subtilis*, but surprisingly not when the chitosan was instead dissolved in acetic or propionic acids [20].

Although natural and edible compounds are safer from a toxicological viewpoint, the substances are still leaching and released into nature; hence, a negative impact on the environment cannot be excluded.

13.6 Fabrication of Contact-active Materials

To make a contact-active material, the antibacterial agent must have both a cell-envelope-damaging effect and be able to attach onto the surface of the material. It can be noted though that the link between the antibacterial action in solution and antibacterial effect on the surface in many cases is unclear; a substance exhibiting a good effect in solution does not necessarily possess the antibacterial effect once on the surface and *vice versa*. Such was the case with the first discovered contact-active compound, a quarternised silane, octadecyldimethyl(3-trimethoxysilylpropyl) ammonium chloride. In 1972, researchers found only a minor effect using common tests in solution, but as the tests continued, they observed an increasing effect [21], as the compound had irreversibly attached to the used glassware. This compound was later commercialised and is today available in several products, including textile fibres for clean room usage and band-aids. Its effect has however, been questioned [22]. The compound has been tested on microfibrillated cellulose in a simple adsorb and cure procedure, but the conclusions were somewhat unclear [23].

After the discovery of the quarternised silane, the research on contact-active materials was quite inactive. It would take until the beginning of the 21st century

until the contact-active surfaces underwent a revival. By this time, the environmental problems and issues with increasing antibiotic resistance had been neglected. But at the time of the pioneering work of Tiller and co-workers [24], making contact-active surfaces modified with cationic amphiphilic polymers, the times had changed. The contact-active materials with their limited range had undergone a revival over the less sustainable leaching surfaces, at least in research terms. In practice, the production and efficiency of the materials outside the lab hinders the development of new commercial products. Still, the benefits make the future of these contact-active materials promising.

13.6.1 Grafting of Polymers

The common method of material surface modification is the chemical grafting of polymers onto the fibre surface. Grafting is usually carried out in several steps and requires harsh conditions, such as high temperatures and organic solvents. Roy and co-workers [25] used reversible addition-fragmentation chain transfer to surface polymerise 2-(dimethylamino)ethyl methacrylate onto filter paper. The polymers were then quartenised with alkyl bromides to obtain a cationic surface charge. In this manner, a material capable of removing *Escherichia coli* was obtained. The researchers found that the chain length of the polymers affected the outcome as well as the obtained positive surface charge; in addition, the wetting behaviour of the filter papers was affected. Other researchers have used different polymerisation techniques. Lee and co-workers [26] used ATRP of tertiary amine 2-(dimethylamino)ethyl methacrylate, which was then quaternised using an alkyl halide. The polymer-modified filter paper surface had antibacterial effects on both *Escherichia coli* and *Bacillus subtilis*. Cen and co-workers [27] copolymerised 4-vinylpyridine and subsequently derivatised, with hexyl bromide *via* the quaternisation of the grafted pyridine groups, into pyridinium groups. This work was also carried out on filter paper.

As the grafting techniques are unsuitable for large-scale production, at least for low-value products, there is a need to replace the unsustainable grafting methods with greener technologies. Enzymatic grafting by laccase is one proposed method for lignocellulosic materials. The enzyme produces phenoxy radicals in the surface lignin matrix, which undergo crosslinking reactions. Elegir and co-workers [28] performed a thorough investigation on the antibacterial effect of laccase-mediated grafting of unbleached kraft liner fibres with phenolic acids, phenolic essential oils components and dopamine. The modification process was carried out as a simple dip-coating process of handsheets and had, depending on the type of grafted compound and concentration, an antibacterial effect against both *Staphylococcus aureus* and *Escherichia coli*. Overall, the Gram-positive bacteria were more sensitive towards the laccase-modified fibres than the Gram-negative. Widsten and co-workers [29] found

similar differences in sensitivity when using natural tannins in a grafting process. For *Escherichia coli*, a reduction lower than the stipulated definition of an antibacterial material, i.e., 99.9% was achieved.

13.6.2 Adsorption of Polymers

An alternative to the grafting process for immobilising polymers onto surfaces is electrostatic adsorption of charged polymers, so-called polyelectrolytes. The adsorption approach has the benefits of being able to be carried out in water-based solutions and at room temperature, which makes the approach very appealing. The surface coverage can however, be considerably lower compared with that achieved using covalent modification and there is usually a prerequisite to use a charged substrate. A method to increase the adsorbed polymer content is to use polyelectrolyte adsorption in multilayers, also called the LbL method. This is achieved by repeating the adsorption step with oppositely charged polyelectrolytes until the desired number of layers is achieved (an illustration for three polyelectrolyte layers is shown in **Figure 13.7.** The method, developed by Decher and co-workers in the late 1990s [30], is versatile and has successfully been applied to materials including forest-based fibres to, e.g., increase the wet strength. We have shown that it is possible to use this method to convey antibacterial properties onto cellulosic fibres by carefully choosing the polymers and process parameters. Hydrophobically modified and unmodified polyvinylamines (PVAm), weak polyelectrolytes with a positive charge in the biological pH ranges, have been evaluated for their activity, together with the anionic polymer polyacrylic acid in multilayers on both regenerated cellulose membranes and on pulp fibres. It was found that the charge effect dominated the possible hydrophobic interaction of the antibacterial properties against both Gram-positive *Bacillus subtilis* and Gram-negative *Escherichia coli* [31]. Moreover, the importance of the introduced cationic charge was shown as the antibacterial effect could be modulated by changing the ionic strength conditions, in the antibacterial tests, and even more so by altering the initial charge of the substrate fibres. The latter was performed by either (2,2,6,6-tetramethylpiperidin-1-yl)oxidanyl oxidation of the original substrate fibres or by choosing a pulp fibre with a higher initial charge, such as chemi-thermomechanical pulp fibres [32]. Although one layer showed an antibacterial effect against the bacteria, three layers of polymers were found to give the optimal effect. On regenerated cellulose, the effect instead continuously increased upon increasing the number of layers [33]. The difference is thought to be an effect of both the adsorbed amount and structure, as more PVAm adsorbed onto the fibres than onto the regenerated cellulose.

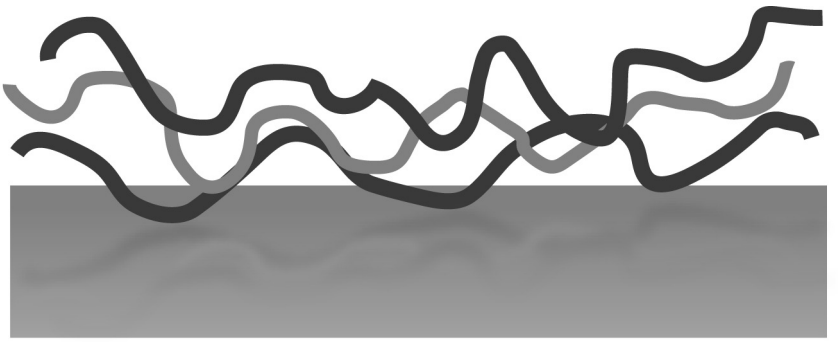

Figure 13.7 Illustration of three layers of polyelectrolytes in a polyelectrolyte multilayer

13.6.3 Other Approaches

As is clear from this review, the most common way to obtain a contact-active antibacterial cellulosic material, and contact-active materials in general, is by immobilising positively charged components. However, it is possible to use biological components such as viruses that specifically target bacteria, so-called bacteriophages. The bacteriophages have a negatively charged head and positively charged tail fibres, which are the method of attachment onto the bacteria during a viral infection. By electrostatically attaching the phages onto regenerated cellulose membranes, given a positive surface charge by the adsorption of polyvinylamine, a higher amount and larger fraction of active phages could be achieved [34]. The treated membranes controlled the growth of *Listeria monocytogenes* and *Escherichia coli* in ready-to-eat and raw meat. Phages can also be genetically modified with cellulose-binding modules, which can aid in the immobilisation of the bacteriophages onto the cellulose fibres [35]. The bacteriophages are approved for use in certain applications, such as to protect ready-to-eat meat; however, the use of viruses is controversial. Although the viruses used in the examples are bacteria-specific, the word virus generates negative associations, especially when genetically modified.

Finally, it is possible to use the photocatalytic TiO_2 as an antibacterial agent. This compound is already used in papermaking as a brightening agent and filler. When titanium dioxide is exposed to ultraviolet (UV) light, highly reactive hydroxyl and free oxygen radicals are formed, which makes the compound interesting for both antibacterial applications and for the degradation of organic pollutants. Daoud and co-workers [36] have described the application of TiO_2 on cellulosic fibres

of unspecified origin, though the effect was quite moderate. One problem is that the material needs UV irradiation during the antibacterial assay, which itself has a disinfectant effect; hence, the effect of the material itself tends to be low compared with the irradiated reference. The titanium dioxide particles described in the literature are often on the nanoscale dimension, due to the increased effect of nanoparticles as discussed previously. The potential negative effects of nanoparticles have not yet, as stated previously, been fully evaluated.

13.7 Testing of Antibacterial Fibres

An important factor to consider when trying to evaluate and compare different antibacterial materials is the manner in which they have been tested. However, direct comparison of the different treatments is difficult, even when only regarding the antibacterial properties and not taking, e.g., environmental factors into consideration. A leaching material is likely to be more efficient against bacteria in the short-term than a contact-active material. The contact-active material will, on the other hand, not be depleted in the same manner as the leaching material. However, the comparison is also made difficult by the fact that the testing conditions used for the antibacterial testing of modified cellulose materials are more or less unregulated, and each tester therefore chooses the conditions she or he finds most appropriate. Although the test method will differ depending on if the testing involves a leaching surface or a surface that works *via* a contact-active mechanism, some fundamental aspects are common, as listed below.

Bacteria: the bacterial strains might show different susceptibility to the antibacterial methods. There might be especially large differences between Gram-positive and Gram-negative strains. Therefore, a minimum requirement of the test is to include both types of bacteria. Type strains are globally available through culture collections such as the American Type Culture Collection (ATCC) and Leibniz-Institut-Deutsche Sammlung von Mikroorganismen und Zellkulturen (DMSZ), which makes it easy to acquire test cultures. In a real situation, the material will most likely be exposed to a mixture of bacteria.

Growth temperature: bacteria have different generation times and optimal growth temperatures. Frequently, the classical microbiology methods are designed for medical tests, which states that the temperature should be 37 °C, i.e., body temperature. This temperature often suits the most common test strains, *Escherichia coli* (Gram-negative bacterium) and different *Bacillus* strains (Gram-positive bacterium) such as *Bacillus subtilis*. However, this does not necessary reflect the temperature at which the antibacterial material will be used; a lower temperature may be more appropriate.

Bacterial growth medium: the type of nutrient source as well as pH and ionic strength will also impact how fast the bacteria grow. Bacterial strains have varied nutritional preferences and will thus respond differently depending on the nutrient composition of the medium. Another often-overlooked fact is that the nutrient, and especially the ionic strength of the nutrient medium, can affect the antibacterial agent material. The effect of antibacterial polyelectrolytes, i.e., charged polymers, such as chitosan, is known to depend on both ionic strength and pH. This is most likely a combined effect of the conformation and impact of electrostatic shielding. It should also be mentioned that the bacteria themselves are affected by the physical properties of the growth medium in a similar manner, as the bacterial cell envelope contains charged constituents. There is also the possibility that the nutrient components found in the growth medium, e.g., proteins and other macromolecules, interact with the antibacterial modification and thereby disturb the intended effect.

Tests exists where no nutrients are added, instead only a reduction of the number of bacteria in the saline suspension is registered; though this technically fulfills the definition of a 99.9% reduction in bacterial load, there is no guarantee that the removed bacteria are not viable, i.e., that they cannot grow. Considering the intended end use of the materials, an environment containing no nutrients is quite artificial.

Test duration: how long should a test last? An antibacterial material must have a quick effect, to work more or less instantly when applied, enabling a fast antibacterial effect to be documented; the material should also be effective throughout the life span of the material. Practically, in many cases, this is difficult to perform, although cellulosic products can have a short-term usage. For the contact-active material there should be sufficient time to allow the test bacteria to make contact with the material.

Substrate: besides considering the absorbent properties, as mentioned in the introduction, the form of the material must also be considered. Are the fibres shaped into a sheet, a fibre pad or are they to be tested free in suspension? The material form might require extra steps to, e.g., separate the fibres from the bacteria, as well as making parts of the material inaccessible to optical detection methods. The material properties may also exclude detection methods based on fluorescence, such as the commercially available live/dead kit which discriminates membrane-damaged bacteria from intact bacteria, as the lignocellulosic fibres may be autofluorescent.

13.7.1 Available Standard Methods

Despite an obvious need for standardisation, a standard method for testing the antibacterial properties of modified lignocellulosic fibres is still not available. However, there are standards developed for other materials, mainly for the textile industry,

which can be partly or fully adapted for testing lignocellulosic antibacterial pulp, as well as methods for testing the microbiological quality of pulp and paper. A list of standard methods that are of interest for testing antibacterial cellulosic fibres is listed in the next subsection, sorted by the responsible organisations. The list includes methods for antifungal detection, as well as methodology which might be of interest for antibacterial purposes. It is also common for antibacterial treatments to have effects on fungi, which fundamentally differ from bacteria in that they are eukaryotic, similar to our cells. The opposite also occurs, where only bacteria are affected. It should also be noted that standard methods allow some flexibility regarding the test organisms and growth medium. To make sure that the comparison of the material is accurate, side-by-side tests in the same laboratory must be performed.

13.7.1.1 American Association of Textile Chemists and Colourists Standards

American Association of Textile Chemists and Colorists Standards (AATCC) 90 – Antibacterial Activity Assessment of Textile Materials: Agar Plate Method: in this qualitative method the test material is molten in the agar, thereby making it possible even for rough, nonflat surfaces to have close contact with the agar.

AATCC TM 100 – Assessment of Antimicrobial Finishes on Textile Materials: this antimicrobial test is a quantitative method in which the test material is fully soaked in a bacterial suspension. After incubation the bacteria is eluted and cultivated. Only a single replicate is demanded.

AATCC TM 147 – Antibacterial Assessment of Textile Materials: Parallel Streak Method Antimicrobial Testing Activity on Textile Materials: for this qualitative method, two parallel streaks of bacteria are made on an agar plate over which the test material is added. If the test sample shows an antibacterial effect, the streaks will be interrupted beneath the material and if leaching, a zone of inhibition surrounding the sample will be observed. This test gives a rough estimation of the efficiency of potential diffusing antimicrobial agents by observing the zone of inhibition. For nonleaching materials, the test is only qualitative. Depending on the type of material, it can be difficult to distinguish the streaks directly under the sample.

13.7.1.2 Japanese Industry Standards

Japanese Industry Standards (JIS) L 1902 – Testing for Antibacterial Activity and Efficacy on Textile Products: a quantitative test in which bacteria are first inoculated and then recovered from the material. It requires the bacterial suspension to be fully

adsorbed into the material to ensure full contact. It differs from AATCC TM 100 in that the nutrients are diluted to 1:20.

13.7.1.3 American Society for Testing and Materials International Standards

American Society for Testing and Materials (ASTM) C1338 – Standard Antimicrobial Test Method for Determining Fungi Resistance of Insulation Materials and Facings: this antimicrobial test method covers the ability of new insulation materials and interfaces to resist fungal growth. As cellulose fibres can be used as insulation material, this test is interesting in that perspective.

ASTM D2020 – Standard Antimicrobial Testing Methods for Mildew (fungus) Resistance of Paper and Paperboard: these antimicrobial testing methods cover the qualitative determination of mildew (fungus) resistance of paper and paperboard.

ASTM D3273 – Standard Antimicrobial Testing Method (ASTM D 3273) for Resistance to Mould on the Surface of Interior Coatings in an Environmental Chamber: this antimicrobial testing method tests the relative resistance of paint films to fungi in a small environmental chamber during a four-week period. This test is of interest for gypsum boards and could be interesting for antibacterial wallpapers.

ASTM E2149 – Standard Antimicrobial Test Method for Determining the Antimicrobial Activity of Immobilised Antimicrobial Agents under Dynamic Contact Conditions: this quantitative method is commonly known as the shake-flask method. Here, the test piece is put into a buffer with bacteria and shaken for one hour. The remaining bacteria in the buffer are then counted *via* cultivation. The growth of bacteria is not determined.

ASTM E2315 – Standard Guide for Assessment of Antimicrobial Activity Using a Time-Kill Study Procedure: this is more of a general method and not specific to antibacterial materials. This test method measures changes of a population of aerobic microorganisms within a specified time period when tested against antimicrobial test materials. There are multiple options to consider when conducting the experiments.

13.7.1.4 International Organization for Standardization

International Organization for Standardization (ISO) 20645:2004 – Textile fabrics – Determination of Antibacterial Activity – Agar Diffusion Plate Test: the test method

works in a similar way to AATCC 90, i.e., the antibacterial substance is leached from the material.

ISO 20743:2007: specifies quantitative test methods to determine the antibacterial activity of antibacterial finished textile products, including nonwovens. The method is largely modelled on JIS L 1902, but allows more flexibility regarding the nutrient source.

ISO 8784-1:2005 – Pulp, paper and board – Microbiological examination – Part 1: total count of bacteria, yeast and mould based on disintegration; part 2 for the detection of microorganisms on the surface of the cellulose-based material is under development.

13.7.1.5 Technical Association of the Pulp and Paper Industry

Technical Association of the Pulp and Paper Industry (TAPPI) T 449 – Bacteriological Examination of Paper and Paperboard: the method is recommended for the bacteriological examination of paper and paperboard intended for use as single-use containers and closures for dairy products.

13.7.1.6 SCAN Methods

Scandinavian Pulps, Paper and Board Testing Committee, SCAN C 60:02, P 81:02 – Microbiological Examination – Total Colony Number – Using the Dry Rehydratable Film Method: it is similar to ISO 8784, but uses film for cultivation.

C 61:02, P 82:02 – Microbiological Examination – Surface Colony Number – Using the Dry Rehydratable Film Method: this method determines the number of microorganisms on the surface, in contrast to the above-described method, by making an imprint of the material on the solid growth film.

13.7.2 Methods for Contact-active Materials

As given by the list of standard methods above, not all methods are suitable for detecting an antibacterial effect of a contact-active fibrous material. The methods based on diffusion, e.g., AATCC 147, which in turn is based on the classical Kirby–Bauer disc diffusion test, is clearly not an option. On the other hand, the Japanese Industry Standard JIS L 1902, ASTM E2149 and ISO 20743 were developed to detect the activity of immobilised antibacterial agents for a preformed product, but not for

free fibres. However, the standard tests do have their drawbacks. ASTM E2149 only tests how many bacteria are removed from the bacterial suspension; if the bacteria are simply attached to the material but not further affected, this will register as a false antibacterial effect. This method is also known to have little correlation to other test methods. The other methods also assume that all bacteria are able to detach from the tested material, which can by no means be guaranteed. On the contrary, the positive charge of the majority of contact-active materials is thought to increase the electrostatic interaction between bacteria and the fibre. For research and development purposes, a higher throughput and flexibility is also desired.

During the course of research on antibacterial cellulosic fibres we have developed a test method that tests both the bacterial reduction, e.g., the removal of the bacteria, as well as the bacterial growth, or viability, in the surrounding media. It is loosely based on the shake-flask method as bacteria are added to a shaken fibrous salt suspension; during this period, no bacterial growth takes place. The conditions of the buffer, regarding salt and pH, are adjusted to be favourable conditions for the bacteria, ensuring that possible pH-changes of the test material do not bias the results. The shaking movement ensures maximal contact opportunities. After this period of shaking, aliquots are diluted and cultivated to elucidate the number of bacteria remaining in the suspension in accordance with ASTM E2149. After this, nutrients (1:10) are added to the remaining fibre and bacteria suspension, and growth is monitored by measuring the increase in optical density (OD). The detection using optical density makes it possible to quickly and simply detect the antibacterial properties, in contrast to cultivation and enumeration on agar plates, which is labour and material-wise intensive. It is therefore possible to test a larger number of samples and also to easily monitor the change in OD over time. However, for testing free fibres an additional, light centrifugation step is necessary to remove fibres which would otherwise interfere. The centrifuge speed must be carefully adjusted to find the balance between removing the fibres and keeping the bacteria in the centrifugate. However, the OD values do not allow a direct translation into bacterial concentration, since the OD-bacterial concentration relationship is not linear over the whole range. It is therefore necessary to make a calibration curve for the specific instrument if the results are to be expressed as colony forming units per ml. Alternatively, constructing a cultivation series is of course possible as an alternative to measuring the OD. This does not require any centrifugation pretreatment, but is time-consuming and thus the time difference between the samples in a large series will vary significantly. This test has been further adjusted to test the influence of ionic strength, as well as pH and bacterial load, with good results. In these cases, it is extremely important to include negative controls for each test point. It is also possible to modify the method to test whether a material is leaching or is truly contact-active. The test samples are then first soaked in the saline buffer solution, with no bacterial addition, and then removed using sterile filtration. The test is then performed using the filtrate in a similar manner

as described above. Surprisingly, few scientific publications address this issue, as in the case of contact-active antibacterial lignocellulosic fibres the materials are mainly at the research stage. To claim a contact-active mechanism some form of leaching test must be performed.

Although the described test shows the main properties of the antibacterial material, i.e., the reduction in both bacterial number and growth, and the contact-active, nonleaching properties, it does not explain what is happening to the bacteria at a cellular level. To show this aspect, microscopic methods can be used. A common method for contact-active antibacterial surfaces in general, independent of substrate, is the fluorescent live/dead assay. The assay consists of two different fluorescent dyes of which the green can freely pass over the cell envelope, while the red dye requires damaged cell membranes in order to enter into the cell. Viewed under a fluorescent microscope, the damaged bacteria then appear red and thus the viability of the bacteria can be determined. For rough or structured materials, the use of confocal microscopy gives a better result. However, we have found that cellulosic pulp fibres can show too much autofluorescence, thus making it difficult or, in the worst cases, impossible, to use this method. It may then be suitable to use other techniques for visualisation. In our case, we chose to use scanning electron micrsocopy and transmission electron microscopy to see the impact of the antibacterial modification. These techniques give excellent resolution and allow the possibility of examining a cross section of the bacterial cells, but do require the samples to be completely dry. To prevent the cells from collapsing due to desiccation, the cell wall is stabilised by fixation with glutaraldehyde, which crosslinks the proteins. The samples can then be carefully dehydrated by solvent exchange with ethanol. This method has been shown to give important information regarding the antibacterial mechanism, as it simultaneously shows the substrate fibres and the bacteria, and thus gives a visual representation of the fibre-bacteria interaction.

13.8 Final Remarks

Presently, there is a large market pull for antibacterial products and, as stated at the beginning of the chapter, there is indeed a need for new methods; the antibacterial materials shown here, based on cellulose fibres, display good potential for the future. However, it is important to fully evaluate the chosen approach regarding the end use and potential side effects, as well as the sustainability of the fabrication process. Far too often, the term antibacterial or antimicrobial becomes just a word used in the marketing campaign; the right antibacterial treatment in the right application can, on the other hand, save lives.

References

1. M. Spenger in *Latest Europe-wide Data on Antibiotic Resistance*, ECDC Director's Presentation, 2011. *http://ecdc.europa.eu/en/aboutus/organisation/DirectorSpeeches/111117_Marc_Sprenger_EAAD-2011.pdf*

2. S. Silver, L. Phung and G. Silver, *Journal of Industrial Microbiology & Biotechnology*, 2006, **33**, 7.

3. C. Marambio-Jones and E. Hoek, *Journal of Nanoparticle Research*, 2010, **12**, 5.

4. A. Svensson in *Miljögifter i Inkommande Avloppsvatten och Slam-Omfattande 8 Reningsverk i Västra Götaland*, Länsstyrelsen Västra Götalands län, Göteborg, Sweden, 2009. [In Swedish]

5. M. Adolfsson-Erici, M. Pettersson, J. Parkkonen and J. Sturve, *Chemosphere*, 2002, **46**, 9.

6. T.A. Dankovich and D.G. Gray, *Environmental Science & Technology*, 2011, **45**, 5.

7. T. Maneerung, S. Tokura and R. Rujiravanit, *Carbohydrate Polymers*, 2008, **72**, 1.

8. R.J.B. Pinto, P.A.A.P. Marques, C.P. Neto, T. Trindade, S. Daina and P. Sadocco, *Acta Biomaterialia*, 2009, **5**, 6.

9. H.S. Barud, C. Barrios, T. Regiani, R.F.C. Marques, M. Verelst, J. Dexpert-Ghys, Y. Messaddeq and S.J.L. Ribeiro, *Materials Science and Engineering: C*, 2008, **28**, 4.

10. R. Tankhiwale and S.K. Bajpai, *Colloids and Surfaces B: Biointerfaces*, 2009, **69**, 2.

11. F. Tang, L. Zhang, Z. Zhang, Z. Cheng and X. Zhu, *Journal of Macromolecular Science, Part A*, 2009, **46**, 10.

12. B. Jia, Y. Mei, L. Cheng, J. Zhou and L. Zhang, *ACS Applied Materials & Interfaces*, 2012, **4**, 6.

13. E.J. Routledge, J. Parker, J. Odum, J. Ashby and J.P Sumpter, *Toxicology and Applied Pharmacology*, 1998, **153**, 1.

14. M. Royo, I. Fernández-Pan and J.I. Maté, *Journal of the Science of Food and Agriculture*, 2010, **90**, 9.

15. X. Ming, G.H. Weber, J.W. Ayres and W.E. Sandine, *Journal of Food Science*, 1997, **62**, 2.

16. J.B. Luchansky and J.E. Call, *Journal of Food Protection*, 2004, **67**, 5.

17. V.T. Nguyen, M.J. Gidley and G.A. Dykes, *Food Microbiology*, 2008, **25**, 3.

18. Z. Jia, D. Shen and W. Xu, *Carbohydrate Research*, 2001, **333**, 1.

19. N. Bordenave, S. Grelier and V. Coma, *Biomacromolecules*, 2009, **11**, 1.

20. J. Vartiainen, R. Motion, H. Kulonen, M. Rättö, E. Skyttä and R. Ahvenainen, *Journal of Applied Polymer Science*, 2004, **94**, 3.

21. A.J. Isquith, E.A. Abbott and P.A. Walters, *Applied and Environmental Microbiology*, 1972, **24**, 6.

22. P.R. Murray, A.C. Niles and R.L. Heeren, *Journal of Clinical Microbiology*, 1988, **26**, 9.

23. M. Andresen, P. Stenstad, T. Moretro, S. Langsrud, K. Syverud, L-S. Johansson and P. Stenius, *Biomacromolecules*, 2007, **8**, 7.

24. J.C. Tiller, C.J. Liao, K. Lewis and A.M. Klibanov, *Proceedings of the National Academy of Sciences of the United States of America*, 2001, **98**, 11.

25. D. Roy, J.S. Knapp, J.T. Guthrie and S. Perrier, *Biomacromolecules*, 2007, **9**, 1.

26. S.B. Lee, R.R. Koepsel, S.W. Morley, K. Matyjaszewski, Y. Sun and A.J. Russell, *Biomacromolecules*, 2004, **5**, 3.

27. L. Cen, K.G. Neoh and E.T. Kang, *Langmuir*, 2003, **19**, 24.

28. G. Elegir, A. Kindl, P. Sadocco and M. Orlandi, *Enzyme and Microbial Technology*, 2008, **43**, 2.

29. P. Widsten, C. Heathcote, A. Kandelbauer, G. Guebitz, G.S. Nyanhongo, E.N. Prasetyo, and T. Kudanga, *Process Biochemistry*, 2010, **45**, 7.

30. G. Decher, *Science*, 1997, **277**, 5330.

31. J. Illergård, U. Römling, L. Wågberg and M. Ek, *Cellulose*, 2012, **19**, 5.

32. J. Illergård in *The Creation of Antibacterial Fibres through Physical Adsorption of Polyelectrolytes*, KTH Royal Institute of Technology, Stockholm, Sweden, 2012.

33. E.H. Westman, M. Ek and L. Wågberg, *Holzforschung*, 2009, **63**, 1.

34. H. Anany, W. Chen, R. Pelton and M.W. Griffiths, *Applied and Environmental Microbiology*, 2011, **77**, 18.

35. Z. Li, M. Tolba, M. Griffiths and T. van de Ven, *Colloids and Surfaces B: Biointerfaces*, 2010, **76**, 2.

36. W.A. Daoud, J.H. Xin and Y-H. Zhang, *Surface Science*, 2005, **599**, 1.

14 Recent Advances in the Processing of Biomass Feedstocks for Biohydrogen Production

Ioannis A. Panagiotopoulos and Emmanuel G. Koukios

14.1 Introduction

The world currently faces important environmental problems, most of which are linked to the issue of climate change. This issue has become very prominent on the global agenda [1–3] and is basically driven by the utilisation of fossil fuels, which mainly include coal, lignite, oil and natural gas, and all originate from plants and animals existing upon the earth during the last 500 million years. In order to tackle climate change, the replacement of fossil fuels by CO_2 neutral energy resources needs to take place. The successful achievement of this replacement will be in the direction of sustainable development, which is currently a hot topic and constitutes a fundamental challenge of the modern world. Economic, environmental, ecological, energy and socio-political sustainability indicates that none of the replacement resources are of sufficient abundance to cover the entirety, but a portfolio of technologies must be used in a collective effort. It is very possible that, under the framework of sustainable development, this portfolio will mainly include technologies of renewable energy, such as solar energy, wind power, biomass, biofuels and others.

Biomass is any organic material made from plants or animals. Domestic biomass sources include agricultural and forestry residues, municipal solid wastes, industrial wastes, and terrestrial and aquatic crops grown solely for energy purposes. The term 'biomass energy' is also interesting and refers to the solar energy stored in plants through the process of photosynthesis. Biomass is expected to have a major role in contributing to the global energy demand in the near future [4–7]. Moreover, biomass-derived energy can be instrumental in reducing the greenhouse gas emissions since the CO_2, which arises from biomass combustion, can be readsorbed by growing plants. In comparison to the CO_2-cycle utilisation of fossil fuels, the short CO_2-cycle of biomass utilisation leads to less accumulation of CO_2 in the atmosphere. Depending on the type of biomass, processing of biomass is needed to render the available carbohydrates accessible for fermentation purposes and biofuel production. Biomass processing usually includes pretreatment and enzymatic hydrolysis. Pretreatment usually refers

to a physical, chemical or biological process, which aims to enhance the accessibility of the carbohydrates in the lignocellulosic biomass [8]. It is typically followed by enzymatic hydrolysis, which mainly aims to convert the cellulose of the pretreated material to soluble, fermentable glucose.

A number of biofuel options are currently under investigation or development worldwide [9–11]. Bioethanol [12–14] and biodiesel [15, 16] are two notable liquid biofuels, and are already being produced worldwide. Currently, almost all bioethanol is produced from grain or sugar cane, while most biodiesel is made from soybean, rapeseed and palm oils. The commercial deployment of the so-called 'second-generation biofuels', which are based on lignocellulosic biomass, is currently a hot issue [11, 17–19], but the processing technologies are relatively immature. Hydrogen is a gaseous biofuel which appears to be a very important biofuel of the long-term future [20–22]. Today, hydrogen is mainly produced from natural gas. However, the use of renewable resources for hydrogen production [23–25] is expected to enhance the contribution of hydrogen energy in the formation of a sustainable energy future [26].

The focus of this chapter is on the fermentative hydrogen production from biomass. Among the different processes, dark fermentation for producing biohydrogen presents considerable advantages. Dark fermentation, commonly termed as 'dark hydrogen fermentation' [27], is the process where the organic compounds, which break down toward hydrogen production, constitute the sole carbon and energy source, providing metabolic energy. Dark fermentation is relatively inexpensive and efficient, and it has low energy demands. Most hydrogen-producing microorganisms cannot directly utilise cellulose or hemicelluloses as a carbon source to grow and produce hydrogen. Therefore, pretreatment and hydrolysis of most of the raw materials are typically required prior to fermentative hydrogen production. An overview of the basic pretreatment processes that have been used or have the potential for future use in biohydrogen production is provided in **Section 14.2**. The role of pretreatment in the efficiency of hydrogen fermentation is reflected by the term 'fermentability' [25], which is discussed in **Section 14.3**, where several features of hydrogen production from sugary and mixed-composition biomass are presented and discussed from a raw material point of view. Similarly, raw material-specific as well as microorganism-specific features of hydrogen production from cellulose-rich biomass are discussed in **Section 14.4**, which is the main focus of this chapter.

14.2 Biomass Pretreatment for Biohydrogen Production

Pretreatment of biomass is needed to render the available carbohydrates accessible for hydrogen fermentation. The degree of the carbohydrate accessibility depends on the type of the raw material. In the case of sugary biomass, such as sugar beet and

sweet sorghum, most of the sugars are readily fermentable, so the pretreatment is relatively simple. For example, the combined extraction and pressing of sugar beet slices has been used to produce a sucrose solution from sugar beet [28]. This technique was designed to simulate industrial sugar beet processing. A similar technique was followed for the extraction of fermentable sucrose from sweet sorghum [29]. In the case of raw materials with 'mixed' chemical composition, such as wheat bran or sugar beet pulp, the pretreatment is usually more complex, often requiring heat and chemicals. Wheat bran which is a coproduct, resulting from the industrial milling of wheat to produce flour, typically contains 12–26% starch, 41–67% nonstarch polysaccharides and up to 10% lignin [30–32]. Sugar beet pulp is a coproduct from the sugar refining industry and contains 20–34% hemicelluloses, 19–27% cellulose, 18–30% pectin and 1–2% lignin [33–35]. Cellulose is by far more difficult to pretreat compared with starch [36], so in the case of typical cellulose-rich materials, such as agricultural or forestry residues, pretreatment is necessary and various pretreatment methods have been extensively described in order to promote the accessibility of polysaccharides in this complex biomass. Typically, the pretreatment step is the first step of the biomass-to-hydrogen process, followed by enzymatic hydrolysis and one or more (see **Section 14.4**) fermentation steps (**Figure 14.1**). The hydrolysis step can be performed by using concentrated acids but today, enzymatic hydrolysis is mostly performed using cellulases and hemicellulases. Fermentation takes place with various hydrogen-producing microorganisms (see **Section 14.4**).

The pretreatments can be classified into four main groups: mechanical pretreatment (including milling and grinding), thermal pretreatment (including steam explosion and liquid hot water (LHW)), chemical pretreatment (including acids, alkalis, ionic liquids, oxidising compounds and so on), and/or their combinations [8, 37]. Hendriks and Zeeman [8] recently reviewed biomass pretreatment methods for biofuel (mainly ethanol and methane) production. Hydrogen production was not studied in that review, because hydrogen is still in the R&D phase. Below, we present the main characteristics of some selected pretreatment methods and we discuss the key work that has been reported on each method, and the potential of each method with regard to hydrogen production.

Mechanical pretreatment leads to a reduction of particle size, which results in an increase of the available specific surface and a reduction of the degree of polymerisation [38]. It is a method with high energy costs that has not been used so far for biohydrogen production. Considering the need to decrease the cost of biomass pretreatment for the economically viable production of biohydrogen [39], it is likely that mechanical pretreatments are not economically feasible. To give the reader a sense for the cost of biohydrogen production, Ljunggren and co-workers [40] performed a techno-economic comparison of the utilisation of barley straw for biological hydrogen production compared with that for second-generation ethanol production. They

concluded that the hydrogen production cost is 422 €/GJ, being about 20 times higher than the ethanol production cost, which is 20 €/GJ.

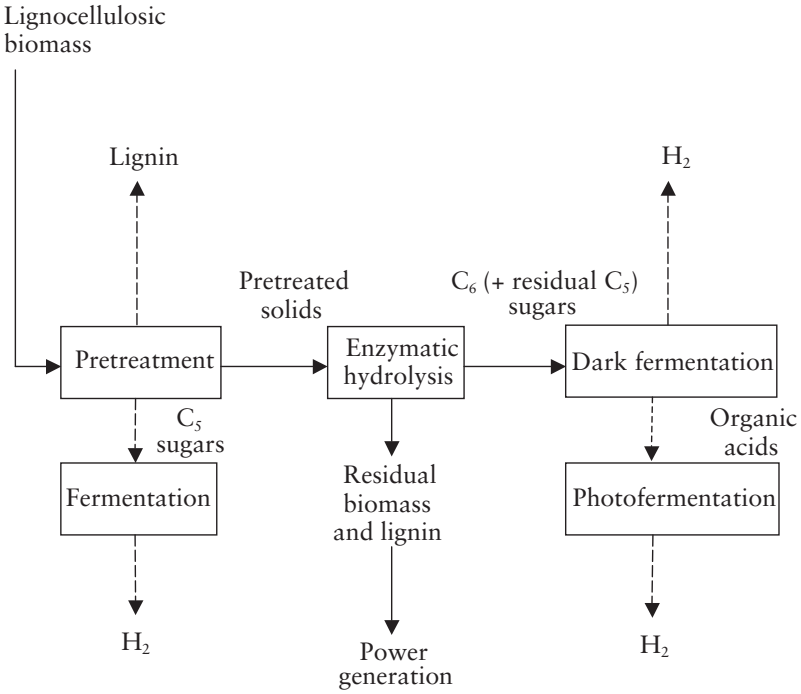

Figure 14.1 A schematic outline of a biohydrogen production-based pretreatment process. The dashed arrows on lignin and C_5 sugars represent the potential of the pretreatment for the fractionation of biomass into high-quality lignin to be used as a substitute for polymeric materials, and C_5 sugars to be used for hydrogen fermentation. This potential depends on the pretreatment method. The dashed arrows on photofermentation represent the potential to couple dark fermentation with photofermentation in order to achieve increased hydrogen yields (see **Section 14.4**)

Steam pretreatment has been studied extensively during the past two decades [41–45] for the conversion of lignocellulosic biomass towards ethanol production, and is expected to be incorporated into many of the first commercial biorefineries that are based on the hydrolysis procedure. Although the method is sometimes referred to as 'steam explosion' describing the disruption of the biomass with the rapid decrease of pressure, it has been shown that an explosion is not required to achieve good

pretreatment and that the main mechanism is rather similar to dilute-acid hydrolysis [46]. Iogen (Ottawa, Canada) have developed their own steam pretreatment process and along with Inbicon (Kalundborg, Denmark) and Abengoa (Salamanca, Spain) they have used the process in a demonstration-scale ethanol plant, indicating that steam pretreatment could be close to commercialisation. In particular, steam pretreatment has been shown to be effective in the processing of agricultural residues and hardwoods such as corn stover [44] and poplar [45]. In steam pretreatment, chips of biomass are conveyed into large vessels and high-pressure steam is applied (at 200–240 °C) for several minutes. At a set time, some steam is rapidly vented from the reactor to reduce the pressure, and the contents are discharged into a large vessel to flash cool the biomass [47, 48].

Concerning the application of steam pretreatment to biohydrogen production, the process has been used with corn stover [49], corn straw [50] and cornstalks [51], giving good results. Given that with steam pretreatment the hemicelluloses is solubilised, thus making the cellulose better accessible for enzymatic hydrolysis, high C5 and C6 sugar yields are achieved with this method. This favours applying steam pretreatment to biohydrogen production because hydrogen-producing microorganisms have been shown to be able to consume both C5 and C6 sugars. In particular, hydrogen-producing microorganisms, such as the extreme thermophilic anaerobic bacterium *Caldicellulosiruptor saccharolyticus* (see **Sections 14.3** and **14.4**), simultaneously consume glucose and xylose [52–54], when these sugars are present in ratios which can be expected in hydrolysates from lignocellulosic biomass, whereas others, such as *Thermotoga neapolitana*, seem to prefer glucose over xylose [53]. Notable is that *C. saccharolyticus* seems to have a preference for xylose if both sugars are present at equal concentrations [55]. Moreover, one of the concerns about using steam pretreatment for biofuel production through fermentative pathways is the generation of fermentation inhibitory compounds [56, 57]. However, given that early research work shows that hydrogen-producing microorganisms [53] are more tolerant to sugar degradation products compared with ethanol-producing microorganisms [56, 58, 59], steam pretreatment could be more efficiently used for cellulosic biohydrogen production rather than cellulosic ethanol production. It should be noted that the inhibition phenomena in dark hydrogen fermentations have not been elucidated yet.

The process of LHW is similar to steam pretreatment, but in this case LHW is used instead of steam. LHW offers the potential for high xylose yields and a reduction in cellulose recalcitrance to enzymatic hydrolysis, while maintaining the levels of inhibitory compounds at low levels. However, the use of this process for hydrogen fermentation purposes has not been reported so far.

Acid pretreatment of lignocellulosic biomass has been studied extensively over the years [60, 61]. Concentrated acids have been traditionally used to treat lignocellulosic

materials, but are toxic and corrosive, and their use disturbs the economic feasibility of biofuel production [62]. Dilute-acid pretreatment [63–70] has been more successful and can significantly improve the hydrolysis of polysaccharides, mainly hemicelluloses. Acid is mixed with the biomass at an acid concentration of 0.1–2%, and the mixture is held at temperatures of 150–200 °C for periods ranging from seconds to minutes (**Figure 14.2**). The hemicelluloses are consequently hydrolysed.

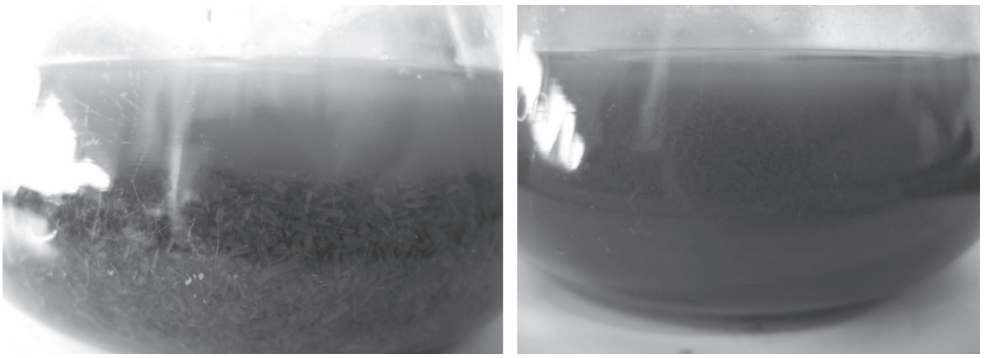

(a) (b)

Figure 14.2 Barley straw (a) before dilute-acid pretreatment, and (b) after dilute-acid pretreatment

However, in addition to hydrolysing the hemicelluloses, dilute-acid pretreatment releases substances that negatively affect the quality of the hydrolysates by decreasing their fermentability [53, 70–72]. These substances, known as inhibitors, include weak acids (mainly acetic acid), furans (mainly 5-hydroxymethylfurfural (HMF), a hexose degradation product and furfural, a pentose degradation product) and phenolic compounds from lignin [73]. Recently, the use of the ratio of Σsugars/Σinhibitors (Σs/Σi) was used for the evaluation of the suitability of barley straw hydrolysates for hydrogen fermentation purposes [70]. The term Σsugars includes glucose, xylose and arabinose, but it depends on the type of lignocellulosic material. For example, if wood is pretreated then mannose or galactose may also need to be considered. However, it should be noted that the method of dilute-acid pretreatment seems to be advantageous for agricultural residues. The term Σinhibitors includes acetic acid, HMF, furfural, levulinic acid and formic acid. The formation of levulinic acid and formic acid takes place with further degradation of HMF. Moreover, formic acid is formed when furfural breaks down [74]. With the Σs/Σi tool, the dilute-acid pretreatment of barley straw has been optimised at the conditions of 170 °C

and 60 min [70]. Under these conditions the production of undesired inhibitors is 2.1 g acetic acid/L, 0.1 g HMF/L, 0.4 g furfural/L, 0.0 g levulinic acid/L and 0.0 g formic acid/L, which should not be problematic for hydrogen production. Various types of agricultural residues have been dilute-acid pretreated for the production of biohydrogen. Cao and co-workers [75] used dilute sulfuric acid to pretreat corn stover for biohydrogen production with *Thermoanaerobacterium thermosaccharolyticum* W16, while the same acid was used by Nguyen and co-workers [76] to pretreat rice straw for biohydrogen production with *Thermotoga neapolitana*. Given that sulfuric acid seems to be effective as a pretreatment agent in producing substrates fermentable to hydrogen, Panagiotopoulos and co-workers [77] investigated the extent to which the dilute sulfuric acid pretreatment of agricultural residues for hydrogen production is raw-material specific. In this study, barley straw, wheat straw, corn stalk and corn cob were dilute-acid pretreated and fermented to produce hydrogen using *Caldicellulosiruptor saccharolyticus*. With use of typical pretreatment conditions it was shown that dilute sulfuric acid pretreatment is more suitable for hydrogen fermentation with the straws, particularly with barley straw, compared with the corn residues. In particular, the fermentability of the aforementioned raw materials was ranked in the order: barley straw > wheat straw > corn stalk > corn cob. It is likely that pretreatment temperatures higher than 160–170 °C are too severe for corn stalk and corn cob, leading to increased HMF concentrations ranging from 0.2 to 0.7 g/L in the fermentation media with corn stalk hydrolysate and increased HMF concentrations (0.2–1.0 g/L) and increased furfural concentrations (0.1–0.6 g/L) in the fermentation media with corn cob hydrolysate. On the other hand, the hemicelluloses fraction of barley straw is likely to be more recalcitrant in comparison with the corn residues, which leads to lower furfural concentrations in the barley straw hydrolysate and therefore better fermentability. It should be noted that the HMF and furfural concentrations of 1–2 g/L have been reported to result in 50% inhibition of hydrogen production [53]. The release of acetic acid during dilute-acid pretreatment does not seem to be a barrier in hydrogen fermentations given that the acetic acid concentrations typically observed with dilute-acid pretreatment should be tolerable by hydrogen-producing microorganisms. For instance, the acetic acid concentration of 9 g/L was recently reported to lead to complete inhibition of the growth of *C. saccharolyticus* [78], being in agreement with a previous study of van Niel and co-workers [79]. *T. neapolitana* is even more tolerant, being able to grow at acetic acid concentrations as high as 18 g/L [78]. According to Panagiotopoulos and co-workers [25] who tested biomass substrates, acetic acid concentrations lower than 3 g/L are fully tolerable by *C. saccharolyticus*. In conclusion, there is currently a lack of a clear relation between the concentration of sugar degradation products in the hydrolysates of dilute-acid pretreated biomass and hydrogen fermentability.

Alkaline pretreatment of lignocellulosic biomass for biofuel production, mostly bioethanol, has received significant attention. Alkaline pretreatments use sodium

[54, 80–83], calcium [84–86], potassium and ammonium hydroxide as reactants. The extensive use of sodium hydroxide over calcium hydroxide is mostly due to the higher solubility of sodium hydroxide and the higher biomass digestibility achieved. In particular, treatment with NaOH causes swelling, leading to an increase in internal surface area, a decrease in the degree of polymerisation, a decrease in crystallinity, separation of structural linkages between lignin and polysaccharides, and disruption of the lignin structure. Notable is that the achieved delignification of biomass may have a significant contribution to the upgraded role of lignin in the biorefinery. De Vrije and co-workers [81] achieved a 77% delignification of *Miscanthus* with the addition of 12% NaOH (w/w dry matter) to the biomass during extrusion at 70 °C, whereas Panagiotopoulos and co-workers [54] observed a 46% delignification of sweet sorghum bagasse with 10% NaOH (w/w dry matter) and milder pretreatment conditions (**Figure 14.3**). Maas [86] reported a 47% delignification of wheat straw with 12% NaOH, while the delignification determined with up to 15% lime was insignificant. In the case when severe experimental conditions are applied, lime pretreatment can result in significant but still low delignification [84].

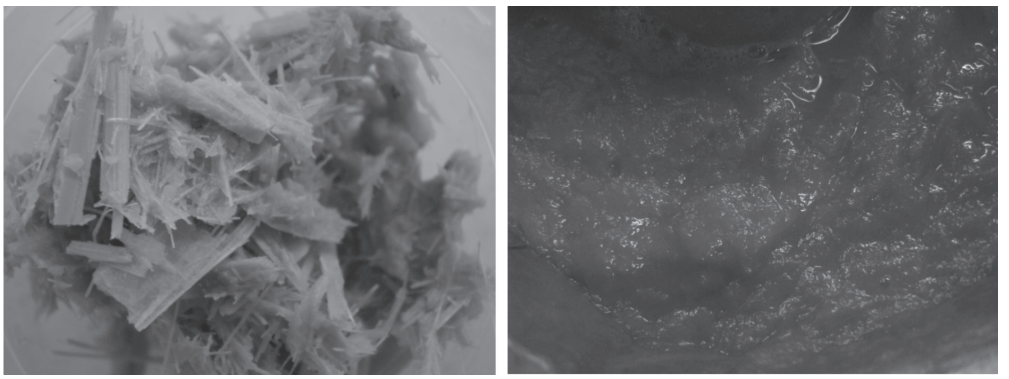

(a) (b)

Figure 14.3 Sweet sorghum bagasse (a) before alkaline pretreatment and (b) after alkaline pretreatment

Alkaline pretreatment is more effective on agricultural residues than on wood materials. Lignin has a role in this because of its relatively low content in agricultural residues and high content in wood materials. Although the organosolv pretreatment is not extensively discussed in this chapter, it should be noted that it is a method based

on the fact that lignin can be solubilised in certain organic solvents, such as ethanol, and is currently the most suitable pretreatment method for the removal of lignin from wood materials [87]. However, as in the case of some alkaline pretreatments, the hemicelluloses component is difficult to recover in the ethanol/lignin-rich post-pulping liquor. In general, the efficient recovery of both lignin and hemicelluloses is a key feature of an ideal pretreatment [88, 89]. Concerning lignin, it is important that the pretreatment recovers it in a high-purity form [90] and with a minimum use of water, although water dilution steps are still required with the current status of development [91]. The loss of hemicelluloses which are present in the nonfermentable lignin-rich liquor, known as dark liquor, is also one of the disadvantages of alkaline pretreatment. The loss of hemicelluloses mainly depends on the type of alkali, the alkali level and the type of biomass. For instance, the loss of hemicelluloses with a NaOH load of 12% (w/w dry matter) has been reported to be 11–13% [54, 86]. Alkaline pretreatment has been previously used in order to enhance biogas production from olive mill effluents [92]. More recently, the application of a NaOH pretreatment to a pulp and paper sludge, in order to improve the methane productivity, was reported [93]. De Vrije and co-workers [53] investigated the fermentability of alkaline pretreated *Miscanthus* hydrolysates for thermophilic hydrogen fermentation. They reported poor fermentability of lime-pretreated *Miscanthus*, whereas the fermentation of a NaOH pretreatment hydrolysate yielded 3.2–3.3 mole hydrogen per mole C6 sugar. These hydrogen yields are amongst the highest yields obtained in the fermentation of sugars in lignocellulosic hydrolysates reported to date (**Table 14.3**). These results are comparable with the results of Panagiotopoulos and co-workers [54] who used the fermentability test (see **Section 14.3**) to adapt the severity of the alkaline pretreatment towards maximum hydrogen production and observed good fermentability of NaOH-pretreated sweet sorghum bagasse. The aforementioned results suggest that the application of alkaline pretreatment has great potential for enhanced hydrogen production in the future. One of the explanations of the good fermentability of the NaOH-pretreated biomass is that with mild pretreatment conditions at relatively low temperatures (70–75 °C) the generation of fermentation inhibitors is avoided, thus ameliorating the hydrogen fermentation.

The method of ionic liquids is a new concept in the fractionation of lignocellulosic biomass and has been applied so far to energy crops such as switchgrass [94, 95], agricultural residues such as sugarcane bagasse [96] and also to woody biomass [97]. One of the challenges of ionic liquids, apart from their very high cost, is the stability and activity of cellulases in the presence of small amounts of ionic liquids coprecipitated with the recovered cellulose [98]. Recently, the effect of ionic liquids on the growth of *Saccharomyces cerevisiae* and bioethanol production was studied [99], but so far no work has been reported on hydrogen-producing microorganisms. Therefore, no detailed discussion on ionic liquids is provided in the current chapter.

Wet oxidation has been applied commercially since the 1960s for treating wastewater and it attracted new attention in the 1980s as an alternative biomass pretreatment method [100]. This process is an effective method in fractionating cellulose from lignin and hemicelluloses, but the main challenge of this process is the loss of sugars which takes place due to nonselective oxidation. In the case of wheat straw, the loss of hemicelluloses can be 40–45% or higher, depending on the process conditions [101, 102]. This is high compared with the hemicelluloses loss encountered during alkaline pretreatments (see text above). Research efforts have focused on the optimisation of the process conditions towards the increase of hemicelluloses recovery. For example, it has been shown that an increase in oxygen pressure results in an increase in hemicelluloses recovery [103, 104]. Palonen and co-workers [105] studied the effect of pH on the hemicelluloses recovery to discover that a decrease of the pH results in an increase of the hemicelluloses recovery from softwood, most likely due to autohydrolysis. Nonselective oxidation also results in the oxidation of lignin, which typically results in the formation of undesired aromatic compounds [102]. This phenomenon can result in the inhibition of hydrogen fermentations and can also decrease the potential income from lignin, on an industrial scale, for biohydrogen production in the biorefinery. In order to decrease the production of fermentation inhibitors, Martin and co-workers [106] used an alkaline pH, which leads to decreased hemicelluloses recovery. Considering all the aforementioned characteristics of wet oxidation and the present status of its development, it is rather unlikely that wet oxidation will be suitable for biohydrogen production any time soon. Although recently, wet oxidised wheat straw was reported in the literature to produce hydrogen with *T. neapolitana* [107]; the aforementioned technical characteristics of wet oxidation, along with the high cost of oxygen, render its application problematic.

14.3 Biohydrogen Production with Processing of Sugar-rich and Mixed-composition Biomass

Sugar-rich raw materials, such as sugar beet and sweet sorghum, have a high content of readily fermentable sugars and are potential substrates for hydrogen fermentations. Sugar beet, with productivity of 8–15 t/ha, contains 64–67% sucrose [28]. It was introduced as a European replacement for sugar cane, which is grown in a tropical climate. Sugar beet is available in the European Union (EU), as well as in the USA, China and Japan, where the climate is temperate. In 2008, with the global annual crop of about 173 million tonnes, sugar beet accounted for 20% of the world sucrose output [108]. In 2008, the EU planted 1.7 Mha of sugar beet crops and produced 16.9 million tonnes of sugar [109], while in 2011 the EU planted 1.5 Mha of sugar beet crops and produced 14.8 million tonnes of sugar [110]. The USA planted 0.5 Mha of sugar beet crops and produced 4.1 million tonnes of sugar in 2009 [111].

Panagiotopoulos and co-workers [25] performed a comparison of the suitability of several raw materials of agricultural origin, including sugar beet, for fermentative hydrogen production. A rapid test, the fermentability test, was applied to evaluate the potential for hydrogen production of each raw material. During the fermentability test, the fermentability of the substrates is tested in small-scale experiments with closed flasks. Typically, flasks of 118 mL with 20 mL culture medium under a nitrogen atmosphere are used. The total concentration of sugars is 20 g/L coming from the pure sugar mixture or the hydrolysate. This sugar concentration is indicatory and the experimenter is encouraged to use other concentrations, e.g., 10 g sugar/L, if appropriate. Diluted samples containing less than 20 g/L sugars from the hydrolysate are filled up with pure sugars, in a similar composition as in the hydrolysates, to a total sugar concentration of 20 g/L to avoid an effect of the sugar concentration on growth. **Table 14.1** shows the experimental set-up of the fermentability test. The first step of the procedure is the inoculation of the flasks with 5% (v/v) of a preculture that is grown overnight on the same pure sugar mixture. After 16 and 40 h of fermentation, samples are withdrawn from the headspace (0.2 mL gas) and the culture medium (1 mL) for further measurements. The quality of the substrate can be determined by measuring various parameters related to the fermentation reactions (**Equations 14.1** and **14.2**) by the thermophilic bacteria (here shown with glucose as the substrate, but similar for some other hexoses and pentoses):

$$C_6H_{12}O_6 + 2H_2O \rightarrow 2CH_3COOH + 2CO_2 + 4H_2 \quad (14.1)$$

$$C_6H_{12}O_6 \rightarrow 2CH_3CHOHCOOH \quad (14.2)$$

Growth of the microorganism (optical density of the culture) (**Figures 14.4** and **14.5**), hydrogen production (**Figure 14.4**) and organic acid (acetate and lactate) production (**Figure 14.5**) are the main parameters considered. The pH decrease and pressure increase in the flasks may also be considered. Typically, hydrogen production and organic acid production is compared with the production in control fermentations with a mixture of the corresponding pure sugars. From an applied research point of view, the fermentability test can be used by researchers involved in biohydrogen-oriented biomass processing. With this test, the methods of pretreatment and hydrolysis can be rapidly adapted to improve the fermentability of the hydrolysate. Although the methodology of the fermentability test is described in the current section, the reader is

encouraged to evaluate the application of the test in some representative lignocellulosic hydrolysates, which are discussed in **Section 14.4** of this chapter.

Table 14.1 Experimental set-up of the fermentability test. C stands for the control media. H stands for the media with the hydrolysate

	Substrate, g/L sugars					
Sample code	**C**	**H5**	**H7.5**	**H10**	**H15**	**H20**
Biomass feedstock	0	5	7.5	10	15	20
Pure sugars	20	15	12.5	10	5	0
Total sugars	20	20	20	20	20	20

Reproduced with permission from I. Panagiotopoulos, R.R. Bakker, M.A.W. Budde, T. de Vrije, P.A.M. Claassen and E.G. Koukios, *Bioresource Technology*, 2009, **100**, 24, 6333. ©2009, Elsevier [25]

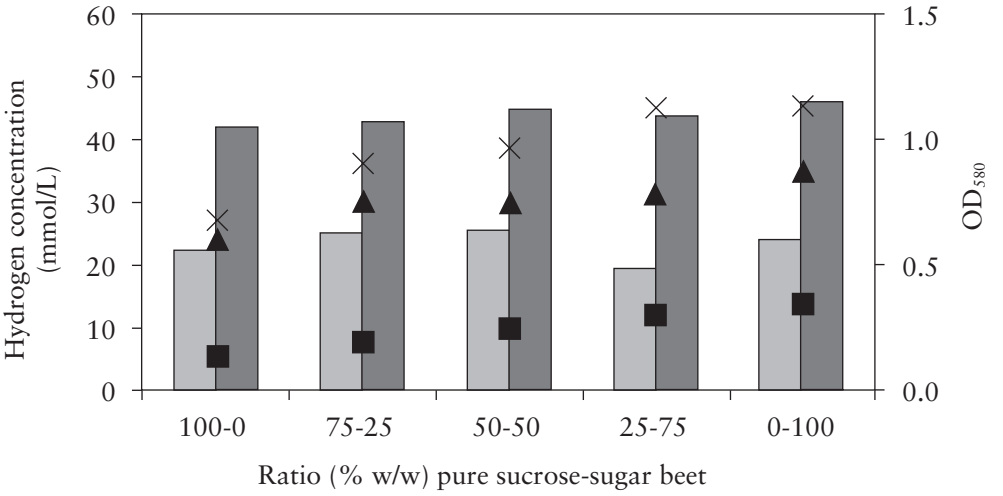

Figure 14.4 Hydrogen production by a culture of *C. saccharolyticus* grown on various ratios of pure sucrose and sugar beet extract. Measurements were performed after 16 (light grey bars) and 40 (dark grey bars) h after the start of fermentation. The growth of *C. saccharolyticus* (OD_{580}) after 0 (■), 16 (▲) and 40 (×) h of fermentation is also indicated. Reproduced with permission from J. Panagiotopoulos, R. Bakker, T. de Vrije, P. Claassen and E. Koukios in *Proceedings of the 18th World Hydrogen Energy Conference 2010 - WHEC 2010: Parallel Sessions Book 2: Hydrogen Production Technologies*, 2010, **Part 1**, 72. ©2010, Forschungszentrum Jülich GmbH, Zentralbibliothek, Verlag [112]

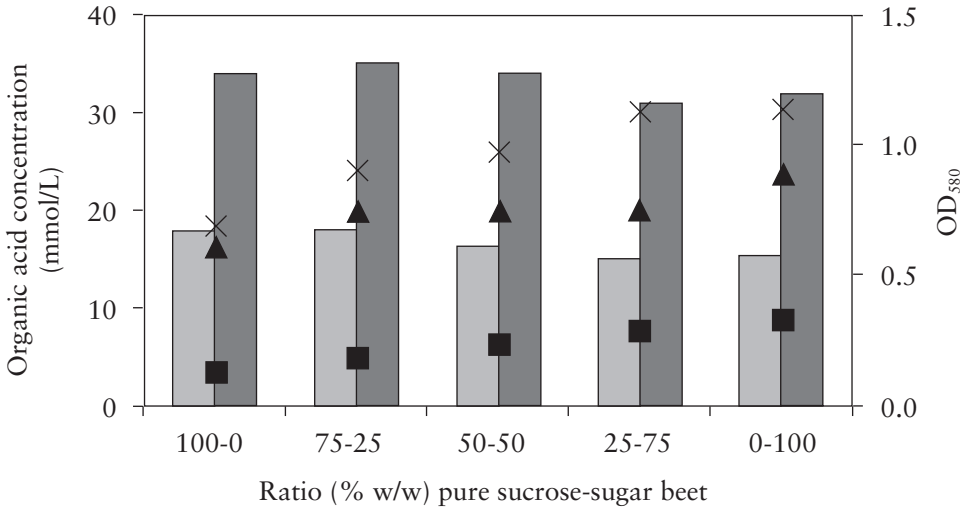

Figure 14.5 Organic acid production by a culture of *C. saccharolyticus* grown on various ratios of pure sucrose and sugar beet extract. See Figure 14.4 caption for details Reproduced with permission from I.A. Panagiotopoulos, R.R. Bakker, M.A.W. Budde, T. de Vrije, P.A.M. Claassen and E.G. Koukios, *Bioresource Technology*, 2009, **100**, 24, 6336. ©2009, Elsevier Ltd [25]

The fermentability of sugar beet extract has been investigated using the fermentability test. Briefly, sugar beet seems to be fermentable for hydrogen production. Using the thermophilic bacterium *C. saccharolyticus*, hydrogen production seems to increase with increasing sugar beet extract (**Figure 14.4**). This is in accordance with the growth of *C. saccharolyticus* which is maximised when 100% sugar beet extract is used. A possible explanation for the increased hydrogen production from the sugar beet juice is that sugar beet naturally contains some of the required nutrients for cell growth and hydrogen production. The juice of sugar beet contains, apart from sucrose, amino acids (e.g., glutamine, glutamic acid, asparaginic acid, leucine, isoleucine and alanine), organic acids (mainly lactic acid) and inorganic acids (mainly phosphoric acid). However, the influence of the concentration of these nutrients on hydrogen production has not been investigated yet.

One key parameter of the fermentability test, which has not yet been elucidated, is the extent to which its results are able to predict the fermentation characteristics of a substrate in large-scale fermentations, under pH- and hydrogen pressure-controlled conditions. At the present stage of development of hydrogen production, the predictability of large-scale fermentations by the fermentability test is uncertain;

however, research is currently ongoing to elucidate this issue. Batch fermentations of sugar beet juice under controlled conditions were recently performed [28] and confirmed previous results observed with the fermentability test [25]. The production of hydrogen from sugar beet seems to be largely equal to or higher than the hydrogen production of the control with pure sucrose.

Two key parameters used to characterise the hydrogen production efficiency in controlled experiments using bioreactors are hydrogen yield, which is expressed as mol hydrogen per mol C6 sugar, and hydrogen productivity, which is typically used in its volumetric version and expressed as mmol hydrogen per L culture medium and h of fermentation. In fermentations of sugar beet juice and sucrose, hydrogen yields of 3.0 and 2.9 mol/mol hexose were respectively determined, corresponding to 73% and 75% of the theoretical value of 4 mol hydrogen/mol hexose (**Table 14.2**). The aforementioned hydrogen yield of 3.0 mol/mol hexose is the highest ever recorded so far in the literature of hydrogen production from sugar-rich and mixed-composition biomass *via* dark fermentation. It was observed with the use of the extreme thermophilic bacterium *Caldicellulosiruptor saccharolyticus*, which is discussed in detail in **Section 14.4** because one of its key characteristics is its capability of using a wide variety of substrates, including cellulose. For comparison reasons, the juice of sweet sorghum (see the discussion at the end of the current section) has been reported to produce hydrogen at a yield of 0.9–2.5 mol/mol hexose (**Table 14.2**), while the use of substrates with more complex chemical composition, such as wheat bran [113] and the coproduct from a wheat flour industry [114], resulted in 1.7 mol hydrogen/mol hexose and 0.9 mol hydrogen/mol hexose, respectively. It should be mentioned that an undefined microbial mixture, thriving on the activated sludge of a paper mill in China, was found relatively recently and seemed to be promising with respect to hydrogen production when used for the consumption of wheat bran sugars [115]. However, the reproducibility of the experiments of that work, as well as of all investigations which employ undefined, mixed microflora, is difficult. Therefore, **Table 14.2**, as well as **Table 14.3**, mainly summarise fermentation experiments which employed well-defined species. Moreover, **Tables 14.2** and **14.3** mainly include data of recent studies where the two basic parameters of hydrogen production, yield and rate, are presented in mol H_2/mol hexose and L H_2/L • day, respectively. Only exceptionally, these tables include data from studies where hydrogen production was normalised as per, for example, chemical oxygen demand or total volatile solids and so on.

Table 14.2 Hydrogen yields and production rates from sugar-rich and mixed-composition biomass

Biomass	Substrate	Microorganism	g sugar/L	Reactor operation mode	Y_{H2} mol/mol C6	Max. Q_{H2} mmol/(L • h)	Ref
Sweet sorghum juice	Sucrose, glucose, fructose	*C. saccharolyticus*	25	Batch	2.3	-	[130]
Sweet sorghum juice	Sucrose	*R. albus*	3	Batch	2.6	-	[131]
Sweet sorghum juice	Total sugar	Heat-treated sludge	25	Batch	2.2	-	[169]
Sweet sorghum juice	Sucrose	Indigenous microbial mesophilic culture	17	Continuous	0.9	8.5[a]	[170]
Sugar beet juice	Sucrose	Mixed culture	10	Batch	1.7	-	[171]
Sugar beet juice	Sucrose	*C. saccharolyticus*	10	Batch	3.0	12.8	[28]
Molasses	Glucose	Mixed mesophilic culture	86[b]	Continuous	-	4.8[a]	[122]
Molasses	Sucrose	*C. saccharolyticus*	15	Batch	2.1	7.1	[172]
Molasses	Sucrose	*C. butyricum* W5	22	Batch	1.6	-	[173]
Artificial medium	Sucrose	*T. thermosaccharolyticum*	20	Batch	2.5	12.1	[138]
Artificial medium	Sucrose	*C. saccharolyticus*	10	Batch	2.9	12.1	[28]
Wheat starch	Glucose	Heat-treated sludge	7.5	Continuous	1.9	5.0	[174]
Corn starch	Glucose	Mixed mesophilic cultures	20[c]	Continuous	0.5	2.6[a]	[123]
Wheat bran	-	Heat-treated sludge	80[d]	Batch	128.2[e]	2.5[f]	[115]
Wheat flour industry coproduct	Total sugar	Heat-treated sludge	3.2	Continuous	0.9	0.5[a]	[114]

[a] L/L • d
[b] kg COD/m^3 • d
[c] g COD/L
[d] g wheat bran/L
[e] mL/g total volatile solids (TVS)
[f] mL/(g TVS • h)

Table 14.3 Hydrogen yields and production rates from lignocellulosic biomass

Biomass	Substrate	Microorganism	g sugar/L	Reactor operation mode	Y_{H2} mol/mol C6	Max. Q_{H2} mmol/(L • h)	Ref
Miscanthus	Glucose, xylose	*T. neapolitana*	14	Batch	3.2	12.3	[53]
Miscanthus	Glucose, xylose	*C. saccharolyticus*	14	Batch	3.3	10.4	[53]
Sweet sorghum bagasse	Glucose, xylose, sucrose	*C. saccharolyticus*	10	Batch	2.6	10.6	[54]
Sweet sorghum bagasse	Glucose, xylose, sucrose	*C. saccharolyticus*	20	Batch	1.3	10.2	[54]
Sweet sorghum bagasse	Glucose, xylose, arabinose	*R. albus*	3	Batch	2.6	-	[131]
Sugar cane bagasse	Glucose, xylose	*C. butyricum*	20[a]	Batch	1.7	1.6[b]	[175]
Wheat straw	Glucose, xylose, arabinose	*T. neapolitana*	5	Batch	2.6	1.2	[107]
Rice straw	Xylose	*C. butyricum*	9.2	Batch	0.8[c]	0.6[b]	[176]
Corn stover	Xylose	*T. thermosaccharolyticum*	9	Batch	2.2[c]	-	[75]
Corn stover	Glucose	Activated sludge	5	Batch	3.0	10.6	[49]
Corn stover	-	Activated sludge	1[a]	Batch	1.5	-	[177]
Carrot pulp	Glucose, fructose	*C. saccharolyticus*	10	Batch	2.8	15.7	[140]
Carrot pulp	Glucose, fructose	*T. neapolitana*	10	Batch	2.7	12.5	[140]
Wood fibres	Cellulose	*C. thermocellum*	1	Batch	1.5	-	[146]
Paper sludge	Glucose, xylose	*C. saccharolyticus*	8	Batch	2.0–2.1	5.3–6.0	[52]
Artificial medium	Glucose, xylose	*C. saccharolyticus*	10	Batch	3.0	17.0	[55]
Artificial medium	a-cellulose	*C. thermocellum*	4	Continuous	1.3	5.1	[178]

[a] g COD/L
[b] L/L • d
[c] mol/mol C5

As mentioned above, sugar beet pulp is an important residue of the sugar refining industry and it has a high carbohydrate content and low lignin content. Its valorisation for energy and fuels has become an important field of research [35, 116–120]. Grabarczyk and co-workers [121] investigated the potential of considering a conventional sugar factory as a beet pretreatment unit to which a fermentation unit can be connected to produce hydrogen. In this study hydrogen production from molasses, raw juice and thick juice was investigated. Moreover, hydrogen production in stand-alone plants located close to beet growing areas was considered. In another study, the potential hydrogen yield from sugar beet pulp per growing area of sugar beet in a two-stage fermentation process was calculated [28]. The potential hydrogen yield from dry and pressed sugar beet pulp can reach 300 kg/ha used for sugar beet growing, and is significant compared with the respective hydrogen yield from sugar beet juice. Considering European climatic data and sugar beet yields, and assuming that 50% of the total quantity of the pulp produced in sugar factories in the EU-27 is used for hydrogen production, a threefold increase in hydrogen potential is possible with use of the pulp. An annual hydrogen potential of 300×10^6 kg hydrogen was estimated for the EU-27. Ren and co-workers [122] focused on the utilisation of molasses in continuous fermentations and determined a hydrogen productivity of 4.8 L H_2/L • day, which is high compared with the hydrogen productivity of 2.6 L H_2/L • day, which was determined again with the use of mixed mesophilic cultures by Arooj and co-workers [123].

Sweet sorghum (*Sorghum bicolor*) is a C4, heat and drought tolerant, highly productive crop, with a high photosynthetic efficiency. One of the most important inherent characteristics of sweet sorghum is its high yields of 20–30 ton dry weight/ha. Fractionation of sweet sorghum can be performed *via* sugar extraction of the stalks to a liquid fraction, rich in sucrose, known as juice, and a remaining solid fraction, known as sweet sorghum bagasse. To date, ethanol is the best-known microbial product from sweet sorghum juice [124–126] or bagasse [127–129]. However, sweet sorghum juice consists mainly of soluble sugars (sucrose, glucose and fructose) that can be fermented to hydrogen production. Claassen and co-workers [130] determined a hydrogen yield of 2.3 mol/mol reported on glucose from the fermentation of sweet sorghum juice using *C. saccharolyticus*. This microorganism was shown to have a preference for the consumption of sucrose over glucose. Another bacterium which seems suitable for efficient hydrogen production from sweet sorghum juice is the rumen bacterium *Ruminococcus albus*, which resulted in a hydrogen yield of 2.6 mol/mol glucose [131]. The initial sugar concentration in the fermentation medium should be considered when comparing the fermentation characteristics of biomass substrates using different microorganisms. Sweet sorghum bagasse consists mainly of 39% cellulose, 21% hemicelluloses and 18% lignin. Panagiotopoulos and co-workers [54] studied biological hydrogen production from sweet sorghum bagasse; the results of this work are discussed in **Section 14.4**.

14.4 Biohydrogen Production with Processing of Lignocellulosic Biomass

Biohydrogen production using complex organic materials, such as agricultural wastes, food wastes, paper wastes and municipal wastes has recently received increasing attention [132]. In particular, dark fermentation is advantageous since it can produce hydrogen all day long without the need for light. Moreover, dark fermentation systems have relatively simple construction and operation presents low energy demands, mainly for mixing. On the other hand, increasing the yield results in the hydrogen fermentation becoming thermodynamically unfavourable and the product gas mixture contains CO_2, which has to be separated [133].

The main principles of hydrogen production *via* dark fermentation, as well as the hydrogen-producing microorganisms are described in detail by de Vrije and Claassen [27]. An update of the principles relevant to the research efforts towards the maximisation of hydrogen production from lignocellulosic biomass and an update of the microorganisms recently studied are provided in the current section of this chapter. In general, hydrogen can be produced either through mixed acidogenic microbial cultures, derived from natural environments such as soil or wastewater sludge, or through defined, pure cultures of hydrogen-producing microorganisms. In particular, dark fermentative hydrogen production can occur with a wide range of hydrogen-producing microorganisms, which include strict anaerobes (*Clostridia*, rumen bacteria, thermophiles, methanogens), facultative anaerobes (*Enterobacter, Escherichia coli*, *Citrobacter*), aerobes (*Alcaligenes*, *Bacillus*), and co- and mixed cultures. The highest hydrogen yields have been obtained by hydrogen-producing extreme thermophilic anaerobic bacteria, with the strictly anaerobic *Clostridia* producing hydrogen with higher yields than facultative anaerobes. The highest hydrogen production rates have been obtained using *Clostridia*, *Enterobacter*, and co- and mixed cultures. Due to the aforementioned reasons, among the hydrogen-producing bacteria, *Clostridia, Enterobacter*, and co- and mixed cultures are the most widely studied.

Recently, thermophiles and in particular, extreme thermophiles (65–80 °C) and hyperthermophiles (> 80 °C), are preferred for the production of hydrogen from lignocellulosic biomass because the increase of temperature in principle improves the reaction kinetics [134]. The main thermophiles that have been recently studied include *Caldicellulosiruptor saccharolyticus* [53, 54, 78, 135–137], *Thermoanaerobacterium thermosaccharolyticum* [75, 138, 139] and *Thermotoga neapolitana* [53, 76, 78, 107, 140]. **Table 14.3** summarises the results from selected studies conducted for hydrogen production *via* dark fermentation with different types of lignocellulosic biomass. Concerning *C. saccharolyticus*, it is notable that *C. owensensis* and *C. kristjanssonii* were reported to be good complementary microorganisms to *C. saccharolyticus*, for the quick and efficient utilisation of glucose and xylose [55]. In general, the use of

defined mixed cultures has good potential for development because it provides control of metabolic pathways and products, resulting in high H_2 yields by controlling the composition of the bacterial consortium [55, 141]. Concerning *T. neapolitana*, it is notable that the hydrogen production rate with this microorganism was 2–3 times higher compared with *T. maritima* [107], which has also attracted significant attention and has potential for hydrogen production [142, 143]. One of the take-home messages of **Table 14.3** is that with the present stage of development of hydrogen production from lignocellulosic biomass, pretreatment of biomass (and subsequent enzymatic hydrolysis) is required to bring the sugars to a soluble, fermentable form and thus result in the efficient conversion of the sugars to hydrogen. For instance, barley hulls have been used without any pretreatment to produce hydrogen at a yield of 0.2 mol H_2/mol glucose [144], which is lower than the hydrogen yields of 2–3 mol/mol glucose most typically observed in recent literature (**Table 14.3**).

The fermentability test (see **Section 14.3**) has been applied to assess the suitability of alkaline pretreatment of sweet sorghum bagasse for its fermentability [54]. It was found that hydrogen production in samples with the sweet sorghum bagasse hydrolysate is mostly higher than in the control experiments with sugars of analytical grade. Subsequently, larger scale batch fermentations were performed under controlled conditions and it was found that *C. saccharolyticus* grows normally on hydrolysates of sweet sorghum bagasse up to a sugar concentration of 20 g/L. The study of the consumption pattern of the biomass sugars is interesting and comparison of the consumption pattern of the pure sugars could provide useful information, with regards to the role of compounds naturally present in biomass, within hydrogen fermentations. It seems that the natural presence of nutrients in the bagasse improves the fermentation conditions for hydrogen production. In particular, on 10 and 20 g/L of sweet sorghum bagasse sugars *C. saccharolyticus* simultaneously consumed glucose, xylose and sucrose, showing a high rate of glucose consumption and a relatively low rate of sucrose consumption. Although it was observed that at the end of the 72 h fermentations a small part of the oligomeric sugars had still not been consumed, the proof that di- and oligomeric sugars can be simultaneously consumed, along with glucose and xylose, for biohydrogen production could be instrumental in the utilisation of sugar streams of different biomass origin in the biorefinery. Besides hydrogen, the main metabolic products detected in the fermentations were acetic and lactic acid. In general, glucose fermentation can be accompanied by the generation of acetate, butyrate and formate, as well as other, undesired by-products such as lactate and propionate which derive directly from pyruvate, and ethanol and butanol which derive from a further step from acetyl CoA metabolism. For example, *C. saccharolyticus* converts sugars to hydrogen, acetate, lactate and traces of ethanol [145]. According to **Equation 14.1,** the maximum theoretical yield of biohydrogen is 4 moles H_2 per mol of glucose. This yield decreases with the generation of undesired by-products which is not accompanied by hydrogen production. The maximal hydrogen yield observed

in batch experiments with sweet sorghum bagasse hydrolysates, under controlled conditions, was 2.6 mol per mol C6 sugar and the maximal volumetric hydrogen production rate ranged from 10.2 to 10.6 mmol/(L • h) [54]. At higher substrate concentrations, the production of lactic acid increased at the expense of hydrogen production (**Figure 14.6**). This was also observed by Levin and co-workers [146], who used the thermophilic bacterium *Clostridium thermocellum* in order to produce hydrogen from delignified wood fibre, and by de Vrije and co-workers [140] who used *C. saccharolyticus* in order to produce hydrogen from carrot pulp. The phenomenon was also observed in the case of potato steam peels using *C. saccharolyticus* [78]. However, fermentations with high concentrations of *Miscanthus* sugars did not result in high lactate production [53], so the phenomenon seems to be raw-material specific [140]. Although it is not yet clear what triggers the shift in the metabolism of the cells, according to van Niel and co-workers [79], lactate and other reduced organic compounds, such as ethanol, are produced when reducing equivalents accumulate in the cell.

To extend the discussion to other microorganisms, the growth of mixed mesophilic cultures is inhibited with increased organic loadings [147, 148] therefore, dilution of the raw waste is typically required in order to decrease the organic loading and thus prevent inhibition of the process. To extend the discussion further, other parameters such as pH [149–151], temperature [152], hydraulic retention time (HRT) of the reactor [123, 148, 153] and gas stripping to avoid high partial hydrogen pressures [154–156] can influence the growth of the microorganisms, the hydrogen yield and productivity, and the economic profile of the process.

Biological hydrogen production by a sequential operation of dark- and photofermentation has attracted a considerable amount of research interest in the last five years [23, 157–161]. In such a system, the anaerobic fermentation of the organic material produces organic intermediates, such as acetic, butyric, lactic and propionic acids (**Equation 14.1**), which can be readily fermented in the second step by photoheterotrophic bacteria (**Equation 14.3**). The overall reactions of the process can be represented as:

$$2CH_3COOH + 4H_2O \rightarrow 8H_2 + 4CO_2 \qquad (14.3)$$

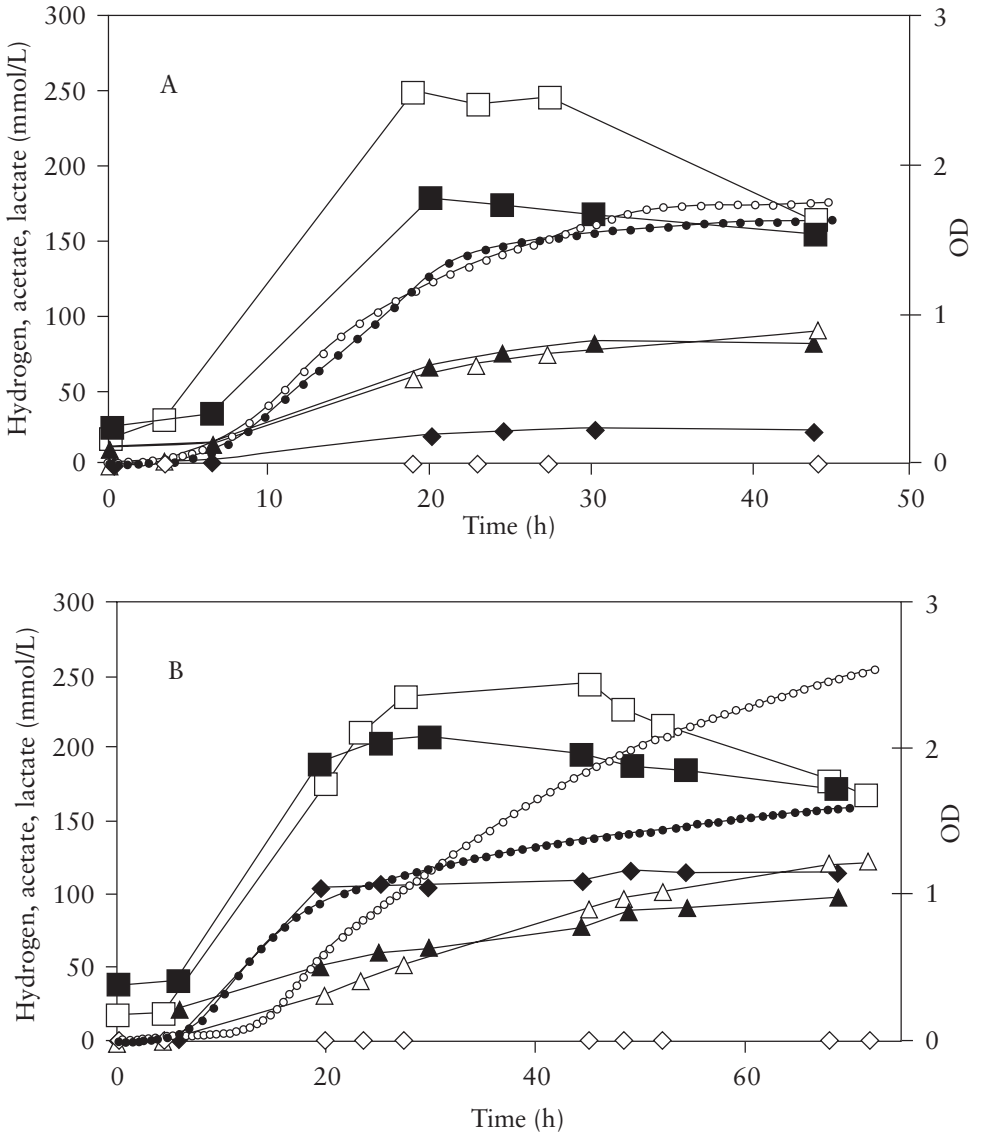

Figure 14.6 Growth (squares), production of hydrogen (circles), acetate (triangles) and lactate (diamonds) in cultures of *C. saccharolyticus* grown on pure sugars (open symbols) and the hydrolysate of sweet sorghum bagasse (filled symbols). The sum of glucose, xylose and sucrose concentrations was (A) 10 g/L and (B) 20 g/L. Optical density (OD) was measured at 580 nm. Reproduced with permission from I.A. Panagiotopoulos, R.R. Bakker, T. de Vrije, E.G. Koukios and P.A.M. Claassen, *International Journal of Hydrogen Energy*, 2010, **35**, 15, 7746. ©2010, Elsevier Ltd [54]

Using glucose as the sole substrate in dark anaerobic fermentation, where acetic acid is the predominant metabolite product, a total of 12 mol hydrogen could be expected in a combined process from one mol of glucose. To give a realistic example, the USA DOE report has set a lower conversion goal of 6 mol hydrogen/mol glucose for hydrogen production from biomass [162]. So far, the research on the sequential operation of dark- and photofermentation has mainly focused on the use of pure sugars as the substrate, and the observed yields with the two-step fermentations have been generally found to be higher than single-step fermentations, ranging from 3 to 7 mol H_2/mol hexose. Moreover, some initial efforts to produce hydrogen in two steps from sugars originating from biomass, such as potato steam peels [161, 163] and cassava starch [164, 165], have been recently reported. For example, Özgür and co-workers [163] investigated the photofermentative hydrogen production on effluents of thermophilic dark fermentations using a potato steam peels hydrolysate and molasses in indoor, batch fermentations. *Caldicellulosiruptor saccharolyticus* was used in the dark fermentation step and *Rhodobacter capsulatus* was used in the photofermentation step. The overall hydrogen yield of the two-step fermentations was higher than the yield of single-step dark fermentations. Addition of buffer and nutrients to dark fermenter effluents was found to improve the overall efficiency of hydrogen production.

One of the key challenges of the sequential operation of dark- and photofermentation is the low photosynthetic efficiency of the second stage of the process, because at even moderate light intensities the main part of captured light is dissipated as heat [166]. This would imply that large surface areas are required resulting in increasing the total cost of hydrogen production. Boran and co-workers [167] operated outdoors a 90 L scaled-up tubular photobioreactor in continuous mode using effluent from the dark fermentation of thick juice as a feedstock. This work reported an average production rate of 0.15 mol $H_2/(m^3 \bullet h)$ and confirmed that the hydrogen productivity depends on the light exposure of the cells. One main disadvantage of the light-dependent processes is the more complex design of the reactors. Due to the need to maintain a suitable proportion between the reactor surface area and volume when scaling-up, research focus is expected to target the design of the reactors, which will ideally allow high light availability, homogeneous distribution of light and high hydrogen production efficiency.

The hydrogen production efficiency and the energy efficiency of this coupled dark- and photofermentation has been compared with steam reforming of biogas. The production efficiency of the coupled dark- and photofermentation seems to be comparable to the reforming of biogas, but its energy efficiency is lower [168]. Moreover, a recent techno-economic comparison between the two-step, biological production of hydrogen from barley straw and biological production of ethanol showed that the production cost of the biohydrogen process is 20 times higher than

the ethanol process, mainly due to low hydrogen productivity [40]. In conclusion, it is expected that in the near future research efforts will focus on the sequential dark- and photofermentation, which will be further developed in order to approach practical application in the long-term future.

14.5 Conclusions

Depending on the type of biomass, processing of biomass is needed to render the available carbohydrates accessible for fermentation towards biohydrogen production. In the case of sugary biomass, such as sugar beet and sweet sorghum, most of the sugars are readily fermentable, so the processing is relatively simple. In the case of lignocellulosic biomass, such as wheat straw, wheat bran and sweet sorghum bagasse, processing usually includes pretreatment and enzymatic hydrolysis. An overview of the basic pretreatment methods that have been used or have the potential for future use in biohydrogen production has been discussed in the current chapter. Although some pretreatment methods, such as steam pretreatment, dilute-acid pretreatment and alkaline pretreatment show apparent advantages, it is unlikely that one method will be suitable for all biomass feedstocks. To date, pretreatment methods have been developed in order to achieve high sugar yield and high enzymatic digestibility of the pretreated biomass. The future research on specific pretreatment for biohydrogen production should be focused on achieving high fermentability. The fermentability test is a rapid test that is applied to evaluate the potential for hydrogen production from a pretreated feedstock. Although the predictability of the characteristics of large-scale fermentations using the fermentability test is uncertain at the present stage of development of hydrogen production, research is ongoing towards this objective.

Acknowledgements

The authors wish to thank all partners in the HYVOLUTION Integrated Project (Commission of the European Communities, 6th Framework Programme, Sustainable Energy Systems, Contract Nr. 019825) for their fruitful collaboration during the project. In particular, we thank Rob Bakker, Truus de Vrije and Pieternel Claassen (Wageningen UR, The Netherlands) for their close experimental collaboration and very helpful discussions on the hydrogen fermentability of pretreated biomass during the project.

References

1. B. Bolin, *Science*, 1998, **279**, 5349, 330.

2. M.E. Mann, *Science*, 2000, **289**, 5477, 253.

3. J.A. Patz, D. Campbell-Lendrum, T. Holloway and J.A. Foley, *Nature*, 2005, **438**, 310.

4. N.D. Diamantidis and E.G. Koukios, *Industrial Crops and Products*, 2000, **11**, 2–3, 97.

5. M. Parikka, *Biomass and Bioenergy*, 2004, **27**, 6, 613.

6. J. Heinimö and M. Junginger, *Biomass and Bioenergy*, 2009, **33**, 9, 1310.

7. M. de Wit and A. Faaij, *Biomass and Bioenergy*, 2010, **34**, 2, 188.

8. A.T.W.M. Hendriks and G. Zeeman, *Bioresource Technology*, 2009, **100**, 1, 10.

9. P.A.M. Claassen, J.B. van Lier, A.M.L. Contreras, E.W.J. van Niel, L. Sijtsma, A.J.M. Stams, S.S. de Vries and R.A. Weusthuis, *Applied Microbiology and Biotechnology*, 1999, **52**, 6, 741.

10. A. Demirbas, *Energy Conversion and Management*, 2008, **49**, 8, 2106.

11. R.E.H. Sims, W. Mabee, J.N. Saddler and M. Taylor, *Bioresource Technology*, 2010, **101**, 6, 1570.

12. C.N. Hamelinck, G.V. Hooijdonk and A.P. Faaij, *Biomass and Bioenergy*, 2005, **28**, 4, 384.

13. A.E. Farrell, R.J. Plevin, B.T. Turner, A.D. Jones, M. O'Hare and D.M. Kammen, *Science*, 2006, **311**, 5760, 506.

14. B. Hahn-Hägerdal, M. Galbe, M.F. Gorwa-Grauslund, G. Lidén and G. Zacchi, *Trends in Biotechnology*, 2006, **24**, 12, 549.

15. F. Ma and M.A. Hanna, *Bioresource Technology*, 1999, **70**, 1, 1.

16. Y. Chisti, *Trends in Biotechnology*, 2008, **26**, 3, 126.

17. C.E. Wyman, *Trends in Biotechnology*, 2007, **25**, 4, 153.

18. P.R.D. Williams, D. Inman, A. Aden and G.A. Heath, *Environmental Science & Technology*, 2009, **43**, 13, 4763.

19. A. Eisentraut, *OECD/IEA Information Paper*, 2010. *http://www.task39.org*

20. T.N. Veziroglu and F. Barbir, *International Journal of Hydrogen Energy*, 1992, **17**, 6, 391.

21. M.L. Wald, *Scientific American*, 2004, **42**, 41.

22. *Hydrogen and Fuel Cells – Fundamentals, Technologies and Applications*, Ed., D. Stolten, Wiley–VCH, Weinheim, Germany, 2010.

23. P.A.M. Claassen and T. de Vrije, *International Journal of Hydrogen Energy*, 2006, **31**, 11, 1416.

24. N. Martínez-Pérez, S.J. Cherryman, G.C. Premier, R.M. Dinsdale, D.L. Hawkes, F.R. Hawkes, G. Kyazze and A.J. Guwy, *Biomass and Bioenergy*, 2007, **31**, 2–3, 95.

25. I.A. Panagiotopoulos, R.R. Bakker, M.A.W. Budde, T. de Vrije, P.A.M. Claassen and E.G. Koukios, *Bioresource Technology*, 2009, **100**, 24, 6331.

26. N.Z. Muradov and T.N. Veziroglu, *International Journal of Hydrogen Energy*, 2008, **33**, 23, 6804.

27. T. de Vrije and P.A.M. Claassen in *Bio-methane & Bio-hydrogen: Status and Perspectives of Biological Methane and Hydrogen Production*, Eds., J.H. Reith, R.H. Wijffels and H. Barten, Smiet Offset, Dutch Biological Hydrogen Foundation, The Hague, The Netherlands, 2003, p.103.

28. I.A. Panagiotopoulos, R.R. Bakker, T. de Vrije, K. Urbaniec, E.G. Koukios and P.A.M. Claassen, *Journal of Cleaner Production*, 2010, **18**, 1, S9.

29. I.A. Panagiotopoulos, R.R. Bakker, M.A.W. Budde, T. de Vrije, P.A.M. Claassen and E.G. Koukios in *Proceedings of the 16th European Biomass Conference & Exhibition*, European Commission DG (Directorate-General) Joint Research Centre, Valencia, Spain, 2008, p.1670.

30. M.E.F. Bergmans, G. Beldman, H. Gruppen and A.G.J. Voragen, *Journal of Cereal Science*, 1996, **23**, 3, 235.

31. C. Maes and J.A. Delcour, *Journal of Cereal Science*, 2001, **34**, 1, 29.

32. M.A. Kabel, F. Carvalheiro, G. Garrote, E. Avgerinos, E. Koukios, J.C. Parajó, F.M. Gírio, H.A. Schols and A.G.J. Voragen, *Carbohydrate Polymers*, 2002, **50**, 1, 47.

33. T. Cheilas, T. Stoupis, P. Christakopoulos, P. Katapodis, D. Mamma, D.G. Hatzinikolaou, D. Kekos and B.J. Macris, *Process Biochemistry*, 2000, **35**, 6, 557.

34. Energy Research Centre of The Netherlands (ECN), *The Composition of Biomass and Waste*, Phyllis, The Netherlands. *http://www.ecn.nl/phyllis/info.asp*

35. Y. Zheng, Y-S. Cheng, C. Yu, R. Zhang, B.M. Jenkins and J.S. VanderGheynst, *Bioprocess and Biosystems Engineering*, 2012, **35**, 9, 1531.

36. D.L. Klass in *Biomass as a Nonfossil Fuel Source*, American Chemical Society, Washington, DC, USA, 1981.

37. P. Kumar, D.M. Barrett, M.J. Delwiche and P. Stroeve, *Industrial & Engineering Chemical Research*, 2009, **48**, 8, 3713.

38. L. Palmowski, J. Muller in *Proceedings of 2nd International Symposium on Anaerobic Digestion of Solid Waste*, International Association on Water Quality, Barcelona, Spain, 1999, p.137.

39. HYVOLUTION Integrated Project, Commission of the European Communities, Deliverable 5.30, *Final Cost Estimation of Fully Integrated Process Routes*, 2010. [Unpublished]

40. M. Ljunggren, O. Wallberg and G. Zacchi, *Bioresource Technology*, 2011, **102**, 20, 9524.

41. J.N. Saddler and D.J. Gregg in *Proceedings of the 1997 Ethanol Research and Development Workshop*, Natural Resources Canada, Ottawa, Canada, 1997, p.135.

42. J. Söderström, L. Pilcher, M. Galbe and G. Zacchi, *Applied Biochemistry and Biotechnology*, 2002, **98–100**, 1–9, 5.

43. M. Linde, M. Galbe and G. Zacchi, *Applied Biochemistry and Biotechnology*, 2006,**130**, 1–3, 546.

44. K. Öhgren, R. Bura, J. Saddler and G. Zacchi, *Bioresource Technology*, 2007, **98**, 13, 2503.

45. R. Bura, R. Chandra and J. Saddler, *Biotechnology Progress*, 2009, **25**, 2, 315.

46. H.H. Brownell, E.K.C. Yu and J.N. Saddler, *Biotechnology and Bioengineering*, 1986, **28**, 6, 792.

47. N. Mosier, C. Wyman, B. Dale, R. Elander, Y.Y. Lee, M. Holtzapple and M. Ladisch, *Bioresource Technology*, 2005, **96**, 6, 673.

48. D.J. Hayes, *Catalysis Today*, 2009, **145**, 1–2, 138.

49. R. Datar, J. Huang, P.C. Maness, A. Mohagheghin and S.C.E. Czernik, *International Journal of Hydrogen Energy*, 2007, **32**, 8, 932.

50. D.M. Li and H.Z. Chen, *International Journal of Hydrogen Energy*, 2007, **32**, 12, 1742.

51. Y. Lu, Q. Lai, C. Zhang, H. Zhao, K. Ma, X. Zhao, H. Chen, D. Liu and X-H. Xing, *Bioresource Technology*, 2009, **100**, 12, 2889.

52. Z. Kádár, T. de Vrije, G.E. van Noorden, M.A.W. Budde, Z. Szengyel and K. Réczey, *Applied Biochemistry and Biotechnology*, 2004, **114**, 1–3, 497.

53. T. de Vrije, R.R. Bakker, M.A.W. Budde, M.H. Lai, A.E. Mars and P.A.M. Claassen, *Biotechnology for Biofuels*, 2009, **2**, 12.

54. I.A. Panagiotopoulos, R.R. Bakker, T. de Vrije, E.G. Koukios and P.A.M. Claassen, *International Journal of Hydrogen Energy*, 2010, **35**, 15, 7738.

55. A.A. Zeidan, *International Journal of Hydrogen Energy*, 2009, **34**, 10, 4524.

56. J.M. Oliva, F. Sáez, I. Ballesteros, A. González, M.J. Negro and P. Manzanares, *Applied Biochemistry and Biotechnology*, 2003, **105**, 1–3, 141.

57. M. Cantarella, L. Cantarella, A. Gallifuoco, A. Spera and F. Alfani, *Biotechnology Progress*, 2004, **20**, 1, 200.

58. J.N. Nigam, *Journal of Biotechnology*, 2001, **87**, 1, 17.

59. M.A. Franden, P.T. Pienkos and M. Zhang, *Journal of Biotechnology*, 2009, **144**, 4, 259.

60. J.D. McMillan in *Enzymatic Conversion of Biomass for Fuels Production*, Eds., M.E. Himmel, J.O. Baker and R.P. Overend, American Chemical Society, Washington, DC, USA, 1994, **566**, p.292.

61. Y. Sun and J.J. Cheng, *Bioresource Technology*, 2005, **96**, 14, 1599.

62. M.V. Sivers and G. Zacchi, *Bioresource Technology*, 1995, **51**, 1, 43.

63. L.R. Lynd and H.E. Grethlein, *Biotechnology and Bioengineering*, 1987, **29**, 1, 92.

64. R. Torget, P. Walter, M. Himmel and K. Grohmann, *Applied Biochemistry and Biotechnology*, 1991, **28–29**, 1, 75.

65. A. Esteghlalian, A.G. Hashimoto, J.J. Fenske and M.H. Penner, *Bioresource Technology*, 1997, **59**, 2–3, 129.

66. R. Wooley, M. Ruth, J. Sheehan and K. Ibsen in *National Renewable Energy Laboratory Technical Report, NREL/TP-580-26157*, US Department of Energy, Golden, CO, USA, 1999.

67. B.C. Saha, L.B. Iten, M.A. Cotta and Y.V. Wu, *Process Biochemistry*, 2005, **40**, 12, 3693.

68. T.A. Lloyd and C.E. Wyman, *Bioresource Technology*, 2005, **96**, 18, 1967.

69. S. Monavari, M. Galbe and G. Zacchi, *Biotechnology for Biofuels*, 2009, **2**, 6.

70. I.A. Panagiotopoulos, R.R. Bakker, T. de Vrije and E.G. Koukios, *Bioresource Technology*, 2011, **102**, 24, 11204.

71. S. Larsson, E. Palmqvist, B. Hahn-Hägerdal, C. Tengborg, K. Stenberg, G. Zacchi and N-O. Nilvebrant, *Enzyme and Microbial Technology*, 1999, **24**, 3–4, 151.

72. I.A. Panagiotopoulos, G. Lignos, R.R. Bakker and E.G. Koukios, *Journal of Cleaner Production*, 2012, **32**, 45.

73. E. Palmqvist and B. Hahn-Hägerdal, *Bioresource Technology*, 2000, **74**, 1, 25.

74. J.R.M. Almeida, T. Modig, A. Petersson, B. Hahn-Hägerdal, G. Liden and M.F. Gorwa-Grauslund, *Journal of Chemical Technology and Biotechnology*, 2007, **82**, 4, 340.

75. G. Cao, N. Ren, A. Wang, D-J. Lee, W. Guo, B. Liu, Y. Feng and Q. Zhao, *International Journal of Hydrogen Energy*, 2008, **34**, 17, 7182.

76. T-A.D. Nguyen, K-R. Kim, M.S. Kim and S.J. Sim, *International Journal of Hydrogen Energy*, 2010, **35**, 24, 13392.

77. I.A. Panagiotopoulos, R.R. Bakker, T. de Vrije, E.W.J. van Niel, E.G. Koukios and P.A.M. Claassen, *Journal of Japan Institute of Energy*, 2011, **90**, 4, 363.

78. A.E. Mars, T. Veuskens, M.A.W. Budde, P.F.N.M. van Doeveren, S.J. Lips, R.R. Bakker, T. de Vrije and P.A.M. Claassen, *International Journal of Hydrogen Energy*, 2010, **35**, 15, 7730.

79. E.W.J. van Niel, P.A.M. Claassen and A.J.M. Stams, *Biotechnology and Bioengineering*, 2003, **81**, 3, 255.

80. D.P. Koullas, P.F. Christakopoulos, D. Kekos, E.G. Koukios and B.J. Macris, *Biomass and Bioenergy*, 1993, **4**, 1, 9.

81. T. de Vrije, G.G. de Haas, G.B. Tan, E.R.P. Keijsers and P.A.M. Claassen, *International Journal of Hydrogen Energy*, 2002, **27**, 11–12, 1381.

82. Y. Zhao, Y. Wang, J.Y. Zhu, A. Ragauskas and Y. Deng, *Biotechnology and Bioengineering*, 2008, **99**, 6, 1320.

83. A. Goshadrou, K. Karimi and M.J. Taherzadeh, *Industrial Crops and Products*, 2011, **34**, 1, 1219.

84. V.S. Chang, M. Nagwani and M.T. Holtzapple, *Applied Biochemistry and Biotechnology*, 1998, **74**, 3, 135.

85. S. Kim and M.T. Holtzapple, *Bioresource Technology*, 2005, **96**, 18, 1994.

86. R.H.W. Maas in *Microbial Conversion of Lignocellulose-derived Carbohydrates into Bioethanol and Lactic Acid*, Wageningen, The Netherlands, 2008. [PhD Thesis]

87. X. Pan, N. Gilkes, J. Kadla, K. Pye, S. Saka, D. Gregg, K. Ehara, D. Xie, D. Lam and J. Saddler, *Biotechnology and Bioengineering*, 2006, **94**, 5, 851.

88. V.B. Agbor, N. Cicek, R. Sparling, A. Berlin and D.B. Levin, *Biotechnology Advances*, 2011, **29**, 6, 675.

89. M. Galbe and G. Zacchi, *Biomass and Bioenergy*, 2012, **46**, 70.

90. X. Pan, C. Arato, N. Gilkes, D. Gregg, W. Mabee, K. Pye, Z. Xiao, X. Zhang and J. Saddler, *Biotechnology and Bioengineering*, 2005, **90**, 4, 473.

91. D. Haverty, K. Dussan, A.V. Piterina, J.J. Leahy and M.H.B. Hayes, *Bioresource Technology*, 2012, **109**, 173.

92. M. Beccari, M. Majone, M.P. Papini and L. Torrisi, *Water Science and Technology*, 2001, **43**, 275.

93. Y. Lin, D. Wang, S. Wu and C. Wang, *Journal of Hazardous Materials*, 2009, **170**, 1, 366.

94. S. Singh, B.A. Simmons and K.P. Vogel, *Biotechnology and Bioengineering*, 2009, **104**, 1, 68.

95. C. Li, B. Knierim, C. Manisseri, R. Arora, H.V. Scheller, M. Auer, K.P. Vogel, B.A. Simmons and S. Singh, *Bioresource Technology*, 2010, **101**, 13, 4900.

96. S.S.Y. Tan, D.R. MacFarlane, J. Upfal, L.A. Edye, W.O.S. Doherty, A.F. Patti, J.M. Pringle and J.L. Scott, *Green Chemistry*, 2009, **11**, 339.

97. N. Sun, M. Rahman, Y. Qin, M.L. Maxim, H. Rodriguez and R.D. Rogers, *Green Chemistry*, 2009, **11**, 646.

98. S. Datta, B. Holmes, J.I. Park, Z. Chen, D.C. Dibble, M. Hadi, H.W. Blanch, B.A. Simmons and R. Sapra, *Green Chemistry*, 2010, **12**, 338.

99. M. Ouellet, S. Datta, D.C. Dibble, P.R. Tamrakar, P.I. Benke, C. Li, S. Singh, K.L. Sale, P.D. Adams, J.D. Keasling, B.A. Simmons, B.M. Holmes and A. Mukhopadhyay, *Green Chemistry*, 2011, **13**, 2743.

100. G.D. McGinnis, W.W. Wilson and C.E. Mullen, *Industrial & Engineering Chemistry Product Research and Development*, 1983, **22**, 2, 352.

101. A.S. Schmidt and A.B. Thomsen, *Bioresource Technology*, 1998, **64**, 2, 139.

102. H.B. Klinke, B.K. Ahring, A.S. Schmidt and A.B. Thomsen, *Bioresource Technology*, 2002, **82**, 1, 15.

103. B.K. Ahring, D. Licht, A.S. Schmidt, P. Sommer and A.B. Thomsen, *Bioresource Technology*, 1999, **68**, 1, 3.

104. E. Arvaniti, A.B. Bjerre and J.E. Schmidt, *Biomass and Bioenergy*, 2012, **39**, 94.

105. H. Palonen, A.B. Thomsen, M. Tenkanen, A.S. Schmidt and L. Viikari, *Applied Biochemistry and Biotechnology*, 2004, **117**, 1, 1.

106. C. Martin, H.B. Klinke and A.B. Thomsen, *Enzyme and Microbial Technology*, 2007, **40**, 3, 426.

107. N.T. Eriksen, M.L. Riis, N.K. Holm and N. Iversen, *Biotechnology Letters*, 2011, **33**, 2, 293.

108. J.A. Panagiotopoulos, R.R. Bakker, P. Harmsen, K. Urbaniec, A. Zarzycki, J. Wu and V. Sardo in *Biomass Crops: Production, Energy and the Environment*, Ed., A.P. Haggerty, Nova Publishers, Hauppauge, NY, USA, 2011, p.89.

109. Comité Européen des Fabricants de Sucre. *http://www.eurosugar.org/pdf/stat2008.pdf*

110. Comité Européen des Fabricants de Sucre. *http://www.eurosugar.org/pdf/stat2011.pdf*

111. S. Haley, *Sugar and Sweeteners Outlook*, 2012. *http://www.ers.usda.gov/ publications/sss/2010/Feb/SSSM258.pdf*

112. J. Panagiotopoulos, R. Bakker, T. de Vrije, P. Claassen and E. Koukios in *Proceedings of the 18th World Hydrogen Energy Conference 2010 - WHEC 2010 : Parallel Sessions Book 2: Hydrogen Production Technologies - Part 1*, Eds., D. Stolten and T. Grube, Forschungszentrum Jülich GmbH, Zentralbibliothek, Verlag, Jülich, Germany, 2010, p.69.

113. T. Noike and O. Mizuno, *Water Science and Technology*, 2000, **42**, 12, 155.

114. F.R. Hawkes, H. Forsey, G.C. Premier, R.M. Dinsdale, D.L. Hawkes, A.J. Guwy, J. Maddy, S. Cherryman, J. Shine and D. Auty, *Bioresource Technology*, 2008, **99**, 11, 5020.

115. C. Pan, Y. Fan and H. Hou, *Industrial & Engineering Chemistry*, 2008, **47**, 16, 5812.

116. M. Hutnan, M. Drtil and L. Mrafkova, *Biodegradation*, 2000, **11**, 4, 203.

117. A. Koppar and P. Pullammanappallil, *Bioresource Technology*, 2008, **99**, 8, 2831.

118. V. Kryvoruchko, A. Machmüller, V. Bodiroza, B. Amon and T. Amon, *Biomass and Bioenergy*, 2009, **33**, 4, 620.

119. S. Kühnel, H. A. Schols and H. Gruppen, *Biotechnology for Biofuels*, 2011, **4**, 14.

120. Y. Zheng, C. Yu, Y-S. Cheng, C. Lee, C.W. Simmons, T.M. Dooley, R. Zhang, B.M. Jenkins and J.S. VanderGheynst, *Applied Energy*, 2012, **93**, 168.

121. R. Grabarczyk, K. Urbaniec, E. Koukios, R. Bakker and G. Vaccari, *Sugar Industry/Zuckerindustrie*, 2011, **136**, 12, 784.

122. N.Q. Ren, H. Chua, S.Y. Chan, Y.F. Tsang, Y.J. Wang and N. Sin, *Bioresource Technology*, 2007, **98**, 9, 1774.

123. M-F. Arooj, S-K. Han, S-H. Kim, D-H. Kim and H-S. Shin, *International Journal of Hydrogen Energy*, 2008, **33**, 22, 6509.

124. L. Laopaiboon, P. Thanonkeo, P. Jaisil and P. Laopaiboon, *World Journal of Microbiology and Biotechnology*, 2007, **23**, 10, 1497.

125. D.K. Kundiyana, D.D. Bellmer, R.L. Huhnke, M.R. Wilkins and P.L. Claypool, *Biomass and Bioenergy*, 2010, **34**, 10, 1481.

126. X. Wu, S. Staggenborg, J.L. Propheter, W.L. Rooney, J. Yu and D. Wang, *Industrial Crops and Products*, 2010, **31**, 1, 164.

127. I. Dogaris, G. Vakontios, E. Kalogeris, D. Mamma and D. Kekos, *Industrial Crops and Products*, 2009, **29**, 2–3, 404.

128. B. Sipos, J. Réczey, Z. Somorai, Z. Kádár, D. Dienes and K. Réczey, *Applied Biochemistry and Biotechnology*, 2009, **153**, 1–3, 151.

129. F. Shen, J. Hu, Y. Zhong, M.L.Y. Liu, J.N. Saddler and R. Liu, *Biomass and Bioenergy*, 2012, **41**, 157.

130. P.A.M. Claassen, T. de Vrije, M.A.W. Budde, E.G. Koukios, A. Glynos and K. Réczey in *Proceedings of the 2nd World Conference on Biomass for Energy, Industry and Climate Protection*, European Commission DG (Directorate-General) Joint Research Centre, US DOE (Department of Energy) and Natural Resources Canada, Rome, Italy, 2004, p.1522.

131. I. Ntaikou, H.N. Gavala, M. Kornaros and G. Lyberatos, *International Journal of Hydrogen Energy*, 2008, **33**, 4, 1153.

132. C.L. Li and H.H.P. Fang, *Critical Reviews in Environmental Science and Technology*, 2007, **37**, 1, 1.

133. D. Das and T.N. Veziroglu, *International Journal of Hydrogen Energy*, 2008, **33**, 21, 6046.

134. D.B. Levin, C.R. Carere, N. Cicek and R. Sparling, *International Journal of Hydrogen Energy*, 2009, **34**, 17, 7370.

135. A.L. VanFossen, M.R.A. Verhaart, S.M.W. Kengen and R.M. Kelly, *Applied and Environmental Microbiology*, 2009, **75**, 24, 7718.

136. I.A. Panagiotopoulos, R.R. Bakker, T. de Vrije, P.A.M. Claassen and E.G. Koukios, *International Journal of Hydrogen Energy*, 2012, **37**, 16, 11727.

137. K. Willquist, *International Journal of Hydrogen Energy*, 2012, **37**, 6, 4925.

138. S. O-Thong, P. Prasertsan, D. Karakashev and I. Angelidaki, *International Journal of Hydrogen Energy*, 2008, **33**, 4, 1204.

139. G-L. Cao, N-Q. Ren, A-J. Wang, W-Q. Guo, J. Yao, Y-J. Feng and Q-L. Zhao, *Bioresource Technology*, 2010, **101**, 6, 2053.

140. T. de Vrije, M.A.W. Budde, S.J. Lips, R.R. Bakker, A.E. Mars and P.A.M. Claassen, *International Journal of Hydrogen Energy*, 2010, **35**, 15, 13206.

141. S. Ozmihci and F. Kargi, *International Journal of Hydrogen Energy*, 2011, **36**, 12, 7089.

142. C. Schroder, M. Selig and P. Schonheit, *Archives of Microbiology*, 1994, **161**, 6, 460.

143. G.J. Schut and M.W.W. Adams, *Journal of Bacteriology*, 2009, **191**, 13, 4451.

144. L. Magnusson, R. Islam, R. Sparling, D. Levin and N. Cicek, *International Journal of Hydrogen Energy*, 2008, **33**, 20, 5398.

145. F.A. Rainey, A.M. Donnison, P.H. Janssen, D. Saul, A. Rodrigo, P.L. Bergquist, R.M. Daniel, E. Stackebrandt and H.W. Morgan, *FEMS Microbiology Letters*, 1994, **120**, 3, 263.

146. D.B. Levin, R. Islam, N. Cicek and R. Sparling, *International Journal of Hydrogen Energy*, 2006, **31**, 11, 1496.

147. G. Davila-Vazquez, F. Alatriste-Mondragon, A. de Leon-Rodriguez and E. Razo-Flores, *International Journal of Hydrogen Energy*, 2008, **33**, 19, 4989.

148. I. Ntaikou, C. Kourmentza, E. Koutrouli, K. Stamatelatou, A. Zampraka, M. Kornaros and G. Lyberatos, *Bioresource Technology*, 2009, **100**, 15, 3724.

149. S. van Ginkel, S. Sung and J.J. Lay, *Environmental Science & Technology*, 2001, **35**, 24, 4726.

150. Y.J. Lee, T. Miyahara and T. Noike, *Journal of Chemical Technology and Biotechnology*, 2002, **77**, 6, 694.

151. G. Antonopoulou, H.N. Gavala, I.V. Skiadas and G. Lyberatos, *International Journal of Hydrogen Energy*, 2010, **35**, 5, 1921.

152. J.L. Wang and W. Wan, *International Journal of Hydrogen Energy*, 2008, **33**, 20, 5392.

153. S.Y. Wu, C.H. Hung, C.Y. Lin, P.J. Lin, K.S. Lee, C.N. Lin, F.Y. Chang and J-S. Chang, *International Journal of Hydrogen Energy*, 2008, **33**, 5, 1542.

154. O. Mizuno, R. Dinsdale, F.R. Hawkes, D.L. Hawkes and T. Noike, *Bioresource Technology*, 2000, **73**, 1, 59.

155. K. Willquis and P.A.M. Claassen, *International Journal of Hydrogen Energy*, 2009, **34**, 11, 4718.

156. M. Ljunggren, K. Willquist and G. Zacchi *Biotechnology for Biofuels*, 2011, **4**, 31.

157. K. Nath, M. Muthukumar, A. Kumar and D. Das, *International Journal of Hydrogen Energy*, 2008, **33**, 4, 1195.

158. B. Uyar, M. Schumacher, J. Gebicki and M. Modigell, *Bioprocess and Biosystems Engineering*, 2009, **32**, 5, 603.

159. C.Y. Chen, K.L. Yeh, Y.C. Lo, H.M. Wang and J.S. Chang, *International Journal of Hydrogen Energy*, 2010, **35**, 24, 13356.

160. T.V. Laurinavichene, B.F. Belokopytov, K.S. Laurinavichius, D.N. Tekucheva, M. Seibert and A.A. Tsygankov, *International Journal of Hydrogen Energy*, 2010, **35**, 16, 8536.

161. N. Afsar, E. Özgür, M. Gürgan, S. Akköse, M. Yücel, U. Gündüz and I. Eroglu, *International Journal of Hydrogen Energy*, 2011, **36**, 1, 432.

162. US Department of Energy, *A Multiyear Plan for the Hydrogen R&D Program, Rationale, Structure and Technology Roadmaps*, Washington, DC, USA, 1999.

163. E. Özgür, N. Afsar N., T. de Vrije, M. Yücel, U. Gündüz, P.A.M. Claassen and I. Eroglu, *Journal of Cleaner Production*, 2010, **18**, 1, S23.

164. H. Su, J. Cheng, J. Zhou, W. Song and K. Cen, *International Journal of Hydrogen Energy*, 2009, **34**, 4, 1780.

165. W. Zong, R. Yu, P. Zhang, M. Fan and Z. Zhou, *Biomass and Bioenergy*, 2009, **33**, 10, 1458.

166. S. Hoekema, R.D. Douma, M. Janssen, J. Tramper and R.H. Wijffels, *Biotechnology and Bioengineering*, 2006, **95**, 4, 613.

167. E. Boran, E. Özgür, M. Yücel, U. Gündüz and I. Eroglu, *Journal of Cleaner Production*, 2012, **31**, 150.

168. A. Miltner, W. Wukovits, T. Pröll and A. Friedl, *Journal of Cleaner Production*, 2010, **18**, 1, S51.

169. P. Saraphirom and A. Reungsang, *International Journal of Hydrogen Energy*, 2010, **35**, 24, 13435.

170. G. Antonopoulou, H.N. Gavala, I.V. Skiadas, K. Angelopoulos and G. Lyberatos, *Bioresource Technology*, 2008, **99**, 1, 110.

171. I. Hussy, F.R. Hawkes, R. Dinsdale and D.L. Hawkes, *International Journal of Hydrogen Energy*, 2005, **30**, 5, 471.

172. E. Özgür, A.E. Mars, B. Peksel, A. Louwerse, M. Yücel, U. Gündüz, P.A.M. Claassen and I. Eroglu, *International Journal of Hydrogen Energy*, 2010, **35**, 2, 511.

173. X.W. Wang, B. Jin and D. Mulcahy, *International Journal of Hydrogen Energy*, 2008, **33**, 19, 4998.

174. I. Hussy, F.R. Hawkes, R. Dinsdale and D.L. Hawkes, *Biotechnology and Bioengineering*, 2003, **84**, 6, 619.

175. S. Pattra, S. Sangyoka, M. Boonmee and A. Reungsang, *International Journal of Hydrogen Energy*, 2008, **33**, 19, 5256.

176. Y-C. Lo, W-C. Lu, C-Y. Chen and J-S. Chang, *Bioresource Technology*, 2010, **101**, 15, 5885.

177. C.Z. Liu and X.Y. Cheng, *International Journal of Hydrogen Energy*, 2010, **35**, 17, 8945.

178. L. Magnusson, N. Cicek, R. Sparling and D. Levin, *Biotechnology and Bioengineering*, 2009, **102**, 3, 759.

Abbreviations

(v/v)	Volume/volume
(w/w)	Weight/weight
^{13}C-NMR	^{13}C Solid-state nuclear magnetic resonance
A	Acid treatment
A	Proton-acceptor nanocentre
AA	Active alkali
AATCC	American Association of Textile Chemists and Colorists Standards
AdCl	Adamantoyl chloride
AFEX	Ammonia fibre explosion
AFM	Atomic force microscopy
AGU	Anhydroglucopyranose unit
AlO_2	Aluminium oxide
AMIMCl	1-*N*-Allyl-3-methylimidazolium chloride
AOX	Adsorbable organic halogens
AQ	Antraquinone
AS	Alkaline sulfite
ASAM	Alkaline sulfite-antraquinone-methanol
ASTM	American Society for Testing and Materials

ATRP	Atom transfer radical polymerisation
b	Bond strength per unit of bonded area
BAT	Reference Document on Best Available Techniques in the Pulp and Paper Industry
BC	Bacterial cellulose
BCP	Bacterial cellulose phosphate
BHKP	Bleached Hardwood Kraft Market Pulp
BMIMBr	1-*N*-Butyl-3-methylimidazolium bromide
BMIMCl	1-*N*-Butyl-3-methylimidazolium chloride
BMPF	9,9-*Bis*(4-hydroxy-3-methylphenyl)fluorine
BOD	Biological oxygen demand
BP	*Broussonetia papyrifera*
BPA	2,2-*Bis*(4-hydroxyphenyl)propane
C	Causticity
C	Chlorine
CA	Cellulose acetate
CAB	Cellulose acetate butyrate
CaO	Calcium oxide
CAP	Cellulose acetate propionate
CBC	Continuous batch cooking
CDA	Cellulose diacetate
CDD and Cdd_0	Critical degree of dilution in water-solution and distilled water
Cdtren	Cadmium-*tris*(2-aminoethyl)amine complex

CED	Cupriethylenediamine
CEPI	Confederation of European Paper Industries
CHO	*Chinese hamster ovary* cells
CIMV	Compagnie Industrielle de la Matière Végétale
CLA	Conjugated linoleic acids
CMC	Carboxymethylcellulose
CMCAB	Carboxymethylcellulose acetate butyrate
CMCP	Carboxymethylcellulose phosphate
CMCP-Na	Carboximethyl cellulose phosphate sodium salt
CNC	Cellulose nanocrystals
COD	Chemical oxygen demand
CO_2	Carbon dioxide
CPH	Combined power and heat
CP/MAS	Cross polarisation/magic angle spinning
CTA	Cellulose triacetate
CTMP	Chemithermomechanical pulping
Cuam	Cuprammonium hydroxide
Cuen	Cupriethylenediamine hydroxide
D	Chlorine dioxide
D	Proton-donor nanocentre
DCM	Dichloromethane
DDW	Drum displacer-washer
DEA	Diethylamine

DEP	Diethylphthalate
DEtA	Diethylamine
D_{HT}	Hot chlorine dioxide
DMA	*N*,*N*-Dimethylacetamide
DMF	*N*,*N*′-Dimethylformamide
DMSO	Dimethylsulfoxide
DNA	Deoxyribonucleic acid
DP	Degree of polymerisation
DR	Degree of reduction of sodium sulfate
DS	Degree of substitution
DTG	Derivative thermogravimetry
E	Alkaline extraction
EA	Effective alkali
EAPap	Electroactive paper
ECF	Elemental chlorine free
EHS	Environmental, health and safety
EMCC	Extended modified continuous cooking
EO	Alkaline extraction and oxygen
EOP	Alkaline extraction, oxygen and peroxide
EP	Alkaline extraction and peroxide
ER	Electrorheological
ESCA	Electron spectroscopy for chemical applications
ESFR	European Synchrotron Radiation Facility

ESR	Electron spin resonance
Etol	Ethanol
EU	European Union
EVA	Poly(ethylene-vinyl acetate)
EW	Earlywood
F	Flexibility coefficient
FAO	Food and Agriculture Organization of the United Nations
FBR	Forest biorefinery
FeI	Felting index
FT-IR	Fourier Transform-infrared
g	Hydration factor
G	Velocity gradient
GAN	Gaseous nitrogen
GGM	Galactoglucomannan
G-layer	Gelatinous Layer
GOX	Gaseous oxygen
H	Hypochlorite
HBMSC	Human bone marrow stromal cells
HBT	1-Hydroxybenzotriazole
HC	High consistency
HE	Hydroentaglement
HexA	Hexenuronic acid
HMF	5-Hydroxymethylfurfural

HMR	Hydroxymataresinol
HOO^-	Hydroperoxide anions
$HOO^\bullet$	Hydroperoxy radicals
HPAEC	High performance anion exchange chromatography
HRT	Hydraulic retention time
IFBR	Integrated forest biorefinery
IL	Ionic liquid(s)
INS	Inelastic neutron scattering
ITC	Isothermal cooking
ISO	International Organization for Standardization
JIS	Japanese Industry Standards
JW	Juvenile wood
K	Kappa number
kDa	kiloDaltons
L	Fibre length
l	Fibre lumen
LAR	Liquefied argon
LbL	Layer by layer
LCC	Lignin-carbohydrates complex
LCST	Low critical solution temperature
LHW	Liquid hot water
LIN	Liquefied nitrogen
LMS	Laccase-mediator system

LODP	Level-off degree of polymerisation
LOX	Liquefied oxygen
LW	Latewood
LWC	Low-weight-coated
MBA	*N*,*N*′-Methylenebisacrylamide
MC	Medium consistency
MCC	Microcrystalline cellulose
MCC	Modified continuous cooking
MFA	Microfibril angle
MFC	Microfibrillated cellulose
$MgSO_4$	Magnesium sulfate
Mj	Megajoules
ML	Middle lamella
MP steam	Medium pressure steam
Mt	Megatonnes
MW	Mature wood
Na_2S	Sodium sulfide
$Na_2S_2O_3$	Sodium thiosulfate
Na_2SO_4	Sodium sulfate
NaOH	Sodium hydroxide
NB	Polynorbornene
NDT	Sodium salt of dichlorotriazine
NFC	Nanofibrillated cellulose

Nitren	Dihydroxo-*tris*(2-aminoethyl)amine-nickel(II)-complex
N_2	Nitrogen gas
NMMO	*N*-Methylmorpholine-*N*-oxide
NMR	Nuclear magnetic resonance
NSSC	Neutral sulfite semichemical
O	Single stage oxygen delignification
$^{\bullet}O_2^-$	Superoxide radical anions
$^{\bullet}O_2^{\bullet}$	Oxygen biradicals
o.d.	Oven dried
OD	Optical density
$OH^{\bullet}$	Hydroxyl radicals
O/O	Double stage oxygen delignification
OX	Halogenated compounds
OXE	Oxidising equivalent
P	Primary wall
P	Peroxide
Paa	Peracetic acid
Pc	Post colour number
PC	Polycarbonate
PCC	Parenchymal cell cellulose
PGW	Pressure groundwood
PHK	Prehydrolysed kraft
PLA	Poly(lactic acid)

PNIPAAm	Poly(*N*-isopropylacrylamide)
PO	Pressurised peroxide
ppm	Parts per million
PPO	Poly(2,6-dimethyl-1,4-phenylene oxide)
PS	Polystyrene
PSA	Pressure swing adsorption
PVAc	Poly(vinyl acetate)
PVAm	Polyvinylamine
Q	Chelating agent
R	Runkel Ratio
RBA	Relative bonded area
RDH	Rapid displacement heating
RMP	Refiner mechanical pulping
RTIL	Room temperature ionic liquid
S	Colloidal suspension
S	Sulfidity
S1	S outermost layer
S2	S middle layer
S3	S innermost layer
SANS	2-D small angle neutron spectroscopy
SAX	Small angle X-ray
SC	Supercalendered
SCHL	Structure change in hydration layers

SEL	Specific edge load
SEM	Scanning electron microscopy
SGW	Stone groundwood
SiO_2	Silicon dioxide
SMA	Poly(styrene-*co*-maleic anhydride)
SQD	Stock quality degree
SR	Degree of pulp beating according to Schopper–Riegler
T	Peracids
TA	Total alkali
TAED	Tetraacetylethylenediamine
TAHT	Trisacryloylhexahydrotriazine
TAPPI	Technical Association of the Pulp and Paper Industry
TBAF	Tetrabutylammonium fluoride trihydrate
TC	Terminal complexes
TCF	Totally chlorine free
TCP	Tricresyl phosphate
TEM	Transmission electron microscopy
TEMPO	2,2,6,6-Tetramethylpiperidine-1-oxyl
TFA	Trifluoroacetic acid
Tg	Glass transition temperature
TGA	Thermogravimetric analysis
TGW	Thermogroundwood
TMP	Thermomechanical pulping

TMS	Trimethylsilyl
TMSC	Trimethylsilylcellulose
TosCl	*p*-Toluenesulfochloride
TRHRS	Thermo-responsive hydrated reticular system
TRS	Total reduced sulfur
TSS	Total suspended solids
UCST	Upper critical solution temperature
UF	Urea-formaldehyde
UV	Ultraviolet
VOC	Volatile organic compounds
VPSA	Vacuum pressure swing adsorption
VSA	Vacuum swing adsorption
w	Cell wall thickness
W	Fibre width
WAX	Wide angle X-ray
WF	Wall fraction
WRV	Water retention value
X	Xylanase treatment
Z	Ozone
Σs/Σi	Σsugars/Σinhibitors

Index

B

C

D

E

F

G

H

I

J

M

N

O

P

Q

R

S

T

U

V

W

X

Y

Z

ISBN 978-1-84735-633-8
90000
9 781847 356338

Published by Smithers Rapra Technology Ltd, 2013

Cellulose represents the most widely spread organic polymer found in nature and for a long time it has been used as a raw material for paper, textiles, film and flexible packing material. Due to its accessibility in huge amounts, *via* the photosynthetic process, it is a renewable material and is presently considered as a chance to answer many problems connected with sustainable development. This explains the great scientific interest in cellulose along with a preoccupation to systematise the accumulated information in reviews and books. This book will present the aspects of cellulose obtained in correlation with its integration into the new concept of biorefining.

Thus, the usual technological steps of pulp manufacture (pulping, bleaching) will be detailed along with the chemical characteristics of by-products and their utilisation, fibre characterisation for obtaining paper, cellulose derivatives and special products as a result of cellulose processing (beads and microspheres, micro- and nanostructures, fibre production, their antibacterial properties, optical functional film and hydrogen).

SMITHERS RAPRA

Shawbury, Shrewsbury, Shropshire, SY4 4NR, UK
Telephone: +44 (0)1939 250383
Fax: +44 (0)1939 251118
Web: www.polymer-books.com